Valery N. Pilipchuk

Oscillators and Oscillatory Signals from Smooth to Discontinuous

Geometrical, Algebraic, and Physical Nature

Second Edition

Springer

Oscillators and Oscillatory Signals from Smooth to Discontinuous

Valery N. Pilipchuk

Oscillators and Oscillatory Signals from Smooth to Discontinuous

Geometrical, Algebraic, and Physical Nature

Second Edition

Springer

Valery N. Pilipchuk
Mechanical Engineering Department
Wayne State University
Detroit, MI, USA

ISBN 978-3-031-37787-7 ISBN 978-3-031-37788-4 (eBook)
https://doi.org/10.1007/978-3-031-37788-4

This Springer imprint is published by the registered company Springer Nature Switzerland AG
The registered company address is: Gewerbestrasse 11, 6330 Cham, Switzerland

Preface

This book represents an updated and enhanced edition of *Nonlinear Dynamics: Between Linear and Impact Limits* originally published as Springer lecture notes 12 years ago. Now it includes an overview of the relevant applications found in the literature after the first edition, and a series of new examples illustrating theoretical statements and analytical tools. The present version still follows the so-called complementarity principle by emphasizing rudimentary spatiotemporal and algebraic roots of linearity and nonlinearity as physical concepts. Although their mathematical definitions are quite clear and straightforward, formalization of a real system is never unique. It may appear to be either linear or nonlinear for the same physical system. A simple thought experiment can clarify this point by imagining an empty Galilean space. How the space should by filled with material objects in the least possible way to observe linearity or nonlinearity? The reason for such a virtual experiment is in revealing the related elementary functions and algebraic relationships that may serve as a general basis for complementary linear and nonlinear tools. Hence, the main purpose of this book is to show that, on one hand, the subgroup of rotations and the regular complex analysis generate linear and weakly nonlinear approaches. On the other hand, translations and reflections with hyperbolic complex numbers point to the essentially nonlinear methodology based on the idea of nonsmooth temporal transformations. In elementary algebraic terms, the two complementary groups of methods appear to associate with two different signs of the equation $j^2 = \pm 1$. It will be shown that, in contrast to the regular imaginary unit, the "nonlinear gene" j is not a fixed algebraic element anymore. It is a piecewise constant discontinuous function, such as the square wave, representing subgroups of translations and reflections. These types of temporal behaviors are inherent physical properties of impact oscillators, and other mechanical systems with discontinuities of dynamic states. In this book, such type of the most severe nonlinearity is postulated as a complementary limiting case to the harmonic and quasi-harmonic cases. It should be noted that the generality of the suggested nonsmooth methodology is rather narrow compared to the universal quasi-linear approach, although the term *general* in nonlinear cases has no unique meaning. Regarding mathematical formalisms, it should be noted

that most methods of dynamics were originally developed within the paradigm of low energy smooth motions based on the classical theory of differential equations. Although the impact dynamics has also quite a long prehistory, any kind of a nonsmooth behavior is still viewed as an exemption rather than a rule since the classical theory of differential equations avoids non-differentiable functions. From such a standpoint, the current practical demands have reached the area of exemptions, namely high-energy phenomena with strongly nonlinear and nonsmooth spatiotemporal behaviors. Recall that such phenomena occur when dealing with dynamical systems under constraint conditions, friction-induced vibrations, structural damages due to cracks, liquid sloshing impacts, and numerous problems of nonlinear physics. In electrical engineering and control, some electronic devices include the so-called Schmitt trigger circuit generating nonsmooth signals whose temporal shapes resemble mechanical vibroimpact processes. In many such cases, smooth methods are adapted by splitting the system phase space in multiple domains and matching different pieces of solutions with discrete mapping. This approach resembles analytical manipulations with spatial cells in material sciences dealing with composite structures and mechanical metamaterials. The goal is to derive homogenized equations with effective moduli of elasticity and/or other global physical characteristics. Local effects are considered separately based on other equations and matching conditions incorporating structural discontinuities. It is shown in final sections of this book that alternative approaches can be developed on a cell-wise discontinuous basis to describe both local and global specifics in a closed analytical form.

The present material was prepared during different years of work for the National University and Technological University (Dnipro, Ukraine), Wayne State University, and Research and Development of General Motors (Michigan, USA). The author greatly appreciates discussions on different subjects and applications related to this book with Professors I.V. Andrianov (Aachen University) who kindly offered his help and useful comments on the text, R.A. Ibrahim (Wayne State University), A.A. Martynyuk (National Academy of Science of Ukraine), Yu.V. Mikhlin (Kharkov Polytechnic Institute), A.F. Vakakis (University of Illinois at Urbana-Champaign) for his collaboration and enthusiastic view on nonsmooth temporal transformations, A.A. Zevin (National Academy of Science of Ukraine), and V.F. Zhuravlev (Russian Academy of Science). The research style was inherited from Professor Leonid I. Manevitch, who is unfortunately no longer with us but continues his spiritual life through the work of his numerous students.

Detroit, MI, USA Valery N. Pilipchuk

Contents

Chapter 1
Introduction

This chapter contains physical and mathematical preliminaries with different introductory remarks. Although some of the statements are informal and rather intuitive, they nevertheless provide hints on selecting complementary generating models and the corresponding analytical tools. The core concept is in the assumption that a technical simplicity of mathematical formalisms is due to their hidden links with subgroups of rigid-body motions representing a primary spatiotemporal base of Euclidean geometry followed by the classical dynamics. Such motions may be qualified as rudimentary macro-dynamic phenomena developed in the physical Galilean space. For instance, since rigid-body rotations are associated with sine waves and therefore (smooth) harmonic analyses, then translations and mirror-wise reflections must reveal some adequate tools for strongly anharmonic and nonsmooth approaches. In the most explicit way, such a complementarity is revealed through the related algebraic structures. The harmonic analyses associate with the regular complex numbers, whereas the suggested set of nonsmooth tools generates the so-called hyperbolic Clifford's algebra, which is essentially enriched by the specific temporal dependence of its imaginary unit. This viewpoint is illustrated by physical examples, problem formulations, and solutions in different sections of this chapter, which is somewhat longer than usual to represent a short snapshot of the entire texts.

1.1 Brief Literature Overview

Linear and weakly nonlinear dynamic theories are covered quite completely in many monographs and textbooks. Analytical methods of conventional nonlinear dynamics are based on the classical theory of differential equations dealing with smooth coordinate transformations, asymptotic integrations, and averaging [16, 34, 69, 69, 82, 101, 104, 117, 120, 126, 129, 148, 149, 151, 152, 156, 161, 203, 204, 256]. The corresponding solutions often include quasi harmonic expansions as a generic

V. N. Pilipchuk, *Oscillators and Oscillatory Signals from Smooth to Discontinuous*,
https://doi.org/10.1007/978-3-031-37788-4_1

feature that explicitly points to the physical basis of these methods, namely, the harmonic oscillator. Generally some of the perturbation methods are also applicable to dynamical systems close to nonlinear integrable, but unfortunately nonlinear generating solutions are seldom available in closed form [16]. As a result, strongly nonlinear methods usually target specific situations and are rather difficult to use in other cases. Generating models for *strongly nonlinear* analytical tools with a wide range of applicability must obviously:

- Capture the most common features of oscillating processes regardless of their nonlinear specifics;
- Possess simple enough solutions to provide efficiency of perturbation schemes;
- Describe essentially nonlinear phenomena out of the scope of the weakly nonlinear methods.

The main goal of the present work is to suggest possible recipes for selecting such models within the set of *nonsmooth* systems while keeping the *smooth* motions still within the range of applicability. Note that different nonsmooth cases have been also considered for several decades by practical and theoretical reasons [2, 22, 24, 32, 37, 38, 49, 52, 60, 62, 63, 70, 75, 86, 88, 89, 96, 110, 111, 116, 124, 125, 128, 165–168, 205, 211, 214, 218, 228, 229, 231, 235, 247, 256, 257]. On the physical point of view, this kind of modeling essentially employs the idea of perfect spatiotemporal localization of strong nonlinearities or impulsive loadings. For instance, sudden jumps of restoring force characteristics are represented by absolutely stiff constraints under the assumption that the dynamics in between the constraints is smooth and simple enough to describe. As a result, the system dynamics is discretized in terms of mappings matching different pieces of solutions.

The present direction is rather close to another group of methods dealing with the differential equations of motion on the entire time interval despite singularity points. Such methods are developed to satisfy the matching conditions automatically by means of specific coordinate transformations on preliminary stages of study. To some extent, these can be qualified as adaptations of the differential equations of motion for further studies by another method. Among such kind of transformations, the Caratheodory substitution [63] can be mentioned first. This *linear* substitution, which includes the unit-step Heaviside function, eliminates Dirac delta-functions participating as summands in differential equations. Much later, nonsmooth *nonlinear* coordinate transformations were suggested in [251, 256] for the class of impact systems. This strongly nonlinear transformation effectively eliminates stiff barriers by unfolding the system configuration space in a mirror-wise manner with respect to the barriers. A similar idea was implemented later regarding the system phase space [96] to resolve certain problems related to non-elastic impacts. Some technical details and discussions on these methods are included below in Sects. 1.5.2 and 1.5.3 for comparison reason. In contrast, the current approach employs time histories of impact systems as new time arguments. Originally such a nonsmooth temporal transformation (NSTT), or a new temporal argument oscillating by the triangle

wave law,[1] was introduced for strongly nonlinear but smooth periodic motions with certain temporal symmetries [172]. Then, it was shown that such an approach still works for general cases by generating specific algebraic structures in terms of the coordinates [173, 185]. The occurrence of such algebraic structures seems to be an essential feature of the approach since it justifies and simplifies most analytical manipulations with non-invertible temporal substitutions, such as NSTT. Further, the technique was applied to different problems of theoretical and applied mechanics [23, 66, 87, 122, 123, 132–134, 143, 212, 213, 220, 224, 227, 230, 239, 241]. However, much of the material presented in this book is either new or significantly updated. A noticeable area of NSTT applications dealing with nonlinear beating effects emerged in recent years after publications [132] and [133]. During the beating dynamics, two interacting oscillators can exchange the energy in a more or less intensive way dictated by their initial states. On the plane of energy distribution versus phase shift, the phase portrait has a cell-wise structure, where stationary points mean the absence of energy flow, whereas cell boundaries represent the most intensive energy exchange. In physical terms, the stationary points associate with the normal mode motions. Then, as noticed in [133], the cell boundaries should be viewed as a natural alternative to the normal modes in compliance with the principle of asymptotic complementarity [6, 14, 20]: "If a system has meaningful asymptotics when some parameter tends to zero, then there exists meaningful asymptotics when this parameter tends to infinity as well." A system path along the cell boundary was defined as *the limiting phase trajectory* (LPT). Since the LPTs' simplicity develops in their temporal shapes at cost of the loss of smoothness, the corresponding solutions for different physical models were approximated analytically with NSTT in further publications [107, 108, 222]. Resonance interactions are of a great importance for the area of mechanical engineering dealing with the idea of targeted energy transfer (TET) [66, 240]. (Recent publications are reviewed in [55].) In these studies, the NSTT was used in combination with shooting method for analyses of periodic motions of the related Hamiltonian systems [122]. In material sciences, periodic temporal patterns of nonlinear normal mode types in granular media were investigated in [226]. Also, NSTT was applied to modeling spatially periodic composites to conduct their homogenization preserving cell scale specifics within closed form solutions [194]; further details are given in Chap. 14. Finally, a rigorous mathematical analysis of differential equations with generalized periodic right-hand side was conducted in [58].

The entire text is organized as follows. As mentioned in the preamble, Chap. 1 contains physical and mathematical preliminaries and different introductory remarks. Then Chap. 2 gives a brief overview of selected analytical methods for smooth oscillating processes. The description focuses on the ideas and technical details that are used further in combinations with nonsmooth approaches. In particular, the method of asymptotic integration of the differential equations

[1] In older publications, the term "sawtooth" was also used for periodic piecewise-linear functions regardless of slopes of their teeth.

of motion based on the Hausdorff equation for Lie operators is reproduced. Chapter 3 includes different examples of smooth vibrating systems that, under some conditions, show close to nonsmooth or even nonsmooth time histories. Such cases are usually most difficult for conventional analyses. Much of the content focuses on nonlinear beat and localization phenomena. Recent interest to this area is driven by the idea of nonlinear energy absorption. Chapter 4 provides a new description of NSTT with proofs of the basic identities and rules for algebraic, differential, and integral manipulations. In particular, final subsections show how to introduce nonsmooth arguments into the differential equations. Such manipulation imposes two main features on the dynamical systems, namely, generates specific algebraic structures for unknown functions and switches formulations to boundary-value problems. Notice that the transformation itself imposes no constraints on dynamical systems and easily applies to both smooth and nonsmooth systems. Any further steps, however, should account for physical properties of the related systems. Chapter 5 preliminary illustrates the NSTT's advantages by introducing power series expansions for general periodic processes. This becomes possible because the new temporal argument—the triangular sine wave—is itself periodic in the original time. Therefore, such expansions can be viewed as some alternative to Fourier series for processing periodic signals especially with stepwise discontinuities. Then a periodic version of the Lie series is introduced. As a result, formal analytical solutions for normal mode motions of dynamical systems are obtained. Chapters 6, 7, and 8 describe NSTT-based analytical tools for linear, weakly nonlinear, and strongly nonlinear vibrating systems, respectively. In particular, applying NSTT to linear and weakly nonlinear systems may be very effective in those cases when nonsmooth loadings are present, and thus harmonic or quasi harmonic approaches require multiple term expansions for capturing essential features of the dynamics. Chapters 9–11 deal with the concept of nonlinear normal modes. In particular, it is shown that NSTT leads to adequate formulations of the normal mode problem for impact systems. Also the idea of nonlinear normal modes for the case of forced vibration is formulated in terms of NSTT. Chapter 12 presents a semi-analytical approach combining NSTT with the shooting method that essentially extends the area of applications. Chapter 13 describes a possible physical basis for NSTT in case of essentially non-periodic processes. Finally, as mentioned above, Chap. 14 illustrates different applications to spatially oscillating structures such as one-dimensional elastic rods with periodic discrete inclusions and two-dimensional media with a periodic nonsmooth boundary source of waves.

1.2 Asymptotic Meaning of the Approach

1.2.1 Two Simple Limits of Lyapunov's Oscillator

This section is to illustrate the main principle on which the whole content of this book is built. For that reason, let us consider first a one-degree-of-freedom model

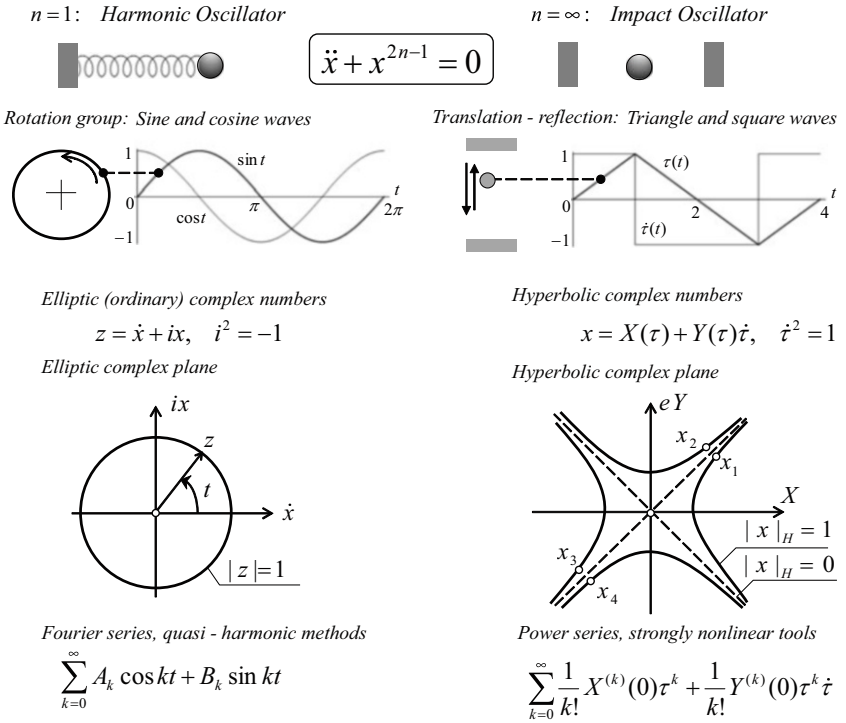

Fig. 1.1 Two complementary asymptotic limits described by elementary functions associated with subgroups of rigid-body motions: regular complex and hyperbolic planes are shown on the left and right, respectively; in contrast to the circle, each of the hyperbola branches is covered exactly once as the hyperbolic angle is varying in the infinite interval

whose differential equation of motion is shown at the top of Fig. 1.1.[2] Such a relatively simple model depicts a gradual evolution from the linear to extremely nonlinear dynamics as the exponent n varies from unity to infinity. Notably, all the temporal mode shapes of the oscillator are described by special functions except for the two boundaries of the interval $1 \leq n < \infty$. Both boundaries represent asymptotic limits within the class of *elementary functions*. The physical cause of such simplifications is explained by the behavior of the potential well $V(x) = x^{2n}/(2n)$, which takes parabolic and square shapes at the boundaries $n = 1$ and $n \to \infty$, respectively. In the latter case, the bottom of the potential well is flat, $V = 0$, within the interval $-1 < x < 1$. As a result, the particle moves with a constant speed in between the vertical potential walls at $x = \pm 1$.

[2] Note that oscillators with power-form characteristics were considered for quite a long time since possibly Lyapunov who obtained such oscillators while investigating degenerated cases in dynamic stability problems; see Chap. 3 for details.

Consider first the limit of harmonic oscillator, $n = 1$, that generates the sine and cosine waves as illustrated on the left column of Fig. 1.1. From the very general geometrical standpoint, a widely known convenience of using this couple of functions can be explained by their certain link to the group of rigid-body motions, namely, the subgroup of rotations. The standard complex plane representation and Euler formula can be mentioned here as related tools. Further, taking the linear combination of harmonic waves with different frequencies and keeping in mind the idea of parameter variations invoke the area of harmonic and quasi harmonic analyses for both signal processing and dynamical systems. Such tools therefore represent more or less complicated dynamic processes as a combination of very simple rigid-body rotations with different angular speeds.

Let us consider now another limit $n = \infty$, when the restoring force vanishes inside the interval $-1 < x < 1$ but becomes infinitely growing as the system reaches the potential barriers at $x = \pm 1$. The physical meaning of this limit is introduced at the top of the right column of the diagram. Despite the strong nonlinearity caused by impact interactions with the potential walls, the limiting case is also described by quite simple elementary functions, such as triangle and square waves, say $\tau(t)$ and $\dot{\tau}(t)$, respectively.[3] These two are associated with another subgroup of the rigid-body motions, namely, translation and reflection.[4] Therefore, analogously to the above case $n = 1$, the upper limit $n = \infty$ can play the same fundamental role by generating a hierarchy of alternative to quasi harmonic tools. On first look, such alternative tools can still be developed within the paradigm of Fourier expansions using appropriate multiple frequency combinations of $\tau(t)$ and $\dot{\tau}(t)$ instead of trigonometric functions. Although such approaches may work for signal processing, it is unclear how to deal with a large number of singularities if substituting the related expansions in differential equations of motion. Indeed nonsmoothness of such Fourier basis seems to contradict the typical formalism of continuous dynamical systems involving time derivatives.[5] In addition, the Fourier expansions are closely linked to the *linear* superposition principle.

Finally, as follows from Figs. 1.1–1.2, both functions, $\tau(t)$ and $\dot{\tau}(t)$, should not be viewed just as a formal periodic combination of straight lines.[6] It is seen that

[3] The term *square wave* will be maintained through the text as more common, although the wave shapes are rather rectangular in many cases.

[4] As mentioned in Preface, there are also electric circuits generating qualitatively similar temporal shapes [219].

[5] Generally speaking, it is possible to start with an expansion for high-order derivatives and then come backward to coordinates by integrations. However, technical complexities of such approaches may overshadow any advantages as compared to the regular Fourier expansions.

[6] It is quite clear that harmonic waves can also be interpreted as those combined of the same pieces of curves, but such a viewpoint would eliminate much of the vibration theory and many physical effects.

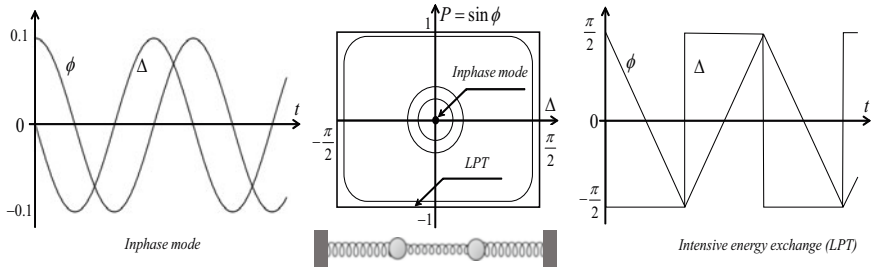

Fig. 1.2 Harmonic and nonsmooth temporal mode shapes with the corresponding phase trajectories of the energy exchange oscillator associated with the internal 1:1 resonance in two mass-spring system (Sect. 1.2.4); whereas the origin $\{\Delta, P\} = \{0, 0\}$ represents the (inphase) normal mode, the rectangle can be interpreted as a natural alternative to normal mode motions [133]

these couple of periodic nonsmooth functions emerge on a real physical basis. Therefore, appropriate mathematical formalism should follow.

Remark on Normalization of Periods

The period of sine wave is normalized to 2π obviously to comply with the geometry of circle, which is a clear representative of rotations. As a result, this normalization principle becomes somewhat baseless if applied to the triangle wave. Instead, as follows from the right part of Fig. 1.1, the unit slope of triangle wave, $\dot{\tau}^2 = 1$, represents a convenient algebraic property. Assuming that the amplitude is one, the unit slope is provided by the period equal to four. Thus the period-frequency relationships as well as the meaning of frequency for the trigonometric sine wave, $\sin \Omega t$, and the triangle wave, $\tau(\omega t)$, will be different. In order to match the periods for both functions, the following condition must be imposed

$$T = \frac{2\pi}{\Omega} = \frac{4}{\omega} \tag{1.1}$$

Below in this text, we usually use the upper case Ω for the conventional (trigonometric) sine wave frequency, whereas the low case ω will denote the triangle wave frequency. According to (1.1), such frequencies differ by the standard factor as

$$\Omega = \frac{\pi}{2}\omega \tag{1.2}$$

Using both notations helps to avoid a frequent presence of factor $\pi/2$ in differential and algebraic manipulations, although the above relationship may have a dipper (geometrical) sense indicating the complementarity of two asymptotic limits revealed by Fig. 1.1. Finally, introducing notation for a quarter of the period, $a = T/4$, gives

$$\omega = \frac{1}{a} \tag{1.3}$$

and therefore temporal scale of the triangle wave can be adjusted in either way as $\tau(\omega t) \equiv \tau(t/a)$.

1.2.2 Smoothing the Triangle Wave

The oscillator $\ddot{x} + x^{2n-1} = 0$, which is carrying the complementary asymptotics of sine and triangle waves (Fig. 1.1), represents just one of possibly several other physical and mathematical examples with similar properties. A well-known physical example of brachistochrone is analyzed in the next subsection. As a related formal example, let us consider here the example of one-parameter family of two periodic functions of the period $T = 4$ with a positive parameter α

$$\tau_\alpha(t) = \frac{2}{\pi} \arcsin\left(\alpha \sin\frac{\pi t}{2}\right), \quad 0 < \alpha < 1 \tag{1.4}$$

$$e_\alpha(t) = \frac{d\tau_\alpha(t)}{dt} = \frac{\alpha}{\sqrt{1 - \alpha^2 \sin^2(\pi t/2)}} \cos\frac{\pi t}{2} \tag{1.5}$$

In contrast to solutions of the oscillator $\ddot{x}+x^{2n-1} = 0$, the function $\tau_\alpha(t)$ belongs to the class of elementary functions for any $\alpha \in (0, 1)$ while still describing the sine wave and triangle wave at the boundaries $\alpha = 0$ and $\alpha = 1$ as, respectively,

$$\tau_\alpha(t) \sim \frac{2\alpha}{\pi} \sin\frac{\pi t}{2}, \quad \alpha \to 0 \tag{1.6}$$

and

$$\tau_\alpha(t) \sim \tau(t), \quad \alpha \to 1 \tag{1.7}$$

Therefore, function (1.4) provides a continuous transition from harmonic (1.6) to the triangular (1.7) temporal shape while including both limits into the same family of *elementary functions*. In a similar manner, we obtain

$$\begin{aligned} e_\alpha(t) &\sim \alpha \cos\frac{\pi t}{2}, \quad \alpha \to 0 \\ e_\alpha(t) &\sim \cos\frac{\pi t}{2} \Big/ \left|\cos\frac{\pi t}{2}\right| = e(t), \quad \alpha \to 1 \end{aligned} \tag{1.8}$$

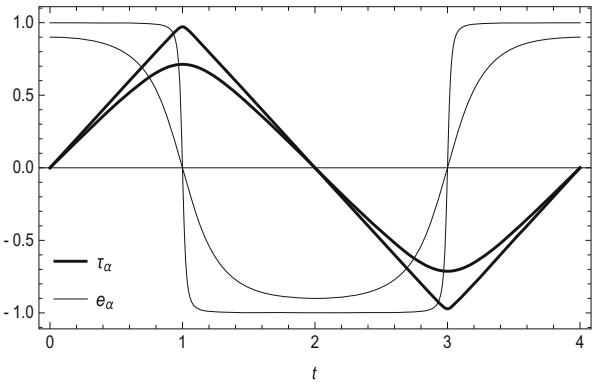

Fig. 1.3 Functions τ_α and e_α describe transition to triangle and square waves, respectively, as α increases from 0.9 to 0.999

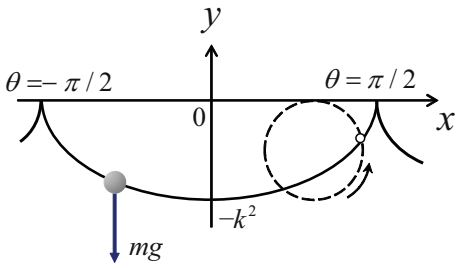

Fig. 1.4 Solution of the brachistochrone problem is given by the trajectory of a point fixed on the edge of a disc rolling along the horizontal $y = 0$ without sliding (cycloid)

Transition to nonsmooth limits (1.7) and (1.8) is illustrated in Fig. 1.3. As mentioned above, the example clarifying physical and geometrical meaning of function (1.4) as well as its asymptotic limits (1.6) and (1.7) is considered in the next subsection.

1.2.3 Complementary Asymptotics in Brachistochrone Dynamics

Figure 1.4 represents the so-called brachistochrone problem of finding the curve down which a bead sliding from the rest and accelerated by gravity will slip without friction from one point to another in the least time. Solution of this problem, which is usually considered as introductory example in calculus of variations, is given by the second-order differential equation for the vertical coordinate of the bead, $y = y(x)$:

$$1 + y'^2 + 2yy'' = 0$$

Using the substitution $y' = z(y)$ brings this equation to the separable form $1 + z^2 + 2yzz'(y) = 0$ that admits general integral

$$y(1+z^2) = y(1+y'^2) = -k^2 \tag{1.9}$$

where k is an arbitrary constant.

It can be verified by direct substitution that Eq. (1.9) describes cycloid in the parametric form

$$\begin{aligned} x &= \frac{1}{2}k^2(2\theta + \sin 2\theta) \\ y &= -\frac{1}{2}k^2(1+\cos 2\theta) \end{aligned} \tag{1.10}$$

Let us derive the differential equation of motion of the bead by using $\theta = \theta(t)$ as a generalized coordinate within the bounded interval $-\pi/2 < \theta < \pi/2$. The related one cycle of brachistochrone is shown in Fig. 1.4. Considering (1.10) as a constraint eliminating transformation to the generalized coordinate θ brings Lagrangian of the bead to the form

$$L = \frac{1}{2}m(\dot{x}^2 + \dot{y}^2) - mgy = k^2 m(2k^2\dot{\theta}^2 + g)\cos^2\theta$$

The corresponding Euler-Lagrange equation

$$\frac{d}{dt}(\dot{\theta}\cos\theta) + \frac{g}{2k^2}\sin\theta = 0 \tag{1.11}$$

admits first integral

$$(\dot{\theta}\cos\theta)^2 = \frac{g}{2k^2}(\alpha^2 - \sin^2\theta) \tag{1.12}$$

where α^2 is an arbitrary constant determined by the initial conditions for θ and $\dot{\theta}$.

Separating variables in (1.12) and integrating give periodic solution in terms of elementary functions

$$\theta = \arcsin(\alpha \sin \Omega t) \equiv A\tau_\alpha(\omega t) \tag{1.13}$$

with parameters

$$0 < \alpha < 1,\ A = \frac{\pi}{2},\ \omega = \frac{2}{\pi}\Omega \tag{1.14}$$

where the function τ_α is defined in (1.4), $\Omega = \sqrt{g/2}/k$ is the regular trigonometric frequency, and an arbitrary phase shift can always be added since the system admits the group of time translations. Note also that the system admits the replacement $\theta \to -\theta$.

As follows from (1.12), $\alpha = 0$ represents the equilibrium state, $\theta = 0$ and $\dot{\theta} = 0$, whereas the upper boundary, $\alpha = 1$, corresponds to oscillations with a maximum possible amplitude $\pi/2$. The corresponding asymptotic estimates are given by

$$\theta(t) \to \begin{cases} \alpha \sin \Omega t \text{ if } \alpha << 1 \\ A\tau\,(\omega t) \text{ if } \alpha \to 1 \end{cases} \tag{1.15}$$

Obviously, the nonsmooth limit $\alpha \to 1$ in (1.15) associates with singularities of cycloid (1.10) since the derivative $dy/dx = \cot\theta$ does not exist at $\theta = \pm\pi/2$.

1.2.4 *Hidden Vibroimpact Dynamics in Weakly Coupled Harmonic Oscillators*

As emphasized in Preface, the choice for coordinates is essential from the standpoint of formal mathematical definitions of linearity and nonlinearity. The following example shows how a perfectly linear vibrating system can reveal severely nonlinear and still physically reasonable effects. Moreover, such effects appear to have a surprisingly direct relation to the complementary sine and triangle wave asymptotics discussed already in the previous subsections. So, let us consider the process of energy exchange between two weakly coupled identical harmonic oscillators

$$\begin{aligned} m\ddot{x}_1 + kx_1 &= -\gamma(x_1 - x_2) \\ m\ddot{x}_2 + kx_2 &= -\gamma(x_2 - x_1) \end{aligned} \tag{1.16}$$

where m and k mass and base spring stiffness of each oscillator, and γ is a positive parameter characterizing the strength of coupling.

The corresponding mass-spring model is shown at the middle of Fig. 1.2. In order to describe specifics of the energy exchange, it is convenient to switch from the coordinate-velocity state variables to energy-phase variables. Details of the corresponding transformations are described in [190, 192] and will be reproduced in Sect. 3.3.1. The original coordinates are expressed through the new state variables $E_0(t)$, $P(t)$, $\Delta(t)$, and $\delta(t)$ as

$$\begin{aligned} x_1 &= \sqrt{E_0(1+P)}\cos\delta \\ x_2 &= \sqrt{E_0(1-P)}\cos(\delta+\Delta) \end{aligned} \tag{1.17}$$

where $E_0 = E_1 + E_2$ is the total energy of two independent oscillators excluding the energy of coupling, $P = (E_1 - E_2)/E_0$ is a quantity characterizing the energy distribution between the oscillators, Δ is the phase shift between the oscillators, and δ is the fast phase, which is identical to time t in the leading order.

As shown in [190, 192], Δ and P represent, respectively, a generalized coordinate and a generalized momentum of the effective energy exchange oscillator of the Hamiltonian form

$$\begin{aligned} \frac{d\Delta}{d\bar{t}} &= -\frac{P}{\sqrt{1-P^2}}\cos\Delta = \frac{\partial H}{\partial P} \\ \frac{dP}{d\bar{t}} &= \sqrt{1-P^2}\sin\Delta = -\frac{\partial H}{\partial \Delta} \end{aligned} \tag{1.18}$$

where $\bar{t} = (\gamma/\sqrt{km})t$ is a slow time whose scale is due to the strength of coupling, and the Hamiltonian is given by

$$H(\Delta, P) = \sqrt{1-P^2}\cos\Delta \tag{1.19}$$

Now using the integral $H(\Delta, P) = H_0$ and conducting the substitution $P = \sin\phi(t)$ give a strongly nonlinear oscillator of the form

$$\frac{d^2\phi}{d\bar{t}^2} + H_0^2\frac{\tan\phi}{\cos^2\phi} = 0 \tag{1.20}$$

where $H_0 = \cos\phi_0\cos\Delta_0$ is a constant determined by the initial angles ϕ_0 and Δ_0, assuming that $-\pi/2 \le \phi_0 \le \pi/2$.

It can be verified by the direct substitution[7] that oscillator (1.20) has exact analytical solution in terms of elementary functions

$$\phi = \arcsin\left[\sin\phi_0\sin\left(\Omega\bar{t} + \frac{\pi}{2}\right)\right] \tag{1.21}$$

where $\Omega = |H_0/\cos\phi_0| = |\cos\Delta_0|$.

Comparing solution (1.21) to function (1.4) gives

$$\phi = A\tau_\alpha\left(\omega\bar{t} + 1\right); \quad \alpha = \sin\phi_0, \quad A = \frac{\pi}{2}, \quad \omega = \frac{2}{\pi}\Omega \tag{1.22}$$

where notations (1.14) are adapted.

Therefore, the complementary sine and triangle wave asymptotics noticed in Sect. 1.2.2 apply to the present case as well. Note that the nonsmooth triangle wave limit, $\alpha \to 1$, associates with the rectangular boundary of the phase cell, which is shown at the middle of Fig. 1.2, whereas all the trajectories inside the phase cell are described with integral (1.19). The boundary equation $H(\Delta, P) = H_0 = 0$ describes a family of straight lines. In contrast, near the origin, one has $H_0 \sim 1$, and hence phase trajectories take almost circular shapes: $(\Delta^2 + P^2)/2 \sim 1 - H_0 << 1$.

[7] See also Sect. 3.2 for further details.

Now recall that the quantity $P = \sin\phi$ characterizes the energy distribution between the oscillators. The condition $|\phi(t)| << 1$ means that a relatively small portion of the total energy is cyclically moving back and forth between the oscillators, and thus $P \sim \phi$. In this case, Eq. (1.20) admits the following linearization

$$m\frac{d^2P}{dt^2} + k_e P = 0, \quad k_e = \frac{\gamma^2}{k}\cos^2\Delta_0 \tag{1.23}$$

where k_e is an equivalent stiffness of the energy partitioning oscillator, and the time variable t is switched back to its original meaning. Note that the equivalent stiffness of this oscillator depends upon the fixed stiffness parameters of the original system as well as its initial conditions through the phase shift Δ_0.

1.2.5 Oscillating Time and Hyperbolic Numbers

The above series of examples are to provide a theoretical legitimacy for the triangle and square waves similar to their trigonometric counterparts. It was shown that both types of functions can emerge as complementary asymptotics from the same physical systems. It can be assumed therefore that some alternative to the harmonic analyses can be developed based on the triangle and square waves. Recall that trigonometric (Fourier) expansions approximate periodic signals by combining sine and cosine waves of different frequencies. As follows from Fig. 1.1, the suggested complementary formalism follows different principle. The fundamental frequency is fixed, while the temporal shape of a signal is approximated by polynomials (power series) or some other functions of the triangle wave τ. Since the periodicity is attributed to the triangle wave, the set of approximating functions is not restricted by the periodicity condition any more. Such formalism is based on the following:

Proposition 1.2.1 *Pilipchuk [173] Any periodic process $x(t)$ of the period normalized to $T = 4$ can be expressed through the dynamic state of impact oscillator, $\{\tau(t), \dot{\tau}(t)\}$, in the form of hyperbolic complex number as*

$$x = X(\tau) + Y(\tau)\,\dot{\tau} \tag{1.24}$$

where $\dot{\tau}^2 = 1$ holds for almost any t.

All the details regarding identity (1.24) are given in Chap. 4, where the functions X and Y are expressed through $x(t)$ as

$$X(\tau) = \frac{1}{2}[x(\tau) + x(2-\tau)], \quad Y(\tau) = \frac{1}{2}[x(\tau) - x(2-\tau)] \tag{1.25}$$

Further algorithms that can be applied to components (1.24) for signal processing are introduced in Chap. 5. If $x(t)$ represents an unknown periodic motion of some dynamical system, then equations for X and Y components are obtained by substituting (1.24) into the corresponding differential equation of motion. Then either analytical or numerical procedures can be applied. For instance, the power series method with respect to powers of the "oscillating time" τ can be applied since the periodicity is built into the new argument τ. Therefore expression (1.24) can be viewed as *nonsmooth temporal transformation,* $t \to \tau$, on the manifold of periodic motions. The extension on a general period, $T = 4a$, is straightforward. For that reason, expressions (1.25) and the temporal scale of the triangle wave must be modified as

$$X(\tau) = \frac{1}{2}\left[x(a\tau) + x(2a - a\tau)\right], \quad Y(\tau) = \frac{1}{2}\left[x(a\tau) - x(2a - a\tau)\right] \tag{1.26}$$

and $\tau = \tau(t/a)$, respectively. Also, the derivative of the triangle wave, $\dot{\tau}$, in identity (1.24) must be taken with respect to its entire argument as $e(t/a) = d\tau(t/a)/d(t/a)$ in order to preserve the unit slope, $e^2 = 1$.

Remark 1.2.1 Below, the terms triangle wave and square wave will be used for the functions $\tau(\varphi)$ and $e(\varphi)$, respectively. The square wave is always first derivative of the triangle wave with respect to its entire argument. The initial phase is fixed as $\tau(0) = 0$ and $e(0) = 1$ to relate the temporal symmetry of the triangle and square waves with trigonometric sine and cosine functions, respectively. For that reason the terms triangular sine and rectangular cosine may emphasize the above specifics, although the terms triangle and square wave are more common in the literature.

Abstract Hyperbolic Structures in Algebra

A unique property of the hyperbolic number generated by relationship (1.24) is that its imaginary unit is not a fixed element any more. It is the square wave, which is a periodic stepwise discontinuous function of time. On one hand, this bridges the gap between the formal (hyperbolic) algebra and nonlinear dynamics. On the other hand, using such types of hyperbolic numbers as substitutions for the differential equations of motion requires proper extensions of the algebraic set of rules. The extensions are introduced later in this introductory chapter on a series of examples. Then further details and mathematical justifications will be given in Chap. 4. The rest of this section focuses on the complementarity of ordinary (elliptic) and hyperbolic complex algebras to further clarify the content of Fig. 1.1.

Note that the algebraic structure of hyperbolic numbers has been known for quite a long time under very different names[8] mostly as a formal extension of the regular elliptic complex numbers with no relation to dynamics and nonsmooth functions. In the mathematical literature, such an extension is often regarded to as a particular case of Clifford's algebras[9] and introduced as follows. Whereas the algebraic equation $e^2 = 1$ has the real number solutions $e = \pm 1$, the existence of a *unipotent* e is assumed such that $e \neq +1$ and $e \neq -1$ but still $e^2 = 1$. Then by considering the elements $\{1, e\}$ as a standard basis, any hyperbolic number $z \in H$ is written in the form $z = x + ye$, where x and y are real numbers. The hyperbolic conjugate of z is defined by $z^- = x - ye$ so that $|z|_H = \sqrt{zz^-}$ is the norm of z. The middle of Fig. 1.1 illustrates the difference between complex and hyperbolic planes. More details and some, rather abstract, applications of this algebraic theory can be found in references [15, 121, 223, 237]. Geometrical interpretations of hyperbolic and other algebraic structures were considered in [102, 106, 248]. As to applied areas, the same kind of algebraic structures occurred in hydrodynamics in connection with characteristics of partial differential equations [121]. Links to non-Euclidean geometry by Lobachevskii and special relativity were noticed in [248], where three different types of complex numbers were associated with three cases for the roots of quadratic equation, $x^2 + px + q = 0$. For that reason, the roots were represented as

$$x_{1,2} = -\frac{p}{2} \pm \frac{1}{2}\sqrt{\Delta} = -\frac{p}{2} \pm \frac{1}{2}\sqrt{|\Delta|}E \equiv a \pm bE \tag{1.27}$$

where $\Delta = p^2 - 4q$ is the discriminant, $a = -p/2$ and $b = \sqrt{|\Delta|}/2$ are real numbers, and E is a specific element whose role is to make solution (1.27) always, regardless of the sign of Δ, "valid." In such a way, the quadratic equation imposes three different interpretations for the element E:

$$\begin{aligned} &\Delta < 0 \Longrightarrow E = i \qquad (i^2 = -1) \\ &\Delta = 0 \Longrightarrow E = \varepsilon \qquad (\varepsilon^2 = 0) \\ &\Delta > 0 \Longrightarrow E = e \qquad (e^2 = 1) \end{aligned} \tag{1.28}$$

These relationships seem to provide some algebraic completeness. In terms of reference [248], the element i associates with *ordinary complex numbers*, ε generates the algebra of *dual numbers*, and the element e moves the combination $a + be$ into the algebra of *double numbers*. In the present text, the terms *elliptic*, *parabolic*, and *hyperbolic* are used, respectively, as more close to the complemen-

[8] Real tessarines (J. Cockle, 1848), Algebraic motors (W. Clifford, 1882), Hyperbolic numbers (J. Vignaux, 1935), Perplex numbers (Poodiack and LeClair, 2009), Double numbers (I. Yaglom [248]).

[9] William Kingdon Clifford (1845–1879), English mathematician who, in particular, developed the idea that space may not be independent of time.

tary asymptotics represented by Fig. 1.1. Note that $e^2 = 1$ but neither only $e = 1$ nor only $e = -1$ but both together as dictated by two roots (1.27). Also, recall that the term *algebra* assumes that a product of two elements is another element from the same set. For instance, taking $a + bE$ squared and enforcing table (1.28) give:

$$\begin{aligned}(a + bi)^2 &= a^2 - b^2 + 2abi \\ (a + b\varepsilon)^2 &= a^2 + 2ab\varepsilon \\ (a + be)^2 &= a^2 + b^2 + 2abe\end{aligned} \tag{1.29}$$

The imaginary units of table (1.28) admit extension on the matrix space through the following real 2×2 matrixes

$$\mathbf{i} = \begin{bmatrix} 0 & -1 \\ 1 & 0 \end{bmatrix}, \qquad \boldsymbol{\varepsilon} = \begin{bmatrix} 0 & 0 \\ 1 & 0 \end{bmatrix}, \qquad \mathbf{e} = \begin{bmatrix} 1 & 0 \\ 0 & -1 \end{bmatrix} \tag{1.30}$$

Taking these matrixes squared gives $\mathbf{i}^2 = -\mathbf{I}$, $\boldsymbol{\varepsilon}^2 = \mathbf{0}$, and $\mathbf{e}^2 = \mathbf{I}$, where $\mathbf{I}$ and $\mathbf{0}$ are 2×2 identity and zero matrixes, respectively.

In a more general *Abelian* complex number system, the role of imaginary unit can be assigned to some element E, whose squared is not necessarily listed in (1.28) but still obeys rules (1.29) as

$$E^2 = c + 2Ed \tag{1.31}$$

where c and d are real.

Then multiplications of elements from the corresponding algebra simply enforce quadratic Eq. (1.31) without solving it for E.

As follows from Fig. 1.1, the elliptic and hyperbolic algebraic structures can be associated with different types of dynamics described with smooth and nonsmooth functions of time, respectively. Furthermore, the related functions point to the link with two different subgroups of rigid body motions. Let us recall now that, as conic sections, ellipse and hyperbola describe, respectively, low- and high-energy trajectories of a satellite in the two-body problem of celestial mechanics, whereas parabola gives a natural boundary separating the low- and high-energy levels. Also, in classical dynamics, the low-energy structural vibrations with smooth temporal shapes are typically described with either linear or quasi linear differential equations. Increasing the energy may lead to the so-called essentially nonlinear effects described with qualitatively different and highly individual mathematical tools. These still superficial remarks may justify the intent to associate the general concepts of linearity and nonlinearity with the elliptic and hyperbolic algebraic structures, respectively.

Square Wave as Imaginary Unit of Hyperbolic Algebra

As already noticed above, identity (1.24) reveals the unipotent in the essentially different way as compared to the formal mathematical definition. It is neither a number nor an element any more but the discontinuous function of a certain physical nature describing the velocity of a small particle freely oscillating between two amplitude limiters. In order to emphasize the algebraic meaning of the corresponding square wave as a unipotent, we also use the notation $e(t) = \dot{\tau}(t)$. Since t is varying, then there is no unique choice for the value of e, whereas always[10] $e^2 = 1$. In addition, identity (1.24) links the hyperbolic structure to the temporal symmetry of periodic processes. Both terms on the right-hand side of (1.24) are essential as those responsible for components with different temporal symmetries. Figure 1.5 illustrates geometrical meaning of the particular case of zero Y-component, when $x(t) \equiv x[a\tau(t/a)] = X(\tau)$.

It is important to note that, under some conditions on X and Y, combination (1.24) can be of any class of smoothness even though the couple $\{\tau, \dot{\tau}\} \equiv \{\tau, e\}$ has singularities at such time instances t where $\tau = \pm 1$. As a result, differentiation of hyperbolic "numbers" (1.24) is conducted in a different way as compared to the case of fixed imaginary units. Let us take a formal derivative keeping in mind that the couple $\{\tau(t), e(t)\}$ does not possess classical derivatives at points $\Lambda = \{t : \tau(t) = \pm 1\}$. Taking into account the notation $e = \dot{\tau}$ and enforcing the property of the imaginary unit, $e^2 = 1$, give

$$\begin{aligned} \frac{dx}{dt} &= \frac{d}{dt}[X(\tau) + Y(\tau)\, e] = X'(\tau)\, e + Y'(\tau)\, e^2 + Y(\tau)\, \dot{e} \\ &= Y'(\tau) + X'(\tau)\, e + Y(\tau)\, \dot{e} \qquad (' \equiv d/d\tau) \end{aligned} \tag{1.32}$$

In terms of distributions, the derivative $\dot{e}$ represents a periodic sequence of δ-functions as shown in Fig. 1.8. Since the pulses are localized at points Λ, the term $Y(\tau)\, \dot{e}$ can be removed from (1.32) by imposing condition

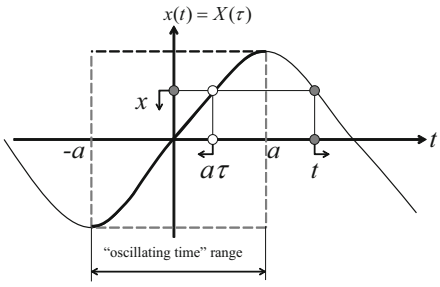

Fig. 1.5 Geometrical interpretation of the particular case with a sine-wave temporal symmetry: observing the coordinate x does not allow to conclude which of the two temporal variables, τ or t, is actually "running"

[10] More precisely, for almost any t.

$$\tau = \pm 1 : Y = 0 \tag{1.33}$$

which is obviously a necessary condition for continuity of $x(t)$. Taking into account (1.33) gives

$$\frac{d}{dt}[X(\tau) + Y(\tau)e] = Y'(\tau) + X'(\tau)e \tag{1.34}$$

The result of differentiation therefore still belongs to the algebra of hyperbolic numbers although the real and imaginary parts of the derivative dx/dt are produced by the imaginary and real parts of the function x, respectively. Further details on both differential and integral operations are described in Chap. 4 and illustrated on different examples dealing with applications.

Nonsmooth Idempotent Basis

Let us note that the hyperbolic plane has another natural basis associated with the two isotropic lines separating the hyperbolic quadrants as shown in Fig. 1.1. The transition from one basis to another is given by $e_\pm = (1 \pm e)/2$ or, inversely, $1 = e_+ + e_-$ and $e = e_+ - e_-$. Therefore,

$$\begin{aligned} x &= X + Ye = X(e_+ + e_-) + Y(e_+ - e_-) \\ &= (X + Y)e_+ + (X - Y)e_- \\ &\equiv X_+(\tau)e_+ + X_-(\tau)e_- \end{aligned}$$

where $x = x(t)$ is any periodic function, as defined in (1.24), whose period is normalized to $T = 4$.

On one hand, the advantage is that the elements e_+ and e_- are mutually annihilating (*idempotents),* $e_+e_- = 0$, whereas $e_-^2 = e_-$ and $e_+^2 = e_+$. It is clear also that $ee_+ = e_+$ and $ee_- = -e_-$. Due to the annihilation property, the idempotent basis significantly eases different algebraic manipulations, for instance,

$$(X_+e_+ + X_-e_-)^2 = X_+^2e_+ + X_-^2e_-$$

On the other hand, this basis usually makes coupled the corresponding smoothness (boundary) conditions for $X-$ and $Y-$components; see Chap. 4 for further details and examples.

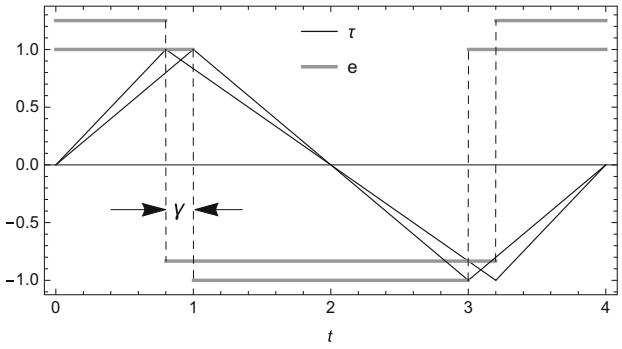

Fig. 1.6 Shifting the peaks of the triangle wave τ is equivalent to transition from hyperbolic to Abelian complex number system in terms of the imaginary unit $e = \dot{\tau}$

Links to Abelian Complex Number Systems

Shifting peaks of the triangle wave will change its positive and negative slopes as shown in Fig. 1.6. The corresponding first derivative is determined on the period in graphical way as

$$e(t,\gamma) = \frac{\partial \tau(t,\gamma)}{\partial t} = \begin{cases} (1-\gamma)^{-1} & \text{for } -1+\gamma \le t \le 1-\gamma \\ -(1+\gamma)^{-1} & \text{for } 1-\gamma \le t \le 3+\gamma \end{cases} \tag{1.35}$$

$$\forall t : e(t+4,\gamma) = e(t,\gamma)$$

Taking (1.35) squared gives another piecewise constant function $[e(t,\gamma)]^2$, which can be expressed through the function $e(t,\gamma)$ by adjusting its amplitude and shifting the outcome along the vertical as

$$[e(t,\gamma)]^2 = \frac{1}{1-\gamma^2} + \frac{2\gamma}{1-\gamma^2} e(t,\gamma) \tag{1.36}$$

Introducing the notations $E = e(t,\gamma)$, $c = \left(1-\gamma^2\right)^{-1}$, and $d = \gamma c$ brings (1.36) to the form of multiplication rule of Abelian complex number system (1.31). Further details with extensions on differential and integral operations are given in Sect. 4.1.8. From the physical standpoint, the peak shifts can be explained by modifying the oscillator with the power characteristic as

$$\ddot{x} + (1+\mu\dot{x})\, x^{2n-1} = 0 \tag{1.37}$$

where the constant coefficient μ may depend upon the number n. If $n \gg 1$, the term $\mu\dot{x}$ absorbs the energy near the maximum value $x \approx 1$ and pumps the energy back into the oscillator near the minimum at $x \approx -1$. Inside the interval $-1 <$

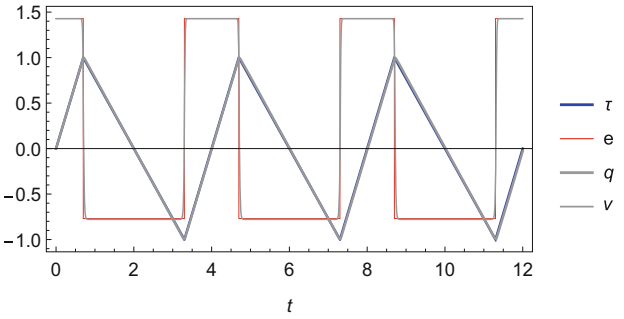

Fig. 1.7 Comparison of the temporal behavior of oscillator (1.37) in terms of the state variables q and $\dot{q} = v$ (1.38) for the initial conditions $q(0) = \tau(0, \gamma)$ and $v(0) = e(0, \gamma) = 1/(1 - \gamma)$, and a sample set of parameters: $\gamma = 0.3$, $\mu = 0.8$, $n = 40$

$x < 1$, the dynamics of system (1.37) is approximated by the equation $\ddot{x} = 0$, which is generating families of straight lines. Note that the power function x^{2n-1} can produce a significant enough restoring force slightly above the unity $|x| = 1$. As follows from the energy conservation law in the conservative case, $\mu = 0$, the actual amplitude is of order $\sim n^{1/(2n)} > 1$. For that reason, let us scale the coordinate x by means of substitution

$$x(t) = Aq(t), \qquad A = \left[n/(1-\gamma)^2\right]^{\frac{1}{2n}} \tag{1.38}$$

where the term $(1 - \gamma)^2$ is inserted to account for the effect of specific initial condition dictated by the graphs of $\tau = \tau(t, \gamma)$ and $e = e(t, \gamma)$ and explained by Fig. 1.7.

When $\gamma \neq 0$, representing the function $\tau\,(t, \gamma)$ in the closed form within the class of elementary functions may be possible although with predictable technical complexities. Alternatively, the functions $\tau\,(t, \gamma)$ and $e\,(t, \gamma)$ can be viewed as a standard couple of functions with their clear algebraic and physical basis. Further applications of this case are discussed in Chaps. 4, 6, and 14. The following examples are devoted mainly to the hyperbolic case, $\gamma = 0$.

1.3 Examples

1.3.1 Remarks on the NSTT Basis Functions

As a basis functions, the triangle and square waves, $\tau(t)$ and $\dot{\tau}(t)$, can be expressed through the standard elementary functions in the closed form as, respectively,

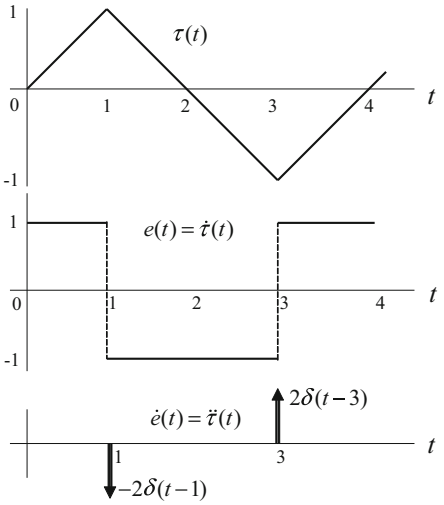

Fig. 1.8 NSTT basis functions of the normalized period $T = 4$: $\tau(t)$-the triangle wave, $e(t)$-square wave, and its generalized derivative, $\dot{e}(t)$

$$\tau(t) = \frac{2}{\pi} \arcsin \sin \frac{\pi t}{2} \tag{1.39}$$

and

$$\dot{\tau}(t) = \cos \frac{\pi t}{2} \left| \cos \frac{\pi t}{2} \right|^{-1} = e(t) \tag{1.40}$$

Obviously the amplitudes of both these waves are unity, and the period is $T = 4$ as shown at the upper right of Fig. 1.1 and detailed in Fig. 1.8. Expression (1.40) holds *almost everywhere* and can be replaced with $e(t) = \text{sgn}\,[\cos(\pi t/2)]$ for calculation purposes. Note that trigonometric formulas (1.39) and (1.40) do not participate in further analytical manipulations nor they have to be involved in numerical calculation. These relationships are given here to confirm that both functions, $\tau(t)$ and $e(t)$, belong to the class of elementary functions. Practically, for a given t, one can calculate the functions $\tau(t)$ and $e(t)$ based on their piecewise-linear graphs even with no tables nor calculators involved. From that standpoint one must admit that sine and cosine waves represent a more complicated although smooth case.

One of the further goals is to show how to deal with insulated singularities of these functions when conducting operations with differential equations. A necessary mathematical background is discussed in reference [185] and will be reproduced in Chap. 4 in more details. At this stage, solutions can be compared with exact solutions obtained in a different, either analytical or numerical, way to validate the technique. Furthermore, during the derivations, there is no need in using expressions (1.39) and (1.40). All the technical manipulations are based on:

- linear independence of the elements 1, e, and $\dot{e}$, as those from different classes of smoothness, and
- the following properties

$$\begin{aligned} \dot{\tau} &= e \\ \dot{e} &= 2\sum_{k=-\infty}^{\infty}\left[\delta\left(t+1-4k\right)-\delta\left(t-1-4k\right)\right] \\ e^2 &= 1 \end{aligned} \tag{1.41}$$

Generally, equalities (1.41) should be interpreted in terms of the distributions due to the presence of singularities that occur whenever $\tau = \pm 1$. However, all the singularities that are either inherently present in the model or occur in derivations are eventually eliminated through the specific boundary conditions. The resultant set of equations represent a classical boundary value problem with no singularities. A series of examples illustrating the technique and outlining those cases when the NSTT may be reasonable to apply is given below.

1.3.2 Overdamped Dynamics Under the Triangle Wave Forcing

Consider first a simple one-dimensional case. A light particle in a viscous fluid is subjected to the triangle wave forcing such that the differential equation of motion is reduced to

$$\dot{x}(t) = q\tau(t) \tag{1.42}$$

where q is the loading amplitude per unit coefficient of viscosity, and the inertia term is ignored.

The general solution of Eq. (1.42) is given by

$$x(t) = x(0) + q\int_0^t \tau(\varphi)d\varphi \tag{1.43}$$

where $x(0)$ is an arbitrary initial position, and the main part of this problem, which is integrating the triangle wave, still persists.

Alternatively, let us represent the periodic solution in the form of hyperbolic number

$$x = X(\tau) + Y(\tau)e \tag{1.44}$$

where $\tau = \tau(t)$ and $e = e(t)$.

Substituting (1.44) in (1.42) and taking into account properties (1.41) give

$$(Y' - q\tau) + X'e + Y\dot{e} = 0 \tag{1.45}$$

where $' \equiv d/d\tau$.

Due to the linear independence of 1, e, and $\dot{e}$, Eq. (1.45) is equivalent to the boundary value problem

$$Y' = q\tau, \qquad X' = 0, \qquad Y|_{\tau=\pm 1} = 0 \tag{1.46}$$

where the boundary condition provides zero factor for all $\delta-$functions of the derivative $\dot{e}$.

Note that problem (1.46) has no singularities. Although the function τ is nonsmooth in the original time variable t, it does no matter since the function τ plays the role of a new temporal argument. In contrast to (1.42), the integration of Eq. (1.46) is straightforward since the variable of integration is τ

$$Y = q\int_{-1}^{\tau} \tau d\tau = \frac{q}{2}(\tau^2 - 1), \qquad X = C \tag{1.47}$$

where the lower limit of integration for Y is chosen to satisfy the boundary condition in (1.46).

Substituting solution (1.47) back in (1.44) gives general solution of the original Eq. (1.42)

$$x = C + \frac{q}{2}(\tau^2 - 1)e \tag{1.48}$$

where C is an arbitrary constant of integration. Then taking into account that $\tau(0) = 0$ and $e(0) = 1$ gives $x(0) = C - q/2$, and therefore solution (1.48) takes the final form

$$x = x(0) + \frac{q}{2} + \frac{q}{2}(\tau^2 - 1)e \tag{1.49}$$

Compared to the direct approach (1.43), the NSTT allowed for integration of the differential equation of motion without dealing with the piecewise structure of the integrand. Besides, comparing solutions (1.43) and (1.49) gives relationship

$$\int_0^t \tau(\varphi)d\varphi = \frac{1}{2}[1 + (\tau^2 - 1)e], \quad \tau = \tau(t), \quad e = e(t) \tag{1.50}$$

which can be verified by differentiating both sides with respect to t.

Note that there are two boundary conditions for Y in (1.46). Since the $Y-$component of the solution appeared to be an even function of the argument τ, then both of the conditions are satisfied although just one arbitrary constant, which is

available for Y. If the forcing function in (1.42) were of even degree with respect to τ, for instance, $q\tau^2$, then the corresponding boundary-value problem would have no solution. This fact is explained by the absence of periodic solutions under the loading $q\tau^2$, which has a non-zero mean, whereas representation (1.44) imposes periodicity on the function $x(t)$. Note that the NSTT is also applicable in case of any odd degree polynomial of τ on the right-hand side of Eq. (1.42),

$$\dot{x}(t) = \sum_{k=1}^{n} q_k \tau^{2k-1}, \qquad \tau = \tau(t) \tag{1.51}$$

where and q_k are constant coefficients of the polynomial.

Analogously to the above particular case, considering the modified equation,

$$Y'(\tau) = \sum_{k=1}^{n} q_k \tau^{2k-1}$$

gives periodic solution

$$x = x(0) + \sum_{k=1}^{n} \frac{q_k}{2k} + \left[\sum_{k=1}^{n} \frac{q_k}{2k} (\tau^{2k} - 1) \right] e \tag{1.52}$$

This solution can be verified by the direct substitution of (1.52) in (1.51).

1.3.3 The Square Wave Input

Let us consider now the case of stepwise discontinuous periodic loading

$$\dot{x}(t) = pe(t) \tag{1.53}$$

Substituting (1.44) in (1.53) gives[11]

$$Y' + (X' - p)e + Y\dot{e} = 0$$

The boundary value problem therefore takes the form

$$Y'(\tau) = 0, \qquad X'(\tau) = p, \qquad Y|_{\tau=\pm 1} = 0 \tag{1.54}$$

In this case, $Y \equiv 0$, and the solution of Eq. (1.53) is

[11] Compare to (1.45).

$$x = x(0) + p\tau(t) \tag{1.55}$$

In this illustrating case, the above solution also follows directly from the definition of $e(t)$ (1.40). As a generalization, let us consider equation

$$\dot{x}(t) = e\sum_{k=0}^{m} p_k \tau^k, \quad \tau = \tau(t), \quad e = e(t) \tag{1.56}$$

where p_k are constant coefficients.

In this case, the following periodic solution does exist for both odd and even degrees of the polynomial in (1.56)

$$x = x(0) + \sum_{k=0}^{m} \frac{p_k}{k+1}\tau^{k+1} \tag{1.57}$$

Finally, combining the right-hand sides of Eqs. (1.51) and (1.56), and considering the corresponding infinite series, gives function

$$f(t) = \sum_{k=1}^{\infty} q_k \tau^{2k-1} + e\sum_{k=0}^{\infty} p_k \tau^k \equiv Q(\tau) + P(\tau)e \tag{1.58}$$

It will be shown later that expansion (1.58) represents a very general class of zero mean periodic functions with the period normalized to $T = 4$. The corresponding periodic solution of the equation $\dot{x}(t) = f(t)$ is obtained by combining solutions (1.52) and (1.57).

A Particle in Viscous Media Under the Square Wave Loading

Now, let us modify Eq. (1.53) as

$$\dot{v} + \lambda v = pe(t) \tag{1.59}$$

where $\lambda > 0$ is a constant parameter, and v can be interpreted as a velocity of the particle subjected to the external square wave loading and linear viscous force.

In this case, the substitution $v = X(\tau) + Y(\tau)e$ brings Eq. (1.59) to the form

$$Y' + \lambda X + (X' + \lambda Y - p)e + Y\dot{e} = 0$$

which is equivalent to the boundary value problem

$$Y' + \lambda X = 0, \qquad X' + \lambda Y = p, \qquad Y|_{\tau=\pm 1} = 0 \tag{1.60}$$

Eliminating the X-component from the second equation gives the differential equation $Y'' - \lambda^2 Y = -\lambda p$ with the general solution

$$Y = C_1 \sinh \lambda\tau + C_2 \sinh \lambda\tau + p/\lambda$$

Then satisfying the boundary conditions in (1.60), determining $X = -Y'/\lambda$, and substituting both X and Y back in (1.44) give the periodic solution of Eq. (1.59)

$$x(t) = \frac{p}{\lambda}\left[\frac{\sinh \lambda\tau}{\cosh \lambda} + \left(1 - \frac{\cosh \lambda\tau}{\cosh \lambda}\right)e\right], \quad \tau = \tau(t), \quad e = e(t) \tag{1.61}$$

Let us emphasize that the current solution procedure, (1.59) through (1.61), avoids typical approaches based on Fourier series expansions, Laplace transforms, or mapping separate pieces of solutions at discontinuity times. These tools would obviously require additional technical efforts in analytical manipulations. Also note that the so-called Wilbraham-Gibbs phenomenon generates quite significant errors of the Fourier expansions near the discontinuity times whose neighborhoods may appear to be of the main interest in dynamics. Instead exact solution (1.61) represents a combination of elementary functions in a closed form.

1.3.4 Oscillatory Pipe Flow Model

As a possible application, let us consider a simplified model of pipe flow driven by the square pressure wave [233]. The pipe flow $Q(t)$ is described by the first-order nonlinear differential equation

$$L\dot{Q} + KQ^2 = P_0 + P_1 e(t/a) \tag{1.62}$$

where L is a lumped inertness of the flow, K is a constant coefficient of quadratic resistance, P_0 and P_1 are constant parameters characterizing the pressure drop, and $T = 4a$ is the period of the square pressure wave.

Scaling the parameters as $k = K/L$, $p_0 = P_0/L$, and $p_1 = P_1/L$ brings Eq. (1.62) to the form

$$\dot{Q} + kQ^2 = p_0 + p_1 e(t/a) \tag{1.63}$$

The temporal behavior of the flow essentially depends on the model parameters and initial conditions. Let us assume that the flow becomes eventually periodic with the period of square pressure wave. The objective is to determine the average steady-state flow. For that reason, the corresponding periodic solution can be represented in the form

$$Q(t) = X(\tau) + Y(\tau)e \tag{1.64}$$

where $\tau = \tau(t/a)$ and $e = e(t/a)$ are triangle and square waves, respectively, of the period $T = 4a$.

Substituting (1.64) in (1.63), and taking into account the relationship $e^2 = 1$, gives

$$a^{-1}(Y' + X'e + Ye') + k(X^2 + Y^2 + 2XYe) = p_0 + p_1 e \tag{1.65}$$

where $e' = de(t/a)/d(t/a)$.

Then, using the linear independence of the elements 1, e, and $\dot{e}$ and collecting separately the related coefficients in Eq. (1.65) give

$$\begin{aligned} Y' + ak(X^2 + Y^2) &= ap_0 \\ X' + 2akXY &= ap_1 \\ Y|_{\tau=\pm 1} &= 0 \end{aligned} \tag{1.66}$$

where the boundary condition for Y provides zero factor for all $\delta-$ functions of the derivative $\dot{e}$ and hence eliminates it completely from the equation.

Introducing the new unknowns $U = X + Y$ and $V = X - Y$ brings the boundary value problem (1.66) to the form

$$\begin{aligned} U' + akU^2 &= aF \\ V' - akV^2 &= -aG \\ (U - V)|_{\tau=\pm 1} &= 0 \end{aligned} \tag{1.67}$$

where $F = p_0 + p_1$ and $G = p_0 - p_1$ are constant, and the differential equations are decoupled at cost of coupling the boundary conditions.

Both equations in (1.67) admit separation of variables with general solutions

$$\begin{aligned} U(\tau, C_1) &= \sqrt{\frac{F}{k}}\left[1 - \frac{2\exp(-2a\sqrt{kF}\tau)}{C_1 + \exp(-2a\sqrt{kF}\tau)}\right] \\ V(\tau, C_2) &= -\sqrt{\frac{G}{k}}\left[1 - \frac{2\exp(-2a\sqrt{kG}\tau)}{C_2 + \exp(-2a\sqrt{kG}\tau)}\right] \end{aligned} \tag{1.68}$$

where C_1 and C_2 are arbitrary constants of integration to be determined from the boundary conditions

$$\begin{aligned} U(1, C_1) - V(1, C_2) &= 0 \\ U(-1, C_1) - V(-1, C_2) &= 0 \end{aligned} \tag{1.69}$$

Each real solution of Eqs. (1.69) for the constants C_1 and C_2 gives a periodic solution of differential equation (1.63). Also, numerical tests show that some of the periodic solutions may appear to be unstable. Finally the pipe flow function Q can be represented in either standard or idempotent basis as

$$\begin{aligned} Q(t) &= X + Ye = \frac{1}{2}(U+V) + \frac{1}{2}(U-V)e \\ &= U(\tau, C_1)e_+ + V(\tau, C_2)e_- \end{aligned} \tag{1.70}$$

where $\tau = \tau(t/a)$ and $e_\pm(t/a) = [1 \pm e(t/a)]/2$ are the elements of idempotent basis.

It will be shown in Chap. 4 that the temporal mean value of a periodic function is determined by averaging its $X(\tau)$-component with respect to τ. For instance, solution (1.70) gives the average steady-state flow as

$$\begin{aligned} \langle Q \rangle \equiv \frac{1}{T}\int_0^T Q(t)dt = \frac{1}{2}\int_{-1}^{1} X(\tau)d\tau = \frac{1}{2}\left(\sqrt{\frac{G}{k}} - \sqrt{\frac{F}{k}}\right) \\ + \frac{1}{4ak}\ln\frac{[1 + C_1\exp(2a\sqrt{kF})][1 + C_2\exp(-2a\sqrt{kG})]}{[1 + C_1\exp(-2a\sqrt{kF}][1 + C_2\exp(2a\sqrt{kG})]} \end{aligned} \tag{1.71}$$

Figure 1.9 shows what happens to the steady-state flow profile as the period of pressure wave becomes twice longer. Note that the average flow for the period $T = 4$ is somewhat smaller compared to the case of longer period $T = 8$.

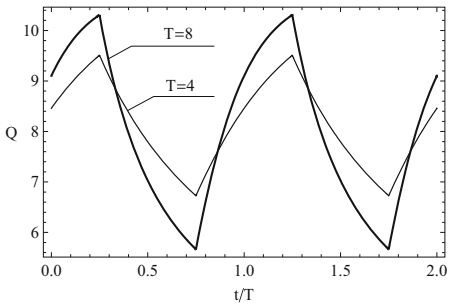

Fig. 1.9 Profiles of steady-state pipe flows obtained for two different periods T of the square pressure wave under the model parameters $k = 0.03$, $p_0 = 2.0$, and $p_1 = 1.5$; case $T = 4$: $C_1 = 8.2248$, $C_2 = -0.3125$ and $< Q >= 8.12292$; case $T = 8$: $C_1 = 11.7200$, $C_2 = -0.2651$, and $< Q >= 8.02996$

1.3.5 Periodic Impulsive Loading

Let us consider the one-dimensional motion of a material point under the periodic impulsive loading inside the linearly viscous fluid. The corresponding differential equation of the particle velocity of motion is

$$\dot{v} + \lambda v = 2p \sum_{k=-\infty}^{\infty} [\delta(t + 1 - 4k) - \delta(t - 1 - 4k)] = p\dot{e} \tag{1.72}$$

where λ and p are a coefficient of viscosity and a half of the pulse amplitude per unit mass, respectively, and the infinite sequence of Dirac functions is represented by the generalized derivative of the square wave $e(t)$ of the period $T = 4$ according to (1.41).

Equation (1.72) contains generalized functions/distributions, and therefore equality must be interpreted in terms of integral identities. Such kind of problem is usually solved by applying either Fourier series or Laplace transform or by considering the equation between the pulses by matching different pieces of the solution at the pulse times. Alternatively, the solution can be obtained in few quick steps by using identity (1.44).

Indeed, substituting (1.44) in (1.72) and taking into account (1.41) give

$$\left(Y' + \lambda X\right) + \left(X' + \lambda Y\right) e + (Y - p)\dot{e} = 0$$

or

$$Y' + \lambda X = 0, \qquad X' + \lambda Y = 0, \qquad Y|_{\tau=\pm 1} = p \tag{1.73}$$

Solving boundary value problem (1.73) in similar way to (1.60) gives the closed form particular solution

$$v = -\frac{p}{\cosh\lambda}\left(\sinh\lambda\tau - e\cosh\lambda\tau\right), \quad \tau = \tau(t/a), \quad e = e(t/a) \tag{1.74}$$

Due to linearity of Eq. (1.72), the entire general solution is obtained by adding the term with an arbitrary constant, $C\exp(-\lambda t)$.

1.3.6 Dirac Comb Loading

Let us consider the case of the one-directional Dirac's pulse loading (Dirac comb) of the period $T = 2$

$$\dot{v} + \lambda v = 2p \sum_{k=-\infty}^{\infty} \delta\,(t + 1 - 2k) = -p\,\mathrm{sgn}(\tau)\dot{e} \tag{1.75}$$

where $\tau = \tau(t)$ and $e = e(t)$ are the triangle and square waves, respectively, with the period $T = 4$.

As follows from Fig. 1.8, the term $\mathrm{sgn}(\tau)$ near the derivative $\dot{e}$ on the right-hand side of Eq. (1.75) makes all the δ-functions of the loading one-directional and positive. As a result, the loading period is as many as twice shorter. Comparing Eq. (1.75) to (1.72) leads to the boundary value problem, which is similar to (1.73) except for the boundary condition

$$Y' + \lambda X = 0, \qquad X' + \lambda Y = 0, \qquad Y|_{\tau=\pm 1} = -p\,\mathrm{sgn}(\tau) \tag{1.76}$$

Solution of this boundary value problem is obtained analogously to (1.61) and (1.74) as

$$v = \frac{p}{\sinh\lambda}\,(\cosh\lambda\tau - e\sinh\lambda\tau) \tag{1.77}$$

Solution (1.77) is illustrated in Fig. 1.10. The mean value of the velocity over one period is calculated by using the formula derived in Chap. 4 and already applied above in (1.71):

$$\langle v\rangle = \frac{1}{2}\int_{-1}^{1} X(\tau)d\tau = \frac{p}{2\sinh\lambda}\int_{-1}^{1}\cosh\lambda\tau d\tau = \frac{p}{\lambda} \tag{1.78}$$

As follows from (1.78), the particle's drift of displacement due to one-directional Dirac comb loading is estimated as $\sim (p/\lambda)t$.

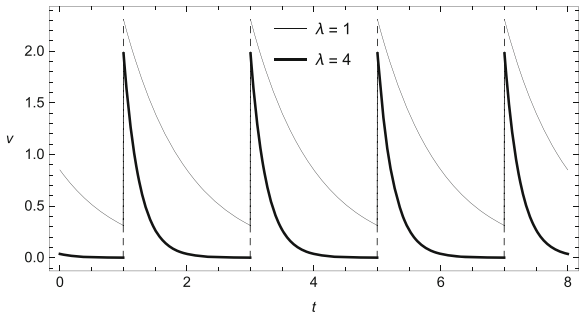

Fig. 1.10 Steady-state periodic velocity response of a particle in the viscous media under Dirac comb loading with parameters: $a = 1$ and $p = 1$

1.3.7 Combined Loading

Consider now the case of combined nonsmooth input described with equation

$$\dot{x} + (1 + \lambda e)x = pe' \tag{1.79}$$

where α and p are constant parameters, $\tau = \tau(t/a)$, $e = e(t/a)$, and e' is the periodic series of δ-functions,[12]

$$e' = \frac{de(t/a)}{d(t/a)} = 2\sum_{k=-\infty}^{\infty}\left[\delta\left(\frac{t}{a} + 1 - 4k\right) - \delta\left(\frac{t}{a} - 1 - 4k\right)\right]$$

$$= 2a\sum_{k=-\infty}^{\infty}\left[\delta\left(t + a - 4ak\right) - \delta\left(t - a - 4ak\right)\right] \tag{1.80}$$

Equation (1.79) therefore includes the periodic stepwise discontinuous parametric term e and the external periodic impulsive term e' with two-directional Dirac δ-functions. Following the previous examples and conducting the substitution $x = X(\tau) + Y(\tau)e$ in Eq. (1.79) give the following boundary value problem

$$\begin{aligned} \frac{1}{a}X' + \lambda X + Y &= 0 \\ \frac{1}{a}Y' + X + \lambda Y &= 0 \\ Y|_{\tau=\pm1} &= p \end{aligned} \tag{1.81}$$

The general solution of linear system (1.81) can be obtained by eliminating X and switching to a single second-order equation for Y. This leads to the following form of solution with two arbitrary constants

$$\begin{aligned} X &= \exp(-\lambda a\tau)\left(C_1\cosh a\tau - C_2\sinh a\tau\right) \\ Y &= \exp(-\lambda a\tau)\left(C_2\cosh a\tau - C_1\sinh a\tau\right) \end{aligned} \tag{1.82}$$

Then, determining C_1 and C_2 from the boundary conditions in (1.81) gives the periodic solution of Eq. (1.79) as

$$x = X + Ye = -ap\exp(-\lambda a\tau) \tag{1.83}$$
$$\times\left[\frac{\cosh\lambda a}{\cosh a}(\sinh a\tau - e\cosh a\tau) + \frac{\sinh\lambda a}{\sinh a}(\cosh a\tau - e\sinh a\tau)\right]$$

[12] Using the property $\delta(\gamma t) = |\gamma|^{-1}\delta(t)$.

Remark 1.3.1 Taking into account that $e^{2j} = 1$ and $e^{2j+1} = e$ for $j = 0, 1, 2, \ldots$ and almost all $t \in (-\infty, \infty)$ gives the hyperbolic version of Euler formula, where the stepwise discontinuous function e plays the role of imaginary unity,

$$\exp(\varphi e) = \sum_{j=0}^{\infty} \frac{(\varphi e)^j}{j!} = \sum_{j=0}^{\infty} \frac{\varphi^{2j}}{(2j)!} + e \sum_{j=0}^{\infty} \frac{\varphi^{2j+1}}{(2j+1)!}$$
$$= \cosh \varphi + e \sinh \varphi \tag{1.84}$$

Replacing $\varphi \to -a\tau$ in (1.84) and using the relationship $e^2 = 1$ give

$$\exp(-a\tau e) = \cosh a\tau - e \sinh a\tau$$
$$-e \exp(-a\tau e) = \sinh a\tau - e \cosh a\tau$$

Using this remark brings solution (1.83) to the form

$$x = -ap \exp[-(\lambda + e)a\tau] \left(\frac{\sinh \lambda a}{\sinh a} - \frac{\cosh \lambda a}{\cosh a} e \right) \tag{1.85}$$

Figure 1.11 illustrates solution (1.85) for two different amplitudes of the parametric loading, λ. It is seen that the parametric loading has a global effect on the system response with no influence on the stepwise discontinuities produced by the external pulses. This happens because every delta pulse of the series pe' on the right-hand side of Eq. (1.79) is balanced only by the derivative $\dot{x}$ on the left. The term $(1 + \lambda e)x$ cannot generate δ-type singularities and hence works only within intervals between the pulses. It is quite easy to prove. If this term had δ-functions, then the derivative $\dot{x}$ would produce unbalanced generalized derivatives of the δ-functions. In addition, the product ex would become questionable since δ-functions with discontinuous multipliers are not uniquely defined in the theory of distributions [63, 65].

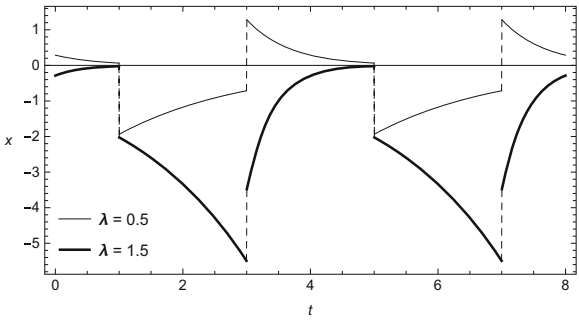

Fig. 1.11 Steady-state periodic velocity response of a particle in the viscous media under the external Dirac's two-directional pulses and parametric stepwise loads with parameters: $a = 1$ and $p = 1$

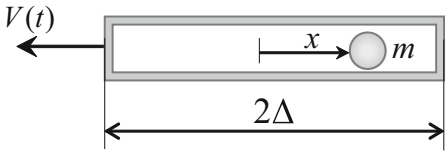

Fig. 1.12 Mass m, whose position inside the moving container is described by the relative coordinate $x(t)$, is subjected to a periodic stepwise loading and reaction impulses from the vertical walls as the container's velocity is varying according to the triangle wave law, $V(t) = V_0\tau(\omega t)$

1.3.8 Vibroimpact Oscillator Under the Stepwise Loading

Consider the dynamic behavior of a small particle of mass m inside the container whose velocity is changing according to the triangle wave law, $V(t) = V_0\tau(\omega t)$, as shown in Fig. 1.12. Using the d'Alembert principle leads to the differential equation of motion $\ddot{x} = \dot{V}(t)$, where $x(t)$ is the container-based (relative) coordinate of the mass. Then, assuming that the particle can strike the container's vertical walls gives the vibroimpact oscillator under the periodic stepwise loading and constraint condition as

$$\ddot{x} = \alpha e(\varphi), \quad |x| \le \Delta \tag{1.86}$$

where $\alpha = V_0\omega$ and $\varphi = \omega t$ are the loading amplitude and phase, respectively, and the condition of impact interactions with the walls, $x = \pm\Delta$, is given by

$$\dot{x}(t_i + 0) = -k\dot{x}(t_i - 0) \tag{1.87}$$

where t_i is the collision time, and k is the so-called coefficient of restitution, $0 \le k \le 1$.

Recall that the period of function $e(\varphi)$ with respect to the phase φ is normalized to four; hence, the loading period is $T = 4/\omega$. Let us show that, for certain frequencies ω, the problem (1.86) and (1.87) admits an exact closed-form periodic solution. First, let us replace (1.86) by an auxiliary model with no constraints

$$\ddot{x} = \alpha e(\varphi) + pe'(\varphi) \tag{1.88}$$

where the reaction of constraints is represented by the periodic series of δ-functions of the amplitude $2p/\omega$ with yet unknown parameter p. Note that systems (1.86) and (1.88) are not completely equivalent. It will be discussed in Chap. 10 that solutions of Eq. (1.88) may violate the constraint condition $|x| \le \Delta$ away from the assumed impact times. This does not happen though under proper conditions imposed on the system parameters.

Let us seek solution of Eq. (1.88) in the form $x = X(\tau) + Y(\tau)e$, where $\tau = \tau(\varphi)$ and $e = e(\varphi)$. Following the procedure described in the previous sections gives

$$X''\omega^2 + (Y''\omega^2 - \alpha)e + (X'\omega^2 - p)e' = 0 \tag{1.89}$$

Then setting separately both components of the hyperbolic number to zero and eliminating the singular term give equations and the boundary condition as, respectively,

$$\omega^2 X'' = 0, \qquad \omega^2 Y'' = \alpha \tag{1.90}$$

and

$$\tau = \pm 1: \quad Y = 0, \qquad \omega^2 X' = p \tag{1.91}$$

General solution of system (1.90) is

$$X = A\tau + B, \qquad Y = C\tau + D + \frac{\alpha\tau^2}{2\omega^2} \tag{1.92}$$

where A, B, C, and D are arbitrary constants.

Let us assume that the constraints $x = \pm\Delta$ are reached at the amplitude points $\tau = \pm 1$. Then taking into account the boundary conditions for Y-component (1.91) gives

$$X(\pm 1) + Y(\pm 1)e = \ X(\pm 1) = \pm\Delta \tag{1.93}$$

Boundary conditions (1.91) and (1.93) allow us to determine A, B, C, and D and express the reaction of constraint p through the yet arbitrary frequency parameter ω. This brings general solution (1.92) to the form

$$X = \Delta\tau, \qquad Y = \frac{\alpha}{2\omega^2}(\tau^2 - 1), \qquad \omega^2\Delta = p \tag{1.94}$$

Note that condition (1.87) still remains unsatisfied; thus, the coefficient of restitution k did not show up in the solution. Satisfying condition (1.87), which is formulated in the original time variable t, represents the main issue in the present problem. To switch to the periodic time variable τ, let us maintain the assumption that collisions take place whenever $\tau = \pm 1$. If, for instance, the collision time t_i corresponds to some amplitude point at which $\tau = -1$, then the function e switches its value from $e = -1$ to $e = +1$ when the system is passing through the collision time t_i. At those collision times, at which $\tau = 1$, the function e switches its value from $e = 1$ to $e = -1$. As a result, condition (1.87) can be replaced by the two relationships [191]

$$\begin{aligned} \tau = -1: \quad & Y' + X' = -k\left(Y' - X'\right) \\ \tau = +1: \quad & Y' - X' = -k\left(Y' + X'\right) \end{aligned} \tag{1.95}$$

Since the components X and Y are odd and even functions of τ, respectively, both of these conditions are satisfied with (1.94) if

$$\omega = \sqrt{\frac{1+k}{1-k}\frac{\alpha}{\Delta}} \tag{1.96}$$

Taking into account the notation $\alpha = V_0\omega$ and solving (1.96) for ω give also

$$\omega = \frac{1+k}{1-k}\frac{V_0}{\Delta} \tag{1.97}$$

This should be viewed as a necessary condition under which the assumed periodic solution of the period $T = 4/\omega$ does exist. Then substituting (1.96) in (1.94) gives the corresponding temporal mode shape and the constraint response p as

$$\begin{aligned} x(t) &= X + Ye = \Delta\left[\tau - \frac{1}{2}\left(\frac{1-k}{1+k}\right)(1-\tau^2)e\right] \\ p &= \omega^2\Delta = \left(\frac{1+k}{1-k}\right)^2\frac{V_0^2}{\Delta} \end{aligned} \tag{1.98}$$

where $\tau = \tau(\omega t)$ and $e = e(\omega t)$.

The temporal shapes of the coordinate and the velocity are illustrated by Fig. 1.13.

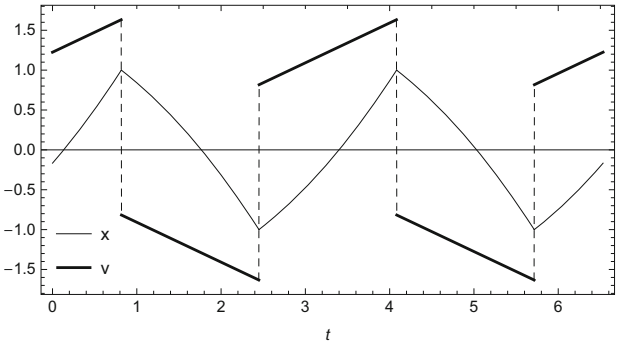

Fig. 1.13 Steady-state response of the basic vibroimpact model to the periodic stepwise loading with energy loss at the barriers: $\alpha = 0.5$, $\Delta = 1.0$, $k = 0.5$, and $\omega = 1.2247$

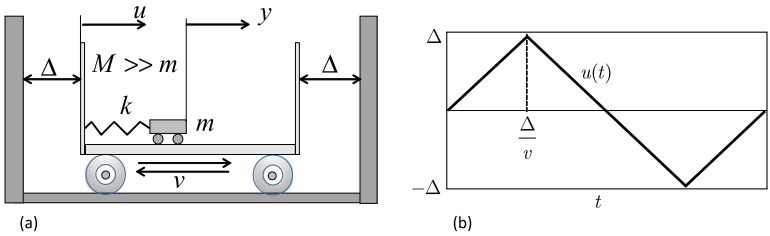

Fig. 1.14 Physical interpretation of the triangle wave support motion of harmonic oscillator, where v is the platform velocity, 2Δ is a clearance to be passed twice per one cycle, and hence a quarter of the period is $a = \Delta/v$

1.3.9 Harmonic Oscillator Under the Triangle Wave Forcing

In order to compare two alternative approaches based on a physical example, let us consider the case of triangle wave support motion for the undamped harmonic oscillator of the mass m represented by Fig. 1.14. A massive platform of the mass M, carrying the oscillator, is moving in the clearance 2Δ between two absolutely stiff walls without energy loss. Assuming that $M >> m$ and thus ignoring the feedback effect of oscillator on the dynamics of platform lead to the following differential equation of motion for the oscillator's *absolute displacement* y in the form $m\ddot{y} = k(u - y)$.

Fourier Series Solution

First, let us obtain steady-state solution by using the Fourier expansion for the support motion

$$u = \Delta\tau\,(\omega t) = \Delta\frac{8}{\pi^2}\sum_{j=1}^{\infty}\frac{(-1)^{j+1}}{(2j-1)^2}\sin\Omega_j t \tag{1.99}$$

$$\Omega_j = (2j-1)\frac{\pi}{2}\omega \quad \left(\omega = \frac{1}{a} = \frac{v}{\Delta}\right) \tag{1.100}$$

Introducing the notations $\Omega_0 = \sqrt{k/m}$ and $F_0 = (k/m)\Delta$ brings its differential equation of motion to the form

$$\ddot{y} + \Omega_0^2 y = F_0\tau\,(\omega t) = F_0\frac{8}{\pi^2}\sum_{j=1}^{\infty}\frac{(-1)^{j+1}}{(2j-1)^2}\sin\Omega_j t \tag{1.101}$$

Assuming no resonance and using the method of undetermined coefficients give the steady-state response of oscillator (1.101)

$$y = F_0 \frac{8}{\pi^2} \sum_{j=1}^{\infty} \frac{(-1)^{j+1}}{(2j-1)^2} \frac{\sin \Omega_j t}{\Omega_0^2 - \Omega_j^2} \tag{1.102}$$

Taking into account notations (1.100) and the condition of possible resonance, $\Omega_0^2 = \Omega_j^2$, from (1.102) gives the corresponding resonance velocities

$$v = \frac{2\Delta}{(2j-1)\pi} \Omega_0 \qquad (j = 1, 2, \ldots) \tag{1.103}$$

Triangle Wave Solution

Now let us apply the triangle wave temporal substitution to find the steady- state response in the form $y = X(\tau)$, where $\tau = \tau(\omega t)$ is the new time argument. Implementing this substitution in Eq. (1.101) gives the equation,

$$\omega^2 (X'' + X' e') + \Omega_0^2 X = F_0 \tau \, (\omega t)$$

which is equivalent to the boundary value problem

$$X'' + r^2 X = \omega^{-2} F_0 \tau, \qquad X'|_{\tau=1} = 0 \qquad (' \equiv d/d\tau) \tag{1.104}$$

where $r = \Omega_0/\omega$ is the adjusted frequency ratio, such that the principal resonance, $\Omega_0 = \Omega = (\pi/2)\omega$, is given by $r = \pi/2$.

The general solution of differential equation in (1.104) is

$$X = A \sin r\tau + B \cos r\tau + \frac{F_0}{\Omega_0^2} \tau \tag{1.105}$$

The arbitrary constants A and B are determined from the boundary conditions

$$\tau = 1 : r(A \cos r - B \sin r) + \frac{F_0}{\Omega_0^2} = 0$$

$$\tau = -1 : r(A \cos r + B \sin r) + \frac{F_0}{\Omega_0^2} = 0$$

as $A = -F_0/(r\Omega_0^2 \cos r)$ and $B = 0$. Then solution (1.105) takes the form

$$y = X = \frac{F_0}{\Omega_0^2} \left(\tau - \frac{\sin r\tau}{r \cos r} \right), \qquad \tau = \tau(\omega t) \tag{1.106}$$

In contrast to (1.102), solution (1.106) was derived in a closed form, which is more convenient for calculations and different analytical manipulations. As follows

from the form of solution (1.106), the resonance condition follows from the roots of equation $\cos r = 0$ and appears to be equivalent to (1.103):

$$r = \frac{\pi}{2}(2j-1) = \frac{\Omega_0}{\omega} = \frac{\Omega_0}{v}\Delta \qquad (j = 1, 2, \ldots)$$

More importantly, differentiation of the series in solution (1.102) essentially affects its convergence, whereas solution (1.106) gives both velocity and acceleration still in a closed form in two steps as

$$\dot{y} = \frac{F_0}{r\Omega_0}\left(1 - \frac{\cos r\tau}{\cos r}\right)e, \qquad e = \frac{d\tau(\omega t)}{d(\omega t)}$$

$$\ddot{y} = \frac{F_0}{r^2}\left(1 - \frac{\cos r\tau}{\cos r}\right)\frac{de(\omega t)}{d(\omega t)} + \frac{F_0}{r}\frac{\sin r\tau}{\cos r}e^2 = \frac{F_0}{r}\frac{\sin r\tau}{\cos r}$$

where the relationship $e^2 = 1$ was used and the term including periodic series of δ-functions, $de(\omega t)/d(\omega t)$, removed based on properties (1.41). Note that the acceleration, $\ddot{y}$, is still a continuous however nonsmooth function.

1.3.10 Strongly Nonlinear Oscillator

As a strongly nonlinear case, let us consider the nonlinear oscillator with reference to Fig. 1.1,

$$\ddot{x} + x^{2n-1} = 0 \tag{1.107}$$

where n is an arbitrary positive integer.

Note that this example gave the asymptotic basis for introducing the triangle wave τ as a new temporal argument [172]. In this case, the argument τ itself becomes solution as $n \to \infty$. The problem here is that the limit is nonsmooth, whereas finite numbers n still lead to smooth oscillations. Let us show that changing the temporal variable, $t \to \tau$, facilitates a natural transition to the limit $n \to \infty$. The temporal symmetry of the oscillator justifies the assumptions, $X(-\tau) \equiv -X(\tau)$ and $Y \equiv 0$, and hence the following representation for periodic solution

$$x = X(\tau), \qquad \tau = \tau(t/a) \tag{1.108}$$

where $a = T/4$ is an unknown quarter of the period.

Substituting (1.108) in (1.107) and taking into account (1.41) give

$$\frac{1}{a^2}(X'' + X'e') + X^{2n-1} = 0 \tag{1.109}$$

Due to the oddness of $X(\tau)$, Eq. (1.109) is equivalent to a one-point boundary value problem

$$X'' = -a^2 X^{2n-1}, \qquad X'|_{\tau=1} = 0 \tag{1.110}$$

where the boundary condition eliminates the singular term e' in Eq. (1.109).

The idea is to take advantage of the fact that the new temporal argument is periodic and bounded, $-1 \leq \tau \leq 1$. For that reason, successive iterations can be applied as a complementary analytical tool to the quasi harmonic methods. This tool requires no small parameter to be present explicitly. On one hand, it provides a much broader applicability. On the other hand, one must rely on the convergence of algorithm. Although the convergence is usually slow,[13] the physical basis of the convergence can always be determined whenever the problem has some physical content. Note that the harmonic balance method does not require any explicit small parameter either by assuming the temporal mode shapes to be close to harmonic. In other words, all the high frequency terms of quasi harmonic expansions just *correct* but not exceed the fundamental harmonic of the solution. In the present case, the solution is approximated by the triangle wave, which is corrected by higher powers of the same triangle wave. On the physical point of view, the model under consideration must be close to the vibroimpact rather than the harmonic oscillator. In terms of the new time variable τ, such an assumption simply means that the right-hand side of the differential equation of motion (1.110) is small enough to justify the following generating system

$$X_0'' = 0 \tag{1.111}$$

This equation describes a family of impact oscillators with the triangular sine wave time histories

$$X_0 = A\tau(t/a) \tag{1.112}$$

where A is an arbitrary constant and another (additive) constant is zero due to the symmetry $X(-\tau) \equiv -X(\tau)$.

The entire iteration algorithm can be designed in different ways. For instance, next approximation can be obtained by substituting (1.112) in the right-hand side of Eq. (1.110) and then integrating it twice as

$$X_1 = A\tau - a^2 A^{2n-1} \frac{\tau^{2n+1}}{2n(2n+1)} \tag{1.113}$$

Note that the linear term $A\tau$ occurred again as a result of integration in (1.110). Keeping the same notation for the arbitrary constant, A, automatically incorporates

[13] This is rather a side effect of the generality of successive approximation techniques.

generating solution (1.112) into the current approximation. Now ignoring (1.112) and satisfying the boundary condition for X_1 in (1.110) give

$$a^2 = \frac{2n}{A^{2n-2}} \tag{1.114}$$

and therefore

$$X_1 = A\left(\tau - \frac{\tau^{2n+1}}{2n+1}\right) \tag{1.115}$$

High-order algorithms of successive approximations are described in Chap. 8. It is shown that expression (1.114) is sequentially improved as follows:

$$a^2 = \frac{2n}{A^{2n-2}}\left(1 + \frac{2n-1}{4n+2}\right), \qquad T = 4a$$

As mentioned above, successive approximation algorithms can be applied to Eq. (1.110) with more general right-hand sides. In the above considered case, the number n relates directly to the idea of algorithm. As a result, solution (1.115) is working better as the exponent n increases. A physically meaningful transition to the limit $n \to \infty$ can be implemented by considering the initial velocity $v_0 = A/a$ instead of the parameter A. The algorithm for next steps of iteration is given in Appendix 1, and further details on the current example under the notation $m = 2n - 1$ are presented in Sect. 8.3.2. Finally, despite the manipulations with nonsmooth and discontinuous functions, solution (1.115) is twice continuously differentiable with respect to the argument t. This can be verified directly by taking first two formal derivatives of (1.115). Generally, the boundary value problem, such as (1.110), may appear to be complicated for any analytical method. In such cases, a combination of NSTT with the shooting method can be effectively used as a semi-analytical approach [185, 201].

1.4 Geometrical Views on Nonlinearity

1.4.1 Geometrical Example

As shown in the previous sections, the asymptotic of linearity has a strongly nonlinear but simple enough counterpart such that both may complement each other as possible approaches to vibration problems. In other words, two couples of basic functions, $\{\sin t, \cos t\}$ and $\{\tau(t), e(t)\}$, naturally associate with the opposite parametric boundaries of different physical systems. Recall that oscillator (1.107) is not a unique example of systems with such properties. Another case is represented by Eq. (1.20) of Sect. 1.2.4 dealing with the energy exchange between two

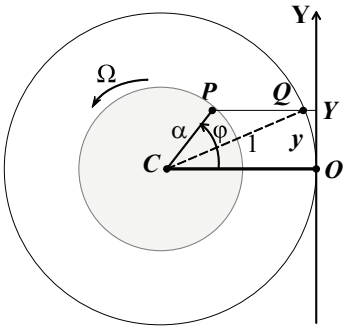

Fig. 1.15 Rigid-body rotation that generates both sine and triangular waves within the same class of elementary functions

resonating weakly coupled identical oscillators. Below, a geometrical (kinematic) interpretation for this case is introduced.[14]

Let us consider a purely geometrical model generating both sine and triangle waves as two asymptotic limits of the same family of periodic functions. With reference to Fig. 1.15, the distance between two fixed points C and O is equal to unity. A disc of the radius $CP = \alpha$ is rotating around its geometrical center C with some angular speed Ω so that the angle between CO and CP is $\varphi = \Omega t$. The edge point P of the rotating disc has its image Q on the co-centered circle of the unit radius. The image is obtained under the condition that, during the rotation, PQ remains parallel to CO. Then position of the image Q is given by either Cartesian coordinate Y or by the arc length y as follows:

$$Y = \alpha \sin\varphi \tag{1.116}$$

$$y = \arcsin(\alpha \sin\varphi) \equiv \frac{\pi}{2}\tau_\alpha\left(\frac{2}{\pi}\varphi\right) \tag{1.117}$$

where τ_α is defined earlier in (1.4).

Expression (1.117) is obtained by equating projections of CP and CQ on the vertical and taking into account that the angle QCO is equal to the corresponding arc length y. Obviously, (1.117) becomes equivalent to (1.116) and thus describes the harmonic sine wave as $\alpha \to 0$. Suppose now that $\alpha \to 1-0$. In this case, (1.117) takes the shape of triangle wave

$$y \to \frac{\pi}{2}\tau\left(\frac{2}{\pi}\varphi\right) \tag{1.118}$$

Interestingly enough, both types of observation of the above rigid-body rotation are associated with different elastic oscillators. On one hand, as a function of time, expression (1.116) satisfies equation

[14] This geometrical interpretation is unrelated to the broadly used term "geometrical nonlinearity".

$$\ddot{Y} + \Omega^2 Y = 0 \tag{1.119}$$

On the other hand, the function $y(t)$ (1.117) satisfies the differential equation of motion of the conservative oscillator

$$\ddot{y} + \frac{\tan y}{\cos^2 y} = 0 \tag{1.120}$$

under condition

$$\alpha^2 + \Omega^{-2} = 1 \tag{1.121}$$

Condition (1.121) implies that the frequency Ω depends upon the disc radius monotonically in such a way that $1 \leq \Omega < \infty$ as $0 \leq \alpha < 1$. Therefore, the nonsmooth limit (1.118) is reached under the infinitely large frequency Ω, when the total energy of oscillator (1.120) becomes infinitely large,

$$H = \frac{\dot{y}^2}{2} + \frac{\tan^2 y}{2} \to \infty \tag{1.122}$$

The reasons for considering oscillator (1.120) as a generating model in nonlinear dynamics will be explained later. At this stage, let us bring attention to the fact that both Eqs. (1.119) and (1.120) actually describe the same rigid-body rotation but in different coordinate systems.

1.4.2 Nonlinear Equations and Nonlinear Phenomena

The purpose of next few subsections is to find a physical support for using *elementary* nonsmooth systems as a basis for analytical algorithms in nonlinear dynamics. Defining the nonlinearity regardless of mathematical formalizations appears to be a challenging task. It is difficult to find appropriate physical principles that would qualify nonlinearity as a natural phenomenon rather than a specific form of mathematical expressions. Intuitively it is clear though that nonlinear phenomena may occur at high energy levels. The following scenario is described in the book [163]: "... once the power or violence of a system is increased, it leaves the familiar linear region and enters the more complex world of nonlinear effects: rivers become turbulent, amplifiers overload and distort, chemicals explode, machines go into uncontrollable oscillations, plates buckle, metals fracture, and structures collapse." The author goes even further by saying that "within such an approach, mind may no longer appear as an alien stuff in a mechanical universe; rather the operation of mind will have resonances to the transformations of matter, and indeed, the two will be found to emerge from a deeper ground." Mathematical approaches can still be helpful based on the following logical identity

$$\text{Nonlinear systems} = \text{All systems} - \text{Linear systems} \tag{1.123}$$

Although this relationship brings little physical contents, it shows that a physical understanding of the nonlinearity can possibly be achieved based on the idea of complementarity. In other words, it may be easier to clarify first what kind of physics is behind the well-known linear simplicity. The standard mathematical definition for linear systems is usually introduced through the superposition principle. Generally, it can be defined in terms of operators. Let L be an operator acting on the system states or may be positional coordinates $\{q\}$. Then the operator L is linear, if for any two states, say q_1 and q_2, and any two constants, C_1 and C_2, the following relationship holds:

$$L(C_1\, q_1 + C_2\, q_2) = C_1\, Lq_1 + C_2\, Lq_2 \tag{1.124}$$

According to (1.123), a system is nonlinear if it is not linear. This mathematical definition appears to be questionable from physical viewpoints. For instance, system

$$\begin{aligned} \ddot{\rho} - \rho\,\dot{\varphi}^2 &= \rho\,(\sin 2\,\varphi - 2) \\ \rho\ddot{\varphi} + 2\dot{\rho}\,\dot{\varphi} &= \rho\cos 2\,\varphi \end{aligned} \tag{1.125}$$

does not satisfy condition (1.124) and must be called *nonlinear*, whereas system

$$\begin{aligned} \ddot{x}_1 + 2x_1 - x_2 &= 0 \\ \ddot{x}_2 - x_1 + 2x_2 &= 0 \end{aligned} \tag{1.126}$$

is *linear*, whose linear differential operator L is acting on the position (vector) matrix $q = [x_1, x_1]^T$ as

$$Lq = \begin{bmatrix} d^2/dt^2 + 2 & -1 \\ -1 & d^2/dt^2 + 2 \end{bmatrix} \begin{bmatrix} x_1 \\ x_2 \end{bmatrix} = \begin{bmatrix} 0 \\ 0 \end{bmatrix} \tag{1.127}$$

The linear superposition principle (1.124) is therefore applicable to system (1.126) and obviously inapplicable to system (1.125). Still both sets of Eqs. (1.125) and (1.126), describe *the same two mass-spring system* in polar and Cartesian coordinates, respectively. On the plane of configurations, the corresponding coordinate transformation is given by

$$x_1 = \rho\cos\,\varphi, \qquad x_2 = \rho\sin\,\varphi \tag{1.128}$$

It is clear that the system is linear from the physical point of view, since the nonlinearity of Eqs. (1.125) is due to the specific choice for the system coordinates. Therefore, a *physical definition* for linear systems must also specify the type of coordinates, for instance: *A mechanical system is linear if its differential*

equations of motions in the inertial Cartesian frame are linear.[15] On one hand, this definition involves some physical principles since the Cartesian frame is uniquely associated with general properties of the physical space. On the other hand, the mathematical concept of coordinate systems is still present. Nonetheless, as known from observations and expressed by the above quotation [163], some dynamic phenomena are perceived as nonlinear without any explicit coordinates. Since all the theories are developed by people, then all the basic theoretical concepts and notions should inevitably inherit our spatiotemporal perceptions. The importance of human sensoring for formulations of physical laws was noticed by H. Poincaré. Since then it is discussed in the literature from different viewpoints [7, 140]. Next two subsections make yet another attempt to figure out why a nonlinear feel is actually possible and what kind of constructive conclusion may follow.

1.4.3 Rigid-Body Motions and Linear Systems

As mentioned at the beginning of this introduction, both sine and cosine waves are associated with the subgroup of rigid-body rotations. The same temporal shapes describe vibrations of deformable linearly elastic bodies such as harmonic oscillators. Therefore, one-dimensional dynamics generated by linearly elastic restoring forces can be represented as free rigid-body rotations in the two-dimensional space. In other words, the linearly elastic forces are effectively eliminated by expanding the dimension of space. In such a way, structural vibrations of linearly elastic systems can be viewed as kinematics of freely spinning discs, where the number of discs represents the number of normal modes. Any asymmetries, interactions, or dissipation must be ignored as effects beyond elementary rigid-body motions. A mathematical formalization of the above analogies can be introduced as follows. Let z be a complex vector frozen in a rigid body (disc), whose position is observed inside the empty space. The concept of *position* becomes quite vague, if there is only one body. Hence the observer represents another physical body, which is a single point. A straight line connecting this point and the center of the disc plays the role of a reference line for determining direction of the vector z. Since the disc is assumed to be rigid then

$$z'\bar{z}' = z\bar{z} \tag{1.129}$$

where the bar means complex conjugate and the prime denotes any new position of the body.

Expression (1.129) associates with the Galilean rotation, whose complex operator G is acting as

[15] Suggested by V.Ph. Zhuravlev during a private discussion at International Conference "Nonlinear Phenomena," Moscow, 1989.

$$z' = Gz \tag{1.130}$$

where G must depend on some parameter, say φ, characterizing the angular shift, $z \to z'$.

Substituting (1.130) in (1.129) gives

$$G\bar{G} = |G|^2 = 1 \Longrightarrow G = \exp(i\varphi), \qquad i^2 = -1 \tag{1.131}$$

As follows from (1.131), the conjugate operator $\bar{G}$ reverses the angular shift produced by G. Since φ is the only parameter of the only one process that can be observed from a free disc, then φ must be qualified as *time* with possibly some scaling factor. Introducing an arbitrary scaling factor, say Ω, gives then

$$G = \exp(i\Omega t) = \cos \Omega t + i \sin \Omega t \tag{1.132}$$

Now a direct calculation shows that

$$\left(\frac{d}{dt} - i\Omega\right) G = 0 \text{ and } \left(\frac{d}{dt} + i\Omega\right) \bar{G} = 0$$

Therefore both operators, G and $\bar{G}$, satisfy the differential equation of harmonic oscillator associated with the operator

$$\left(\frac{d}{dt} - i\Omega\right)\left(\frac{d}{dt} + i\Omega\right) = \frac{d^2}{dt^2} + \Omega^2 \tag{1.133}$$

Consider now n rotating discs with different angular velocities, $\Omega_1,\ldots,\Omega_n$, by generalizing product (1.133) as

$$\left(\frac{d}{dt} - i\Omega_1\right)\left(\frac{d}{dt} + i\Omega_1\right)\ldots\left(\frac{d}{dt} - i\Omega_n\right)\left(\frac{d}{dt} + i\Omega_n\right) \tag{1.134}$$
$$= \prod_{j=1}^{n}\left(\frac{d^2}{dt^2} + \Omega_j^2\right)$$

Operator (1.134) represents an arbitrary n-degrees-of-freedom linear elastic system. Replacing $d/dt \to \lambda i$ gives the corresponding characteristic equation in the form

$$\prod_{j=1}^{n}\left(\lambda^2 - \Omega_j^2\right) = 0 \tag{1.135}$$

Finally, let us consider the limit $n \to \infty$. In order to calculate the limit, the frequency dependence on its index j must be specified. If, for instance, $\Omega_j = ja$

with some constant a, then Eq. (1.135) gives

$$\prod_{j=1}^{n}\left(\lambda^2 - j^2a^2\right) = n!\prod_{j=1}^{n}\left(\frac{\lambda^2}{j^2a^2} - 1\right) = 0 \tag{1.136}$$

Skipping the nonzero factor $n!$ and considering the limit $n \to \infty$ bring Eq. (1.136) to its equivalent form

$$\sin\frac{\pi\lambda}{a} = 0 \qquad (\lambda \neq 0) \tag{1.137}$$

Equation (1.137) associates with the boundary value problem for a linearly elastic string of the length $l = \pi$ with two fixed ends

$$\frac{\partial^2 u\,(t,x)}{\partial t^2} - a^2\frac{\partial^2 u\,(t,x)}{\partial x^2} = 0; \qquad u\,(t,0) = u\,(t,\pi) = 0 \tag{1.138}$$

Therefore, it is shown that the basic linearly elastic vibrating systems can be logically derived from the kinematics of freely rotating discs or even from a more fundamental concept given by expression (1.129), which is the so-called rigid transformation preserving the lengths (*isometry)*. To some extent, this may explain why *nonlinearity* is perceptible as a physical phenomenon. Indeed it was shown that the linear dynamics associate with the *usual perception* of the space through the rigid body rotations. All the other spatiotemporal events except for the simple translation alone should therefore relate to *nonlinear* phenomena. The Galilean translation has no dynamic effect and hence is meaningless unless combined with reflections; see Sect. 1.4.5.

1.4.4 Remarks on the Multidimensional Case

The multidimensional example below gives another (purely geometrical) viewpoint on the link between rigid-body motions and the concept of linearity. First, recall that by definition, the mapping $f : R^n \longrightarrow R^n$ is an *isometry* if relation

$$\|f\,(\mathbf{v}) - f\,(\mathbf{w})\| = \|\mathbf{v} - \mathbf{w}\| \tag{1.139}$$

holds for all $\mathbf{v}, \mathbf{w} \in R^n$.

This definition requires distances between any two images and their pre-images to be same; this is a generalization of relationship (1.129). Let us consider such isometries with a fixed point $\mathbf{O}$ in R^n that is symbolically $f\,(\mathbf{O}) = \mathbf{O}$. Let us show that *an isometry that fixes the origin is a linear mapping*

$$f\,(a\mathbf{v} + b\mathbf{w}) = af\,(\mathbf{v}) + bf\,(\mathbf{w}) \tag{1.140}$$

where a and b are arbitrary scalars.

First, note that the relations

$$\|f(\mathbf{v})\| = \|\mathbf{v}\| = \|-\mathbf{v}\| = \|f(-\mathbf{v})\|$$

and

$$\|f(\mathbf{v}) - f(-\mathbf{v})\| = \|\mathbf{v} - (-\mathbf{v})\| = 2\|\mathbf{v}\|$$

hold due to (1.139), and thus $f(\mathbf{v})$ and $f(-\mathbf{v})$ are antipodal: $f(-\mathbf{v}) = -f(\mathbf{v})$.

Second, taking into account the latter result and definition (1.139) transforms the polarization identity as follows:

$$\begin{aligned}\mathbf{v}\cdot\mathbf{w} &= \frac{1}{2}\left(\|\mathbf{v}+\mathbf{w}\|^2 - \|\mathbf{v}\|^2 - \|\mathbf{w}\|^2\right)\\ &= \frac{1}{2}\left(\|f(\mathbf{v}) - f(-\mathbf{w})\|^2 - \|f(\mathbf{v})\|^2 - \|f(-\mathbf{w})\|^2\right)\\ &= \frac{1}{2}\left(\|f(\mathbf{v}) + f(\mathbf{w})\|^2 - \|f(\mathbf{v})\|^2 - \|f(\mathbf{w})\|^2\right)\\ &= f(\mathbf{v})\cdot f(\mathbf{w})\end{aligned}$$

Therefore, the inner product is preserved. Now, if $\{\mathbf{u}_i\}$ is the orthogonal basis in R^n, then $\{f(\mathbf{u}_i)\}$ is another orthogonal basis. Taking the dot product of the both sides of identity (1.140) with the arbitrary basis vector $f(\mathbf{u}_i)$ gives

$$f(a\mathbf{v}+b\mathbf{w})\cdot f(\mathbf{u}_i) = af(\mathbf{v})\cdot f(\mathbf{u}_i) + bf(\mathbf{w})\cdot f(\mathbf{u}_i)$$

or

$$(a\mathbf{v}+b\mathbf{w})\cdot\mathbf{u}_i \equiv a\mathbf{v}\cdot\mathbf{u}_i + b\mathbf{w}\cdot\mathbf{u}_i$$

The above relation proves identity (1.140) in terms of the coordinates associated with the basis $\{f(\mathbf{u}_i)\}$.

All linear isometries of R^n are denoted by the symbol $O(n)$. By choosing a basis for R^n, one can represent every element of $O(n)$ as a matrix. It can be shown that $O(n)$ consists of all $n \times n$ matrixes such that $A^{-1} = A^T$:

$$\begin{aligned}1 = \det I &= \det\left(AA^{-1}\right) = \det\left(AA^T\right)\\ &= \det A \det A^T = (\det A)^2\end{aligned} \tag{1.141}$$

Relationship (1.141) is therefore a multidimensional orthogonal matrix analogy of the relationship (1.131). In the present content, the dimension is set to be $n = 3$. Generally, orthogonal matrixes with determinant $+1$ are rotations, and those with

determinant -1 are reflections. Since rotations were linked with linearity, then reflections represent a complementary to the linearity side, which is nonlinearity. Let us summarize it as

$$\begin{array}{l} \det A = +1 \Longrightarrow rotations \quad \Longrightarrow linearity \\ \det A = -1 \Longrightarrow reflections \Longrightarrow nonlinearity \end{array} \tag{1.142}$$

Hence the singular matrix, $\det A = 0$, is a formal boundary between the linearity and nonlinearity. Figure 1.1 of this Introduction and the above series of examples give already a preview on the constructive outcome of the present discussion. Namely, the natural base for a complementary nonlinear methodology can be found within the class of *elementary nonsmooth functions* associated with reflections. Note that the idea of using nonsmooth functions for dynamic problems is not new. Space unfolding nonsmooth transformations have been applied in a geometrical way to straighten trajectories in the theory of billiards. Similar approach was suggested to derive the differential equations of motion for impact systems in a closed form without mapping; see Sects. 1.5.2 and 1.5.3 for illustrations with a detailed comparison to NSTT. Briefly, the NSTT absorbs the reflections by switching the direction of time. As a result, both reflections and smooth U-turns can be processed in the same way.

1.4.5 Natural Time of Rudimentary Nonlinearities

Let us consider now the temporal coordinate of Galilean spatiotemporal continuum. The idea of a "perfectly rigid time" is expressed by relationship

$$dt'^2 = dt^2 \iff \left(\frac{dt'}{dt}\right)^2 = 1 \tag{1.143}$$

which is a temporal analogy of condition (1.129).

Considering (1.143) as a differential equation with respect to $t' = s\,(t)$ gives two solutions

$$t' = \pm\,(t - a) \tag{1.144}$$

where a is an arbitrary temporal shift.

Now, combining different branches of (1.144) for $t < a$ and $t > a$ gives

$$t' = s\,(t) = |t - a| \tag{1.145}$$

Function (1.145) also satisfies Eq. (1.143), for all t except maybe single point $t = a$, where the classical derivative of $s\,(t)$ has no certain value, and equality (1.143) holds for almost all t except maybe $t = a$. Solution (1.145) admits an obvious

physical interpretation since it describes a free material point moving in the space split into two subspaces by a stiff plane assuming that the velocity is scaled by condition

$$\dot{s}^2 = 1 \tag{1.146}$$

Since the perception of empty space rejects any built-in stiff planes, then a sudden V-turn of the particle will represent *unusual*, in other words, *strongly nonlinear* event. This is obviously the most elementary nonlinear event whose simplicity nevertheless will be employed further in less trivial cases.

1.4.6 Example of Simplification in Nonsmooth Limits

The idea that transition to the most severe nonlinearity may actually simplify a system response finds its support in very different examples. Consider, for instance, the differential equation of motion

$$\ddot{x} = \exp\left(-\frac{2x}{\epsilon^2}\right) \tag{1.147}$$

where ϵ is a small parameter compared to unity. The nonlinear force on the right-hand side gives the "rigid body" limit as the parameter ϵ approaches zero. Let us assume that $\dot{x} = -1$ and $x \to \infty$ as $t \to -\infty$. In this case, Eq. (1.147) has exact solution

$$x(t) = \epsilon^2 \ln\left(\epsilon \cosh \frac{t-a}{\epsilon^2}\right) \tag{1.148}$$

where a is an arbitrary parameter such that $\dot{x}(a) = 0$; see Fig. 1.16, where $a = 1$.

Now let us consider the asymptotic limit $\epsilon \to 0$. Taking into account the evenness of cosh-function brings solution (1.148) to the form

$$x = \epsilon^2 \ln\left(\epsilon \cosh \frac{|t-a|}{\epsilon^2}\right) = \epsilon^2 \ln\left(\epsilon \cosh \frac{s}{\epsilon^2}\right) \tag{1.149}$$

This manipulation represents a useful preliminary step for asymptotic estimates, because the new temporal argument, s, remains always positive as the original time runs in the interval $-\infty < t < \infty$. Further algebraic manipulations bring solution (1.149) to the form

$$x = s + \epsilon^2 \ln\left[\frac{\epsilon}{2}\left(1 + \exp\left(-\frac{2s}{\epsilon^2}\right)\right)\right] \tag{1.150}$$

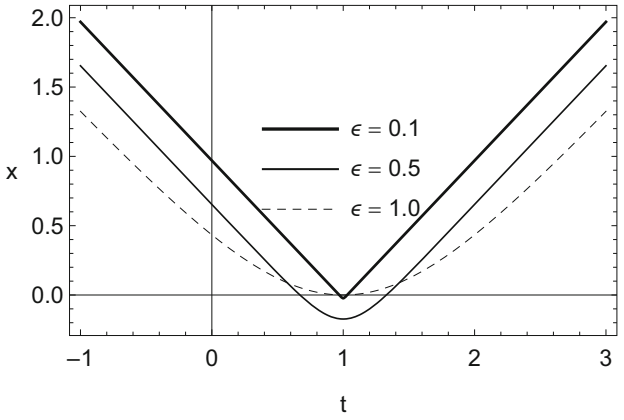

Fig. 1.16 Time histories of the particle when the barrier approaches rigid-body limit, $\epsilon \to 0$

Taking into account that $0 < \exp\left(-2s/\epsilon^2\right) < 1$ gives the "rigid-body" limit

$$x \to s = |t - a| \tag{1.151}$$

as $\epsilon \to 0$.

This example shows that (1.145) can be viewed as a natural time associated with the temporal symmetry of a V-turn. Note that the new temporal argument is both nonsmooth and non-invertible with respect to the original time. As a result, using (1.145) for temporal substitutions in the differential equations of motion has certain specifics as discussed below.

1.4.7 Preliminaries on Nonsmooth Time Arguments

The goal of this subsection is to show why the inversion of nonsmooth time arguments generates hyperbolic algebraic structures. As mentioned above, the piecewise linear function, $s(t)$, (1.145) can play the role of a natural temporal argument associated with the elementary nonlinear events such as dynamic V-turns. The temporal symmetry of V-turns is captured by the function $s(t)$ regardless of possible shapes of the potential barriers. Therefore, using the function $s(t)$ as a temporal argument should ease further analyses since the information about V-turns is built into the new argument. The corresponding time substitution is not straightforward since its inverse version does not exist in the form $t = t(s)$. A correct version requires the following generalization $t = t(s, \dot{s})$. Below, this case is discussed first. Then the periodic version is introduced that reveals a structural similarity of expressions since periodic motions can be viewed as regular sequences of U-turns. More details are given in Chap. 4.

Nonperiodic Case

Let us start with the inverse version of (1.145), which includes both the image s and its time derivative $\dot{s}$ as follows:

$$t = t(s, \dot{s}) = a + s\dot{s} \tag{1.152}$$

As follows from (1.146), combination (1.152) represents an element of hyperbolic structure with the basis $\{1, \dot{s}\}$. In other words, time belongs to the algebra of hyperbolic complex numbers with the table of products generated by (1.146). For instance, taking (1.152) squared gives another hyperbolic number

$$t^2 = a^2 + s^2 + 2as\dot{s} \tag{1.153}$$

Hyperbolic numbers are known to be isomorphic to symmetric 2×2-matrixes. For instance, relationship (1.153) can be represented as

$$t^2 = (a + s\dot{s})^2 \longleftrightarrow \begin{pmatrix} a & s \\ s & a \end{pmatrix}^2 = \begin{pmatrix} a^2 + s^2 & 2as \\ 2as & a^2 + s^2 \end{pmatrix} \tag{1.154}$$

Moreover, it is easy to prove for any function $x(t)$ that[16]

$$x\,(t) = X\,(s) + Y\,(s)\,\dot{s} \tag{1.155}$$

where

$$X\,(s) = \frac{1}{2}\left[x\,(a + s) + x\,(a - s)\right]$$

$$Y\,(s) = \frac{1}{2}\left[x\,(a + s) - x\,(a - s)\right]$$

For instance, setting $a = 0$ in the case $x(t) = \exp t$ gives

$$\exp\,(\dot{s}s) = \cosh s + \dot{s}\sinh s \tag{1.156}$$

In contrast to the conventional complex algebra, division is not always possible. For instance, the following relationship is meaningless for $|a| = s$ or $t = 0$:

$$\frac{1}{t} = \frac{1}{a + s\dot{s}} = \frac{(a - s\dot{s})}{(a + s\dot{s})\,(a - s\dot{s})} = \frac{a}{a^2 - s^2} - \frac{s}{a^2 - s^2}\dot{s}$$

[16] See Sect. 4.1.2.

In the particular case of even function $x\,(t)$, with respect to $t = a$, one can set $Y\,(s) \equiv 0$ in (1.155).

Periodic Case

The periodic version of nonsmooth time transformations, which is introduced in Sect. 1.2.5, involves triangle and square waves described by the periodic piecewise-linear function

$$\tau\,(t) = \frac{2}{\pi}\arcsin\sin\frac{\pi t}{2} = \begin{cases} t & \text{for } -1 \le t \le 1 \\ -t+2 & \text{for } 1 \le t \le 3 \end{cases}, \qquad \tau\,(t) \overset{\forall t}{=} \tau\,(4+t)$$

and its Schwartz derivative $e(t) = \dot{\tau}\,(t)$; see Figs. 1.1 and 1.8.

Recall that, from the physical point of view, the functions $\tau\,(t)$ and $e\,(t)$ describe dynamic states of a particle oscillating between two rigid walls with no energy loss as shown in Fig. 1.17. The spatiotemporal coordinates are normalized as

$$dt^2 = d\tau^2 \Longleftrightarrow e^2 = \dot{\tau}^2 = 1 \tag{1.157}$$

Note that relationship (1.157) is a periodic version of (1.146) whereas, for any periodic function of the period $T = 4$, representation (1.24) is a periodic version of (1.155). In other words, any periodic motion uniquely associates with the standard impact vibration, for instance, as follows:

$$x\,(t) = A\sin\frac{\pi t}{2} + B\cos\frac{\pi t}{2} = A\sin\frac{\pi\tau}{2} + B\cos\frac{\pi\tau}{2}e \tag{1.158}$$

where $\tau = \tau\,(t)$, $e = \dot{\tau}\,(t)$, and A and B are arbitrary constants.

Exercise 1.4.1 By taking formal derivatives of $x(t) = X(\tau) + Y(\tau)e$, show that differentiation keeps the result within the set of hyperbolic numbers provided that the signal $x(t)$ is smooth enough. For instance,

$$d^{2n-1}\left(A\sin\frac{\pi\tau}{2} + B\cos\frac{\pi\tau}{2}e\right)/dt^{2n-1} = \left(\frac{\pi}{2}\right)^{2n-1}\left(-B\sin\frac{\pi\tau}{2} + A\cos\frac{\pi\tau}{2}e\right)$$

$$d^{2n}\left(A\sin\frac{\pi\tau}{2} + B\cos\frac{\pi\tau}{2}e\right)/dt^{2n} = \left(\frac{\pi}{2}\right)^{2n}\left(A\sin\frac{\pi\tau}{2} + B\cos\frac{\pi\tau}{2}e\right)$$

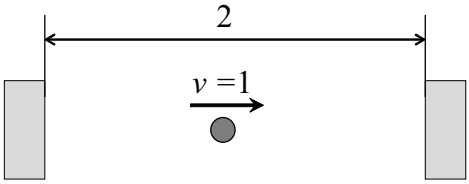

Fig. 1.17 Mechanical model whose dynamic states are described with the triangular and square wave functions, $\tau\,(t)$ and $\dot{\tau}\,(t)$, respectively

$$(n = 1, 2, \ldots)$$

1.4.8 Examples of NSTT for Periodic Signals

The Fourier analysis is based on the standard trigonometric functions $\{\sin \Omega t, \cos \Omega t\}$ or $\{\exp(i\Omega t), \exp(-i\Omega t)\}$ so that periodic signals are described by linear combinations of these functions with appropriate sets of frequencies $\{\Omega_k\}$. For instance, the dynamic states of the impact oscillators are represented as

$$\begin{aligned}
\tau(t) &= \frac{8}{\pi^2}\left(\sin\frac{\pi t}{2} - \frac{1}{3^2}\sin\frac{3\pi t}{2} + \frac{1}{5^2}\sin\frac{5\pi t}{2} - \ldots\right) \\
&= \frac{4i}{\pi^2}\sum_{k=-\infty}^{\infty}\frac{(-1)^k}{(2k-1)^2}\exp(i\Omega_k t) \\
e(t) &= \frac{4}{\pi}\left(\cos\frac{\pi t}{2} - \frac{1}{3}\cos\frac{3\pi t}{2} + \frac{1}{5}\cos\frac{5\pi t}{2} - \ldots\right) \\
&= \frac{2}{\pi}\sum_{k=-\infty}^{\infty}\frac{(-1)^{k+1}}{(2k-1)^2}\exp(i\Omega_k t)
\end{aligned} \tag{1.159}$$

where $\Omega_k = (2k-1)\pi/2$.

The well-known convenience of Fourier series for handling partial and ordinary differential equations is due to the fact that $\exp(i\Omega t)$ is an eigen function of the time derivative, in other words, $d\exp(i\Omega t)/dt = i\Omega\exp(i\Omega t)$. This important advantage is unfortunately missing when using a generalized nonsmooth basis for Fourier expansions.

The proposed alternative is based on *power series* expansions since, in terms of the oscillating time τ, the power series remain periodic, for instance:

$$\begin{aligned}
\sin\frac{\pi t}{2} &= \sin\frac{\pi\tau}{2} = \frac{\pi\tau}{2} - \frac{1}{3!}\left(\frac{\pi\tau}{2}\right)^3 + \frac{1}{5!}\left(\frac{\pi\tau}{2}\right)^5 - \ldots \\
\cos\frac{\pi t}{2} &= \cos\frac{\pi\tau}{2}e = \left[1 - \frac{1}{2!}\left(\frac{\pi\tau}{2}\right)^2 + \frac{1}{4!}\left(\frac{\pi\tau}{2}\right)^4 - \ldots\right]e
\end{aligned} \tag{1.160}$$

These truncated series preserve periodicity at cost of smoothness loss though; see Fig. 1.18 for explanation. Fortunately, the nonsmoothness times $\Lambda = \{t : \tau(t) = \pm 1\}$ are same for every term of the series, and this enables one of smoothing the series by re-ordering their terms as follows (Chap. 5):

$$\sin\frac{\pi t}{2} = \sin\frac{\pi\tau}{2} = \frac{\pi}{2}\left(\tau - \frac{\tau^3}{3}\right) + \left(\frac{\pi}{2} + \frac{\pi^3}{16}\right)\left(\frac{\tau^3}{3} - \frac{\tau^5}{5}\right)$$

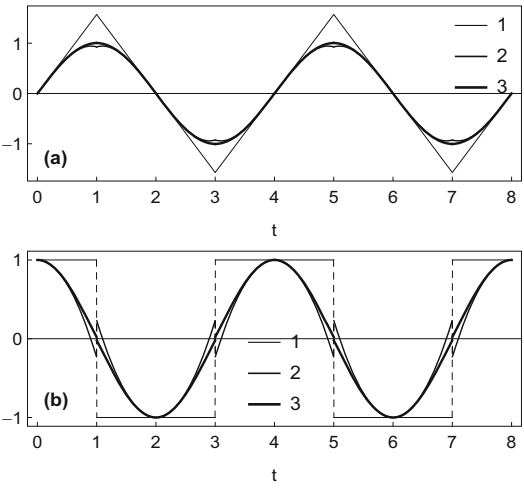

Fig. 1.18 Truncated Maclaurin's NSTT expansions with respect to τ for (**a**) $\sin(\pi t/2)$ and (**b**) $\cos(\pi t/2)$ including (1) one, (2) two, and (3) three first terms of the expansions shown by the curves of increasing thickness

$$+\left(\frac{\pi}{2}+\frac{\pi^3}{16}+\frac{\pi^5}{768}\right)\left(\frac{\tau^5}{5}-\frac{\tau^7}{7}\right)+\ldots \tag{1.161}$$

$$\cos\frac{\pi t}{2}=\cos\frac{\pi\tau}{2}e=\left[1-\tau^2+\left(1-\frac{\pi^2}{8}\right)\left(\tau^2-\tau^4\right)\right.$$
$$\left.+\left(1-\frac{\pi^2}{8}+\frac{\pi^4}{384}\right)\left(\tau^4-\tau^6\right)+\ldots\right]e$$

Figure 1.19 illustrates both convergence and smoothness of the transformed series as compared with the diagrams in Fig. 1.18. Moreover, it will be shown in Chap. 5 that the power series of τ can be re-ordered in such a manner that their particular sums become as smooth as necessary whenever the signal $x(t)$ is smooth. Still the convenience of such kind of series is that they can accurately approximate nonsmooth or close to them processes just by first few terms.

Finally, there are many physical processes easily described by very simple combinations of the triangle and square waves, which otherwise would require quite long Fourier sums; see Fig. 1.20, for examples.

1.4.9 Differential Equations of Motion and Distributions

Any nonsmooth substitution in the differential equations of motion must be examined since the differentiation is involved. In many physically meaningful cases, mathematical justifications can be achieved by understanding the equalities as integral identities. For illustration purposes, let us consider conservative oscillator

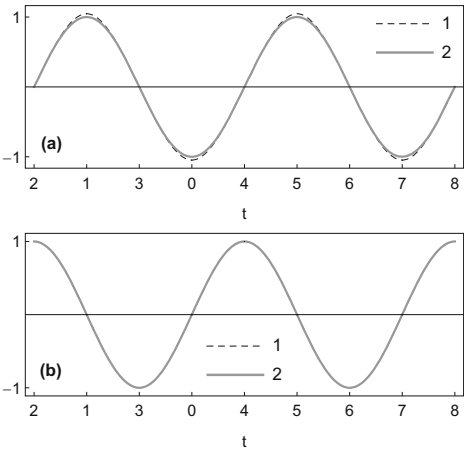

Fig. 1.19 First term of the modified NSTT series with respect to τ for (**a**) $\sin(\pi t/2)$ and (**b**) $\cos(\pi t/2)$; 0—original functions, 1—first term of the series

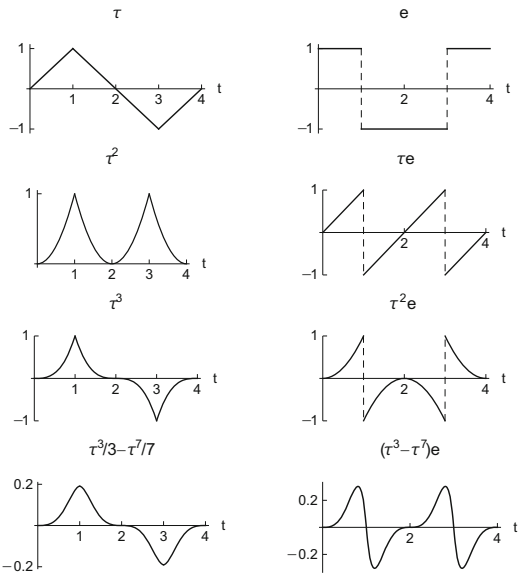

Fig. 1.20 Sample temporal shapes of periodic signals described by combinations of the triangle and square waves

$$\ddot{x} + V'(x) = 0 \tag{1.162}$$

where $V(x)$ is the potential energy.

Classical pointwise interpretations of the differential equations require no discontinuities to occur on the left-hand side of (1.162). Therefore, real motions must be described by at least twice continuously differentiable functions of time, $x(t) \in C^2(R)$. Practically, however, physical systems cannot be observed at every time instance. In other words, the point-wise interpretation of equality (1.162) appears to be restrictive from the physical standpoint. As an extension of classical approaches,

the left-hand side of Eq. (1.162) can be considered as some force producing zero work on arbitrary path variations δx during the observation interval, $t_1 < t < t_2$:

$$\int_{t_1}^{t_2} \left[\ddot{x} + V'(x)\right] \delta x dt = 0 \tag{1.163}$$

or

$$-\delta \int_{t_1}^{t_2} \left[\frac{1}{2}\dot{x}^2 - V(x)\right] dt = -\delta S = 0 \tag{1.164}$$

where S is the action by Hamilton.

Expression (1.164) represents Hamiltonian principle, where the integral can be calculated for less smooth functions, say $x(t) \in C(R)$. Therefore, it is possible to essentially extend the class of solutions based on interpretation (1.163) rather than Eq. (1.162). Note that Eq. (1.162) may be strongly nonlinear; however, the highest derivative must participate in a linear way as a summand; otherwise, transition from (1.163) to (1.164) may become impossible.

1.5 Nonsmooth Coordinate Transformations

1.5.1 Caratheodory Substitution

Including Dirac's δ-functions in nonlinear differential equations complicates mathematical justifications of the modeling. It is important how δ-functions participate in equations [63, 65]. Let, for instance, the differential equation to include δ-function as a summand

$$\dot{x} = kx^3 + q\delta(t - t_1) \tag{1.165}$$

where k, q, and t_1 are constant parameters.

In this case, the δ-function input generates a stepwise discontinuity of the response $x(t)$ at $t = t_1$. Still the nonlinear operation in (1.165) is meaningful. Moreover, the δ-function is easily excluded from Eq. (1.165) by substitution

$$x(t) = y(t) + qH(t - t_1) \tag{1.166}$$

where $y(t)$ is a new unknown function and $H(t - t_1)$ is the unit-step Heaviside function.

Substituting (1.166) in (1.165) and taking into account that $\dot{H}(t-t_1) = \delta(t-t_1)$, $H^2(t-t_1) = H(t-t_1)$, and $H^3(t-t_1) = H(t-t_1)$ give

$$\dot{y} = k[y^3 + (q^3 + 3yq^2 + 3y^2q)H(t-t_1)] \tag{1.167}$$

where $y(t)$ is now continuous on the entire time interval, including the point t_1.

1.5.2 Transformation of Positional Variables

One-Dimensional Case

Now let us discuss the method of nonsmooth coordinate transformation (NSCT) for mechanical systems with perfectly stiff constraints [252]. According to this approach, the new coordinates are introduced in order to automatically satisfy the constraint conditions. Let us reproduce the idea based on the one-degree-of-freedom Lagrangian system

$$L = \frac{1}{2}\dot{x}^2 - V(x) \tag{1.168}$$

whose motion is limited by interval

$$-1 \le x \le 1 \tag{1.169}$$

It is assumed that the particle collides with the obstacles $x = \pm 1$ with no energy loss.

Note that relationships (1.168) and (1.169) give no unique differential equation of motion on the entire time domain since every collision with constraints indicates transition from one system to another. Even though the form of Lagrangian (1.168) remains the same, one must deal with different solutions before and after every collision, say $x^-(t)$ and $x^+(t)$. Matching such solutions is usually not straightforward since collision times are a priori unknown.

The main reason for applying NSCT is that it gives a single differential equation of motion for the entire time interval with no constraint conditions. As a result, the mapping procedure becomes unnecessary. In addition, as a result of the transformation, a new system appears to be well suited for averaging since no impact forces are involved any more.

Regarding Eqs. (1.168) and (1.169), the NSCT is introduced as follows:[17]

$$x = \tau(s) \tag{1.170}$$

[17] Note that both notations and normalization for the period for the triangle wave function differ from the original work [252].

where $s(t)$ is a new positional coordinate.

Substituting (1.170) into (1.168) gives

$$L = \frac{1}{2}[\tau'(s)\dot{s}]^2 - V(\tau(s)) = \frac{1}{2}\dot{s}^2 - V(\tau(s)) \tag{1.171}$$

where the prime indicates differentiation with respect to s, and the relationship $[\tau'(s)]^2 = [e(s)]^2 = 1$ has been taken into account.

Now, condition (1.169) is satisfied automatically since $-1 \leq \tau(s) \leq 1$, whereas the Hamiltonian principle gives the differential equation of motion with no constraints

$$\ddot{s} + \frac{dV}{d\tau}e(s) = 0 \tag{1.172}$$

On geometrical point of view, transformation (1.170) unfolds the configuration space by switching the coordinate direction on opposite whenever the particle collides with an obstacle. As a result, the new configuration space acquires a cell-wise non-local structure as illustrated in [242] and [196]. This usually makes the differential equation essentially nonlinear even when the system in between the constraints is linear. Let, for instance, the potential energy function represent the harmonic oscillator, $V(x) = \Omega^2 x^2/2$. Then the coordinate transformation (1.170) brings system

$$\ddot{x} + \Omega^2 x = 0, \qquad -1 \leq x \leq 1 \tag{1.173}$$

to the form

$$\ddot{s} + \Omega^2 \tau(s)e(s) = 0, \qquad -\infty < s < \infty \tag{1.174}$$

Note that, as a side effect of the elimination of constraints, the differential equation has lost its linearity. The original system is strongly nonlinear as well because linear differential equation (1.173) alone does not describe the entire system. The nonlinearity is hidden in condition (1.169).

The comparison between NSCT and NSTT can be summarized as follows [184]:

Coordinate transformation	Time transformation
Unfolds the space with no effect on the time variable	Folds the time, and generates the hyperbolic algebraic structures in space
Targets rigid barriers (constraints)	Barriers do no matter
Dynamic regime independent	Assumes certain temporal symmetries of motion
Applies to a function (image)	Transforms an argument (pre-image)
Essentially changes the ODE structure, for instance, linear on strongly nonlinear	Preserves most structural properties of ODEs

As follows from this comparison, NSCT is quite the opposite to NSTT from both physical and mathematical viewpoints.

Multidimensional Case

For illustrating purposes, consider also the following N-degrees-of-freedom Lagrangian system

$$L = \frac{1}{2}\sum_{i=1}^{N} \dot{x}_i^2 - \frac{1}{2}\sum_{i=0}^{N} k_i (x_{i+1} - x_i)^2 \tag{1.175}$$

$$|x_i(t)| \le 1 \tag{1.176}$$

$$x_0(t) \equiv x_{N+1}(t) \equiv 0 \tag{1.177}$$

This is a chain of unit-mass particles connected by linearly elastic springs of stiffness k_i. Stiff constraints are imposed on each of the coordinates according to (1.176). Although Lagrangian (1.175) generates linear differential equations, these equations alone do not completely describe the system. Due to the presence of constraints (1.176), the system is strongly nonlinear, and this becomes obvious in the adequately chosen coordinates. Transition to such coordinates is given by space unfolding transformation

$$x_i = \tau(s_i) \tag{1.178}$$

where τ is the triangle wave of spatial coordinates s_i $(i = 1, \ldots, N)$.

The coordinate transformation (1.178) brings system (1.175) through (1.177) to the form

$$L = \frac{1}{2}\sum_{i=1}^{N} \dot{s}_i^2 - \frac{1}{2}\sum_{i=0}^{N} k_i [\tau(s_{i+1}) - \tau(s_i)]^2 \tag{1.179}$$

$$s_0(t) \equiv s_{N+1}(t) \equiv 0. \tag{1.180}$$

It is seen from (1.179) that transformation (1.178) preserves the quadratic form of the kinetic energy while constraint conditions (1.176) are satisfied automatically due to the property $|\tau(s_i)| \le 1$. In contrast to (1.175), Lagrangian (1.179) completely describes the model on the entire time interval $0 \le t < \infty$. Instead, in terms of the new coordinates, the potential energy acquired a non-local cell-wise structure so that the corresponding differential equations of motion are essentially nonlinear as seen from Eqs. (1.181) below. After the transformation, every impact interaction with constraints is interpreted as a transition from one cell to another as illustrated below on the case $N = 2$. In this case, Lagrangian (1.179) gives the differential equations of motion on the infinite plane $-\infty < s_i < \infty$ $(i = 1, 2)$ with no constraints

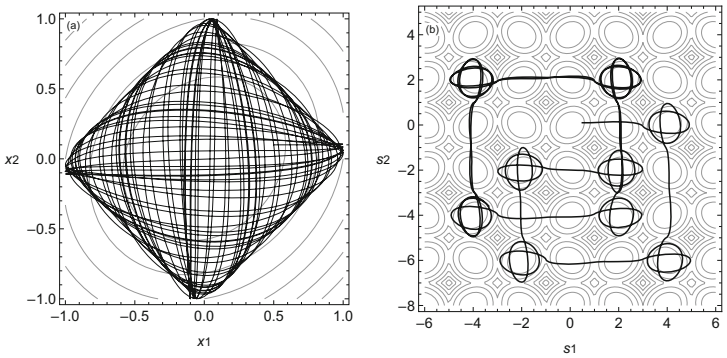

Fig. 1.21 Potential energy levels and a sample trajectory of the system obtained under the initial conditions at $t = 0$: $x_1 = 0.5$, $x_2 = 0.0$, $\dot{x}_1 = 1.0$, and $\dot{x}_2 = 0.0$: (**a**) system configuration plane in the original coordinates, and (**b**) unfolded configuration plane

$$\begin{aligned} \ddot{s}_1 + [(k_0 + k_1)\tau(s_1) - k_1\tau(s_2)]\tau'(s_1) = 0 \\ \ddot{s}_2 + [(k_1 + k_2)\tau(s_2) - k_1\tau(s_1)]\tau'(s_2) = 0 \end{aligned} \tag{1.181}$$

Figure 1.21b shows the corresponding equipotential energy levels and a sample trajectory of the beat-wise dynamics. It is seen that the system is trapped in different cells sometimes for the energy exchange process. After one of the two masses accumulated the energy, which is sufficient to reach the barrier, the impact event happens with a transition to another cell. The fact of energy exchange inside a trapping cell is confirmed by the transversality of incoming and outcoming pieces of the trajectory. As long as the mass remains in impact regime, its trajectory is passing through one cell to another until the system is trapped again in another cell for a new energy exchange process. A similar geometrical interpretation but for *impact normal mode* dynamics was introduced earlier in [242], where the impact modes were associated with originally hidden geometrical symmetries of the periodic patterns of equipotential lines as shown in Fig. 1.21b. Compared to just two axes of symmetry ($x_2 = \pm x_1$), associated with the elliptic curves in Fig. 1.21a, the unfolded configuration plane has four axes of symmetry ($s_2 = \pm s_1$, $s_2 = 0$, and $s_1 = 0$). Obviously the axes, $s_2 = 0$ and $s_1 = 0$, admit parallel shifts due to the periodicity of the potential field.

Whereas the axes $s_2 = \pm s_1$ dictate exact solutions, the additional symmetries, $s_2 = 0$ and $s_1 = 0$, represent the dynamic regimes in asymptotic high-energy limits with extremely intensive strikes against the amplitude limiters.

1.5.3 Transformation of State Variables

Under some restrictions, the NSCT can still be adapted to the case of non-elastic interactions with constraints in a purely geometrical way [256]. However,

generalized approaches to such cases should involve both coordinates and velocities [96, 97] as illustrated below based on two different examples.

Bouncing Ball Problem

Let us consider a small ball of mass m, which is dropped from some height, $z = h > 0$, onto a level floor, $z = 0$, in a viscous environment with the coefficient of linear viscosity c. When the ball hits the floor, the velocity u reverses with the coefficient of restitution k. Components of the state vector, $\{z, u\}$, are therefore described as

$$\dot{z} = u$$
$$\dot{u} = -g - \frac{c}{m}u \tag{1.182}$$
$$u_+ = -ku_- \quad \text{if} \quad z = 0 \tag{1.183}$$

where u_+ and u_- are velocities of the ball immediately after and before the contact with the floor, respectively.

Despite the linearity of the differential equations, the entire system is obviously strongly nonlinear due to condition (1.183). This is why eliminating condition (1.183) makes the nonlinearity explicit. The corresponding transformation of state variables $\{z, u\} \to \{s, v\}$ is introduced in reference [97] as

$$z = s\ \mathrm{sgn}(s)$$
$$u = \mathrm{sgn}(s)[1 - \kappa\ \mathrm{sgn}(sv)]v \tag{1.184}$$
$$\kappa = \frac{1-k}{1+k}$$

Applying (1.184) to (1.182) gives[18]

$$\dot{s} = [1 - \kappa \mathrm{sgn}(sv)]v \tag{1.185}$$
$$\dot{v} = -\frac{c}{m}v - \frac{g}{1-\kappa^2}[\mathrm{sgn}(s) + \kappa \mathrm{sgn}(v)]$$

As compared to (1.182), system (1.185) automatically accounts for condition (1.183) at cost of strong nonlinearity of the resultant differential equations. Nonetheless, the advantage of new system (1.185) is that it represents the dynamic process over the entire time interval, $0 \le t < \infty$, with no conditioning at $z = 0$.

[18] Note that differentiation of sgn-functions will produce Dirac delta-functions with effectively zero factors however.

Harmonic Oscillator with One-Sided Barrier

As another example, let us consider the case of harmonic oscillator under the constraint condition

$$\dot{\mathbf{x}} = \mathbf{A}\mathbf{x}, \qquad x_1 > 0 \tag{1.186}$$

where $\mathbf{x} = [x_1(t), x_2(t)]^T$ is the state vector such that $x_2 = \dot{x}_1$, and

$$\mathbf{A} = \begin{bmatrix} 0 & 1 \\ -\Omega^2 & 0 \end{bmatrix} \tag{1.187}$$

It is assumed that every collision with the barrier $x_1 = 0$ results in a momentary energy loss characterized by the restitution coefficient k. The idea is to unfold the *phase space* in such way that the energy loss would automatically occur whenever the system crosses a preimage of the line $x_1 = 0$. The corresponding transformation is given in the matrix form as

$$\mathbf{x} = \mathbf{S}\mathbf{y} \tag{1.188}$$

where $\mathbf{y} = [s(t), v(t)]^T$ is a new state matrix/vector, and

$$\mathbf{S} = \begin{bmatrix} 1 & 0 \\ 0 & 1 - \kappa \operatorname{sgn}(sv) \end{bmatrix} \operatorname{sgn}(s) \tag{1.189}$$

where $\kappa = (1 - k)/(1 + k)$.

Transformation (1.188) is strongly nonlinear due to nonsmooth dependence (1.189). Substituting (1.188) in (1.186) gives equation

$$\dot{\mathbf{y}} = (\mathbf{S}^{-1}\mathbf{A}\mathbf{S})\mathbf{y} \tag{1.190}$$

In the component-wise form, expressions (1.188) and (1.190) are written as, respectively,

$$\begin{aligned} x_1 &= x_1(s, v) \equiv s \operatorname{sgn}(s) \\ x_2 &= x_2(s, v) \equiv \operatorname{sgn}(s)[1 - \kappa \operatorname{sgn}(sv)]v \end{aligned} \tag{1.191}$$

and

$$\begin{aligned} \dot{s} &= [1 - \kappa \operatorname{sgn}(sv)]v \\ \dot{v} &= -\Omega^2 s[1 + \kappa \operatorname{sgn}(sv)]/(1 - \kappa^2) \end{aligned} \tag{1.192}$$

where both unknown components of the state vector are continuous, while the specific of non-elastic collisions is captured by transformation (1.191).

General Case of Nonlinear Oscillator

Finally, consider the general case of one-degree-of-freedom nonlinear oscillator

$$\begin{aligned} \dot{x}_1 &= x_2 \\ \dot{x}_2 &= -f(x_1, x_2, t) \end{aligned} \tag{1.193}$$

whose motion is restricted to the positive half plane by the barrier $x_1 = 0$ with the restitution coefficient k.

Applying transformation (1.191) to system (1.193) gives

$$\begin{aligned} \dot{s} &= [1 - \kappa \mathrm{sgn}(sv)]v \\ \dot{v} &= -f(x_1(s, v), x_2(s, v), t)\mathrm{sgn}(s)[1 + \kappa \mathrm{sgn}(sv)]/(1 - \kappa^2) \end{aligned} \tag{1.194}$$

Although the above illustrations are one-dimensional, similar coordinate transformations can be introduced also for multiple degree-of-freedom systems in which one of the coordinates is normal to the constraint. The corresponding analytical manipulations can be conducted in terms of Routh functions such that the normal to the constraint coordinate is Lagrangian whereas other generalized coordinates and associated momenta are Hamiltonian.

Figure 1.22 illustrates a sample trajectory of the harmonic oscillator in its original (a) and transformed (b) phase planes, respectively. It is seen from the fragment (b) that both unknown components of the transformed state vector are continuous, whereas effects of non-elastic collisions with the amplitude limiter are incorporated geometrically in transformation (1.191)

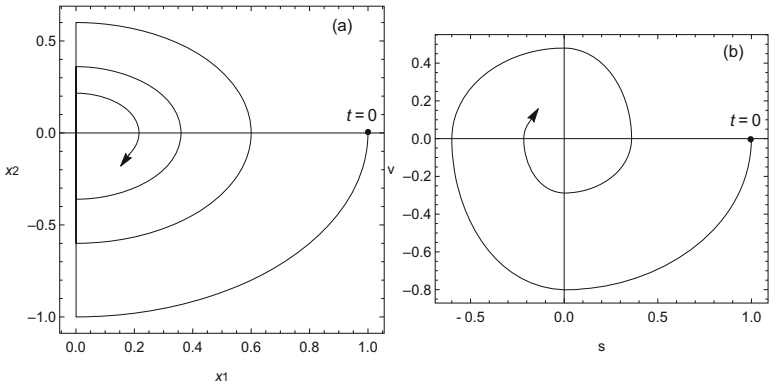

Fig. 1.22 Phase plane of the harmonic oscillator with a one-sided stiff but inelastic amplitude limiter: (**a**) the original coordinates and (**b**) auxiliary coordinates; $\Omega = 1.0$ and $\kappa = 0.25$

Chapter 2
Smooth Oscillating Processes

This chapter gives an overview of selected analytical methods for smooth oscillating processes. Most of such methods are quasi-linear by nature. The corresponding technical implementations usually employ the harmonic oscillator as a generating model. The description focuses on such ideas and technical details that are further combined with nonsmooth methods. The related procedures of the asymptotic integration usually include the stage of a preliminary transformation of the original system to the form that admits a straightforward solution. In particular, the averaging algorithm based on the Hausdorff equation for operators Lie is reproduced.

2.1 Linear and Weakly Nonlinear Approaches

By both practical and theoretical reasons, the quantitative methods of dynamics were developed first for smooth processes. As a rule, smooth oscillations can be directly observed under no special conditions. For instance, projection of any fixed point of a body rotating with constant angular speed makes a perfect impression about harmonic oscillations. Interestingly, in 1693, Leibniz derived the differential equation for sine geometrically by considering a circle. Much later, original analytical ideas of nonlinear vibrations emerged from the celestial mechanics considering perturbations of circular orbits of rigid-body motions rather than any mass-spring oscillators. Robert Hooke (1635–1703) was probably first who suggested the basic elastic mass-spring model, whereas Galileo and Huygens were investigating the pendulum. Later, d'Alembert, Daniel Bernoulli, and Euler considered a one-dimensional continual model of a string. It was found that the vibrating string represents the infinity of harmonic oscillators corresponding to different mode shapes of the string. It is well-known that a serious discussion occurred about whether or not the sum of smooth functions, such as sines, can

V. N. Pilipchuk, *Oscillators and Oscillatory Signals from Smooth to Discontinuous*,
https://doi.org/10.1007/978-3-031-37788-4_2

represent a nonsmooth shape of the string. These discussions were finalized by the Fourier theorem.

Let us reproduce the result for a periodic function of time $f(t)$ of the period T in the complex form

$$f(t) = \sum_{k=-\infty}^{\infty} c_k \exp(ik\Omega t) \tag{2.1}$$

$$c_k = \frac{1}{T}\int_0^T f(t)\exp(-ik\Omega t)dt, \quad \Omega = \frac{2\pi}{T}$$

This relation generates a one-to-one mapping between the function $f(t)$ and its Fourier coefficients

$$f(t) \longleftrightarrow \{\ldots c_{-2}, c_{-1}, c_1, c_2, \ldots\} \tag{2.2}$$

Note that mathematical expressions (2.1) do not necessarily imply that the periodic signal $f(t)$ must be produced by a linear system even though the right-hand side of (2.1) combines free vibrations of linear oscillators.[1] Therefore, the Fourier analysis with its associates should be viewed as a *linear language* for *nonlinear systems* regardless of specifics of analytical algorithms. Most quantitative methods for weakly nonlinear periodic motions, one way or another, recover Fourier coefficients of the corresponding solutions. On one hand, such tools possess a high level of generality. On the other hand, even elementary strongly nonlinear phenomena, as defined in Chap. 1, may become quite difficult to describe in the linear language. Nevertheless, the quantitative theory of nonlinear vibration has been advanced by new asymptotic techniques developed originally in a formal way for solving nonlinear differential equations. Most traditional methods are essentially based on the ideas of perturbation or averaging [69]. Similar results can be obtained within the theory of Poincaré normal forms [153], which retains resonance terms, whereas all non-resonance terms are eliminated by means of a coordinate transformation. Such a normal form is qualified as the simplest possible form of the equations of motion.

2.2 A Brief Overview of Smooth Methods

2.2.1 Periodic Motions of Quasi-linear Systems

Consider a weakly nonlinear oscillator of the form

$$\ddot{x} + \Omega_0^2 x = \varepsilon f(x, \dot{x}) \tag{2.3}$$

[1] Recall rigid-body analogies in Sect. 1.4.3.

where ε is a small parameter from the interval $0 < \varepsilon \ll 1$, and $f(x, \dot{x})$ is a smooth enough function of both arguments.

Periodic solutions of Eq. (2.3) can be found by splitting the nonlinear system into a sequence of linear oscillators by means of the power series of the small parameter ε

$$x = x_0 + \varepsilon x_1 + \varepsilon^2 x_2 + \ldots \tag{2.4}$$

The perturbation on the right-hand side of Eq. (2.3) changes the fundamental frequency of the oscillator as

$$\Omega^2 = \Omega_0^2(1 + \varepsilon\gamma_1 + \varepsilon^2\gamma_2 + \ldots) \tag{2.5}$$

The new frequency, Ω, is introduced explicitly into the differential equation of motion by switching to the phase argument

$$\varphi = \Omega t \tag{2.6}$$

As a result, series (2.4) appears to be composed of trigonometric functions of multiple phases φ, 2φ, 3φ,.... The numbers γ_1, γ_2,... are used for canceling the so-called secular terms from the solution.

A similar idea was implemented by Lyapunov for systems of first-order equations, such as

$$\begin{aligned} \dot{x}_1 &= a_{11}x_1 + a_{12}x_2 + f_1(x_1, x_2) \\ \dot{x}_2 &= a_{21}x_1 + a_{22}x_2 + f_2(x_1, x_2) \end{aligned} \tag{2.7}$$

where f_1 and f_2 are nonlinear functions, it is assumed that system (2.7) admits first analytical integral, and the corresponding linearized system has only periodic solutions. Then periodic solutions of (2.7) admit power series expansions with respect to the amplitude.

There exist at least two extensions of Lyapunov theory, such as local and global approaches to nonlinear normal modes, see, for instance, [136, 155, 241].

2.2.2 *One-Phase Averaging*

Averaging with Van der Pol Amplitude-Phase Variables

Let us illustrate different implementations of the averaging by reproducing some technical details. The description focuses on such tools that remain applicable to nonconservative systems.

To illustrate van der Pol's averaging procedure, let us represent Eq. (2.3) as a system of two first-order equations by introducing the velocity variable, v, as

$$\begin{aligned} \dot{x} &= v \\ \dot{v} &= -\Omega_0^2 x + \varepsilon f(x, v) \end{aligned} \tag{2.8}$$

The next step includes transition to the amplitude-phase variables on the system phase plane as $\{x,\ v\} \to \{a, \varphi\}$:

$$x = a\cos\varphi, \quad v = -a\Omega_0 \sin\varphi \tag{2.9}$$

Now substituting (2.9) in (2.8) and considering the result as a system of two algebraic equations with respect to the derivatives $\dot{a}$ and $\dot{\varphi}$ give

$$\begin{aligned} \dot{a} &= -\frac{\varepsilon}{\Omega_0} f(a\ \cos\varphi, -a\Omega_0 \sin\varphi) \sin\varphi \\ \dot{\varphi} &= \Omega_0 - \frac{\varepsilon}{\Omega_0 a} f(a\ \cos\varphi, -a\Omega_0 \sin\varphi) \cos\varphi \end{aligned} \tag{2.10}$$

This system is still an exact equivalent of the original equation (2.3). Despite the formal complexity, system (2.10) has the essential advantage due to different time scales of the variables, a and φ. Noticing that the new system is 2π-periodic with respect to the fast phase φ suggests its elimination from the right-hand side of the system by applying the operator of averaging

$$< \cdots >_\varphi \equiv \frac{1}{2\pi} \int_0^{2\pi} \cdots d\varphi$$

as follows:

$$\dot{a} = -\frac{\varepsilon}{\Omega_0} < f(a\ \cos\varphi, -a\Omega_0 \sin\varphi) \sin\varphi >_\varphi \tag{2.11}$$

$$\dot{\varphi} = \Omega_0 - \frac{\varepsilon}{\Omega_0 a} < f(a\ \cos\varphi, -a\Omega_0 \sin\varphi) \cos\varphi >_\varphi \tag{2.12}$$

Solutions of system (2.12) are considered as approximate leading-order averaged solutions of the original system (2.10). The main achievement from the above manipulations is due to independence of the amplitude equation from the phase φ.

Example of Rayleigh-Duffing Oscillator

Very often, amplitude equation (2.11) can be solved exactly by separation of variables as illustrated below based on Rayleigh-Duffing oscillator:

$$\ddot{x} + \Omega_0^2 x = \varepsilon \left[\left(1 - \frac{1}{3}\dot{x}^2 \right) \dot{x} - \alpha x^3 \right] \tag{2.13}$$

In this case, substituting (2.9) in $f(x, v) = \left(1 - v^2/3\right) v - \alpha x^3$ and then conducting the averaging in (2.12) give

$$\begin{aligned} \dot{a} &= \frac{1}{2}\varepsilon \left(a - \frac{1}{4}\Omega_0^2 a^3 \right) \\ \dot{\varphi} &= \Omega_0 + \varepsilon \frac{3\alpha}{8\Omega_0} a^2 \end{aligned} \tag{2.14}$$

where the amplitude a is described by a separable equation, which is independent on the phase variable, φ.

Assuming the initial condition $a(0) = a_0$ and separating the variables give explicit solution:

$$a = \frac{2a_0}{\sqrt{a_0^2 \Omega_0^2 \left[1 - \exp(-\varepsilon t)\right] + 4\exp(-\varepsilon t)}} \tag{2.15}$$

Now the phase φ can be obtained from the second equation in (2.14) by the direct integration as

$$\varphi = \Omega_0 t + \frac{3\alpha}{2\Omega_0^3} \ln \left\{ 1 + \frac{1}{4} a_0^2 \Omega_0^2 \left[\exp(\varepsilon t) - 1 \right] \right\} + \varphi_0 \tag{2.16}$$

where $\varphi_0 = \varphi(0)$.

Solution (2.15) and (2.16) should be considered as solutions in the leading asymptotic order of the averaging procedure. Such types of approximations are often sufficient for practical estimations as follows from Fig. 2.1. Comparing the graphs shows a sufficient agreement of the result of direct numerical integration of Eq. (2.13) with the analytical approximation given by (2.15) and (2.16).

Krylov-Bogolyubov Generalization

This above averaging procedure was essentially generalized in the 1930s of the last century [34] by combining the Lindstedt-Poincaré and van der Pol's ideas to obtain high asymptotic orders of the averaging. Let us outline the corresponding formalism based on the general one-phase system

$$\begin{aligned} \dot{x} &= \varepsilon X(x, y) \\ \dot{y} &= \Omega(x) + \varepsilon Y(x, y) \end{aligned} \tag{2.17}$$

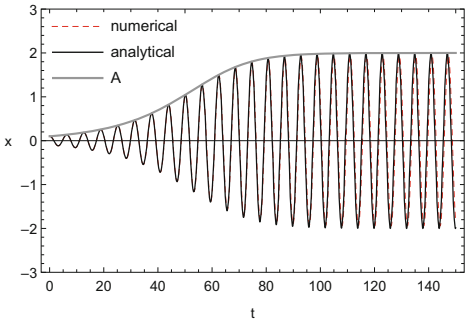

Fig. 2.1 Time history response of Rayleigh-Duffing oscillator under the following parameters and initial conditions: $\varepsilon = 0.1$, $\alpha = 0.3$, $\Omega_0 = 1.0$, $A_0 = 0.1$, $\varphi_0 = 0$

where y and x are scalar and vector variables, respectively, and the right-hand side is assumed to be 2π-periodic with respect to y.

In contrast to (2.10), the frequency Ω in (2.17) depends on the slow varying vector-function x, which may represent a set of amplitudes of an $n-$degrees-of-freedom vibrating system, $x = (a_1, \ldots, a_n)$. Sometimes, such kind of systems is called essentially nonlinear since the condition $\varepsilon = 0$ does not make the frequency state independent. Note that, if $\varepsilon = 0$, the system has no fast phase on the right-hand side. Thus the problem is to find a close to identical transformation

$$\begin{aligned} x &= q + \varepsilon u_1(q, \psi) + \varepsilon^2 u_2(q, \psi) + \ldots \\ y &= \psi + \varepsilon v_1(q, \psi) + \varepsilon^2 v_2(q, \psi) + \ldots \end{aligned} \tag{2.18}$$

which eliminates the fast phase entirely from the system and brings it to the form

$$\begin{aligned} \dot{q} &= \varepsilon A_1(q) + \varepsilon^2 A_2(q) + \ldots \\ \dot{\psi} &= \Omega_0(q) + \varepsilon \Omega_1(q) + \varepsilon^2 \Omega_2(q) + \ldots \end{aligned} \tag{2.19}$$

This problem is solved by substituting expansions (2.18) in Eqs. (2.17), enforcing Eqs. (2.19) to eliminate the derivatives $\dot{q}$ and $\dot{\psi}$, and then separating different orders of ε. Then the resultant system is solved iteratively. In zero-order of ε, the second equation in (2.17) gives $\Omega_0(q) = \Omega(q)$. As a result, the problem of order ε takes the form

$$\Omega(q)\frac{\partial u_1}{\partial \psi} = X(q, \psi) - A_1(q) \tag{2.20}$$

$$\Omega(q)\frac{\partial v_1}{\partial \psi} = Y(q, \psi) + \Omega'(q)u_1 - \Omega_1(q) \tag{2.21}$$

These partial differential equations are solved for u_1 and v_1 under the condition that solutions must be bounded with respect to the fast phase ψ. For that reason, the average of the right-hand side of both equations must be zero, which is achieved by setting

$$A_1(q) = < X(q,\psi) >_\psi \tag{2.22}$$

$$\Omega_1(q) = < Y(q,\psi) >_\psi + \Omega'(q) < u_1 >_\psi \tag{2.23}$$

Then, integration gives

$$u_1 = \frac{1}{\Omega(q)} \int_0^\psi [X(q,\psi) - < X(q,\psi) >_\psi] d\psi \tag{2.24}$$

$$v_1 = \frac{1}{\Omega(q)} \int_0^\psi [Y(q,\psi) - < Y(q,\psi) >_\psi] d\psi \tag{2.25}$$

$$+ \frac{\Omega'(q)}{\Omega(q)} \int_0^\psi [u_1 - < u_1 >_\psi] d\psi$$

Strictly speaking, both these solutions should include arbitrary functions of q as summands. These arbitrary functions are chosen to be zero assuming that both the old and new variables, $\{x, y\}$ and $\{q, \psi\}$ in (2.18), satisfy the same initial conditions. On the next step of asymptotic integration, values (2.22) through (2.25) are substituted in equations

$$\Omega(q) \frac{\partial u_2}{\partial \psi} = u_1 \frac{\partial}{\partial q} X(q,\psi) + v_1 \frac{\partial}{\partial \psi} X(q,\psi) \tag{2.26}$$

$$- A_1(q) \frac{\partial u_1}{\partial q} - \Omega_1(q) \frac{\partial u_1}{\partial \psi} - A_2(q)$$

and

$$\Omega(q) \frac{\partial v_2}{\partial \psi} = u_1 \frac{\partial}{\partial q} Y(q,\psi) + v_1 \frac{\partial}{\partial \psi} Y(q,\psi) \tag{2.27}$$

$$- A_1(q) \frac{\partial v_1}{\partial q} - \Omega_1(q) \frac{\partial v_1}{\partial \psi} + \Omega'(q) u_2 + \frac{1}{2} \Omega''(q) u_1^2 - \Omega_2(q)$$

Despite a more complicated form, these equations have the same structure as Eqs. (2.20) and (2.21). Moreover, it is easy to see that this structure will be maintained for any order with an obvious increase of the technical complexity though. Practically, high-order approximations can be obtained by means of automatic systems of symbolic manipulations.

Example of Rayleigh Equation

Let us represent Rayleigh's equation, $\ddot{z} + \Omega^2 z = \varepsilon\left(1 - \dot{z}^2/3\right)\dot{z}$, as a set of two first-order equations

$$\begin{aligned} \dot{z} &= v \\ \dot{v} &= -\Omega^2 z + \varepsilon\left(1 - \frac{1}{3}v^2\right)v \end{aligned} \tag{2.28}$$

The coordinate transformation, $z = x\cos y$ and $v = -x\Omega\sin y$, brings system (2.28) to the form of system (2.17), where

$$X(x, y) = x\left(1 - \frac{1}{3}x^2\Omega^2\sin^2 y\right)\sin^2 y \tag{2.29}$$

$$Y(x, y) = \frac{1}{6}\left(3 - x^2\Omega^2\sin^2 y\right)\sin 2y \tag{2.30}$$

and Ω is constant.

Substituting (2.29) and (2.30) in (2.22) through (2.25), conducting integration, and substituting the result in (2.19) and (2.18) give, respectively,

$$\dot{q} = \frac{1}{2}\varepsilon\left(q - \frac{1}{4}\Omega^2 q^3\right) + O(\varepsilon^3) \tag{2.31}$$

$$\dot{\psi} = \Omega - \frac{1}{256\Omega}\varepsilon^2\left(32 - 24\Omega^2 q^2 + 5\Omega^4 q^4\right) + O(\varepsilon^3) \tag{2.32}$$

and

$$x = q - \frac{1}{48\Omega}\varepsilon q[12 - (4 - \cos 2\psi)q^2\Omega^2]\sin 2\psi + O(\varepsilon^2) \tag{2.33}$$

$$y = \psi + \frac{1}{12\Omega}\varepsilon\left(6 - q^2\Omega^2\sin^2\psi\right)\sin^2\psi + O(\varepsilon^2) \tag{2.34}$$

The original variable is given by $z = x\cos y$. Taking into account first-order approximation and setting the right-hand side of Eqs. (2.26) and (2.27) to zero give $A_2 = 0$ whereas $\Omega_2 \neq 0$ as seen from Eqs. (2.31) and (2.32).

Solutions of Rayleigh's equation in first and second asymptotic orders are compared in Fig. 2.2. Both solutions are in a sufficient agreement with the result of direct numerical integration even for the parameter ε, which is not very small as compared to unity. The effect of improvement in the order ε^2 still can be observed after multiple cycles of oscillation as follows from Fig. 2.2b.

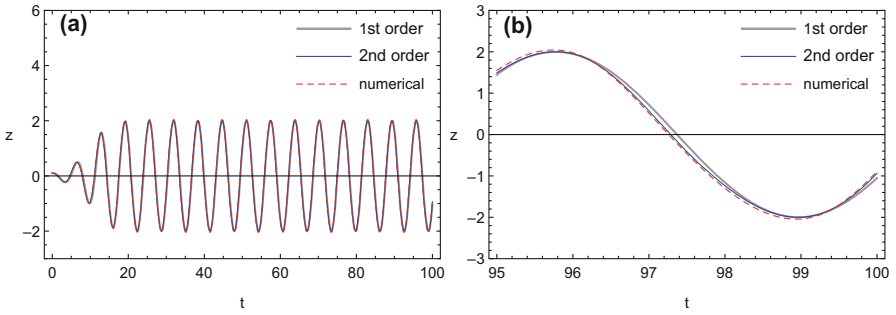

Fig. 2.2 Solutions of Rayleigh's equation in first and second asymptotic orders for the parameters $\varepsilon = 0.5$, $\Omega = 1.0$, and the initial conditions $q(0) = 0.1$, $\psi(0) = 0.0$: (**a**) developing steady state and (**b**) comparison of temporal mode shapes after multiple cycles

2.2.3 Two-Phase Averaging for Mathew Equation

In a multiple frequency case, the averaging procedure may require an extra step of the system adaptation. For illustrating purpose, consider Mathew's equation with damping

$$\ddot{x} + 2\zeta\Omega_0\dot{x} + \Omega_0^2(1 + \varepsilon\cos\Omega t)x = 0 \tag{2.35}$$

where the damping ratio ζ is assumed to be a small parameter of order ε, and $\Omega = 2$ as required by the standard form of Mathew's equation. Therefore, in addition to the natural frequency Ω_0, there is one more frequency, Ω, associated with the parametric loading term.

It will be shown below that the dissipative term $2\zeta\Omega_0\dot{x}$ can be eliminated from the equation by means of a substitution as soon as the equation remains linear. However, keeping in mind possible generalizations on nonlinear cases, this term will be maintained through the manipulations. Let us introduce the phase variable $\psi = \Omega t$ and represent Eq. (2.35) in the form of two first-order equations

$$\begin{aligned} \dot{x} &= v \\ \dot{v} &= -\Omega_0^2 x + F(x, v) \end{aligned} \tag{2.36}$$

where

$$F = -2\zeta\Omega_0 v - \varepsilon\Omega_0^2 x\cos\psi \quad \sim \varepsilon \tag{2.37}$$

Applying transformation (2.9) to (2.36) gives the system with two fast phases, φ and ψ, as

$$\begin{aligned}
\dot{a} &= -\zeta a\Omega_0(1-\cos 2\varphi) + \frac{1}{4}\varepsilon a\Omega_0\,[\sin(2\varphi-\psi)+\sin(2\varphi+\psi)] \\
\dot{\varphi} &= \Omega_0(1-\zeta\sin 2\varphi) + \frac{1}{4}\varepsilon\Omega_0\,[2\cos\psi+\cos(2\varphi-\psi)+\cos(2\varphi+\psi)] \\
\dot{\psi} &= \Omega
\end{aligned} \tag{2.38}$$

Averaging the right-hand side of system (2.38) separately over φ and ψ would lead to the system $\dot{a} = -\zeta a\Omega_0$, $\dot{\varphi} = \Omega_0$, and $\dot{\psi} = \Omega$, in which the effect of parametric loading is vanished. As seen from the right-hand side of system (2.38), such an averaging becomes inadequate when $2\Omega_0 \sim \Omega$, and therefore $2\dot{\varphi} - \dot{\psi} \sim \varepsilon$. This means that, in addition to the amplitude a, another slow variable, $2\varphi - \psi = \theta$, occurs in the system. As a result, both terms $\sin(2\varphi-\psi) = \sin\theta$ and $\cos(2\varphi-\psi) = \cos\theta$ must be interpreted as frozen when averaging with respect to either φ or ψ. The corresponding formalization is conducted by excluding one of the fast phases, say ψ by means of relationship

$$\psi = 2\varphi - \theta \tag{2.39}$$

Substituting (2.39) in (2.38), taking into account that $\Omega = 2$, and applying the averaging with respect to φ give

$$\begin{aligned}
\dot{a} &= -\zeta\,\Omega_0 a + \frac{1}{4}\varepsilon\Omega_0 a\sin\theta \\
\dot{\theta} &= 2(\Omega_0 - 1) + \frac{1}{2}\varepsilon\Omega_0\cos\theta \\
\dot{\varphi} &= \Omega_0 + \frac{1}{4}\varepsilon\Omega_0\cos\theta
\end{aligned} \tag{2.40}$$

The second equation of this system shows that the phase θ is a slow varying quantity if $\Omega_0 - 1 \sim \varepsilon$. In this case, system (2.40) describes the two slow variables, a and θ, and one fast phase, φ. In other words, compared to the non-resonance case of Sect. 2.2.2, the dimension of the so-called slow manifold is increased by one due to the internal resonance condition.

The original variable is given by the relationship $x = a\cos\varphi$, where the slow phase θ does not explicitly show up but affects the amplitude a and phase φ through system (2.40). The stationary case, $\dot{a} = \dot{\theta} = 0$, determines a family of periodic solutions whenever the system parameters satisfy condition

$$\zeta^2 + \left(1 - \frac{1}{\Omega_0}\right)^2 = \frac{\varepsilon^2}{16} \tag{2.41}$$

or

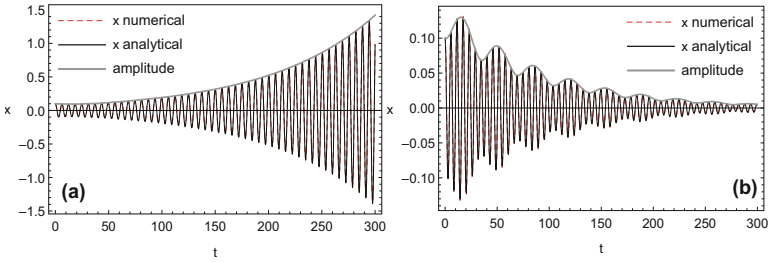

Fig. 2.3 Comparison of the analytical approximation and numerical solution of equation (2.35) for parameter values $\zeta = 0.01$ and $\varepsilon = 0.08$: (**a**) $\Omega = 1$-inside instability zone, (**b**) $\Omega = 1.1$-outside instability zone

$$\Omega_0 = \left[1 \pm \sqrt{\frac{\varepsilon^2}{16} - \zeta^2}\right]^{-1} \tag{2.42}$$

Condition (2.41) is obtained by setting the right-hand side of the first two equations of system (2.40) to zero and then eliminating the phase angle θ. From the geometrical viewpoint, Eq. (2.41) represents boundaries of the main instability zone in the parameter plane $\Omega_0 - \varepsilon$. Figure 2.3 illustrates what happens to the dynamics when crossing the boundary and confirms that the result of averaging and numerical solutions remain in a reasonable agreement. When $\zeta = 0$, Eq. (2.42) gives $\Omega_0 = 1 \pm \varepsilon/4 + O(\varepsilon^2)$. Note that a complete set of boundaries is often given for Mathew's equation of the form $\ddot{y} + (\delta + 2\epsilon \cos 2t)y = 0$, which can be obtained from Eq. (2.35) by means of the substitution $x(t) = \exp(-\zeta \Omega_0 t)y(t)$. Such a substitution leads to the above Mathew's equation, if $\delta = \Omega_0^2(1 - \zeta)$ and $2\epsilon = \Omega_0^2 \varepsilon$.

2.2.4 *Averaging in Complex Variables*

In physical literature, vibration problems are usually considered in terms of complex variables [120]. The idea of averaging can be implemented as follows. If $\varepsilon = 0$ then general solution of Eq. (2.3) is represented in the complex form

$$x = \frac{1}{2}[A \exp(i\Omega_0 t) + \bar{A} \exp(-i\Omega_0 t)] \tag{2.43}$$

where A and $\bar{A}$ are arbitrary complex conjugate constants, and the numerical factor $1/2$ is introduced for further convenience of calculation, although it is not strictly necessary.

Following the idea of parameter variations, let us assume that A and $\bar{A}$ are time-dependent quantities hopefully to satisfy Eq. (2.3) with non-zero right-hand side, $\varepsilon \neq 0$. Under such an assumption, differentiating (2.43) gives

$$\dot{x} = \frac{1}{2}\left[\frac{dA}{dt}\exp(i\Omega_0 t) + \frac{d\bar{A}}{dt}\exp(-i\Omega_0 t)\right] \tag{2.44}$$
$$+\frac{1}{2}i\Omega_0[A\exp(i\Omega_0 t) - \bar{A}\exp(-i\Omega_0 t)]$$

Further, the following condition is imposed on the arbitrary functions, $A(t)$ and $\bar{A}(t)$, with the intent to eliminate the derivatives of amplitudes from (2.44)

$$\frac{dA}{dt}\exp(i\Omega_0 t) + \frac{d\bar{A}}{dt}\exp(-i\Omega_0 t) = 0 \tag{2.45}$$

This condition brings derivative (2.44) to the form

$$\dot{x} = \frac{1}{2}i\Omega_0[A\exp(i\Omega_0 t) - \bar{A}\exp(-i\Omega_0 t)] \tag{2.46}$$

Differentiating (2.46) and taking into account (2.43) give

$$\begin{aligned}\ddot{x} &= \frac{1}{2}i\Omega_0\left[\frac{dA}{dt}\exp(i\Omega_0 t) - \frac{d\bar{A}}{dt}\exp(-i\Omega_0 t)\right] \\ &\quad -\frac{1}{2}\Omega_0^2[A\exp(i\Omega_0 t) + \bar{A}\exp(-i\Omega_0 t)] \\ &= \frac{1}{2}i\Omega_0\left[\frac{dA}{dt}\exp(i\Omega_0 t) - \frac{d\bar{A}}{dt}\exp(-i\Omega_0 t)\right] - \Omega_0^2 x\end{aligned} \tag{2.47}$$

Now, substituting (2.47) in the original equation (2.3) gives second equation for $A(t)$ and $\bar{A}(t)$ in the form

$$\frac{1}{2}i\Omega_0\left[\frac{dA}{dt}\exp(i\Omega_0 t) - \frac{d\bar{A}}{dt}\exp(-i\Omega_0 t)\right] = \varepsilon f \tag{2.48}$$

where the function $f = f(x, \dot{x})$ must be expressed through $A(t)$ and $\bar{A}(t)$ by means of relationships (2.43) and (2.46).

Solving the linear system (2.45) and (2.48) for the derivatives of complex amplitudes gives

$$\frac{dA}{dt} = \frac{\varepsilon}{i\Omega_0}\exp(-i\Omega_0 t) f \tag{2.49}$$

$$\frac{d\bar{A}}{dt} = \frac{\varepsilon}{-i\Omega_0}\exp(i\Omega_0 t) f \tag{2.50}$$

where $f = f(x, \dot{x})$ must be expressed through (2.43) and (2.46).

System (2.49) and (2.50) is still exact equivalent of the original equation (2.3) and represents the result of changing the state variables

$$\{x, \dot{x}\} \to \{A, \bar{A}\} \tag{2.51}$$

The advantage of using the complex variables is that it is sufficient to consider only one amplitude equation, for instance, (2.49) since the other one is simply its complex conjugate. Besides, solving Eqs. (2.43) and (2.46) for A gives the so-called complex amplitude, which is often used in both physics and nonlinear mechanics,

$$A = \frac{1}{i\Omega_0} \exp(-i\Omega_0 t)(\dot{x} + i\Omega_0 x) \tag{2.52}$$

Note that similar formal manipulations remain valid in degenerated cases of multiple degrees of freedom systems. For instance, Eq. (2.3) can be interpreted as a vector equation with the scalar factor Ω_0^2.

Finally, if the parameter ε is small, then the amplitude A is slow; hence the averaging can be applied as

$$\frac{dA}{dt} = \frac{1}{2\pi i}\varepsilon \int_0^{2\pi/\Omega_0} \exp(-i\Omega_0 t) f dt \tag{2.53}$$

Complex Form Solution for Van der Pol Oscillator

For example, let us consider oscillator

$$\ddot{x} + x = \varepsilon f(x, \dot{x}) \tag{2.54}$$

where

$$f(x, \dot{x}) = -(x^2 - 1)\dot{x} \tag{2.55}$$

Substituting (2.55) in Eq. (2.53) gives the following equation for the complex amplitude

$$\dot{A} = \frac{\varepsilon}{2\pi i} \int_0^{2\pi} \exp(-it)(1 - x^2)\dot{x} dt \tag{2.56}$$

where x and $\dot{x}$ are given by (2.43) and (2.46), respectively, after setting $\Omega_0 = 1$.

Conducting the corresponding algebraic manipulations and then integration with respect to time over the period 2π gives

$$\dot{A} = \frac{1}{8}\varepsilon(4 - |A|^2)A \tag{2.57}$$

To solve this equation, let us switch to the exponential form of the complex amplitude

$$A = \rho \exp(i\theta) \tag{2.58}$$

where $\rho = \rho(t)$ and $\theta = \theta(t)$ are the modulus and argument, respectively. Substituting (2.58) in (2.57) and separating imaginary and real parts give

$$\dot{\theta} = 0, \qquad \dot{\rho} = \frac{1}{8}\varepsilon(4 - \rho^2) \tag{2.59}$$

Therefore, θ is a constant phase, while ρ is determined by separating the variables as

$$\rho = \frac{2}{\sqrt{1 + (4\rho_0^{-2} - 1)\exp(-\varepsilon t)}} \tag{2.60}$$

where $\rho_0 = \rho(0)$.

The reverse transition to the original variable $x(t)$ through (2.43) and (2.58) finally gives a general solution of van der Pol's equation in the leading asymptotic order

$$x = \frac{2\cos(t + \theta)}{\sqrt{1 + (4\rho_0^{-2} - 1)\exp(-\varepsilon t)}} \tag{2.61}$$

In the particular case of zero initial velocity, one can set $\theta = 0$ and $\rho_0 = x(0)$ within the same asymptotic order.

2.3 Lie Groups Formalism

The one-parameter Lie[2] group approaches are motivated by the idea of matching the tool and the object of study as explained in references [253] and [256]. Briefly, it is suggested to seek transformation (2.18) among solutions of some dynamical systems rather than the class of the arbitrary nonlinear transformations. Original materials and overviews of the mathematical structure of Lie groups, Lie algebras, and Lie transforms with applications to nonlinear differential equations can be

[2] Marius Sophus Lie (1842–1899), Norwegian mathematician; different mathematical objects are named after him, for instance, groups, operators, algebras, and series.

found in [29, 46, 50, 81, 127]. An essential ingredient of this version of asymptotic integration is the Hausdorff formula, which relates Lie group operators of the original and new systems and the operator of coordinate transformation. According to [254] and [256], most of the averaging techniques just reproduce this formula every time implicitly, during the transformation process. Hence it is more reasonable to start with Hausdorff's relationship rather than recover it during the transformation procedure. This enables one of optimizing the number of manipulations for high-order approximations of asymptotic integration [109].

2.3.1 Hausdorff Equation

The theory of Lie groups deals with a set of transformations. In other words, some dynamical system

$$\dot{x} = f(x) \tag{2.62}$$

is transformed into another system

$$\dot{q} = g(q, \varepsilon), \qquad 0 < \varepsilon \ll 1 \tag{2.63}$$

by means of a near identical coordinate transformation $x \to q$, which is produced by a solution of the initial value problem for a third dynamical system

$$\frac{dx}{d\varepsilon} = s\,(x)\,, \qquad x|_{\varepsilon=0} = q \tag{2.64}$$

Here, the choice for the right-hand side, $s\,(x)$, is dictated by the desired properties of the transformed system. The parameter of group, ε, is interpreted as an independent variable. As follows from the initial condition in (2.64), the transformation is assumed to be identical, $x = q$, when $\varepsilon = 0$, and therefore

$$g(q, 0) = f(q) \tag{2.65}$$

Hausdorff's formula determines the right-hand side of Eq. (2.63) for nonzero ε. For illustrating purpose, consider the one-dimensional case, $x, q \in R^1$ by noticing that the final relationship can be applied to a multidimensional case too. The idea is to conduct the transformation, (2.62)→(2.64)→(2.63), in terms of the operators Lie as

$$F = f(x)\frac{\partial}{\partial x} \longrightarrow S = s(x)\frac{\partial}{\partial x} \longrightarrow G = g(q, \varepsilon)\frac{\partial}{\partial q} \tag{2.66}$$

Using operators (2.66) opens a formal way to representing the above dynamical systems in the linear form as

$$\dot{x} = Fx \longrightarrow \left\{ \frac{dx}{d\varepsilon} = Sx, \qquad x|_{\varepsilon=0} = q \right\} \longrightarrow \dot{q} = Gq \tag{2.67}$$

Now the problem is to find the new operator, G, produced by the operator of transformation, S, from the old operator, F. As follows from (2.67), if the operator S is known, then the related transformation, $x \longrightarrow q$, takes the form of Lie series

$$x = \exp(\varepsilon S)q = (1 + \varepsilon S + \ldots)q = q + \varepsilon s(q) + \ldots \tag{2.68}$$

One of the advantages of this approach is that relationship (2.68) easily generates the inverse transformation, $\exp(-\varepsilon S)x = q$, where the variable q is replaced with x in the operator S.

To derive Hausdorff formula, let us take first time derivative of both sides of transformation (2.68) and enforce Eqs. (2.62) and (2.63) to exclude $\dot{x}$ and $\dot{q}$. This gives

$$f(q + \varepsilon s + \ldots) = (1 + \varepsilon \frac{\partial s}{\partial q} + \ldots)g(q, \varepsilon) \tag{2.69}$$

Using power series expansions for the functions f and g, taking into account relationship (2.65), and rearranging the terms bring (2.69) to the form

$$\frac{\partial}{\partial \varepsilon} g = s \frac{\partial}{\partial q} g - g \frac{\partial}{\partial q} s \qquad \text{as } \varepsilon \longrightarrow 0 \tag{2.70}$$

Multiplying both sides of Eq. (2.70) by the differential operator $\partial/\partial q$ on the right on both sides and using notations (2.66) give Hausdorff equation

$$\frac{\partial}{\partial \varepsilon} G = SG - GS \equiv [S, G] \tag{2.71}$$

where the operator of transformed system, G, satisfies the initial condition

$$G|_{\varepsilon=0} = F = f(q) \frac{\partial}{\partial q} \tag{2.72}$$

according to the assumption that $x = q$ when $\varepsilon = 0$.

A power series solution of the initial value problem (2.71)–(2.72) for operators Lie is given by Hausdorff formula [29]:

$$G = F + \varepsilon [S, F] + \frac{1}{2!} \varepsilon^2 [S, [S, F]] + \ldots \tag{2.73}$$

This formula relates operators F, S, and G according to (2.66) and can be used for the asymptotic integration of the original system (2.62) as follows.

2.3.2 Asymptotic Integration in Terms of Operators Lie

Let the right-hand side of system (2.62) depend upon a small parameter ε as $f = f_0(x) + \varepsilon f_1(x)$, assuming that the system $\dot{x} = f_0(x)$ admits a straightforward integration. Respectively, let us represent the operator of original system, F, the operator of transformation, S, and the operator of transformed system, G, in the power series form

$$\begin{aligned} F &= F_0 + \varepsilon F_1 \\ S &= S_0 + \varepsilon S_1 + \varepsilon^2 S_2 + \ldots \\ G &= G_0 + \varepsilon G_1 + \varepsilon^2 G_2 + \ldots \end{aligned} \tag{2.74}$$

The problem is to iteratively obtain the operator of transformation, such that operator of transformed system possesses the same useful property as the operator of original system at $\varepsilon = 0$. If this problem is solved then the new system, $\dot{q} = Gq$, can be integrated the same way as the system $\dot{x} = f_0(x)$. Such an asymptotic procedure is formalized by substituting (2.74) in Hausdorff formula (2.73) and matching terms of the same power of ε as

$$G_0 = F_0 \tag{2.75}$$

$$G_1 = F_1 + [S_0, F_0] \tag{2.76}$$

$$G_2 = F_2 + [S_0, F_1] + [S_1, F_0] + \frac{1}{2!}[S_0, [S_0, F_0]] \tag{2.77}$$

$$\ldots$$

Note that all the operator relationships remain applicable to multidimensional cases in the same form.

In order to illustrate the averaging procedure in a two-dimensional case, let us consider system (2.17) assuming that the frequency Ω is fixed:

$$\begin{aligned} \dot{x} &= \varepsilon X(x, y) \\ \dot{y} &= \Omega + \varepsilon Y(x, y) \end{aligned} \tag{2.78}$$

The operator Lie of this system is given by

$$F = F_0 + \varepsilon F_1 \tag{2.79}$$

$$F_0 = \Omega \frac{\partial}{\partial y}, \qquad F_1 = X(x, y)\frac{\partial}{\partial x} + Y(x, y)\frac{\partial}{\partial y} \tag{2.80}$$

When $\varepsilon = 0$, system (2.78) does not have the fast variable y on the right-hand side. The problem is to find the transformation $\{x, y\} \longrightarrow \{q, \psi\}$, such that the

transformed system possesses the same property for nonzero ε, namely, its right-hand side does not have the fast variable (phase) ψ. Thus the problem is formulated in the same way to Krylov-Bogolyubov, which is formalized by Eqs. (2.17), (2.18), and (2.19). In contrast, the present approach does not require the substitution (2.18) in (2.17). The operator of transformed system, G, is given by (2.75) through (2.77) after the replacement of variables $\{x, y\}$ with $\{q, \psi\}$, for instance, as

$$G_0 = \Omega \frac{\partial}{\partial \psi} \tag{2.81}$$

$$G_1 = F_1 - \Omega \frac{\partial}{\partial \psi} S_0 \tag{2.82}$$

Applying the operator G_0 to $\{q, \psi\}$ eliminates the fast phase ψ on the right-hand side of transformed system

$$\{\dot{q}, \dot{\psi}\} = G_0\{q, \psi\} = \{0, \Omega\}$$

The same property is assigned to the operator G_1 by averaging the right-hand side of (2.82) as

$$G_1 = < F_1 >_\psi = < X(q, \psi) >_\psi \frac{\partial}{\partial q} + < Y(q, \psi) >_\psi \frac{\partial}{\partial \psi} \tag{2.83}$$

Note that the integration with respect to the variable ψ does not affect the differential operator $\partial/\partial\psi$. This relationship should be also viewed as a definition for averaging of operators Lie. Since condition (2.83) is imposed on the left-hand side of Eq. (2.82), the equality can be achieved by a proper choice for the operator S_0, which is still unknown. Thus, substituting (2.83) in (2.82) and integrating with respect to ψ give the corresponding approximation for the operator of transformation:

$$\begin{aligned} S_0 &= \frac{1}{\Omega} \int_0^\psi (F_1 - < F_1 >_\psi) d\psi = \frac{1}{\Omega} \int_0^\psi (F_1 - G_1) d\psi \\ &= \frac{1}{\Omega} \int_0^\psi (X - < X >_\psi) d\psi \frac{\partial}{\partial q} + \frac{1}{\Omega} \int_0^\psi (Y - < Y >_\psi) d\psi \frac{\partial}{\partial \psi} \end{aligned} \tag{2.84}$$

Taking into account that $F_2 = 0$ and calculating the commutator $[S_1, F_0]$ bring Eq. (2.77) to the form

$$G_2 = [S_0, F_1] + \frac{1}{2!}[S_0, [S_0, F_0]] - \Omega \frac{\partial}{\partial \psi} S_1 \tag{2.85}$$

Now reiterating manipulations of the previous step gives

$$G_2 = < [S_0, F_1] >_{\psi} + \frac{1}{2!} < [S_0, [S_0, F_0]] > \psi \tag{2.86}$$

and

$$S_1 = \frac{1}{\Omega} \int_0^{\psi} \left([S_0, F_1] + \frac{1}{2!} [S_0, [S_0, F_0]] - G_2 \right) d\psi \tag{2.87}$$

The operators of transformation, S_0 and S_1, and the operators of averaged system, G_1 and G_2, generate solution of system (2.17) in the second asymptotic order and the corresponding averaged system as, respectively,

$$x = \exp(\varepsilon S) q = (1 + \varepsilon S_0 + \varepsilon^2 S_1) q + O(\varepsilon^3) \tag{2.88}$$

$$y = \exp(\varepsilon S) \psi = (1 + \varepsilon S_0 + \varepsilon^2 S_1) \psi + O(\varepsilon^3) \tag{2.89}$$

and

$$\dot{q} = (G_0 + \varepsilon G_1 + \varepsilon^2 G_2) q + O(\varepsilon^3) \tag{2.90}$$

$$\dot{\psi} = (G_0 + \varepsilon G_1 + \varepsilon^2 G_2) \psi + O(\varepsilon^3) \tag{2.91}$$

Solution of Rayleigh Equation in Terms of Operators Lie

For comparison reason, let us consider the example of Rayleigh equation (2.28). According to (2.29) and (2.30), in terms of van der Pol's variables, the corresponding operator Lie is

$$\begin{aligned} F_0 = \Omega \frac{\partial}{\partial \psi}, \qquad F_1 &= X(q, \psi) \frac{\partial}{\partial q} + Y(q, \psi) \frac{\partial}{\partial \psi} \\ &= q \left(1 - \frac{1}{3} q^2 \Omega^2 \sin^2 \psi \right) \sin^2 \psi \frac{\partial}{\partial q} \\ &+ \frac{1}{6} \left(3 - q^2 \Omega^2 \sin^2 \psi \right) \sin 2\psi \frac{\partial}{\partial \psi} \end{aligned} \tag{2.92}$$

where the replacement $\{x, y\} \longrightarrow \{q, \psi\}$ has been made according to the above-described algorithm.

Conducting the averaging in (2.83), (2.84), (2.86), and (2.87) and then substituting the result in (2.88) and (2.89) give

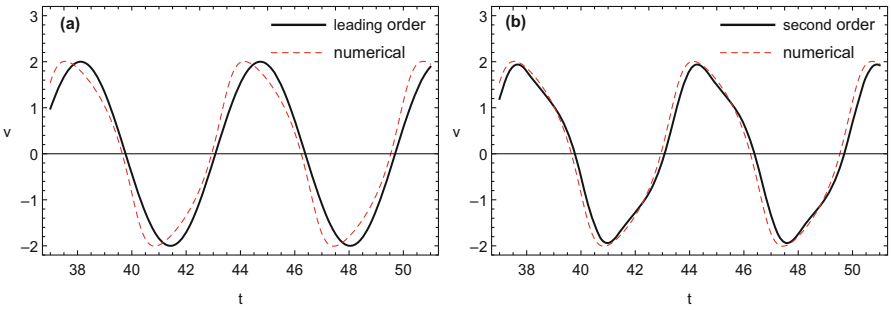

Fig. 2.4 Comparison of numerical solution of Rayleigh equation (2.28) to the leading order (**a**) and second order (**b**) approximations for $v = \dot{z}$ obtained by means of Lie group operators; $\varepsilon = 0.9$, $\Omega = 1$, $q(0) = 0.1$, and $\psi(0) = 0$

$$
\begin{aligned}
x &= q - \frac{\varepsilon}{48\Omega} q[12 - (4 - \cos 2\psi) q^2\Omega^2] \sin 2\psi - \frac{\varepsilon^2}{192\Omega^2} \\
&\quad \times q[48 - \left(12 - q^2\Omega^2\right)\left(6 - q^2\Omega^2 \sin^2\psi\right)] \sin^2\psi + O(\varepsilon^3) \\
y &= \psi + \frac{\varepsilon}{12\Omega}\left(6 - q^2\Omega^2 \sin^2\psi\right) \sin^2\psi + \frac{\varepsilon^2}{1536\Omega^2} \\
&\quad \times [96 - q^2\Omega^2\left(24 - 5q^2\Omega^2\right)(4 - \cos 2\psi)] \sin 2\psi + O(\varepsilon^3)
\end{aligned}
\tag{2.93}
$$

where the functions $q = q(t)$ and $\psi = \psi(t)$ are given by the averaged system (2.90) and (2.91) leading to (2.31) and (2.32). Note that the terms of order ε coincide with those in (2.33) and (2.34).

The effectiveness of second-order approximation is illustrated by Fig. 2.4, where the parameter ε was intentionally chosen to be close to unity since the terms of order ε^2 appeared to have quite small numerical factors in solutions (2.93). The graphs represent temporal shapes of the velocity, $v = \dot{z}$, in order to better observe the effect of anharmonicity.

2.3.3 Linearization Near Equilibrium Manifold

Methods considered in the previous sections of this chapter essentially employ solutions of linearized systems. The linearization procedure assumes the system to remain near a single (stationary) equilibrium point. This condition cannot be guaranteed if the total energy of the system is above the potential barrier on the way to another equilibrium point. As a result, the problem becomes nonlocal and usually multidimensional since the path connecting both points is not necessarily

straight. Following reference [170], let us illustrate this situation based on a two-mode approximation for a simply supported cylindrical panel of thickness h with a sinusoidal initial imperfection of the amplitude α

$$\begin{aligned} \ddot{q}_1 + \varepsilon^2 (q_1 - 1) + \frac{1}{4}\left({q_1}^2 + 4{q_2}^2 - 1\right) q_1 = 0 \\ \ddot{q}_2 + 16\varepsilon^2 q_2 + \left({q_1}^2 + 4{q_2}^2 - 1\right) q_2 = 0 \end{aligned} \tag{2.94}$$

where q_1 and q_2 are time-dependent amplitudes of the first and second sine wave modes, respectively, and ε is a small parameter characterizing the panel flexibility as

$$\varepsilon^2 = \frac{1}{12}\left(\frac{h}{\alpha}\right)^2 \ll 1$$

Model (2.94) can be represented by its Lagrangian as

$$L = \frac{1}{2}(\dot{q}_1^2 + \dot{q}_2^2) - V(q_1, q_2) \tag{2.95}$$

with the potential energy of elastic deformations given by

$$V(q_1, q_2) = \frac{1}{2} f(q_1, q_2)^2 + \varepsilon^2 \Phi(q_1, q_2) \tag{2.96}$$

$$f(q_1, q_2) = \frac{\sqrt{2}}{4}\left(q_1^2 + 4q_2^2 - 1\right) \tag{2.97}$$

$$\Phi(q_1, q_2) = \frac{1}{2}[(q_1 - 1)^2 + 16q_2^2] \tag{2.98}$$

where the functions f and Φ associate with the tension-compression and bending deformations, respectively. A typical shape of the potential energy with a sample trajectory inside the potential well is shown in Fig. 2.5. If $\varepsilon = 0$, system (2.94) has one equilibrium point $P_0(0, 0)$ on the plane $q_1 q_2$ corresponding to a horizontal configuration of the panel, which is obviously unstable by Lyapunov due to the extreme compression. Also, there is a continuous manifold of the elliptic shape, ${q_1}^2 + 4{q_2}^2 = 1$, along which the panel can move with zero strain of its center line. If $\varepsilon \neq 0$, this manifold disappears by generating four equilibrium points, of which two are located on the straight line $q_2 = 0$ and correspond to the original and inverted positions of the panel: $P_1(1, 0)$ and $P_2(-(1 + \sqrt{1 - 16\varepsilon^2})/2, 0)$, respectively. The other two points are unstable equilibria involving the second (sine wave) spatial

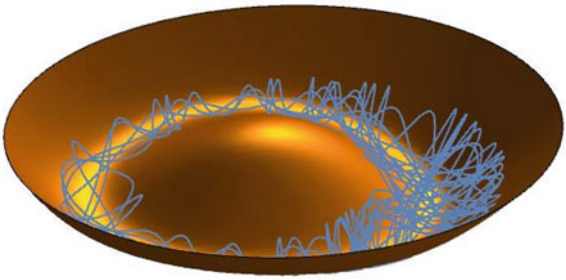

Fig. 2.5 Top-side qualitative view of the potential well V with a sample system trajectory inside the well under the flexibility $\varepsilon = 0.1$, and other parameters as: $a_1 = 1, a_2 = 0, q_1(0) = 1, q_2(0) = 0, \dot{q}_1(0) = 1, \dot{q}_2(0) = 0.25$

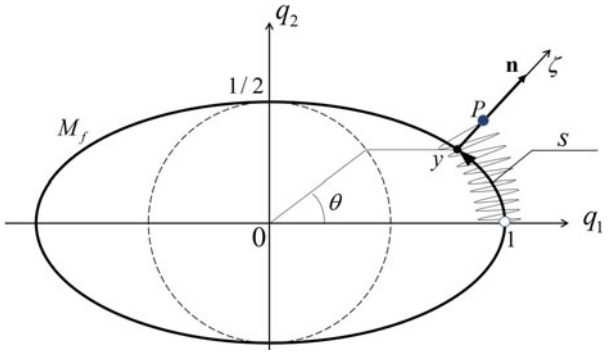

Fig. 2.6 Planar geometry of the coordinate transformation $\{q_1, q_2\} \to \{\zeta, s\}$ with interpretation of the arclength parametrization $s = s(\theta)$

mode: $P_{3,4}(-1/3, \pm\sqrt{2 - 36\varepsilon^2}/3)$. The point P_0 remains on the line $q_2 = 0$ with some shift from zero: $P_0((\sqrt{1 - 16\varepsilon^2} - 1)/2, 0)$. All of the above equilibria exist under the condition $\varepsilon < \sqrt{2}/6$. The minimum potential barrier on the path between two stable equilibrium points, P_1 and P_2, is calculated by substituting the coordinates of one of the two symmetric saddle points, $P_{3,4}$, in (2.96) as

$$V_* = \frac{8}{3}\varepsilon^2 - 16\varepsilon^4 \tag{2.99}$$

The methodology is based on a global linearization of Eqs. (2.94) near the elliptic manifold of equilibrium positions of the perfectly flexible panel, $\varepsilon = 0$. In the present case of just two modes, such a linearization is conducted by means of two new generalized coordinates, such as the deviation ζ from the ellipse and the angular coordinate θ (Fig. 2.6)

$$\begin{aligned} q_1 &= y_1(\theta) + \varepsilon n_1(\theta)\zeta \\ q_2 &= y_2(\theta) + \varepsilon n_2(\theta)\zeta \end{aligned} \tag{2.100}$$

where $\{y_1, y_2\}$ is a projection of the point $P(q_1, q_2)$ onto the ellipse

$$y_1(\theta) = \cos\theta, \quad y_2(\theta) = \frac{1}{2}\sin\theta \tag{2.101}$$

and $\{n_1, n_2\}$ is the corresponding unit vector

$$n_1 = \frac{1}{\omega}\frac{\partial f(y_1, y_2)}{\partial y_1}, \quad n_2 = \frac{1}{\omega}\frac{\partial f(y_1, y_2)}{\partial y_2} \tag{2.102}$$

$$\omega = \sqrt{\left(\frac{\partial f}{\partial y_1}\right)^2 + \left(\frac{\partial f}{\partial y_2}\right)^2} = \frac{\sqrt{2}}{2}\sqrt{1 + 3\sin^2\theta}$$

The nonlinear coordinate transformation $\{q_1, q_2\} \longrightarrow \{\zeta, \theta\}$ (2.100) is conducted by means of Routh function combining the Lagrangian and Hamiltonian formulations for the normal and tangential to the ellipse motion components, respectively [150]. Another approach was using a local Cartesian frame following the point P along the ellipse [136]. Although the nonlinear coordinate transformation technically complicates the differential equations of motion as compared to system (2.94), the new coordinates become closer to the system physical meaning: the fast coordinate ζ associates with the tension-compression of the panel, whereas the slow coordinate θ describes the bending deformations. As a result, the system is reduced based on the idea of separation of motions followed by the averaging procedure. The leading order asymptotic integration gives finally

$$\ddot{\zeta} + \omega^2\zeta = O(\varepsilon) \tag{2.103}$$

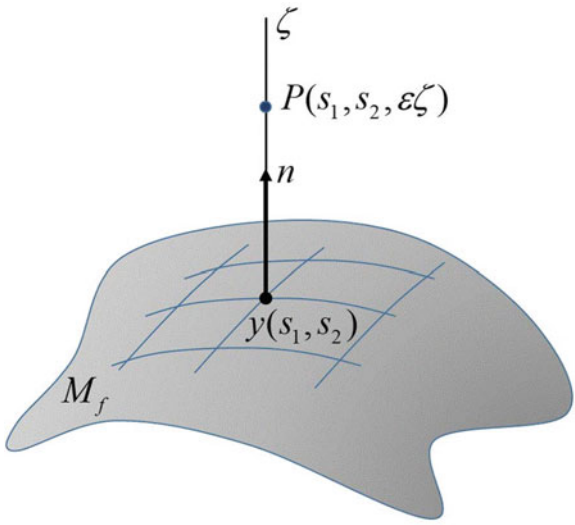

Fig. 2.7 Three-dimensional illustration of zero strain manifold, $M_f = \{q : f(q) = 0\}$, and the corresponding generalized Lagrangian coordinates: $\{\zeta, s_1, s_2\}$

and

$$\frac{1}{2}\left(\omega\frac{d\theta}{dt}\right)^2+\varepsilon^2\left[2(1-\cos\theta)+3\sin^2\theta\right]=E=\text{const.} \tag{2.104}$$

According to (2.99), the least energy level of system (2.94), at which the global motion may become possible, is of order ε^2. Analyzing Eqs. (2.103) and (2.104) for the vanishing ε recalls the discussion on rigid-body motions from the standpoint of linearity and nonlinearity concepts. In the present case, Eqs. (2.103) and (2.104) associate with rotations and translations, respectively, as discussed in Chap. 1.

Figure 2.7 gives an outline for increasing the number of flexural modes of the panel. Although the dimension of essentially nonlinear component can be reduced by one, a parametrization of the equilibrium manifold would lead to significant technical complexities.

Chapter 3
Nonsmooth Processes as Asymptotic Limits

The objective of this chapter is to show that nonsmooth processes may naturally occur as high-energy asymptotics in different oscillatory models with no intentionally introduced stiff constraints or external impacts. In other words, nonsmooth temporal mode shapes may be as natural as sine waves generated by same oscillators under low-energy conditions. Essentially nonlinear phenomena, such as nonlinear beats and energy localization, are also considered. It is shown that energy exchange between two oscillators may possess hidden nonsmooth behaviors.

3.1 Lyapunov's Oscillator

Let us consider a family of oscillators described by the differential equation

$$\ddot{x} + x^{2n-1} = 0 \tag{3.1}$$

where n is a positive integer; see Fig. 1.1.

In the particular case $n = 1$, one has the harmonic oscillator whose natural frequency is unity. When $n > 1$ the system becomes essentially nonlinear and cannot be linearized within the class of vibrating systems. Moreover, as the parameter n increases, the temporal mode shape of oscillator (3.1), while remaining smooth, is gradually approaching the triangle wave nonsmooth limit. Such transitions usually represent a challenging problem from both physical and mathematical viewpoints. Hence it is important to understand some basic cases, such as oscillator (3.1) and those considered in the next section. These special cases admit exact solutions showing explicitly how smooth motions are approaching their nonsmooth limits. It is known regarding oscillator (3.1) that, for an arbitrary positive integer n, its general

V. N. Pilipchuk, *Oscillators and Oscillatory Signals from Smooth to Discontinuous*,
https://doi.org/10.1007/978-3-031-37788-4_3

solution can be expressed in terms of special Lyapunov functions [76, 101, 126], such as $\mathrm{sn}\theta$ and $\mathrm{cs}\theta$ defined by expressions[1]

$$\theta = \int_0^{\mathrm{sn}\theta} \left(1 - nz^2\right)^{\frac{1-2n}{2n}} dz, \qquad \mathrm{cs}^{2n}\theta + n\,\mathrm{sn}^2\theta = 1$$

These functions possess the properties,

$$\mathrm{cs}0 = 1, \qquad \mathrm{sn}0 = 0, \qquad \frac{d\mathrm{sn}\theta}{d\theta} = \mathrm{cs}^{2n-1}\theta, \qquad \frac{d\mathrm{cs}\theta}{d\theta} = -\mathrm{sn}\theta$$

and their normalized period is given by

$$T = 4\sqrt{n}\int_0^1 \frac{dx}{\sqrt{1-x^{2n}}} = 2\sqrt{\frac{\pi}{n}}\frac{\Gamma\left(\frac{1}{2n}\right)}{\Gamma\left(\frac{n+1}{2n}\right)}$$

The general solution of Eq. (3.1) can be written as

$$x = A\mathrm{cs}\left(A^{n-1}t + \alpha\right) \tag{3.2}$$

where A and α are arbitrary constants.

Note that the scaling factors A and A^{n-1} are easily predictable based on the form of Eq. (3.1) since the equation admits the group of transformations $x = A\bar{x}(\bar{t})$, where $\bar{t} = A^{n-1}t$.

For $n = 1$ the functions $\mathrm{sn}\theta$ and $\mathrm{cs}\theta$ give the standard pair of trigonometric functions $\sin\theta$ and $\cos\theta$, respectively. Interestingly enough, the strongly nonlinear limit $n \to \infty$ also gives a quite simple pair of periodic functions. Despite some mathematical challenges, this case admits interpretation by means of the total energy

$$\frac{\dot{x}^2}{2} + \frac{x^{2n}}{2n} = \frac{1}{2} \tag{3.3}$$

where the number $1/2$ on the right-hand side corresponds to the initial conditions $x(0) = 0$ and $\dot{x}(0) = 1$.

Taking into account that the coordinate of the oscillator reaches its amplitude value at zero kinetic energy gives the estimate $-n^{1/(2n)} \le x(t) \le n^{1/(2n)}$ for any time t. Since $n^{1/(2n)} \longrightarrow 1$ as $n \longrightarrow \infty$ then the limiting motion is restricted by the interval $-1 \le x(t) \le 1$. Inside of this interval, the second term on the left-hand side of expression (3.3) vanishes and hence, $\dot{x} = \pm 1$ or $x = \pm t + \alpha_{\pm}$, where

[1] Another version of special functions for Eq. (3.1) was considered in [209].

$\alpha_{\pm}$ are constants. By manipulating with the signs and constants, one can construct the triangle wave, $\tau(t)$, since there is no other way to providing the periodicity condition.

Thus the family of oscillators (3.1) includes the two quite simple complementary asymptotics associated with the boundaries of the interval $1 \leq n < \infty$ as illustrated by Fig. 1.1. Respectively, there are two couples of periodic functions

$$\{x, \dot{x}\} = \{\sin t, \cos t\}, \quad \text{if } n = 1 \tag{3.4}$$

and

$$\{x, \dot{x}\} \to \{\tau(t), e(t)\}, \quad \text{if } n \to \infty \tag{3.5}$$

where $e(t) = \dot{\tau}(t)$ is a generalized derivative of the triangle wave, which is the square wave.[2]

Earlier, the power-form characteristics with integer exponents were employed for phenomenological modeling of the amplitude limiters of vibrating elastic structures [242] and illustrations of impact asymptotics [172, 176]. It should be noted that such phenomenological approaches to the modeling of impacts are designed to capture the integral effect of interaction with physical constraints while bypassing its local details near constraints. Such details obviously depend upon both the material properties of interacting bodies and physical conditions of interactions. In many cases, Hertz model of interaction is used to describe the local dynamics near constraint surfaces [84]. Note that direct replacement of the characteristic x^{2n-1} by the Hertzian restoring force $kx^{3/2}$ in (3.1) gives no oscillator. The equation,

$$\ddot{x} + kx^{3/2} = 0 \tag{3.6}$$

which is a particular case considered in [84], must be obviously accompanied by the condition $0 \leq x$, where $x = 0$ corresponds to the state at which the moving body and constraint barely touch each other with still zero interaction force.

The following modification brings system (3.6) into the class of oscillators with odd characteristics

$$\ddot{x} + k\text{sgn}(x)|x|^{3/2} = 0 \tag{3.7}$$

However, oscillator (3.7) essentially differs from oscillator (3.1) since Eq. (3.7) cannot describe any gap (clearance) in between the left and right constraint surfaces. In other words models (3.1) and (3.7) represent physically different situations. The gap 2Δ with its center at the origin, $x = 0$, can be introduced in Eq. (3.7) as follows:

$$\ddot{x} + k[H(x - \Delta)|x - \Delta|^{3/2} - H(-x - \Delta)|x + \Delta|^{3/2}] = 0 \tag{3.8}$$

where H is Heaviside unit-step function.

[2] The terms *triangular sine* and *rectangular cosine* can be also used to emphasize the choice for the initial time point, $\tau(0) = 0$ and $e(0) = 1$, and unit amplitudes.

This is a generalization of model (3.7), which is now derived from (3.8) by setting $\Delta = 0$. Equation (3.8) can be viewed as a physical impact oscillator that accounts for elastic properties of its components. As compared to phenomenological model (3.1), Eq. (3.8) was obtained on certain physical basis given by the Hertz contact theory.

Finally, oscillators with power-form characteristics, including their generalizations, can be found in physical literature [33, 78, 157], [80, 130] and different areas of applied mathematics and mechanics [5, 8, 9, 18, 45, 61, 67, 83, 113, 141, 142, 146, 207, 244]. In reference [195], the power-form restoring forces were introduced to simulate the liquid sloshing impacts; regarding this phenomenon, see also review article [90].

3.2 Nonlinear Oscillators Solvable in Elementary Functions

A class of strongly nonlinear oscillators admitting surprisingly simple exact general solutions at any level of the total energy is described below. Although the fact of exact solvability of these oscillators has been known for quite a long time [103], it did not attract much attention possibly due to the specific form of the oscillator characteristics with uncertain physical interpretations. It is clear however that, in a phenomenological way, such characteristics capture sufficiently general physical situations with hardening and softening behavior of the restoring forces. For instance, these oscillators were recently used as a phenomenological basis for describing different practically important physical and mechanical systems [53, 54, 158]. The hardening characteristic is close to linear for relatively small amplitudes but becomes infinity growing as the amplitude approaches certain limits. As a result, the corresponding temporal mode of vibration changes its shape from smooth quasi harmonic to the nonsmooth triangle wave of the rapidly growing frequency. In contrast, the softening characteristic behaves in a non-monotonic way such that the vibration shape is approaching the square wave as the amplitude is increasing. Earlier, amplitude-phase equations were obtained for a coupled array of the hardening oscillators [187]. It will be shown below that such oscillators admit explicit action-angle variables within the class of elementary functions. As a result, conventional averaging procedures become applicable to a wide range of nonlinear motions including transitions from high- to low-energy dynamics under small damping conditions. These solutions are in a good agreement with the corresponding numerical solutions at any energy level even within the first-order asymptotic approximation.

Hardening and softening cases of these oscillators are, respectively,

$$H = \frac{1}{2}(v^2 + \tan^2 x) \Rightarrow \ddot{x} + \frac{\tan x}{\cos^2 x} = 0 \tag{3.9}$$

and

$$H = \frac{1}{2}(v^2 + \tanh^2 x) \Rightarrow \ddot{x} + \frac{\tanh x}{\cosh^2 x} = 0 \tag{3.10}$$

where the mass is set to unity and thus $v = \dot{x}$ is interpreted as a generalized momentum of the Hamiltonian H, whereas x is a generalized coordinate.

Further objectives are to investigate the high-energy asymptotics with transitions to nonsmooth temporal mode shapes to show that both of the above oscillators can play the role of generating systems for regular perturbation procedures within the class of elementary functions.

Notice that oscillators (3.9) and (3.10) complement each other as those with stiff and soft characteristics represented in Fig. 3.1a and b, respectively. These oscillators can be represented also in the form

$$\ddot{x} + \tan x + \tan^3 x = 0 \tag{3.11}$$

$$\ddot{x} + \tanh x - \tanh^3 x = 0 \tag{3.12}$$

Further analyses of Eqs. (3.11) and (3.12) can be conducted by means of substitutions $q = \tan x$ and $q = \tanh x$, respectively. Interestingly enough, oscillators (3.11) and (3.12) without the cubic terms were considered by Timoshenko and Yang [232]. But, despite the simplified form, the corresponding solutions are expressed in terms of special functions.

3.2.1 Hardening Case

Consider first stiff oscillator (3.9), whose solution is

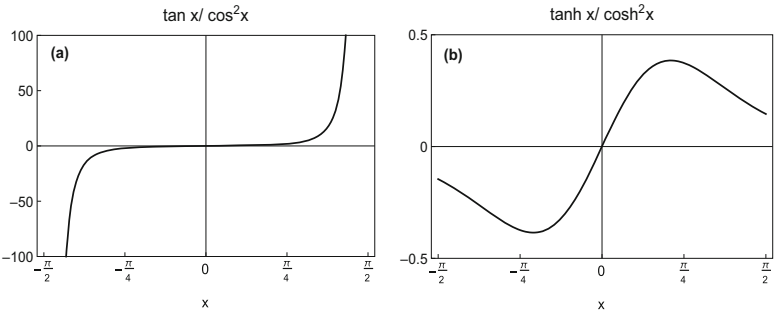

Fig. 3.1 Restoring force characteristics of exactly solvable strongly nonlinear oscillators (3.9) and (3.10): (**a**) hardening characteristic and (**b**) softening characteristic

$$x = \arcsin\left[\sin A \sin\left(\frac{t}{\cos A}\right)\right] \tag{3.13}$$

where A is an arbitrary constant, and another constant is introduced through the time shift $t- > t + const.$, since the equations admit the group of temporal shifts.

Therefore, function (3.13) represents a general periodic solution of the period $T = 2\pi \cos A$, while the total energy is expressed through the amplitude, A, as

$$E = \frac{1}{2}\tan^2 A \tag{3.14}$$

In zero energy limit, when the amplitude is close to zero, the oscillator linearizes, whereas solution (3.13) gives the corresponding sine-wave temporal shape. On the other hand, the energy becomes infinitely large as the parameter A approaches the upper limit $\pi/2$. In this case, the period vanishes while the oscillation takes the triangle wave shape as follows from expression (3.13). Figure 3.2a illustrates the evolution of the vibration shape as a function of phase, $\varphi = t/\cos A$, where $\alpha = \sin A$.

Action-Angle Variables

Below, the action-angle variables are introduced in terms of elementary functions. This enables one of considering non-periodic motions by using exact solution (3.13) as a starting point of the averaging procedure. For a single degree-of-freedom conservative oscillator, the action coordinate I is known to be the area bounded by the system path on the phase plane divided by 2π, whereas the angle φ coordinate is simply phase angle [16, 161, 164]. In the case of hardening restoring force characteristic (3.9), one obtains

$$I = \frac{1}{2\pi}\oint v dx = \frac{1}{\cos A} - 1 \tag{3.15}$$

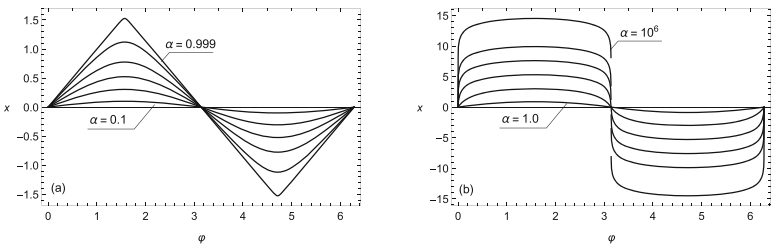

Fig. 3.2 Normalized temporal mode shapes of the oscillators with stiffening and softening restoring force characteristics in the displacement versus phase coordinates: (**a**) $x = \arcsin(\alpha \sin\varphi)$ and (**b**) $x = \text{arcsinh}(\alpha \sin\varphi)$

and

$$\varphi = \frac{t}{\cos A} \tag{3.16}$$

respectively.

The original coordinate and the velocity are expressed through the action-angle variables as follows:[3] [188]

$$x = \arcsin\left(\frac{\sqrt{2I + I^2}}{1 + I}\sin\varphi\right), \quad v = \frac{(1 + I)\sqrt{2I + I^2}\cos\varphi}{\sqrt{1 + \left(2I + I^2\right)\cos^2\varphi}} \tag{3.17}$$

To observe the convenience of action-angle coordinates, let us choose the Hamiltonian description of the oscillator. Taking into account expressions (3.14) and (3.15), and eliminating the amplitude A, gives the total energy and thus Hamiltonian

$$H = I + \frac{1}{2}I^2 \tag{3.18}$$

The corresponding differential equations of motion are derived as follows:

$$\dot{\varphi} = \frac{\partial H}{\partial I} = 1 + I, \quad \dot{I} = -\frac{\partial H}{\partial \varphi} = 0 \tag{3.19}$$

As it is seen, the oscillator is linearized with respect to the action-angle coordinates and hence possesses the exact general solution

$$I = I_0, \quad \varphi = (1 + I_0)\,t + \varphi_0 \tag{3.20}$$

where $I_0 > 0$ and φ_0 are arbitrary constants. By substituting (3.20) in (3.17), one can express the solution via the original coordinates. The meaning of the initial action is clear from the energy relationship

$$E = I_0 + \frac{1}{2}I_0^2 = \frac{1}{2}\tan^2 A \tag{3.21}$$

Note that the linearity of the Hamiltonian equations is due to the specific strongly nonlinear form of the coordinate transformation (3.17). *In other words, the system nonlinearity has been "absorbed" in a purely geometric way by the nonlinear coordinate transformation.*

As mentioned at the beginning, simplicity of the transformed system and that of the corresponding solution can be essentially employed for the purpose of

[3] The relationship for x was known earlier [164]. However, the complete set is required for nonconservative velocity-dependent perturbations.

perturbation analysis. Let us consider the differential equation of motion in the Newtonian form

$$\ddot{x} + \frac{\tan x}{\cos^2 x} = \varepsilon f\,(x, \dot{x}) \tag{3.22}$$

where ε is a small parameter.

This system is weakly nonconservative and therefore has no Hamiltonian. It is still possible nonetheless to consider expressions (3.17) as a transformation of state variables, $\{x, v\} \longrightarrow \{I, \varphi\}$. For that reason, let us represent equation (3.22) as a system of two first-order equations for the state variables, x and v,

$$\begin{aligned} \dot{x} &= v \\ \dot{v} &= -\frac{\tan x}{\cos^2 x} + \varepsilon f\,(x, v) \end{aligned} \tag{3.23}$$

Substituting (3.17) in (3.23) and then solving the system for $\dot{\varphi}$ and $\dot{I}$ give

$$\begin{aligned} \dot{\varphi} &= 1 + I - \frac{\varepsilon f(x, v) \sin\varphi}{(1 + I)\sqrt{\left(2I + I^2\right)\left[1 + \left(2I + I^2\right)\cos^2\varphi\right]}} \\ \dot{I} &= \frac{\varepsilon f(x, v)\sqrt{2I + I^2}\cos\varphi}{\sqrt{1 + \left(2I + I^2\right)\cos^2\varphi}} \end{aligned} \tag{3.24}$$

where the function $f(x, v)$ still must be expressed through the action-angle coordinates by means of (3.17).

Example of Linear Viscous Damping

In case of the linear damping, $f(x, v) \equiv -v$, Eqs. (3.24) take the form

$$\begin{aligned} \dot{\varphi} &= 1 + I + \frac{\varepsilon \cos\varphi \sin\varphi}{1 + \left(2I + I^2\right)\cos^2\varphi} \\ \dot{I} &= -\frac{\varepsilon\,(1 + I)\left(2I + I^2\right)\cos^2\varphi}{1 + \left(2I + I^2\right)\cos^2\varphi} \end{aligned} \tag{3.25}$$

Let us implement just one step of the averaging procedure and evaluate its effectiveness. Applying the operator of averaging with respect to the phase, φ, in (3.25) gives the corresponding first-order averaged system in the linear form

$$\dot{\varphi} = 1 + I, \quad \dot{I} = -\varepsilon I \tag{3.26}$$

Substituting the general solution of system (3.26) in (3.17) finally gives

$$x = \arcsin\left\{\frac{\sqrt{2I_0\exp(-\varepsilon t)+I_0^2\exp(-2\varepsilon t)}}{1+I_0\exp(-\varepsilon t)}\right. \\ \left.\times\sin\left[t+I_0\frac{1-\exp(-\varepsilon t)}{\varepsilon}+\varphi_0\right]\right\} \tag{3.27}$$

where I_0 and φ_0 are arbitrary constants. The corresponding time history records and phase plane diagrams for different damping coefficients are shown in Fig. 3.3. Even the leading order approximation appears to be in a good agreement with numerical solution for all the range of amplitudes. The analytical and numerical curves can be distinguished only at relatively large magnitudes of the damping parameter ε. Also, the graphs show that the temporal mode is gradually changing its shape from the triangular to harmonic as time increases and the amplitude decays.

Nonlinear Localized Damping

Let us consider the case of nonlinear damping

$$\ddot{x}+\frac{\tan x}{\cos^2 x}=-2\varepsilon\dot{x}\tan^2 x \tag{3.28}$$

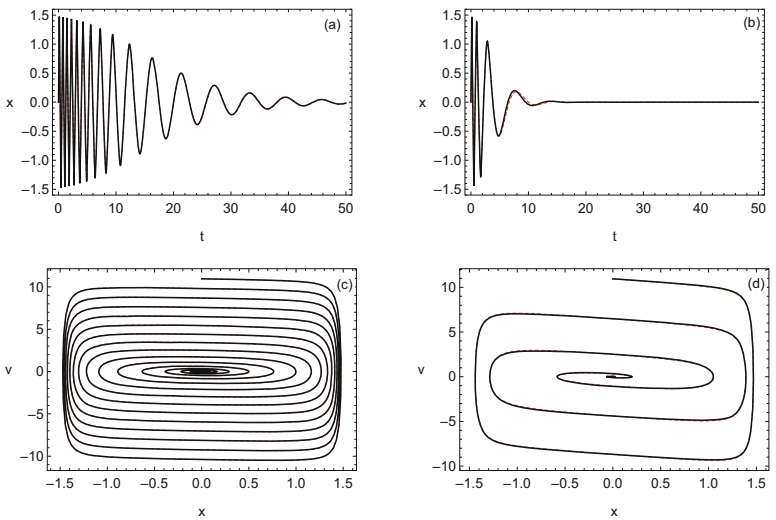

Fig. 3.3 The response of hardening oscillator (3.22) in case of the linear viscous damping, $f(x,v)\equiv -v$, under the initial conditions $I_0=10$ and $\varphi_0=0$, and two different damping parameters: $\varepsilon=0.2$ (**a**, **c**) and $\varepsilon=0.8$ (**b**, **d**); the numerical solution of the differential equation is represented for the time history (**a**, **b**) and phase plane diagrams (**c**, **d**) by the dashed curves

In this case, the perturbation is given by $f(x, v) \equiv -2v \tan^2 x$. Such a damping is rapidly growing near the boundaries of the interval $-\pi/2 \leq x \leq \pi/2$, but it becomes negligible when the amplitude is small, $|x| << 1$.

In the action-angle coordinates, first-order averaging gives

$$\dot{\varphi} = 1 + I, \quad \dot{I} = -\varepsilon I^2$$

and thus

$$\varphi = t + \frac{1}{\varepsilon} \ln(1 + \varepsilon I_0 t) + \varphi_0, \quad I = \frac{I_0}{1 + \varepsilon I_0 t}$$

Using the coordinate transformation (3.17) gives solution

$$x = \arcsin\left\{ \frac{\sqrt{I_0(2 + I_0 + 2\varepsilon I_0 t)}}{1 + I_0 + \varepsilon I_0 t} \sin\left[t + \frac{\ln(1 + \varepsilon I_0 t)}{\varepsilon} + \varphi_0 \right] \right\} \tag{3.29}$$

where I_0 and φ_0 are arbitrary constants.

Note that the amplitude decay of solutions (3.27) and (3.29) is qualitatively different. For instance, the amplitude of vibration (3.29) originally decays in a fast rate and then becomes very slow. In contrast, the amplitude of vibration (3.27) first decays slowly, and then the decay rate abruptly increases and then slows down again.

3.2.2 *Softening Case*

Let us consider now softening oscillator (3.10), whose exact solution is

$$x = \operatorname{arc\,sinh}\left[\sinh A \sin\left(\frac{t}{\cosh A} \right) \right] \tag{3.30}$$

Figure 3.2b shows that the temporal shape of high-energy vibrations approaches the square wave and thus essentially differs of that observed in the stiff case. To compare the shapes for different periods, the dependencies are given with respect to the phase variable $\varphi = t/\cosh A$ using the parameter $\alpha = \sinh A$. Based on solution (3.30), the action-angle coordinates are introduced as

$$x = \operatorname{arc\,sinh}\left(\frac{\sqrt{2I - I^2}}{1 - I} \sin\varphi \right), \quad v = \frac{(1 - I)\sqrt{2I - I^2}\cos\varphi}{\sqrt{1 - (2I - I^2)\cos^2\varphi}} \tag{3.31}$$

where the action is expressed through the parameter A as

$$I = 1 - \frac{1}{\cosh A} \tag{3.32}$$

All the analytical manipulations are analogous to those conducted for the stiff case. Taking into account (3.32) gives the total energy as a function of the action I

$$E = \frac{1}{2}\tanh^2 A = I - \frac{1}{2}I^2 \tag{3.33}$$

In the presence of the linear viscous damping,

$$\ddot{x} + \frac{\tanh x}{\cosh^2 x} = -\varepsilon \dot{x} \tag{3.34}$$

the averaging procedure gives the linear system

$$\dot{\varphi} = 1 - I, \quad \dot{I} = -\varepsilon I \tag{3.35}$$

which differs by sign in the first equation compared to system (3.26).

Integrating system (3.35) and substituting the result in (3.31) give general solution of the original equation

$$x = \operatorname{arc\,sinh}\left\{\frac{\sqrt{2I_0 \exp(-\varepsilon t) - I_0^2 \exp(-2\varepsilon t)}}{1 - I_0 \exp(-\varepsilon t)} \times \sin\left[t - I_0 \frac{1 - \exp(-\varepsilon t)}{\varepsilon} + \varphi_0\right]\right\} \tag{3.36}$$

The corresponding time history graphs and phase plane diagrams are shown in Fig. 3.4 for different damping coefficients. The leading order approximation appears to match the corresponding numerical solution for all range of amplitudes, unless the initial action I_0 approaches the magnitude 1. As follows from expressions (3.33), this magnitude corresponds to the maximum value of the total energy of the oscillator. Note that the energy of the hardening oscillator has no maximum.

3.3 Nonsmoothness Hidden in Smooth Processes

In this section, nonlinear beats phenomena are considered as another source of nonsmooth behavior that brings a certain physical meaning to oscillator (3.22). Note that nonlinear beats became of growing interest few decades ago from different viewpoints of physics and nonlinear dynamics [79, 112, 119, 131, 238]. Interestingly enough, phase variables of interacting oscillators with close natural frequencies may show nonsmoothness of temporal behavior during the beating [79], for instance,

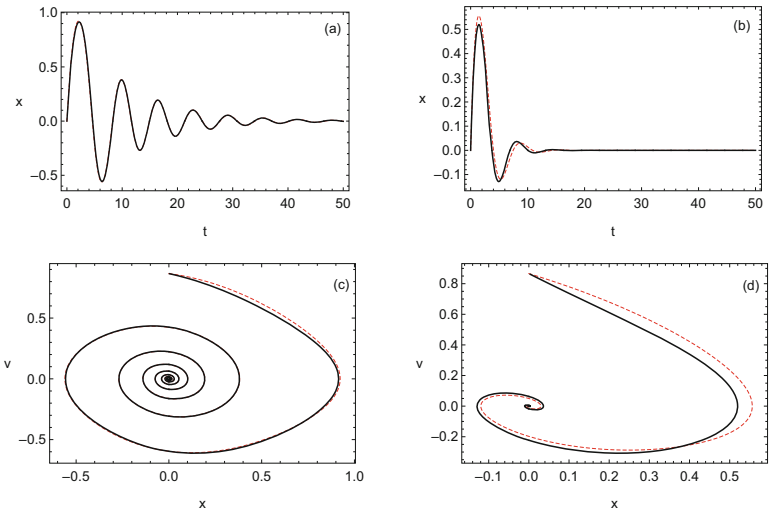

Fig. 3.4 The dynamics of the linearly damped softening oscillator under the initial conditions $I_0 = 0.5$, $\varphi_0 = 0$, and two different damping parameters: $\varepsilon = 0.2$ (**a**, **c**) and $\varepsilon = 0.8$ (**b**, **d**); numerical solution of the differential equation is represented for the time history (**a**, **b**) and phase plane diagrams (**c**, **d**) by the dashed curves

similar to that of a vibroimpact process [132, 133]. Such limiting dynamics were defined as a complementary nonstationary alternative to the normal mode motions. Below a new set of descriptive functions is introduced to analyze the beating effects directly in energy variables.

3.3.1 *Descriptive Functions for Interaction of Identical Oscillators*

Let us consider an ensemble of two identical harmonic oscillators with the natural frequency Ω:

$$\ddot{q}_k + \Omega^2 q_k = 0 \quad (k = 1, 2) \tag{3.37}$$

Although there is no interaction between oscillators (3.37) in terms of forces, there is still certain coupling through the time variable t. Namely, both oscillators have the same natural temporal scale $\delta = \Omega t$ with the same initial point. In other words two independent oscillators (3.37) still represent a system. Now let us denote $v_k = \dot{q}_k$ $(k = 1, 2)$ and then introduce symmetric 2×2 matrix

$$E_{kj} = \frac{1}{2}(v_k v_j + \Omega^2 q_k q_j) \tag{3.38}$$

and the following combinations of its elements [190]

$$\begin{aligned} E_{11} + E_{22} &= E \\ \frac{E_{11} - E_{22}}{E} &= P, \quad -1 \le P \le 1 \\ \frac{E_{12}}{\sqrt{E_{11}E_{22}}} &= Q, \quad -1 \le Q \le 1 \end{aligned} \tag{3.39}$$

where E is the total energy of both oscillators per unit mass and P is a unitless index characterizing the distribution of energy between the oscillators as

$$E_{11} = \frac{1}{2}E(1+P), \quad E_{22} = \frac{1}{2}E(1-P) \tag{3.40}$$

Relationships (3.40) are derived by solving the first two equations in (3.39) for E_{11} and E_{22}. To clarify the meaning of quantity Q and express the original state variables through E, P, and Q, let us assume that the oscillators are described by

$$q_1 = A_1 \cos\delta, \qquad q_2 = A_2 \cos(\delta + \Delta) \tag{3.41}$$

where $\delta = \Omega t$, A_1 and A_2 are constant amplitudes, and Δ is a phase shift. Then, substituting (3.41) in (3.38) gives

$$\begin{aligned} E_{12} &= \frac{1}{2}\Omega^2 A_1 A_2 [\sin\delta \sin(\delta+\Delta) + \cos\delta\cos(\delta+\Delta)] \\ &= \frac{1}{2}\Omega^2 A_1 A_2 \cos\Delta \\ E_{11}E_{22} &= \frac{1}{4}\Omega^4 A_1^2 A_2^2 \end{aligned} \tag{3.42}$$

Substituting (3.42) in (3.39) shows that the quantity Q represents the phase shift of oscillations as

$$Q = \frac{E_{12}}{\sqrt{E_{11}E_{22}}} = \cos\Delta \tag{3.43}$$

Now, substituting (3.41) in (3.40) and taking into account (3.38) give $\Omega^2 A_1^2 = E(1+P)$ and $\Omega^2 A_2^2 = E(1-P)$. Solving these equations for the amplitudes and taking into account (3.41) finally give the transformation from E, P, Δ, and δ back to the original state variables of both oscillators

$$\begin{aligned} q_1 &= \frac{1}{\Omega}\sqrt{E(1+P)}\cos\delta \\ v_1 &= -\sqrt{E(1+P)}\sin\delta \end{aligned}$$

$$q_2 = \frac{1}{\Omega}\sqrt{E(1-P)}\cos(\delta+\Delta) \qquad (3.44)$$
$$v_2 = -\sqrt{E(1-P)}\sin(\delta+\Delta)$$

Note that, in case of non-interacting linear oscillators (3.37), the quantities E, P, and Δ are constant. Therefore, in line with the idea of parameter variations and averaging, these can be assumed to be slowly varying functions under the presence of relatively small perturbations, such as coupling and nonlinearities. The advantage of such descriptive variables is due to their physical meaning given by (3.38) and (3.39). Also, in contrast to other types of characteristics, quantities (3.38) and (3.39) can be evaluated directly from numerical or experimental signals for state variables. However, the convenience of these variables becomes most obvious whenever the problem formulation deals with the effects of energy transfer or with the modal content of oscillations. In such cases, variables (3.39) reveal the necessary information in a straightforward way. For instance, as follows from (3.39) and confirmed by (3.44), the number $P = 0$ indicates the energy equipartition, $E_{11} = E_{22}$, whereas at $P = 1$ or $P = -1$ all the energy belongs to the first or to the second oscillator, respectively. Regarding the modal content, the numbers $Q = 1$ and $Q = -1$ correspond to the inphase ($\Delta = 0$) and antiphase ($\Delta = \pi$) vibration modes, respectively. In these cases, transformation (3.44) gives the corresponding couple of straight lines on configuration plane $q_1 - q_2$:

$$q_2 = \pm\sqrt{\frac{1-P}{1+P}}q_1 \qquad (3.45)$$

If $Q = 0$ ($\Delta = \pi/2$), then, according to (3.44), the system follows the elliptic path in either clockwise or counterclockwise direction:

$$\frac{q_1^2}{1+P} + \frac{q_2^2}{1-P} = \frac{E}{\Omega^2} \qquad (3.46)$$

Geometrical meaning of the *coherency index* Q is explained in Fig. 3.5. As already mentioned, in case of system (3.37), the numbers P and Q are fixed and can be determined from the initial conditions by means of relationships (3.38) and

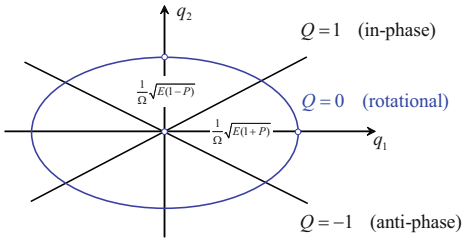

Fig. 3.5 Geometrical interpretation of the coherency index Q on the configuration plane

(3.39). In the general transient case, the temporal behavior of numbers P and Q reveals which of the above three modes is dominant during a certain time interval.

As noticed in Sect. 2.2.4, in physical literature, harmonic oscillations are often represented by rotating vectors on the complex plane. For that reason, let us express quantities (3.39) through the complex coordinates [120] $\psi_j = v_j + i\Omega q_j$, or inversely,

$$v_j = \frac{1}{2}\left(\psi_j + \bar{\psi}_j\right), \qquad q_j = \frac{1}{2i\Omega}\left(\psi_j - \bar{\psi}_j\right) \tag{3.47}$$

Substituting (3.47) in (3.38) gives

$$E_{kj} = \frac{1}{2}(v_k v_j + \Omega^2 q_k q_j) = \frac{1}{4}(\bar{\psi}_k \psi_j + \psi_k \bar{\psi}_j) \tag{3.48}$$

Hence the total energy of two oscillators excluding coupling, E, the energy distribution, P, and the index of coherency, Q, are calculated through the complex coordinates as:

$$E = E_{11} + E_{22} = \frac{1}{2}\left(\left|\psi_1\right|^2 + \left|\psi_2\right|^2\right) \tag{3.49}$$

$$P = \frac{E_{11} - E_{22}}{E_{11} + E_{22}} = \frac{\left|\psi_1\right|^2 - \left|\psi_2\right|^2}{\left|\psi_1\right|^2 + \left|\psi_2\right|^2}, \quad -1 \le P \le 1 \tag{3.50}$$

$$Q = \frac{E_{12}}{\sqrt{E_{11}E_{22}}} = \frac{\bar{\psi}_1\psi_2 + \psi_1\bar{\psi}_2}{2\left|\psi_1\right|\left|\psi_2\right|}, \quad -1 \le Q \le 1 \tag{3.51}$$

The example of analysis using these descriptive variables is considered in the next subsection.

3.3.2 *Systems with 1:1 Resonance*

Let us derive equations describing temporal behaviors of the new variables by considering a system of two interacting oscillators

$$\begin{aligned} \ddot{q}_1 + \Omega^2 q_1 + f_1(q_1, \dot{q}_1, q_2, \dot{q}_2) &= 0 \\ \ddot{q}_2 + \Omega^2 q_2 + f_2(q_1, \dot{q}_1, q_2, \dot{q}_2) &= 0 \end{aligned} \tag{3.52}$$

where the terms f_1 and f_2 are small enough to be viewed as perturbations.

In the state space, system (3.52) is represented in the form of four first-order differential equations

$$\begin{aligned}\dot{q}_1 &= v_1\\ \dot{v}_1 &= -\Omega^2 q_1 - f_1\\ \dot{q}_2 &= v_2\\ \dot{v}_2 &= -\Omega^2 q_2 - f_2\end{aligned} \tag{3.53}$$

where $f_k = f_k(q_1, v_1, q_2, v_2)$ $(k = 1, 2)$.

Due to the presence of perturbations, quantities (3.39) become time varying in a temporal rate dictated by the magnitude of perturbations, f_k, as follows from the derivative of the energy matrix

$$\frac{d}{dt}\begin{bmatrix} E_{11} & E_{12}\\ E_{21} & E_{22}\end{bmatrix} = -\frac{1}{2}\begin{bmatrix} 2f_1v_1 & f_1v_2 + f_2v_1\\ f_1v_2 + f_2v_1 & 2f_2v_2\end{bmatrix} \tag{3.54}$$

which is obtained from (3.38) by enforcing equations (3.53).

As noticed above, relationships (3.44) can be considered as a coordinate transformation in the system state space using the idea of parameter variations as

$$\{q_1, v_1, q_2, v_2\} \longrightarrow \{E(t), P(t), \Delta(t), \delta(t)\} \tag{3.55}$$

where E, P, and Δ are now slowly varying quantities, whose temporal rates are determined by the magnitude of terms f_1 and f_2 according to (3.54); recall expressions (3.39).

Note that, in the presence of perturbation, the time-dependent quantity E is losing its meaning of the system's total energy due to both possible nonconservative terms and the ignored energy of coupling. Nonetheless, under the assumption of small perturbation, the quantity E still can serve as a convenient estimate for the total excitation level of the system in line with the idea of Lyapunov functions.

Substituting (3.44) in (3.53) and solving the resultant equations for the derivatives of new state variables give

$$\begin{aligned}\frac{dE}{dt} &= \sqrt{E}\left[\sqrt{1-P}\,f_2\sin(\delta+\Delta) + \sqrt{1+P}\,f_1\sin\delta\right]\\ \frac{dP}{dt} &= -\frac{P}{\sqrt{E}}\left[\sqrt{1-P}\,f_2\sin(\delta+\Delta) + \sqrt{1+P}\,f_1\sin\delta\right]\\ &\quad -\frac{1}{\sqrt{E}}\left[\sqrt{1-P}\,f_2\sin(\delta+\Delta) - \sqrt{1+P}\,f_1\sin\delta\right]\\ \frac{d\Delta}{dt} &= \frac{1}{\sqrt{E}}\left[\frac{f_2\cos(\delta+\Delta)}{\sqrt{1-P}} - \frac{f_1\cos\delta}{\sqrt{1+P}}\right]\end{aligned} \tag{3.56}$$

and

$$\frac{d\delta}{dt} = \Omega + \frac{f_1 \cos\delta}{\sqrt{E(1+P)}} \tag{3.57}$$

where both functions f_1 and f_2 must be expressed through E, P, Δ and δ by means of (3.44).

At this point, Eqs. (3.56) and (3.57) still represent the exact equivalent of original system (3.53). Further, assuming that $f_k \sim \varepsilon$ $(0 < \varepsilon << 1, k = 1, 2)$, different procedures of asymptotic integration can be applied to system (3.56) and (3.57). Practically acceptable approximate solutions can be often obtained by the direct one-step averaging of the right-hand side of system (3.56) and (3.57) with respect to the fast phase δ over the period 2π by means of the integral operator

$$< \cdots >_\delta = \frac{1}{2\pi}\int_0^{2\pi} \cdots d\delta \tag{3.58}$$

Energy Localization in Coupled Identical Duffing Oscillators

Let us consider the example of two coupled Duffing oscillators by assuming

$$\begin{aligned} f_1 &= 2\zeta\Omega v_1 + \beta(q_1 - q_2) + \alpha q_1^3 \\ f_2 &= 2\zeta\Omega v_2 + \beta(q_2 - q_1) + \alpha q_2^3 \end{aligned} \tag{3.59}$$

Substituting (3.59) in (3.56) and (3.57), taking into account (3.44), and applying averaging (3.58) to the right-hand side of the resultant system give

$$\begin{aligned} \frac{dE}{dt} &= -2\zeta\Omega E \\ \frac{dP}{dt} &= \frac{\beta}{\Omega}\sqrt{1-P^2}\sin\Delta \\ \frac{d\Delta}{dt} &= -\frac{3\alpha}{4\Omega^3}EP - \frac{\beta\cos\Delta}{\Omega\sqrt{1-P^2}}P \end{aligned} \tag{3.60}$$

and

$$\frac{d\delta}{dt} = \Omega + \frac{3\alpha}{8\Omega^3}E(1+P) + \frac{\beta}{2\Omega}\left(1 - \sqrt{\frac{1-P}{1+P}}\cos\Delta\right) \tag{3.61}$$

Let us introduce new temporal argument $\bar{t}$ and the total excitation level $\kappa(\bar{t})$ as

$$t = \frac{\Omega}{\beta}\bar{t}, \qquad E(t) = \frac{4\beta\Omega^2}{3\alpha}\kappa(\bar{t}) \tag{3.62}$$

Substituting (3.62) in (3.60) and solving the first equation for κ bring the averaged system to the form

$$\begin{aligned} \kappa &= \kappa_0 \exp\left(-2\frac{\zeta}{\beta}\Omega^2 \bar{t}\right) \\ \frac{dP}{d\bar{t}} &= -\frac{\partial H}{\partial \Delta} = \sqrt{1-P^2}\sin\Delta \\ \frac{d\Delta}{d\bar{t}} &= \frac{\partial H}{\partial P} = -P\left(\kappa + \frac{\cos\Delta}{\sqrt{1-P^2}}\right) \end{aligned} \tag{3.63}$$

where $\kappa_0 = \kappa(0)$ and

$$H = H(P, \Delta, \bar{t}) = -\frac{1}{2}\kappa(\bar{t})P^2 + \sqrt{1-P^2}\cos\Delta \tag{3.64}$$

It is seen that P and Δ can play the role of Hamiltonian generalized momentum and generalized coordinate, respectively. Note that the Hamiltonian structure occurs despite the presence of dissipation in the original system. Obviously, Hamiltonian (3.64) is not conserved, unless $\zeta = 0$, and thus, enforcing system (3.63) gives

$$\frac{dH}{d\bar{t}} = \frac{\zeta}{\beta}\Omega^2 P^2 \kappa \tag{3.65}$$

Thus it is found that the resonance energy flow between the two interacting oscillators is described with an effective Hamiltonian oscillator. In order to consider the oscillatory dynamics, the damping ratio ζ will be assumed to be small enough to have the adiabatic effect on system (3.63). This system therefore can be viewed as a dynamical system on the phase plane $\Delta - P$ whose phase flow depends upon the total excitation level, κ. Since the right-hand side of system (3.63) is 2π-periodic with respect to Δ, it is sufficient to investigate two cells of the phase portrait including the stationary points $(\Delta, P) = (0, 0)$ and $(\Delta, P) = (\pi, 0)$, corresponding to the inphase and antiphase modes, respectively. As follows from the right-hand side of (3.63), the inphase mode is unique at any positive κ, whereas the antiphase mode can bifurcate to give rise for two new modes, when the total excitation level κ exceeds the critical level

$$\kappa^* = 1 \Longrightarrow E^* = \frac{4\beta\Omega^2}{3\alpha} \tag{3.66}$$

The corresponding stationary points are given by

$$(\Delta, P) = (0, \pm\sqrt{1-\kappa^{-2}}), \qquad 1 \le \kappa \tag{3.67}$$

Both critical and supercritical phase portraits are shown in Fig. 3.6a and b, respectively. These illustrate the bifurcation of the antiphase stationary point from

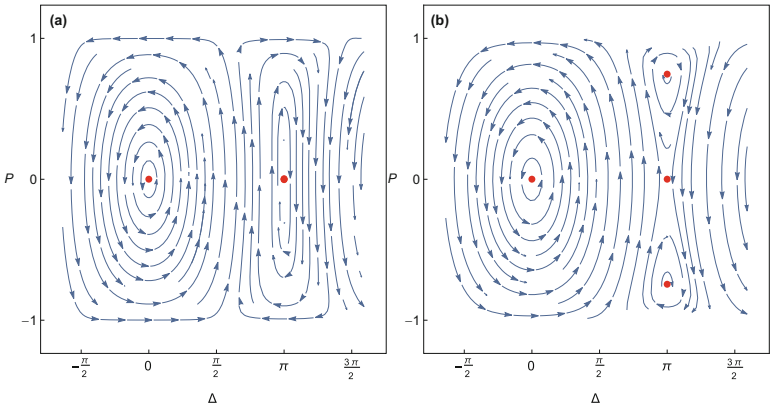

Fig. 3.6 Phase portraits of system (3.63) at fixed excitation levels: (**a**) $\kappa = 1$—critical, (**b**) $\kappa = 1.5$—supercritical

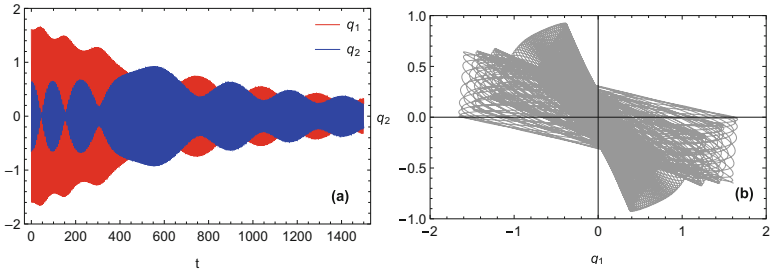

Fig. 3.7 Transition from local to antiphase mode due to the adiabatic energy loss: (**a**) time history response and (**b**) configuration plane under the following parameters and initial conditions: $\Omega = 1.0$, $\zeta = 0.001$, $\alpha = 0.08$, $\beta = 0.03$, $E(0) = 1.5$ ($\kappa(0) = 3.0$), $P(0) = 0.72$, $\Delta(0) = \pi - 0.001$

center to saddle and two centers, creating two local modes. Such effects are usually referred to as the symmetry breaking bifurcation in a perfectly symmetric system leading to the possibility of energy localization. As follows from (3.67), the energy localization/trapping effect can occur on a high-energy level. Assuming that the model remains adequate as the energy is increasing, one can reach the limit in which all the energy becomes localized at just one of the two oscillators

$$(\Delta, P) \sim (0, \pm 1), \qquad 1 \ll \kappa \tag{3.68}$$

Practically however, if no energy inflow is maintained, the dissipation effect will cause a gradual decrease of the quantity κ. As a result, the local modes will eventually disappear followed by the reciprocal beatwise oscillations as seen from Figs. 3.7 and 3.8.

Let us consider the conservative system, $\zeta = 0$, when κ is a fixed number. In this case, as follows from (3.65), system (3.63) admits the following integral:

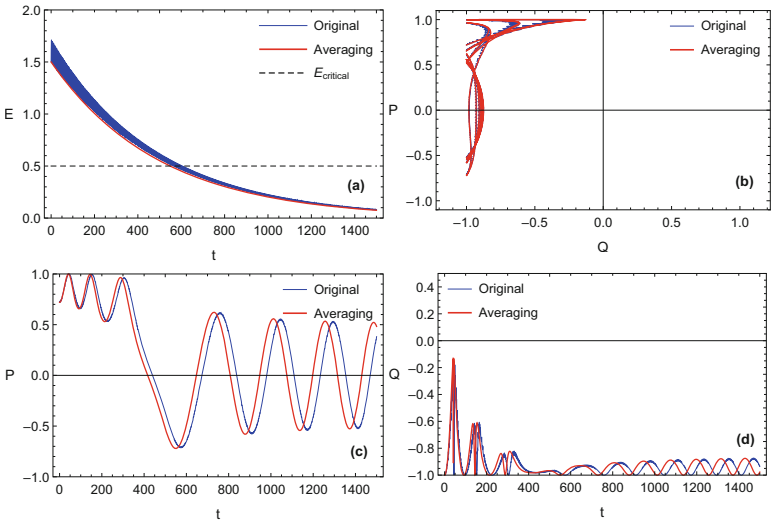

Fig. 3.8 Illustration of the delocalization process (Fig. 3.7) in terms of the variables $\{E, P, Q\}$ obtained from numerical solutions of the original and averaged systems in comparison: (**a**) total excitation level, (**b**) $P - Q$ diagram, (**c**) the evolution of energy distribution, and (**d**) coherency index

$$H(P, \Delta) = H_0 = H(P, \Delta)|_{\tilde{t}=0} \tag{3.69}$$

Substituting $P = \sin\phi$ $(-\pi/2 \le \phi \le \pi/2)$ in (3.63) and (3.69) and then eliminating the phase shift Δ give a strongly nonlinear conservative oscillator for the new variable ϕ describing the resonance beatwise energy flow

$$\frac{d^2\phi}{d\tilde{t}^2} + \left(H_0 + \frac{1}{2}\kappa\right)^2 \frac{\tan\phi}{\cos^2\phi} - \frac{1}{8}\kappa^2 \sin 2\phi = 0 \tag{3.70}$$

where H_0 is expressed through the parameter κ and initial angles ϕ_0 and Δ_0 as

$$H_0 = -\frac{1}{2}\kappa \sin^2\phi_0 + \cos\phi_0 \cos\Delta_0, \qquad \kappa = \frac{3\alpha E}{4\beta\Omega^2} \tag{3.71}$$

Oscillator (3.70) has the effective potential energy described by

$$V(\phi) = \frac{1}{2}\left(H_0 + \frac{1}{2}\kappa\right)^2 \tan^2\phi - \frac{1}{8}\kappa^2 \sin^2\phi \tag{3.72}$$

Note that using oscillator (3.70) is complicated by the fact that the number H_0 depends upon the initial conditions given by

$$\sin\phi_0 = P_0, \qquad \left.\frac{d\phi}{d\bar{t}}\right|_{\bar{t}=0} = \sin\Delta_0 \tag{3.73}$$

where the second relationships follow from (3.63).

Hidden Nonsmooth Effects in Weakly Coupled Harmonic Oscillators

It follows from (3.62) that the parameter κ takes zero value if the original system (3.52) and (3.59) is linear, $\alpha = 0$. In this case oscillator (3.70) has exact analytical solution in terms of elementary functions

$$\phi = \arcsin\left[\sin\phi_0 \sin\left(|\cos\Delta_0|\bar{t} + \frac{\pi}{2}\right)\right] \tag{3.74}$$

In this case, the energy distribution, $P = \sin\phi$, behaves as a harmonic oscillator according to the sine wave law

$$P = P_0 \sin\left(|\cos\Delta_0|\bar{t} + \frac{\pi}{2}\right) \tag{3.75}$$

where $P_0 = \sin\phi_0$ is the initial energy distribution.

The phase ϕ behaves in a quite different way. As discussed briefly in Sect. 1.2.4, solution (3.74) admits two simple limits, such as the sine wave

$$\phi \sim \phi_0 \sin\left(|\cos\Delta_0|\bar{t} + \frac{\pi}{2}\right), \quad |P_0| \ll 1 \tag{3.76}$$

and the triangle wave

$$\phi \sim \frac{\pi}{2}\tau\left(\frac{2}{\pi}|\cos\Delta_0|\bar{t} + 1\right), \quad |P_0| \sim 1 \tag{3.77}$$

Figure 3.9 illustrates temporal mode shapes of the phase variables ϕ and Δ at different parameter of total excitation values κ. The initial distribution is close to predominantly one of the two oscillators, $P(0) \sim 1$. It is seen that such an uneven initial distribution results in oscillations of the angle ϕ within almost its entire interval $(-\pi/2, \pi/2)$ with a close to the triangle wave shape described by (3.77).

As mentioned in the preamble to this section, the most intensive energy exchange between subsystems can be viewed as a logical alternative to the stationary case with no energy exchange at all. Since the latter case associates with the normal mode motions, such alternative provides an adequate asymptotic limit for interpretations of different physical effects that cannot be described with conventional normal mode expansions.

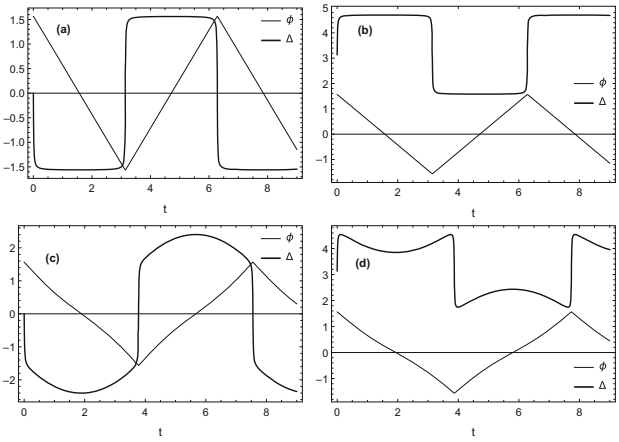

Fig. 3.9 Temporal shapes of the phase variables at $P(0) \sim 1$ ($\phi_0 = \pi/2 - 0.01$): (**a**) $\kappa = 0$, $\Delta = -0.001$, (**b**) $\kappa = 0$, $\Delta = \pi - 0.001$, (**c**) $\kappa = 1.5$, $\Delta = -0.001$, and (**d**) $\kappa = 1.5$, $\Delta = \pi - 0.001$

3.3.3 Energy Exchange Oscillator

As shown in Sect. 3.3.1, the energy exchange strongly nonlinear oscillator (3.70) admits the exact solution in terms of elementary functions, if the original system is linear, $\kappa = 0$. Now let us apply the methodology of Sect. 3.2 to the case $\kappa \neq 0$, when exact analytical solution cannot be expressed through elementary functions. First, let us represent the oscillator (3.70) in the following form:

$$\frac{d^2\phi}{dp^2} + \frac{\tan\phi}{\cos^2\phi} = \mu \sin 2\phi \tag{3.78}$$

where $p = |H_0 + \kappa/2|\,\bar{t}$ is a new temporal argument, whose parameters H_0 and κ are defined in (3.71), and

$$\mu = \frac{1}{2}\frac{\kappa^2}{(2H_0 + \kappa)^2} = \frac{1}{2}\frac{\kappa^2}{(\kappa\cos^2\phi_0 + 2\cos\phi_0\cos\Delta_0)^2} \tag{3.79}$$

The corresponding initial conditions can be obtained from (3.73) by taking into account the temporal substitution $p \to \bar{t}$. There are two possible ways to asymptotic simplifications of the essentially nonlinear equation (3.78).

Asymptotic of Equipartition

The first way is using the assumption that the initial energy is distributed almost equally between the oscillators of the ensemble (3.52), namely $|P_0| << 1$ or

$|\phi_0| << 1$. In this case, Eq. (3.78) can be reduced to the following Duffing equation:

$$\frac{d^2\phi}{dp^2} + (1-2\mu)\phi + \frac{4}{3}(1+\mu)\phi^3 = 0 \tag{3.80}$$

When $\mu < 1/2$, Eq. (3.80) describes periodic energy exchange. The period of the energy exchange process is given by the corresponding solution of Duffing equation (3.80). However, the point $(\phi, d\phi/dp) = (0,0)$ on the phase plane of oscillator (3.80) is changing its type from center to saddle when

$$\mu > \frac{1}{2} = \mu^* \tag{3.81}$$

Note that the critical number $\mu = \mu^*$ makes sense only for the neighborhood of antiphase mode (see Fig. 3.6b) as follows from relationship (3.79) after the following substitutions:

$$\mu|_{\{\Delta_0=\pi,\phi_0=0\}} = \frac{1}{2}\frac{\kappa^2}{(\kappa-2)^2} \tag{3.82}$$

$$\mu|_{\{\Delta_0=0,\phi_0=0\}} = \frac{1}{2}\frac{\kappa^2}{(\kappa+2)^2} \tag{3.83}$$

It is seen that formula (3.82) gives μ^* at $\kappa = \kappa^*$, whereas (3.83) gives μ, which is below μ^* at any positive κ.

Phase trajectories of oscillator (3.78) are shown in Fig. 3.10 for both critical and supercritical numbers μ. In order to keep μ fixed on the entire family of trajectories, we have to admit different κ on different trajectories. In particular, the numbers κ in Fig. 3.10 are obtained by substituting the fixed initial phase $\Delta_0 = \pi$ and different initial ϕ_0 in the inverse of (3.79)

$$\kappa = \frac{8(\sqrt{2\mu}\cos\phi_0 - 2\mu\cos^3\phi_0)\cos\Delta_0}{4\mu\cos 2\phi_0 + \mu\cos 4\phi_0 + 3\mu - 4} \tag{3.84}$$

The transition in phase diagrams of Fig. 3.10 is similar to that in Fig. 3.6 near the antiphase mode, except for different meaning and orientation of axes.

Low-Energy-Intensive Beats

The second way of asymptotic simplification of Eq. (3.78) is less conventional. We skip the condition $|\phi_0| << 1$ by allowing the energy to be distributed in any proportion while assuming that μ is sufficiently small. As follows from (3.79) and (3.71), the condition of small μ requires the quantity $\kappa = 3\alpha E/(4\beta\Omega^2)$ to be small. When $\mu \to 0$, the equation of energy exchange oscillator (3.78) still remains

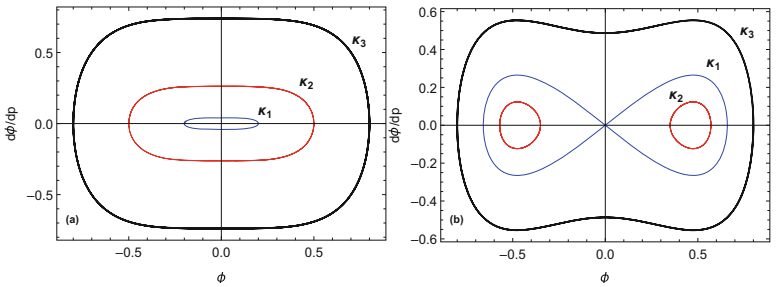

Fig. 3.10 Phase trajectories of the energy exchange oscillator: (**a**) $\mu = 1/2$—critical, $\kappa_1 = 0.999797$, $\kappa_2 = 0.991534$, $\kappa_3 = 0.938073$, and (**b**) $\mu = 0.8$—supercritical, $\kappa_1 = 1.11696$, $\kappa_2 = 1.12299$, $\kappa_3 = 1.09204$

strongly nonlinear but becomes exactly solvable in elementary functions. To employ this fact, let us introduce action-angle variables as described in Sect. 3.2

$$\phi = \arcsin\left(\frac{\sqrt{2I + I^2}}{1 + I}\sin\varphi\right)$$
$$v = \frac{(1 + I)\sqrt{2I + I^2}\cos\varphi}{\sqrt{1 + \left(2I + I^2\right)\cos^2\varphi}} \tag{3.85}$$

Following the procedure of Sect. 3.2 gives still exact equivalent of oscillator (3.78) in action-angle variables

$$\frac{dI}{dp} = \mu\frac{I(2 + I)}{(1 + I)^2}\sin 2\varphi$$
$$\frac{d\varphi}{dp} = 1 + I - \frac{2\mu}{(1 + I)^3}\sin^2\varphi \tag{3.86}$$

A direct averaging with respect to the phase φ can be applied to the right-hand side of system (3.86) to obtain the averaged system in the leading order approximation

$$\frac{dI}{dp} = 0, \qquad \frac{d\varphi}{dp} = 1 + I - \frac{\mu}{(1 + I)^3} \tag{3.87}$$

and its solution as

$$I = I_0 = const., \qquad \varphi = \left[1 + I_0 - \frac{\mu}{(1 + I_0)^3}\right]p \tag{3.88}$$

Substituting (3.88) in (3.85) gives the corresponding relationships in terms of the original variables.

High-order approximations can be obtained with canonical transformations of the Hamiltonian of oscillator (3.78). Such Hamiltonian can be expressed through the action-angle variables (3.85) as

$$H_\phi(I,\varphi,\mu)=\frac{1}{2}I(I+2)+\mu\frac{1+I(I+2)\cos 2\varphi}{2(I+1)^2} \tag{3.89}$$

Obviously, Eqs. (3.86) now follow from the Hamiltonian equations

$$\frac{dI}{dp}=-\frac{\partial H_\phi}{\partial\varphi},\qquad \frac{d\varphi}{dp}=\frac{\partial H_\phi}{\partial I} \tag{3.90}$$

Recall that $\{I,\varphi\}$ represent the action-angle variables of oscillator (3.78) only for the unperturbed case, $\mu=0$. This is why the angle φ is still present in Hamiltonian (3.89) although through the term of order μ. A high-order averaging can be implemented as a canonical transformation $\{I,\varphi\}\to\{J,\psi\}$ eliminating the fast phase from Hamiltonian (3.89). The main advantage of the Hamiltonian approach is that, instead of manipulating differential equations (3.90), the procedure deals with just one descriptive function $H_\phi(I,\varphi,\mu)$. In the leading order, the corresponding variable transformation must be identical since Hamiltonian (3.89) already has no fast phase at $\mu=0$. Using the automatic system of symbolic manipulations *Mathematica*$^{(R)}$ gives the transformation in the first asymptotic order as

$$\begin{aligned} I&=J-\mu\frac{J(2+J)}{2(1+J)^3}\cos 2\psi+O(\mu^2)\\ \varphi&=\psi-\mu\frac{J^2+2J-2}{4(1+J)^4}\sin 2\psi+O(\mu^2)\end{aligned} \tag{3.91}$$

This transformation brings Hamiltonian (3.89) to the form with no fast phase in the first-order of μ

$$H_\phi\to H_\psi=\frac{1}{2}J(J+2)+\frac{\mu}{2(1+J)^2}+O(\mu^2) \tag{3.92}$$

As a result, the new system takes the form, which is similar to (3.87) with the error of order $O(\mu^2)$

$$\frac{dJ}{dp}=-\frac{\partial H_\psi}{\partial\psi}=O(\mu^2),\qquad \frac{d\psi}{dp}=\frac{\partial H_\psi}{\partial J}=1+J-\frac{\mu}{(1+J)^3}+O(\mu^2) \tag{3.93}$$

Also, the form of solution for the fast phase is similar to (3.88)

$$J = J_0, \qquad \psi = \left[1 + J_0 - \frac{\mu}{(1+J_0)^3}\right] p \tag{3.94}$$

where $J_0 = const$. The inverse transformation to the original variables $\{\phi, v\}$ becomes more complicated than (3.85) due to the extra step according to (3.91).

3.3.4 Interaction of Liquid Sloshing Modes

The terminology of liquid sloshing covers both the physics of sloshing dynamics and the related mathematical methods [1, 57, 87, 90]. Many finite degrees-of-freedom sloshing models are obtained by representing the free liquid surface, say $\eta = \eta(t, x, y)$ (see Fig. 3.11), as a linear combination of some modal functions $\{U_k(x, y)\}$ with unknown time-dependent amplitudes

$$\eta(t, x, y) = \sum_k q_k(t) U_k(x, y) \tag{3.95}$$

Then applying Galerkin or similar method gives a set of ordinary differential equations for the amplitudes $\{q_k(t)\}$. The modal functions often represent a mathematically convenient orthogonal basis obtained as eigen functions of the corresponding linearized model of zero-viscosity fluid. Although such modal functions are conventionally called (linear) *sloshing modes*, in reality, physical sloshing modes may appear to be quite different due to viscous and nonlinear coupling effects. The sloshing waves observed in experiments usually associate with some stationary solutions of the entire nonlinear system for the modal amplitudes $\{q_k(t)\}$ and thus may combine two or even more predominant *linear sloshing modes* (LSMs). Since nonlinearity is essential for determining such combinations, the term *nonlinear sloshing modes* (NSMs) is meant in the present text. Below we follow reference [190], where the equations for modal amplitudes derived in [93] are used. Note that details of such derivations from the fluid dynamic equations are technically complicated and somewhat irrelevant to the present content. The model assumes irrotational flows of incompressible and originally inviscid fluid inside the tank with perfectly stiff walls. The tank has a square base whose side length is unity, $w = l = 1$, so that the fluid depth h is measured in the units of side wall length as shown in Fig. 3.11. On one hand, the assumption of square base brings formal simplifications to the governing differential equations of motion. On the other hand, the symmetry-induced 1:1 resonance coupling between the first two dominating modes essentially complicates the system dynamics, since the linear superposition principle does not hold in nonlinear cases.

A reasonable modal reduction therefore must include couples of symmetric modes, for instance,

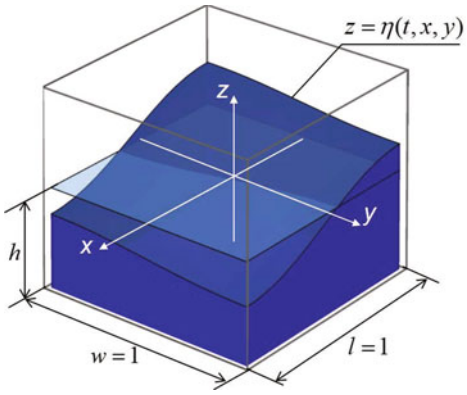

Fig. 3.11 Liquid sloshing in square tank

$$\eta(t, x, y) = q_1(t) \sin \pi x + q_2(t) \sin \pi y \tag{3.96}$$

Due to the perfect symmetry of square base, the first two modes satisfy exactly the 1:1 resonance condition $\Omega_1 = \Omega_2 \equiv \Omega$, and the corresponding differential equations of motion take the symmetric form

$$\begin{aligned} \ddot{q}_1 + 2\zeta\Omega\dot{q}_1 + \Omega^2 q_1 + f(q_1, q_2, \dot{q}_1, \dot{q}_2) &= 0 \\ \ddot{q}_2 + 2\zeta\Omega\dot{q}_2 + \Omega^2 q_2 + f(q_2, q_1, \dot{q}_2, \dot{q}_1) &= 0 \end{aligned} \tag{3.97}$$

where the phenomenological damping ratios are assumed to be the same, $\zeta = 0.0005$, and the nonlinear terms are given by the polynomial derived in [92]

$$f(q_1, q_2, \dot{q}_1, \dot{q}_2) \equiv S_3 q_1 \dot{q}_1{}^2 + S_4 q_1 \dot{q}_2{}^2 + S_5 q_2 \dot{q}_1 \dot{q}_2 + S_8 q_1{}^3 + S_9 q_1 q_2{}^2 \tag{3.98}$$

The quantities $S_i (i = 3, 4, 5, 8, 9)$ depend upon the tank depth h assuming that other dimensions are unity as shown in Fig. 3.11. In particular, $S_3 = 2.46654$, $S_4 = 4.9348$, $S_5 = -1.94182$, $S_8 = -2.53216$, and $S_9 = -1.05117$, when $h = 0.45$. Note also that, in references [92] and [190], the equations are scaled in such a way that $\Omega = 1$.

To bridge (3.97) with the standard form (3.53) of Sect. 3.3.1, let us set

$$f_1 = 2\zeta\Omega v_1 + f(q_1, q_2, v_1, v_2), \qquad f_2 = 2\zeta\Omega v_2 + f(q_2, q_1, v_2, v_1) \tag{3.99}$$

Then applying the averaging procedure of Sect. 3.3.1 gives equations[4]

[4] Note that, in reference [190], the origin $\Delta = 0$ corresponds to the antiphase mode. Therefore, transformation (3.44) must be adapted with the phase shift $\Delta \to \Delta + \pi$ in order to match the version used in [190]; Eqs. (3.100) and (3.101) still remain the same.

$$\begin{aligned}\frac{dE}{dt} &= -2\zeta\Omega E\\ \frac{dP}{dt} &= A\left(1-P^2\right)\sin 2\Delta\\ \frac{d\Delta}{dt} &= P(B-A\cos 2\Delta)\end{aligned} \tag{3.100}$$

and

$$\frac{d\delta}{dt} = \Omega + \frac{1}{2}[C - BP - A(1-P)\cos 2\Delta] \tag{3.101}$$

where A, B, and C are time-dependent quantities proportional to the total excitation level $E = E(t)$:

$$\begin{aligned}A = A(t) &= \frac{E(t)}{4\Omega^3}[\Omega^2(S_4 - S_5) - S_9]\\ B = B(t) &= \frac{E(t)}{4\Omega^3}[\Omega^2(-S_3 + 2S_4) - 3S_8 + 2S_9]\\ C = C(t) &= \frac{E(t)}{4\Omega^3}[\Omega^2(S_3 + 2S_4) + 3S_8 + 2S_9]\end{aligned} \tag{3.102}$$

The first equation in (3.100) describes the exponential energy decay of the first two modes combined:

$$E(t) = E(0)\exp(-2\zeta\Omega t) \tag{3.103}$$

The fast phase δ, described by the last equation in (3.100), determines the principal temporal scale, which is usually of little interest. Any way, Eq. (3.101) is solved for $\delta(t)$ by the direct integration as soon as the functions $P(t)$ and $\Delta(t)$ are known. As follows from (3.102), all the coefficients of the second and third equations in (3.100) decay with the same time rate according to (3.103). As a result, one can introduce a variable temporal scale, say $s(t)$, associated with the rate of energy dissipation. The corresponding function is given by the differential equation $ds(t) = A(t)dt$ under the initial condition $s(0) = 0$ as follows

$$s = A(0)\int_0^t \exp(-2\zeta\Omega t)dt = \frac{A(0)}{2\zeta\Omega}[1 - \exp(-2\zeta\Omega t)] \tag{3.104}$$

Now assuming that $P = P(s)$ and $\Delta = \Delta(s)$ and applying the substitution $t \to s$ as $d/dt = A\, d/ds$ brings system (3.100) to the effective Hamiltonian form for the couple of conjugate variables $\{\Delta, P\}$

$$\frac{dP}{ds} = -\frac{\partial H}{\partial \Delta} \equiv \left(1-P^2\right)\sin 2\Delta$$

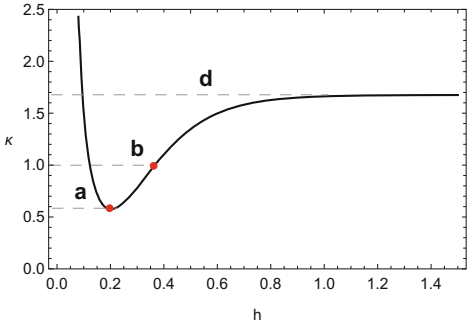

Fig. 3.12 The dependence of parameter κ versus fluid depth for the square tank, $w = l = 1$, based on the data of reference [91]: (**a**) minimum; (**b**) critical value; and (**d**) asymptotic maximum

$$\frac{d\Delta}{ds} = \frac{\partial H}{\partial P} \equiv (\kappa - \cos 2\Delta) P \tag{3.105}$$

with Hamiltonian,

$$H = H(P, \Delta) \equiv \frac{1}{2}\kappa P^2 + \frac{1}{2}\left(1 - P^2\right)\cos 2\Delta \tag{3.106}$$

where $\kappa = B/A$ is a constant parameter linked to the tank geometry namely the fluid depth as shown in Fig. 3.12.

The physical meaning of this result is that the energy level of sloshing has no effect on the resonance dynamics except for the slowing down of their temporal scale. From the mathematical standpoint, this is explained by the form of nonlinearity in (3.98). Since the polynomial f is *homogeneous*, $f(\lambda q_1, \lambda q_2, \lambda \dot{q}_1, \lambda \dot{q}_2) = \lambda^3 f(q_1, q_2, \dot{q}_1, \dot{q}_2)$, all the proportions between different terms of such polynomials remain fixed regardless of the amplitude levels λ. As follows from (3.105), κ is a single parameter of the effective oscillator.

The phase plane diagrams of system (3.105) represent level lines of the Hamiltonian $H = H(P, \Delta)$ versus the parameter κ and are shown in Fig. 3.13. The major qualitative transition takes place when $\kappa = 1$. Namely, the two cells I and A, surrounding the stationary Points (centers), collapse into vertical lines by giving rise two saddle points. This transition is accompanied by developing phase channels near the upper and lower cell boundaries $P = \pm 1$. In terms of NSMs, both inphase and antiphase NSMs become unstable, while only circular/rotational modes remain; see Fig. 3.5 for interpretation on the configuration plane $q_1 - q_2$. Compared to the case of linear elastic coupling of identical oscillators, which is represented by Fig. 3.6, the period of phase portrait along the coordinate Δ is shorter as many as twice. This follows also from the comparison of effective Hamiltonians (3.64) and (3.106). The reason is that the inphase and antiphase sloshing modes are physically equivalent due to the symmetry of square tank with respect to both its diagonals. As a result, system (3.97) admits either of the two replacements $q_1 \to -q_1$ or $q_2 \to -q_2$. In case of a mass-spring system with elastic coupling, the antiphase mode is carrying

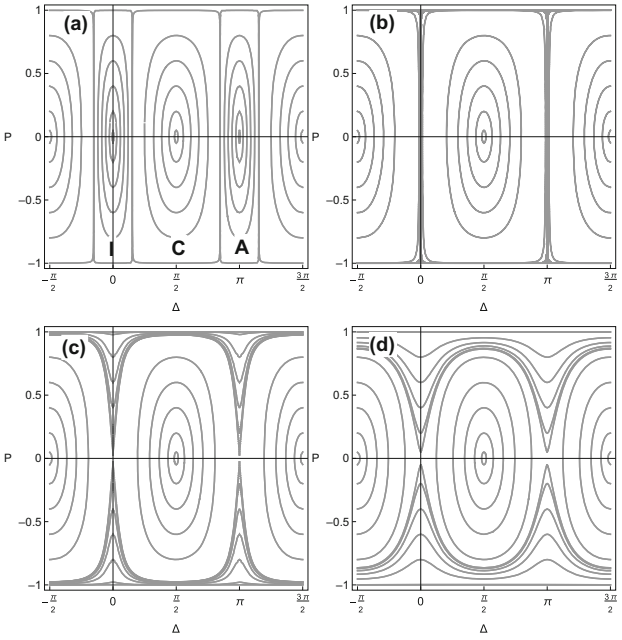

Fig. 3.13 Phase plane $\Delta - P$ diagrams of the effective Hamiltonian system at different κ: (**a**) $\kappa = 0.5753$—minimum reached at $h = 0.20156$, C—cells of circular modes, I—cells of inphase mode, and A—cells of antiphase mode; (**b**) $\kappa = 1.0$—critical value reached at $h = 0.3666$; (**c**) $\kappa = 1.1$—slightly supercritical value reached at $h = 0.3992$; (**d**) $\kappa = 1.6754$—asymptotic limit at $h \to \infty$; see Fig. 3.12

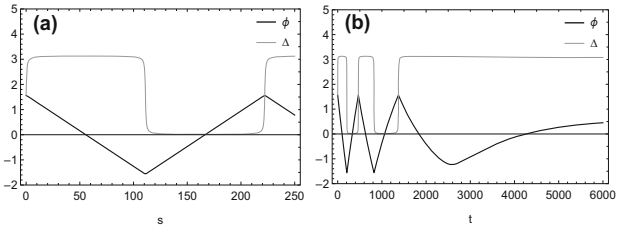

Fig. 3.14 Sample behavior of the phase angles ϕ and Δ at critical fluid height, $h = 0.3666$, and the initial conditions: $P(0) = 0.9999$, $\Delta(0) = \pi/2$, $E(0) = 0.25$: (**a**) variable time scale and (**b**) the original time

more energy of elastic deformations than the inphase mode, and this makes both modes physically different.

Figure 3.14 illustrates the behavior of excitation distribution between the modes in terms of the angle $\phi = \arcsin P$ and the phase shift Δ corresponding to the case (b) of Fig. 3.13. The initial conditions correspond to the rotating mode on the configuration plane $q_1 - q_2$. It is seen that the excitation exchange happens in a nonsmooth way due to the fact that only one of the two NSMs was predominantly

excited at $t = 0$. In this case almost all the energy will drift from one mode to another.

3.3.5 Model of Weakly Coupled Autogenerators

Following [114] consider an ensemble of two linearly coupled generalized van der Pol-Duffing autogenerators that differ from each other by only one coefficient including the so-called frequency detuning parameter σ:

$$\begin{aligned} &\ddot{u}_1 + u_1 + 8\alpha\varepsilon {q_1}^3 + 2\beta\varepsilon(u_1 - u_2) \\ &+ 2\varepsilon(\gamma - 4b{u_1}^2 + 8d{u_1}^4)\dot{u}_1 = 0 \\ &\ddot{u}_2 + (1 + 4\varepsilon\sigma)u_2 + 8\alpha\varepsilon {u_2}^3 + 2\beta\varepsilon(u_2 - u_1) \\ &+ 2\varepsilon(\gamma - 4b{u_2}^2 + 8d{u_2}^4)\dot{u}_2 = 0 \end{aligned} \tag{3.107}$$

In this case, setting $\Omega = 1$ and applying the averaging operator (3.58) to system (3.56) and (3.57) give, respectively,

$$\dot{E} = -2\varepsilon E[\gamma - bE + dE^2 - (b - 3dE)EP^2] \tag{3.108}$$

$$\dot{P} = 2\varepsilon\left[E(b - 2dE)P(1 - P^2) + \beta\sqrt{1 - P^2}\sin\Delta\right] \tag{3.109}$$

$$\dot{\Delta} = 2\varepsilon\left[\sigma - 3\alpha EP - \beta\frac{P}{\sqrt{1 - P^2}}\cos\Delta\right] \tag{3.110}$$

and

$$\dot{\delta} = 1 + \varepsilon\left[3\alpha E(1 + P) + \beta\left(1 - \sqrt{\frac{1 - P}{1 + P}}\cos\Delta\right)\right] \tag{3.111}$$

In the conservative case, when no dissipative terms are present in the original system (3.107), equation of (3.108) takes the form $\dot{E} = 0$, and thus the averaged total energy of both oscillators remains constant during the vibrating process. Otherwise, this energy is varying unless the right-hand side of Eq. (3.108) is zero:

$$\gamma - bE + dE^2 - (b - 3dE)EP^2 = 0 \tag{3.112}$$

It is easy to see the particular case, $E = b/(3d)$ and $\gamma = 2b^2/(9d)$, in which condition (3.112) takes place. Substituting these values of E and γ in (3.109) and (3.110) give the reduced system on the phase plane $\Delta - P$ as

$$\frac{dP}{d\bar{t}} = \frac{b^2}{9\beta d} P(1-P^2) + \sqrt{1-P^2}\sin\Delta$$

$$\frac{d\Delta}{d\bar{t}} = \frac{\sigma}{\beta} - \frac{\alpha b}{\beta d} P - \frac{P}{\sqrt{1-P^2}}\cos\Delta \tag{3.113}$$

where $\bar{t} = 2\varepsilon\beta t$.

The result of numerical integration at the stationary excitation level $E = b/(3d)$ is illustrated in Fig. 3.15. In particular, fragment (a) shows that the temporal mode shapes of phase angles ϕ and Δ tend to stabilize close to the triangle and square waves, respectively. Fragment (b) explains what happens in terms of the excitation distribution index P and the phase shift Δ. As follows from the coherency index Q, which is obtained by the direct integration of the original system, the generators oscillate coherently in the dynamic regime close to the elliptic rotational mode as seen from the fragment (c). During this rotational mode, the excitation is transmitted from one generator to another. The corresponding trajectory in the configuration plane of original variables is shown in fragment (d). Phase transitions happen quickly in a stepwise manner, when only one of the two generators is excited. A fixed phase shift means that oscillators are synchronized. In the case under consideration, the phase shift is practically fixed except for relatively short intervals

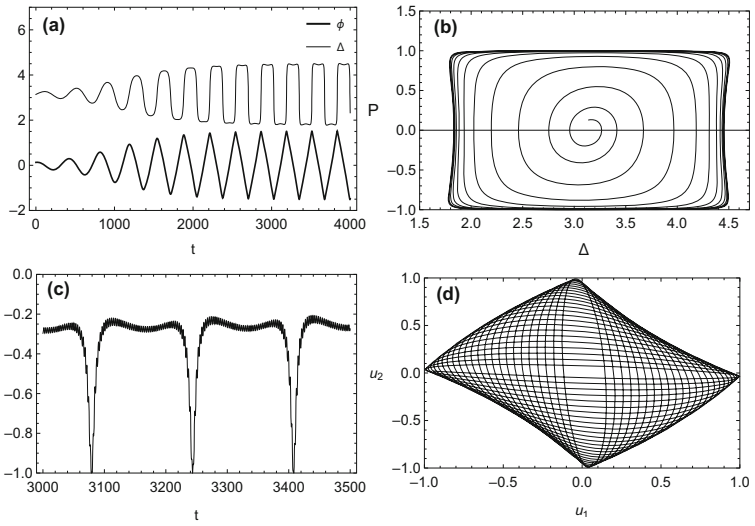

Fig. 3.15 The dynamics of weakly coupled autogenerators in different variables obtained by numerical integration of the original and averaged equations under the stationary total excitation level given by $E(0) = b/(3d)$ and the following values of parameters and initial conditions: $\varepsilon = 0.01$, $\beta = 1.0$, $\alpha = 0.268$, $d = 0.8$, $b = 1.2$, $\sigma = 0$, $\gamma = 2b^2/(9d)$, $\Delta(0) = \pi - 0.001$, $P(0) = 0.128844$

of stepwise switches. Such type of synchronization was noticed and defined as nonconventional synchronization in [135] and then documented in [115].

3.3.6 *Localization of Friction-Induced Vibrations*

The variables$\{E, P, \Delta, \delta\}$ can be used for investigation of different dynamic effects in a coupled set of two coupled oscillators with equal or close to each other natural frequencies regardless of physical meaning of the problem. Following [193], let us consider a chain of n linearly coupled nonlinear oscillators of the mass m driven by friction forces due to the interaction with a continuous stiff surface moving with a constant speed V_b as shown in Figs. 3.16–3.17. The restoring force characteristic of oscillators corresponds to Duffing model, where k_g and k_3 are linear and cubic stiffness coefficients, respectively. In addition to the friction force, each oscillator is subjected to the linear viscous damping with the coefficient of viscosity c. The oscillators are coupled by linear springs of stiffness k. Each mass is under the constant normal load, p. The friction force acting on the jth mass is expressed through its relative velocity as

$$F_j = p\mu(V_b - \dot{q}_j) \tag{3.114}$$

where μ is the so-called friction coefficient, which is usually introduced in a phenomenological way as, for instance [59],

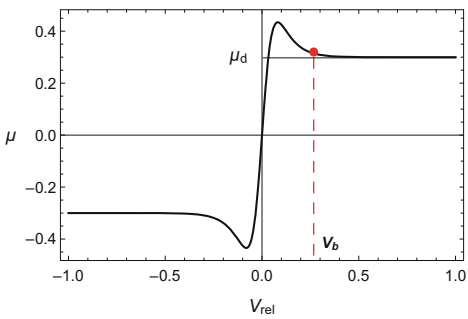

Fig. 3.16 Friction coefficient versus relative velocity (3.115) for the following numerical values: $\alpha_f = \beta_f = 15$, $\mu_\sigma = 0.7$, $\mu_d = 0.3$, and $V_b = 0.23$

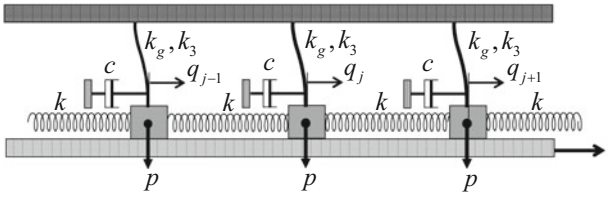

Fig. 3.17 Finite element model of friction interphase

$$\mu(V_{rel}) = \left[\mu_d + \frac{\mu_\sigma - \mu_d}{\cosh(\alpha_f V_{rel})}\right] \tanh(\beta_f V_{rel}) \tag{3.115}$$

Let us introduce the natural frequency of a linearized individual oscillator, $\Omega = \sqrt{k_g/m}$, and scale the parameter of normal load as $\varepsilon = p\Omega/k_g$, assuming that the load is relatively weak. Also, let us introduce two parameters, α and β, characterizing the level of nonlinearity and the strength of coupling, as $k_3/k_g = \varepsilon\alpha$ and $k/k_g = 2\varepsilon\beta$, respectively. The corresponding differential equations of motion are represented in the form

$$\begin{aligned} &\frac{d^2 q_j}{d\bar{t}^2} + q_j + \varepsilon\alpha q_j^3 - 2\varepsilon\beta\left(q_{j-1} - 2q_j + q_{j+1}\right) \\ &\quad = -\varepsilon\left[a\frac{dq_j}{d\bar{t}} + b\left(\frac{dq_j}{d\bar{t}}\right)^3 + d\left(\frac{dq_j}{d\bar{t}}\right)^5\right] \end{aligned} \tag{3.116}$$

where $\bar{t} = \Omega t$ is a natural temporal scale associated with individual linearized oscillators, and a polynomial expansion of the dependence (3.115) was applied to give the following coefficients: $a = \mu'(V_b) + c/p$, $b = \Omega^2\mu^{(3)}(V_b)/6$, and $d = \Omega^4\mu^{(5)}(V_b)/120$.

Below a two mass-spring case is considered by assuming that only one coupling spring is present. As a result, system (3.116) gives the system of two coupled non-conservative oscillators

$$\frac{dq_j}{d\bar{t}} = v_j, \quad \frac{dv_j}{d\bar{t}} = -q_j - f_j; \quad j = 1, 2 \tag{3.117}$$

where

$$\begin{aligned} f_1 &= \varepsilon\alpha q_1^3 + 2\varepsilon\beta(q_1 - q_2) + \varepsilon\left[a\frac{dq_1}{d\bar{t}} + b\left(\frac{dq_1}{d\bar{t}}\right)^3 + d\left(\frac{dq_1}{d\bar{t}}\right)^5\right] \\ f_2 &= \varepsilon\alpha q_2^3 + 2\varepsilon\beta(q_2 - q_1) + \varepsilon\left[a\frac{dq_2}{d\bar{t}} + b\left(\frac{dq_2}{d\bar{t}}\right)^3 + d\left(\frac{dq_2}{d\bar{t}}\right)^5\right] \\ &\quad + 4\varepsilon\sigma q_2 \end{aligned} \tag{3.118}$$

Following Sect. 3.3.2 let us substitute (3.118) in Eqs. (3.56) and (3.57) by setting $\Omega = 1$. Then applying the operator of averaging (3.58) with respect to the fast phase δ gives

$$\begin{aligned} \frac{dE}{d\bar{t}} &= -\frac{1}{8}\varepsilon E\left[8a + 6bE + 5dE^2 + \left(6bE + 15dE^2\right)P^2\right] \\ \frac{dP}{d\bar{t}} &= \frac{1}{4}\varepsilon\left[\left(3bE + 5dE^2\right)P\left(P^2 - 1\right) + 8\beta\sqrt{1 - P^2}\sin\Delta\right] \end{aligned} \tag{3.119}$$

$$\frac{d\Delta}{d\bar{t}} = \frac{1}{4}\varepsilon\left(8\sigma - 3\alpha E P - \frac{8\beta P}{\sqrt{1-P^2}}\cos\Delta\right)$$

$$\frac{d\delta}{d\bar{t}} = 1 + \frac{3}{8}\varepsilon\alpha E(1+P) + \varepsilon\beta\left(1 - \sqrt{\frac{1-P}{1+P}}\cos\Delta\right) \tag{3.120}$$

Analyzing the right-hand side of the first equation in (3.119) reveals the stationary excitation level, $E = E_{stat} = -(2/5)b/d$, which is possible under the condition $d = (1/5)b^2/a$. Taking into account these two relationships brings another two equations of system (3.119) to the form

$$\frac{dP}{ds} = \frac{a}{4\beta}P(1-P^2) + \sqrt{1-P^2}\sin\Delta$$

$$\frac{d\Delta}{ds} = \frac{\sigma}{\beta} + \frac{3a}{4b}\frac{\alpha}{\beta}P - \frac{P}{\sqrt{1-P^2}}\cos\Delta \tag{3.121}$$

where $s = 2\varepsilon\beta\bar{t}$ is a slow time scale associated with the strength of coupling.

System (3.121) represents an autonomous planar case; hence, using phase plane diagrams for its parametric study becomes possible. For instance, analyzing the equilibrium points of system (3.121) versus the cubic nonlinearity, α, shows that the antiphase mode, $(\Delta, P) = (\pi, 0)$ experiences center to saddle bifurcation at $\alpha_* = -4\beta b/(3a)$ by giving rise to the local modes as illustrated in Fig. 3.18.

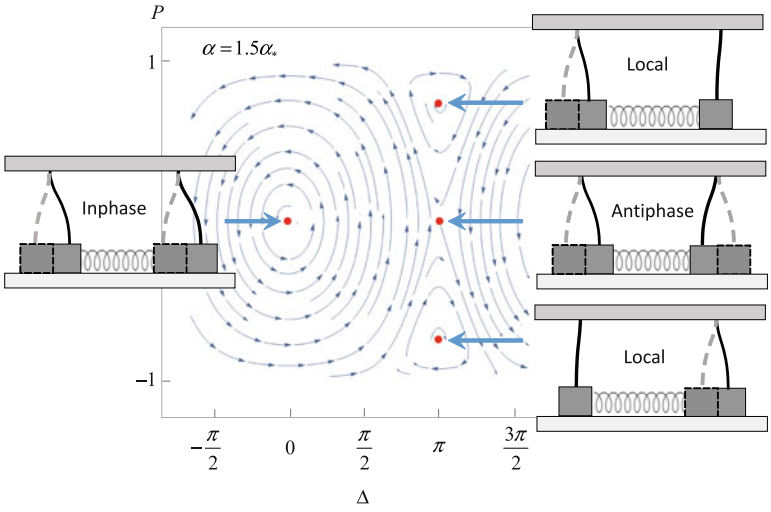

Fig. 3.18 Developed nonlinear mode localization at supercritical nonlinearity according to (3.121) under parameter values [193]: $V_b = 0.23$, $a = 0.1406$, $\beta = 1.0$, $b = -10.43$, $d = 154.72$, and thus $\alpha_* = 98.9015$

3.4 Transition from Normal to Local Modes

The transient mode localization phenomenon is considered below in a mechanical model combined of a simply supported beam with two localized mass attachments enforced by nonlinear springs with hardening characteristics. Two different approaches to the model reduction, such as normal and local mode representations for the beam's center line, are discussed. It is concluded that the local mode discretization brings advantages for the transient localization analysis. Based on the specific coordinate transformations and the idea of averaging, explicit equations describing the energy exchange between the local modes and the corresponding localization conditions are obtained. It was shown that, when the energy is slowly pumped into the system then, at some point, the energy equipartition around the system suddenly breaks and one of the two local modes becomes the dominant energy receiver. The phenomenon is interpreted in terms of the related phase plane diagram. The diagram shows qualitative changes near the image of antiphase mode as the total energy of the system has reached its critical level. A simple closed form expression is obtained for the corresponding critical time estimate. The material below is an update of reference [189].

3.4.1 Model Description

The model under investigation represents a simply supported elastic beam of length l with two masses attached to the beam and connected to the base by nonlinear springs as shown in Fig. 3.19. The corresponding differential equation of motion and boundary conditions are, respectively,

$$\rho A \frac{\partial^2 w}{\partial t^2} + EI \frac{\partial^4 w}{\partial y^4} = f_1(t)\delta(y - y_1) + f_2(t)\delta(y - y_2) \tag{3.122}$$

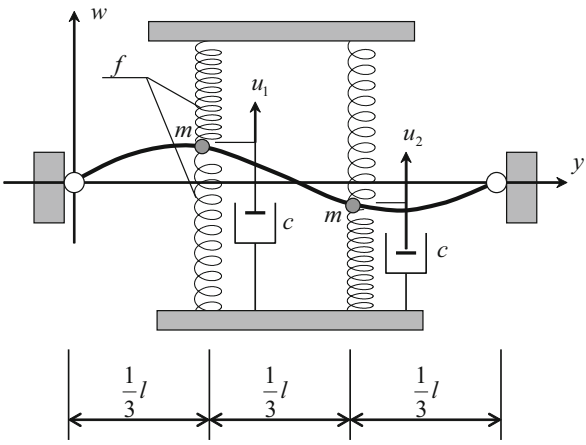

Fig. 3.19 The mechanical model admitting both normal and local mode motions; all the springs have hardening restoring force characteristics

and

$$w(t, y)|_{y=0,l} = 0, \quad \frac{\partial^2 w(t, y)}{\partial y^2}|_{y=0,l} = 0 \tag{3.123}$$

where

$$f_i(t) = -f[w(t, y_i)] - c\frac{\partial w(t, y_i)}{\partial t} - m\frac{\partial^2 w(t, y_i)}{\partial t^2}; \quad i = 1, 2 \tag{3.124}$$

are transverse forces applied to the beam from masses attached at the points $y = y_{1,2}$.

It will be assumed that the structure is symmetric with respect to the middle of the beam, $y = l/2$, such that

$$y_1 = l/3 \quad \text{and} \quad y_2 = 2l/3 \tag{3.125}$$

Below we consider the case of the hardening restoring force characteristics of the springs and show that, under appropriate conditions, a slow energy inflow leads to the localization of vibration modes. As a result, the system energy is spontaneously shifted to either the left or the right side of the beam due to the so-called symmetry breaking effect. The adiabatic (slow) energy increase means that the energy source has a minor or no direct effect on the mode shapes. For simulation purposes, such energy inflow is provided by the assumption that the viscous damping coefficient c is sufficiently small and negative; the physical basis for such an assumption was discussed in [187, 188]. This remark, which is substantiated below by the corresponding numerical values of the parameters, is important to follow; otherwise, the phenomenon, which is the focus of this paper, may not be developed. In contrast, the dissipation ($c > 0$) can lead to a spontaneous dynamic transition from local to normal modes, when the total energy reaches its sub-critical level.

Recall that the presence of Dirac δ-functions in Eq. (3.122) requires a generalized interpretation of the differential equation of motion in terms of distributions [208]. The corresponding compliance is provided by further model reduction based on the Bubnov-Galerkin approach, which actually switches from the point-wise to the integral interpretation of equations.

3.4.2 Normal and Local Mode Coordinates

Normal Mode Coordinates

Let us evaluate two possible ways to discretizing the model (3.122). The minimum number of modes (two) will be maintained to capture the effect of interest. The conventional normal mode representation for the boundary value problem (3.122)–(3.123) is

$$w(t, y) = w_1(t) \sin \frac{\pi y}{l} + w_2(t) \sin \frac{2\pi y}{l} \tag{3.126}$$

Substituting (3.126) in (3.122) and applying the standard Bubnov-Galerkin procedure give

$$\ddot{w}_1 + \frac{3}{3m + Al\rho} \left(c\dot{w}_1 + \frac{\pi^4 EI}{3l^3} w_1 \right) + F_1(w_1, w_2) = 0 \tag{3.127}$$
$$\ddot{w}_2 + \frac{3}{3m + Al\rho} \left(c\dot{w}_2 + 16\frac{\pi^4 EI}{3l^3} w_2 \right) + F_2(w_1, w_2) = 0$$

where $F_i(w_1, w_2) = F(w_1 + w_2) + (-1)^{i+1} F(w_1 - w_2)$, and

$$F(z) = \frac{\sqrt{3}}{3m + Al\rho} f\left(\frac{\sqrt{3}}{2} z \right) \tag{3.128}$$

Equations (3.127) are decoupled in the linear terms related to the elastic beam center line, whereas the modal coupling is due to the spring nonlinearities participating in $F(z)$.

Local Mode Coordinates

Alternatively, the model can be discretized by introducing the local mode coordinates determined by the spring locations

$$u_i(t) = w(t, y_i); \quad i = 1, 2 \tag{3.129}$$

Substituting (3.125) in (3.126) and taking into account (3.129) reveal simple links between the normal and local coordinates as

$$u_1 = \frac{\sqrt{3}}{2}(w_1 + w_2), \quad u_2 = \frac{\sqrt{3}}{2}(w_1 - w_2) \tag{3.130}$$

or, inversely,

$$w_1 = \frac{\sqrt{3}}{3}(u_1 + u_2), \quad w_2 = \frac{\sqrt{3}}{3}(u_1 - u_2) \tag{3.131}$$

Substituting (3.131) in (3.126) gives the local mode representation for the beam center line

$$w(t, y) = u_1(t)\psi_1 \left(\frac{\pi y}{l} \right) + u_2(t)\psi_2 \left(\frac{\pi y}{l} \right) \tag{3.132}$$

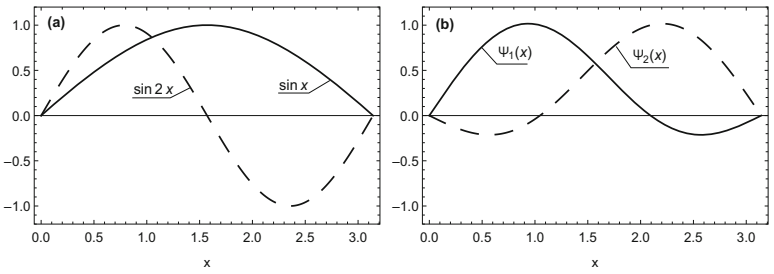

Fig. 3.20 Two types of spatial basis for simply supported beams: (**a**) normal modes and (**b**) local mode shape functions

where the local mode shape functions are defined as

$$\begin{bmatrix} \psi_1(x) \\ \psi_2(x) \end{bmatrix} = \frac{\sqrt{3}}{3} \begin{bmatrix} 1 & 1 \\ 1 & -1 \end{bmatrix} \begin{bmatrix} \sin x \\ \sin 2x \end{bmatrix} \tag{3.133}$$

Both normal and local mode shape functions are shown in Fig. 3.20a and b, respectively. Transformation (3.133) can be generalized for a greater number of modes. Note that functions (3.133) satisfy the following orthogonality condition

$$\int_0^{\pi} \psi_i(x)\, \psi_j(x)\, dx = \frac{\pi}{3}\delta_{ij} \tag{3.134}$$

where δ_{ij} is the Kronecker symbol.

The differential equations for the local mode amplitudes, $u_1(t)$ and $u_2(t)$, can be derived by substituting (3.132) in the partial differential equation (3.122) and then applying Bubnov-Galerkin procedure with orthogonality condition (3.134). Alternatively the equations can be obtained by substituting (3.131) in (3.127) and conducting straightforward algebraic manipulations. Finally the local mode equations take the form

$$\ddot{u}_1 + \frac{3}{3m + Al\rho}\left[c\dot{u}_1 + \frac{\pi^4 EI}{6l^3}(17u_1 - 15u_2) + f(u_1)\right] = 0 \tag{3.135}$$

$$\ddot{u}_2 + \frac{3}{3m + Al\rho}\left[c\dot{u}_2 + \frac{\pi^4 EI}{6l^3}(17u_2 - 15u_1) + f(u_2)\right] = 0$$

Further consider Duffing's type polynomial approximation for the springs restoring force characteristic, $f(z) = kz + az^3$.

Symmetry Breaking with Energy Localization

Let us represent equations (3.135) as a set of four first-order equations for the system state variables

$$\begin{aligned} \dot{u}_1 &= v_1 \\ \dot{u}_2 &= v_2 \\ \dot{v}_1 &= -\Omega^2 u_1 - f_1 \\ \dot{v}_2 &= -\Omega^2 u_2 - f_2 \end{aligned} \tag{3.136}$$

where

$$\begin{aligned} f_1 &= \varepsilon(-\Omega^2 u_2 + \zeta v_1 + \alpha u_1^3) \\ f_2 &= \varepsilon(-\Omega^2 u_1 + \zeta v_2 + \alpha u_2^3) \end{aligned} \tag{3.137}$$

and the following set of parameters and assumptions are introduced:

$$\Omega = \sqrt{\frac{6kl^3 + 17\pi^4 EI}{2l^3(3m + Al\rho)}} = O(1), \quad \varepsilon = \frac{15\pi^4 EI}{6kl^3 + 17\pi^4 EI} << 1 \tag{3.138}$$

$$\zeta = \frac{3c}{(3m + Al\rho)\varepsilon} = O(1), \quad \alpha = \frac{3a}{(3m + Al\rho)\varepsilon} = O(1)$$

From the physical standpoint, relationships (3.138) mean that the beam is flexible enough compared to the linear stiffness of springs, whereas both the viscosity effect and nonlinearity are relatively weak as compared to the beam bending rigidity. Note that localized spring forces may practically trigger high modes of the flexible beam and thus invalidate the two modes' approximation represented by relationship (3.126). Nonetheless, in the current illustrating model, a role of the beam is secondary. As follows from system (3.136), the beam just provides a weak coupling between the oscillators. Therefore a more detailed modeling could incorporate the high modes as a perturbation to the coupling effect.

Following Sect. 3.3.1, substituting (3.137) in (3.56) and (3.57), and conducting the averaging give

$$\begin{aligned} \dot{E} &= -\varepsilon\zeta E \\ \dot{P} &= \varepsilon\Omega\sqrt{1 - P^2}\sin\Delta \\ \dot{\Delta} &= -\varepsilon\Omega\left(\frac{3\alpha}{4\Omega^4}E + \frac{\cos\Delta}{\sqrt{1 - P^2}}\right)P \end{aligned} \tag{3.139}$$

and

$$\dot{\delta} = \Omega + \frac{3\varepsilon\alpha}{8\Omega^3}E(1+P) - \frac{1}{2}\varepsilon\Omega\sqrt{\frac{1-P}{1+P}}\cos\Delta \tag{3.140}$$

If the viscosity is negative,[5] $\zeta < 0$, then Eqs. (3.139) describe transition to the local mode as the system energy increases; see Fig. 3.21 for illustration. The energy partitioning parameter P is varying within the interval $-1 \le P \le 1$. The ends of the interval obviously correspond to the local modes, whereas its center $P = 0$ corresponds to the normal modes: $\Delta = 0$-inphase, and $\Delta = \pi$-antiphase; recall transformation (3.44). Linearizing system (3.139) in the vicinity of stationary points $(\Delta, P) = (0, 0)$ and $(\Delta, P) = (\pi, 0)$, assuming the variable E is "frozen," and eliminating the phase variable give

$$\ddot{P} + \varepsilon^2\Omega^2\left(1 \pm \frac{3\alpha}{4\Omega^4}E\right)P = 0 \tag{3.141}$$

where plus or minus sign in the parenthesis corresponds to the inphase or antiphase mode, respectively.

It follows from the form of Eq. (3.141) that a localized mode can branch out of the antiphase mode, when $E = E^* = 4\Omega^4/(3\alpha)$. In the case of negative viscosity, the first equation in (3.139) gives $E = E_0\exp(\varepsilon|\zeta|t)$. Therefore, the critical system excitation level E^* will be reached regardless of the initial number E_0, when $t = t^*$:

$$t^* = \frac{1}{\varepsilon|\zeta|}\ln\frac{4\Omega^4}{3\alpha E_0} \tag{3.142}$$

The data of Fig. 3.21 gives $E_0 = 1.36585 \times 10^{-5}$, $E^* = 1.42116 \times 10^{-2}$, and expression (3.142) generates the number $t^* = 3580.42$, in a reasonable agreement with Fig. 3.21.

3.5 Autolocalized Modes in Nonlinear Coupled Oscillators

Below, the term *autolocalized* means that the system itself may come into the nonlinear local mode regime and stay there regardless of initial energy distribution among its particles. As follows from Poincaré recurrence theorem, such phenomena are rather impossible within the class of conservative systems [16]. Nonetheless, interactions between the system particles can be designed in specific ways in order to achieve desired phenomena. It is assumed that such a design can be implemented practically by using specific electric circuits and possibly mechanical actuators. On macro-levels, the autolocalization may help to optimize vibration suppression.

[5] Possible physical mechanisms of the negative viscosity are not discussed here since the negative damping is used only for simulation of a slow energy inflow into the system.

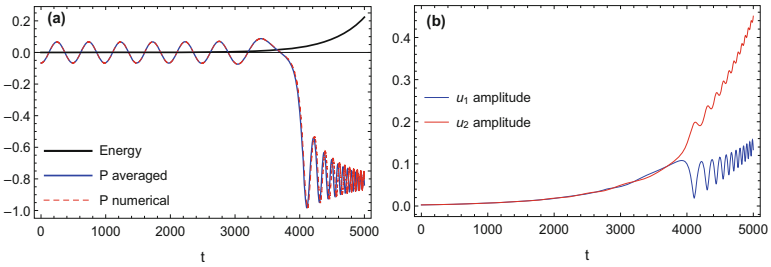

Fig. 3.21 Symmetry breaking followed by sudden transition from normal to local mode vibration as the system energy has reached its critical value: (**a**) energy distribution and (**b**) local mode amplitudes; the following parameters were taken for numerical simulations: $\varepsilon = 0.009$, $\zeta = -0.2156$, $\Omega = 1.4217$, $\alpha = 383.29$, and the initial normal mode amplitudes at zero velocities are $w_1(0) = 0.0001$ and $w_2(0) = -0.003$

Some results from the previous publication [179] are reproduced below after some notation modifications for a better coherency with the current text. Let us consider an array of N harmonic oscillators, such that each of the oscillators interacts with only the nearest neighbors. The corresponding differential equations of motion are of the form

$$\ddot{x}_j + \Omega^2 x_j = \beta(x_{j-1} - 2x_j + x_{j+1}) +$$

$$+ \alpha[(E_j - E_{j-1})E_{j-1} - (E_{j+1} - E_j)E_{j+1}]\dot{x}_j \tag{3.143}$$

$$E_j = \frac{1}{2}(\dot{x}_j^2 + \Omega^2 x_j^2); \qquad j = 1, ..., N \tag{3.144}$$

where $E_j = E_j(t)$ is the total energy[6] of the jth oscillator under the boundary conditions of fixed ends, $E_0(t) \equiv E_{N+1}(t) \equiv 0$; and Ω, β, and α are constant parameters of the model.

On the right-hand side of Eq. (3.143), two groups of terms describe the coupling between the oscillators. If $\alpha = 0$ then the only linear coupling remains. In this case, under special initial conditions, N different coherent periodic motions, i.e., linear normal modes, can exist. Any other motion is combined of the linear normal mode motions, whereas the energy is conserved on each of the modes the way it was initially distributed between the modes. In other words, no energy localization is possible on individual particles if $\alpha = 0$.

Another group of terms, including the common factor α, has the opposite to the linear elastic interaction effect. These nonlinear terms are to simulate a

[6] Note that the concept of energy for individual oscillators becomes somewhat ambiguous in the presence of coupling and nonconservative terms. Hence expression (3.144) should rather be viewed as Lyapunov function.

possible competition between the oscillators leading to a one-way energy flow to the neighbor whose energy is greater. Such kind of interaction dominates when the total system energy is large enough to involve high degrees of the coordinates and velocities.

Let us introduce the complex conjugate variables $\{A_j(t), \bar{A}_j(t)\}$ into Eqs. (3.143) according to relationships

$$x_j = \frac{1}{2}[A_j \exp(i\Omega t) + \bar{A}_j \exp(-i\Omega t)]$$
$$\dot{x}_j = \frac{1}{2} i\Omega [A_j \exp(i\Omega t) - \bar{A}_j \exp(-i\Omega t)] \tag{3.145}$$

where the following compatibility condition is imposed

$$\frac{dA_j}{dt} \exp(i\Omega t) + \frac{d\bar{A}_j}{dt} \exp(-i\Omega t) \tag{3.146}$$

In terms of the complex amplitudes, the total energy of individual oscillator (3.144) takes the form

$$E_j = \frac{1}{2}\Omega^2 A_j \bar{A}_j = \frac{1}{2}\Omega^2 |A_j|^2 \tag{3.147}$$

When $\beta = \alpha = 0$, the system is decomposed into N uncoupled oscillators leading to a constant solution in the new variables. In general case, substituting (3.145) in (3.143), taking into account (3.146), and applying the averaging with respect to the phase $z = \Omega t$, give the set of equations

$$\dot{A}_j = -\frac{i\beta}{2\Omega}(A_{j-1} - 2A_j + A_{j+1}) +$$
$$+ \frac{\alpha\Omega^4}{8}\left[\left(|A_j|^2 - |A_{j-1}|^2\right)|A_{j-1}|^2 - \left(|A_{j+1}|^2 - |A_j|^2\right)|A_{j+1}|^2\right] A_j \tag{3.148}$$
$$(j = 1, ..., N)$$

where the conjugate equations are omitted.

Let us consider first the case of two coupled oscillators ($N = 2$), when system (3.148) is reduced to

$$\dot{A}_1 = -\frac{i\beta}{2\Omega}(A_2 - 2A_1) + \frac{\alpha\Omega^4}{8}\left(|A_1|^2 - |A_2|^2\right)|A_2|^2 A_1 \tag{3.149}$$
$$\dot{A}_2 = -\frac{i\beta}{2\Omega}(A_1 - 2A_2) + \frac{\alpha\Omega^4}{8}\left(|A_2|^2 - |A_1|^2\right)|A_1|^2 A_2$$

This system has the integral

$$K = |A_1|^2 + |A_2|^2 = 2(E_1 + E_2)/\Omega^2 = const.$$

As a result, the dimension of phase space is reduced by introducing the phases $\varphi_1(t)$, $\varphi_2(t)$ and $\psi(t)$ as

$$A_1 = \sqrt{K}\cos\psi\exp(i\varphi_1), \qquad A_2 = \sqrt{K}\sin\psi\exp(i\varphi_2) \tag{3.150}$$

where ψ determines the energy distribution between the oscillators as

$$\tan\psi = \frac{|A_2|}{|A_1|} = \sqrt{\frac{E_2}{E_1}} \qquad (0 \le \psi < \pi/2) \tag{3.151}$$

Substituting (3.150) in system (3.149) and then considering separately its real and imaginary parts give

$$\begin{aligned}
\dot{\varphi}_1 &= \frac{\beta}{\Omega} - \frac{\beta}{2\Omega}\tan\psi\cos(\varphi_2 - \varphi_1) \\
\dot{\varphi}_2 &= \frac{\beta}{\Omega} - \frac{\beta}{2\Omega}\cot\psi\cos(\varphi_2 - \varphi_1) \\
\dot{\psi} &= -\frac{\beta}{2\Omega}\sin(\varphi_2 - \varphi_1) - \frac{1}{32}\alpha K^2\Omega^4\sin 4\psi
\end{aligned} \tag{3.152}$$

Introducing the phase shift $\Delta = \varphi_2 - \varphi_1$ and new temporal variable $p = \Omega t/\beta$ give

$$\begin{aligned}
\frac{d\Delta}{dp} &= -\cot 2\psi\cos\Delta \\
\frac{d\psi}{dp} &= -\frac{1}{2}(\sin\Delta + \lambda\sin 4\psi)
\end{aligned} \tag{3.153}$$

where λ is a dimensionless parameter related to the total energy of both oscillators as

$$\lambda = \frac{\alpha K^2\Omega^5}{16\beta} = \frac{\Omega\alpha}{4\beta}(E_1 + E_2)^2 \tag{3.154}$$

System (3.153) is periodic with respect to both phases, Δ and ψ. As a result, its phase plane has the periodic cell-wise structure. Let us consider just one cell,

$$R_0 = \left\{-\frac{\pi}{2} < \Delta < \frac{\pi}{2}, 0 < \Psi < \frac{\pi}{2}\right\} \tag{3.155}$$

including the stationary point

$$(\Delta, \psi) = (0, \pi/4) \tag{3.156}$$

As follows from (3.150) and (3.151), point (3.156) represents the inphase vibration with $E_1 = E_2$. Linearizing system (3.153) near this stationary and then solving the corresponding characteristic equation give the following couple of roots:

$$r_{1,2} = \lambda \pm i\sqrt{1-\lambda^2} \tag{3.157}$$

Expression (3.157) determines the low excitation interval $0 < \lambda < 1$ of a qualitatively similar system behavior. Point (3.156) is unstable by Lyapunov for positive λ, while no other stationary points exist within the rectangular cell (3.155). As a result, the system trajectory is eventually attracted to the boundary of rectangular R_0 (3.155) as shown in Fig. 3.22a and b. This is a periodic limit cycle whose period is found in a closed form,

$$T = 2\int_0^{\pi/2} \frac{d\psi}{1-\lambda\sin 4\psi} - 2\int_{\pi/2}^{0} \frac{d\psi}{1+\lambda\sin 4\psi} = \frac{2\pi}{\sqrt{1-\lambda^2}} \tag{3.158}$$

where the horizontal pieces of the boundary ∂R_0 have zero contribution as those passed momentarily by the system (3.153). This is confirmed also by the diagrams in Fig. 3.23a, c and b, d showing stepwise jumps of the variable $\Delta(p)$ in steady-state limits.

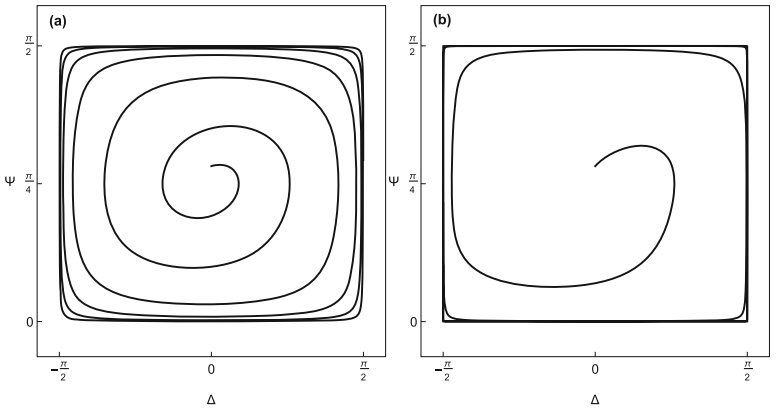

Fig. 3.22 (**a**) Low-energy transition to the nonsmooth limit cycle; numerical solution obtained for the following system parameter and initial conditions: $\lambda = 0.2$; $\Delta(0) = 0.0$, $\Psi(0) = \pi/4 + 0.1$. (**b**) Transition to the nonsmooth limit cycle under the energy level approaching its critical value; the numerical solution obtained for the following system parameter and initial conditions: $\lambda = 0.6$; $\Delta(0) = 0.0$, $\Psi(0) = \pi/4 + 0.1$

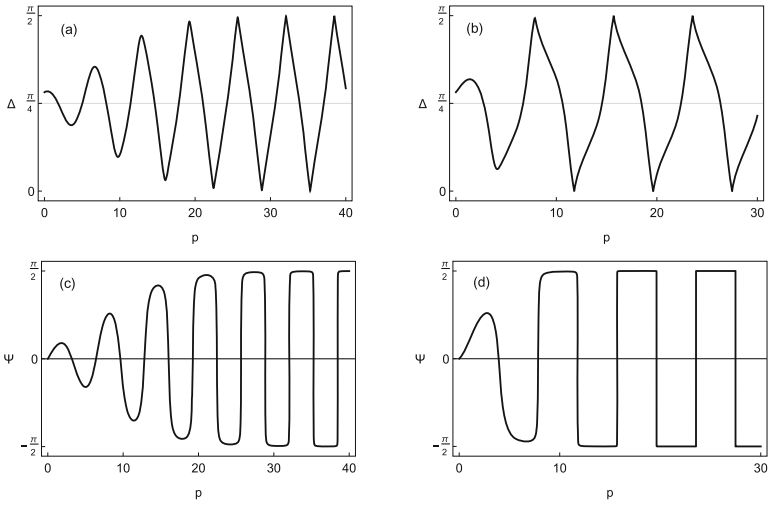

Fig. 3.23 (**a**) and (**c**): Low-energy transition to the "impact" limit cycle of phase variables at $\lambda = 0.2$; (**b**) and (**d**) Transition to the "impact" limit cycle of phase variables at $\lambda = 0.6$

Expression (3.158) shows that $T \to \infty$ as $\lambda \to 1$. The infinity long period means that there is only one-way energy flow in the system. As a result, the energy is eventually localized on one of the oscillators. The corresponding total critical energy value is determined by substituting $\lambda = 1$ in (3.154). This gives

$$E_1 + E_2 = 2\sqrt{\frac{\beta}{\Omega\alpha}} = E^* \tag{3.159}$$

If $E_1 + E_2 < E^*$ then periodic energy exchange with the period $T = \beta P/\Omega$ takes place, but no localization is possible. Therefore, in order to be localized on one of the oscillators, the total system energy must be large enough. Note that the transition to localized mode of this model happens through nonsmooth limit cycle along which the dynamics of phase variables, Ψ and Δ, resembles the behavior of coordinate and velocity of impact oscillator;[7] see Fig. 3.23. It was found later that such types of trajectories represent quite a general situation that may occur in the dynamics of interacting oscillators in terms of the specific phase coordinates. As a result the concept of limiting phase trajectories (LPT) was introduced in [133] as complementary nonstationary alternative to (stationary) normal mode motions.

[7] As already mentioned, the possibility of "vibro-impact dynamics" of phase variables was noticed later in [133] when considering another model of nonlinear beats.

Chapter 4
Nonsmooth Temporal Transformations (NSTT)

In this chapter, different versions of nonsmooth argument substitutions, specifically nonsmooth time, are introduced with proofs of the related identities. Basic rules for algebraic, differential, and integral manipulations are described. Final subsections show how to implement nonsmooth argument substitutions in the differential equations. These impose two principal features on the dynamical systems by generating specific algebraic structures and leading to boundary value problems. Notice that the transformation itself assumes no constraints on dynamical systems and easily applies to both smooth and nonsmooth systems. Any further steps should account for physical properties of the related systems following the principle of compliance between tools and objects of study. Briefly, linear coordinate transformations can significantly simplify analyses of the linear dynamic. Weakly nonlinear coordinate transformations often play the core role in the quasi-linear theory. Hence, the investigation of dynamical systems with discontinuities can be simplified by means of appropriate nonsmooth transformations of variables.

4.1 Nonsmooth Time and Induced Algebra

Major features induced by nonsmooth temporal substitutions can be briefly listed as follows:

- Introducing nonsmooth temporal arguments, in particular triangle wave, takes the coordinates into the algebra of hyperbolic numbers with a nonsmooth time-dependent imaginary unit;[1]

[1] Algebra of complex numbers, $X + Ye$, where $e^2 = 1$; see details in the next subsections.

V. N. Pilipchuk, *Oscillators and Oscillatory Signals from Smooth to Discontinuous*,
https://doi.org/10.1007/978-3-031-37788-4_4

- Under appropriate conditions, differentiation or integration of the coordinates keeps the result within the same algebra and therefore eases the corresponding manipulations with the dynamic systems;
- Explicit time argument can be used together with the nonsmooth time in order to describe amplitude and/or frequency modulated signals.

Usually NSTT itself is a preliminary stage of analysis finalized by specific boundary value problems on standard intervals. Then, different methods can be applied to the boundary value problems according to their physical content and the purpose of study.

4.1.1 Positive Time

To begin with a simple illustration of the nonsmooth positive time, consider the series

$$\ln\left(2\cosh\frac{t}{2}\right) = \frac{t}{2} + \exp(-t) - \frac{1}{2}\exp(-2t) + \frac{1}{3}\exp(-3t) - \ldots \tag{4.1}$$

which is convergent for $t \geq 0$ but obviously becomes divergent if $t < 0$; the convergence is conditional at $t = 0$. A simple replacement, $t \longrightarrow |t|$, makes this series convergent within the entire interval $-\infty < t < \infty$ as follows:

$$\begin{aligned}\ln\left(2\cosh\frac{t}{2}\right) &\equiv \ln\left(2\cosh\frac{|t|}{2}\right) \\ &= \frac{|t|}{2} + \exp(-|t|) - \frac{1}{2}\exp(-2|t|) + \frac{1}{3}\exp(-3|t|) - \ldots\end{aligned} \tag{4.2}$$

A side effect of such manipulation is that finite sums of the series are losing differentiability at zero, $t = 0$, whereas the original function is smooth everywhere. However, it will be shown later that the series can be rearranged in such a manner that any truncated series becomes differentiable at $t = 0$ as many times as needed.

Note that the *transformation* $t \longrightarrow |t|$ *is non-invertible. As a result, the manipulation illustrated by example (4.2) may not work for other cases*. In the above example though, the substitution $t \longrightarrow |t|$ holds for both positive and negative time t due to the evenness of the original function. To extend the above idea on the general case, let us represent the time argument in the form

$$t = |t|\,|t|^{\cdot} \tag{4.3}$$

Now, taking into account the relationship $(|t|^{\cdot})^2 = 1$ gives sequentially

$$t^{2n} = |t|^{2n} \quad \text{and} \quad t^{2n+1} = |t|^{2n+1}\,|t|^{\cdot}, \quad n = 1, 2, \ldots \tag{4.4}$$

Example 4.1.1 Combining identities (4.4) and the power series expansion of the exponential function gives

$$\exp(t) \equiv \exp(|t|\,|t|^{\cdot}) = 1 + \frac{|t|^2}{2!} + ... + \left(|t| + \frac{|t|^3}{3!} + ...\right)|t|^{\cdot}$$

or

$$\exp(t) = \cosh(|t|) + \sinh(|t|)\,|t|^{\cdot} \tag{4.5}$$

Expression (4.5) represents the exponential function as a sum of the even and odd components.

Let us take a general function, $x(t)$, and assume that

$$x(t) = x(|t|\,|t|^{\cdot}) = X(|t|) + Y(|t|)\,|t|^{\cdot} \tag{4.6}$$

This gives the following set of equations for the components, $X(|t|)$ and $Y(|t|)$,

$$\begin{aligned} x(|t|) &= X(|t|) + Y(|t|) \qquad \text{for } |t|^{\cdot} = 1 \\ x(-|t|) &= X(|t|) - Y(|t|) \qquad \text{for } |t|^{\cdot} = -1 \end{aligned}$$

and, finally,

$$\begin{aligned} X(|t|) &= \frac{1}{2}[x(|t|) + x(-|t|)] \\ Y(|t|) &= \frac{1}{2}[x(|t|) - x(-|t|)] \end{aligned} \tag{4.7}$$

Therefore, identity (4.6) holds under condition (4.7). It is seen that the right-hand side of expression (4.6) represents an element of the algebra with the basis $\{1, |t|^{\cdot}\}$. The corresponding table of products is generated by the relationship $(|t|^{\cdot})^2 = 1$. This leads to other useful algebraic relationships, such as

$$X + Y|t|^{\cdot} = 0 \Longleftrightarrow \{X = 0, Y = 0\}$$

and

$$f(X + Y|t|^{\cdot}) = R_f(X, Y) + I_f(X, Y)\,|t|^{\cdot} \tag{4.8}$$

where

$$\begin{aligned} R_f(X, Y) &= \frac{1}{2}[f(X + Y) + f(X - Y)] \\ I_f(X, Y) &= \frac{1}{2}[f(X + Y) - f(X - Y)] \end{aligned} \tag{4.9}$$

Thus, introducing the nonsmooth positive time $|t|$ imposes the specific complexification on the system coordinate

$$x(t) \longrightarrow \{X(|t|), Y(|t|)\} \tag{4.10}$$

As shown in different sections of this chapter, the nonsmooth argument substitutions are always accompanied by such type of complexifications.

4.1.2 Single-Tooth Substitution

As a simple generalization of the positive time, $|t|$, let us introduce the temporal shift, say a, as

$$s = |t - a| \equiv s(t) \tag{4.11}$$

Obviously, $\dot{s} = -1$ for $t - a < 0$ and $\dot{s} = 1$ for $t - a > 0$, and therefore $\dot{s}^2 = 1$ for almost all t, at least.

Proposition 4.1.1 *A general function $x(t)$ can be represented in the form*

$$x(t) = X(s) + Y(s)\dot{s} \tag{4.12}$$

where $s = s(t)$ is given by (4.11).

Proof By analogy to (4.3),

$$t = a + s\dot{s} \tag{4.13}$$

Substituting (4.13) in the left-hand side of (4.12) gives

$$\begin{aligned} x(a - s) &= X(s) - Y(s) \qquad \text{for } \dot{s} = -1 \\ x(a + s) &= X(s) + Y(s) \qquad \text{for } \dot{s} = 1 \end{aligned}$$

and thus,

$$\begin{aligned} X(s) &= \frac{1}{2}[x(a + s) + x(a - s)] \\ Y(s) &= \frac{1}{2}[x(a + s) - x(a - s)] \end{aligned} \tag{4.14}$$

Therefore, identity (4.12) holds for any $x(t)$ under condition (4.14).

4.1.3 Broken Time Substitution

Another generalization of the positive time $|t|$ is given by the piecewise linear function

$$\tau = \begin{cases} v_1 t & \text{for } t \leq 0 \\ v_2 t & \text{for } t \geq 0 \end{cases} \tag{4.15}$$

where $v_1 \neq v_2$.

The inverse relationship can be represented in the form

$$t = A(\tau) + B(\tau)\dot{\tau} \tag{4.16}$$

where

$$A = \left(\frac{1}{v_1} + \frac{1}{v_2}\right)\tau \quad \text{and} \quad B = -\frac{1}{v_1 v_2}\tau$$

and

$$\dot{\tau}^2 = -v_1 v_2 + (v_1 + v_2)\dot{\tau} \tag{4.17}$$

Further, applying a general function x to both sides of equality (4.16) gives

$$x(t) = X(\tau) + Y(\tau)\dot{\tau} \tag{4.18}$$

where the components, X and Y, are determined analogously to (4.6) through (4.7) as

$$\begin{aligned} X(\tau) &= \frac{1}{v_2 - v_1}\left[v_2 x\left(\frac{\tau}{v_1}\right) - v_1 x\left(\frac{\tau}{v_2}\right)\right] \\ Y(\tau) &= -\frac{1}{v_2 - v_1}\left[x\left(\frac{\tau}{v_1}\right) - x\left(\frac{\tau}{v_2}\right)\right] \end{aligned} \tag{4.19}$$

Now, assuming that another function f is applied to both sides of (4.18) gives

$$f(x) = R_f(X, Y) + I_f(X, Y)\dot{\tau} \tag{4.20}$$

where

$$\begin{aligned} R_f &= \frac{1}{v_2 - v_1}\left[v_2 f(X + Y v_1) - v_1 f(X + Y v_2)\right] \\ I_f &= -\frac{1}{v_2 - v_1}\left[f(X + Y v_1) - f(X + Y v_2)\right] \end{aligned} \tag{4.21}$$

Comparing the right-hand sides of expressions (4.16), (4.18), and (4.20) shows that the algebraic structure generated by the nonsmooth time substitution is preserved after different functional manipulations with the corresponding elements of the algebra.[2]

4.1.4 Triangle Wave Temporal Substitution

Let us consider the periodic version of nonsmooth time (4.11) which is based on the triangle wave

$$\tau(t) = \begin{cases} t & \text{for } -1 \le t \le 1 \\ -t+2 & \text{for } 1 \le t \le 3 \end{cases}, \qquad \tau(t) \overset{\forall t}{=} \tau(4+t) \tag{4.22}$$

Recall that function (4.22) describes position of a bead oscillating between two stiff parallel barriers with no energy loss. In other words, function (4.22) describes the motion of the standard impact oscillator; see Chap. 1 for illustrations. This function can be expressed also in the closed form by means of trigonometric functions as

$$\tau(t) = (2/\pi)\arcsin[\sin(\pi t/2)] \tag{4.23}$$

The period is normalized to four while the amplitude is unity to provide the unit slope,

$$\dot{\tau}^2 = 1 \tag{4.24}$$

Proposition 4.1.2 ([173]) *Any periodic process, whose period is normalized to $T = 4$, is expressed through the triangle wave $\tau(t)$ and the square wave $\dot{\tau}(t)$ as*

$$x(t) = X(\tau) + Y(\tau)\dot{\tau} \tag{4.25}$$

where the X- and Y-component are given by

$$\begin{aligned} X(\tau) &= \frac{1}{2}[x(\tau) + x(2-\tau)] \\ Y(\tau) &= \frac{1}{2}[x(\tau) - x(2-\tau)] \end{aligned} \tag{4.26}$$

[2] Abelian complex algebraic structure, which becomes hyperbolic when $v_1 + v_2 = 0$ and $v_1 v_2 < 0$; see Sect. 1.2.5 for terminology and details.

In other words, any periodic signal is uniquely expressed through the state variables, such as the coordinate τ and velocity $\dot{\tau}$, of the standard impact oscillator.

Proof *([185])* It can be verified by inspection that

$$t = 1 + (\tau - 1)\,\dot{\tau} \qquad \text{if } -1 < t < 3 \tag{4.27}$$

Note that the function $\dot{\tau}(t)$ has a stepwise discontinuity at $t = 1$, which is suppressed however by the continuous factor, $\tau(t) - 1$, of zero value at $t = 1$. Based on this remark, property (4.24) will be considered as true everywhere on the interval $-1 < t < 3$, since $\dot{\tau}$ is either explicitly or implicitly accompanied by the factor $\tau(t) - 1$ whenever it appears in algebraic manipulations. For instance, identity

$$t^2 = 1 + (\tau - 1)^2 + 2\,(\tau - 1)\,\dot{\tau}$$

holds everywhere on the interval $-1 < t < 3$. Further, applying the method of mathematical induction gives

$$t^n = A_n(\tau) + B_n(\tau)\dot{\tau} \tag{4.28}$$

where n is any positive integer and A_n and B_n are polynomials of the degree n or $n-1$. Expression (4.28) shows that any analytic function $x(t)$ that admits the power series expansion on the interval $-1 < t < 3$ can be represented in the form

$$x(t) = x\,[1 + (\tau - 1)\,\dot{\tau}] = X\,(\tau) + Y\,(\tau)\,\dot{\tau} \tag{4.29}$$

where $X\,(\tau)$ and $Y\,(\tau)$ are power series of τ. Now, let us assume that expression (4.29) holds even though the function $x(t)$ is not analytic. In this case, one must show that the X- and Y-component can be determined with no power series expansions. Indeed, since either $\dot{\tau} = 1$ or $\dot{\tau} = -1$ on the entire interval $-1 < t < 3$, except may be the point $t = 1$, then expression (4.29) gives two equations, $x\,(\tau) = X\,(\tau) + Y\,(\tau)$ and $x\,(2 - \tau) = X\,(\tau) - Y\,(\tau)$. Solving these equations for X and Y and substituting the solution in (4.29) give the identity,

$$x(t) = \frac{1}{2}\,[x\,(\tau) + x\,(2 - \tau)] + \frac{1}{2}\,[x\,(\tau) - x\,(2 - \tau)]\,\dot{\tau} \tag{4.30}$$

which obviously holds on the interval $-1 < t < 3$, except may be $t = 1$. If the function $x(t)$ is continuous at $t = 1$, then identity (4.30) is also true at $t = 1$ because the stepwise discontinuity of the square wave $\dot{\tau}(t)$ at $t = 1$ is suppressed by the factor

$$2Y\,(\tau) = x\,(\tau) - x\,(2 - \tau) \to x\,(1 - 0) - x\,(1 + 0) \to 0 \tag{4.31}$$

as $t \to 1 \pm 0$; see Definition (4.22). Now if the function $x(t)$ is periodic of the period $T = 4$, then identity (4.30) holds almost everywhere on the interval $-\infty < t < \infty$, because the right-hand side of (4.30) depends on the time argument t through the pair of periodic functions $\tau(t)$ and $\dot{\tau}(t)$ of the same period $T = 4$. Finally, if the function $x(t)$ is continuous also at $t = -1$, and thus $t = 3$ due to the periodicity, then identity (4.30) is true for every t. Hence let us consider the point $t = -1$ at which the function $\dot{\tau}(t)$ has the stepwise discontinuity. Taking into account that $\tau(-1 \pm 0) = -1 + 0$ and the periodicity condition $x(t) = x(t-4)$ gives

$$\begin{aligned} 2Y(\tau) &= x[\tau(-1 \pm 0)] - x[2 - \tau(-1 \pm 0)] \\ &= x(-1+0) - x(3-0) = x(-1+0) - x(-1-0) \to 0 \end{aligned} \tag{4.32}$$

as $t \to -1 \pm 0$ due to the continuity of the function $x(t)$ at $t = -1$. Hence, the stepwise discontinuity of the function $\dot{\tau}(t)$ at the point $t = -1$ is suppressed as well due to (4.32). Thus, it is proved that if $x(t)$ is continuous then identity (4.30) or (4.25) holds everywhere on the interval $-\infty < t < \infty$. The periodic version of conditions (4.31) and (4.32) is

$$Y|_{\tau=\pm 1} = 0 \tag{4.33}$$

As noticed in Chap. 1, the extension on any period $T = 4a$ is implemented by scaling the argument of the triangle wave as $\tau = \tau(t/a)$ followed by expressions (1.26).

Remark 4.1.1 If the function $x(t)$ is stepwise discontinuous at the instances $\Lambda = \{t : \tau(t) = \pm 1\}$, then limits (4.31) and (4.32) are nonzero. In this case, the discontinuities of the function $\dot{\tau}(t)$ are not suppressed to represent the behavior of the original function $x(t)$.

Proposition 4.1.3 *Elements (4.25) belong to the algebra of hyperbolic numbers due to (4.24); see Sect. 1.2.5. As a result,*

$$f(X + Y\dot{\tau}) = R_f + I_f\dot{\tau} \tag{4.34}$$

$$R_f = \frac{1}{2}[f(X+Y) + f(X-Y)]$$

$$I_f = \frac{1}{2}[f(X+Y) - f(X-Y)]$$

provided that both values $f(X \pm Y)$ are defined.

Relationship (4.34) is verified by setting sequentially $\dot{\tau} = 1$ and $\dot{\tau} = -1$. The right-hand side of expression (4.25) therefore admits interpretation as a hyperbolic complex number with real, X, and imaginary, Y, components. The corresponding imaginary unit $\dot{\tau}$ creates a cyclical group, such as: $\dot{\tau}^2 = 1$, $\dot{\tau}^3 = \dot{\tau}$, $\dot{\tau}^4 =$

1,.... This remark significantly simplifies all the mathematical manipulations with representation (4.25). For example,

$$(X + Y\dot{\tau})^2 = X^2 + Y^2 + 2XY\dot{\tau}$$
$$(X + Y\dot{\tau})^3 = X^3 + 3XY^2 + \left(Y^3 + 3YX^2\right)\dot{\tau}$$

The right-hand sides of these expressions appear to belong to the same hyperbolic structure as the element $X + Y\dot{\tau}$ itself.

Another example resembles Euler formula in the algebra of ordinary complex numbers; however, hyperbolic functions replace trigonometric ones as

$$\exp(X + Y\dot{\tau}) = \exp(X)\left[\cosh(Y) + \sinh(Y)\,\dot{\tau}\right] \tag{4.35}$$

Further, by taking into account that $\dot{\tau}^2 = 1$, one obtains

$$\frac{1}{X + Y\dot{\tau}} = \frac{X}{X^2 - Y^2} - \frac{Y}{X^2 - Y^2}\dot{\tau} \quad \text{if} \quad X \neq \pm Y$$

This example explains why division is not always possible, which is the essential difference as compared to the conventional complex analysis.

Remark 4.1.2 Very often, the triangle wave function is assumed to depend on some phase variable, say $\varphi(t)$. In all such cases, the imaginary element is given by the derivative with respect to the phase variable, $e(\varphi) = \tau'(\varphi)$ as defined in Chap. 1. Now the relation

$$e^2 = 1 \tag{4.36}$$

holds regardless of the argument of the triangle wave.

Example 4.1.2 Introduce the triangle wave time into the functions $\sin t$ and $\cos t$.

Solution. In order to deal with the period normalized to four, let us introduce new argument $\varphi = 2t/\pi$ as

$$\sin t = \sin\left(\frac{\pi}{2}\frac{2t}{\pi}\right) = \sin\left(\frac{\pi}{2}\varphi\right)$$

Now, applying representation (4.25) to the new argument φ gives

$$X(\tau) = \frac{1}{2}\left\{\sin\left(\frac{\pi}{2}\tau\right) + \sin\left[\frac{\pi}{2}(2 - \tau)\right]\right\} = \sin\left(\frac{\pi}{2}\tau\right)$$
$$Y(\tau) = \frac{1}{2}\left\{\sin\left(\frac{\pi}{2}\tau\right) - \sin\left[\frac{\pi}{2}(2 - \tau)\right]\right\} = 0$$

and therefore

$$\sin t \equiv \sin\left[\frac{\pi}{2}\tau\left(\frac{2t}{\pi}\right)\right]$$

Analogously,

$$\cos t = \cos\left[\frac{\pi}{2}\tau\left(\frac{2t}{\pi}\right)\right] e\left(\frac{2t}{\pi}\right)$$

Example 4.1.3 Combining the results from previous example with the Euler formula for complex exponential functions gives

$$\exp(ikt) = \sin\left(\frac{k\pi}{2}\tau\right) i + \cos\left(\frac{k\pi}{2}\tau\right) e \qquad \text{for} \qquad k = 1, 3, 5, ...$$

$$\exp(ikt) = \cos\left(\frac{k\pi}{2}\tau\right) + \sin\left(\frac{k\pi}{2}\tau\right) ie \qquad \text{for} \qquad k = 0, 2, 4, ...$$

where τ and e still depend on the same argument $2t/\pi$. The right-hand sides of these equalities can be viewed as elements of a more complicated algebra, $z = \alpha + \beta e + \gamma i + \delta ei$, with the basis elements $\{1, e, i, ei\}$. The corresponding table of products is given by

$$\begin{array}{cccccc}
\times & 1 & e & i & ei \\
1 & 1 & e & i & ei \\
e & e & 1 & ei & i \\
i & i & ei & -1 & -e \\
ei & ei & i & -e & -1
\end{array}$$

4.1.5 NSTT and Matrix Algebras

As discussed in Chap. 1, hyperbolic numbers represent a simple example of so-called Clifford geometric algebras with isomorphism to the matrix algebra. It is known [137] that complex numbers associate with skew-symmetric 2×2 matrixes with equal diagonal entries, whereas the hyperbolic numbers correspond to the symmetric matrixes as follows:

$$a + ib \longleftrightarrow \begin{bmatrix} a & b \\ -b & a \end{bmatrix}$$

$$X + eY \longleftrightarrow \begin{bmatrix} X & Y \\ Y & X \end{bmatrix}$$

The above correspondences are isomorphisms because both summations and multiplications with the numbers associate with the corresponding matrix operations, for instance,

$$(X_1 + eY_1)(X_2 + eY_2) = (X_1X_2 + Y_1Y_2) + (X_1Y_2 + Y_1X_2)e \tag{4.37}$$

$$\begin{bmatrix} X_1 & Y_1 \\ Y_1 & X_1 \end{bmatrix} \begin{bmatrix} X_2 & Y_2 \\ Y_2 & X_2 \end{bmatrix} = \begin{bmatrix} X_1X_2 + Y_1Y_2 & X_1Y_2 + Y_1X_2 \\ X_1Y_2 + Y_1X_2 & X_1X_2 + Y_1Y_2 \end{bmatrix} \tag{4.38}$$

As was already mentioned, the algebra of hyperbolic numbers and Clifford algebras were developed in an abstract way as manipulations with specific elements with no relation to any nonsmooth transformations. However, the uncovered links may appear to be useful for conducting automatic symbolic manipulations with NSTT. Indeed, most of the corresponding packages have built-in tools to handling the matrix operations, whereas defining the operations with hyperbolic numbers may require some programming work.

4.1.6 *Differentiation and Integration Rules*

Regarding applications to differential equations, it is essential that, under some conditions, the differential operations also preserve the hyperbolic structure of elements [173]. For example,

$$\dot{x} = Y' + X'\dot{\tau} \quad + \underline{Y\ddot{\tau}} \tag{4.39}$$

where primes mean derivatives with respect to τ.

The derivative $\ddot{\tau}$ represents the periodic series of δ-functions

$$\ddot{\tau} = 2\sum_{k=-\infty}^{\infty} [\delta(t + 1 - 4k) - \delta(t - 1 - 4k)] \tag{4.40}$$

This derivative is active exactly at those points Λ where the factor Y is equal to zero due to (4.33). Hence, the last (underlined) term in (4.39) must be ignored whenever the function $x(t)$ is continuous.

In a similar manner, one can sequentially consider high-order derivatives. For example, the second derivative is given by

$$\ddot{x} = X'' + Y''\dot{\tau} \tag{4.41}$$

under the boundary condition

$$X'|_{\tau=\pm1} = 0 \tag{4.42}$$

Further, an arbitrary odd derivative is given by

$$x^{(2k-1)}(t) = Y^{(2k-1)}(\tau) + X^{(2k-1)}(\tau)\, e \tag{4.43}$$

provided that

$$\begin{aligned} Y(\tau)|_{\tau=\pm 1} &= 0 \\ X'(\tau)|_{\tau=\pm 1} &= 0 \\ &\ldots \\ Y^{(2k-2)}(\tau)|_{\tau=\pm 1} &= 0 \end{aligned} \tag{4.44}$$

Also an arbitrary even derivative is

$$x^{(2k)}(t) = X^{(2k)}(\tau) + Y^{(2k)}(\tau)\, e \tag{4.45}$$

if

$$\begin{aligned} Y(\tau)|_{\tau=\pm 1} &= 0 \\ X'(\tau)|_{\tau=\pm 1} &= 0 \\ &\ldots \\ X^{(2k-1)}(\tau)|_{\tau=\pm 1} &= 0 \end{aligned} \tag{4.46}$$

Finally, integration also gives the hyperbolic number

$$\int (X + Y\dot{\tau})dt = Q + P\dot{\tau} \tag{4.47}$$

whose components are

$$Q(\tau) = \int_0^{\tau} Y d\tau + C \qquad \text{and} \qquad P(\tau) = \int_{-1}^{\tau} X d\tau$$

where C is an arbitrary constant, and the following condition must be satisfied:

$$\int_{-1}^{1} X(\tau) d\tau = 0 \tag{4.48}$$

Relationship (4.47) is verified by the differentiation with respect to t. The role of condition (4.48) is to provide a zero mean value of the integrand in (4.47).

4.1.7 NSTT Averaging

Lemma 4.1.1 *Let $x(t)$ be a general periodic function of the period $T = 4a$ so that presentation (4.25) holds*

$$x(t) = X(\tau(\phi)) + Y(\tau(\phi))e(\phi) \tag{4.49}$$

where $\phi = t/a$, $e(\phi) = \tau'(\phi)$ and

$$X(\tau) = \frac{1}{2}[x(a\tau) + x(2a - a\tau)] \tag{4.50}$$
$$Y(\tau) = \frac{1}{2}[x(a\tau) - x(2a - a\tau)]$$

Then the mean value of $x(t)$ over its period is

$$\frac{1}{T}\int_0^T x(t)dt = \frac{1}{2}\int_{-1}^{1} X(\tau)d\tau \tag{4.51}$$

In other words, the imaginary component Ye of the hyperbolic number (4.49) makes zero contribution into the mean value.

Proof With no loss of generality, let us assume that $a = 1$; thus $T = 4$ and $\phi \equiv t$. Then, during one period $-1 < t < 3$,

$$\tau'(t) = e(t) = 1 \quad \text{and} \quad dt = d\tau \quad \text{for} \quad -1 < t < 1$$
$$\tau'(t) = e(t) = -1 \quad \text{and} \quad dt = -d\tau \quad \text{for} \quad 1 < t < 3$$

Taking into account (4.49) gives

$$\frac{1}{T}\int_0^T x(t)dt = \frac{1}{4}\left[\int_{-1}^{1} x(t)dt + \int_1^3 x(t)dt\right]$$

$$= \frac{1}{4}\int_{-1}^{1}[X(\tau) + Y(\tau)]d\tau - \frac{1}{4}\int_1^{-1}[X(\tau) - Y(\tau)]d\tau = \frac{1}{2}\int_{-1}^{1} X(\tau)d\tau$$

Example 4.1.4 Let $x(t)$ be a periodic function of the period $T = 4a$. Taking into account (4.49) gives

$$x^2 = (X + Ye)^2 = X^2 + Y^2 + 2XYe$$

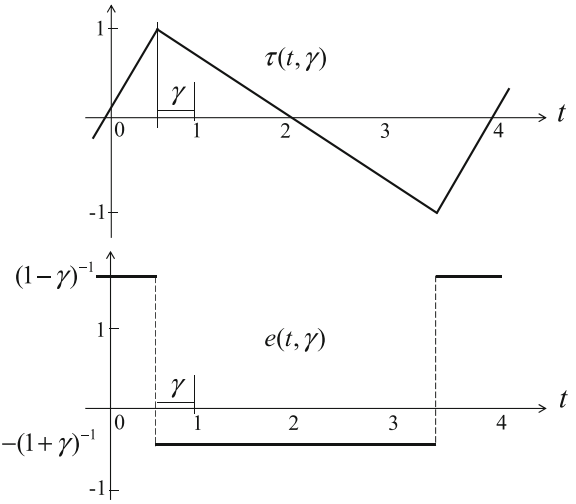

Fig. 4.1 Asymmetric triangle wave and square (rectangle) wave obtained for the number $\gamma = 0.5$

Then, applying the above Lemma leads to

$$< x^2 >\equiv \frac{1}{T}\int_0^T x^2 dt = \frac{1}{2}\int_{-1}^{1}(X^2 + Y^2)d\tau \tag{4.52}$$

Example 4.1.5 Consider the case $x(t) = A\sin t + B\cos t$, where $T = 2\pi$ and $a = \pi/2$. In this case, relationships (4.50) give $X(\tau) = A\sin(\pi\tau/2)$ and $Y(\tau) = B\cos(\pi\tau/2)$. Therefore, $< x^2 >= (A^2 + B^2)/2$.

4.1.8 Generalizations on Asymmetrical Triangle Wave

It has been shown in [177] and [197] that an arbitrary periodic function $x(t)$ whose period is normalized to four can still be represented in the form (4.25), even though the triangular wave, τ, has asymmetrical slopes such that[3]

$$\tau(t,\gamma) = \begin{cases} t/(1-\gamma) & \text{for } -1+\gamma \le t \le 1-\gamma \\ (-t+2)/(1+\gamma) & \text{for } 1-\gamma \le t \le 3+\gamma \end{cases} \tag{4.53}$$

$$\dot{\tau}(t,\gamma) = \frac{\partial\tau(t,\gamma)}{\partial t} = e(t,\gamma) \tag{4.54}$$

where $\gamma \in (-1, 1)$ is a parameter characterizing the inclination of the saw as shown in Fig. 4.1.

[3] The function $\tau(t,\gamma)$ can be viewed as a generalized sawtooth (sine) wave.

In this case, the inverse transformation of time on the period, $-1+\gamma \leq t \leq 3+\gamma$, has the form

$$t = \frac{1-\gamma^2}{2} \times \left\{ [(1-\gamma)\tau] \left(\frac{1}{1+\gamma} + e \right) + [2-(1+\gamma)\tau] \left(\frac{1}{1-\gamma} - e \right) \right\} \tag{4.55}$$

By using this expression, one can show that

$$x(t) = X[\tau(t,\gamma)] + Y[\tau(t,\gamma)]\, e(t,\gamma) \tag{4.56}$$

$$X = \frac{1}{2\alpha} \left\{ \frac{1}{1+\gamma} x[(1-\gamma)\tau] + \frac{1}{1-\gamma} x[2-(1+\gamma)\tau] \right\}$$
$$Y = \frac{1}{2\alpha} \{ x[(1-\gamma)\tau] - x[2-(1+\gamma)\tau] \} \tag{4.57}$$

$$e^2 = \alpha + \beta e \tag{4.58}$$

where $\alpha = 1/\left(1-\gamma^2\right)$ and $\beta = 2\gamma\alpha$.

As compared to (4.36), relationship (4.58) complicates algebraic and differential operations as, respectively,

$$f(X+Ye) = R_f(X,Y) + I_f(X,Y)\, e \tag{4.59}$$

$$R_f(X,Y) = \frac{1}{2\alpha} \left[\frac{1}{1+\gamma} f(Z_+) + \frac{1}{1-\gamma} f(Z_-) \right]$$
$$I_f(X,Y) = \frac{1}{2\alpha} [f(Z_+) - f(Z_-)]$$
$$Z_\pm = X \pm \frac{Y}{1 \mp \gamma}$$

and

$$\dot{x} = \alpha Y' + \left(X' + \beta Y'\right) e + Y \underline{\frac{\partial e}{\partial t}} \tag{4.60}$$

where $f(Z_+)$ and $f(Z_-)$ must be defined, primes indicate differentiation with respect to τ, and

$$\frac{\partial e}{\partial t} = 2\alpha \sum_{k=-\infty}^{\infty} [\delta(t+1-\gamma-4k) - \delta(t-1+\gamma-4k)] \tag{4.61}$$

If the function $x\,(t)$ is continuous at time instances $\Lambda = \{t : \tau\,(t, \gamma) = \pm 1\}$, then the singular term $\partial e/\partial t$ is suppressed by the boundary condition $Y\,|_{t\in\Lambda} = Y\,|_{\tau=\pm 1} = 0$ analogously to the symmetric case. Otherwise, the periodic singular term remains in expression (4.60).

It is convenient to calculate high-order derivatives by means of the matrix-operator D acting on the vector-column $[X, Y]^T$ sequentially as

$$\begin{aligned} D &= \begin{bmatrix} 0 & \alpha \\ 1 & \beta \end{bmatrix} \frac{d}{d\tau} \\ D \begin{bmatrix} X \\ Y \end{bmatrix} &= \begin{bmatrix} \alpha Y' \\ X' + \beta Y' \end{bmatrix} \\ D^2 \begin{bmatrix} X \\ Y \end{bmatrix} &= \begin{bmatrix} \alpha X'' + \alpha\beta Y'' \\ \beta X'' + (\alpha + \beta^2) Y'' \end{bmatrix} \end{aligned} \tag{4.62}$$

Therefore, applying D and D^2 gives

$$\begin{aligned} \dot{x} &= \alpha Y' + (X' + \beta Y')e \\ \ddot{x} &= \alpha X'' + \alpha\beta Y'' + [\beta X'' + (\alpha + \beta^2) Y'']e \end{aligned}$$

under the boundary conditions

$$\begin{aligned} Y|_{\tau=\pm 1} &= 0 \\ (X' + \beta Y')|_{\tau=\pm 1} &= 0 \end{aligned}$$

Note that rules (4.62) are still valid in the symmetric case $\gamma = 0$, when the differential matrix operator takes the form

$$D = \begin{bmatrix} 0 & 1 \\ 1 & 0 \end{bmatrix} \frac{d}{d\tau}$$

Finally, the result of integration (4.47) has the components

$$Q = \int \left[Y\,(\tau) - \frac{\beta}{\alpha} X\,(\tau) \right] d\tau \quad \text{and} \quad P = \frac{1}{\alpha} \int_{-1}^{\tau} X\,(\xi)\, d\xi$$

under condition (4.48).

4.1.9 Multiple Frequency Case

Practical applications of NSTT to the class of multiple frequency motions face problems similar to those caused by small denominators in quasi-linear approaches. Formal generalizations of the basic relationships are illustrated below.

Let P_φ and N_φ be operators acting on some periodic function $x(\varphi)$ of the period $T = 4$ as follows:

$$P_\varphi x\,(\varphi) = \frac{1}{2}\{x[\tau\,(\varphi)] + x[2 - \tau\,(\varphi)]\} \equiv X[\tau\,(\varphi)] \tag{4.63}$$
$$N_\varphi x\,(\varphi) = \frac{1}{2}\{x[\tau\,(\varphi)] - x[2 - \tau\,(\varphi)]\} \equiv Y[\tau\,(\varphi)]$$

where functions $X\,(\tau)$ and $Y\,(\tau)$ are defined according to (4.26).

In such notations, representation (4.25) takes the form

$$x(\varphi) = (P_\varphi + eN_\varphi)x(\varphi), \qquad e = \tau'\,(\varphi) \tag{4.64}$$

Let us consider now a function of multiple arguments $x = x\left(\varphi_1, ..., \varphi_n\right)$ of the period $T = 4$ with respect to each of its n arguments. This function describes a multiple frequency quasi-periodic process if $\varphi_1 = \Omega_1 t$,..., $\varphi_n = \Omega_n t$ with a set of positive incommensurable frequencies, Ω_1,..., Ω_n. In this case, transformation (4.64) is independently applicable to each of the n arguments as follows:

$$x\left(\varphi_1, ..., \varphi_n\right) = \prod_{j=1}^{n}(P_{\varphi_j} + e_j N_{\varphi_j})x\left(\varphi_1, ..., \varphi_n\right) \tag{4.65}$$

where the new notations, $\tau_j = \tau(\varphi_j)$ and $e_j = \tau'(\varphi_j)$, are introduced.

Note that all the operators included in this product are commutating as those applied to different arguments of the function. Moreover, the number of cofactors of the product can differ from one to n.

Let us consider the case of two arguments. Introducing the notations $e_0 \equiv 1$ and $e_3 = e_1 e_2$, and expanding the product in (4.65) give

$$x\,(\varphi_1, \varphi_2) = X\,(\tau_1, \tau_2)\,e_0 + Y\,(\tau_1, \tau_2)\,e_1 + Z\,(\tau_1, \tau_2)\,e_2 + W\,(\tau_1, \tau_2)\,e_3 \tag{4.66}$$

where

$$X = P_{\varphi_1} P_{\varphi_2} x\,(\varphi_1, \varphi_2)\,, \qquad Y = N_{\varphi_1} P_{\varphi_2} x\,(\varphi_1, \varphi_2)$$
$$Z = P_{\varphi_1} N_{\varphi_2} x\,(\varphi_1, \varphi_2)\,, \qquad W = N_{\varphi_1} N_{\varphi_2} x\,(\varphi_1, \varphi_2)$$

The basis elements of (4.66) obey the table of products

$$\begin{array}{cccccc} \times & e_0 & e_1 & e_2 & e_3 \\ e_0 & e_0 & e_1 & e_2 & e_3 \\ e_1 & e_1 & e_0 & e_3 & e_2 \\ e_2 & e_2 & e_3 & e_0 & e_1 \\ e_3 & e_3 & e_2 & e_1 & e_0 \end{array} \tag{4.67}$$

Further, applying some function f to the element (4.66) gives

$$f(Xe_0 + Ye_1 + Ze_2 + We_3) = R_f e_0 + I_f^1 e_1 + I_f^2 e_2 + I_f^3 e_3 \tag{4.68}$$

where the coefficients at the right-hand side are defined by the system of linear equations

$$\begin{aligned} R_f + I_f^1 + I_f^2 + I_f^3 &= f\,(X + Y + Z + W) \\ R_f + I_f^1 - I_f^2 - I_f^3 &= f\,(X + Y - Z - W) \\ R_f - I_f^1 + I_f^2 - I_f^3 &= f\,(X - Y + Z - W) \\ R_f - I_f^1 - I_f^2 + I_f^3 &= f\,(X - Y - Z + W) \end{aligned} \tag{4.69}$$

Equations (4.69) are obtained by substituting different combinations of $e_1 = \pm 1$ and $e_3 = \pm 1$ in (4.68). Some application of the multiple frequency case will be illustrated at the end of Chap. 5 and also in Chap. 14.

4.2 Idempotent Basis Generated by the Triangle Wave

4.2.1 Definitions and Algebraic Rules

In addition to the standard basis $\{1, e\}$, the hyperbolic plane has another natural basis $\{e_+, e_-\}$ associated with the two isotropic lines separating the hyperbolic quadrants as described in Chap. 1. The transition from one basis to another is given by (see Fig. 4.2)

$$\begin{aligned} e_+ &= \frac{1}{2}(1 + e) \\ e_- &= \frac{1}{2}(1 - e) \end{aligned} \tag{4.70}$$

or, inversely,

$$\begin{aligned} 1 &= e_+ + e_- \\ e &= e_+ - e_- \end{aligned} \tag{4.71}$$

Therefore,

$$\begin{aligned} x = X + Ye &= X(e_+ + e_-) + Y(e_+ - e_-) \\ &= (X + Y)e_+ + (X - Y)e_- \end{aligned}$$

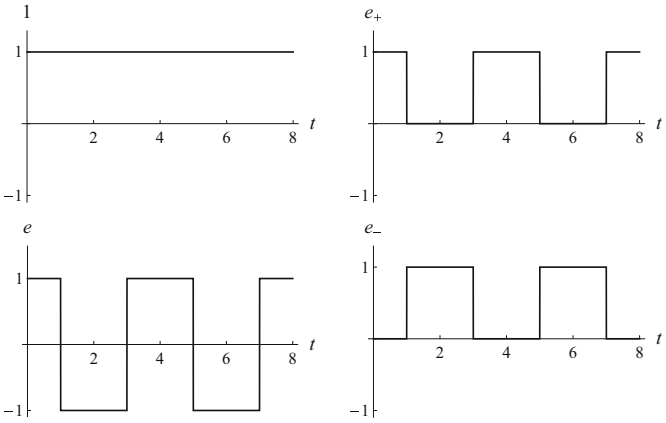

Fig. 4.2 The standard basis and idempotent basis shown on the left and right, respectively

where $x = x(t)$ is any periodic function whose period is normalized to $T = 4$, and therefore $e = e(t)$.

Taking into account (4.26) gives

$$x = X_+(\tau)e_+ + X_-(\tau)e_- \tag{4.72}$$

where $\tau = \tau(t)$, $e_+ = e_+(t)$, $e_- = e_-(t)$, and

$$\begin{aligned} X_+ &= X + Y = x(\tau) \\ X_- &= X - Y = x(2-\tau) \end{aligned} \tag{4.73}$$

The elements e_+ and e_- are mutually annihilating. They are called *idempotents* due to their properties

$$\begin{aligned} e_+e_- &= 0 \\ e_-^2 &= e_- \\ e_+^2 &= e_+ \end{aligned} \tag{4.74}$$

As follows from (4.71), $ee_+ = e_+$ and $ee_- = -e_-$. Obviously, the matrix representation of (4.72) is

$$X_+e_+ + X_-e_- \longleftrightarrow \begin{bmatrix} X_+ & 0 \\ 0 & X_- \end{bmatrix}$$

Properties (4.74) make the idempotent basis very convenient to use in different analytical manipulations. For instance, for any real number α,

$$(X_+e_+ + X_-e_-)^\alpha = X_+^\alpha e_+ + X_-^\alpha e_- \tag{4.75}$$

One can extend relationship (4.75) on a general function f as[4]

$$f(X_+e_+ + X_-e_-) = f(X_+)e_+ + f(X_-)e_- \tag{4.76}$$

provided that $f(X_+)$ and $f(X_-)$ are defined.

As a result, the major advantage of using the idempotent basis is that the differential equations of motion in terms of the components $X_+(\tau)$ and $X_-(\tau)$ appear to be decoupled regardless of nonlinearity. Instead, the corresponding boundary conditions become coupled. The nature of this fact is explained in the next subsection.

The time variable t can be represented in the idempotent basis during one period, $T = 4$, of a periodic signal. This can be shown by substituting (4.71) in (4.27), where $\dot{\tau}(t) = e(t)$, and then conducting the following manipulations

$$\begin{aligned} t &= 1 + (\tau - 1)\, e = (e_+ + e_-) + (\tau - 1)\,(e_+ - e_-) \\ &= \tau e_+ + (2 - \tau)e_- \qquad (-1 < t < 3) \end{aligned} \tag{4.77}$$

Further, using properties (4.74) gives, for instance,

$$\begin{aligned} t^2 &= \tau^2 e_+ + (2 - \tau)^2 e_- \\ t^\alpha &= \tau^\alpha e_+ + (2 - \tau)^\alpha e_- \\ (\alpha &> 0) \end{aligned} \tag{4.78}$$

Note that expressions (4.78) provide the direct proof of representation (4.72), at least for the class of analytical periodic functions $x(t)$.

4.2.2 Time Derivatives in the Idempotent Basis

Taking into account definitions (4.70) and (4.71) gives time derivatives of the basis elements

$$\dot{e}_+ = -\dot{e}_- = \frac{1}{2}\dot{e} \tag{4.79}$$

where $\dot{e}_+$ is a periodic series of δ-functions

$$\dot{e}_+ = \sum_{k=-\infty}^{\infty} [\delta(t + 1 - 4k) - \delta(t - 1 - 4k)]$$

[4] The so-called functional linearity property.

Thus, differentiating (4.72) gives

$$\begin{aligned}\dot{x} &= X'_+ e e_+ + X'_- e e_- + X_+ \dot{e}_+ + X_- \dot{e}_- \\ &= X'_+ e_+ - X'_- e_- + \frac{1}{2}(X_+ - X_-)\dot{e}\end{aligned}$$

Assuming the continuity condition

$$(X_+ - X_-)|_{\tau=\pm 1} = 0 \tag{4.80}$$

leads to

$$\dot{x} = X'_+ e_+ - X'_- e_- \tag{4.81}$$

Analogously, assuming the continuity condition for $\dot{x}(t)$,

$$(X'_+ + X'_-)|_{\tau=\pm 1} = 0 \tag{4.82}$$

gives then

$$\ddot{x} = X''_+ e_+ + X''_- e_-$$

It is seen that the algebraic structure with the idempotent basis is maintained when taking derivatives.

Example 4.2.1 Suppose the equation $\dot{x} = f(x)$, where $x(t) \in R^n$, has a family of periodic solutions of the period $T = 4a$. Introducing the triangle wave time, $\tau = \tau(t/a)$, and using the idempotent basis bring the equation to the form

$$(X'_+ e_+ - X'_- e_-)\frac{1}{a} = f(X_+ e_+ + X_- e_-) = f(X_+)e_+ + f(X_-)e_-$$

Then collecting separately terms with different basis elements gives

$$\begin{aligned}X'_+ &= a f(X_+) \\ X'_- &= -a f(X_-)\end{aligned} \tag{4.83}$$

under condition (4.80). As mentioned above, the triangle wave time substitution implemented in the idempotent basis leads to the decoupled set of equations such as (4.83), whereas boundary condition (4.80) is coupled. It is practically sufficient to solve only first equation of system (4.83). Then solution of the second equation is obtained by the replacement $\tau \to -\tau$ in the first solution.

4.3 Idempotent Basis Generated by Asymmetric Triangle Wave

4.3.1 Definition and Algebraic Properties

Let us introduce basic rules for algebraic manipulations with the idempotent basis generated by the asymmetric triangle wave (4.53). The standard basis is given by the set $\{1, e\}$ and shown on the left in Fig. 4.3, where $e = e(t, \gamma)$ is defined by (4.54) as a generalized square wave with stepwise discontinuities at the points $\Lambda_\gamma = \{t : \tau(t, \gamma) = \pm 1\}$.

In this case, the idempotent basis is introduced as

$$\begin{aligned} e_+ &= \frac{1}{2}[1 - \gamma + (1 - \gamma^2)e] \\ e_- &= \frac{1}{2}[1 + \gamma - (1 - \gamma^2)e] \end{aligned} \tag{4.84}$$

or, inversely,

$$\begin{aligned} 1 &= e_+ + e_- \\ e &= \frac{1}{1-\gamma}e_+ - \frac{1}{1+\gamma}e_- \end{aligned} \tag{4.85}$$

where $e_+ = e_+(t, \gamma)$ and $e_- = e_-(t, \gamma)$, and the parameter of asymmetry γ is included in order to normalize the range of change for the basis elements as $0 \le e_+ \le 1$ and $0 \le e_- \le 1$; see the diagrams on the right in Fig. 4.3.

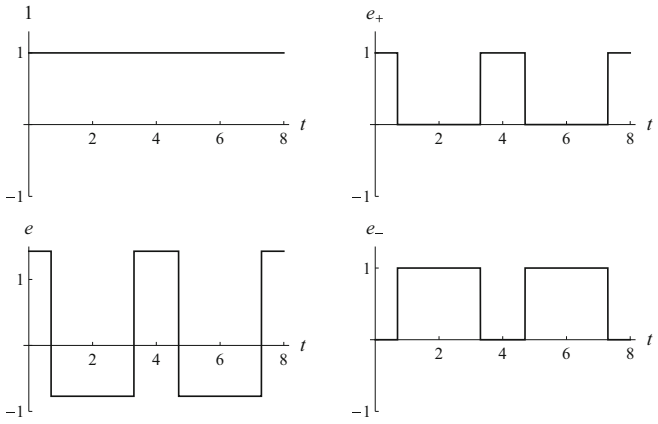

Fig. 4.3 The standard basis and idempotent basis (on the left and right, respectively) generated by the asymmetric triangle wave with $\gamma = 0.3$

Definition (4.84) brings (4.55) to the form

$$t = (1-\gamma)\,\tau e_+ + [2-(1+\gamma)\,\tau]\,e_- \tag{4.86}$$

If $\gamma = 0$, then definition (4.84) becomes equivalent to (4.70). The new elements, e_+ and e_-, are still mutually annihilating and create *idempotents* even though $\gamma \neq 0$. Hence, the table of products (4.74) still holds for any $\gamma \in (-1, 1)$. Also, it follows from (4.74) and (4.85) that

$$\begin{aligned} ee_+ &= \frac{1}{1-\gamma}e_+ \\ ee_- &= -\frac{1}{1+\gamma}e_- \end{aligned} \tag{4.87}$$

Now, substituting (4.85) into identity (4.56) gives

$$\begin{aligned} x = X + Ye &= X(e_+ + e_-) + Y\left(\frac{1}{1-\gamma}e_+ - \frac{1}{1+\gamma}e_-\right) \\ &= \left(X + \frac{1}{1-\gamma}Y\right)e_+ + \left(X - \frac{1}{1+\gamma}Y\right)e_- \end{aligned} \tag{4.88}$$

where $x = x(t)$ is any periodic function whose period is normalized to $T = 4$.

Substituting (4.57) in (4.88) and conducting algebraic manipulations give

$$x = X_+(\tau, \gamma)e_+ + X_-(\tau, \gamma)e_- \tag{4.89}$$

where $\tau = \tau(t, \gamma)$ is defined above by (4.53), and the components are given by

$$X_+(\tau, \gamma) = x((1-\gamma)\tau) \qquad \text{and} \qquad X_-(\tau, \gamma) = x(2-(1+\gamma)\tau) \tag{4.90}$$

Obviously, the basic algebraic properties, (4.75) and (4.76), remain valid.

4.3.2 *Differentiation Rules*

Taking into account definitions (4.84) and (4.85) gives time derivatives of the idempotent basis, produced by the asymmetric triangle wave, as

$$\frac{\partial e_+}{\partial t} = -\frac{\partial e_-}{\partial t} = \frac{1}{2}(1-\gamma^2)\frac{\partial e}{\partial t} \tag{4.91}$$

where $\partial e/\partial t$ is a periodic sequence of Dirac δ-functions acting whenever $t \in \Lambda_\gamma$. In this section, the symbol of partial derivative ∂ is used due to the dependence of basis upon two arguments, t and γ, although γ is just a fixed parameter here.

Taking into account that $\partial\tau/\partial t = e$ and differentiating (4.89) give

$$\dot{x} = \frac{\partial X_+}{\partial \tau} e e_+ + \frac{\partial X_-}{\partial \tau} e e_- + X_+ \frac{\partial e_+}{\partial t} + X_- \frac{\partial e_-}{\partial t} \tag{4.92}$$

Substituting (4.87) and (4.91) in (4.92) brings (4.92) to the form

$$\dot{x} = \frac{1}{1-\gamma}\frac{\partial X_+}{\partial \tau} e_+ - \frac{1}{1+\gamma}\frac{\partial X_-}{\partial \tau} e_- + \frac{1}{2}(1-\gamma^2)(X_+ - X_-)\frac{\partial e}{\partial t} \tag{4.93}$$

Assuming the continuity of $x(t)$ leads to boundary conditions

$$(X_+ - X_-)|_{\tau=\pm 1} = 0 \tag{4.94}$$

These conditions eliminate the singular term $\partial e/\partial t$ from expression (4.93), which takes the form

$$\dot{x} = \frac{1}{1-\gamma}\frac{\partial X_+}{\partial \tau} e_+ - \frac{1}{1+\gamma}\frac{\partial X_-}{\partial \tau} e_- \tag{4.95}$$

As seen from (4.95), the algebraic structure of representation (4.89) is preserved after the differentiation. Thus, under the continuity condition, the result of differentiation is obtained by the following replacements in (4.89):

$$X_+ \to \frac{1}{1-\gamma}\frac{\partial X_+}{\partial \tau} \qquad \text{and} \qquad X_- \to -\frac{1}{1+\gamma}\frac{\partial X_-}{\partial \tau} \tag{4.96}$$

Due to property (4.96), high-order derivatives can be obtained iteratively by making substitutions (4.96) in (4.93). For instance, second derivative is given by

$$\begin{aligned} \ddot{x} = {} & \frac{1}{(1-\gamma)^2}\frac{\partial^2 X_+}{\partial \tau^2} e_+ + \frac{1}{(1+\gamma)^2}\frac{\partial^2 X_-}{\partial \tau^2} e_- \\ & + \frac{1}{2}(1-\gamma^2)\left(\frac{1}{1-\gamma}\frac{\partial X_+}{\partial \tau} + \frac{1}{1+\gamma}\frac{\partial X_-}{\partial \tau}\right)\frac{\partial e}{\partial t} \end{aligned} \tag{4.97}$$

The singular term $\partial e/\partial t$ in (4.97) is eliminated by condition

$$\left(\frac{1}{1-\gamma}\frac{\partial X_+}{\partial \tau} + \frac{1}{1+\gamma}\frac{\partial X_-}{\partial \tau}\right)|_{\tau=\pm 1} = 0 \tag{4.98}$$

As a result, the second derivative $\ddot{x}$ takes the form of expansion with the basis $\{e_+, e_-\}$. Such differentiation can be continued step-by-step as soon as derivatives remain continuous in Λ_γ.

4.3.3 Oscillators in the Idempotent Basis

To illustrate the application of idempotent basis to vibration problems, let us consider oscillator

$$\ddot{x} + f(x) = F_+ e_+(\omega t, \gamma) + F_- e_-(\omega t, \gamma) \tag{4.99}$$

where ω is triangle wave frequency,[5] $F_\pm = F_\pm(\tau, \gamma)$ are components of the external loading represented in the idempotent basis with the period $T = 4a = 4/\omega$, and $\tau = \tau(\omega t, \gamma)$.

No specific conditions are imposed on the characteristic $f(x)$, but it is assumed that oscillator (4.99) possesses periodic solution with the period of external loading, T. Such a solution admits representation (4.89). Due to the presence of time scaling factor, expressions for the time derivatives from the previous subsection must be modified by the replacement $\partial\tau \to a\partial\tau = \omega^{-1}\partial\tau$. Now, substituting (4.89) in (4.99), taking into account (4.94) through (4.98) and the property of functional linearity, $f(X_+e_+ + X_-e_-) = f(X_+)e_+ + f(X_-)e_-$, gives equations

$$\frac{\omega^2}{(1-\gamma)^2}\frac{d^2X_+}{d\tau^2} + f(X_+) = F_+(\tau, \gamma) \tag{4.100}$$

$$\frac{\omega^2}{(1+\gamma)^2}\frac{d^2X_-}{d\tau^2} + f(X_-) = F_-(\tau, \gamma) \tag{4.101}$$

under the boundary conditions (4.94) and (4.98).

The obvious advantage of using the idempotent basis is that Eqs. (4.100) and (4.101) are in a better match with the form of original equation (4.99). The equations are decoupled and hence solvable in a similar way. Although the entire boundary value problem is still coupled through the boundary conditions, the problem caused by the coupling is eased.

4.3.4 Exact Closed Form Solution for Piecewise Linear Oscillator

For a practical example of manipulations with the idempotent basis, let us consider the oscillator with a piecewise linear restoring force characteristic described by equation

$$\ddot{x} + \Omega_0^2[1 + \mu H(x)]x = 0, \qquad -1 < \mu < \infty \tag{4.102}$$

where Ω_0 and μ are constant parameters, and $H(x)$ is Heaviside unit step function.

[5] As defined in Sect. 1.2.1.

Let us seek periodic solution in the form $x = X_+e_+ + X_-e_-$ (4.89) assuming that X_+ and X_- associate with positive ($x > 0$) and negative ($x < 0$) branches of the solution, respectively. Therefore,

$$X_+ \geq 0 \qquad \text{and} \qquad X_- \leq 0 \tag{4.103}$$

Such a separation is dictated by the temporal shapes of the idempotent basis, $e_+(t, \gamma)$ and $e_-(t)$, in Fig. 4.3. Oscillator (4.102) spends a shorter time in the region $x > 0$ and a longer time in the region $x < 0$ since its characteristic is stiffer when $x > 0$ and softer when $x < 0$, respectively. Assumptions (4.103) therefore are based on the fact that the rectangle pulses of functions, $e_+(t)$ and $e_-(t)$, are acting shorter and longer time intervals, respectively.

Substituting (4.89) in Eq. (4.102) and following differential and algebraic manipulations, as outlined above in this section, give Eqs. (4.100) and (4.101), where the right-hand sides must be set to zero, $F_\pm \equiv 0$, since no external loading is applied in the present case. Compared to Eq. (4.99), the restoring force characteristic is transformed in somewhat specific way due to the presence of stepwise Heaviside function. The goal is to absorb its discontinuity by the basis functions, $e_\pm(t)$, and hence eliminate the discontinuity from the resultant equations. Taking into account (4.103), the functional linearity property, and the definition for Heaviside function gives the relationship

$$H(X_+e_+ + X_-e_-) = H(X_+)e_+ + H(X_-)e_- = H(X_+)e_+ = e_+$$

The restoring force characteristic of oscillator (4.102) is therefore transformed as

$$\Omega_0^2[1 + \mu H(x)]x = \Omega_0^2(1 + \mu e_+)(X_+e_+ + X_-e_-)$$

$$= \Omega_0^2(1 + \mu)X_+e_+ + \Omega_0^2 X_-e_-$$

Finally, the component-wise equations are

$$\frac{d^2X_+}{d\tau^2} + \Omega_+^2 X_+ = 0, \qquad \frac{d^2X_-}{d\tau^2} + \Omega_-^2 X_- = 0 \tag{4.104}$$

where $r = \Omega_0/\omega$ is the adjusted frequency ratio, $\Omega_+ = r(1 - \gamma)\sqrt{1 + \mu}$ and $\Omega_- = r(1 + \gamma)$; note that the triangle wave frequency, ω, and the slope, γ, are yet unknown.

In the present case, the boundary condition of continuity (4.94) for the coordinate x is satisfied automatically by a stronger continuity condition at zero, $x = 0$, where the restoring force changes its slope,

$$\tau = \pm 1 : X_+ = X_- = 0 \tag{4.105}$$

Therefore, in contrast to condition (4.94), setting both components, X_+ and X_-, individually to zero is required by the physical specific of the system under

consideration. Condition (4.98) for continuity of the velocity $\dot{x}$ is still the same and can be represented as

$$\tau = \pm 1 : \frac{dX_-}{d\tau} = -\frac{1+\gamma}{1-\gamma}\frac{dX_+}{d\tau} \tag{4.106}$$

The above boundary value problem, (4.104) through (4.106), is solved in two steps. First, boundary conditions (4.105) are applied to the general solution of system (4.104)

$$X_+ = A_+ \cos \Omega_+ \tau + B_+ \sin \Omega_+ \tau$$
$$X_- = A_- \cos \Omega_- \tau + B_- \sin \Omega_- \tau$$

This gives $B_+ = B_- = 0$ with two equations, $\cos \Omega_\pm = 0$, under which a non-trivial solution with $A_\pm \neq 0$ is possible. Choosing the same principal root for both quantities, $\Omega_\pm = \pi/2$, gives $X_\pm = A_\pm \cos(\pi\tau/2)$. Substituting this couple of functions in (4.106) determines the ratio $A_-/A_+ = -(1+\gamma)/(1-\gamma)$. As a result, solution of Eq. (4.102) takes the form

$$x = X_+ e_+ + X_- e_- = A\left(e_+ - \frac{1+\gamma}{1-\gamma}e_-\right)\cos\frac{\pi\tau}{2} \tag{4.107}$$

where $A = A_+$ is an arbitrary amplitude parameter, while another arbitrary constant can be introduced as a phase shift, $t \longrightarrow t + t_0$, since Eq. (4.102) admits the group of time translations.

Substituting (4.84) in (4.107) brings solution to its final form

$$x(t) = A\left[(1+\gamma)\, e(\omega t, \gamma) - \frac{2\gamma}{1-\gamma}\right]\cos\left[\frac{1}{2}\pi\tau(\omega t, \gamma)\right] \tag{4.108}$$

where the triangle wave frequency, ω, and the parameter of slope, γ, are determined from the two equations $\Omega_\pm = \pi/2$ as

$$\omega = \frac{2}{\pi}(1+\gamma)\Omega_0 \qquad \text{and} \qquad \gamma = \frac{\sqrt{1+\mu}-1}{\sqrt{1+\mu}+1} \tag{4.109}$$

Solution (4.108) is validated by comparing it to the result of numerical integration of differential equation (4.102). The result of comparison is represented in Fig. 4.4, where the graphs for $\tau = \tau(\omega t, \gamma)$ and $e = e(\omega t, \gamma)$ reveal how two different pieces of solution are combined by means of the standard functions τ and e.

Finally, Fig. 4.5 shows how the idempotent basis functions, $e_+(t, \gamma)$ and $e_-(t, \gamma)$, are picking and matching the proper pieces from the components $X_+(t, \gamma)$ and $X_-(t, \gamma)$.

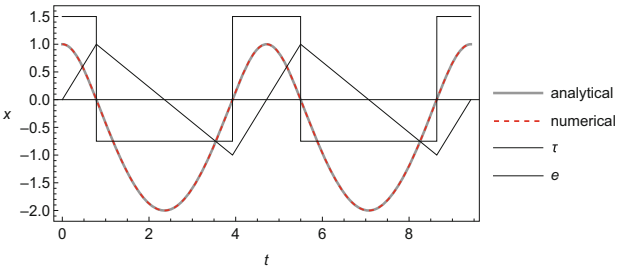

Fig. 4.4 Numerical validation of analytical solution (4.108) for the following parameters: $A = 1.0$, $\Omega_0 = 1.0$, $\mu = 3$, and $\gamma = 1/3$

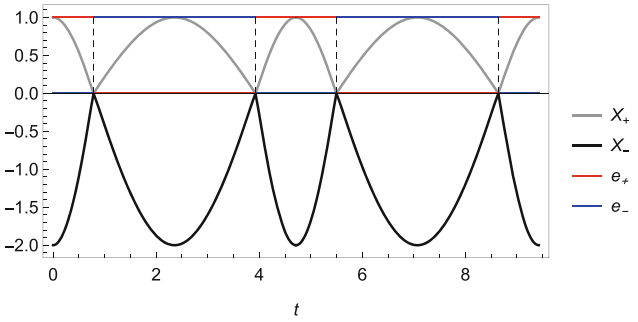

Fig. 4.5 Components of solution (4.107) in the idempotent basis and the basis functions for the parameters used in Fig. 4.4

4.3.5 Integration in the Idempotent Basis

Let $x(t)$ be a periodic function of the period normalized to $T = 4$ with zero mean value on the period T. Then, integrating the right-hand side of (4.89) gives

$$\int [X_+(\tau,\gamma)e_+ + X_-(\tau,\gamma)e_-]dt = P_+(\tau,\gamma)e_+ + P_-(\tau,\gamma)e_- \tag{4.110}$$

where

$$P_+(\tau,\gamma) = (1-\gamma)\int_{-1}^{\tau} X_+(z,\gamma)dz + C$$

$$P_-(\tau,\gamma) = -(1+\gamma)\int_{-1}^{\tau} X_-(z,\gamma)dz + C \tag{4.111}$$

Note that both expressions in (4.111) have the same arbitrary constant of integration C. As a result, substituting (4.111) in (4.110) and taking into account (4.85) give a single constant of integration as follows: $Ce_+ + Ce_- = C(e_+ + e_-) = C$.

Proof of relationships (4.111) is obtained by taking time derivative of both sides of equality (4.110). Under the condition of continuity of the right-hand side of (4.110), the differentiation leads to the boundary value problem

$$\begin{aligned} \frac{1}{1-\gamma}\frac{\partial P_+(\tau,\gamma)}{\partial \tau} &= X_+(\tau,\gamma) \\ -\frac{1}{1+\gamma}\frac{\partial P_-(\tau,\gamma)}{\partial \tau} &= X_-(\tau,\gamma) \\ (P_+ - P_-)|_{\tau=\pm 1} &= 0 \end{aligned} \tag{4.112}$$

This boundary value problem has solution (4.111) under the following condition though

$$(1-\gamma)\int_{-1}^{1} X_+(\tau,\gamma)d\tau + (1+\gamma)\int_{-1}^{1} X_-(\tau,\gamma)d\tau = 0 \tag{4.113}$$

The meaning of this condition is clarified by substituting (4.90) in (4.113) and taking into account the standard properties of definite integrals as follows:

$$\int_{-1}^{1} x[(1-\gamma)\tau]d[(1-\gamma)\tau] + \int_{-1}^{1} x[2-(1+\gamma)\tau]d[(1+\gamma)\tau]$$

$$= \int_{-(1-\gamma)}^{(1-\gamma)} x(z)dz - \int_{2+(1+\gamma)}^{(1-\gamma)} x(z)dz = \int_{-1+\gamma}^{3+\gamma} x(z)dz = \int_{0}^{T} x(t)dt = 0$$

In other words, condition (4.113) requires zero mean value for $x(t)$ on the period. Otherwise, the result of integration would appear to be out of the class of periodic functions by invalidating the algebraic structure of right-hand side of (4.110).

4.4 Discussions, Remarks, and Justifications

4.4.1 Group Properties of Conservative Oscillators and the Triangle Wave

Let us show that the triangle wave temporal argument τ (t) associates with the very general group properties of the conservative oscillator

$$\frac{d^2x}{dt^2} + f(x) = 0 \tag{4.114}$$

Suppose that another oscillating time parameter, say g, is introduced as $x(t) = X[g(t)]$, where $g(t)$ is a periodic function, which is not necessarily triangle wave. This kind of substitution brings the differential equation of motion to the form

$$\left(\frac{dg}{dt}\right)^2 \frac{d^2X}{dg^2} + \frac{d^2g}{dt^2}\frac{dX}{dg} + f(X) = 0 \tag{4.115}$$

A general side effect of such substitution is that the system has lost its original Newtonian form. In order to keep the differential equation of motion in Newtonian form, the following conditions must be imposed on Eq. (4.115)

$$\left(\frac{dg}{dt}\right)^2 = 1 \quad \text{and} \quad \frac{d^2g}{dt^2}\frac{dX}{dg} = 0 \tag{4.116}$$

Conditions (4.116) are satisfied by

$$g = \alpha + t \quad \text{or} \quad g = \beta - t \tag{4.117}$$

where α and β are arbitrary constants.

Relationships (4.117) simply represent the group of time transformations which is admitted by the original system (4.114). Let us recall however that the function $g(t)$ was assumed to be periodic. Therefore, according to (4.117), $g(t)$ must be a piecewise linear periodic function. The simplest one-frequency case is given by the triangular wave, $g(t) \equiv \tau(t)$. In this case the first equality of (4.116) is equivalent to the basic algebraic relationship (4.24), whereas the second equality holds for all t under the condition (4.42). As a result, the new equation (4.115) takes the same form as (4.114).

Therefore, the triangular wave time substitution $\tau(t)$ possesses the unique property among all periodic time substitutions as it preserves the form of differential equations of conservative oscillators.

4.4.2 *Remarks on Nonsmooth Solutions in the Classical Dynamics*

Problems of classical dynamics are usually formulated in terms of second- order differential equations of motion for the system coordinates. Hence the corresponding solutions must be at least twice continuously differentiable functions of time. The existence and uniqueness theorem imposes also special conditions on the system characteristics and external forcing functions. As a result, using discontinuities or

distributions for modeling dynamical systems takes the corresponding differential equations out of frames of the classic theory of differential equations. This requires additional examination of such formulations in order to insure that solutions actually exist. One of the NSTT roles is to bring models back into the area of classic theory. However, some preliminary analyses of correctness of original models are still required especially in nonlinear cases. In this and next subsections, some details and examples are introduced on nonlinear formulations with discontinuities and δ-functions.

For illustration purposes, let us consider a one-dimensional forced oscillator

$$\ddot{x} + f(x, \dot{x}) = q(t) \tag{4.118}$$

where the functions $q(t)$, $f(x, \dot{x})$ and $\partial f(x, \dot{x}) / \partial \dot{x}$ must be continuous according to the Cauchy theorem.

Let the system be subjected to an impulsive external loading applied at $t = t_0$. In this case, the external forcing function can be expressed by Dirac δ-function[6]

$$\ddot{x} + f(x, \dot{x}) = I\delta(t - t_0) \tag{4.119}$$

where I is a constant linear momentum per unit mass.

The differential equation of motion (4.119) cannot be treated within the classic theory of differential equations. It is also impossible to find a solution in the class of twice differentiable functions. However, a physically meaningful interpretation of Eq. (4.119) is suggested by the theory of distributions. For example, in terms of function-theoretic approaches, the distributions are not classical functions any more but linear functionals acting on manifolds of appropriate differentiable functions, $\{\varphi(t)\}$. Further, equalities are thought to be integral identities rather then point-wise relationships. Therefore, a "real meaning" of Eq. (4.119) is given by the identity

$$\int_{-\infty}^{\infty} [\ddot{x} + f(x, \dot{x})] \varphi(t)\, dt = I \int_{-\infty}^{\infty} \delta(t - t_0) \varphi(t)\, dt \tag{4.120}$$

which is supposed to be true for any "testing function" $\varphi(t)$.

Taking into account the definition of δ-function and integrating by parts give

$$\int_{-\infty}^{\infty} [-\dot{x}\dot{\varphi}(t) + f(x, \dot{x}) \varphi(t)]\, dt = I\varphi(t_0) \tag{4.121}$$

[6] The Dirac δ-function belongs to the class of so-called generalized Functions introduced by Sergei Sobolev in 1935 and re-introduced by Laurent Schwartz in the late 1940s, who developed a theory of distributions.

On one hand, this expression allows to weaken the smoothness condition on the class of solutions. On the other hand, the integral identity (4.120) appears to have quite clear physical meaning since its both sides represent the work done on arbitrary virtual displacements, $\varphi(t)$. Note that the solution $x(t)$ itself is not considered as a functional unless the function f is linear. For example, let us consider the case $f(x, \dot{x}) = 2\lambda\dot{x} + \Omega^2 x$, where λ and Ω are constant parameters. In this case, by proceeding with integration by parts in Eq. (4.121), one obtains

$$\int_{-\infty}^{\infty} \left[\ddot{\varphi}(t) - 2\lambda\dot{\varphi}(t) + \Omega^2\varphi(t)\right] x(t)\, dt = I\varphi(t_0)$$

Therefore, $x(t)$ generates a linear functional of the form $\int_{-\infty}^{\infty} (...)\, x(t)\, dt$ and thus can be qualified as a *generalized solution*.[7]

In nonlinear cases, the concept of generalized solution does not work, but Eq. (4.121) still holds and enables one to use the concept of the so-called "weak solution" [65]. This concept is involved to justify manipulations with the nonsmooth functions at intermediate steps of the approach.

4.4.3 Caratheodory Equation

Since δ-function is defined as a linear functional, then nonlinear operations with δ-functions are generally illegal. Nonetheless Dirac δ-function still can participate in nonlinear differential equations in a linear way as a summand. Such cases were examined in details by Caratheodory [63]. Let us consider the differential equation $\dot{x} = f(t, x)$, where the right-hand side satisfies the Caratheodory conditions as follows. In the domain D of the (t, x) space: the function $f(t, x)$ is defined and continuous with respect x for almost all t; the function $f(t, x)$ is measurable in t for each x; and $|f(t, x)| \leq m(t)$, where function $m(t)$ is summable.

The above conditions are less restrictive than those required by the classical existence theorem, namely, the function $f(t, x)$ is allowed to be stepwise discontinuous in t. Such an extension becomes possible if the right-hand side of the equivalent integral equation is calculated by Lebesgue,

$$x(t) - x(t_0) = \int_{t_0}^{t} f(\xi, x(\xi))\, d\xi$$

[7] *Sometimes the very presence of δ-functions in any nonlinear equation is rejected by the reason that nonlinearity is incompatible with the notion of linear functionals. In differential equations of motion, however, singular forces and the corresponding accelerations usually participate as summands, whereas velocities and coordinates include no δ-type singularities and thus can be subjected to nonlinear operations.*

Now, let the right-hand side of the equation to include the δ-function as a summand

$$\dot{x} = f(t, x) + v\delta(t - a) \tag{4.122}$$

where a and v are constant parameters. In this case, the right-hand side does not satisfy any more the Caratheodory conditions. However, changing the variable

$$x(t) \longrightarrow y(t): \quad x(t) = y(t) + vH(t - a) \tag{4.123}$$

where H is Heaviside unit-step brings the differential equation to the form

$$\dot{y} = f[t, y + vH(t - a)] \equiv F(t, y) \tag{4.124}$$

where Dirac function has been eliminated due to the equality $\dot{H}(t - a) = \delta(t - a)$; as a result the right-hand side, $F(t, y)$, satisfies the Caratheodory conditions.

Note that, due to the presence of discontinuous function $H(t - a)$, the right-hand side of the transformed equation, $F(t, y)$, is generally piecewise continuous in t, even though the function $f(t, x)$ may be continuous.

Relationships (4.122) through (4.124) admit direct extensions on the vector space so that many mechanical and physical models can be represented in the form (4.122).

Example 4.4.1 Parametrically excited Duffing's oscillator subjected to the external impact at $t = a$ is described by equation

$$\ddot{u} + \Omega_0^2(1 + \varepsilon \cos 2t)u - \beta u^3 = 2p\delta(t - a) \tag{4.125}$$

Equation (4.125) is transformed to (4.122) by introducing the following vector-functions:

$$x = \begin{bmatrix} u \\ \dot{u} \end{bmatrix} = \begin{bmatrix} x_1 \\ x_2 \end{bmatrix}, \qquad v = \begin{bmatrix} 0 \\ 2p \end{bmatrix}$$

$$f(t, x) = \begin{bmatrix} x_2 \\ \beta x_1^3 - \Omega_0^2(1 + \varepsilon \cos 2t)x_1 \end{bmatrix}$$

Example 4.4.2 Center lines of linearly elastic beams resting on elastic foundations can be described by the dimensionless differential equation

$$\frac{d^4W}{d\xi^4} + \gamma(\xi)W = q\delta(\xi - a) \tag{4.126}$$

where $W = W(\xi)$ is the center line coordinate, $\gamma(\xi)$ is a variable stiffness of the foundation, and q is a transverse force localized at $\xi = a$. Equation (4.126)

is brought to the form (4.122) by considering t as a spatial coordinate ξ and introducing the matrixes

$$x = \begin{bmatrix} W \\ dW/d\xi \\ d^2W/d\xi^2 \\ d^3W/d\xi^3 \end{bmatrix}, \qquad f(\xi, x) = \begin{bmatrix} 0 & 1\,0\,0 \\ 0 & 0\,1\,0 \\ 0 & 0\,0\,1 \\ -\gamma(\xi) & 0\,0\,0 \end{bmatrix} x, \qquad v = \begin{bmatrix} 0 \\ 0 \\ 0 \\ q \end{bmatrix}$$

In order to completely formulate the problem, the corresponding boundary conditions must be added.

Let us show now that introducing the nonsmooth argument (4.11) eliminates the δ-function in Eq. (4.122) in such a way that no stepwise discontinuity occurs in the new equation. Substituting (4.12) and (4.13) into Eq. (4.122) and taking into account expression $\ddot{s} = 2\delta(t - a)$ give

$$Y' + R_f(s, X, Y) + \left[X' + I_f(s, X, Y)\right]\dot{s} + (2Y - v)\,\delta(t - a) = 0 \tag{4.127}$$

where expressions

$$R_f = \frac{1}{2}\left[f(a + s, X + Y) + f(a - s, X - Y)\right]$$
$$I_f = \frac{1}{2}\left[f(a + s, X + Y) - f(a - s, X - Y)\right]$$

are obtained analogously to (4.34).

Eliminating the δ-function in (4.127) and equating separately both components of the remaining hyperbolic element to zero give the boundary value problem

$$\begin{aligned} X' + I_f(s, X, Y) &= 0 \\ Y' + R_f(s, X, Y) &= 0 \\ Y|_{s=0} &= \frac{1}{2}v \end{aligned} \tag{4.128}$$

Although Eqs. (4.128) have a more complicated form as compared to (4.122), the stepwise discontinuous function, $H(t - a)$, is not involved any more; also it may become important that the new argument s is half-limited: $0 \le s < \infty$.

4.4.4 *Other Versions of Periodic Time Substitutions*

Following Sect. 4.4.1, it will be shown here that the symmetric triangle wave generates the most simple algebraic structure among other possible versions of

non-invertible time substitutions. Note that periodic temporal arguments have been considered in the literature for a long time. The main idea of these approaches is to make a new temporal argument limited and therefore expand the class of usable algorithms. For example, the harmonic transformation of time in combination with the power series method was used by Ince [94] for investigation of periodic motions. In particular, by introducing the new variables

$$\tau = \sin t \qquad \text{and} \qquad x(t) = X[\tau(t)] \tag{4.129}$$

in the Mathieu equation,

$$\ddot{x} + (a + b\cos 2t)\, x = 0$$

one obtains the equation

$$\left(1 - \tau^2\right) X''_{\tau^2} - \tau X'_{\tau} + \left(a + b - 2b\tau^2\right) X = 0$$

which admits periodic solutions in terms of the power series with respect to the new temporal argument $|\tau| \leq 1$ [246].

Transformation (4.129) with the power series methods was employed for nonlinear vibrating systems as well [144, 206, 250]. Non-harmonic time transformations dealing with Jacobian functions can be also found in the literature [28]. As it is known that such time substitutions are restricted by special cases and *cannot be applied to any periodic motion.* From the mathematical point of view, it is caused by the fact that an inverse transformation does not exist on the whole period.

In this section, different versions of the periodic time are introduced in such a way that the corresponding transformations are valid for any periodic motion. This is reached through a special complexification of the coordinates.

Let us start with a generalization of substitution (4.129). For the sake of compactness, notations

$$\tau = \tau(\varphi) \equiv \sin\varphi \qquad \text{and} \qquad e = e(\varphi) \equiv \cos\varphi \tag{4.130}$$

will be used below, where $e(\varphi) = \tau'(\varphi)$.

Proposition 4.4.1 *Any sufficiently smooth periodic function $x(\varphi)$ of the period $T = 2\pi$ can be represented in the form*

$$x(\varphi) = X[\tau(\varphi)] + Y[\tau(\varphi)]e(\varphi) \tag{4.131}$$

where X and Y are of the power series form with respect to τ.

Proof By collecting separately terms with odd and even wave numbers in the corresponding Fourier series, one obtains

$$x(\varphi) = \frac{A_0}{2} + \sum_{n=1}^{\infty} [A_{2n} \cos 2n\varphi + A_{2n-1} \cos(2n-1)\varphi] + \sum_{n=1}^{\infty} [B_{2n} \sin 2n\varphi + B_{2n-1} \sin(2n-1)\varphi] \tag{4.132}$$

Then, introducing notations (4.130) into the tabulated expressions [71] (Formulas No. 1.332) gives

$$\cos 2n\varphi = \sum_{i=0}^{n} a_{2i}\tau^{2i}, \qquad \cos[(2n-1)\varphi] = \left(\sum_{i=1}^{n} a_{2i-1}\tau^{2i-2}\right) e$$
$$\sin 2n\varphi = \left(\sum_{i=1}^{n} b_{2i-2}\tau^{2i-1}\right) e, \quad \sin[(2n-1)\varphi] = \sum_{i=1}^{n} b_{2i-1}\tau^{2i-1} \tag{4.133}$$

where the coefficients are listed in [71]. Substituting (4.133) in (4.132) and reordering the terms complete the proof.

As it is seen from identities (4.133), the second component in representation (4.131) is due to the odd cosine-terms and even sine-terms of the Fourier expansion.

Note that combination (4.131) possesses algebraic properties similar to those generated by the triangle wave time substitution. Namely, *differentiation, integration, or any sufficiently smooth function of representation (4.131) gives an element of the same two-component structure as (4.131).* This is due to the fact that none of the listed above operations destroys periodicity of the function, and hence, identity (4.131) can be applied to the result of the operations as well. Practically, results of the operations are obtained by taking into account the trigonometric identities

$$\tau'(\varphi) = e(\varphi), \quad e'(\varphi) = -\tau(\varphi) \tag{4.134}$$

and

$$e^2 = 1 - \tau^2 \tag{4.135}$$

Note also that the components of representation (4.131) apparently are linearly independent and thus the whole combination is zero if and only if its both components are zero.

In order to illustrate manipulations with (4.131), let us introduce the temporal argument $\tau = \sin \Omega t$ into the Duffing oscillator with no linear stiffness term [236]

$$\ddot{x} + \zeta \dot{x} + x^3 = F \sin \Omega t \tag{4.136}$$

Considering periodic solutions and taking into account (4.134) and (4.135) on every step of the transformation give

$$\left[\left(1-\tau^2\right)X''-\tau X'\right]\Omega^2+\zeta\left[\left(1-\tau^2\right)Y'-\tau Y\right]\Omega \tag{4.137}$$
$$+3\left(1-\tau^2\right)XY^2+X^3=F\tau$$

$$\left[\left(1-\tau^2\right)Y''-3\tau Y'-Y\right]\Omega^2+\zeta X'\Omega \tag{4.138}$$
$$+3X^2Y+\left(1-\tau^2\right)Y^3=0$$

The unknown functions, X and Y, must satisfy conditions of analytical continuation on the boundaries of the interval $-1\le\tau\le 1$. These conditions are obtained by substituting $\tau=\pm 1$ in Eqs. (4.137) and (4.138) as follows:

$$\left[-\tau X'\Omega^2-\tau\zeta Y\Omega+X^3-F\tau\right]|_{\tau=\pm 1}=0 \tag{4.139}$$

$$\left[-\left(3\tau Y'+Y\right)\Omega^2+\zeta X'\Omega+3X^2Y\right]|_{\tau=\pm 1}=0 \tag{4.140}$$

The above system does not admit a family of solutions on which $Y(\tau)\equiv 0$ due to the damping; therefore, transformation (4.129) is not valid in this case.

Interestingly enough, the form of representation (4.131) remains the same in the case of triangular wave, although the basic algebraic operation (4.135) is different.

For the comparison reason, let us consider equation (4.136) with the forcing function $F\tau\,(t/a)$, where τ is the triangle wave of the period $4a$. Let us represent periodic solutions in the form (4.131), where the new temporal argument is the triangle wave (4.22) of the phase variable $\varphi=t/a$. Then, substituting (4.131) in Eq. (4.136) and considering the result as a two-component element of the algebra, one obtains the boundary value problem

$$X''a^{-2}+\zeta Y'a^{-1}+XY^2+X^3=F\tau \tag{4.141}$$

$$Y''a^{-2}+\zeta X'a^{-1}+3YX^2+Y^3=0 \tag{4.142}$$

$$Y|_{\tau=\pm 1}=0,\qquad X'|_{\tau=\pm 1}=0 \tag{4.143}$$

where the boundary conditions (4.143) are to eliminate the periodic series of Dirac functions from the first and second derivatives of the coordinate.

4.4.5 General Case of Non-invertible Time and Its Physical Meaning

Let us consider now a general class of functions $\{\tau(\varphi), e(\varphi)\}$ produced by the conservative oscillator $\ddot{x} + V'(x) = 0$, where $V(x)$ is the potential energy of the oscillator. To normalize the amplitude to unity, let us scale the potential energy and the phase variable as $P(x) = V(x)/V(1)$ and $\varphi = \sqrt{2V(1)}t$, respectively. As a result, the differential equation of motion and the energy integral are represented as, respectively,

$$\frac{d^2x}{d\varphi^2} + \frac{1}{2}P'(x) = 0 \qquad \text{and} \qquad \left(\frac{dx}{d\varphi}\right)^2 = 1 - P(x) \tag{4.144}$$

Let $x = \tau(\varphi)$ be the system coordinate determined implicitly from the energy integral

$$\int_0^{\tau(\varphi)} \frac{ds}{\sqrt{1 - P(s)}} = \varphi \tag{4.145}$$

Then second expression from (4.144) gives

$$e^2 = 1 - P(\tau) \tag{4.146}$$

where

$$e(\varphi) = \tau'(\varphi) \qquad \text{and} \qquad e'(\varphi) = -\frac{1}{2}P'(\tau) \tag{4.147}$$

Now let us formulate without proof

Proposition 4.4.2 *Any periodic function $x(\varphi)$ whose period is normalized to*

$$T = 4\int_0^1 \frac{ds}{\sqrt{1 - P(s)}}$$

can be represented in the form (4.131), where the functions $\tau(\varphi)$ and $e(\varphi)$ are given by (4.145) and (4.147).

For example, one can transform equation (4.136) based on the potential energy function $P(x) = x^{2n}$. Then the boundary value problems (4.137) through (4.140) and (4.141) through (4.143) can be derived as particular cases $n = 1$ and $n \longrightarrow \infty$, respectively.

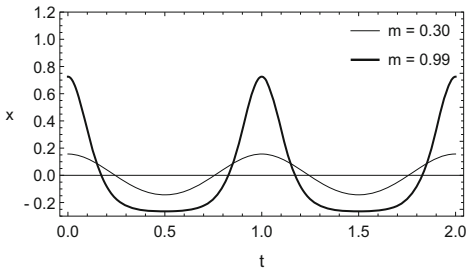

Fig. 4.6 Transition from quasi-harmonic ($m = 0.3$) to cnoidal ($m = 0.9$) wave

4.4.6 NSTT and Cnoidal Waves

There are other methodological sources of approximate solutions in terms of power series with respect to different type of periodic functions. In case of oscillators with even nonlinearities, it was suggested to approximate solutions by power series of the elliptic Jacobi cn-function [48]

$$x(t) = A + \sum_{n=1}^{N} B_n \mathrm{cn}^{2n}(\Omega t + \alpha_n, k^2) \tag{4.148}$$

where A and B_n are constants, Ω is the frequency parameter, and k is the modulus.

The reason for using series (4.148) is that Jacobi function effectively captures strongly anharmonic temporal shapes of periodic motions near separatrix loops. However, mathematical properties of Jacobi functions may require certain efforts while manipulating with solutions especially when the solutions are involved into further perturbation procedures.

Note the particular case of expression (4.148) $N = 1$, which resembles the well-known case of cnoidal wave [234].

$$x(t) = -\frac{E(m)}{K(m)} + \mathrm{dn}^2[2K(m)t] \tag{4.149}$$

where $K(m)$ and $E(m)$ are compete elliptic integrals of first kind and second kind, respectively, $m = k^2$ is the parameter (Jacobi), and the period is normalized to unity.

If the parameter m is small enough, function (4.149) takes almost harmonic shapes. When m is getting larger, then $x(t)$ describes so-called cnoidal waves as shown in Fig. 4.6.

From the physical point of view, function (4.149) with specific scaling factors exactly describes temporal behavior of the interaction force between particles of Toda lattice

$$f = a[\exp(-br) - 1], \qquad ab > 0 \tag{4.150}$$

where r is the distance between adjacent particles and a and b are arbitrary parameters.

Periodic function (4.149) admits the exact Fourier expansion

$$x(t) = \frac{\pi^2}{[K(m)]^2} \sum_{l=1}^{\infty} \frac{l \cos(2\pi l t)}{\sinh[\pi l K(1-m)/K(m)]} \tag{4.151}$$

Interestingly enough, function (4.149) can be also represented as a sum of localized waves (solitons) shifted one with respect to other by the same interval as

$$x(t) = -\frac{\pi}{2K(m)K(1-m)} + \frac{\pi^2}{[2K(1-m)]^2} \sum_{l=-\infty}^{\infty} \cosh^{-2}[\pi(t-l)K(m)/K(1-m)] \tag{4.152}$$

Practical reasons for using either of series (4.151) or (4.152) are that terms of both series consist of elementary functions[8] of time while executing different principles of approximation. Namely, each term of the Fourier series is carrying global information about the periodic process, whereas each term of series (4.152) provides just local description in some interval near the time point determined by the number l. Although both series describe the process exactly from the theoretical standpoint, the only limited number of terms is possible to keep in calculations. As a result, the abovementioned difference in principles of approximation may become essential as discussed further in this subsection.

Now, adapting transformation (4.72) to the case $T = 1$ and then applying the result to periodic function (4.152) give

$$x_{n,p}(t) = -\frac{\pi(e_+ + e_-)}{2K(m)K(1-m)} + \frac{\pi^2}{[2K(1-m)]^2} \times \left\{ \sum_{l=-n}^{n} \cosh^{-2}[\lambda(m)(\tau - 4l)]e_+ + \sum_{l=-p}^{p+1} \cosh^{-2}[\lambda(m)(\tau - 2 + 4l)]e_- \right\} \tag{4.153}$$

$$\lambda(m) = \frac{\pi K(m)}{4K(1-m)}$$

where the infinite limits of summation have been replaced by the integers $n > 0$ and $p > 0$; the triangle wave time, $\tau = \tau(4t)$, and the idempotent basis, $e_+ = [1 + e(4t)]/2$ and $e_- = [1 - e(4t)]/2$, are introduced; the substitution $1 = e_+ + e_-$ is used to emphasize that the entire expression (4.153) has the form of hyperbolic number represented in the idempotent basis.

[8] Exponential functions with real and imaginary exponents.

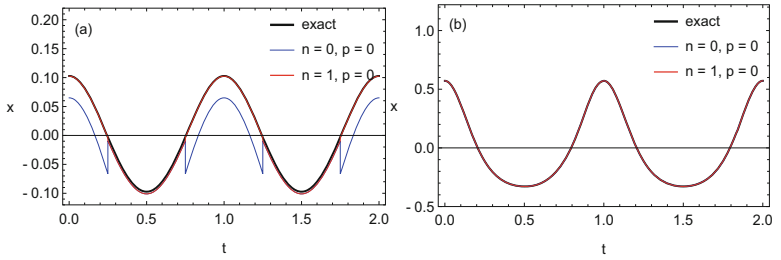

Fig. 4.7 NSTT of the periodic cnoidal wave for different number of terms in series (4.153) and two different values of Jacobi parameter: (**a**) $m = 0.2$ and (**b**) $m = 0.9$

Obviously, $x_{\infty,\infty}(t) = x(t)$, and hence (4.153) becomes the exact equivalent to (4.152). Still convergence properties of series (4.153) are significantly improved as compared to (4.152). As time t is growing in (4.152), one must switch from one term to another to keep a sufficient precision of approximation. In other words, in the infinite time interval, $-\infty < t < \infty$, the entire series (4.152) is needed. In contrast, the temporal argument of series (4.153) is always bounded by the standard interval $-1 \leq \tau \leq 1$, whereas the periodicity of wave is captured by the basis functions rather than multiple terms of the series. As a result, terms of series (4.153) are exponentially decaying as the summation index increases. As follows from the graphs in Fig. 4.7, for the range of Jacobi parameter $m > 0.2$, just five terms in (4.153) are sufficient to capture both quasi-harmonic and cnoidal wave shapes with a good precision. For a greater m, when the wave becomes essentially cnoidal, only three terms provide a good agreement with the exact shape. As seen from the upper fragment in Fig. 4.7, the three-term approximation gives essential discontinuous error for very small Jacobi parameter $m = 0.08$. However, in this almost harmonic range, it is more effective to use few or even one-term Fourier series (4.151) rather than series (4.152). Another essential advantage of series (4.153) is that, in the range of cnoidal shapes, different algebraic manipulations with truncated series are essentially eased due to the property of idempotents.

Chapter 5
Periodic Power Series

In this chapter, we introduce polynomials and power series expansions with respect to the triangular sine-wave. These can be used for approximations of periodic signals and unknown periodic solutions of dynamical systems. Such approximations may appear to be effective in those cases when trigonometric series converge slowly due to stepwise discontinuities or spikes. Another reason for using polynomial expansions is that they are usually more convenient for algebraic manipulations. In contrast to Fourier series, determining Taylor coefficients does not require integration procedures. If the process under consideration is smooth, then sufficient class of smoothness of approximations is achieved by imposing specific constraints on the coefficients of triangle wave polynomials. Other equations for the coefficients may appear either as a result of optimization procedures minimizing the error of approximation or as an outcome of iterative procedures dictated by the differential equations of motion. It is also shown that using operators Lie associated with dynamical systems essentially facilitates construction of the periodic power series.

5.1 Power Series of Triangle Wave

5.1.1 Smoothing Procedures

Consider a smooth periodic function $x(t)$ of the period $T = 4$ represented in the form $x(t) = X(\tau) + Y(\tau)\dot{\tau}$, where $\tau = \tau(t)$. Obviously, both components, X and Y, admit power series expansions with respect to the argument τ with no loss of periodicity in the original time t. As a side effect, note that keeping the finite number of terms in such series may violate the smoothness conditions at $\tau = \pm 1$ since functions and their truncated series may behave differently near the boundaries $\tau = \pm 1$. For that reason, let us introduce formal algorithms that can be applied to the truncated series in order to improve their smoothness properties. First, consider

V. N. Pilipchuk, *Oscillators and Oscillatory Signals from Smooth to Discontinuous*,
https://doi.org/10.1007/978-3-031-37788-4_5

the expansion

$$X(\tau) = \sum_{i=0}^{2N} \frac{X^{(i)}(0)}{i!}\tau^i + O\left(\tau^{2N+1}\right) \tag{5.1}$$

Obviously, finite sums in (5.1) are generally non-differentiable on the set of points $\Lambda = \{t : \tau(t) = \pm 1\}$. In contrast, the binomials

$$\phi_i(\tau) = \frac{\tau^i}{i} - \frac{\tau^{i+2}}{i+2}; \quad i = 1, 2, \ldots \tag{5.2}$$

are twice differentiable with respect to t on Λ that can be verified by taking derivatives with respect to t. For instance, first two generalized derivatives are

$$\frac{d\phi_i(\tau)}{dt} = \tau^{i-1}(1-\tau^2)\dot{\tau}(t)$$
$$\frac{d^2\phi_i(\tau)}{dt^2} = (i-1)\tau^{i-2} - (i+1)\tau^i$$

where the term $\tau^{i-1}(1-\tau^2)\ddot{\tau}$ has been removed from the second derivative due to the presence of factor $1-\tau^2$ that takes zero value whenever $\ddot{\tau} \neq 0$. Thus functions (5.2) are twice continuously differentiable with respect to t even though each of the functions is combination of two non-differentiable terms. This is achieved by the specific choice for the coefficients and signs in (5.2) such that the power terms have same jumps of slopes but with the opposite signs.

Now, considering (5.2) as equations with respect to different powers of τ gives, respectively, odd and even powers, as

$$\begin{aligned}
\tau &= \phi_1(\tau) + \ldots + \phi_{2N+1}(\tau) + \frac{\tau^{2N+3}}{2N+3} \\
\tau^3 &= 3\left[\phi_3(\tau) + \ldots + \phi_{2N+1}(\tau) + \frac{\tau^{2N+3}}{2N+3}\right] \\
\tau^{2N+1} &= (2N+1)\left[\phi_{2N+1}(\tau) + \frac{\tau^{2N+3}}{2N+3}\right]
\end{aligned} \tag{5.3}$$

and

$$\begin{aligned}
\tau^2 &= 2\left[\phi_2(\tau) + \ldots + \phi_{2N+2}(\tau) + \frac{\tau^{2N+2}}{2N+2}\right] \\
\tau^4 &= 4\left[\phi_4(\tau) + \ldots + \phi_{2N+2}(\tau) + \frac{\tau^{2N+2}}{2N+2}\right]
\end{aligned} \tag{5.4}$$

$$\tau^{2N} = 2N\left[\phi_{2N}(\tau) + \frac{\tau^{2N+3}}{2N+2}\right]$$

where N is an arbitrary positive integer.

Substituting (5.3) and (5.4) in (5.1) and setting $N \to \infty$ give

$$X(\tau) = X(0) + \sum_{i=1}^{\infty}\sum_{k=1}^{i}\left[\frac{X^{(2k-1)}(0)}{(2k-2)!}\phi_{2i-1}(\tau) + \frac{X^{(2k)}(0)}{(2k-1)!}\phi_{2i}(\tau)\right] \tag{5.5}$$

In contrast to (5.1), particular sums of series (5.5) are twice continuously differentiable functions of t. Since the Y-component usually appears with the stepwise discontinuous multiplier, $\dot{\tau}(t)$, the related series must be re-organized in a somewhat different way by taking into account the corresponding necessary condition of continuity: $Y(\pm 1) = 0$. In this case, appropriate polynomials are designed as

$$\psi_i(\tau) = \tau^i - \tau^{i+2}; \quad i = 0, 1, 2, \ldots \tag{5.6}$$

These polynomials provide the continuity for the term $\psi_i[\tau(t)]\dot{\tau}(t)$ as well as its first derivative

$$\frac{d[\psi_i(\tau)\dot{\tau}]}{dt} = \psi_i'(\tau)\dot{\tau}^2 = i\tau^{i-1} - (i+2)\tau^{i+1}$$

where the term $\psi_i(\tau)\ddot{\tau}$ has been eliminated due to the boundary conditions $\psi_i(\pm 1) = 0$.

Second derivative still appears to be a stepwise discontinuous function at times Λ,

$$\frac{d^2[\psi_i(\tau)\dot{\tau}]}{dt^2} = \left[i(i-1)\tau^{i-2} - (i+2)(i+1)\tau^i\right]\dot{\tau}$$

Therefore, particular sums of the new series

$$Y(\tau)\dot{\tau} = \sum_{i=0}^{\infty}\sum_{k=0}^{i}\left[\frac{Y^{(2k-1)}(0)}{(2k-1)!}\psi_{2i-1}(\tau) + \frac{Y^{(2k)}(0)}{(2k)!}\psi_{2i}(\tau)\right]\dot{\tau} \tag{5.7}$$

are less smooth than those obtained for the X-component (5.5).

Combining (5.5) and (5.7) and considering an arbitrary period, $T = 4a$, give

$$x(t) = X(0) + \sum_{i=1}^{\infty} K_X(i)\left(\frac{\tau^i}{i} - \frac{\tau^{i+2}}{i+2}\right) + e\sum_{i=0}^{\infty} K_Y(i)\left(\tau^i - \tau^{i+2}\right) \tag{5.8}$$

where $\tau = \tau\,(t/a)$ and $e = \tau'\,(t/a)$ and the coefficients are calculated as follows:

$$K_X\,(2i-s) = \sum_{k=1}^{i} \frac{X^{(2k-s)}\,(0)}{(2k-1-s)!}$$

$$K_Y\,(2i-s) = \sum_{k=0}^{i} \frac{Y^{(2k-s)}\,(0)}{(2k-s)!} \tag{5.9}$$

$$(s = 0,\, 1)$$

Series (5.8) may represent periodic solutions of dynamical systems. Formal solutions are obtained by considering the differential equations of motion when calculating the derivatives in coefficients (5.9). It can be done by means of the operator Lie as discussed in the next section. Examples of the power series including smoothing algorithms are introduced below with the corresponding algorithms given in Appendix 2.

Example 5.1.1 For illustration of expansion (5.8), we introduce first the triangle wave argument according to relationships (1.26) and then apply expansion (5.8) to the components X and Y as

$$f(t) = \ln\,(2+\cos t) = X(\tau) + Y(\tau)e$$

$$= \frac{1}{2}\ln\left(4-\cos^2\frac{\pi\tau}{2}\right) + \frac{1}{2}\ln\left[\frac{2+\cos(\pi\tau/2)}{2-\cos(\pi\tau/2)}\right]e$$

$$= \frac{\ln 3}{2} + \frac{\pi^2}{12}\left(\frac{\tau^2}{2}-\frac{\tau^4}{4}\right) + \left(\frac{\pi^2}{12}-\frac{\pi^4}{48}\right)\left(\frac{\tau^4}{4}-\frac{\tau^6}{6}\right)+\ldots$$

$$+\left[\frac{\ln 3}{2}\left(1-\tau^2\right) + \left(\frac{\ln 3}{2}-\frac{\pi^2}{12}\right)\left(\tau^2-\tau^4\right)\right. \tag{5.10}$$

$$\left.+\left(\frac{\ln 3}{2}-\frac{\pi^2}{12}+\frac{\pi^4}{192}\right)\left(\tau^4-\tau^6\right)+\ldots\right]e$$

where $\tau = \tau\,(2t/\pi)$ and $e = e\,(2t/\pi)$. The effectiveness of this truncated series is illustrated in Fig. 5.1.

Example 5.1.2 To compare Taylor truncated τ-series to the smoothed expansions, consider the following example:

$$f(t) = \sin^3\frac{\pi t}{2} = \sin^3\frac{\pi\tau}{2}, \qquad a = 1 \tag{5.11}$$

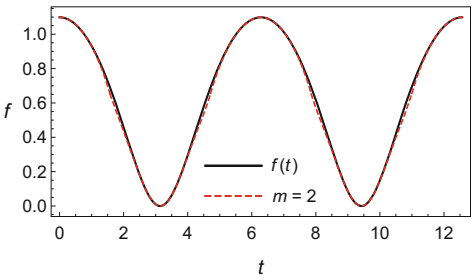

Fig. 5.1 Comparison of the function $f(t)$ to its smoothed expansion (5.10), where the number m defines the highest degree of τ in the truncated series as $2m + 2$

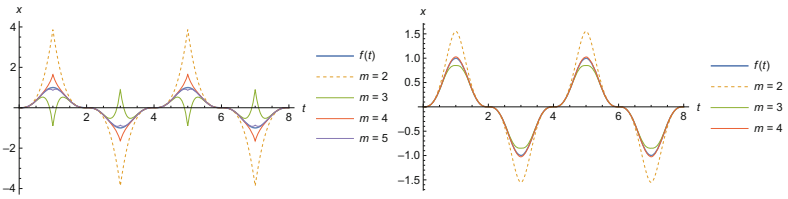

Fig. 5.2 First m terms of the direct polynomial expansion for the function $f(t) = \sin^3(\pi t/2)$ with respect to the triangle wave τ (on the left) and the effect of one-step smoothing algorithm (on the right)

Calculating Taylor coefficients and then applying smoothing algorithm (5.8) give

$$f(t) = \frac{3}{8}\pi^3\left(\frac{\tau^3}{3} - \frac{\tau^5}{5}\right) + \left(\frac{3\pi^3}{8} - \frac{5\pi^5}{64}\right)\left(\frac{\tau^5}{5} - \frac{\tau^7}{7}\right) \tag{5.12}$$
$$+ \left(\frac{3\pi^3}{8} - \frac{5\pi^5}{64} + \frac{91\pi^7}{15360}\right)\left(\frac{\tau^7}{7} - \frac{\tau^9}{9}\right) + \dots$$

where $\tau = \tau(t)$. A smoothing effect is illustrated in Fig. 5.2 by comparing graphs for different number of terms in both types of expansions. It seen that the direct Taylor's expansion develops some "tailing effect" near the boundaries $\tau(t) = \pm 1$. As the number of terms is increasing, the error, while still considerable, becomes localized near the points $\{t : \tau(t) = \pm 1\}$. As follows from the graphs, the discontinuity of slope will be rather maintained regardless of the number of terms in Taylor's expansion. This situation resembles the well-known Wilbraham-Gibbs phenomenon in approximations of stepwise discontinuous periodic functions with Fourier series. There is no such phenomenon in the present case of smooth function (5.11), whose Fourier series has just two terms. Instead, the polynomial tailing occurs as a side effect of approximation of the smooth function with the nonsmooth triangle wave. Fortunately, combining a polynomial τ-expansion with the suggested smoothing algorithm helps to suppress the tailing effect as follows from the right fragment of Fig. 5.2.

Remark 5.1.1 Finally, the above smoothing algorithms can be reiterated as many times as needed until necessary smoothness of the particular sums is achieved. For instance, the expressions (5.2) and (5.6) reveal next steps of the smoothing as

$$\begin{aligned}\phi_i(\tau) &= \frac{\tau^i}{\left(\tau^i\right)'|_{\tau=1}} - \frac{\tau^{i+2}}{\left(\tau^{i+2}\right)'|_{\tau=1}} \in C^2\\ \varphi_i(\tau) &= \frac{\phi_i(\tau)}{\phi_i^{(3)}(\tau)|_{\tau=1}} - \frac{\phi_{i+2}(\tau)}{\phi_{i+2}^{(3)}(\tau)|_{\tau=1}} \in C^4\end{aligned} \tag{5.13}$$

and

$$\begin{aligned}\psi_i(\tau)\dot{\tau} &= \left(\tau^i - \tau^{i+2}\right)\dot{\tau} \in C^1\\ \chi_i(\tau)\dot{\tau} &= \left(\frac{\psi_i(\tau)}{\psi_i^{(2)}(\tau)|_{\tau=1}} - \frac{\psi_{i+2}(\tau)}{\psi_{i+2}^{(2)}(\tau)|_{\tau=1}}\right)\dot{\tau} \in C^3\end{aligned} \tag{5.14}$$

respectively, where the symbol C indicates the class of smoothness in the interval $-\infty < t < \infty$. Second sets of equations in (5.13) and (5.14) have to be inverted for $\phi_i(\tau)$ and $\psi_i(\tau)$ in a similar way to (5.3) and (5.4). Then, by using the corresponding expressions, one can introduce functions $\varphi_i(\tau)$ and $\chi_i(\tau)$ into series (5.5) and (5.7), respectively.

There are multiple ways to designing τ-polynomial approximations with a prescribed class of smoothness. The choice is determined by specific needs for such approximations. Below, we consider two functions, $\tau_\alpha(t)$ and $e_\alpha(t)$, whose nature and asymptotic properties were discussed in Sect. 1.2.1.

Example 5.1.3 First, let us consider the function $\tau_\alpha(t)$ after scaling its amplitude as

$$f(t) = \frac{1}{\alpha}\tau_\alpha(t) = \frac{2}{\alpha\pi}\arcsin\left(\alpha\sin\frac{\pi t}{2}\right), \quad 0 < \alpha < 1 \tag{5.15}$$

Taking into account the period $T = 4$ and applying relationships (1.26) lead to the representation of function $\tau_\alpha(t)$ through its nonsmooth limit, $\alpha \to 1$,

$$f(t) = \frac{2}{\alpha\pi}\arcsin\left(\alpha\sin\frac{\pi\tau}{2}\right) \equiv X(\tau), \qquad \tau = \tau(t) \tag{5.16}$$

Let us consider now a polynomial approximation of this function combining different powers of smooth binomials as

$$X(\tau) = \sum_{i=0}^{m} A_i\left(\tau - \frac{\tau^{2k+1}}{2k+1}\right)^i \tag{5.17}$$

where the coefficients $\{A_i\}$ can be determined by matching different degrees of τ with the corresponding degrees in (5.1). For instance, setting $k = 2$ and $m = 5$ gives

$$A_1 = X'(0), \qquad A_2 = \frac{1}{2!}X''(0), \qquad A_3 = \frac{1}{3!}X^{(3)}(0)$$
$$A_4 = \frac{1}{4!}X^{(4)}(0), \qquad A_5 = \frac{1}{5!}[X^{(5)}(0) + 24X'(0)], \ldots \tag{5.18}$$

As a result, polynomial approximation (5.17) for function (5.16) takes the form

$$X(\tau) = \tau - \frac{\tau^5}{5} - \frac{1}{24}\pi^2\left(1-\alpha^2\right)\left(\tau - \frac{\tau^5}{5}\right)^3 + \frac{384 + \pi^4\left(1 - 10\alpha^2 + 9\alpha^4\right)}{1920}\left(\tau - \frac{\tau^5}{5}\right)^5 \tag{5.19}$$

Note the specific structure of the list of coefficients (5.18), which is linked to the number k. In the present case, $k = 2$, the degree τ^5 occurs twice in summation (5.17): first time when $i = 1$ and, the next time, when $i = 5$. This leads to a coupling between the coefficients, A_1 and A_5, and Taylor coefficient $X^{(5)}(0)/5!$ in the set of algebraic equations for $\{A_i\}$. This is why A_5 is the first coefficient to appear in solution (5.18), which is combining two terms. The effectiveness of periodic polynomial approximation (5.19) is illustrated in Fig. 5.3 for two different values of the parameter α.

Example 5.1.4 Now let us consider the smoothed version of square wave function, $e_\alpha(t)$, which is discussed in Sect. 1.2.1. Scaling its amplitude and switching to the triangle wave argument gives, respectively,

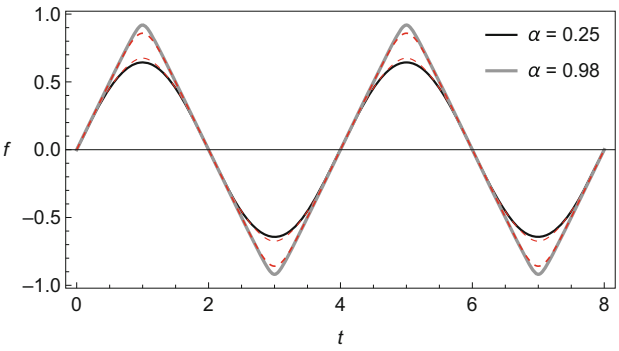

Fig. 5.3 Comparison of function (5.16) to its periodic polynomial approximation (5.19), shown by red dashed lines, for $k = 2$, $m = 5$, and two different values of α

$$f(t) = \frac{1}{\alpha} e_\alpha(t) = \frac{\cos(\pi t/2)}{\sqrt{1 - \alpha^2 \sin^2(\pi t/2)}} \tag{5.20}$$

and

$$f(t) = \frac{\sqrt{2}\cos(\pi \tau/2)}{\sqrt{2 - \alpha^2(1 - \cos \pi \tau)}} e \equiv Y(\tau) e \tag{5.21}$$

where $\tau = \tau(t)$ and $e = e(t)$. Let us assume a polynomial approximation for the function $Y(\tau)$ as

$$Y(\tau) = \left(1 - \tau^{2k}\right) \sum_{i=0}^{m} B_i \tau^i \tag{5.22}$$

where the multiplier $\left(1 - \tau^{2k}\right)$ is to eliminate possible stepwise discontinuities of the term $Y(\tau)\, e$ at points $\{t : \tau(t) = \pm 1\}$, and the coefficients $\{B_i\}$ are determined by matching different degrees of τ with the corresponding degrees of the Taylor's expansion for $Y(\tau)$. For instance, setting $k = 2$ and $m = 4$ and solving the corresponding set of linear algebraic equations give

$$\begin{aligned} &B_0 = Y(0), \qquad B_1 = Y'(0), \qquad B_2 = \frac{1}{2!} Y''(0) \\ &B_3 = \frac{1}{3!} Y^{(3)}(0), \qquad B_4 = \frac{1}{4!}[Y^{(4)}(0) + 24Y(0)], \ldots \end{aligned} \tag{5.23}$$

and finally the following polynomial approximation for the component Y in (5.21)

$$\begin{aligned} Y(\tau) = \left(1 - \tau^4\right) \Bigg[1 - \frac{1}{8}\left(1 - \alpha^2\right) \pi^2 \tau^2 \\ + \left(1 + \frac{1 - 10\alpha^2 + 9\alpha^4}{384}\right) \pi^4 \tau^4 \Bigg] \end{aligned} \tag{5.24}$$

In Fig. 5.4, graphs of function (5.21) are shown in comparison with its polynomial approximations for two different values of the parameter α. It is seen that the periodic polynomial works better for the temporal shape, which is closer to the square wave. Analyzing a broader range of the parameter α for different values of k and m reveals that different α may require different sets of numbers k and m for achieving the best result.

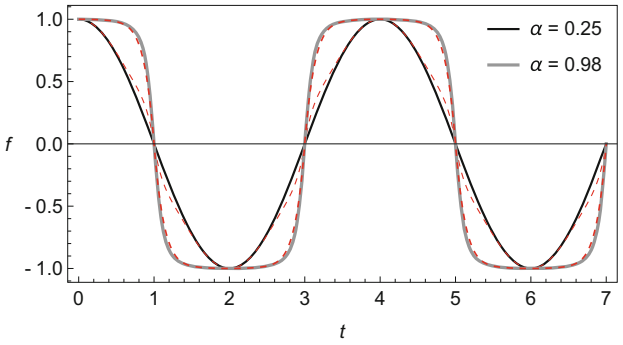

Fig. 5.4 Comparison of function (5.21) to its periodic polynomial approximation, shown by red dashed lines, for $k = 2$, $m = 4$, and two different values of α

5.1.2 Discussion

Regarding the periodic power series, the complementarity principle (Chap. 1) works as usual. In some cases, when the entire Fourier expansion consists of a couple of terms, the periodic power series would require a significant number of terms to achieve a reasonable result. It usually happens when a periodic signal under consideration is strongly non-monotonic on one half of the period. To explain the situation, let us consider function (5.11), whose periodic power series is given by (5.12). Fourier series of this function is obtained by means of the trigonometric identity and has just two terms

$$f(t) = \sin^3 \frac{\pi t}{2} = \frac{3}{4} \sin \frac{\pi t}{2} - \frac{1}{4} \sin \frac{3\pi t}{2} \tag{5.25}$$

Introducing the triangle wave time argument gives

$$f(t) = \frac{3}{4} \sin \frac{\pi \tau(t)}{2} - \frac{1}{4} \sin \frac{3\pi \tau(t)}{2} \tag{5.26}$$

The period of first term of function (5.25) is three times longer as many compared to the period of its second term. The triangle wave, $\tau(t)$, has the longest of the two periods to cover both terms in (5.26). Hence Taylor series for the second terms must include multiple powers to approximate all its halfwaves on the interval $-1 \le \tau \le 1$. This can be avoided by introducing two triangle waves of different periods for different sine waves in (5.25) as

$$f(t) = \frac{3}{4} \sin \frac{\pi \tau(t)}{2} - \frac{1}{4} \sin \frac{\pi \tau(3t)}{2} \tag{5.27}$$

Now the interval $-1 \le \tau \le 1$ covers one halfwave of both terms in (5.27), and thus no extra terms of polynomial for the second term are required. In such a way, one can adapt any number of trigonometric terms by means of the following general formulas:

$$\sin \Omega t = \sin\left[\frac{\pi}{2}\tau(\omega t)\right], \qquad \cos \Omega t = \cos\left[\frac{\pi}{2}\tau(\omega t)\right] e(\omega t), \tag{5.28}$$

where $\omega = (2/\pi)\Omega$ according to (1.2). For instance,

$$F(t) = \frac{A_0}{2} + \sum_{k=1}^{\infty}\left\{A_k \cos\left[\frac{\pi}{2}\tau(\omega_k t)\right] e(\omega_k t) + B_k \sin\left[\frac{\pi}{2}\tau(\omega_k t)\right]\right\} \tag{5.29}$$

$$\omega_k = \frac{2}{\pi}\Omega_k \qquad (k = 1, \ldots, n)$$

If the function $F(t)$ is periodic of the period $T = 2\pi$, then $\Omega_k = k$, and (5.29) is its standard Fourier series. Otherwise (5.29) can represent a general quasi periodic signal. The reason for such a manipulation with trigonometric sums is that both sine and cosine waves can now be approximated with smooth binomials as (5.2) and (5.6), respectively. For instance, using the lowest degree binomials, $\phi_1(\tau)$ and $\psi_0(\tau)$, gives

$$F(t) \approx \frac{A_0}{2} + \sum_{k=1}^{n}\left\{A_k\left[1 - \tau(\omega_k t)^2\right] e(\omega_k t) + B_k \frac{3}{2}\left[\tau(\omega_k t) - \frac{1}{3}\tau(\omega_k t)^3\right]\right\} \tag{5.30}$$

where the factor $3/2$ is inserted to adjust the amplitude of $\phi_1(\tau)$ to unity.

All the coefficients A_k and B_k are assumed to be known. Algorithms for determining these coefficients based on representation (5.30) can involve different optimization procedures. Note that, in contrast to the sine and cosine waves, some subsets of the approximating binomials, ϕ and ψe, are not orthogonal. Their completeness is not analyzed here.

Finally, complex form of Fourier series for a periodic function $F(t)$ of the period $T = 2\pi$ is modified as

$$F(t) = \sum_{k=-\infty}^{\infty} c_k \exp(ikt) \tag{5.31}$$

$$= \sum_{k=-\infty}^{\infty}\left\{c_k e(\omega_k t) \exp\left[ie(\omega_k t)\frac{\pi\tau(\omega_k t)}{2}\right]\right\}, \qquad \omega_k = \frac{2k}{\pi}$$

This transformation can be verified by means of Euler formula. Note that, compared to Example 4.1.3, the elements $e = e(\omega_k t)$ depend upon different arguments and hence cannot create the four-dimensional basis $\{1, e, i, ei\}$.

5.2 Nonlinear Normal Modes with Lie Series

5.2.1 *Periodic Version of Lie Series*

Lie series with respect to the physical time parameter are considered below. Note that the corresponding procedure essentially differs of those used for asymptotic integration of the differential equations of motion, where Lie series associate with a small parameter of perturbation [82, 256].

Let us consider the differential equation of motion for the position vector-function $x\,(t) \in R^n$

$$\ddot{x} + f\,(x, \dot{x}, t) = 0 \tag{5.32}$$

under the initial conditions

$$x_0 = x|_{t=0} \quad \text{and} \quad \dot{x}_0 = \dot{x}|_{t=0} = v_0$$

where the vector-function f is differentiable with respect to its arguments as many times as needed.

The standard Cauchy form of dynamical system (5.32) for the coordinate and velocity vectors is

$$\begin{aligned} \dot{x} &= v \\ \dot{v} &= -f(x, v, t) \\ \dot{t} &= 1 \end{aligned} \tag{5.33}$$

The dynamics of system (5.33) can be locally described by the Lie series [94]

$$x = \exp[(t - t_0)G]x_0 \equiv \left[1 + (t - t_0)G + \frac{1}{2!}(t - t_0)^2 G^2 + \cdots\right] x_0 \tag{5.34}$$

$$G = v_0 \cdot \frac{\partial}{\partial x_0} - f(x_0, v_0, t_0) \cdot \frac{\partial}{\partial v_0} + \frac{\partial}{\partial t_0} \tag{5.35}$$

where G is Lie operator associated with system (5.33), and $\{x_0, v_0, t_0\}$ is some initial point in the phase space of the system; the dot between two quantities indicates dot products as

$$v_0 \cdot \frac{\partial}{\partial x_0} \equiv v_{01} \frac{\partial}{\partial x_{01}} + \cdots + v_{0n} \frac{\partial}{\partial x_{0n}}$$

Series (5.34) are simply Taylor series whose coefficients are calculated by enforcing equations (5.33). Unfortunately, this general idea is still of little use

for oscillatory processes probably due to locality of expansion (5.34). Even entire expansion (5.34) cannot explicitly reveal such global characteristics of oscillations as their amplitude and period. Moreover, the corresponding truncated series produce increasingly growing errors as the time t runs away from the selected initial point t_0. In order to overcome these disadvantages, it is suggested to adapt the Lie series solution for the class of periodic motions as follows.

Theorem 5.2.1 ([186]) *Assume that system (5.33) admits a periodic solution $x(t)$ of the period $T = 4a$ such that $x(t+4a) = x(t)$ for any t, and some point $\{x_0, v_0, t_0\}$ belongs to this solution. Then solution can be expressed in the form*

$$x = \exp(aG)\{\cosh[a(\tau - 1)G] + e \sinh[a(\tau - 1)G]\}x_0 \tag{5.36}$$

where τ and e are triangle and square waves, whose periods are normalized to four and amplitudes are unity as

$$\tau(\varphi) = (2/\pi) \arcsin \sin(\pi\varphi/2) \tag{5.37}$$

and

$$e(\varphi) = sgn[\cos(\pi\varphi/2)], \tag{5.38}$$

respectively, and $\varphi = (t - t_0)/a$ is a scaled time. If, in addition, the solution is odd with respect to one half of the period, $x(t + 2a) = -x(t)$, then expression (5.36) simplifies to

$$\begin{aligned} x &= [\sinh(a\tau G) + e \cosh(a\tau G)]x_0 \\ &\equiv \left[a\tau G + \frac{1}{3!}(a\tau G)^3 + \cdots\right]x_0 + e\left[1 + \frac{1}{2!}(a\tau G)^2 + \cdots\right]x_0 \end{aligned} \tag{5.39}$$

Proof Expression (5.36) is obtained by substituting the identity [185]

$$\varphi = 1 + [\tau(\varphi) - 1]e(\varphi), \qquad (-1 < \varphi < 3) \tag{5.40}$$

in (5.34) and taking into account that

$$e^2 = 1 \tag{5.41}$$

at almost every time instance.[1] In order to prove the particular case (5.39), one should keep in mind that $\exp(2aG)x_0 = x(t_0+2a) = -x_0$, as it follows from (5.34), and the oddness condition assumed.

[1] The set of isolated points $\{\varphi : \tau(\varphi) = \pm 1\}$ appears to have no effect on the results [185].

Recall that τ and e are quite simple piecewise linear functions; the above analytical expressions (5.37) and (5.38) just define them in the unit-form which enables one to avoid conditioning of computation in the original temporal scale, $t_0 \le t < \infty$. This possibility becomes essential when the dynamics includes some evolutionary component.

Physical meaning of relationship (5.40) is that, during the whole period, the time variable φ is expressed through the coordinate τ and velocity e of a classical particle, which is freely oscillating between the two absolutely stiff barriers with no energy loss. Due to (5.41), this relationship possesses the algebraic structure of hyperbolic complex numbers as revealed by (5.36).

Let us outline possible applications of expressions (5.36) and (5.39). For the sake of simplicity, consider the particular case (5.39). Formal expression (5.39) does not guarantee the existence of periodic solutions. In case some periodic solution does exist, one should be able to find the corresponding vectors x_0 and v_0 from appropriate conditions. In autonomous case, the period, $T = 4a$, is also unknown and must be determined. The related conditions are formulated as a requirement of smoothness of expression (5.39), which is generally nonsmooth or even discontinuous due to the presence of nonsmooth and discontinuous functions τ and e, respectively. The smoothing conditions are obtained by eliminating the stepwise discontinuities of the coordinate and velocity vectors imposing the constraints

$$\cosh(aG)x_0 = 0, \qquad \cosh(aG)v_0 = 0 \tag{5.42}$$

In the autonomous case, algebraic equations (5.42) represent a nonlinear eigen-value problem, where a is an eigen-value, and $\{x_0, v_0\}$ is a combined (state) eigen-vector. By narrowing the class of periodic motions to those on which the system passes its trajectory twice in the configurations space during the same period, one obtains a subclass of normal mode motions. For further physically meaningful definitions and discussions, see reference [241]. Let us formulate the corresponding problem based on the periodic Lie series solutions.

Consider the vibrating system

$$\ddot{x} + f(x) = 0, \qquad x \in R^n \tag{5.43}$$

where $f(-x) = -f(x)$, and the initial conditions are $x|_{t=0} = x_0 = 0$ and $\dot{x}|_{t=0} = v_0$.

The normal mode solutions of system (5.43) are obtained as a particular case of (5.39) and (5.42)

$$x = \sinh(a\tau G)x_0|_{x_0=0} \tag{5.44}$$

$$\cosh(aG)v_0|_{x_0=0} \tag{5.45}$$

where the initial vector, $x_0 = 0$, is substituted into the expressions only after all degrees of the differential operator

$$G = v_0 \cdot \frac{\partial}{\partial x_0} - f(x_0) \cdot \frac{\partial}{\partial v_0}$$

have been applied.

Relationship (5.44) can be interpreted as a parametric equation of normal mode trajectories of the system with the parameter interval $-1 \le \tau \le 1$.

Let us illustrate relationships (5.44) and (5.45) based on the linear system so that the result could be compared with the well-known solution.

Example 5.2.1 Suppose that $f(x) = Kx$, where K is a positively defined symmetric $n \times n$-matrix with the eigen-system $\{v_0, \Omega^2\}$ such that $Kv_0 = \Omega^2 v_0$. In this case, by applying the operator G twice, one obtains that v_0 is also an eigen-vector of the operator G^2, namely, $G^2 v_0 = -\Omega^2 v_0$. Then, keeping in mind the power series form of expressions (5.44) and (5.45) as those in (5.39) and sequentially applying the operator G^2 give $x = (v_0/\Omega)\sin(a\Omega\tau)$ and $\cos(a\Omega) = 0$, respectively. Notably, the last equation shows that there exist an infinite number of roots $\{a\}$ related to the same eigen-frequency Ω! However, it is easy to find that all the roots produce the same solution in terms of the original time t. The minimal quarter of the period is $a = \pi/(2\Omega)$; therefore $x = (v_0/\Omega)\sin(\pi\tau/2)$, and $\tau = (2/\pi)\arcsin\sin\Omega t$.

5.3 Lie Series of Transformed Systems

5.3.1 Second-Order Non-autonomous Systems

In the previous section, the triangle wave temporal argument was introduced into Lie series solutions. Alternatively, it can be introduced first in the differential equations of motion before the Lie series procedure is applied. Let the dynamical system be described by the set of second-order equations (5.32), where the vector-function f is periodic with respect to t with the period $T = 4a$. Thus periodic motions of the period T are considered below. In the autonomous case, the period is a priori unknown. Following the differential and algebraic rules introduced in Chap. 4 and conducting the substitutions $t \to \tau(t/a)$ and $x(t) = X(\tau) + Y(\tau)e$ in (5.32) lead to the boundary value problem[2]

$$\begin{aligned} X'' + a^2 R_f\left(X, Y, X', Y', \tau\right) &= 0 \\ Y'' + a^2 I_f\left(X, Y, X', Y', \tau\right) &= 0 \end{aligned} \tag{5.46}$$

[2] See Appendix 3 for automatic algorithms.

$$Y\,|_{\tau=\pm1} = 0, \quad X'|_{\tau=\pm1} = 0 \tag{5.47}$$

where $' \equiv d/d\tau$ and

$$\left\{ \begin{matrix} R_f \\ I_f \end{matrix} \right\} = \frac{1}{2}\left\{ f\left(X+Y,\ \frac{Y'+X'}{a},\ a\tau\right) \pm f\left(X-Y,\ \frac{Y'-X'}{a},\ 2a-a\tau\right)\right\} \tag{5.48}$$

Let us represent system (5.46) as a system of five first-order equations by introducing two more unknown vector-functions, $V(\tau)$ and $U(\tau)$, as

$$\begin{aligned} X' &= V \\ Y' &= U \\ V' &= -a^2 R_f\,(X, Y, V, U, \tau) \\ U' &= -a^2 I_f\,(X, Y, V, U, \tau) \\ \tau' &= 1 \end{aligned} \tag{5.49}$$

This system is formally autonomous. Analogously to (5.35), its operator Lie acting at some initial point of the phase space, $P_0 = \{X_0, Y_0, V_0, U_0, \tau_0\}$, is defined as

$$G = V_0 \cdot \frac{\partial}{\partial X_0} + U_0 \cdot \frac{\partial}{\partial Y_0} - a^2 R_f^0 \cdot \frac{\partial}{\partial V_0} - a^2 I_f^0 \cdot \frac{\partial}{\partial U_0} + \frac{\partial}{\partial \tau_0} \tag{5.50}$$

where $R_f^0 = R_f(P_0)$ and $I_f^0 = I_f(P_0)$.

The idea of Lie series enables one of representing solution of system (5.49) in the power series form with respect to the triangle wave argument, τ, under the initial conditions at P_0, where τ_0 is eventually set to zero, $\tau_0 = 0$. After completing calculations with Lie series, the quantities X_0, Y_0, V_0, and U_0, corresponding to a periodic solution of the period $T = 4a$, can be determined from the smoothing boundary conditions (5.47)

$$Y(X_0, Y_0, V_0, U_0, \tau)|_{\tau=\pm1} = 0, \quad V(X_0, Y_0, V_0, U_0, \tau)|_{\tau=\pm1} = 0 \tag{5.51}$$

Recall that boundary conditions (5.51) guarantee smoothness of the coordinate, x, and therefore continuity of the velocity, $\dot{x}$, at points $\{t : \tau = \pm1\}$. In nonlinear cases, equations (5.51) can be solved numerically by assigning different values for the period T or frequency $\Omega = 2\pi/T = \pi/(2a)$. Alternatively, instead of solving equations (5.51), the smoothing procedure of Sect. 5.1.1 can be applied. In this case, conditions (5.51) are satisfied automatically, whereas quantities X_0, Y_0, V_0, and U_0 remain undetermined. This enables one of extending the smoothness conditions on the acceleration, $\ddot{x}$, as

$$\frac{\partial U(X_0, Y_0, V_0, U_0, \tau)}{\partial \tau}|_{\tau=\pm 1} = 0, \quad \frac{\partial^2 V(X_0, Y_0, V_0, U_0, \tau)}{\partial \tau^2}|_{\tau=\pm 1} = 0 \tag{5.52}$$

Equations (5.51) or (5.52) for X_0, Y_0, V_0, and U_0 are generally quite complicated. In different particular cases, the problem can be simplified by taking into account possible symmetries of the system. For instance, let us consider equation

$$\ddot{x} + f(x, t) = 0 \tag{5.53}$$

where the vector-function $f(x, t)$ is odd with respect to the positional vector x and even with respect to the quarter of the period, $t = a$. In this case, the boundary-value problem, (5.46) and (5.47), admits a family of solutions with zero Y-component, such that the boundary value problem takes the form

$$\begin{aligned} X' &= V \\ V' &= -a^2 f(X, a\tau) \\ \tau' &= 1 \end{aligned} \tag{5.54}$$

and

$$V|_{\tau=1} = 0 \tag{5.55}$$

The operator Lie associated with dynamic system (5.54) is

$$G = V \cdot \frac{\partial}{\partial X} - a^2 f(X, a\tau) \cdot \frac{\partial}{\partial V} + \frac{\partial}{\partial \tau} \tag{5.56}$$

Let us adapt now smooth polynomial expansion (5.5) by keeping only odd powers of τ as

$$X(\tau) = \sum_{i=1}^{\infty} \sum_{k=1}^{i} \frac{X^{(2k-1)}(0)}{(2k-2)!} \left(\frac{\tau^{2i-1}}{2i-1} - \frac{\tau^{2i+1}}{2i+1} \right) \tag{5.57}$$

Condition (5.55) is satisfied automatically. The idea of Lie series is in the sequential calculation of the derivatives $X^{(2k-1)}(0)$ by enforcing the related dynamical system (5.54) in terms of its operator Lie (5.56). First two derivatives are

$$\begin{aligned} X' &= V \equiv GX \\ X'' &= V' = G(GX) \equiv G^2 X \end{aligned}$$

Then,

$$
\begin{aligned}
X''' &= \frac{d}{d\tau}G^2X = \frac{dX}{d\tau}\cdot\frac{\partial}{\partial X}(G^2X) + \frac{dV}{d\tau}\cdot\frac{\partial}{\partial V}(G^2X) + \frac{\partial}{\partial \tau}(G^2X) \\
&= V\cdot\frac{\partial}{\partial X}(G^2X) - a^2 f(X, a\tau)\cdot\frac{\partial}{\partial V}(G^2X) + \frac{\partial}{\partial \tau}(G^2X) \\
&\equiv G^3X
\end{aligned}
$$

A sequential extension of the above process on high-order derivatives shows that $X^{(2k-1)} = G^{2k-1}X$, and hence expansion (5.57) takes the form

$$
x(t) = X(V_0, \tau) = \sum_{i=1}^{\infty}\sum_{k=1}^{i}\frac{G^{2k-1}X|_{\tau=0}}{(2k-2)!}\left(\frac{\tau^{2i-1}}{2i-1} - \frac{\tau^{2i+1}}{2i+1}\right) \tag{5.58}
$$

where $\tau = \tau(t/a)$, and the initial position is zero, $X_0 = \mathbf{0}$, due to the assumption of oddness with respect to τ.

The constant vector V_0 is determined from equation

$$
\frac{\partial^3 X(V_0, \tau)}{\partial \tau^3}|_{\tau=1} = 0 \tag{5.59}
$$

Example 5.3.1 To illustrate the above approach in component-wise form, let us consider now a two-degree-of-freedom oscillating system

$$
\frac{d^2}{dt^2}\begin{bmatrix} x_1 \\ x_2 \end{bmatrix} + \begin{bmatrix} \zeta(2x_1 - x_2) + x_1^3 - P\sin\Omega t \\ \zeta(2x_2 - x_1) + x_2^3 \end{bmatrix} = \begin{bmatrix} 0 \\ 0 \end{bmatrix}
$$

In this case, the parameter $a = \pi/(2\Omega)$ is the quarter of the period of the external forcing function. Introducing the triangle wave temporal argument, $\tau = \tau(t/a)$, and representing the system as a system of first-order equations in the phase space $\{X_1, X_2, V_1, V_2, \tau\}$ generate the following operator Lie:

$$
\begin{aligned}
G = {} & V_1\frac{\partial}{\partial X_1} + V_2\frac{\partial}{\partial X_2} - a^2\left[\zeta(2X_1 - X_2) + X_1^3 - P\sin\frac{\pi\tau}{2}\right]\frac{\partial}{\partial V_1} \\
& -a^2[\zeta(2X_2 - X_1) + X_2^3]\frac{\partial}{\partial V_2} + \frac{\partial}{\partial \tau}
\end{aligned} \tag{5.60}
$$

Let the initial point be

$$
[X_1, X_2, V_1, V_2, \tau]\,|_{\tau=0} = [0, 0, A_1, A_2, 0] \tag{5.61}
$$

where A_1 and A_2 are constants to be determined from the smoothing conditions (5.59). Using (5.60) and (5.61) to calculate the first three terms of series (5.58) gives

$$X_1 = \left(\tau - \frac{\tau^3}{3}\right) A_1 + \left(\frac{\tau^3}{3} - \frac{\tau^5}{5}\right) \left[A_1 + \frac{1}{4}(a^2\, P\, \pi - 4\, a^2\, \zeta\, A_1 + 2a^2\, \zeta\, A_2)\right]$$
$$+\left(\frac{\tau^5}{5} - \frac{\tau^7}{7}\right) \left\{A_1 + \frac{1}{4}(a^2\, P\, \pi - 4\, a^2\, \zeta\, A_1 + 2a^2\, \zeta\, A_2)\right.$$
$$\left. - \frac{1}{192}\left[a^2\, P\, \pi^3 + 8a^4\, P\, \pi\, \zeta - 8A_1\, \left(5\, a^4\, \zeta^2 - 6\, a^2\, {A_1}^2\right) + 32\, a^4\, \zeta^2\, A_2\right]\right\}$$

and

$$X_2 = \left(\tau - \frac{\tau^3}{3}\right) A_2 + \left(\frac{\tau^3}{3} - \frac{\tau^5}{5}\right) \left[A_2 + \frac{1}{2}(a^2\, \zeta\, A_1 - 2\, a^2\, \zeta\, A_2)\right.$$
$$+\left(\frac{\tau^5}{5} - \frac{\tau^7}{7}\right) \left\{A_2 + \frac{1}{2}(a^2\, \zeta\, A_1 - 2\, a^2\, \zeta\, A_2)\right.$$
$$\left. \left. + \frac{1}{48}\left[a^4\, P\, \pi\, \zeta - 8\, a^4\, \zeta^2\, A_1 + 2A_2\, \left(5\, a^4\, \zeta^2 - 6\, a^2\, {A_2}^2\right)\right]\right\}$$

In this case, the vector-form equation (5.59) gives two algebraic equations for A_1 and A_2 as

$$\frac{\partial^3 X_1\,(A_1, A_2, \tau)}{\partial \tau^3}|_{\tau=1} = 0, \quad \frac{\partial^3 X_2\,(A_1, A_2, \tau)}{\partial \tau^3}|_{\tau=1} = 0 \tag{5.62}$$

where the first and the second equations guarantee smoothness of the accelerations $\ddot{x}_1\,(t)$ and $\ddot{x}_2\,(t)$, respectively. Intersections of curves (5.62) on Cartesian plane $A_1 A_2$ visualize the roots of system (5.62), as shown in Fig. 5.5. For instance, setting $\zeta = 1.0$, $P = 0.2$, and $\Omega = \sqrt{0.99}$ gives $(A_1, A_2) = (0.74915, 0.644886)$. This solution corresponds to a weakly nonlinear perturbation of the inphase linear mode. Similarly, in the neighborhood of the second frequency, $\Omega = \sqrt{3.01}$, one finds the solution $(A_1, A_2) = (0.5971, -0.8181)$, which is close to the antiphase linear mode. The corresponding temporal mode shapes are shown in Fig. 5.6 in comparison with numerical solutions. Interestingly enough, the right fragment of Fig. 5.5 shows also two other roots indicated by the pair of blue dots, $(2.33145, 2.28638)$ and $(-2.2065, -2.2548)$. Both these roots represent the *inphase* vibrations (Fig. 5.7) even though the frequency of the external forcing function is close to that of the *antiphase* linear mode. This effect may take place due to large amplitudes such that the inphase *nonlinear* frequency becomes close to the antiphase *linear* frequency.

Since the initial conditions, corresponding to the periodic regimes, are known, one can integrate the differential equations of motion numerically in order to check the analytical solutions. In the latter example, one would obtain that both results are in a good agreement. It must be noted that some of the periodic solutions may appear to be unstable. As a result, even a very small imperfection in the initial conditions

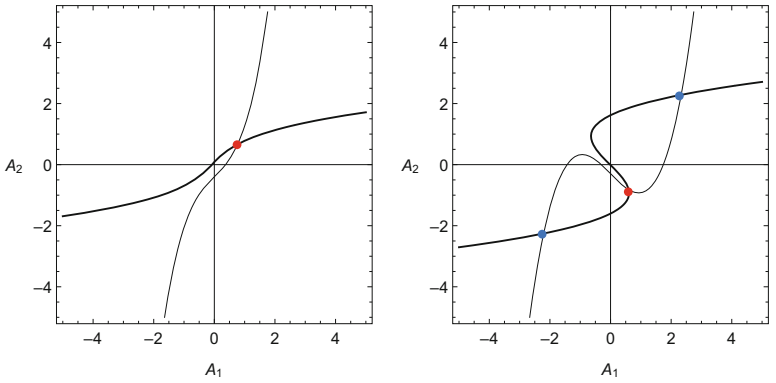

Fig. 5.5 The curves of smoothness for the accelerations $\ddot{x}_1(t)$ and $\ddot{x}_2(t)$ shown by thin and solid lines, respectively: for $\Omega = \sqrt{0.99}$ on the left, and $\Omega = \sqrt{3.01}$ on the right; the intersections correspond to solutions of system (5.62)

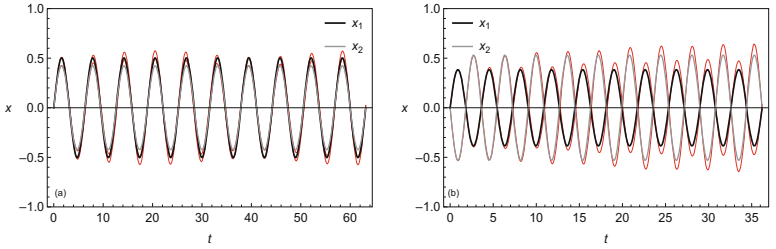

Fig. 5.6 The system response curves for: (**a**) $\Omega = \sqrt{0.99}$—close to the first natural frequency of a linearized system and (**b**) $\Omega = \sqrt{3.01}$—close to the second natural frequency; in both cases, thin red lines represent numerical solutions obtained under the initial conditions corresponding to the analytical solutions

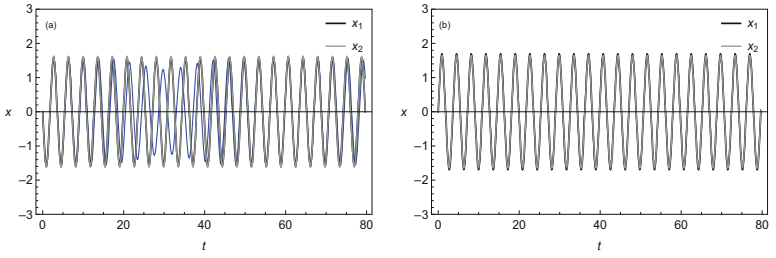

Fig. 5.7 Large amplitude inphase vibrations associated with the blue dots in the right fragment of Fig. 5.5 and corresponding to the frequency $\Omega = \sqrt{3.01}$, which is close to the antiphase natural frequency of linear vibrations

will lead to a significant divergence of the results. Moreover, the tails of polynomial expansions may give roots representing no real solution. Nonetheless, the above approaches seems to make sense as compared to those based on the direct Fourier expansions since the number of algebraic equations in (5.42), (5.51), or (5.62) is independent on the number of terms in the series.

5.3.2 NSTT of Lagrangian and Hamiltonian Equations

In different theoretical areas, describing systems in terms of the analytical dynamics brings some advantages because, until certain stage, it is sufficient to deal with a single scalar function such as Lagrangian or Hamiltonian rather than manipulate with a set of differential equations. Suppose the triangle wave temporal argument is introduced in Lagrangian or Hamiltonian. Let us show that the corresponding differential equations of motion are still derivable from the transformed descriptive functions in the standard way of the analytical dynamics.

Consider first Lagrangian that depends on time t periodically with the period $T = 4a$,

$$L = L(x, \dot{x}, t) \tag{5.63}$$

On the manifold of smooth periodic motions of the same period T, the vector-function $x(t)$ is represented as $x(t) = X(\tau) + Y(\tau)\, e$, where $\tau = \tau(t/a)$ and $e = e(t/a)$. As a result, Lagrangian (5.63) takes the form

$$L(x, \dot{x}, t) = R_L\left(X, Y, X', Y', \tau\right) + I_L\left(X, Y, X', Y', \tau\right) e \tag{5.64}$$

where both components on the right-hand side are determined analogously to expressions (5.48).

It can be verified by inspection that the differential equations of periodic motions can be represented now in either of the two equivalent Euler-Lagrange forms

$$\frac{d}{d\tau}\frac{\partial R_L}{\partial X'} - \frac{\partial R_L}{\partial X} = 0, \qquad \frac{d}{d\tau}\frac{\partial R_L}{\partial Y'} - \frac{\partial R_L}{\partial Y} = 0$$

or

$$\frac{d}{d\tau}\frac{\partial I_L}{\partial Y'} - \frac{\partial I_L}{\partial Y} = 0, \qquad \frac{d}{d\tau}\frac{\partial I_L}{\partial X'} - \frac{\partial I_L}{\partial X} = 0$$

Now let us consider the Hamiltonian

$$H = H(p, q, t) \tag{5.65}$$

which may be periodic with respect to time with the period $T = 4a$.

On the manifold of periodic motions of the period T, the generalized coordinates and momenta are represented as

$$q = X(\tau) + Y(\tau)\, e \quad \text{and} \quad p = U(\tau) + V(\tau)\, e$$

respectively, where $\tau = \tau(t/a)$ and $e = e(t/a)$.

Let us transform the Hamiltonian (5.65) as

$$H \longrightarrow aH(p, q, t) = R_{aH}(U, V, X, Y, \tau) + I_{aH}(U, V, X, Y, \tau)\, e$$

where

$$\left\{ \begin{matrix} R_{aH} \\ I_{aH} \end{matrix} \right\} = \frac{a}{2} \left[H(U + V, X + Y, a\tau) \pm H(U - V, X - Y, 2a - a\tau) \right]$$

The corresponding differential equations of periodic motions are

$$\frac{dX}{d\tau} = \frac{\partial R_{aH}}{\partial U}, \quad \frac{dY}{d\tau} = \frac{\partial R_{aH}}{\partial V}, \quad \frac{dU}{d\tau} = -\frac{\partial R_{aH}}{\partial X}, \quad \frac{dV}{d\tau} = -\frac{\partial R_{aH}}{\partial Y}$$

or

$$\frac{dX}{d\tau} = \frac{\partial I_{aH}}{\partial V}, \quad \frac{dY}{d\tau} = \frac{\partial I_{aH}}{\partial U}, \quad \frac{dU}{d\tau} = -\frac{\partial I_{aH}}{\partial Y}, \quad \frac{dV}{d\tau} = -\frac{\partial I_{aH}}{\partial X}$$

Besides, in autonomous cases, the operator Lie associates with the Poisson bracket, for instance,

$$GX = \{X, R_{aH}\}$$

Thus introducing the triangle wave temporal argument for periodic motions preserves both Lagrangian and Hamiltonian structures of the differential equations of motion.

5.3.3 *Remark on Multiple Argument Cases*

In multiple frequency cases, the smoothing procedures can be applied sequentially to each of the arguments. For instance, in the case of two arguments, $\tau_1 = \tau(t/a_1)$ and $\tau_2 = \tau(t/a_2)$, the X-component would take the form

$$X(\tau_1, \tau_2) = X(0, 0) + \sum_{i=1}^{N_1} \sum_{i=1}^{N_2} K_X(i, j) \left(\frac{\tau_1^i}{i} - \frac{\tau_1^{i+2}}{i+2} \right) \left(\frac{\tau_2^j}{j} - \frac{\tau_2^{j+2}}{j+2} \right) \tag{5.66}$$

where $K_X(i, j)$ are constant coefficients.

Analytical manipulations with 2D polynomials (5.66) are quite complicated because algebraic and differential operations affect the structure of participating binomials. Still expansions of type (5.66) can be used as approximations for solutions in different two-period cases. In static of 2D cell-wise composite structures, the parameters a_1 and a_2 are usually given by design, whereas the coefficients can be obtained by means of variational principles with automatic systems of symbolic manipulations followed by numerical algorithms.

Chapter 6
NSTT for Linear and Piecewise-Linear Systems

The tool of nonsmooth argument substitutions was introduced first to describe strongly nonlinear vibrations whose temporal mode shapes are asymptotically close to nonsmooth ones. Such cases are known to be most difficult for analyses because different quasi-harmonic methods are already ineffective, whereas the nonsmooth mapping is still inapplicable. It is quite clear however that the nonsmooth arguments can be introduced regardless of the strength of nonlinearity or the form of dynamical systems in general. For instance, it is shown in this chapter that the nonsmooth temporal substitutions can facilitate the analyses of different linear models with nonsmooth or discontinuous inputs.

6.1 Free Harmonic Oscillator: Temporal Quantization of Solutions

Introducing the triangle wave temporal argument into the differential equations of motion may bring some specific features into the corresponding solutions. For illustrating purposes, let us consider the harmonic oscillator

$$\ddot{x} + \Omega_0^2 x = 0 \tag{6.1}$$

First, let us obtain exact general solution of the oscillator (6.1) in terms of the triangle wave temporal argument by using the substitution

$$x = X(\tau) + Y(\tau)\, e \tag{6.2}$$

where $\tau = \tau(t/a)$ and $e = e(t/a)$ are the standard triangle and square wave functions, respectively.

V. N. Pilipchuk, *Oscillators and Oscillatory Signals from Smooth to Discontinuous*,
https://doi.org/10.1007/978-3-031-37788-4_6

Substituting (6.2) in (6.1) gives the boundary value problem

$$a^{-2}X''(\tau) + \Omega_0^2 X(\tau) = 0 \tag{6.3}$$

$$a^{-2}Y''(\tau) + \Omega_0^2 Y(\tau) = 0 \tag{6.4}$$

$$X'(\pm 1) = 0, Y(\pm 1) = 0 \tag{6.5}$$

By considering the parameter a as an eigen-value of the problem, one obtains the set of eigen-values and the corresponding solutions as, respectively,

$$a_j = \frac{j\pi}{2\Omega_0} \tag{6.6}$$

and

$$X_j = \sin\left(\frac{j\pi\tau}{2} + \varphi_j\right), \quad Y_j = \cos\left(\frac{j\pi\tau}{2} - \varphi_j\right) \tag{6.7}$$

where $\varphi_j = (\pi/4)[1 + (-1)^j]$, $\tau = \tau(t/a_j)$, and j is any positive real integer.

Therefore, introducing the triangle wave oscillating time produced the discrete family of solutions for harmonic oscillator (6.1). The nature of such kind of quantization is due to the temporal symmetry of periodic motions. In other words, the quantization is associated with a multiple choice for the period

$$T_j = 4a_j = jT \tag{6.8}$$

where $T = 2\pi/\Omega_0$ is the natural period of oscillator (6.1).

In terms of the original temporal variable t, the number j plays no role for the temporal mode shape, given by

$$\begin{aligned} x(t) = A\sin\left[\frac{j\pi}{2}\tau\left(\frac{2\Omega_0 t}{j\pi}\right) + \varphi_j\right] \\ + B\cos\left[\frac{j\pi}{2}\tau\left(\frac{2\Omega_0 t}{j\pi}\right) - \varphi_j\right] e\left(\frac{2\Omega_0 t}{j\pi}\right) \end{aligned} \tag{6.9}$$

where A and B are arbitrary constants, and $x(t)$ is the same harmonic wave regardless of the number j.

In this section, the free linear oscillator was considered for illustrating purposes. There is no other pragmatic reason for introducing the triangle wave time into Eq. (6.1). The situation drastically changes however in non-autonomous cases of nonsmooth or discontinuous inputs. It is shown below that, in such cases, the triangle wave time variable facilitates determining particular solutions. The above-noticed effect of temporal quantization, which is just an identical transformation in the autonomous case, becomes helpful at the presence of external excitations. For instance, according to (6.9), the so-called combination resonances appear to be an inherent property of oscillators.

6.2 Non-autonomous Case

6.2.1 Unipotent Basis

Consider the linear harmonic oscillator under the external forcing described by the linear combination of triangle and square wave functions

$$\ddot{x} + \Omega_0^2 x = F\tau\left(\frac{t}{a}\right) + Ge\left(\frac{t}{a}\right) \tag{6.10}$$

where F and G are constant amplitudes and a is a quarter of the period.

Substituting (6.2) in (6.10) leads to the boundary value problem

$$a^{-2}X''(\tau) + \Omega_0^2 X(\tau) = F\tau \tag{6.11}$$

$$a^{-2}Y''(\tau) + \Omega_0^2 Y(\tau) = G \tag{6.12}$$

under the boundary conditions (6.5).

In contrast to autonomous case (6.1), the parameter a is known. Equations (6.11) and (6.12), are non-homogeneous, and their non-zero solution exists for any a and can be found in few elementary steps. The particular periodic solution of the original Eq. (6.10) takes the form

$$x_p(t) = X(\tau) + Y(\tau)\, e = \frac{F}{\Omega_0^2}\left\{\tau\left(\frac{t}{a}\right) - \frac{\sin\left[a\Omega_0\tau\,(t/a)\right]}{a\Omega_0\cos(a\Omega_0)}\right\}$$
$$+\frac{G}{\Omega_0^2}\left\{1 - \frac{\cos\left[a\Omega_0\tau\,(t/a)\right]}{\cos(a\Omega_0)}\right\} e\left(\frac{t}{a}\right) \tag{6.13}$$

The corresponding general solution is $x(t) = A\cos(\Omega_0 t - \varphi) + x_p(t)$, where A and φ are arbitrary amplitude and phase parameters. Note that solution (6.13) immediately shows all possible resonance combinations $a\Omega_0 = (2k+1)\pi/2$ or

$$\frac{\Omega_0}{\Omega} = 2k + 1 \tag{6.14}$$

where $k = 1, 2, 3\ldots$ and $\Omega = 2\pi/T = \pi/(2a)$ is the fundamental frequency of the external forcing.

Let us compare solution (6.13) to solution obtained by using Fourier series

$$\tau\left(\frac{t}{a}\right) = \frac{8}{\pi^2}\sum_{k=0}^{\infty}\frac{(-1)^k}{(2k+1)^2}\sin[(2k+1)\,\Omega t] \tag{6.15}$$

$$e\left(\frac{t}{a}\right) = \frac{4}{\pi}\sum_{k=0}^{\infty}\frac{(-1)^k}{(2k+1)}\cos[(2k+1)\,\Omega t]$$

These lead to the particular solution of Eq. (6.10) in the form

$$x_p(t) = \sum_{k=0}^{\infty} \frac{(-1)^k}{\Omega_0^2 - (2k+1)^2 \Omega^2} \times \\ \times \left[\frac{8F}{\pi^2 (2k+1)^2} \sin[(2k+1)\Omega t] + \frac{4G}{\pi (2k+1)} \cos[(2k+1)\Omega t] \right] \tag{6.16}$$

Solution (6.16) reveals the same resonance conditions, (6.14). However, the infinite trigonometric series are less convenient for calculations, especially when dealing with derivatives of solutions since differentiation slows down convergence of the series.

6.2.2 Idempotent Basis

Consider the linear oscillator including viscous damping under the square wave external loading

$$\ddot{x} + 2\zeta \Omega_0 \dot{x} + \Omega_0^2 x = pe\left(\frac{t}{a}\right) \tag{6.17}$$

The purpose is to obtain periodic steady-state solution with the period of external loading, $T = 4a$. Recall that the idempotent basis is introduced by means of the linear transformation

$$\{1, e\} \longrightarrow \{e_+, e_-\}: \qquad e_\pm = \frac{1}{2}(1 \pm e) \tag{6.18}$$

or, inversely, $1 = e_+ + e_-$ and $e = e_+ - e_-$, where $e_\pm^2 = e_\pm$ and $e_+ e_- = 0$; see Chaps. 1 and 4.

Now, the periodic solution and external loading are represented in the new basis as

$$x(t) = U(\tau) e_+ + V(\tau) e_- \\ pe = p(e_+ - e_-) \tag{6.19}$$

where $e_\pm = e_\pm(t/a)$ and $U(\tau)$ and $V(\tau)$ are unknown functions of the triangle wave, $\tau = \tau(t/a)$.

Substituting (6.19) in (6.17) and sequentially eliminating derivatives of the square wave, as described in Chap. 4, give equations

$$U'' + 2\zeta \Omega_0 a U' + (\Omega_0 a)^2 U = pa^2 \\ V'' - 2\zeta \Omega_0 a V' + (\Omega_0 a)^2 V = -pa^2 \tag{6.20}$$

with boundary conditions

$$(U - V)|_{\tau=\pm1} = 0$$
$$(U' + V')|_{\tau=\pm1} = 0 \tag{6.21}$$

All the coefficients and right-hand sides of both equations in (6.20) are constant, and the equations are decoupled. As a result, solution of boundary value problem, (6.20) and (6.21), is obtained in the closed form

$$U(\tau) = \frac{p}{\Omega_0^2} - \frac{2p\exp(-\alpha\tau)}{\beta\Omega_0^2(\cos 2\beta + \cosh 2\alpha)} \tag{6.22}$$
$$\times[\cos\beta\cosh\alpha(\beta\cos\beta\tau + \alpha\sin\beta\tau) + \sin\beta\sinh\alpha(\alpha\cos\beta\tau - \beta\sin\beta\tau)]$$

$$V(\tau) = -\frac{p}{\Omega_0^2} + \frac{2p\exp(\alpha\tau)}{\beta\Omega_0^2(\cos 2\beta + \cosh 2\alpha)} \tag{6.23}$$
$$\times[\cos\beta\cosh\alpha(\beta\cos\beta\tau - \alpha\sin\beta\tau) + \sin\beta\sinh\alpha(\alpha\cos\beta\tau + \beta\sin\beta\tau)]$$

where $\alpha = a\zeta\Omega_0$ and $\beta = a\Omega_0\sqrt{1-\zeta^2}$.

Substituting (6.22) and (6.23) in (6.19) gives the closed form particular solution of original Eq. (6.17). Transition to the original temporal variable is given by the functions $\tau(\varphi) = (2/\pi)\arcsin[\sin(\pi\varphi/2)]$ and $e(\varphi) = \mathrm{sgn}[\cos(\pi\varphi/2)]$. Since the system under consideration is linear, the general solution of Eq. (6.17) can be obtained by adding general solution of the corresponding equation with zero right-hand side.

6.3 Systems Under Periodic Pulsed Excitation

Instantaneous impulses acting on a mechanical system can be modeled either by imposing specific matching conditions on the system state vector at pulse times or by introducing Dirac functions into the differential equations of motion. The first approach deals with the differential equations of a free system separately between the impulses; therefore, a sequence of systems under the matching conditions are considered. The second method gives a single set of equations over the whole time interval without any conditions of matching. In latter case, the analysis can be carried out correctly in terms of distributions that requires additional mathematical justifications in nonlinear cases. Both of the above approaches are used for different quantitative and qualitative analyses. The analytical tool, which is described below, eliminates the singular terms from the equations. As a result, solutions are obtained in a closed form of a single analytical expression for the whole time interval.

6.3.1 Regular Periodic Impulses

Introducing the triangle wave temporal argument may significantly simplify solutions whenever loading functions are combined of the triangular wave and its derivatives. For instance, let us seek a particular solution of the first-order differential equation[1]

$$\dot{v} + \lambda v = \mu \sum_{k=-\infty}^{\infty} \left[\delta\left(t + 1 - 4k\right) - \delta\left(t - 1 - 4k\right)\right] \tag{6.24}$$

where λ and μ are constant parameters.

For positive λ, Eq. (6.24) describes the velocity of a particle moving in a viscous media under the periodic impulsive force. The corresponding physical model is shown in Fig. 6.1, where the freely moving massive tank experiences perfectly elastic reflections from the stiff obstacles. By scaling the variables, one can bring the differential equation of motion of the particle to the form (6.24), where $v\left(t\right) = \dot{x}\left(t\right)$.

First, note that the right-hand side of Eq. (6.24) can be expressed through the generalized derivative of the square wave as follows:

$$\dot{v} + \lambda v = \frac{\mu}{2} \dot{e}\left(t\right) \tag{6.25}$$

Now let us represent the particular solution in the form

$$v\left(t\right) = X\left(\tau\left(t\right)\right) + Y\left(\tau\left(t\right)\right) e\left(t\right) \tag{6.26}$$

Substituting (6.26) in (6.25) gives

$$Y' + \lambda X + \left(X' + \lambda Y\right) e\left(t\right) + \underline{\left(Y - \frac{\mu}{2}\right) \dot{e}\left(t\right)} = 0 \tag{6.27}$$

Apparently, the elements $\{1, e\}$ and $\dot{e}$ on the left-hand side of Eq. (6.27) are linearly independent as functions of different classes of smoothness. Therefore,

$$Y' + \lambda X = 0, \qquad X' + \lambda Y = 0, \qquad Y|_{\tau=\pm 1} = \frac{\mu}{2} \tag{6.28}$$

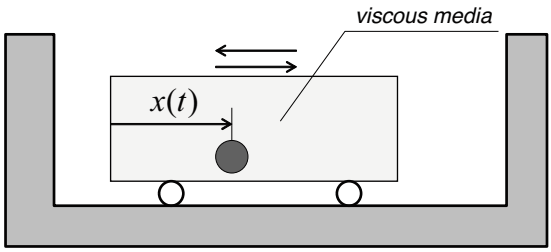

Fig. 6.1 If mass of the particle is very small compared to the total mass of the tank, then the inertia force applied to the particle inside the tank has a periodic pulse-wise character

[1] The case of Dirac comb input was considered in Chap. 1.

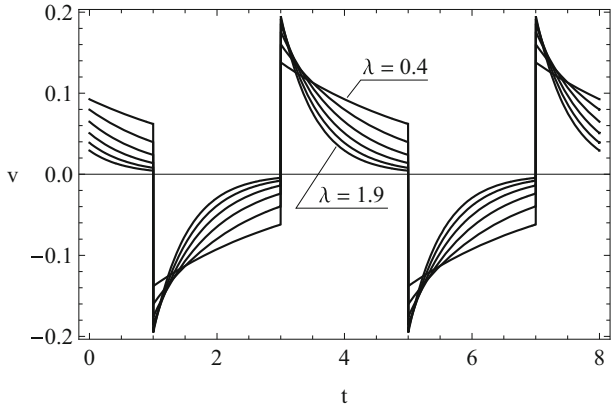

Fig. 6.2 The family of discontinuous periodic solutions for different viscosity parameter of the media inside the tank (Fig. 6.1)

In contrast to Eq. (6.24), this boundary value problem includes no discontinuities, whereas the new independent variable belongs to the standard interval, $-1 \leq \tau \leq 1$. Solving the boundary value problem (6.28) and taking into account substitution (6.26) give the periodic solution of Eq. (6.24) as

$$v = X + Ye = \frac{\mu}{2\cosh\lambda}\left(-\sinh\lambda\tau + e\cosh\lambda\tau\right)$$

or

$$v = \frac{\mu}{2\cosh\lambda}\exp\left[-\lambda\tau\left(t\right)e\left(t\right)\right]e\left(t\right) \tag{6.29}$$

Figure 6.2 illustrates solution (6.29) for $\mu = 0.2$ and different magnitudes of λ.

Note that the discontinuous solution $v\left(t\right)$ is described by the closed form expression (6.29) through the two elementary functions $\tau\left(t\right)$ and $e\left(t\right)$.

6.3.2 *Harmonic Oscillators Under the Periodic Impulsive Loading*

Resonances in Zero Damping Case

Let us consider the harmonic oscillator subjected to periodic pulses

$$\ddot{x} + \Omega_0^2 x = 2p\sum_{k=-\infty}^{\infty}\left[\delta\left(\omega t + 1 - 4k\right) - \delta\left(\omega t - 1 - 4k\right)\right] \tag{6.30}$$

where p, Ω_0 and ω are constant parameters.

The right-hand side of Eq. (6.30) can be expressed through the first derivative of the square wave as follows:

$$\ddot{x} + \Omega_0^2 x = p \frac{de\,(\omega t)}{d\,(\omega t)} \tag{6.31}$$

Let us seek a periodic solution of the period $T = 4/\omega$ in the form

$$x\,(t) = X\,(\tau\,(\omega t)) + Y\,(\tau\,(\omega t))\,e\,(\omega t) \tag{6.32}$$

Substituting (6.32) in (6.31) under the necessary condition of continuity for the coordinate, $x\,(t)$, gives

$$\omega^2 X'' + \Omega_0^2 X + \left(\omega^2 Y'' + \Omega_0^2 Y\right) e + \underline{\left(\omega^2 X' - p\right) \frac{de\,(\omega t)}{d\,(\omega t)}} = 0 \tag{6.33}$$

Analogously to the previous subsection, Eq. (6.33) gives the boundary value problem

$$X'' + \left(\frac{\Omega_0}{\omega}\right)^2 X = 0, \qquad Y'' + \left(\frac{\Omega_0}{\omega}\right)^2 Y = 0 \tag{6.34}$$

$$X'|_{\tau=\pm 1} = \frac{p}{\omega^2}, \qquad Y|_{\tau=\pm 1} = 0$$

Solving problem (6.34) and taking into account (6.32) give the periodic solution of the original Eq. (6.30) in the form

$$x = X\,(\tau\,(\omega t)) = \frac{p}{\omega \Omega_0} \frac{\sin\left[(\Omega_0/\omega)\,\tau\,(\omega t)\right]}{\cos\,(\Omega_0/\omega)} \tag{6.35}$$

where $Y \equiv 0$.

Solution (6.35) is continuous although nonsmooth at those times t where $\tau\,(\omega t) = \pm 1$. All possible resonances are given by

$$\omega = \frac{2}{\pi} \frac{\Omega_0}{k}; \qquad k = 1, 3, 5, \ldots \tag{6.36}$$

where the factor $2/\pi$ is due to different normalization of the periods for sine and triangle waves.

Viscous Damping Case

Now let us consider the case of standard harmonic oscillator described by the differential equation of motion

$$\ddot{x} + 2\zeta\Omega_0\dot{x} + \Omega_0^2 x = p\frac{de(\omega t)}{d(\omega t)} \tag{6.37}$$

where ζ is the damping ratio.

In this case, the boundary value problem becomes coupled

$$X'|_{\tau=\pm1} = \frac{p}{\omega^2}, \qquad Y|_{\tau=\pm1} = 0$$

$$\begin{aligned} X'' + 2\zeta r Y' + r^2 X &= 0 \\ Y'' + 2\zeta r X' + r^2 Y &= 0 \end{aligned} \tag{6.38}$$

where $r = \Omega_0/\omega$ is the adjusted natural over loading frequency ratio. Recall that the sine wave frequency is given by $\Omega = (\pi/2)\omega$. The principal resonance ratio is therefore $r = \pi/2$, which is obviously equivalent to $\Omega_0 = \Omega$.

As a result, the periodic solution has both X and Y components and is given by

$$\begin{aligned} x = X + Ye = &\frac{p}{\beta\omega^2\left(\cos^2\beta\cosh^2\alpha + \sin^2\beta\sinh^2\alpha\right)} \\ &\times[\cosh\alpha\cos\beta\cosh\alpha\tau\sin\beta\tau - \sinh\alpha\sin\beta\sinh\alpha\tau\cos\beta\tau \\ &+ (\sinh\alpha\cos\beta\tau\cosh\alpha\tau\sin\beta - \sinh\alpha\tau\sin\beta\tau\cosh\alpha\cos\beta)\,e] \end{aligned} \tag{6.39}$$

where $\tau = \tau(\omega t)$, $e = e(\omega t)$; $\alpha = r\zeta$ and $\beta = r\sqrt{1-\zeta^2}$.

Figure 6.3 illustrates qualitatively different responses of the system when varying the input frequency. In different proportions, the responses combine properties of the harmonic damped motion and the nonsmooth motion due to the impulsive loading. For instance, when $\omega >> \Omega_0$ and $\omega >> \zeta\Omega_0$, the system is near the limit of a free particle under the periodic impulsive force. In this case, the boundary value problem is reduced to

$$X'' = 0, \qquad Y'' = 0; \qquad X'|_{\tau=\pm1} = \frac{p}{\omega^2}, \qquad Y|_{\tau=\pm1} = 0 \tag{6.40}$$

This gives the triangle wave temporal shape, $x = p\tau(\omega t)/\omega^2$, which is close to the shape in Fig. 6.3d.

Multiple Degrees-of-Freedom Case

Finally, let us consider N-degrees-of-freedom system

$$M\ddot{\mathbf{y}} + K\mathbf{y} = \mathbf{p}\frac{de(\omega t)}{d(\omega t)} \tag{6.41}$$

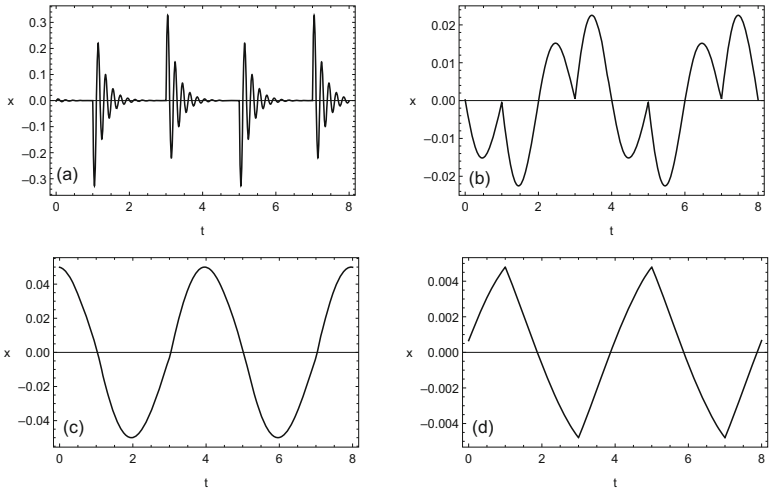

Fig. 6.3 Evolution of the response of the damped harmonic oscillator under the periodic impulsive excitation for $p = 0.1$, $\zeta = 0.125$, $\Omega_0 = 4.0$, and different impulse frequencies $\Omega = (\pi/2)\omega$: (**a**) $\Omega = 0.2$—low-frequency Impulses, (**b**) $\Omega = 2.0$, (**c**) $\Omega = \Omega_0$, and (**d**) $\Omega = 8.0$

where $\mathbf{y}(t)$ is N-dimensional vector-function, $\mathbf{p}$ is a constant vector, and M and K are constant $N \times N$ mass and stiffness matrixes, respectively.

Let $\{\mathbf{e}_1, \ldots, \mathbf{e}_N\}$ and $\Omega_1, \ldots, \Omega_N$ be the normal mode basis vectors and the corresponding natural frequencies, respectively, such that

$$K\mathbf{e}_j = \Omega_j^2 M\mathbf{e}_j, \qquad \mathbf{e}_k^T M\mathbf{e}_j = \delta_{kj}$$

for any $k = 1, \ldots, N$ and $j = 1, \ldots, N$.

Introducing the principal coordinates $x^j(t)$,

$$\mathbf{y} = \sum_{j=1}^{N} x^j(t)\,\mathbf{e}_j \tag{6.42}$$

gives a decoupled set of impulsively forced harmonic oscillators of the form (6.31),

$$\ddot{x}^j + \Omega_j^2 x^j = p^j \frac{de(\omega t)}{d(\omega t)} \tag{6.43}$$

where $p^j = \mathbf{e}_j^T \mathbf{p}$.

Therefore, using solution (6.35) for each of the oscillators (6.43) and taking into account (6.42) give

$$\mathbf{y} = \sum_{j=1}^{N} \frac{(\mathbf{e}_j^T \mathbf{p})\mathbf{e}_j}{\omega\Omega_j} \frac{\sin\left[\left(\Omega_j/\omega\right)\tau(\omega t)\right]}{\cos\left(\Omega_j/\omega\right)} \tag{6.44}$$

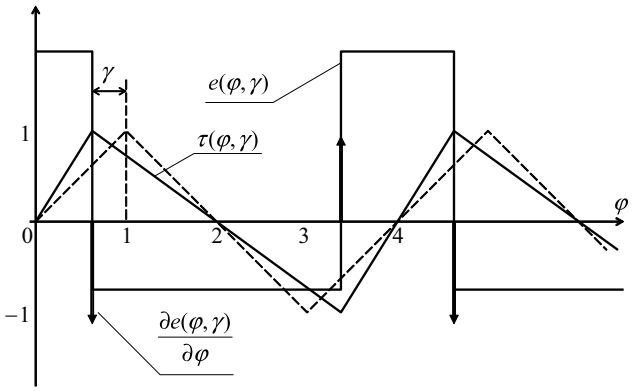

Fig. 6.4 Basic NSTT asymmetric wave functions

The corresponding resonances are determined by the condition

$$\omega = \frac{2}{\pi}\frac{\Omega_j}{k}$$

where $k = 1, 3, 5, \ldots$ and $j = 1, \ldots, N$.

6.3.3 *Periodic Impulses with a Temporal Dipole Shift*

Let us consider the impulsive excitation with a dipole wise shift of pulse times. In this case, the right-hand side of Eq. (6.25) can be expressed by second derivative of the asymmetric triangle wave with some incline[2] characterized by the parameter γ as shown in Fig. 6.4

$$\dot{v} + \lambda v = p\frac{\partial^2 \tau\,(\omega t, \gamma)}{\partial\,(\omega t)^2} = p\frac{\partial e\,(\omega t, \gamma)}{\partial\,(\omega t)} \tag{6.45}$$

$$= \frac{2p}{1-\gamma^2}\sum_{k=-\infty}^{\infty}\left[\delta\,(\omega t + 1 - \gamma - 4k) - \delta\,(\omega t - 1 + \gamma - 4k)\right]$$

Based on the NSTT identities introduced in Chap. 4, periodic solutions of Eq. (6.45) still can be represented in the form

$$v = X\,(\tau) + Y\,(\tau)\,e \tag{6.46}$$

where $\tau = \tau\,(\omega t, \gamma)$ and $e = e\,(\omega t, \gamma)$; see Fig. 6.4 for graphic illustrations.

[2] Can be viewed as a generalized sawtooth function.

Substituting (6.46) in Eq. (6.45) gives

$$\omega\alpha Y' + \lambda X + \left[\omega\left(X' + \beta Y'\right) + \lambda Y\right] e + (\omega Y - p)\frac{\partial e(\omega t, \gamma)}{\partial(\omega t)} = 0 \tag{6.47}$$

where $\alpha = 1/\left(1 - \gamma^2\right)$, $\beta = 2\gamma\alpha$, and the identity $e^2 = \alpha + \beta e$ has been taken into account.

Equation (6.47) is equivalent to the boundary-value problem

$$\begin{aligned} \omega\left(X' + \beta Y'\right) &= -\lambda Y \\ \omega\alpha Y' &= -\lambda X \\ \omega Y|_{\tau=\pm 1} &= p \end{aligned} \tag{6.48}$$

The corresponding solution is

$$\begin{aligned} Y &= \frac{p}{\omega}\left[\cosh\left(\gamma\frac{\lambda}{\omega}\right)\frac{\cosh\left(\frac{\lambda}{\omega}\tau\right)}{\cosh\frac{\lambda}{\omega}} - \sinh\left(\gamma\frac{\lambda}{\omega}\right)\frac{\sinh\left(\frac{\lambda}{\omega}\tau\right)}{\sinh\frac{\lambda}{\omega}}\right]\exp\left(\gamma\frac{\lambda}{\omega}\tau\right) \\ X &= -\frac{\omega\alpha}{\lambda}Y' \end{aligned} \tag{6.49}$$

where the X-component is defined by differentiation due to the second equation in (6.48).

6.4 Parametric Excitation

In this section, two different cases of parametric excitation are considered based on relatively simple linear models. Piecewise-constant and impulsive excitations are described by means of the functions $e(\omega t, \gamma)$ and $\partial e(\omega t, \gamma)/\partial(\omega t)$, respectively. There are at two least reasons for using NSTT as a preliminary analytical step. First, NSTT automatically gives conditions for matching solutions at discontinuity points. Second, due to the automatic matching through the NSTT functions, the corresponding solutions appear to be in the closed form that is important feature when further manipulations with the solutions are required by problem formulations.

6.4.1 Piecewise-Constant Excitation

Let us consider the linear oscillator under the periodic piecewise-constant parametric excitation

$$\ddot{x} + \Omega_0^2[1 + \varepsilon e(\omega t, \gamma)]x = 0 \tag{6.50}$$

where Ω_0, ω, γ, and ε are constant parameters.

We seek periodic solutions with the period of excitation $T = 4/\omega$ in the form

$$x = X(\tau) + Y(\tau)\, e \tag{6.51}$$

where $\tau = \tau(\omega t, \gamma)$ and $e = e(\omega t, \gamma)$.

As follows from the form of Eq. (6.50), the acceleration $\ddot{x}$ may have stepwise discontinuities due to the presence of the function $e(\omega t, \gamma)$, whereas the coordinate $x(t)$ and the velocity $\dot{x}(t)$ must be continuous. Hence neither velocity $\dot{x}(t)$ nor acceleration $\ddot{x}(t)$ can include Dirac δ-functions. Taking first derivative of (6.51) gives

$$\dot{x}(t) = \left[\alpha Y' + (X' + \beta Y')e + \underline{Y \frac{\partial e(\omega t, \gamma)}{\partial(\omega t)}}\right]\omega \tag{6.52}$$

where the last term that consists of the periodic sequence of δ-functions must be excluded by imposing the boundary condition for Y-component

$$Y\,|_{\tau=\pm 1} = 0 \tag{6.53}$$

Under condition (6.53), the second derivative takes the form

$$\begin{aligned}\ddot{x}(t) = \omega^2[\alpha(X'' + \beta Y'')] + \omega^2[\beta X'' + (\alpha + \beta^2)Y'']e \\ + \underline{\omega^2(X' + \beta Y')\frac{\partial e(\omega t, \gamma)}{\partial(\omega t)}}\end{aligned} \tag{6.54}$$

In this case, the singular term, which is underlined in (6.54), is eliminated by condition

$$\left(X' + \beta Y'\right)|_{\tau=\pm 1} = 0 \tag{6.55}$$

Substituting (6.51) and (6.54) in the differential equation of motion (6.50) and taking into account the algebraic properties of hyperbolic numbers bring the left-hand side of the equation to the form $\{\cdots\} + \{\cdots\}e$. Then, setting separately each of the two algebraic components to zero gives a set of the differential equations for $X(\tau)$ and $Y(\tau)$ in the following matrix form:

$$\begin{bmatrix} \alpha & \alpha\beta \\ \beta & \alpha + \beta^2 \end{bmatrix} \frac{d^2}{d\tau^2} \begin{bmatrix} X \\ Y \end{bmatrix} + r^2 \begin{bmatrix} 1 & \alpha\varepsilon \\ \varepsilon & 1 + \beta\varepsilon \end{bmatrix} \begin{bmatrix} X \\ Y \end{bmatrix} = 0 \tag{6.56}$$

where $r = \Omega_0/\omega$

Further, any particular solution of linear differential equations with constant coefficients (6.56) is represented in the exponential form

$$\begin{bmatrix} X \\ Y \end{bmatrix} = B \begin{bmatrix} 1 \\ \mu \end{bmatrix} \exp(\lambda\tau) \tag{6.57}$$

where B, μ, and λ are constant parameters.

Substituting (6.57) in (6.56) and using the relationships, $\alpha = 1/\left(1-\gamma^2\right)$ and $\beta = 2\gamma\alpha$, lead to the characteristic equation with two pairs of roots determined by

$$\begin{aligned} \lambda^2 &= \left[-(1-\gamma)\,\varepsilon - (1-\gamma)^2\right] r^2 \equiv \pm k^2 \\ \lambda^2 &= \left[(1+\gamma)\,\varepsilon - (1+\gamma)^2\right] r^2 \equiv \pm l^2 \end{aligned} \tag{6.58}$$

where signs of the notations $\pm k^2$ and $\pm l^2$ depend on the parameters ε and γ.

Let us consider the case of negative signs on the right-hand side of (6.58), when the following condition holds:

$$-(1-\gamma) < \varepsilon < (1+\gamma) \tag{6.59}$$

Due to condition (6.59), the stiffness coefficient in Eq. (6.50) is always positive, whereas (6.58) gives $\lambda = \pm ki$ and $\lambda = \pm li$.As a result, the general solution of Eqs. (6.56) takes the form

$$\begin{aligned} X &= B_1 \sin k\tau + B_2 \cos k\tau + B_3 \sin l\tau + B_4 \cos l\tau \\ Y &= \mu_1 (B_1 \sin k\tau + B_2 \cos k\tau) + \mu_2 (B_3 \sin l\tau + B_4 \cos l\tau) \end{aligned} \tag{6.60}$$

where $B_1,\ldots,B_4$ are arbitrary constants, and

$$\mu_1 = -\frac{1}{\alpha}\frac{\alpha k^2 - r^2}{\beta k^2 - \varepsilon r^2} \qquad \text{and} \qquad \mu_2 = -\frac{1}{\alpha}\frac{\alpha l^2 - r^2}{\beta l^2 - \varepsilon r^2}$$

Substituting (6.60) in boundary conditions (6.53) and (6.55) gives the homogeneous set of four linear algebraic equations with respect to the arbitrary constants whose matrix is

$$\begin{bmatrix} \mu_1 \sin k & \mu_1 \cos k & \mu_2 \sin l & \mu_2 \cos l \\ -\mu_1 \sin k & \mu_1 \cos k & -\mu_2 \sin l & \mu_2 \cos l \\ k(1+\beta\mu_1)\cos k & -k(1+\beta\mu_1)\sin k & l(1+\beta\mu_2)\cos l & -l(1+\beta\mu_2)\sin l \\ k(1+\beta\mu_1)\cos k & k(1+\beta\mu_1)\sin k & l(1+\beta\mu_2)\cos l & l(1+\beta\mu_2)\sin l \end{bmatrix}$$

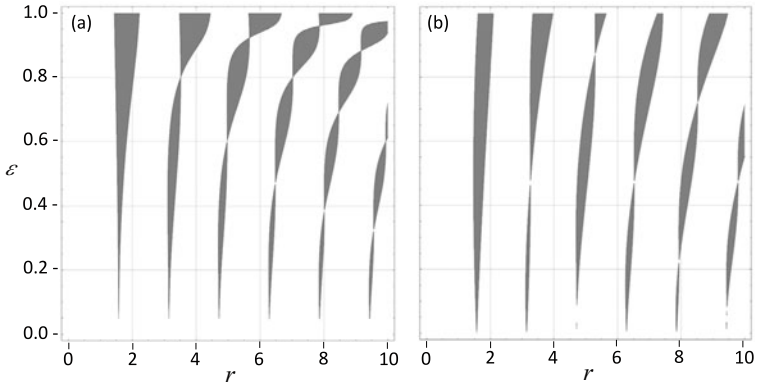

Fig. 6.5 Instability zones of oscillator (6.50) under the piecewise constant parametric excitation for (**a**) $\gamma = 0.0$ and (**b**) $\gamma = 0.7$, where $r = \Omega_0/\omega$

Calculation of the determinant can be eased essentially after a proper summation and subtraction of its rows. Then setting it to zero gives a condition for non-zero solutions in the form

$$\begin{aligned}&\left[\mu_1\left(1+\beta\mu_2\right)l\cos k\sin l-\mu_2\left(1+\beta\mu_1\right)k\cos l\sin k\right]\\&\quad\times\left[\mu_1\left(1+\beta\mu_2\right)l\cos l\sin k-\mu_2\left(1+\beta\mu_1\right)k\cos k\sin l\right]=0\end{aligned}\tag{6.61}$$

Equation (6.61) describes the family of curves separating stability and instability zones on the plane (r, ε) as shown in Fig. 6.5, where the instability zones are shadowed.

The diagrams in Fig. 6.5 are interpreted in a similar way to Ince-Strutt diagrams showing the transition curves in the parameters' plane. The curves divide the plane into regions corresponding to unbounded/unstable and regions of bounded/stable solutions.

6.4.2 Parametric Impulsive Excitation

Let us consider the case of parametric impulsive excitation whose temporal shape is given by first derivative of the generalized square wave, $e(\omega t, \gamma)$, [177]

$$\ddot{x}+\Omega_0^2\left[1+\varepsilon\frac{\partial e\left(\varphi,\gamma\right)}{\partial\varphi}\right]x=0\tag{6.62}$$

where $\varphi = \omega t$, and

$$\frac{\partial e(\varphi,\gamma)}{\partial \varphi} = \frac{\partial^2 \tau(\varphi,\gamma)}{\partial \varphi^2} = \frac{2}{1-\gamma^2}\sum_{k=-\infty}^{\infty}\left[\delta(\varphi+1-\gamma-4k)-\delta(\varphi-1+\gamma-4k)\right]$$

In this case, when substituting (6.51) and (6.54) in Eq. (6.62), the singular term of second derivative (6.54) must be preserved in order to compensate the singularity in Eq. (6.62). The result of such a compensation leads to the boundary conditions (compare to (6.55))

$$\tau = \pm 1: \qquad \omega^2(X' + \beta Y') + \varepsilon \Omega_0^2 X = 0 \tag{6.63}$$

Note that substitution of (6.51) in Eq. (6.62) generates the term $(\partial e/\partial\varphi)eY$, which is generally undefined in the theory of distributions. This term represents a periodic series of δ-functions, $\partial e/\partial\varphi$, "multiplied" by the function e whose stepwise discontinuities coincide with the times of δ-functions, $\{\varphi : \tau(\varphi,\gamma) = \pm 1\}$. Some interpretations of such terms are still possible only within specific contents assuming the common physical nature for both singularities as discussed in the next section. In the present case, the term $(\partial e/\partial\varphi)eY$ is simply removed from the equation since the point-wise singularities at $\{\varphi : \tau(\varphi,\gamma) = \pm 1\}$ are suppressed by continuity condition (6.53) for the coordinate x: $Y\,|_{\tau=\pm 1} = 0$. Then combining separately two group of terms associated with different structural parts of the hyperbolic number gives

$$\begin{bmatrix} \alpha & \alpha\beta \\ \beta & \alpha+\beta^2 \end{bmatrix} \frac{d^2}{d\tau^2}\begin{bmatrix} X \\ Y \end{bmatrix} + r^2 \begin{bmatrix} 1 & 0 \\ 0 & 1 \end{bmatrix}\begin{bmatrix} X \\ Y \end{bmatrix} = 0 \tag{6.64}$$

where $r = \Omega_0/\omega$.

Further steps follow the previous section. Substituting (6.57) in (6.64) leads to the characteristic equation whose two pairs of roots λ and the corresponding amplitude ratios μ are given by

$$\lambda = \pm ki = \pm r(1+\gamma)i, \qquad \mu_1 = -1+\gamma$$
$$\lambda = \pm li = \pm r(1-\gamma)i, \qquad \mu_2 = 1+\gamma$$

where the notations $\alpha = 1/\left(1-\gamma^2\right)$ and $\beta = 2\gamma\alpha$ were taken into account.

Then, substituting (6.60) in boundary conditions, (6.53) and (6.63), gives a homogeneous linear algebraic system for the constants $B_1, \ldots, B_4$. Setting its determinant to zero gives the condition of existence of the period, $T = 4/\omega$, as

$$\varepsilon^2 = \frac{2\left(1-\gamma^2\right)^2 \sin^2 2r}{r^2(\cos 4r - \cos 4\gamma r)} \tag{6.65}$$

The dependence of ε on r at fixed γ has a branched zone-like structure on the plane (r, ε) which is typical for different cases of parametrically excited oscillators. Interestingly enough, different subsequences of zones may disappear as the parameter γ varies. For instance, the number $\gamma = 1/2$ eliminates every second zone, whereas the number $\gamma = 1/5$ removes every fifth zone. The effect of collapsing instability zones can be explained by considering the regions of definition for condition (6.65), $\cos 4r - \cos 4\gamma r > 0$. This inequality holds inside the white regions on the plane (r, γ) as shown in Fig. 6.6. It is seen that the bottom horizontal line, $\gamma = 1/5$, intersects four white regions before it starts crossing two shadowed areas with no white one in between. It happens because the line intersects the (blue) point at the corners of two shadowed regions. The corresponding vertical straight line, which is intersecting the same point, corresponds to one of the roots of the equation $\sin 2r = 0$. This root, $r = 5\pi/2$, locates the point on the r-axis, from which the missing instability zone would branch out if the line $\gamma = 1/5$ were slightly shifted up or down. Another horizontal line, $\gamma = 1/5$, gives the example, when every second zone is missing.

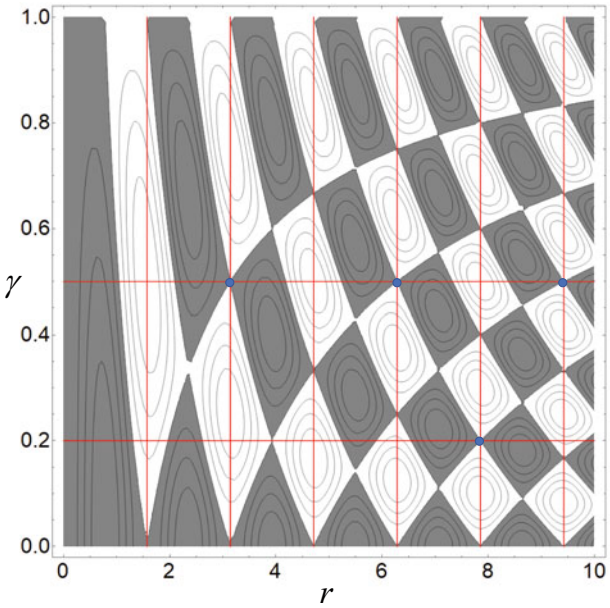

Fig. 6.6 The regions of definition for condition (6.65) are shown in white color; the locations of blue dots explain why the corresponding zones of Ince-Strutt diagrams collapse; see the main text for more details

6.4.3 General Case of Periodic Parametric Excitation

Below, the problem formulation only is discussed for the case of periodic parametric loading with both regular and singular components. It is assumed that there are two discontinuities and two singularities on each period at the same time points. The differential equation of motion is represented in the vector form

$$\ddot{x} + \left[Q(\tau) + P(\tau) e + p \frac{\partial e}{\partial \varphi} \right] x = 0 \tag{6.66}$$

where $x(t) \in R^n$ is the coordinates' vector-column,$\tau = \tau(\varphi, \gamma)$, $e = e(\varphi, \gamma)$, $\varphi = \omega t$ is the phase variable, p is a constant $n \times n$ matrix, and $Q(\tau(\varphi, \gamma))$ and $P(\tau(\varphi, \gamma))$ are periodic matrixes of the period $T = 4$ with respect to the phase φ.

In Eq. (6.66), the first two terms of the coefficient can represent any periodic function $q(\varphi)$ with stepwise discontinuities on $\Lambda = \{t : \tau(\varphi, \gamma) = \pm 1\}$. In case the original function $q(\varphi)$ is continuous, one has $P = 0$ on Λ.

Let us represent periodic solutions of the period $T = 4$ in the form (6.51). Substituting (6.51) in Eqs. (6.66), taking into account the equality $e^2 = \alpha + \beta e$, the necessary condition of continuity of the vector function $x(t)$, (6.53), and using (6.52) and (6.54) give equations

$$\begin{gathered} \omega^2 \left(\alpha X'' + \alpha \beta Y'' \right) + QX + \alpha PY = 0 \\ \omega^2 \left[\left(\alpha + \beta^2 \right) Y'' + \beta X'' \right] + PX + QY + \beta PY = 0 \end{gathered} \tag{6.67}$$

and the boundary condition

$$\left[\omega^2 \left(X' + \beta Y' \right) + pX \right] |_{\tau = \pm 1} = 0 \tag{6.68}$$

In the case of fixed sign of impulses, the matrix p should be provided with the factor $\operatorname{sgn}(\tau)$. Together with (6.53), relations (6.67) and (6.68) represent a boundary-value problem for determining the vector functions X and Y and the corresponding conditions for existence of periodic solutions.

Note that substitution (6.51) in Eq. (6.66) generates the specific term $e \partial e / \partial \varphi$. Let us show that, within the theory of distributions, these terms can be interpreted as

$$e \frac{\partial e}{\partial \varphi} = \frac{1}{2} \beta \frac{\partial e}{\partial \varphi} \tag{6.69}$$

The relationship (6.69) is the result of a formal differentiation of both sides of the relation $e^2 = \alpha + \beta e$ with respect to the phase φ. To justify it in terms of distributions, let us assume that $\omega = 1$ so that $\varphi \equiv t$ and consider expression (6.53) locally, near the point $t = 1 - \gamma$, which is a typical point for the entire set of discontinuities at times $\Lambda = \{t : \tau(t) = \pm 1\}$.

Generally speaking, the "product" $f(t)\delta(t)$ requires the function $f(t)$ to be at least continuous at $t = 0$. However, it is possible to provide the left-hand side of (6.69) with a certain meaning due to the fact that both terms of the product are generated by the same family of smooth functions. In order to illustrate this remark and prove equality (6.69), let us consider a family of smooth functions $\{\delta_\epsilon(t)\}$ such that

$$\int_{-\epsilon}^{\epsilon} \delta_\epsilon(t)\, dt = 1 \tag{6.70}$$

for all positive ϵ, and $\delta_\epsilon(t) = 0$ outside the interval $-\epsilon < t < \epsilon$.

Therefore, in terms of weak limits, $\delta_\epsilon(t) \to \delta(t)$ as $\epsilon \to 0$. Now, a family of smooth functions approximating e and $\partial e/\partial t$ in the neighborhood of point $t = 1-\gamma$ within the interval $-1+\gamma < t < 3+\gamma$ can be chosen as, respectively,

$$e_\epsilon = \frac{1}{1-\gamma} - \frac{\beta}{\gamma}\theta_\epsilon(t-1+\gamma) \quad \text{and} \quad \frac{\partial e_\epsilon}{\partial t} = -\frac{\beta}{\gamma}\delta_\epsilon(t-1+\gamma) \tag{6.71}$$

where $\theta_\epsilon(t) = \int_{-\infty}^{t} \delta_\epsilon(\xi)\, d\xi$ is a smoothed version of Heaviside unit-step function associated with $\delta_\epsilon(t)$.

Based on definitions (6.71) for e_ϵ and $\partial e_\epsilon/\partial t$, one has $e_\epsilon \to e$ and $\partial e_\epsilon/\partial t \to \partial e/\partial t$ as $\epsilon \to 0$ in the interval $-1+\gamma < t < 3+\gamma$.

Substituting (6.71) in equality (6.69) instead of e and $\partial e/\partial\varphi$ reduces the problem to the proof of identity

$$\theta_\epsilon(t-1+\gamma)\delta_\epsilon(t-1+\gamma) = \frac{1}{2}\delta_\epsilon(t-1+\gamma) \to \frac{1}{2}\delta(t-1+\gamma) \qquad \text{as } \epsilon \to 0 \tag{6.72}$$

For simplicity reason, let us shift the origin to the point $t = 1-\gamma$ and show that the left-hand side of (6.72) gives $\delta(t)/2$ as $\epsilon \to 0$ in the sense of a weak limit. The proof below is based on general properties of the functions $\{\delta_\epsilon\}$ regardless of specifics of their shapes. It is important nonetheless to maintain the relationship $d\theta_\epsilon/dt = \delta_\epsilon$ as shown in Fig. 6.7. First, the area bounded by $\theta_\epsilon\delta_\epsilon$ is

$$\int_{-\epsilon}^{\epsilon} \theta_\epsilon\delta_\epsilon dt = \int_{-\epsilon}^{\epsilon} \theta_\epsilon \frac{d\theta_\epsilon}{dt} dt = \frac{1}{2}\theta_\epsilon^2 \,|_{-\epsilon}^{\epsilon} = \frac{1}{2}$$

Then, let $\phi(t)$ belong to the class of continuous testing functions, which is usually considered in the theory of distributions. By definition, in some ϵ-neighborhood of the point $t = 0$, one has $|\,\phi(t) - \phi(0)\,| < 2\eta$, where η is as small as needed whenever ϵ is sufficiently small. Therefore,

$$\left|\int_{-\epsilon}^{\epsilon} \theta_\epsilon(t)\,\delta_\epsilon(t)\,\phi(t)\,dt - \frac{1}{2}\phi(0)\right| \le \int_{-\epsilon}^{\epsilon} \theta_\epsilon(t)\,\delta_\epsilon(t)\,|\,\phi(t) - \phi(0)\,|\,dt \le \eta$$

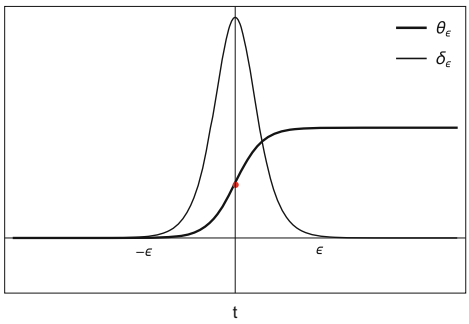

Fig. 6.7 Clarification for the product $\delta(t)\theta(t)$ based on the smooth families of functions $\delta_\epsilon(t)$ and $\theta_\epsilon(t)$

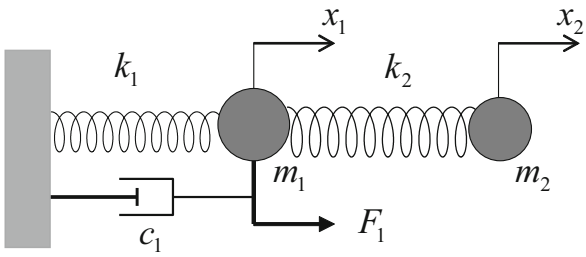

Fig. 6.8 Two mass-spring model

In other words,

$$\int_{-\epsilon}^{\epsilon} \theta_\epsilon(t)\,\delta_\epsilon(t)\,\phi(t)\,dt \to \frac{1}{2}\phi(0)$$

as $\epsilon \to 0$.

This completes the proof.

6.5 Input-Output Systems

The input-output form of dynamical systems may be convenient for different reasons, for instance, when dealing with control problems. In many linear cases, input-output systems are represented in the form of a single high order equation

$$a_n \frac{d^n y}{dt^n} + \ldots + a_1 \frac{dy}{dt} + a_0 y = b_m \frac{d^m u}{dt^m} + \ldots + b_1 \frac{du}{dt} + b_0 u \tag{6.73}$$

where $u = u(t)$ and $y = y(t)$ are input and output, respectively, and $a_n, \ldots, a_1, a_0$, $b_m, \ldots, b_1, b_0$ are constant coefficients.

For illustration purposes, a two-degrees-of-freedom model as shown in Fig. 6.8 is considered, although the general case (6.73) can be handled in the same way.

Eliminating $x_2(t)$ from the system gives a single higher-order equation with respect to the other coordinate, $x_1(t)$, in the form

$$m_1\frac{d^4x_1}{dt^4}+c_1\frac{d^3x_1}{dt^3}+\left(k_1+k_2+\frac{m_1}{m_2}k_2\right)\frac{d^2x_1}{dt^2}+\frac{c_1}{m_2}k_2\frac{dx_1}{dt}+\frac{k_1k_2}{m_2}x_1$$
$$=\frac{d^2F_1}{dt^2}+\frac{k_2}{m_2}F_1 \tag{6.74}$$

System (6.74) is a particular case of (6.73), where $n = 4$ and $m = 2$. Let us consider the stepwise discontinuous periodic function $F_1(t) = u(t) = e(\omega t)$ and represent Eq. (6.74) in the form

$$a_4\frac{d^4y}{dt^4}+\ldots+a_1\frac{dy}{dt}+a_0y=b_2\omega^2e''+b_1\omega e'+b_0e \tag{6.75}$$

where $' \equiv d/d(\omega t)$, and all the coefficients and variables are identified by comparing (6.74)–(6.75).

The right-hand side of Eq. (6.75) contains discontinuous and singular functions; hence, Eq. (6.75) must be treated in terms of distributions. Nonetheless, on the manifold of periodic solutions, Eq. (6.75) is equivalent to some classical boundary-value problem.

To confirm this statement, let us represent the output in the form

$$y(t)=X(\tau)+Y(\tau)e \tag{6.76}$$

where $\tau = \tau(\omega t)$ and $e = e(\omega t)$.

When differentiating expression (6.76) step-by-step, one should eliminate the singular term e' in the first two derivatives by sequentially setting boundary conditions as follows:

$$\frac{dy}{dt}=(Y'+X'e)\omega, \qquad Y|_{\tau=\pm1}=0 \tag{6.77}$$
$$\frac{d^2y}{dt^2}=(X''+Y''e)\omega^2, \qquad X'|_{\tau=\pm1}=0$$

Then, it is dictated by the form of the input in (6.75) that the singular terms e' and e'' must be preserved on the next two steps:

$$\frac{d^3y}{dt^3}=(Y'''+X'''e+Y''e')\omega^3 \tag{6.78}$$
$$\frac{d^4y}{dt^4}=(X^{(4)}+Y^{(4)}e+X'''e'+Y''e'')\omega^4$$

The fourth-order derivative in (6.78) takes into account the equality $ee' = 0$, which easily follows from (6.53) in the symmetric case $\beta = 0$. Substituting (6.77) and (6.78) in (6.75) and considering the elements $\{1, e, e', e''\}$ as a linearly independent give equations

$$\begin{aligned} a_4\omega^4 X^{IV} + a_3\omega^3 Y''' + a_2\omega^2 X'' + a_1\omega Y' + a_0 X = 0 \\ a_4\omega^4 Y^{IV} + a_3\omega^3 X''' + a_2\omega^2 Y'' + a_1\omega X' + a_0 Y = b_0 \end{aligned} \tag{6.79}$$

under the boundary conditions at $\tau = \pm 1$:

$$\begin{aligned} Y = 0, \qquad X' = 0 \\ \omega^2 Y'' = \frac{b_2}{a_4}, \qquad \omega^3 X''' = \frac{1}{a_4}\left(b_1 - \frac{a_3}{a_4} b_2\right) \end{aligned} \tag{6.80}$$

In contrast to Eq. (6.75), the boundary value problem (6.79) and (6.80) does not include discontinuous terms any more. Although the number of equations in (6.79) is doubled as compared to (6.75), such a complication is rather formal due to the symmetry of the equations. Introducing the new variables, $U = X + Y$ and $V = X - Y$, decouples system (6.79) in such a way that the corresponding roots of the characteristic equations differ just by signs. (Besides, this fact reveals the possibility of using the idempotent basis for decoupling the resultant set of equations as discussed in Chap. 4 and will be discussed later in this chapter.) In addition, the type of the symmetry suggests that $X(\tau)$ and $Y(\tau)$ are odd and even functions, respectively. This enables one of reducing the general form of solution to a family of solutions with four arbitrary constants

$$\begin{aligned} X = \sum_{j=1}^{2} \left[A_j \cosh\left(\frac{\alpha_j}{\omega}\tau\right) \sin\left(\frac{\beta_j}{\omega}\tau\right) + B_j \sinh\left(\frac{\alpha_j}{\omega}\tau\right) \cos\left(\frac{\beta_j}{\omega}\tau\right) \right] \\ Y = \sum_{j=1}^{2} \left[A_j \sinh\left(\frac{\alpha_j}{\omega}\tau\right) \sin\left(\frac{\beta_j}{\omega}\tau\right) + B_j \cosh\left(\frac{\alpha_j}{\omega}\tau\right) \cos\left(\frac{\beta_j}{\omega}\tau\right) \right] + \frac{b_0}{a_0} \end{aligned} \tag{6.81}$$

where $\alpha_j \pm \beta_j i$ are complex conjugate roots of the characteristic equation

$$a_4 p^4 + \ldots + a_1 p + a_0 = 0 \tag{6.82}$$

The assumption that both of the roots are complex reflects the physical meaning of the example. Finally, substituting (6.81) in (6.80) gives a linear algebraic set of four independent equations with respect to four constants: A_1, A_2, B_1, and B_2. Although the corresponding analytical solution is easy to obtain by using the standard *Mathematica*® commands, the result is somewhat complicated for reproduction. Practically, it may be reasonable to determine the constants by setting

the system parameters to their numerical values moreover that only numerical solution is often possible for characteristic equations.

6.6 Piecewise-Linear Oscillators with Asymmetric Characteristics

Piecewise-linear oscillators are often considered as finite degrees-of-freedom models of cracked elastic structures [3, 41, 243], but may occur also due to specific design solutions. In many cases, the corresponded periodic solutions can be combined of different pieces of linear solutions valid for two different subspaces of the configuration space [42, 99, 243]. In this section, it will be shown that the nonsmooth transformation of time results in a closed form analytical solution matching both pieces of the solution automatically by means of elementary functions.

6.6.1 Amplitude-Phase Equations

Let us consider a piecewise linear oscillator of the form

$$m\ddot{q} + k[1 - \varepsilon H(q)]q = 0 \tag{6.83}$$

where $H(q)$ is Heaviside unit-step function; m and k are mass and stiffness parameters, respectively; and $|\varepsilon| \ll 1$; therefore, $k_- = k$ and $k_+ = k(1 - \varepsilon)$ are elastic stiffness of the oscillator for $q < 0$ and $q > 0$, respectively.

The exact general solution of oscillator (6.83) can be obtained by satisfying the continuity conditions for q and $\dot{q}$ at the matching point $q = 0$, where the characteristic has a break. The exact *closed form* solution for a similar oscillator was obtained in Sect. 4.3.4 in terms of NSTT. Such approaches are often facing quite challenging algebraic problems, as the number of degrees of freedom increases or external forces are involved. This is mainly due to the fact that times of crossing the boundary, $q = 0$, are a priori unknown. The problems become even more complicated in the presence of other types of nonlinearities. In this section, it will be shown that applying a combination of asymptotic expansions with respect to ε and NSTT gives a closed form solution for oscillator (6.83) with a possibility of generalization on the normal mode motions of multiple degrees-of-freedom systems. In particular, the nonsmooth temporal transformation:

- Provides an automatic matching of the motions from different subspaces of constant stiffness, and
- justifies quasi-linear asymptotic solutions for the specific nonsmooth case of piecewise linear characteristics.

Let us clarify the above two remarks. Introducing the notation $\Omega^2 = k/m$ brings Eq. (6.83) to the standard form of a weakly nonlinear oscillator

$$\ddot{q} + \Omega^2 q = \varepsilon \Omega^2 H(q) q \tag{6.84}$$

The nonlinear perturbation on the right-hand side of oscillator (6.84) is a continuous but nonsmooth function of the coordinate q. Since the major algorithms of quasi-linear theory assume smoothness of nonlinear perturbations, then such algorithms are not applicable in this case unless appropriate modifications and extensions have been made. Even though deriving first-order asymptotic solutions usually require no differentiation of characteristics, dealing with two pieces of the solution may complicate any further stages.

Let us show that combining quasi-linear methods of asymptotic integration, such as Krylov-Bogolyubov averaging,[3] with nonsmooth temporal transformations results in a closed form analytical solution for piecewise linear oscillator (6.83). Note that oscillator (6.83) plays an illustrative role for the approach developed below. Then a more complicated case will be considered.

Let us introduce the amplitude-phase coordinates $\{A(t), \varphi(t)\}$ on the phase plane of oscillator (6.83) through relationships

$$\begin{aligned} q &= A\cos\varphi \\ \dot{q} &= -\Omega A \sin\varphi \end{aligned} \tag{6.85}$$

The following compatibility condition is imposed on transformation (6.85)

$$\dot{A}\cos\varphi - A\sin\varphi\dot{\varphi} = -\Omega A \sin\varphi \tag{6.86}$$

Substituting (6.85) in (6.84) and taking into account (6.86) give

$$\begin{aligned} \dot{A} &= -\frac{1}{2}\varepsilon\Omega A H(A\cos\varphi)\sin 2\varphi \\ \dot{\varphi} &= \Omega - \varepsilon\Omega H(A\cos\varphi)\cos^2\varphi \end{aligned} \tag{6.87}$$

The right-hand sides of Eqs. (6.87) are 2π-periodic with respect to the phase variable, φ. Therefore, nonsmooth transformation of the phase variable applies through the couple of functions

$$\tau = \tau\left(\frac{2}{\pi}\varphi\right) \qquad \text{and} \qquad e = e\left(\frac{2}{\pi}\varphi\right) \tag{6.88}$$

Assuming that $A \geq 0$ and taking into account identities

[3] See Sect. 2.2.2.

$$\begin{aligned} \sin\varphi &= \sin\left(\frac{\pi}{2}\tau\right) \\ \cos\varphi &= \cos\left(\frac{\pi}{2}\tau\right)e \\ H(A\cos\varphi) &= \frac{1}{2}(1+e) \\ e^2 &= 1 \end{aligned} \tag{6.89}$$

bring (6.87) to the form

$$\dot{A} = -\frac{1}{4}\varepsilon\Omega(1+e)A\sin\pi\tau \tag{6.90}$$

$$\dot{\varphi} = \Omega - \frac{1}{2}\varepsilon\Omega(1+e)\cos^2\frac{\pi\tau}{2} \tag{6.91}$$

Note that the right-hand sides of (6.90) and (6.91) are nonsmooth but continuous with respect to the phase φ since the stepwise discontinuities of the square wave $e(2\varphi/\pi)$ are suppressed by the factors $\sin\pi\tau$ and $\cos^2(\pi\tau/2)$, respectively.

6.6.2 *Amplitude Solution*

Let us show that Eq. (6.90) has an exact 2π-periodic solution with respect to the phase variable, φ. According to the algorithm of NSTT, any periodic solution can be represented in the form

$$A = X(\tau) + Y(\tau)e \tag{6.92}$$

where τ and e are defined by (6.88).

Substituting (6.92) in (6.90) and taking into account (6.91) give boundary-value problem

$$\begin{aligned} (X-Y)' &= 0 \\ \frac{(X+Y)'}{X+Y} &= -\frac{\varepsilon\pi}{4}\frac{\sin\pi\tau}{1-\varepsilon\cos^2\frac{\pi\tau}{2}} \end{aligned} \tag{6.93}$$

$$Y|_{\tau=\pm1} = 0 \tag{6.94}$$

where $' \equiv d/d\tau$.

Solution of the boundary value problem, (6.93) and (6.94), is obtained by integration. Then representation (6.92) gives

$$A(\varphi) = \alpha[1 + \zeta(\tau)] - \alpha[1 - \zeta(\tau)]e \tag{6.95}$$
$$\zeta(\tau) = \left(1 - \varepsilon \cos^2 \frac{\pi\tau}{2}\right)^{-1/2}$$

where the functions τ and e of the phase φ are defined in (6.88), and α is an arbitrary positive constant.

Note that solution (6.95) exactly captures the amplitude in both subspaces $q < 0$ and $q > 0$. However, the temporal mode shape and the period essentially depend on the phase variable φ described by Eq. (6.91). Generally, this equation admits exact integration, but the result would appear to have implicit form. Alternatively, it is shown below that solution for the phase variable can be approximated by asymptotic series in the explicit form

$$\begin{aligned}\varphi = \phi &- \frac{1}{8}\varepsilon[\pi\tau + (1+e)\sin\pi\tau] \\ &- \frac{1}{128}\varepsilon^2\{4(2-\cos\pi\tau)(\pi\tau + \sin\pi\tau) \\ &- [4\pi\tau(1+\cos\pi\tau) - 8\sin\pi\tau + \sin 2\pi\tau]e\} + O(\varepsilon^3)\end{aligned} \tag{6.96}$$

where the triangle and rectangle waves depend on the new phase variable, $\tau = \tau(2\phi/\pi)$, $e = e(2\phi/\pi)$, and

$$\phi = \Omega\left[1 - \frac{1}{4}\varepsilon - \frac{3}{32}\varepsilon^2 + O(\varepsilon^3)\right]t \tag{6.97}$$

6.6.3 Phase Solution

In this subsection, a second-order asymptotic procedure for phase equations with nonsmooth periodic perturbations is introduced. If applied to Eq. (6.91), the developed algorithm gives solution (6.96).

Let us consider some phase equation of the general form

$$\dot{\varphi} = \Omega[1 + \varepsilon f(\varphi)] \tag{6.98}$$

where $f(\varphi)$ is a 2π-periodic, nonsmooth, or even stepwise discontinuous function, and ε is a small parameter, $|\varepsilon| \ll 1$.

Using the basic NSTT identity for $f(\varphi)$ brings Eq. (6.98) to the form

$$\dot{\varphi} = \Omega + \varepsilon\Omega\,[G(\tau) + M(\tau)e] \tag{6.99}$$

where the functions $G(\tau)$ and $M(\tau)$ are expressed through $f(\varphi)$, and the functions τ and e of the phase φ are defined in (6.88).

Note that the class of smoothness of the periodic perturbation in Eq. (6.99) depends on the behavior of functions $G(\tau)$ and $M(\tau)$ and their derivatives at the boundaries $\tau = \pm 1$. If, for instance, $M(\pm 1) \neq 0$, then the perturbation is stepwise discontinuous in φ whenever $\tau = \pm 1$.

Let us introduce the asymptotic procedure for Eq. (6.99) by noticing that, in case $\varepsilon = 0$, the phase φ has a constant temporal rate, $\dot{\varphi} = \Omega$. Hence, following the idea of asymptotic integration, let us find a phase transformation

$$\varphi = \phi + \varepsilon F_1(\phi) + \varepsilon^2 F_2(\phi) + \ldots \tag{6.100}$$

where functions $F_i(\phi)$ are such that the new phase variable, ϕ, also has a constant temporal rate even when $\varepsilon \neq 0$.

In other words, transformation (6.100) should bring Eq. (6.99) to the form

$$\dot{\phi} = \Omega(1 + \varepsilon\gamma_1 + \varepsilon^2\gamma_2 + \ldots) \tag{6.101}$$

where γ_i are constant coefficients to be determined together with $F_i(\phi)$ during the asymptotic procedure.

Note that the procedure, which is described below, has several specific features due to the presence of nonsmooth periodic functions. In particular, high-order approximations require a non-conventional interpretation for the power series expansions as discussed in Remark 6.6.1 at the end of this section. Other modifications occur already in the leading order approximation.

Substituting (6.100) in Eq. (6.99) and then enforcing Eq. (6.101) and collecting the terms of order ε give

$$F_1'(\phi) = G(\tau) + eM(\tau) - \gamma_1 \tag{6.102}$$

where the triangle and square waves depend now on the new phase variable ϕ as $\tau = \tau(2\phi/\pi)$ and $e = e(2\phi/\pi)$, respectively.

According to the conventional averaging procedure, the constant γ_1 is selected to achieve a zero mean on the right-hand side of Eq. (6.102) and thus provide periodicity of the solution, $F_1(\phi)$. In the algorithm below, the periodicity is due to the form of representation for periodic solutions, whereas the operator of averaging occurs automatically from the corresponding conditions of smoothness that is boundary conditions for the solution components. Following this remark, let us seek solution of Eq. (6.102) in the form

$$F_1(\phi) = U_1(\tau) + eV_1(\tau) \tag{6.103}$$

Substituting (6.103) in (6.102) and applying NSTT procedure give the boundary-value problem

$$\begin{aligned} U_1'(\tau) &= \frac{\pi}{2} M(\tau) \\ V_1'(\tau) &= \frac{\pi}{2} [G(\tau) - \gamma_1] \\ V_1(\pm 1) &= 0 \end{aligned} \tag{6.104}$$

There are two conditions on the function $V_1(\tau)$ described by the first-order differential equation in (6.104). There is also a choice for γ_1, which is to satisfy one of the two conditions. As a result, solution of boundary-value problem (6.104) is obtained by integration in the form

$$\begin{aligned} U_1(\tau) &= \frac{\pi}{2} \int_0^{\tau} M(z) dz \\ V_1(\tau) &= \frac{\pi}{2} \int_{-1}^{\tau} [G(z) - \gamma_1] dz \\ \gamma_1 &= \frac{1}{2} \int_{-1}^{1} G(\tau) d\tau \end{aligned} \tag{6.105}$$

Further, collecting the terms of order ε^2 gives

$$F_2'(\phi) = G_2(\tau) + eM_2(\tau) + P_2(\tau)e' - \gamma_2 \tag{6.106}$$

where $e' \equiv de(2\phi/\pi)/d(2\phi/\pi)$ is a periodic series of δ-functions, and

$$\begin{aligned} M_2(\tau) &= \frac{2}{\pi} [U_1(\tau)G'(\tau) + V_1(\tau)M'(\tau)] - M(\tau)\gamma_1 \\ G_2(\tau) &= \frac{2}{\pi} U_1(\tau)M'(\tau) - G(\tau)\gamma_1 + \gamma_1^2 \\ P_2(\tau) &= \frac{2}{\pi} U_1(\tau)M(\tau) \end{aligned} \tag{6.107}$$

In contrast to first-order Eq. (6.102), the Eq. (6.106) includes the singular term $P_2(\tau)e'$ produced by the power series expansion of the perturbation in Eq. (6.99). If the perturbation is smooth, then $P_2(\pm 1) = 0$ and such singular term disappears. Nonetheless, the second-order approximation makes sense even in discontinuous case, when $P_2(\pm 1) \neq 0$. To clarify the details, let us represent solution of Eq. (6.106) in the form

$$F_2(\phi) = U_2(\tau) + eV_2(\tau) \tag{6.108}$$

Substituting (6.108) in (6.106) gives boundary-value problem

$$\begin{aligned} U_2'(\tau) &= \frac{\pi}{2} M_2(\tau) \\ V_2'(\tau) &= \frac{\pi}{2}[G_2(\tau) - \gamma_2] \\ V_2(\pm 1) &= \frac{\pi}{2} P_2(\pm 1) \end{aligned} \tag{6.109}$$

In contrast to (6.104), the current boundary-value problem has generally non-homogeneous boundary conditions for V_2. These conditions compensate the singular term e' from differential equation (6.106). As a result Eqs. (6.109) are free of any singularities and admit solution analogously to first-order Eqs. (6.104),

$$\begin{aligned} U_2(\tau) &= \frac{\pi}{2} \int_0^\tau M_2(z) dz \\ V_2(\tau) &= \frac{\pi}{2} \int_{-1}^\tau [G_2(z) - \gamma_2] dz + \frac{\pi}{2} P_2(-1) \\ \gamma_2 &= \frac{1}{2} \int_{-1}^1 G_2(\tau) d\tau + \frac{1}{2}[P_2(-1) - P_2(1)] \end{aligned} \tag{6.110}$$

Example 6.6.1 Now, let us revisit the illustrating model. In particular case (6.91), one has

$$G(\tau) \equiv M(\tau) \equiv -\frac{1}{2} \cos^2 \frac{\pi \tau}{2} \tag{6.111}$$

and

$$\begin{aligned} G(\pm 1) &= M(\pm 1) = 0 \\ G'(\pm 1) &= M'(\pm 1) = 0 \\ G''(\pm 1) &= M''(\pm 1) = -\pi^2/4 \end{aligned} \tag{6.112}$$

where $' \equiv d/d\tau$. First two of Eqs. (6.112) provide continuity for the right-hand side of (6.99) and its first derivative at those φ where $\tau = \pm 1$. As follows from (6.107) and (6.111), for this class of smoothness, one has $P_2(\pm 1) = 0$ and hence no singular terms occur in the first two steps of asymptotic procedure. Finally, taking into account (6.111) and (6.112) and conducting integration in (6.105) and (6.110) bring solution (6.100) to the form (6.96) and (6.97). Figure 6.9 compares analytical solution (6.85), (6.95), and (6.96) shown by the solid line and numerical solution shown by the dashed line. As expected, the amplitude shows the perfect match, whereas some phase shift develops after several cycles.

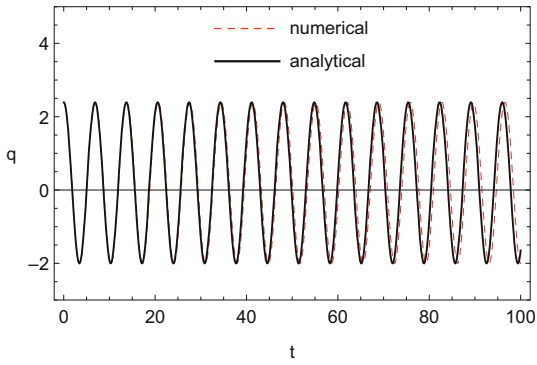

Fig. 6.9 Second-order asymptotic and numerical solutions shown by solid and dashed lines, respectively

6.6.4 The Amplitude-Phase Problem in Idempotent Basis

Recall that the idempotent basis is given by $e_+ = (1+e)/2$ and $e_- = (1-e)/2$ so that $e_+^2 = e_+$, $e_-^2 = e_-$, and $e_+ e_- = 0$. Equations (6.90) and (6.91) therefore take the form

$$\dot{A} = -\frac{1}{2}\varepsilon\Omega e_+ A \sin\pi\tau \tag{6.113}$$

$$\dot{\varphi} = \Omega - \varepsilon\Omega e_+ \cos^2\frac{\pi\tau}{2} \tag{6.114}$$

Let us represent the amplitude as a function of φ in the form

$$A(\varphi) = X_+(\tau)e_+ + X_-(\tau)e_- \tag{6.115}$$

where $e_+ = e_+(2\varphi/\pi)$, $e_- = e_-(2\varphi/\pi)$, and $\tau = \tau(2\varphi/\pi)$.

Substituting (6.115) in (6.113) and taking into account (6.114) give

$$\frac{2}{\pi}(X'_+ e_+ - X'_- e_-)\left(\Omega - \varepsilon\Omega e_+ \cos^2\frac{\pi\tau}{2}\right) = -\frac{1}{2}\varepsilon\Omega e_+(X_+ e_+ + X_- e_-)\sin\pi\tau$$

or

$$\left(1 - \varepsilon\cos^2\frac{\pi\tau}{2}\right)X'_+ = -\frac{\pi}{4}\varepsilon X_+ \sin\pi\tau$$

$$X'_- = 0 \tag{6.116}$$

under the boundary condition

$$(X_+ - X_-)|_{\tau=\pm1} = 0 \tag{6.117}$$

The boundary-value problem (6.116) and (6.117) admits exact solution so that (6.115) gives finally

$$A(\varphi) = \alpha \left[\left(1 - \varepsilon \cos^2 \frac{\pi \tau}{2} \right)^{-1/2} e_+ + e_- \right] \tag{6.118}$$

where α is an arbitrary positive constant.

Remark 6.6.1 In the classical analysis, nonsmooth functions cannot be represented by Taylor series near their singular points. This can be justified however in terms of distributions as confirmed by the following example. Nonsmoothness of the triangular sine is similar to that function $|t|$ has at zero. Let us consider its formal power series

$$|t + \varepsilon| = |t| + |t|' \varepsilon + \frac{1}{2!} |t|'' \varepsilon^2 + \ldots \tag{6.119}$$

where $\varepsilon > 0$ and $-\infty < t < \infty$, and prime indicates Schwartz derivative. It is clear that equality (6.119) has no regular point-wise meaning. For instance, equality (6.119) is obviously not true on the interval $-\varepsilon < t < 0$. In addition, the right-hand side of (6.119) is uncertain at $t = 0$, whereas the left-hand side gives ε. Nevertheless, let us show that equality (6.119) admits a generalized interpretation and holds in terms of distributions. Let $\psi(t)$ be a *test function* in terms of the distribution theory; more precisely, $\psi(t)$ is infinitely differentiable with compact support that is identically zero outside of some bounded interval. Integrating by parts and then shifting the variable of integration give

$$\begin{aligned} &\int_{-\infty}^{\infty} \left(|t| + |t|' \varepsilon + \frac{1}{2!} |t|'' \varepsilon^2 + \ldots \right) \psi(t) dt \\ &= \int_{-\infty}^{\infty} |t| \left[\psi(t) - \psi'(t) \varepsilon + \frac{1}{2!} \psi''(t) \varepsilon^2 - \ldots \right] dt \\ &= \int_{-\infty}^{\infty} |t| \psi(t - \varepsilon) dt = \int_{-\infty}^{\infty} |t + \varepsilon| \psi(t) dt \end{aligned} \tag{6.120}$$

Therefore, equality (6.119) holds in the integral sense of distributions.

6.7 Multiple Degrees-of-Freedom Case

Let us consider a multiple degrees-of-freedom piecewise-linear system of the form

$$M\ddot{x} + Kx = \varepsilon H(Sx) Bx \tag{6.121}$$

where $x(t) \in R^n$ is a vector-function of the system coordinates, M is a mass matrix, H denotes the Heaviside unit-step function, and S is a normal vector to the plane splitting the configuration space into two parts with different elastic properties, so that the stiffness matrix is K when $Sx < 0$ and $K - \varepsilon B$ when $Sx > 0$. It is assumed that the stiffness jump is small, $|\varepsilon| \ll 1$.

The number of possible iterations of the classical perturbation tools usually depends on a class of smoothness of the perturbation. The perturbation term on the right-hand side of (6.121) is continuous but nonsmooth. Therefore, only first-order asymptotic solution can be obtained within the classic theory of differential equations. Also, the piecewise character of the perturbation complicates the form of the solution due to the necessity of matching the different pieces of the solution.

Let us show that NSTT gives a closed-form solution by automatically matching the pieces of solution in two different configuration subspaces of different stiffness properties. We seek a 2π-periodic, with respect to the phase φ, solution of system (6.121) in the form of the following asymptotic expansions:

$$\begin{aligned} x(\varphi) &= A_j \cos\varphi + \varepsilon x^{(1)}(\varphi) + O(\varepsilon^2) \\ \varphi &= \Omega_j \sqrt{1 + \varepsilon\gamma^{(1)} + O(\varepsilon^2)}\, t \end{aligned} \tag{6.122}$$

where Ω_j and A_j are arbitrary eigen-frequency and eigen vector (normal mode) of the linearized system:

$$\left(-\Omega_j^2 M + K\right) A_j = 0 \qquad (j = 1, \ldots, n) \tag{6.123}$$

Substituting (6.122) in (6.121), taking into account identities (6.89), assuming that algebraic equation (6.123) holds, and collecting terms in the first order of ε give

$$\Omega_j^2 M \frac{d^2 x^{(1)}}{d\varphi^2} + K x^{(1)} = \left[\frac{1}{2} B A_j + \left(\frac{1}{2} B A_j + \gamma^{(1)} K A_j\right) e\right] \cos\frac{\pi\tau}{2} \tag{6.124}$$

where $\tau = \tau(2\varphi/\pi)$, $e = e(2\varphi/\pi)$, and the relationship $(1 + \varepsilon\gamma^{(1)})^{-1} = 1 - \varepsilon\gamma^{(1)} + O(\varepsilon^2)$ was enforced.

Since the function $x^{(1)}(\varphi)$ is sought to be 2π-periodic with respect to φ, it should admit NSTT representation

$$x^{(1)} = X(\tau) + Y(\tau) e \tag{6.125}$$

Substituting (6.125) in (6.124) and conducting NSTT procedure give the boundary-value problem

$$\left(\frac{2\Omega_j}{\pi}\right)^2 MX'' + KX = \frac{1}{2}BA_j \cos\frac{\pi\tau}{2}, \qquad X'|_{\tau=\pm1} = 0 \tag{6.126}$$

$$\left(\frac{2\Omega_j}{\pi}\right)^2 MY'' + KY = \left(\frac{1}{2}BA_j + \gamma^{(1)}KA_j\right)\cos\frac{\pi\tau}{2} \tag{6.127}$$

$$Y|_{\tau=\pm1} = 0$$

Representing the corresponding solution in terms of the normal mode coordinates

$$X = \sum_{i=1}^{n} A_i X_i(\tau), \qquad Y = \sum_{i=1}^{n} A_i Y_i(\tau) \tag{6.128}$$

and taking into account M-orthogonality of the set of eigen-vectors give

$$\left(\frac{2\Omega_j}{\pi}\right)^2 X_i'' + \Omega_i^2 X_i = \beta_{ij}\cos\frac{\pi\tau}{2}, \qquad X_i'|_{\tau=\pm1} = 0 \tag{6.129}$$

$$\left(\frac{2\Omega_j}{\pi}\right)^2 Y_i'' + \Omega_i^2 Y_i = (\beta_{ij} + \gamma^{(1)}\varkappa_{ij})\cos\frac{\pi\tau}{2}, \quad Y_i|_{\tau=\pm1} = 0 \tag{6.130}$$

where

$$\beta_{ij} = \frac{1}{2}\frac{A_i BA_j}{A_i MA_i}, \qquad \varkappa_{ij} = \frac{A_i KA_j}{A_i MA_i} \tag{6.131}$$

are dimensionless coefficients.

Note that, despite the similar representation for solution (6.122), the current asymptotic procedure differs from the Poincaré-Lindstedt method due to the specific of representation (6.125). According to the Poincaré-Lindstedt method, the frequency correction term, $\gamma^{(1)}$, is to eliminate the so-called secular terms in the asymptotic expansions. In the present case, the secular terms appear to be periodic due to the inherent periodicity of the new temporal argument. Instead solutions are required to satisfy the boundary-value problems, such as (6.129) and (6.130). If $i \neq j$, the term $\gamma^{(1)}$ disappears from (6.130) due to $\varkappa_{ij} = 0$. Then both boundary-value problems, (6.129) and (6.130), admit solutions

$$X_i = \frac{\beta_{ij}}{\Omega_i^2 - \Omega_j^2}\left(\cos\frac{\pi\tau}{2} - \frac{\Omega_j}{\Omega_i}\cos\frac{\pi\Omega_i\tau}{2\Omega_j}\csc\frac{\pi\Omega_i}{2\Omega_j}\right) \tag{6.132}$$

$$Y_i = \frac{\beta_{ij}}{\Omega_i^2 - \Omega_j^2}\cos\frac{\pi\tau}{2} \tag{6.133}$$

When $i = j$, problem (6.129) still has solution, but problem (6.130) generally does not due to the resonance $\Omega_i = \Omega_j$. Fortunately, in this case $\varkappa_{jj} \neq 0$, and hence

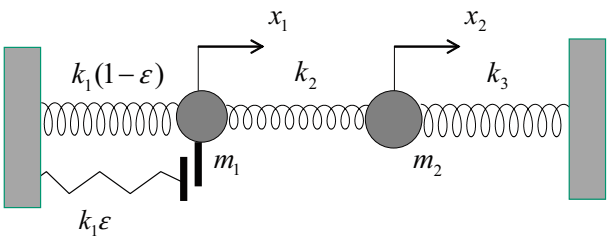

Fig. 6.10 Two degrees-of-freedom piecewise-linear system can be viewed as a model of a rod with a small crack

the right-hand side of the equation can be set to zero by means of the condition on yet undetermined as

$$\gamma^{(1)} = -\frac{\beta_{jj}}{\varkappa_{jj}} \tag{6.134}$$

Due to this condition, problem (6.130) admits zero solution, and thus

$$X_j = \frac{\pi\beta_{jj}}{4\Omega_j^2}\left(\tau \sin\frac{\pi\tau}{2} + \frac{2}{\pi}\cos\frac{\pi\tau}{2}\right) \tag{6.135}$$

$$Y_j = 0 \tag{6.136}$$

Expressions (6.125), (6.128), and (6.132) through (6.136) completely determine the first-order approximation $x^{(1)}(\varphi)$.

Example 6.7.1 Let us consider a two-degrees-of-freedom example of mass-spring model (Fig. 6.10)

$$\begin{aligned} m_1\ddot{x}_1 + (k_1+k_2)x_1 - k_2x_2 &= \varepsilon k_1 H(x_1)x_1 \\ m_2\ddot{x}_2 - k_2x_1 + (k_2+k_3)x_2 &= 0 \end{aligned} \tag{6.137}$$

Equations (6.119) can be represented in the form (6.121), where

$$M = \begin{bmatrix} m_1 & 0 \\ 0 & m_2 \end{bmatrix}, \qquad K = \begin{bmatrix} k_1+k_2 & -k_2 \\ -k_2 & k_2+k_3 \end{bmatrix}, \qquad B = \begin{bmatrix} k_1 & 0 \\ 0 & 0 \end{bmatrix}$$

$$x = \begin{bmatrix} x_1 \\ x_2 \end{bmatrix}, \qquad S = \begin{bmatrix} 1 & 0 \end{bmatrix}$$

In this case, the first-order asymptotic solution for the inphase ($j = 1$) and out-of-phase ($j = 2$) takes the form, respectively,

$$x_1 = e\cos\frac{\pi\tau}{2} + \frac{\varepsilon\pi}{16}\left(\frac{2}{\pi}\cos\frac{\pi\tau}{2} + \tau\sin\frac{\pi\tau}{2}\right) + O(\varepsilon^2)$$

$$x_2 = e\cos\frac{\pi\tau}{2} - \frac{\varepsilon k_1}{8k_2}\left[e\cos\frac{\pi\tau}{2} + \cos\frac{\pi\tau}{2}\right. \tag{6.138}$$

$$\left. - \left(1 + 2\frac{k_2}{k_1}\right)^{-1/2}\cos\left(\sqrt{1 + 2\frac{k_2}{k_1}}\frac{\pi\tau}{2}\right) / \sin\left(\sqrt{1 + 2\frac{k_2}{k_1}}\frac{\pi}{2}\right)\right] + O(\varepsilon^2)$$

$$\varphi = \sqrt{\frac{k_1}{m}}\sqrt{1 - \frac{\varepsilon}{4} + O(\varepsilon^2)}t$$

and

$$x_1 = -e\cos\frac{\pi\tau}{2} + \frac{\varepsilon k_1}{8k_2}\left[e\cos\frac{\pi\tau}{2} + \cos\frac{\pi\tau}{2} - \left(1 + 2\frac{k_2}{k_1}\right)\right.$$

$$\left. \times\cos\left(\frac{\pi\tau}{2}/\sqrt{1 + 2\frac{k_2}{k_1}}\right) / \sin\left(\frac{\pi}{2}/\sqrt{1 + 2\frac{k_2}{k_1}}\right)\right] + O(\varepsilon^2) \tag{6.139}$$

$$x_2 = e\cos\frac{\pi\tau}{2} + \frac{\varepsilon k_1\pi}{16(k_1 + 2k_2)}\left(\frac{2}{\pi}\cos\frac{\pi\tau}{2} + \tau\sin\frac{\pi\tau}{2}\right) + O(\varepsilon^2)$$

$$\varphi = \sqrt{\frac{k_1 + 2k_2}{m}}\sqrt{1 - \frac{\varepsilon k_1}{4(k_1 + 2k_2)} + O(\varepsilon^2)}t$$

where $m = m_1 = m_2$ is assumed. Solutions (6.138) and (6.102) show that the piecewise linear restoring force may have quite different effect on different modes. In particular, solution (6.138) reveals the possibility of internal resonances, when

$$\sin\left(\frac{\pi\Omega_2}{2\Omega_1}\right) = 0, \qquad \frac{\Omega_2}{\Omega_1} = \sqrt{1 + 2\frac{k_2}{k_1}} \tag{6.140}$$

If, for instance, the system is close to the frequency ratio $\Omega_2/\Omega_1 = 2$, then the inphase mode may be affected significantly by a crack even under very small magnitudes of the parameter ε. In contrary, solution (6.102) has the denominator $\sin[(\pi/2)\Omega_1/\Omega_2]$, which is never close to zero because $0 < \Omega_1/\Omega_2 < 1$. Therefore, in current asymptotic approximation, the influence of crack on the out-of-phase mode is always of order ε provided that $k_2/k_1 = O(1)$.The influence of the bilinear stiffness on inphase mode trajectories in the closed to internal resonance case is seen from Fig. 6.11, where both analytical and numerical solutions are shown for comparison reasons. The frequency ratio $\Omega_2/\Omega_1 = 2.0025$ is achieved by conditioning the spring stiffness parameters as follows $k_2 = (3/2)k_1 + 0.005$.

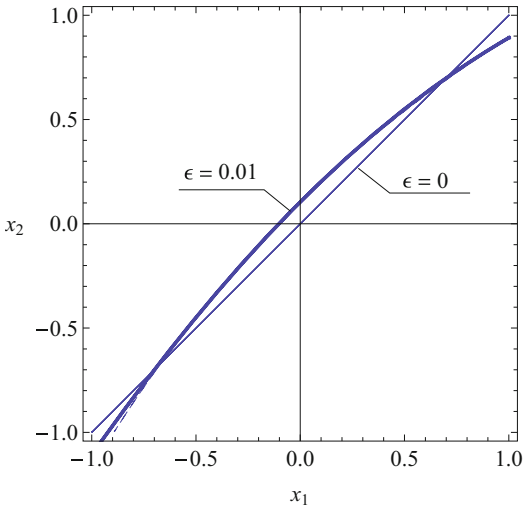

Fig. 6.11 The influence of a small crack, $\varepsilon = 0.01$, on the inphase mode trajectory near the frequency ratio $\Omega_2/\Omega_1 = 2$; the dashed line shows the numerical solution, and the thin solid line corresponds to the linear case, $\varepsilon = 0$

Chapter 7
Periodic and Transient Nonlinear Dynamics Under Discontinuous Loading

In this chapter, two-variable expansions are introduced, where the fast temporal scale is represented by the triangle wave. In contrast to the well-known two-variable procedure, the differential equations for the slow dynamics emerge from the boundary conditions eliminating discontinuities instead of resonance terms. For illustrating purposes, an impulsively loaded one degree-of-freedom model with cubic damping and no elastic force is considered. Further, the method is applied to Duffing's oscillator under the periodic impulsive excitation whose fundamental frequency is close to the linear resonance frequency. Note that the selected illustrating models are weakly nonlinear. Nonetheless, the triangle wave temporal argument adequately captures the main specific of the impulsive loading and provides closed-form asymptotic solutions.

7.1 Nonsmooth Two-Variable Method

Solutions of Cauchy problems under arbitrary initial conditions are generally aperiodic. In the case of amplitude or frequency modulated motions, the averaging may help to obtain the corresponding solutions. A proper formalization can be developed by introducing slow temporal variables in addition to the fast oscillating time τ. Consider, for instance, first-order impulsively loaded system

$$\dot{v} + \varepsilon v^3 = p\frac{de\,(t)}{dt} \tag{7.1}$$

under the initial condition

$$v\,|_{t=0} = v^0 \tag{7.2}$$

V. N. Pilipchuk, *Oscillators and Oscillatory Signals from Smooth to Discontinuous*,
https://doi.org/10.1007/978-3-031-37788-4_7

where ε is a small enough positive parameter and p is a constant parameter characterizing the strength of impulses.

The Cauchy problem, (7.1) and (7.2), describes one-dimensional motions of a material point under the periodic series of impulses and nonlinear damping forces. Note that any standard formulation of the idea of averaging is difficult to apply directly to Eq. (7.1) since its right-hand side is neither smooth nor even continues function of time. Analyzing both sides of Eq. (7.1) shows that solutions should have stepwise discontinuities at times $\Lambda = \{t : \tau(t) = \pm 1\}$. Let us represent such solutions in the form

$$v = X\left(\tau, t^0\right) + Y\left(\tau, t^0\right) e \tag{7.3}$$

where $\tau = \tau(t)$, $e = e(t)$ and $t^0 = \varepsilon t$; therefore, the solution is assumed to depend upon the two time scales, such as the fast oscillating time τ and the slow time t^0.

Substituting now (7.3) in (7.1) gives

$$\frac{\partial Y}{\partial \tau} + \varepsilon\left(\frac{\partial X}{\partial t^0} + X^3 + 3XY^2\right)$$

$$+\left[\frac{\partial X}{\partial \tau} + \varepsilon\left(\frac{\partial Y}{\partial t^0} + 3YX^2 + Y^3\right)\right] e + (Y - p)\dot{e} = 0$$

Following NSTT formalism leads to the set of partial differential equations

$$\begin{aligned} \frac{\partial X}{\partial \tau} &= -\varepsilon\left(\frac{\partial Y}{\partial t^0} + 3YX^2 + Y^3\right) \\ \frac{\partial Y}{\partial \tau} &= -\varepsilon\left(\frac{\partial X}{\partial t^0} + X^3 + 3XY^2\right) \end{aligned} \tag{7.4}$$

under boundary conditions

$$Y\,|_{\tau=\pm 1} = p \tag{7.5}$$

According to the procedure of the two-variable expansions, solution of the boundary value problem (7.4) and (7.5) is represented in the form of asymptotic series

$$X = \sum_{i=0}^{\infty} \varepsilon^i X_i\left(\tau, t^0\right), \qquad Y = \sum_{i=0}^{\infty} \varepsilon^i Y_i\left(\tau, t^0\right) \tag{7.6}$$

Substituting (7.6) into (7.4) and (7.5) and matching coefficients of the same powers of ε gives a sequence of simplified boundary value problems. In particular, zero-order problem is given by

$$\frac{\partial X_0}{\partial \tau} = 0, \qquad \frac{\partial Y_0}{\partial \tau} = 0$$
$$Y_0|_{\tau=\pm 1} = p$$

Both these equations and the boundary condition are satisfied by solution

$$X_0 = A_0\left(t^0\right), \qquad Y_0 = p \tag{7.7}$$

where A_0 is an arbitrary function of the slow time.

Taking into account (7.7) gives the first-order problem

$$\begin{aligned} \frac{\partial X_1}{\partial \tau} &= -\left(3pA_0^2 + p^3\right) \\ \frac{\partial Y_1}{\partial \tau} &= -\left(\frac{dA_0}{dt^0} + A_0^3 + 3A_0p^2\right) \\ Y_1\ |_{\tau=\pm 1} &= 0 \end{aligned} \tag{7.8}$$

Integrating Eq. (7.8) gives general solution

$$\begin{aligned} X_1 &= -\left(3pA_0^2 + p^3\right)\tau + A_1\left(t^0\right) \\ Y_1 &= -\left(\frac{dA_0}{dt^0} + A_0^3 + 3A_0p^2\right)\tau + C_1\left(t^0\right) \end{aligned} \tag{7.9}$$

where $A_1\left(t^0\right)$ and $C_1\left(t^0\right)$ are arbitrary functions.

The boundary condition for Y_1 in (7.8) dictates $C_1\left(t^0\right) \equiv 0$ and

$$\frac{dA_0}{dt^0} + A_0^3 + 3A_0p^2 = 0 \tag{7.10}$$

Therefore $Y_1 \equiv 0$, whereas function $A_1\left(t^0\right)$ in the expression for X_1 remains unknown. Equation (7.10) admits exact solution

$$A_0 = \left[-\frac{1}{3p^2} + \alpha_0 \exp\left(6p^2t^0\right)\right]^{-1/2}$$

where α_0 is a constant of integration to be determined from the initial condition.

Finally, the leading order asymptotic solution of the Caushy problem is written as

$$v(t) = \pm\left\{-\frac{1}{3p^2} + \left[\frac{1}{3p^2} + \left(v^0 - p\right)^{-2}\right]\exp\left(6p^2\varepsilon t\right)\right\}^{-1/2} \tag{7.11}$$

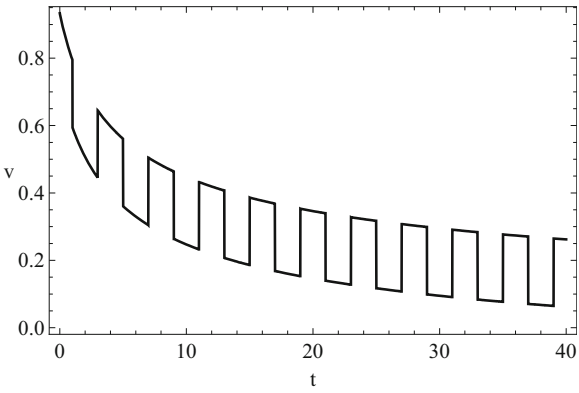

Fig. 7.1 Velocity of the nonlinearly damped material point under the periodic impulsive excitation

$$+pe\,(t) + O\,(\varepsilon)$$

where plus or minus sign is taken if $v^0 - p > 0$ or $v^0 - p < 0$, respectively.

Substituting asymptotic solution (7.11) in Eq. (7.1) satisfies the equation with the error $\sim \varepsilon R(\varepsilon t)e\,(t)$, where $R(\varepsilon t)$ is a function of the slow time scale. Although the error is of the same order of magnitude as the perturbation, it relates only to the singular component of the equation with a scaling factor of order one. In other words, for such kind of systems, regular and singular error components should be considered separately. Note that the first term in expression (7.11) is a transient response of the system that vanishes with time; see Fig. 7.1. It is seen from solution (7.11) that the amplitude of impulses may have a strong effect on the time scale of transient response of the system. Note also that the amplitude of steps in the response is maintained. It already follows directly from the structure of Eq. (7.1). It reveals that the series of δ-functions, $pe\,(t)\,/dt$, can be balanced only by the derivative, $\dot{v}$, whereas the term εv^3 does not have any effect on the steps of the response, v. This observation hints at the possibility of substitution

$$v = y(t) + pe(t) \tag{7.12}$$

which is a periodic version of substitution (1.166).

Substituting (7.12) in Eq. (7.1) eliminates the series of δ-functions on its right-hand side to give the equation with only stepwise discontinuities

$$\dot{y} + \varepsilon \left[y^3 + 3yp^2 + \left(p^3 + 3py^2 \right) e(t) \right] = 0 \tag{7.13}$$

where the basic property of the hyperbolic imaginary unit, $e^2 = 1$, was enforced. Furthermore, on the manifold of periodic solutions, even the stepwise discontinuity can be effectively removed by means of NSTT substitution in the form of hyperbolic number, $y = X(\tau) + Y(\tau)e$. This would replace Eq. (7.13) by a boundary value problem for X and Y according to NSTT procedure.

7.2 Resonances in Duffing's Oscillator Under Impulsive Loading

Let us consider the Duffing's oscillator under the periodic impulsive excitation

$$\ddot{x} + \Omega_0^2 x = -\varepsilon \left[x^3 - p \frac{de\,(\omega t)}{d\,(\omega t)} \right] \tag{7.14}$$

Introducing the detuning parameter σ into the differential equation (7.14) as

$$\Omega_0^2 = \left(\frac{n\pi}{2} \omega \right)^2 + \varepsilon\sigma \tag{7.15}$$

gives

$$\ddot{x} + \left(\frac{n\pi}{2} \omega \right)^2 x = -\varepsilon \left[\sigma x + x^3 - p \frac{de\,(\omega t)}{d\,(\omega t)} \right] \tag{7.16}$$

where n is an odd positive integer.

Recall that, in the near resonance condition (7.15), the factor $\pi/2$ occurs due to the specific normalization of the triangle wave period, $T = 4$.

Let us represent solutions of Eq. (7.16) in the form

$$x(t) = X\left(\tau\,(\omega t), t^0\right) + Y\left(\tau\,(\omega t), t^0\right) e\,(\omega t) \tag{7.17}$$

where $t^0 = \varepsilon t$ is the slow time used in the previous section.

Based on the continuity condition for $x\,(t)$,

$$Y\,|_{\tau=\pm 1} = 0 \tag{7.18}$$

one obtains

$$\dot{x} = \omega \frac{\partial Y}{\partial \tau} + \varepsilon \frac{\partial X}{\partial t^0} + \left(\omega \frac{\partial X}{\partial \tau} + \varepsilon \frac{\partial Y}{\partial t^0} \right) e \tag{7.19}$$

Then, substituting (7.17) and (7.19) in (7.16) eventually gives the boundary value problem (7.18),

$$\omega^2 \frac{\partial X}{\partial \tau}|_{\tau=\pm 1} = \varepsilon p \tag{7.20}$$

and

$$\omega^2 \frac{\partial^2 X}{\partial \tau^2} + 2\varepsilon\omega \frac{\partial^2 Y}{\partial \tau \partial t^0} + \varepsilon^2 \frac{\partial^2 X}{\partial t^{02}} + \left(\frac{n\pi}{2} \omega \right)^2 X$$

$$
\begin{aligned}
&= -\varepsilon\left(\sigma X + X^3 + 3Y^2X\right) \\
&\omega^2\frac{\partial^2 Y}{\partial\tau^2} + 2\varepsilon\omega\frac{\partial^2 X}{\partial\tau\partial t^0} + \varepsilon^2\frac{\partial^2 Y}{\partial t^{02}} + \left(\frac{n\pi}{2}\omega\right)^2 Y \\
&= -\varepsilon\left(\sigma Y + Y^3 + 3X^2Y\right)
\end{aligned}
\tag{7.21}
$$

Due to substitution (7.17), the boundary value problem, (7.18), (7.20) and (7.21), includes no singular functions. Therefore, further averaging procedures can be correctly applied. Following the formalism of two-variable expansions, we seek asymptotic solutions in the form of power series

$$
\begin{aligned}
X &= X_0\left(\tau, t^0\right) + \varepsilon X_1\left(\tau, t^0\right) + \varepsilon^2 X_2\left(\tau, t^0\right) + \ldots \\
Y &= Y_0\left(\tau, t^0\right) + \varepsilon Y_1\left(\tau, t^0\right) + \varepsilon^2 Y_2\left(\tau, t^0\right) + \ldots
\end{aligned}
\tag{7.22}
$$

Substituting (7.22) in (7.18), (7.20), and (7.21), and matching coefficients of the same degrees of ε, gives a series of boundary value problems, where the leading order problem is

$$
\begin{aligned}
&\frac{\partial^2 X_0}{\partial\tau^2} + \left(\frac{n\pi}{2}\right)^2 X_0 = 0, \qquad \frac{\partial X_0}{\partial\tau}|_{\tau=\pm1} = 0 \\
&\frac{\partial^2 Y_0}{\partial\tau^2} + \left(\frac{n\pi}{2}\right)^2 Y_0 = 0, \qquad Y_0|_{\tau=\pm1} = 0
\end{aligned}
\tag{7.23}
$$

These equations and the boundary conditions are satisfied by solution

$$
X_0 = A_0\left(t^0\right)\sin\frac{n\pi\tau}{2}, \qquad Y_0 = D_0\left(t^0\right)\cos\frac{n\pi\tau}{2}
\tag{7.24}
$$

where $A_0\left(t^0\right)$ and $D_0\left(t^0\right)$ are arbitrary functions of the slow time scale to be determined on the next step of iteration.

Collecting all terms of order ε gives the boundary value problem of the next asymptotic order as

$$
\begin{aligned}
\omega^2\left[\frac{\partial^2 X_1}{\partial\tau^2} + \left(\frac{n\pi}{2}\right)^2 X_1\right] &= -\left(2\omega\frac{\partial^2 Y_0}{\partial\tau\partial t^0} + \sigma X_0 + X_0^3 + 3Y_0^2X_0\right) \\
\omega^2\frac{\partial X_1}{\partial\tau}|_{\tau=\pm1} &= p
\end{aligned}
\tag{7.25}
$$

$$
\omega^2\left[\frac{\partial^2 Y_1}{\partial\tau^2} + \left(\frac{n\pi}{2}\right)^2 Y_1\right] = -\left(2\omega\frac{\partial^2 X_0}{\partial\tau\partial t^0} + \sigma Y_0 + Y_0^3 + 3X_0^2Y_0\right)
$$

$$Y_1|_{\tau=\pm 1} = 0$$

The right-hand sides of Eqs. (7.25) implicitly depend on the slow time t^0 through still unknown functions $A_0\left(t^0\right)$ and $D_0\left(t^0\right)$ and their derivatives $A_0^{'}\left(t^0\right)$ and $D_0^{'}\left(t^0\right)$. Taking into account (7.24) leads to the following general solution of the differential equations (7.25):

$$\begin{aligned} X_1 = {} & A_1\left(t^0\right)\sin\frac{n\pi\tau}{2} + B_1\left(t^0\right)\cos\frac{n\pi\tau}{2} \\ & + \frac{1}{\omega}\left[\frac{A_0}{n\pi\omega}\left(\sigma + \frac{3}{4}A_0^2 + \frac{3}{4}D_0^2\right) - D_0'\right]\tau\cos\frac{n\pi\tau}{2} \\ & - \frac{1}{n\pi\omega}\left[\frac{A_0}{n\pi\omega}\left(\sigma + \frac{7}{8}A_0^2 + \frac{3}{8}D_0^2\right) - D_0'\right]\sin\frac{n\pi\tau}{2} \\ & - \frac{A_0}{8n^2\pi^2\omega^2}\left(A_0^2 - 3D_0^2\right)\sin\frac{3n\pi\tau}{2} \end{aligned} \tag{7.26}$$

and

$$\begin{aligned} Y_1 = {} & C_1\left(t^0\right)\sin\frac{n\pi\tau}{2} + D_1\left(t^0\right)\cos\frac{n\pi\tau}{2} \\ & - \frac{1}{\omega}\left[\frac{D_0}{n\pi\omega}\left(\sigma + \frac{3}{4}A_0^2 + \frac{3}{4}D_0^2\right) + A_0'\right]\tau\sin\frac{n\pi\tau}{2} \\ & - \frac{1}{n\pi\omega}\left[\frac{D_0}{n\pi\omega}\left(\sigma + \frac{3}{8}A_0^2 + \frac{7}{8}D_0^2\right) + A_0'\right]\cos\frac{n\pi\tau}{2} \\ & - \frac{D_0}{8n^2\pi^2\omega^2}\left(3A_0^2 - D_0^2\right)\cos\frac{3n\pi\tau}{2} \end{aligned} \tag{7.27}$$

Now the boundary condition for X_1 gives

$$B_1\left(t^0\right) \equiv 0$$

and

$$D_0^{'} = \frac{A_0}{n\pi\omega}\left[\sigma + \frac{3}{4}\left(A_0^2 + D_0^2\right)\right] + \frac{2p}{n\pi\omega}\sin\frac{n\pi}{2} \tag{7.28}$$

Then, the boundary condition for Y_1 gives

$$C_1\left(t^0\right) \equiv 0$$

and

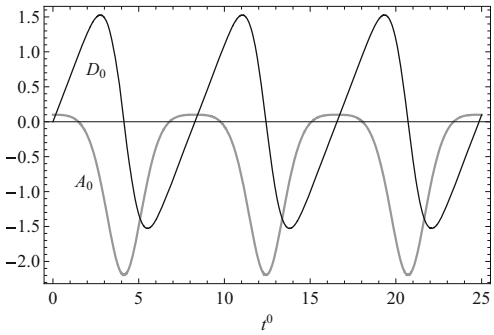

Fig. 7.2 The amplitudes $A_0(t^0)$ and $D_0(t^0)$ in the slow time scale, $t^0 = \varepsilon t$, shown by the gray and black lines, respectively

$$A_0^{'} = -\frac{D_0}{n\pi\omega}\left[\sigma + \frac{3}{4}\left(A_0^2 + D_0^2\right)\right] \tag{7.29}$$

In current approximation, another two arbitrary functions of the slow time scale can be chosen as $A_1\left(t^0\right) \equiv 0$ and $D_1\left(t^0\right) \equiv 0$. The same type of terms are included already into the generating solution (7.24). Substituting derivatives from (7.28) and (7.29) in (7.26) and (7.27) and taking into account (7.24) gives

$$\begin{aligned} X = A_0 \sin\frac{n\pi\tau}{2}\left[1 - \frac{\varepsilon}{2n^2\pi^2\omega^2}\left(A_0^2 - 3D_0^2\right)\cos^2\frac{n\pi\tau}{2}\right] \\ -\frac{2\varepsilon p}{n^2\pi^2\omega^2}\sin\frac{n\pi}{2}\left(n\pi\tau\cos\frac{n\pi\tau}{2} - \sin\frac{n\pi\tau}{2}\right) + O(\varepsilon^2) \end{aligned} \tag{7.30}$$

$$Y = D_0\cos\frac{n\pi\tau}{2}\left[1 + \frac{\varepsilon}{2n^2\pi^2\omega^2}\left(3A_0^2 - D_0^2\right)\sin^2\frac{n\pi\tau}{2}\right] + O(\varepsilon^2) \tag{7.31}$$

Substituting (7.30) and (7.31) in (7.17) finally gives the closed form approximate solution $x(t)$, despite of the discontinuous impulsive loading.

Figures 7.2, 7.3, and 7.4 illustrate the results of calculations under the following parameters and initial conditions: $n = 1$, $\omega = 1.0$, $\sigma = 0.1$, $p = 1.0$, $\varepsilon = 0.1$, $A_0(0) = 0.1$, $D_0(0) = 0.0$. The coordinate-velocity diagram shows two velocity jumps per one cycle due to the periodic impulsive excitation.

7.3 Strongly Nonlinear Oscillator Under Periodic Pulses

Let us consider the case of strongly nonlinear exactly solvable oscillator described in Chap. 3 by adding periodic impulsive loading on the right-hand side as follows:

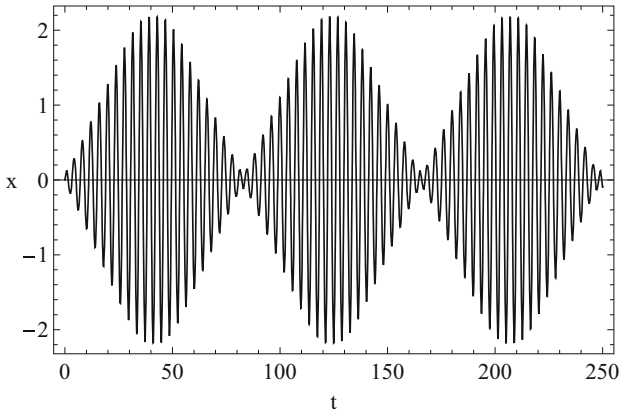

Fig. 7.3 The time history of the oscillator response near the fundamental resonance

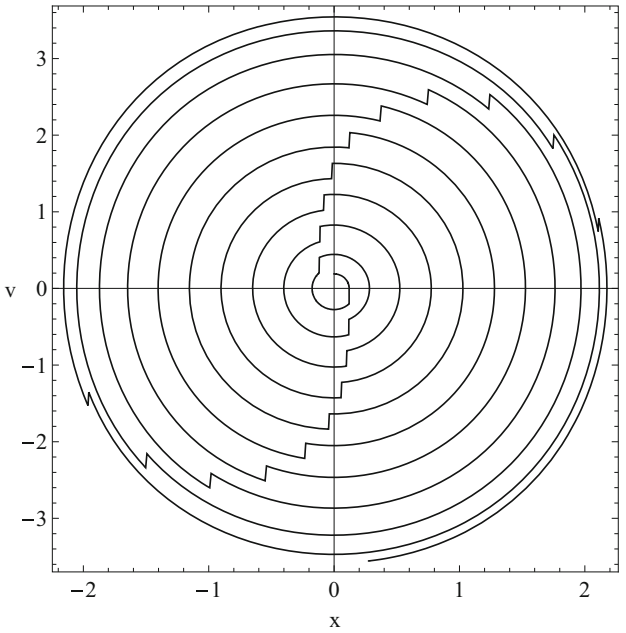

Fig. 7.4 The coordinate-velocity plane with the oscillator trajectory during the interval $0 < t < 40$

$$\ddot{x} + \tan x + \tan^3 x = \frac{F}{a}\frac{de\,(t/a)}{d\,(t/a)}$$
$$= 2F \sum_{n=-\infty}^{\infty} (-1)^n \delta[t - (2n-1)a] \tag{7.32}$$

Here the parameter values $2F > 0$ and $4a = T > 0$ characterize the amplitude and period of the impulsive loading.

Making substitutions $x = X(\tau)$ and $\tau = \tau(t/a)$ in Eq. (7.32) gives

$$a^{-2}\frac{d^2X}{d\tau^2} + \tan X + \tan^3 X = a^{-2}\left(aF - \frac{dX}{d\tau}\right)\frac{de\,(t/a)}{d\,(t/a)}$$

or

$$a^{-2}\frac{d^2X}{d\tau^2} + \tan X + \tan^3 X = 0 \tag{7.33}$$

under the following continuity condition for $x(t)$,

$$\frac{dX}{d\tau}\,|_{\tau=\pm1} = aF \tag{7.34}$$

Boundary value problems (7.33) and (7.34) describe the class of steady-state periodic motions of the period T. With reference to Chap. 3, Eq. (7.33) has exact solution of the form

$$X(\tau) = \arcsin[\sin A \sin(a\tau/\cos A)] \tag{7.35}$$

where A is an arbitrary constant, which is sufficient to satisfy both conditions in (7.34) due to the oddness of solution (7.35) with respect to τ.

Substituting (7.35) in (7.34) gives a trigonometric equation for a quarter of the period, $a = T/4$. The corresponding solution has four different branches of solution that can be combined as

$$a_0 = \cos A\left(\arccos\frac{F\cos^2 A}{|\sin A|\sqrt{1 - F^2\cos^2 A}}\right) \tag{7.36}$$

$$a_k = k\pi\cos A \pm a_0, \qquad (k = 1, 2, 3, \ldots) \tag{7.37}$$

Note that solution (7.35) represents a one-parameter set of particular solutions imposing the initial conditions on the original variables as $x(0) = 0$ and $\dot{x}(0) > 0$. In (7.36) and (7.37), such type of the initial conditions associates with even k, whereas the odd numbers reveal another subset of the periodic solutions with the negative initial velocities. Both of the subsets are covered by the following modification of solution (7.35) in terms of the original variables

$$x_k(t) = (-1)^k \arcsin\left\{\sin A \sin\left[\frac{a_k}{\cos A}\tau\left(\frac{t}{a_k}\right)\right]\right\} \tag{7.38}$$

where a_k is a quarter of the period given by (7.36) and (7.37) and A is an arbitrary parameter restricted by interval whose meaning is discussed below

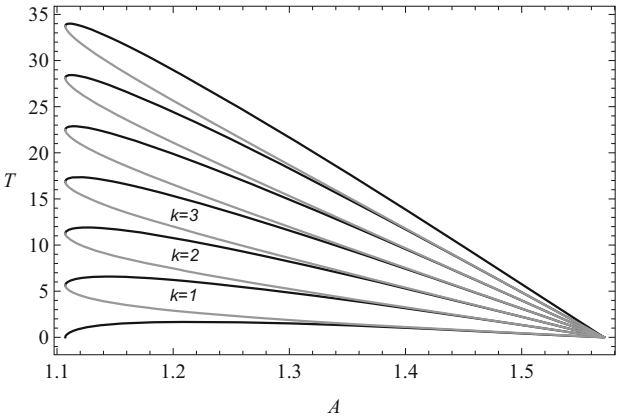

Fig. 7.5 First seven amplitude-period curves, $T = 4a_k$ ($k = 0, 1, \ldots, 6$) according to (7.36) and (7.37) of the oscillator (7.32) at $F = 2.0$

$$\arccos \frac{1}{\sqrt{1+F^2}} = A_{\min} < A < A_{\max} = \frac{\pi}{2} \tag{7.39}$$

Figure 7.5 illustrates the sequence of branches of solutions (7.36) and (7.37) at different numbers k and the parameter $F = 2.0$. The diagram gives such combinations of the period and amplitude at which oscillator (7.32) can have the periodic response with the period of external impulses, $T = 4a$. The upper and lower branches of each loop correspond to plus and minus signs in expression (7.37), respectively. Solution (7.36) corresponds to the number $k = 0$ and has the only upper branch. For the selected magnitude of $F = 2$, the minimal parameter of amplitude is found to be $A_{\min} = 1.10715$, which corresponds to the left edges of the amplitude-period loops in Fig. 7.5. As a result, further slight increase of the amplitude is accompanied by a bifurcation of solutions for every k as shown in Fig. 7.6 in time domain. Only first three couples of solutions ($k = 1, 2, 3$) from the infinite set are shown. Graphs of the left and right columns converge to each other in such a way that impulses are acting twice per one period exactly at $x = 0$ as $A \to A_{\min}$. This is seen from the sharp peaks moving toward the axis $x = 0$ along the vertical as $A \to A_{\min}$. The influence of external pulses on the temporal shapes is decreasing as the amplitude grows. When the parameter A is approaching its maximum $A_{\max} = \pi/2$, the oscillator itself generates high-frequency impacts as discussed in Chap. 3. The effect of external pulses eventually becomes negligible, and their times coincide with some of the pulses produced by the restoring force. Note that the oscillator moves freely every $k - 1$ cycles before the next pulse is applied (Fig. 7.6).

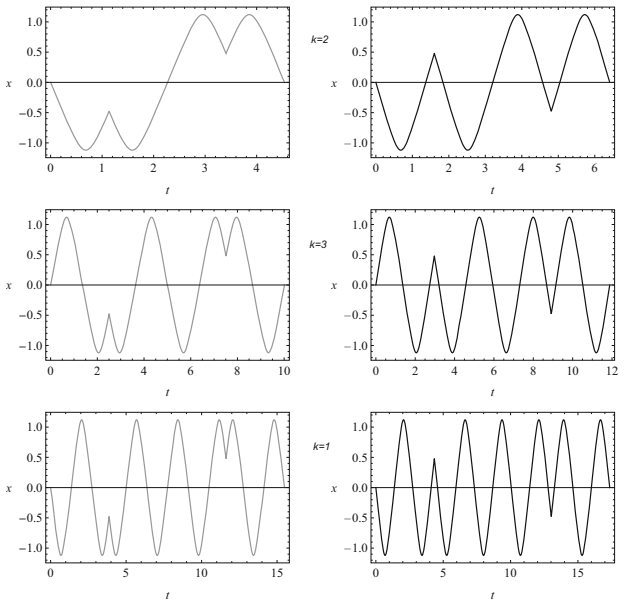

Fig. 7.6 Temporal shapes of the oscillator response near the minimum amplitude $A = 1.12$ and the loading impulse parameter $F = 2.0$, where the left and right columns correspond to the lower and upper branches of loops shown in Fig. 7.5 with gray and black curves, respectively

7.4 Impact Oscillators Under Impulsive Loading

Consider nonlinear oscillator under the periodic impulsive excitation of the following general form

$$\ddot{x} + 2\zeta\dot{x} + f\,(x, \omega t) = p\frac{de\,(\omega t)}{d\,(\omega t)} \tag{7.40}$$

where ζ, ω and p are constant parameters and the function $f\,(x, \omega t)$ is periodic with respect to the argument ωt with the period $T = 4$.

It is assumed that the coordinate x is subjected to either the constraint condition

$$0 \leq x\,(t) \tag{7.41}$$

or

$$-1 \leq x\,(t) \leq 1 \tag{7.42}$$

According to the idea of nonsmooth transformation of positional coordinates[1] [251, 256], the constraints (7.41) and (7.42) are eliminated by unfolding the space as

$$x(t) \longrightarrow l(t) : x = S(l) \tag{7.43}$$

where $S(l) \equiv |l|$ in case (7.41) or $S(l) \equiv \tau(l)$ in case (7.42). As a result, the new coordinate l belongs to the entire infinite interval, $l(t) \in (-\infty, \infty)$, in contrast to (7.41) or (7.42).

Taking into account the identity $[S'(l)]^2 = 1$ gives the final result of transformation (7.43) in the form

$$\frac{d^2 l}{dt^2} + 2\zeta \frac{dl}{dt} + S'(l) f[S(l), \omega t] = pS'(l) \frac{de(\omega t)}{d(\omega t)} \tag{7.44}$$

where the new coordinate $l(t)$ is free of any constraints.

Note that the right-hand side of Eq. (7.44) makes sense within the distribution theory under the condition that times of interaction with constraints (7.41) or (7.42) never coincide with the external pulse times.

Consider now the class of periodic motions of the period of external loading, $T = 4/\omega$. As follows from Chap. 6 and the previous sections of this chapter, within such class of motions, the external pulses are eliminated by introducing the new time argument

$$t \longrightarrow \tau : \tau = \tau(\omega t), \quad l = X(\tau) + Y(\tau) e \tag{7.45}$$

Substituting (7.45) into Eq. (7.44) gives

$$\begin{aligned} &\omega^2 X''(\tau) + 2\zeta\omega Y'(\tau) + R(X, Y, \tau) \\ &+ \left[\omega^2 Y''(\tau) + 2\zeta\omega X'(\tau) + I(X, Y, \tau)\right] e \\ &= \left[pR_S(X, Y) + pI_S(X, Y) e - \omega^2 X'(\tau)\right] \frac{de(\omega t)}{d(\omega t)} \end{aligned} \tag{7.46}$$

where

$$\left\{ \begin{matrix} R \\ I \end{matrix} \right\} = \frac{1}{2} \left\{ S'(X + Y) f[S(X + Y), \tau] \pm S'(X - Y) f[S(X - Y), 2 - \tau] \right\}$$

and

[1] See Sect. 1.5.2.

$$\left\{ \begin{array}{c} R_S \\ I_S \end{array} \right\} = \frac{1}{2} \left\{ S'(X+Y) \pm S'(X-Y) \right\}$$

under the necessary condition of continuity for $l(t)$,

$$Y(\pm 1) = 0 \tag{7.47}$$

Equation (7.46) is equivalent to the following boundary value problem

$$\begin{aligned} \omega^2 X''(\tau) + 2\zeta\omega Y'(\tau) + R(X, Y, \tau) = 0 \\ \omega^2 Y''(\tau) + 2\zeta\omega X'(\tau) + I(X, Y, \tau) = 0 \end{aligned} \tag{7.48}$$

$$[X'(\tau) - \omega^{-2} p S'(X)]|_{\tau=\pm 1} = 0 \tag{7.49}$$

where boundary condition (7.49) is simplified by enforcing condition (7.47).

After solution of the boundary value problem (7.47) through (7.49) has been obtained, the original coordinate is given by the composition of transformations (7.43) and (7.45) as

$$x(t) = S(X(\tau) + Y(\tau) e) \tag{7.50}$$

where $\tau = \tau(\omega t)$ and $e = e(\omega t)$.

The advantage of such a boundary value problem formulation is that the effect of both internal and external impulses is captured by the composition of two transformations (7.50). As a result, the final system is free of any singular terms. Some particular cases and examples were considered earlier in [180].

Chapter 8
Strongly Nonlinear Vibrations

This chapter presents analytical successive approximations algorithms for different oscillators with strongly nonlinear characteristics. In general terms, such algorithms approximate temporal mode shapes of vibrations by polynomials and other simple functions of the triangle wave. In order to develop the algorithms, the triangle wave is introduced into dynamical systems as a new temporal argument. The corresponding manipulations with dynamical systems are described in the next three sections. Then the description focuses on the algorithm implementations for different essentially anharmonic cases including oscillators whose characteristics may approach nonsmooth or even discontinuous limits.

8.1 Periodic Solutions for First-Order Dynamical Systems

Let us consider a dynamical system described by first-order differential equation with respect to the vector-function $x(t) \in R^n$,

$$\dot{x} = f(x) \tag{8.1}$$

where $f(x)$ is a continuous vector-function and the over dot indicates time derivative.

Consider the class of periodic motions of the period $T = 4a$, which is unknown in the autonomous case. Periodic solutions usually require specific initial conditions. Practically, such kind of the specific initial conditions is determined in a backward way, after some periodic family of solutions is obtained under the assumption of periodicity. In the present case, the assumption of periodicity is imposed automatically by the form of representation for periodic solutions

$$x = X(\tau) + Y(\tau)e \tag{8.2}$$

V. N. Pilipchuk, *Oscillators and Oscillatory Signals from Smooth to Discontinuous*,
https://doi.org/10.1007/978-3-031-37788-4_8

where $\tau = \tau(t/a)$ and $e = e(t/a)$ are the standard triangle and square waves, respectively, and $X(\tau)$ and $Y(\tau)$ are unknown components of the solution.

Substituting (8.2) in (8.1) gives

$$(Y' - aR_f) + (X' - aI_f)e \ + Ye' = 0$$

where

$$R_f = R_f(X, Y) = \frac{1}{2}[f(X + Y) + f(X - Y)]$$

$$I_f = I_f(X, Y) = \frac{1}{2}[f(X + Y) - f(X - Y)]$$

Eliminating the periodic singular term $e' = de(t/a)/d(t/a)$ by means of the boundary condition for $Y(\tau)$ gives the nonlinear boundary value problem on the standard interval, $-1 \le \tau \le 1$,

$$\begin{aligned} Y' &= aR_f(X, Y) \\ X' &= aI_f(X, Y) \\ Y|_{\tau=\pm1} &= 0 \end{aligned} \tag{8.3}$$

Note that the entire interval $-1 \le \tau \le 1$ is completely covered by a half of the period, $-a \le t \le a$, while representation (8.2) unfolds the corresponding fragment on the entire time interval $-\infty < t < \infty$.

8.2 Second-Order Dynamical Systems

Consider now the differential equation of motion in the standard Newtonian form

$$\ddot{x} + f(x, \dot{x}, t) = 0 \tag{8.4}$$

where $x(t) \in R^n$ is a positional vector-function and the vector-function f is assumed to be sufficiently smooth and periodic with respect to the explicit time t with the period $T = 4a$, which is unknown the autonomous case.

Substituting (8.2) into (8.4), using the differential and algebraic properties of substitution (8.2), and imposing the boundary (smoothness) conditions give

$$(X'' + a^2R_f) + (Y'' + a^2I_f)e = 0$$

where

$$R_f = \frac{1}{2}\left[f\left(X+Y,\ \frac{X'+Y'}{a},\ a\tau\right)+f\left(X-Y,\ -\frac{X'-Y'}{a},\ 2a-a\tau\right)\right] \tag{8.5}$$

$$I_f = \frac{1}{2}\left[f\left(X+Y,\ \frac{X'+Y'}{a},\ a\tau\right)-f\left(X-Y,\ -\frac{X'-Y'}{a},\ 2a-a\tau\right)\right] \tag{8.6}$$

This leads to the boundary value problem

$$X'' + a^2 R_f(X, Y, X', Y', \tau) = 0, \quad X'|_{\tau=\pm 1} = 0 \tag{8.7}$$

$$Y'' + a^2 I_f(X, Y, X', Y', \tau) = 0, \quad Y\,|_{\tau=\pm 1} = 0 \tag{8.8}$$

Let us discuss the form of Eqs. (8.7) and (8.8). Firstly, despite of the obvious formal complication, Eqs. (8.7) and (8.8) possess certain symmetries dictated by substitution (8.2). For instance, introducing the new unknown variables

$$U(\tau) = X(\tau) + Y(\tau)$$
$$V(\tau) = X(\tau) - Y(\tau)$$

brings the boundary value problem, (8.7) and (8.8), to the form

$$\begin{aligned} U'' + a^2 f\left(U,\ U'/a,\ 2a - a\tau\right) &= 0 \\ V'' + a^2 f\left(V,\ -V'/a, 2a -\ a\tau\right) &= 0 \\ U' + V'|_{\tau=\pm 1} &= 0 \\ U - V|_{\tau=\pm 1} &= 0 \end{aligned} \tag{8.9}$$

where the differential equations are decoupled at cost of coupling the boundary conditions though.

In case when analytical methods are applied, the differential equations (8.9) for $U(\tau)$ and $V(\tau)$ can be usually solved in a similar way. The previous boundary value problem, (8.7) and (8.8), may appear to have some advantages for analyses. In some particular cases, the problem admits families of solutions with either $Y(\tau) \equiv 0$ or $X(\tau) \equiv 0$.

Secondly, due to substitution (8.2), the major qualitative property of solutions, such as periodicity, is captured in advance by the new argument, τ. As a result, the following simplified system can be employed as a generating model for analytical algorithms of successive approximations

$$\begin{aligned} X'' &= 0 \\ Y'' &= 0 \end{aligned} \tag{8.10}$$

Indeed, substituting obvious solutions of Eqs. (8.10) in (8.2) gives a family of nonsmooth *periodic* motions with respect to the original time parameter, t,

$$x(t) = X(0) + X'(0)\tau(t/a) + \left[Y(0) + Y'(0)\tau(t/a)\right] e(t/a) \tag{8.11}$$

Thirdly, from the physical standpoint, linear equations (8.10) describe a strongly nonlinear (nonsmooth) generating model. In particular, if $Y(0) = 0$ and $Y'(0) = 0$, then vector-function (8.11) describes vibrations of basic vibroimpact models.

The analytical algorithms developed below are based on the idea of approximation of smooth vibrating systems by the basic vibroimpact models. In other words, the triangle wave is assumed to be a dominant component of temporal mode shapes of vibrations. Such an idea indeed follows the analogy with the quasi-harmonic approaches. In particular, the harmonic balance method approximates vibrating systems by effective harmonic oscillators regardless types or powers of the system nonlinearities. This is justified by the fact that Fourier coefficients usually decay in a fast enough rate, such that, for instance, the second term can be considered as a small correction to the first term. The corresponding "small parameter" is therefore hidden in the iterative procedure itself rather than explicitly present in the differential equations of motion. Finally note that Eqs. (8.10) make sense due to the temporal substitution $t \longrightarrow \tau(t/a)$. In terms of the original variables, the corresponding equation, $\ddot{x} = 0$, contains too little information about the original system (8.4) and captures no global properties of the dynamics.

8.3 Periodic Solutions of Conservative Systems

8.3.1 The Vibroimpact Approximation

Let us consider the case of n-degrees-of-freedom conservative system

$$\ddot{x} + f(x) = 0 \tag{8.12}$$

where $f(x)$ is an odd analytical vector-function of the positional vector-column $x(t) \in R^n$.

A one-parameter family of periodic solutions will be built such that $X(-\tau) \equiv -X(\tau)$. Since Eq. (8.12) admits the group of time translations, then another arbitrary parameter can be always added to the time variable. Taking into account the symmetry of system (8.12) enables one of considering the particular case of substitution (8.2)

$$x(t) = X(\tau(t/a)), \quad Y \equiv 0 \tag{8.13}$$

Based on the conditions assumed, the boundary value problem (8.7) and (8.8) is reduced to the following one

$$X'' + a^2 f(X) = 0, \quad X'|_{\tau=1} = 0 \tag{8.14}$$

We seek solutions of the boundary value problem (8.14) in the form of series of successive approximations

$$X = X^0(\tau) + X^1(\tau) + X^2(\tau) + \ldots \tag{8.15}$$

$$a^2 = h_0(1 + \gamma_1 + \gamma_2 + \ldots) \tag{8.16}$$

To organize the corresponding iterative procedure, it is assumed that

$$\begin{gathered} O(\|X^i\|) \gg O(\|X^{i+1}\|) \\ O(\gamma_{i+1}) \gg O(\gamma_{i+2}) \\ (i = 0, 1, 2, \ldots) \end{gathered} \tag{8.17}$$

where the norm of vector-functions is defined by $\|X\| = \max_{\tau} \|X\|_{R^n}$.

Based on assumptions (8.17), series (8.15) and (8.16) generate the sequences of equations and boundary conditions as, respectively,

$$X^{0\prime\prime} = 0 \tag{8.18}$$

$$X^{1\prime\prime} = -h_0 f(X^0) \tag{8.19}$$

$$X^{2\prime\prime} = -h_0[\gamma_1 f(X^0) + f'_x(X^0)X^1] \tag{8.20}$$

$$\ldots$$

and

$$(X^{0\prime} + X^{1\prime})|_{\tau=1} = 0 \tag{8.21}$$

$$X^{2\prime}|_{\tau=1} = 0 \tag{8.22}$$

$$\ldots$$

Note that condition (8.21) includes first two approximations as the only way to proceed with a non-zero generating solution. In particular, the generating solution is found from Eq. (8.18) in the form

$$X^0 = A^0\tau \tag{8.23}$$

where $A^0 \in R^n$ is an arbitrary constant vector and the oddness condition has been enforced in order to set to zero another constant vector.

In line with the discussion at the end of the previous section, solution (8.23) describes a multi-dimensional vibroimpact oscillator between two absolutely stiff and perfectly elastic barriers such that A^0 is the normal vector to both barriers. Direction of the vector A^0 will be defined on the next step of successive approximations, whereas its length will appear to be coupled with the parameter h_0 by some relationship due to boundary condition (8.21). So substituting (8.23) in (8.19) and integrating give solution

$$X^1 = A^1\tau - h_0 \int_0^\tau (\tau - \xi) f(A^0\xi) d\xi \tag{8.24}$$

where A^1 is another arbitrary constant vector.

Note that the first term in expression (8.24) is similar to generating solution (8.23) and hence contributes nothing new into the entire solution within the first two steps of the procedure. Therefore, let us take $A^1 = 0$ and then substitute the combination $X^0 + X^1$ in the boundary condition (8.21). This gives a nonlinear eigenvalue problem with respect to the vector A^0 in the form

$$\int_0^1 f(A^0\tau) d\tau = \frac{1}{h_0} A^0 \tag{8.25}$$

Equation (8.25) represents a set of n scalar equations relating the components of vector A^0 and the parameter h_0. The combination A^0 and $1/h_0$ will be interpreted as an eigenvector and eigenvalue of the nonlinear eigenvector problem (8.25). Taking scalar product of both sides of Eq. (8.25) with A^{0T} gives

$$h_0 = \frac{A^{0T} A^0}{A^{0T} \int_0^1 f(A^0\tau) d\tau} \tag{8.26}$$

where the upper index T stays for transpose operation.

To clarify the meaning of expressions (8.25) and (8.26), let us consider the linear case $f(x) \equiv Kx$, where K is an $n \times n$ stiffness matrix. The corresponding relationships will differ from those of the exact linear theory by specific constant factors because the temporal mode shape of vibrations is not exact but approximated by the triangular sine wave. Nevertheless, in nonlinear cases, expression (8.26) can provide estimates for amplitude-frequency response characteristics. Further, integrating Eq. (8.20) gives

$$X^2 = A^2\tau - h_0 \int_0^\tau (\tau - \xi)[\gamma_1 f(A^0\xi) + f'_x(A^0\xi)X^1(\xi)]d\xi \tag{8.27}$$

where A^2 is an arbitrary constant vector and $f'_x(\ A^0\xi\ )$ is the $n \times n$-Jacobian matrix of first partial derivatives.

Then boundary condition (8.22) gives

$$A^2 = h_0 \int_0^1 [\gamma_1 f(A^0\tau) + f'_x(A^0\tau)X^1(\tau)]d\tau \tag{8.28}$$

where the coefficient γ_1 is yet unknown.

In order to determine the coefficient γ_1, some additional condition for the vector A^2 can be imposed, for instance, as follows

$$A^{0T}A^2 = 0 \tag{8.29}$$

This condition means that the vector A^2 must be orthogonal to the corresponding vector of the generating solution A^0 in order to keep the amplitude fixed. Substituting (8.28) in (8.29) gives

$$\gamma_1 = -\frac{A^{0T}\int_0^1 f'_x(A^0\tau)X^1 d\tau}{A^{0T}\int_0^1 f(A^0\tau)d\tau} \tag{8.30}$$

This completes the second step of successive approximations. All the further steps can be passed in the same way. In general terms, convergence properties of the above procedure are due to the following integral operator

$$F[X] \equiv a^2 \left\{ \tau \int_\tau^1 f(X(\xi))d\xi + \int_0^\tau \xi f(X(\xi))d\xi \right\} \tag{8.31}$$

where

$$a^2 = h_0 \frac{A^{0T}\int_0^1 f(A^0\tau)d\tau}{A^{0T}\int_0^1 f(X)d\tau} \tag{8.32}$$

Based on definition (8.31), the original boundary value problem (8.14) admits representation in the form $X = F[X]$. Therefore, the convergence condition is

$$\frac{\|F'_X[X^0]\delta X\|}{\|\delta X\|} < 1 \tag{8.33}$$

where δX is an arbitrary vector-function from a small enough neighborhood of X^0.

In the case of linearized system, condition (8.33) leads to the set of inequalities $\Omega_i/\Omega_j < 1$ for all $i \neq j$, where Ω_j is the eigenfrequency of the linear normal mode, which is chosen to be a generating solution.

Remark 8.3.1 Note that convergence of series (8.16) for a^2 can be improved significantly by means of Padè transform [26] as shown in Sect. 8.3.5 and Appendix 1.

8.3.2 One Degree-of-Freedom General Conservative Oscillator

In the one-degree-of-freedom case with odd characteristic, the boundary condition at $\tau = 1$ is reduced to a single equation, which is sequentially satisfied by the factor h_0 and terms $\gamma_1, \gamma_2, \ldots$ of series (8.16). As a result, the process of successive approximations eases by setting $A^0 = A$ and $A^i = 0$ for $i = 1, 2, \ldots$. Let us introduce notations $h_i = h_0\gamma_i$ and represent series (8.15) and (8.16) in the form

$$\begin{aligned} X &= X_0(\tau) + X_1(\tau) + X_2(\tau) + \ldots \\ a^2 &= h_0 + h_1 + h_2 + \ldots \end{aligned} \tag{8.34}$$

where $X_i(\tau)$ is a scalar function of the triangular sine wave $\tau = \tau(t/a)$.

Due to the reduction of one-dimensional case, all terms of the expansions are iteratively determined by the explicit relationships. First two steps of the iterative procedure are coupled by the smoothing boundary condition (8.21) that provides the leading order smooth estimate for the temporal mode shape by coupling the parameters, $h_0 = h_0(A)$, as follows

$$X_0 = A\tau \tag{8.35}$$

$$\begin{aligned} X_1 &= -h_0 \int_0^\tau (\tau - \xi) f(A\xi) d\xi \\ h_0 &= A/\int_0^1 f(A\xi) d\xi \end{aligned} \tag{8.36}$$

All the next steps of the procedure are passed then in a similar way based on relationships

$$X_i = -\sum_{j=1}^{i} h_{j-1} \int_0^{\tau} (\tau - \xi) R_{i-j} d\xi$$

$$h_{i-1} = -\sum_{j=1}^{i-1} \alpha_{i-j} h_{j-1} \tag{8.37}$$

$$(i = 2, 3, \ldots)$$

where the coefficients and integrands are generated by means of the formal auxiliary parameter, ε, as follows

$$\alpha_i = \int_0^1 R_i d\xi \Big/ \int_0^1 R_0 d\xi \tag{8.38}$$

$$R_i = \frac{1}{i!} \frac{d^i f(X^0 + \varepsilon X^1 + \varepsilon^2 X^2 + \cdots)}{d\varepsilon^i}|_{\varepsilon=0}$$

$$(i = 0, 1, 2, \ldots)$$

The way of using the parameter ε is in compliance with assumptions (8.17). Respectively, such parameter splits the restoring force according to (8.38) and then disappears from expressions. The convergence of suggested iterative series of successive approximations is illustrated by the example below. As noticed at the end of the previous subsection, applying Padè transform to the series for a^2 improves the convergence and hence gives a better estimate for the period (see Appendix 1 for the corresponding algorithm and graphical illustration)

$$T = 4\sqrt{h_0} \left(1 - \frac{h_1}{h_0} + \frac{h_1^2 - h_0 h_2}{h_0^2} - \frac{h_1^3 - 2h_0 h_2 h_1 + h_0^2 h_3}{h_0^3} + \cdots\right)^{-1/2} \tag{8.39}$$

Example 8.3.1 Let us consider the oscillator

$$\ddot{x} + x^m = 0$$

where m is an odd positive integer. This oscillator was already discussed in Chap. 3 under the notation $m = 2n - 1$. Now, applying two iterations according to the above scheme, (8.36) and (8.37), gives solution

$$X = A\left[\tau - \frac{\tau^{m+2}}{m+2} + \frac{m}{2(m+2)}\left(\frac{\tau^{2m+3}}{2m+3} - \frac{\tau^{m+2}}{m+2}\right) - R_3 - R_4 - \cdots\right] \tag{8.40}$$

$$a^2 = \frac{m+1}{A^{m-1}}\left\{1 + \frac{m}{2(m+2)}\left[1 + \frac{(m+1)^2}{(m+2)(2m+3)}\right] + r_3 + r_4 + \cdots\right\} \tag{8.41}$$

where expressions

$$0 < R_i(m,\tau) < \frac{m\,|\tau|^{m+2}}{2^{i-1}(m+2)^2} \tag{8.42}$$

$$0 < r_i(m) < \frac{m}{2^i(m+2)}$$

provide estimates for high-order terms of the successive approximations. In particular, expressions (8.42) indicate that series (8.40) and (8.41) may converge quite slowly. However, the asymptotic of large exponents m essentially improves precision of the truncated series even though first few terms of the series are included. The temporal mode shapes of different iterations are shown in Fig. 8.1, whereas Fig. 8.2 illustrates the period as a function of the number m for the fixed initial velocity, in one and three iterations followed by Padè transform (8.44) in comparison to the exact solution. Figure 8.1 shows that high-order iterations are localized near the amplitude points. For instance, the first iteration, X_1, compensates the discontinuities of slope of the generating solution X_0 with a minor effect on the rest of the triangular wave. Further, Fig. 8.2 confirms that expansion (8.41) gives a better estimate for the period than the harmonic balance as the exponent m increases. Note that the entire series (8.40) and (8.41) are not asymptotic with respect to m or $1/m$ in the sense of Poincaré; however the suggested iterative expansions still capture the asymptotic of impact oscillator as $m \to \infty$ quite effectively. Taking into account the number of iterations in (8.41) and using Padè transform (8.39) give the period

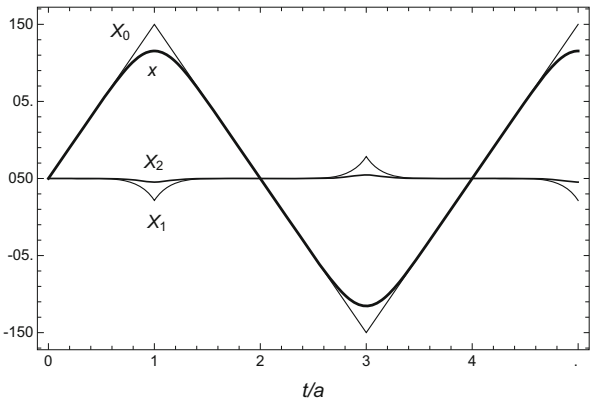

Fig. 8.1 The first three terms of iteration (thin lines) and their sum (solid line) for the temporal mode shape of the oscillator $\ddot{x} + x^5 = 0$

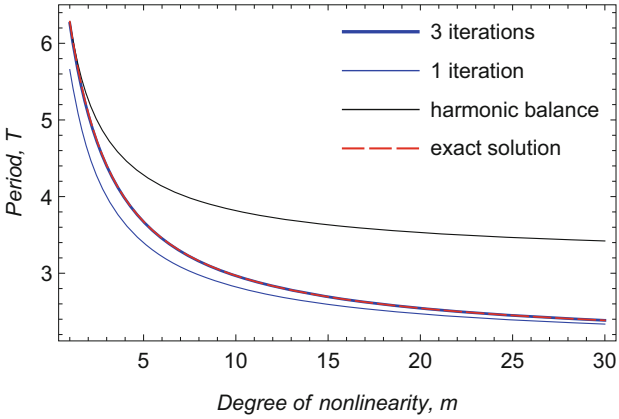

Fig. 8.2 The period of the oscillator with power characteristic at different exponents m obtained by three different methods for the initial velocity $v_0 = 2$

$$T = 4\sqrt{h_0}\left(1 - \frac{h_1}{h_0} + \frac{h_1^2 - h_0 h_2}{h_0^2} - \cdots\right)^{-1/2} \tag{8.43}$$
$$= 8\sqrt{\frac{m+1}{A^{m-1}}}\sqrt{\frac{(m+2)(2m+3)}{m(4m+21)+24}}$$

Differentiating (8.40) with respect to time t at $t = 0$ gives $A = v_0 a = v_0 T/4$, where v_0 is the initial velocity. Substituting this in (8.43) leads to the dependence of period T on the initial velocity

$$T = \left(\frac{4}{v_0}\right)^{\frac{m-1}{m+1}}\left[\frac{64(m+1)(m+2)(2m+3)}{m(4m+21)+24}\right]^{\frac{1}{m+1}} \tag{8.44}$$

As follows from this relationship, $T \longrightarrow 4/v_0$ as $m \longrightarrow \infty$, which corresponds to the vibroimpact limit of a freely oscillating particle with the constant speed v_0 within the interval $-1 \le x \le 1$.

8.3.3 *Energy Absorbers Based on Analogies with Soft-Wall Billiards*

Analytical solution (8.40) was applied to the analysis of energy absorbing devices and mechanical metamaterials based on stochastic soft-wall billiards [169], [171]. The suggested basic model is illustrated in Fig. 8.3, where the mass M of harmonic

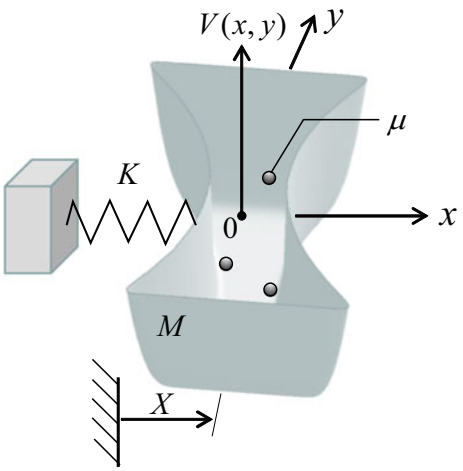

Fig. 8.3 A massive potential container oscillating with a small particle(s) interacting with potential walls of different "stiffness" and shapes represented by function (8.45)

oscillator represents a two-dimensional container including one or few light particles such that the interaction of particles with the container walls is described by the potential energy

$$V(x,y)=\frac{\gamma}{2n}\left[\left(\frac{x}{\alpha+\beta(y^2-1)}\right)^{2n}+y^{2n}\right] \tag{8.45}$$

This phenomenological expression provides a convenient way to modeling qualitatively different shapes of two-dimensional containers with "soft walls," where β is the main geometrical parameter linked to the contour's, $V(x,y)=const.$, curvature as

$$\kappa=\frac{2\beta}{(1+4\beta^2y^2)^{3/2}} \tag{8.46}$$

for $x>0$, $-1<y<1$, as $n\longrightarrow\infty$. Therefore β is a one half of the curvature at $y=0$. Figure 8.4 illustrates the effect of β on the container shape by a typical contour of the potential energy in the non-inertial Cartesian frame xy. The container includes k relatively light non-interacting particles driven by their interactions with the potential walls as the container is given some initial energy. The total mass of particles, $m<<M$, is fixed, while their number k can be different; thus $\mu=m/k$ is a mass of each particle. A practical macro-level design for such model may include k parallel containers in order to exclude interactions between the particles. As follows from (8.46), model (8.45) gives soft analogs of two different types of stiff boundaries: a soft-walled version of billiards with scattering boundaries [221] for $\beta>0$ and a soft approximation for the so-called Bunimovich stadiums [39] for $\beta<0$. The wall effective stiffness is controlled by the number $n\gg1$, such that walls become asymptotically stiff as $n\longrightarrow\infty$. The

role of softening the cell walls is twofold. On one hand, it makes the container model closer to a real cell. On the other hand, in contrast to the conventional theory of billiards, the model can be described within the classical theory of differential equations without geometrically complicated nonsmooth mappings. For instance, it was shown in reference [169] that conditions of chaoticity can be linked to instabilities of nonlinear normal modes [241] rather than the repelling properties of mappings. Further, no phenomenological dissipation in the system is intentionally assumed; hence the total energy of the oscillator with inclusions is conserved. Note that elastic collisions of the light inclusions with the container's walls affect also the dynamics of container however in a less dramatic way. The presence of such a feedback, which is usually ignored in statistical studies, is a key assumption whose purpose is to observe the recurrence effect versus contour shapes of the container. Another difference with the typical statistical studies of non-interacting gas models is that the number of particles, $1 \leq k \leq 5$, is rather insufficient to provide the statistics of large numbers.

Ignoring the effect of gravity, the model dynamics is described by Lagrangian

$$L = \frac{1}{2}\dot{X}^2 - \frac{1}{2}X^2 + \sum_{j=1}^{k}\left\{\frac{\mu}{2}\left[\left(\dot{X}+\dot{x}_j\right)^2 + \dot{y}_j^2\right] - V(x_j, y_j)\right\} \tag{8.47}$$

where $X(t)$ is the displacement of the container with respect to the fixed base and $\{x_j, y_j\}$ are the coordinates of the jth particle in the container-based noninertial frame xy (Fig. 8.3).

As follows from Fig. 8.4, the dynamics of system (8.47) may essentially depend upon the value β, which is responsible for the curvature of the contour boundaries.

When contours possess convexities toward the inside area ($\beta > 0$), the presence of irregularities comes of no surprise due to the scattering segments of boundaries. The case $\beta < 0$ appears to be more complicated since both chaotic and regular motions are possible in different intervals of the curvature. A geometrical nature of such phenomena is likely similar to that was revealed in the case of Bunimovich stadia [39].

As mentioned, the container walls are softened to apply the nonlinear normal modes stability concept with regular analytical tools of Floquet theory. In the case of a single particle, $k = 1$, there is a normal mode whose trajectory is described by the equation $y_1 = 0$ as dictated by the symmetry of potential well. Although such trajectory can be observed under specific initial conditions, its local stability properties appear to have a global effect on the dynamics of particles inside the well. In order to investigate stability of the trajectory $y_1 = 0$, let us linearize the differential equations of motion given by Lanrangian (8.47) with respect to the coordinate y_1 and then re-scale the coordinates and time as

$$\{\bar{x}, \bar{y}, \bar{X}, \bar{t}\} = \frac{1}{\alpha - \beta}\left\{x_1, y_1, X, t\sqrt{\frac{\gamma}{\mu}}\right\} \tag{8.48}$$

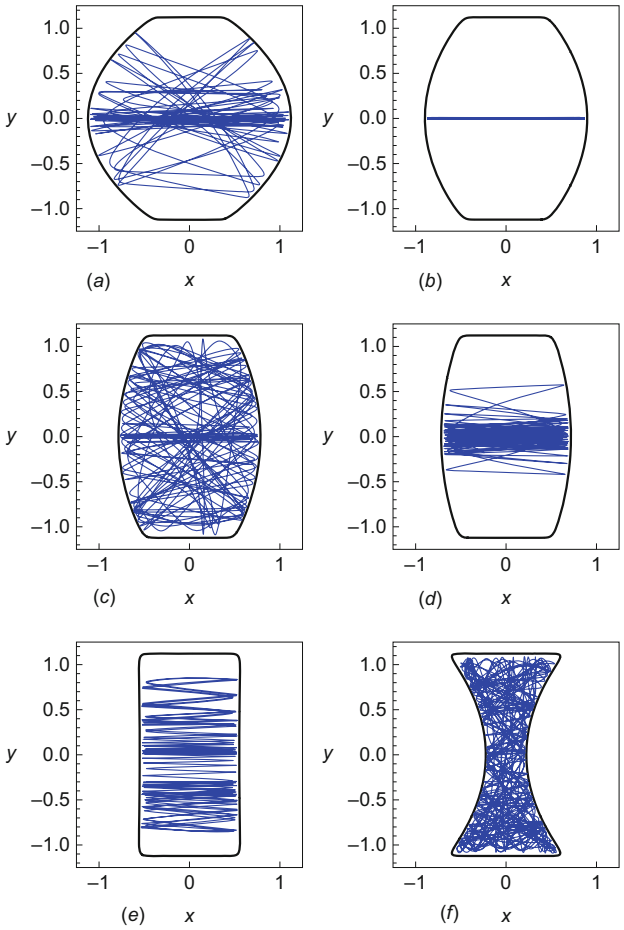

Fig. 8.4 Contour shapes with sample trajectories of a single particle, $k = 1$, inside the potential container during the "short-term" interval, $0 \le t \le 100$, obtained for $\alpha = 1/2$, $\gamma = 1$, $n = 10$, and different contour shapes: (**a**) $\beta = -0.5$, (**b**) $\beta = -0.3$, (**c**) $\beta = -0.2$, (**d**) $\beta = -0.14$, (**e**) $\beta = 0.009$, and (**f**) $\beta = 0.3$; in all these cases, the initial position of the particle is $(x, y) = (0.0, 0.01)$ with zero velocity

where the number $\alpha - \beta$ becomes the least distance from the origin to the potential wall along the horizontal axis in the rigid-body limit $n \to \infty$.

Skipping the overbars in notations (8.48) brings the differential equations of motion for the particle inside the potential well to the form

$$\ddot{x} + x^{2n-1} = O(\mu) \tag{8.49}$$

$$\ddot{y} + \lambda x^{2n} y = 0 \tag{8.50}$$

where $\lambda = -2\beta(\alpha - \beta)$, and the right-hand side of Eq. (8.49) is ignored due to the assumption $\mu \ll 1$.

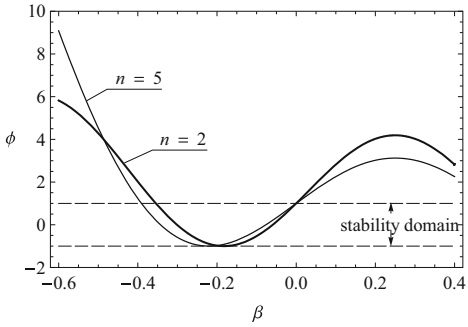

Fig. 8.5 Stability diagram of the nonlinear normal mode $y = 0$ for softer ($n = 2$) and stiffer ($n = 5$) walls, where the range of stability is bounded by the dashed horizontal lines, $\phi^2 = 1$

Equation (8.49) possesses periodic solution (8.40) of the period $T_n = 4a$ under the notation $m = 2n - 1$; hence Eq. (8.50) represents Hill's equation. The corresponding Floquet multipliers, $\rho_{1,2} = \phi \pm \sqrt{\phi^2 - 1}$, are calculated through the number $\phi = [y_1(T_n) + \dot{y}_2(T_n)]/2$, where $y_1(t)$ and $y_2(t)$ are two fundamental solutions of Eq. (8.50), such that $y_1(0) = 1$, $\dot{y}_1(0) = 0$ and $y_2(0) = 0$, $\dot{y}_2(0) = 1$, respectively. Based on the number ϕ, the solution $y(t)$ is unstable if $\phi^2 > 1$ and stable if $\phi^2 < 1$. If $\phi^2 = 1$, there exists a periodic solution of Eq. (8.50). Figure 8.5 illustrates the dependence $\phi = \phi(\beta)$, where the number β determines the curvature κ (8.46). Note that the Floquet stability analysis is justified locally, near the axis of symmetry $y = 0$. In addition, ignoring the right-hand side of Eq. (8.49) is equivalent to a fixed potential container. Nonetheless, a series of simulations reveals that the local stability properties of the trajectory $y = 0$ determine qualitative features of the global dynamics of the entire system (8.47) [169]. Comparing the graphs of Fig. 8.6 to the corresponding graphs of Fig. 8.4 points to the link between the chaoticity of trajectories inside containers with the energy-absorbing properties of the inclusion. For instance, comparing same fragments, (a), (c), (f), of Fig. 8.4 and Fig. 8.6 points to a clear link between the chaoticity of trajectories on the x-y plane and the effect of energy transfer between the donor (D) and receiver (R). The roles of donor and receiver are played by the potential container and its light inclusion (particle), respectively. Further, the trajectories in fragments (e) and (b) of Fig. 8.4 are quite regular. As a result, fragments (e) and (b) of Fig. 8.6 reveal no one-directional trend in energy outflow from the donor to receiver. Finally, a barely seen onset of chaoticity in Fig. 8.4d caused a beat wise exchange by some portion of the energy between the donor and receiver with a relatively slow trend.

As a possible transition to design of mechanical metamaterials [51, 85, 139] using the above effect of energy absorption, a one-dimensional chain of S three-dimensional soft-wall billiards (Fig. 8.7) was analyzed in [171]. The model Lagrangian is represented in the form

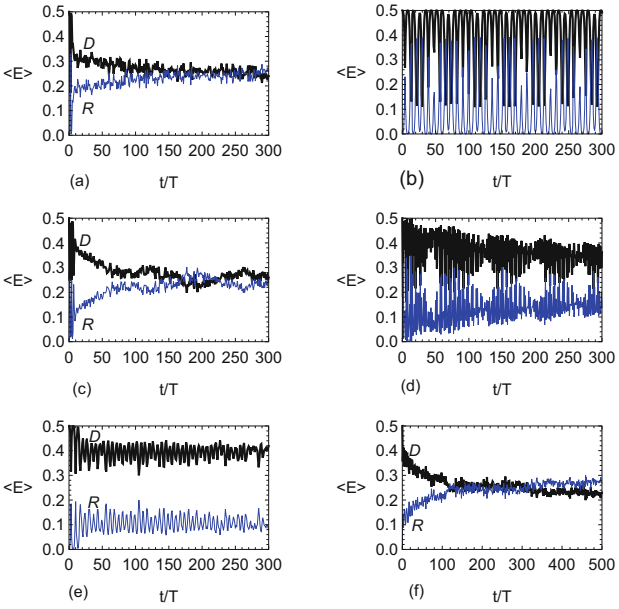

Fig. 8.6 Short-term time histories of the energy of main oscillator (donor—D, black line) and the particle (receiver—R, blue line) corresponding to different contour shapes shown in Fig. 8.4; $< E >$ is the mean value over the ensemble of $N = 50$ runs with randomly chosen initial positions of the particle in a small neighborhood of zero; $k = 1$, $\alpha = 1/2$, $n = 10$

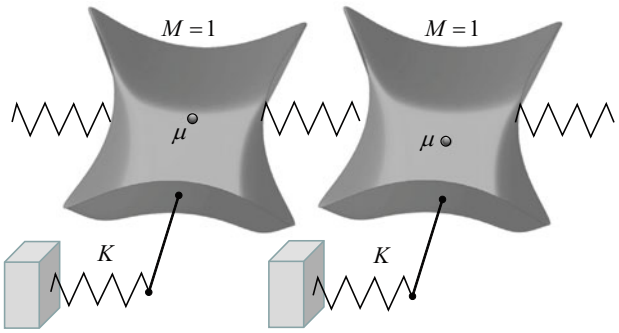

Fig. 8.7 Mass-spring chain model of 3D soft-wall billiards with inclusions; billiard shapes represented by one half of the potential level surface to show the inner side

$$L = \frac{1}{2}\sum_{j=1}^{S}\left\{\left(\frac{dX_j}{dt}\right)^2 + \mu\left[\left(\frac{dx_j}{dt} + \frac{dX_j}{dt}\right)^2 + \left(\frac{dy_j}{dt}\right)^2 + \left(\frac{dz_j}{dt}\right)^2\right]\right\}$$
$$-\sum_{j=1}^{S}\left[\frac{1}{2}KX_j^2 + \frac{1}{2}\left(X_j - X_{j-1}\right)^2 + V\left(x_j, y_j, z_j\right)\right]$$

where the mass of every potential container and its inclusion are $M = 1$ and μ, respectively; the strength coupling and the stiffness ground springs, are unity and K, respectively; X_j is a longitudinal displacement of the jth container; $\{x_j, y_j, z_j\}$ are container-based noninertial coordinates of the inclusion inside the jth container with the origin at geometrical center of the container, and the 3D potential well is described by

$$V(x, y, z) = \frac{\gamma}{2n}\left[\left(\frac{x}{\beta\left(y^2 + z^2 - 1\right) + 1}\right)^{2n} + \left(\frac{y}{\beta\left(x^2 + z^2 - 1\right) + 1}\right)^{2n}\right.$$
$$\left.+\left(\frac{z}{\beta\left(x^2 + y^2 - 1\right) + 1}\right)^{2n}\right]$$

where β determines container shapes, γ is a fixed parameter, and $n \gg 1$.

Note that the cell walls become stiff as $n \longrightarrow \infty$. Initially inclusions are in rest with respect to the absolute space, whereas a sine wave propagates through the chain of cells. Then the light inclusions are gradually involved in the dynamics due to the interaction with container walls. The inclusions start moving chaotically inside the cells by gradually absorbing the energy from the massive cells leading to the wave attenuation with chaotization of its spatial shape.

8.3.4 *A Nonlinear Mass-Spring Model That Becomes Linear at High Amplitudes*

As another example of conservative oscillator, let us consider a single mass vibrating system, which is illustrated in Fig. 8.8 and described by the Lagrangian

$$L = \frac{m\dot{w}^2}{2} - kl^2\left(\sqrt{1 + \frac{w^2}{l^2}} - 1\right)^2$$

Here, m is mass, k is the linear stiffness of each spring, l is the length of each spring at the equilibrium position at which the springs are horizontal, and w is the particle vertical coordinate.

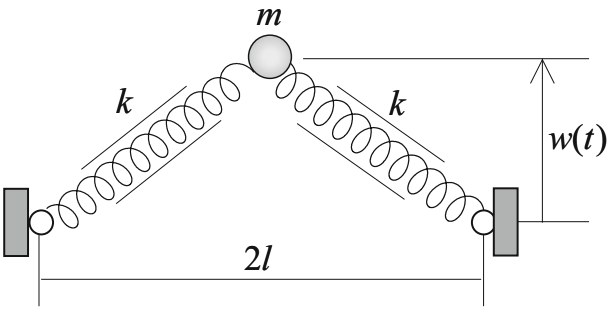

Fig. 8.8 The system, which is strongly nonlinear at small amplitudes and weakly nonlinear at large amplitudes

In terms of the dimensionless coordinate $x = w/l$ and phase $\varphi = (2k/m)^{1/2}t$, the corresponding differential equation of motion takes the form

$$\frac{d^2x}{d\varphi^2} + x - \frac{x}{\sqrt{1+x^2}} = 0 \tag{8.51}$$

Then, applying substitution (8.13) as $x = X(\tau)$ and $\tau = \tau(\varphi/a)$ leads to the boundary problem

$$X'' = -h\left(X - \frac{X}{\sqrt{1+X^2}}\right) \equiv -hf(X)$$
$$X'|_{\tau=1} = 0 \tag{8.52}$$

where $h = a^2$.

First two steps of the successive approximation procedure give

$$X_0 = A\tau$$
$$h_0 = \left(\frac{1}{2} - \frac{\sqrt{1+A^2}-1}{A^2}\right)^{-1}$$

and

$$X_1(\tau) = -\frac{h_0}{2A^2}\left[\frac{1}{3}(A\tau)^3 + 2A\tau - A\tau\sqrt{1+(A\tau)^2} - \operatorname{arcsinh}(A\tau)\right] \tag{8.53}$$
$$\gamma_1 = \frac{h_0}{A^3}\left[\frac{6A+A^3}{12} + \frac{9A-A^3}{6\sqrt{1+A^2}} - \left(1 + \frac{1}{\sqrt{1+A^2}}\right)\operatorname{arcsinh}(A)\right]$$

Interestingly enough, this model is essentially nonlinear at small amplitudes but becomes linear as the amplitudes are infinitely large. Indeed, taking the corresponding limits shows that

$$\frac{X_1}{A} \to -\frac{1}{5}\tau^5, \quad h_0 A^2 \to 8, \quad \gamma_1 \to \frac{3}{10} \quad \text{as} \quad A \to 0 \tag{8.54}$$

and

$$\frac{X_1}{A} \to -\frac{1}{3}\tau^3, \quad h_0 \to 2, \quad \gamma_1 \to \frac{1}{6} \quad \text{as} \quad A \to \infty \tag{8.55}$$

The asymptotic (8.54) obviously corresponds the nonlinear oscillator, whereas the limit case (8.55) associates with the harmonic oscillator. Still solution (8.53) is valid for both large and small amplitudes. Both limit cases follow from Eq. (8.51). In the case of small amplitudes, $|x| \ll 1$, enforcing the estimate $(1 + x^2)^{-1/2} \sim 1 - x^2/2$ in Eq. (8.51) gives

$$d^2x/d\varphi^2 + x^3/2 = 0 \tag{8.56}$$

In the case of large amplitudes, it follows even from Fig. 8.8 that the distance between the spring fixed ends becomes negligible if as compared to l. As a result, the mechanical model becomes effectively close to a mass-spring oscillator of mass m with a single spring of stiffness $2k$. In terms of the differential equations of motion, we also obtain the corresponding limit from exact Eq. (8.51) by assuming that, during most of the time of vibration cycle, the condition $|x| \gg 1$ and hence $\sqrt{1 + x^2} \sim |x|$ holds. As a result, Eq. (8.51) is replaced by

$$d^2x/d\varphi^2 + x - \text{sgn}(x) = 0 \tag{8.57}$$

where the term $\text{sgn}(x)$ has to be neglected due to the same condition $|x| \gg 1$ that gives the standard linear oscillator.

Alternatively, the discontinuous term in Eq. (8.57) can be saved and then considered as a perturbation of the harmonic oscillator. Note that Eq. (8.57) admits another form as follows

$$d^2x/d\varphi^2 + \text{sgn}(x)(|x| - 1) = 0 \tag{8.58}$$

The restoring force characteristic of oscillator (8.58) represents a particular case of the characteristic, $p(x) = \text{sgn}(x)\, f(|x|)$, which is considered later in this chapter.

8.3.5 *Strongly Nonlinear Characteristic with a Stepwise Discontinuity at Zero*

Let us consider the case of symmetric exponentially growing restoring force characteristic with a stepwise discontinuity at zero such that

$$f(x) = \begin{cases} \exp(x) & \text{for } x > 0 \\ -\exp(-x) & \text{for } x < 0 \end{cases} \tag{8.59}$$

Although force (8.59) has no certain value at the point $x = 0$, this still can play the role of equilibrium position. From the physical standpoint, this is equilibrium of a small bead at the bottom of V-shaped potential well. The local dynamics in a small neighborhood of such type of equilibria is considered later in this chapter; see the text in Fig. 8.16. It follows from (8.59) that $f(-x) = -f(x)$. Therefore, periodic motions of the corresponding oscillator can be described by the function $x = X(\tau)$, where $X(-\tau) = -X(\tau)$ and $\tau = \tau(t/a)$. In terms of these NSTT variables, the oscillator of a unit mass is described by the boundary value problem

$$\begin{array}{l} X'' + h\exp(X) = 0, \quad X'|_{\tau=1} = 0 \qquad \text{for } \tau \in (0, 1] \\ X'' - h\exp(-X) = 0, \quad X'|_{\tau=-1} = 0 \text{ for } \tau \in [-1, 0) \end{array} \tag{8.60}$$

where $h = a^2$.

This problem is exactly solvable, and the solution that satisfies the continuity of state condition at $\tau = 0$ has the form

$$\begin{aligned} X_{\pm}(\tau) \equiv A\tau \pm 2\ln[1 + \exp(-A)] \\ \mp 2\ln\left[1 + \frac{h}{2h_0}\exp(\pm A\tau - A)\right] \end{aligned} \tag{8.61}$$

where X_+ and X_- are taken for positive and negative subintervals of τ, respectively, and

$$h = 2h_0 = \frac{2A^2}{\exp(A)[1 + \exp(-A)]^2} \tag{8.62}$$

Note that both the differential equation of oscillator and its solution admit closed form representations as, respectively,

$$\ddot{x} + \mathrm{sgn}(x)\exp(|x|) = 0 \tag{8.63}$$

and

$$X = \mathrm{sgn}(\tau)\left[A|\tau| + 2\ln\frac{1 + \exp(-A)}{1 + \frac{h}{2h_0}\exp(A|\tau| - A)}\right] \tag{8.64}$$

The parameter h is obtained from equation

$$X'|_{\tau=1} = 0 \tag{8.65}$$

or

$$1 - \frac{h}{h_0}\left(1 + \frac{h}{2h_0}\right)^{-1} = 0 \tag{8.66}$$

This exactly solvable case can play the role of a majorant for evaluation of convergence properties of successive approximations. For that reason, we introduce a formal small parameter, $\varepsilon = 1$, and represent solution of Eq. (8.66) in the form

$$h = 2h_0 = \varepsilon h_0 \left(1 - \frac{\varepsilon}{2}\right)^{-1} \tag{8.67}$$

Taking into account (8.67) brings (8.64) to the form

$$X = \mathrm{sgn}(\tau) \left\{ A|\tau| + 2 \ln \frac{1 - \varepsilon[1 - \exp(-A)]/2}{1 - \varepsilon[1 - \exp(A|\tau| - A)]/2} \right\} \tag{8.68}$$

It can be shown by direct calculations that the power series expansions of (8.67) and (8.68) with respect to ε lead to the same series as those obtained by means of the iterative procedure introduced in this section for a general one-degree-of-freedom oscillator. Moreover, the structure of expression (8.67) suggests that considering the modified series,

$$h = \frac{\varepsilon h_0}{1 - \varepsilon\lambda_1 - \varepsilon^2\lambda_2 - \ldots} \tag{8.69}$$

leads to the exact value h already on the second step of the procedure. This fact can be employed for other cases in order to improve efficiency of the successive approximation series (8.16). For instance, according to the idea of Padè transform [26], the following equality must hold in every order of ε

$$\frac{\varepsilon h_0}{1 - \varepsilon\lambda_1 - \varepsilon^2\lambda_2 - \ldots} = \varepsilon h_0 (1 + \varepsilon\gamma_1 + \varepsilon^2\gamma_2 - \ldots) \tag{8.70}$$

This is equivalent to

$$(1 + \varepsilon\gamma_1 + \varepsilon^2\gamma_2 - \ldots)(1 - \varepsilon\lambda_1 - \varepsilon^2\lambda_2 - \ldots) = 1 \tag{8.71}$$

Taking the product of series on the left-hand side of (8.71) and considering different orders of ε generate a sequence of equations for the coefficients λ_1, λ_2, ... Then, substituting the corresponding solutions in (8.69) gives a particular case of Padè transform of (8.16) in the form

$$h = \frac{\varepsilon h_0}{1 - \varepsilon\gamma_1 - \varepsilon^2(\gamma_2 - \gamma_1^2) - \ldots} \tag{8.72}$$

In many cases, expansion (8.72) appears to be more effective than (8.16). Note that it is also possible to organize the successive approximations procedure by using expansion (8.69) instead of (8.16).

8.3.6 A Generalized Case of Odd Characteristics

This subsection deals with some generalization of the standard one-degree-of-freedom conservative oscillator

$$\ddot{x} + f(x) = 0 \tag{8.73}$$

where $f(x)$ is a smooth odd characteristic,

$$f(-x) = -f(x) \tag{8.74}$$

It was shown in this chapter that periodic solutions of the oscillator (8.73) admit the form $x = X(\tau)$, where

$$X(-\tau) = -X(\tau) \tag{8.75}$$

and, in addition, $X(\tau)\tau \geq 0$ for $-1 \leq \tau \leq 1$.

Consider now the following type of oscillators

$$\ddot{x} + \text{sgn}(x) f(|x|) = 0 \tag{8.76}$$

In the case of odd characteristic, $f(x)$, oscillator (8.76) is equivalent to the original one (8.73). The extension is due to the fact that the oscillator (8.76) always has an odd characteristic regardless whether or not the function $f(x)$ itself is odd. In general case, the characteristic, $\text{sgn}(x) f(|x|)$, may be nonsmooth at the equilibrium point, $x = 0$. As a result, the direct implementation of iterative procedures with high-order derivatives of the oscillator characteristics becomes quite limited. As illustrated below, the group properties of Eq. (8.76) can help to effectively build solution of Eq. (8.76) based on the solution of Equation $\ddot{x} + f(x) = 0$ for $x > 0$ by ignoring the point $x = 0$. Obviously, if $V(x)$ is the potential energy of oscillator (8.73), then $V(|x|)$ is the potential energy corresponding to oscillator (8.76). The following example explains why Eq. (8.76) covers a broader class of oscillators than (8.73).

Example 8.3.2 $\ddot{x}+\text{sgn}(x)|x|^{3/2} = 0$ is an oscillator, but $\ddot{x} + x^{3/2} = 0$ is not; see also Chap. 3 for the related discussion.

Based on the transition from Eqs. (8.73)–(8.76) and the general symmetry properties (8.74) and (8.75), we introduce the following representation for periodic solutions of Eq. (8.76)

$$x = \text{sgn}(\tau) X(|\tau|) \tag{8.77}$$

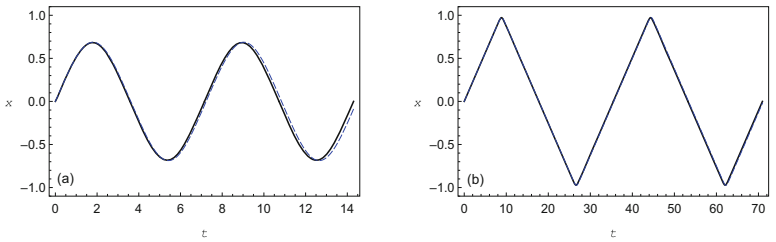

Fig. 8.9 Analytical and numerical solutions of the modified oscillator shown by continuous and dashed lines, respectively: (**a**) $\alpha = 2/3$ and (**b**) $\alpha = \sqrt{2023}$

Such an extension enables one to obtain "closed form" analytical solutions for a large number of oscillators by a simple adaptation of already known solutions, $X(\tau)$, for different cases of smooth characteristics.

Example 8.3.3 Applying transformation (8.77) to solution (8.40), which was derived for the power form characteristic x^{α} with an odd positive exponent $\alpha = m$, gives

$$X = A\,\mathrm{sgn}(\tau)\left[|\tau| - \frac{|\tau|^{\alpha+2}}{\alpha+2} + \frac{\alpha}{2(\alpha+2)}\left(\frac{|\tau|^{2\alpha+3}}{2\alpha+3} - \frac{|\tau|^{\alpha+2}}{\alpha+2}\right)\right] \tag{8.78}$$

where $\tau = \tau(t/a)$ and the expansion (8.41) for a^2 requires only the replacement $m \to \alpha$. Expansion (8.78) represents an approximate solution of the equation

$$\ddot{x} + \mathrm{sgn}(x)|x|^{\alpha} = 0 \tag{8.79}$$

where the notation α substitutes m in order to emphasize that the new exponent can take any positive real value, such as even, odd, rational, or irrational. Figure 8.9a and b illustrates solution (8.78) compared to numerical solution for two different exponents α and the same parameter $A = 1$. As both figures show, the analytical and numerical solutions are in a better match under the large exponent α due to the influence of vibroimpact asymptotic, $\alpha \to \infty$.

A common feature of the algorithms and examples of this section is that generating solutions for successive approximations are represented by triangle waves of proper amplitudes and periods. Such generating solutions belong to the real component of the hyperbolic complex number, $x = X + Ye$. In contrast, the next section introduces algorithms of successive approximations based on the imaginary component. It will be seen that these two approaches have different physical contents.

8.4 Periodic Motions Close to Separatrix Loop

In this section, the classic mathematical pendulum is considered as an example, although the developed algorithm may be applicable to other cases of one-degree-of-freedom systems with multiple equilibrium positions. Let us illustrate the algorithm based on the differential equation of motion

$$\ddot{x} + \sin x = 0 \tag{8.80}$$

It is assumed that the pendulum oscillates inside the separatrix loop around the stable equilibrium $(x, \dot{x}) = (0, 0)$ in between two physically identical unstable saddle points $(x, \dot{x}) = (\pm\pi, 0)$. The separatrix loop also represents a trajectory of the system with the total energy

$$E_s \equiv \int_0^{\pi} \sin x dx = 2 \tag{8.81}$$

The pendulum remains close to the separatrix loop in the area of periodic motions if the total energy, E, belongs to the range

$$0 < 1 - \frac{E}{E_s} << 1 \tag{8.82}$$

Let us show that, under condition (8.82), a successive approximation solution can be derived from the particular case of boundary value problem (8.7) and (8.8). Such particular case is given by setting $X \equiv 0$ so that

$$x(t) = Y(\tau(t/a))e(t/a) \tag{8.83}$$

Substituting (8.83) in Eq. (8.80) and following NSTT procedure yield

$$Y'' = -a^2 \sin Y \tag{8.84}$$

and

$$Y|_{\tau=1} = 0, \quad Y(-\tau) \equiv Y(\tau) \tag{8.85}$$

Let us seek solution of the boundary value problem, (8.84) and (8.85), in the form of series of successive approximations

$$Y = \pi + \varepsilon Y_1(\tau) + \varepsilon^3 Y_3(\tau) + \varepsilon^5 Y_5(\tau) + \ldots \tag{8.86}$$

$$a^2 = p^2 / \left(1 - \varepsilon^2 \lambda_2 - \varepsilon^4 \lambda_4 - \ldots\right) \tag{8.87}$$

where $\varepsilon = 1$ is an auxiliary parameter that helps to organize the iterative process.

According to the formal expansion (8.86), the generating solution is represented by the square wave of the amplitude π, $x(t) = \pi e(t/a)$, which is a stepwise discontinuous function. Such temporal mode shapes occur near the separatrix loop in the natural time scale of the pendulum because the system spends most of the time during one period near the unstable equilibrium position $x = \pi$ and its physically identical position $x = -\pi$. Therefore, expansion (8.86) is designed to be a high-energy expansion near the unstable equilibrium, rather than around the stable equilibrium position, $x = 0$.

Substituting expansions (8.86) and (8.87) into Eq. (8.84) and collecting terms with the same power of ε lead to the sequence of equations

$$\frac{d^2Y_1}{d\tau^2} - p^2 Y_1 = 0 \tag{8.88}$$

$$\frac{d^2Y_3}{d\tau^2} - p^2 Y_3 = p^2\left(\lambda_2 Y_1 - \frac{1}{6}Y_1^3\right) \tag{8.89}$$

$$\frac{d^2Y_5}{d\tau^2} - p^2 Y_5 = p^2\left[\left(\lambda_2^2 + \lambda_4\right)Y_1 - \frac{\lambda_2}{6}Y_1^3 + \frac{1}{120}Y_1^5 + \lambda_2 Y_3 - \frac{1}{2}Y_1^2 Y_3\right] \tag{8.90}$$

$$\ldots$$

Further, the family of even solutions of Eq. (8.88) can be represented in the form

$$Y_1 = -A\frac{\cosh p\tau}{\cosh p} \tag{8.91}$$

where A is an arbitrary constant accompanied by the factor $-\cosh^{-1} p$, which is convenient for further calculations due to the relationship $Y_1(1) = -A$. In particular, this provides the same order of magnitude for the arbitrary constant A as both the parameter p and period $T = 4a$ tend to infinity.

Further procedure is formally similar to the standard Poincaré-Lindstedt algorithm for nonlinear conservative oscillators with positive linear stiffness. For example, substituting (8.91) into the right part of Eq. (8.89) gives a "resonance term" on the right-hand side of the equation, which is proportional to $\cosh p\tau$. This generates "hyperbolic secular terms" of the form $\tau \cosh p\tau$ and $\tau \cosh p\tau$ in the particular solution of Eq. (8.89). The occurrence of such terms can be prevented analogously to the Poincaré-Lindstedt method by setting

$$\lambda_2 = \frac{A^2}{8\cosh^2 p} \tag{8.92}$$

As a result, the particular solution of Eq. (8.89) takes the form

$$Y_3 = \frac{A^3 \cosh 3p\tau}{192\cosh^3 p} \tag{8.93}$$

At the next step, Eq. (8.90) gives solution

$$Y_5 = \frac{A^5}{4096\cosh^5 p}\left(\cosh 3p\tau - \frac{1}{5}\cosh 5p\tau\right) \tag{8.94}$$

under the condition

$$\lambda_4 = -\frac{3A^4}{512\cosh^4 p} \tag{8.95}$$

Substituting (8.91) through (8.92) in (8.86) and (8.87), and setting $\varepsilon = 1$, gives approximate solution

$$Y = \pi - \frac{A\cosh p\tau}{\cosh p} + \frac{A^3\cosh 3p\tau}{192\cosh^3 p} \tag{8.96}$$

$$+ \frac{A^5}{4096\cosh^5 p}\left(\cosh 3p\tau - \frac{1}{5}\cosh 5p\tau\right)$$

and

$$h = p^2\left(1 - \frac{A^2}{8\cosh^2 p} + \frac{3A^4}{512\cosh^4 p}\right)^{-1} \tag{8.97}$$

where $\tau = \tau\,(t/a)$ and $a = \sqrt{h}$.

The truncated series of successive approximations (8.96) and (8.97) depend upon two parameters, A and p, coupled by the boundary (continuity) condition (8.85) as follows

$$A = \pi + \frac{A^3\cosh 3p}{192\cosh^3 p} + \frac{A^5}{4096\cosh^5 p}\left(\cosh 3p - \frac{1}{5}\cosh 5p\right) \tag{8.98}$$

Equation (8.98) should be interpreted as implicit function $A = A(p)$ near the point $A = \pi$. Therefore, expansions (8.96) and (8.97) represent a one-parameter family of periodic solutions with the parameter p.

Figure 8.10a and b shows that the analytical and numerical solutions are in better agreement for larger periods as the system trajectory becomes closer to the separatrix loop.

Note that Eq. (8.80) admits the group of time translations. As a result, another arbitrary parameter, say t_0, is introduced by substitution $t \to t + t_0$.

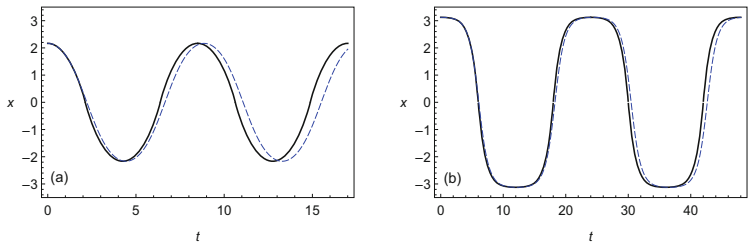

Fig. 8.10 Analytical (solid line) and numerical (dashed) solutions for two different periods: (**a**) $T = 8.5$ ($p = 2$) and (**b**) $T = 24.5$ ($p = 6$)

8.5 Self-Excited Oscillator

This section illustrates the case when both X and Y components of solutions participate in the iterative process.

In particular, we consider periodic self-sustained vibrations described in the differential equation of motion

$$\ddot{x} + g(x)\dot{x} + f(x) = 0 \tag{8.99}$$

where $f(x)$ and $g(x)$ are analytic functions, such that (Lienard's conditions)

(a) $G(x) = \int_0^x g(u)du$ is an odd function such that $G(0) = G(\pm\mu) = 0$ for some $\mu > 0$

(b) $G(x) \to \infty$ if $x \to \infty$, and $G(x)$ is a monotonously increasing function for $x > \mu$

(c) $f(x)$ is an odd function such that $f(x) > 0$ for $x > 0$

The above conditions guarantee that system (8.99) has a single stable limit cycle. In this case, the boundary-value problem (8.7) and (8.8) takes the form

$$\begin{aligned} X'' &= -a^2 R_f - a\left(R_g Y' + I_g X'\right) \equiv -\varepsilon F_X,\ X'|_{\tau=\pm1} = 0 \\ Y'' &= -a^2 I_f - a\left(I_g Y' + R_g X'\right) \equiv -\varepsilon F_Y,\ Y\,|_{\tau=\pm1} = 0 \end{aligned} \tag{8.100}$$

where the period of limit cycle $T = 4a$ is unknown, expressions R_f and I_f as well as R_g and I_g are obtained by applying (8.5) and (8.6) to each of the functions $f(x)$ and $g(x)$, and notations εF_X and εF_Y are introduced with the formal factor $\varepsilon = 1$ for further convenience.

Let us seek solution of the boundary value problem (8.100) in the form of series of successive approximations

$$\begin{aligned} X &= X_0(\tau) + \varepsilon X_1(\tau) + \varepsilon^2 X_2(\tau) + \cdots \\ Y &= Y_0(\tau) + \varepsilon Y_1(\tau) + \varepsilon^2 Y_2(\tau) + \cdots \end{aligned} \tag{8.101}$$

$$a = q_0 + \varepsilon q_1 + \varepsilon^2 q_2 + \cdots \tag{8.102}$$

Further solution procedure can be simplified by taking into account the symmetry properties $X(-\tau) \equiv -X(\tau)$ and $Y(-\tau) \equiv Y(\tau)$ due to the above conditions (a) through (c). Substituting (8.101) and (8.102) into (8.100) and matching the coefficients of the respective powers of ε give the following sequence of boundary value problems

$$\begin{aligned} X_0'' &= 0 \\ Y_0'' &= 0, \quad Y_0|_{\tau=1} = 0 \end{aligned} \tag{8.103}$$

$$\begin{aligned} X_1'' &= -F_{X,0}, \quad (X_0 + X_1)'|_{\tau=1} = 0 \\ Y_1'' &= -F_{Y,0}, \quad Y_1|_{\tau=1} = 0 \end{aligned} \tag{8.104}$$

$$\begin{aligned} X_{i+1}'' &= -F_{X,i}, \quad X_{i+1}'|_{\tau=1} = 0 \\ Y_{i+1}'' &= -F_{Y,i}, \quad Y_{i+1}|_{\tau=1} = 0 \\ (i &= 1, 2, \ldots) \end{aligned} \tag{8.105}$$

where

$$F_{X,i} = \frac{1}{i!}\frac{d^i F_X}{d\varepsilon^i}|_{\varepsilon=0}, \quad F_{Y,i} = \frac{1}{i!}\frac{d^i F_Y}{d\varepsilon^i}|_{\varepsilon=0} \tag{8.106}$$

Note that zero-order and first-order approximations are coupled through the boundary condition for X-component in (8.104), whereas no boundary condition is imposed on X_0 in (8.103). This specific represents a formalization of the physical assumption regarding the dominating component in the temporal mode shape of vibration, which is assumed to be close to the triangle wave rather than square wave. As a result, the generating system (8.103) gives solution

$$X_0 = A\tau, \; Y_0 \equiv 0 \tag{8.107}$$

where A is an arbitrary constant.

Substituting (8.107) in the right-hand side of Eq. (8.104) and integrating yield

$$X_1 = -q_0^2 \int_0^\tau (\tau - \xi) f(A\xi) d\xi, \quad Y_1 = -Aq_0 \int_0^\tau (\tau - \xi) g(A\xi) d\xi \tag{8.108}$$

Then, substituting (8.108) in the boundary conditions in (8.104) gives the following two equations for parameters q_0 and A

$$q_0^2 \int_0^1 f(A\xi)d\xi = A, \quad \int_0^1 (1-\xi)g(A\xi)d\xi = 0 \tag{8.109}$$

Relationships (8.107) through (8.109) complete first basic steps of the iterative procedure. Further iterations are organized then in a similar way as follows

$$X_{i+1} = -\int_0^\tau (\tau - \xi)F_{X,i}(\xi)d\xi, \quad Y_{i+1} = -\int_1^\tau d\zeta \int_0^\zeta F_{Y,i}(\xi)d\xi \tag{8.110}$$

$$\int_0^1 F_{X,i}(\xi)d\xi = 0; \quad i = 1, 2, \ldots. \tag{8.111}$$

Note that the boundary conditions for Y_{i+1} are satisfied automatically due to the lower limit of the outer integral in (8.110), whereas the boundary conditions for X_{i+1} generate Eq. (8.111) for determining the coefficients of series (8.102). Practically, high-order approximations can be obtained by using computer systems of symbolic manipulations.

Example 8.5.1 Consider a self-excited oscillator with the power form stiffness of the degree $m = 3$,

$$\ddot{x} + (bx^2 - 1)\dot{x} + x^3 = 0$$

In this case, $g(x) = bx^2 - 1$ and $f(x) = x^3$. Conducting elementary integrations in (8.109) gives the algebraic system

$$\frac{1}{4}q_0^2 A^3 = A, \quad \frac{1}{12}q_0 A\left(6 - bA^2\right) = 0$$

with non-trivial solution

$$q_0 = \sqrt{\frac{2b}{3}}, \quad A = \sqrt{\frac{6}{b}}$$

As a result, integrating (8.108) yields

$$X_1 = -\sqrt{\frac{6}{b}}\frac{\tau^5}{5}, \quad Y_1 = \tau^2 - \tau^4$$

All further steps of the procedure are conducted according to the same scheme (8.110) and (8.111). For instance, first two steps of the procedure give approximate solution

$$x = \sqrt{\frac{6}{b}}\{\tau - \frac{\tau^5}{5} + \frac{1}{3150}[105\tau^9 + 900\tau^7 b - 21\tau^5(70b + 9) + 350\tau^3 b]\}$$
$$+(1-\tau^2)\{\tau^2 - \frac{1}{420}[20 - 43\tau^2 + 20\tau^4 + 216\tau^6]\}e$$

and the period

$$T = 4a = 8\sqrt{\frac{b}{6}}\left(1 + \frac{3}{20}\right)$$

Two more steps of the procedure correct the above expression for the period as follows

$$T = 4a = 8\sqrt{\frac{b}{6}}\left(1 + \frac{3}{20} + \frac{2960b + 2121}{50400} + \frac{7367360b^2 + 4554992b + 8659035}{605404800}\right)$$

Figures 8.11 and 8.12 show limit cycle trajectories described by the analytical solutions in one and two iterations, respectively. For comparison reason, the numerical solution for transition to the limit cycle is also presented. Then, Fig. 8.13 illustrates the dependence of the quarter of period, $a = T/4$, versus the quantity $b^{-1/2}$, which can be viewed as an estimate for the amplitude of limit cycle.

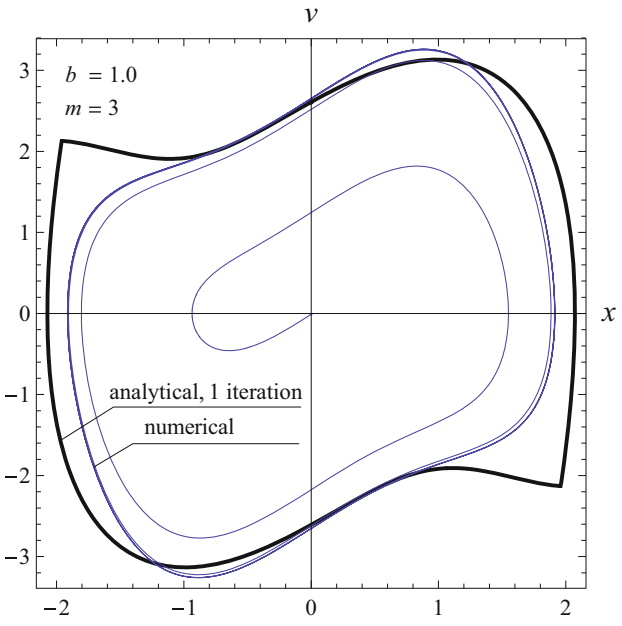

Fig. 8.11 Trajectories of numerical solution and the analytical limit cycle solution in one iteration

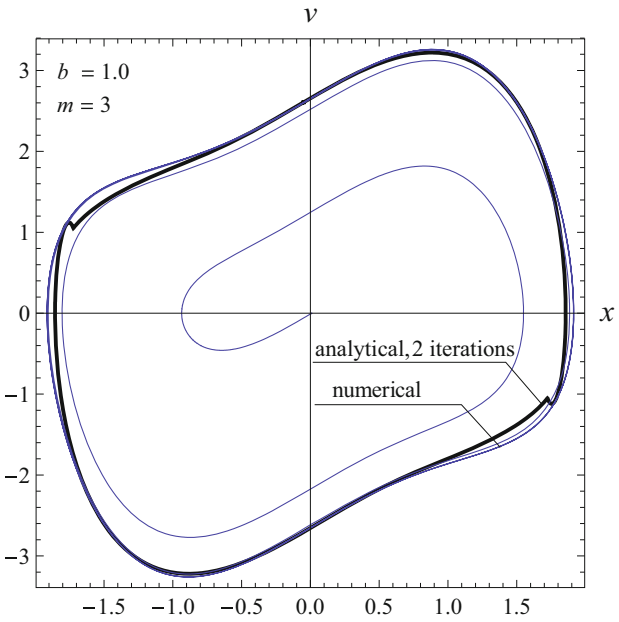

Fig. 8.12 Trajectories of numerical solution and approximate (two iterations) analytical limit cycle solution

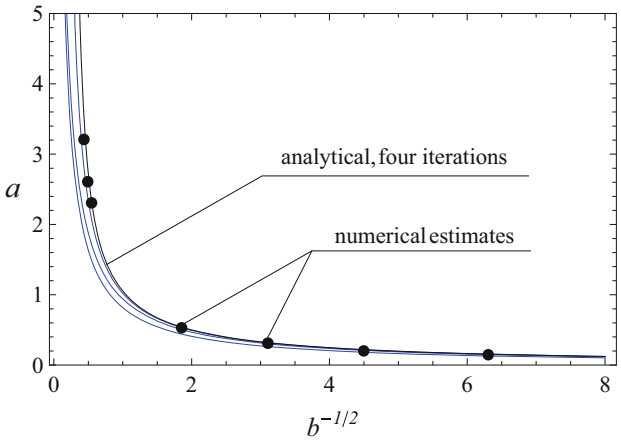

Fig. 8.13 Illustration of convergence of the iterative procedure on the parameter plane

8.6 Strongly Nonlinear Oscillator with Viscous Damping

This section describes the successive approximation procedure combined with the asymptotic of small energy dissipation that leads to a slow amplitude decay. The scheme of the algorithm is closed to that was introduced earlier in [176].

Consider a strongly nonlinear oscillator under the viscous damping

$$\ddot{x} + 2\mu\dot{x} + f(x) = 0 \tag{8.112}$$

where $f(x)$ is an odd function such that $xf(x) \geq 0$ and $0 < \mu << 1$.

The idea of two-variable expansions will be employed below in combination with the triangle wave time substitution. Let us assume that $\tau(\varphi)$ is a fast time scale, whose phase, φ, depends on the slow time scale, $t^0 = \mu t$, according to the following differential equation

$$\dot{\varphi} = \omega(t^0) \tag{8.113}$$

where the right-hand side is a priori unknown.

Let us represent the unknown solution of Eq. (8.112) in the form

$$x = x(\varphi, t^0) = X(\tau(\varphi), t^0) + Y(\tau(\varphi), t^0)e(\varphi) \tag{8.114}$$

Substituting (8.114) in Eq. (8.112) and imposing the smoothness conditions as

$$Y|_{\tau=\pm 1} = 0, \quad \frac{\partial X}{\partial \tau}|_{\tau=\pm 1} = 0 \tag{8.115}$$

give two partial differential equations

$$\begin{aligned} \omega^2 \frac{\partial^2 X}{\partial \tau^2} &= -R_f - \mu H \frac{\partial Y}{\partial \tau} - \mu^2 LX \\ \omega^2 \frac{\partial^2 Y}{\partial \tau^2} &= -I_f - \mu H \frac{\partial X}{\partial \tau} - \mu^2 LY \end{aligned} \tag{8.116}$$

where, as follows from (8.5) and (8.6),

$$\begin{aligned} R_f &= R_f(X, Y) = \frac{1}{2}[f(X + Y) + f(X - Y)] \\ I_f &= I_f(X, Y) = \frac{1}{2}[f(X + Y) - f(X - Y)] \end{aligned}$$

and two linear differential operators are introduced

$$H \equiv 2\omega\left(1+\frac{\partial}{\partial t^0}\right)+\frac{d\omega}{dt^0} \tag{8.117}$$

$$L \equiv \frac{\partial^2}{\partial t^{02}}+2\frac{\partial}{\partial t^0}$$

Note that the fast and slow temporal scales are associated with different physical processes developed in the system. The slow energy dissipation process is represented by the explicit small parameter μ, but there is no explicit parameter associated with perturbations of the triangle wave, which is supposed to be a generating solution of the iterative process. However, as discussed earlier in this section, introducing the triangle wave temporal argument implies that the entire right-hand side of system (8.116) is small. Otherwise, the triangle wave cannot be considered as a dominating component of the temporal mode shape of oscillations. Recall that, in a similar way, selecting the harmonic wave as a dominating solution in quasi-harmonic approaches implies that nonlinearities are small regardless the system parameters. Therefore, iterative procedure for boundary value problem (8.115) and (8.116) should incorporate two different procedures, as those described above in this section, and a proper asymptotic procedure related to the dissipation process. Let us emphasize that the quasi-harmonic methods face similar situation when dealing with weakly nonlinear systems under small damping conditions. For instance, if being applied to such cases, the method of multiple scales accounts for both anharmonicity and dissipation, after appropriate assumption regarding the relation between nonlinearity and damping parameters has been made. Very often, such parameters are assumed to be of the same order of magnitude. As to the boundary value problem (8.115) and (8.116), similar assumption can be introduced by providing the terms R_f and I_f and the parameter μ with the same formal "small factor" $\varepsilon = 1$. Then, the multiple scales or two-variable expansions can be organized by using the auxiliary parameter ε [176]. In the case of linear oscillator, such an algorithm recovers the exact solution of the linear differential equation of motion however in the specific form

$$x = X(\tau, t^0) = C\frac{\omega\exp(-t^0)}{\sqrt{\varepsilon(1-\varepsilon\mu^2)}}\sin\left[\frac{\sqrt{\varepsilon(1-\varepsilon\mu^2)}}{\omega}\tau(\omega t)\right] \tag{8.118}$$

and

$$\omega^2 = \frac{\varepsilon(1-\varepsilon\mu^2)}{4\arcsin^2\sqrt{\varepsilon/2}}$$

where C is an arbitrary constant and another arbitrary constant can be introduced through the arbitrary time shift.

Note that solution (8.118) includes no Y-component because, at every stage of the iterative process, it appears to be possible to satisfy condition

$$H(\partial X/\partial\tau) = 0 \tag{8.119}$$

Thus, the second equation of system (8.116) is satisfied by setting $Y \equiv 0$. Practically, condition (8.119) generates the common factor $\exp(-t^0)$ for all successive approximations. In general nonlinear case, it is rather impossible to satisfy condition (8.119) at every stage of the process, but it still works for the leading order approximate solutions.

Example 8.6.1 Consider the weakly damped oscillator of the m degree power form restoring force characteristic

$$\ddot{x} + 2\mu\dot{x} + x^m = 0 \tag{8.120}$$

At this stage, the exponent m is an odd positive number. It will be shown later that a broader class of power characteristics can also be considered. Note that, for this kind of oscillators, whether or not the damping is small depends on the level of amplitude and the exponent, m. This is due to the fact that, for small enough amplitudes, the elastic force becomes negligible regardless the magnitude of damping. By assuming that the influence of damping is negligible during one cycle of vibration, one can use expressions (8.41) for estimations of magnitudes of damping and elastic forces. As a result, the condition of small damping derives in the form

$$\mu^2 \ll \frac{1}{4}(m+1)A^{m-1} \tag{8.121}$$

One step of the procedure gives approximate solution [176]

$$x = C\exp\left(\frac{-4\mu t}{m+3}\right)\left(\tau - \frac{\tau^{m+2}}{m+2}\right) \tag{8.122}$$

where $\tau = \tau(\varphi)$ and the phase variable is approximated by

$$\varphi = \varphi_\infty\left[1 - \exp\left(-2\mu\frac{m-1}{m+3}t\right)\right] \tag{8.123}$$

$$\varphi_\infty = \frac{1}{2\mu}\frac{m+3}{m-1}\frac{C^{(m-1)/2}}{\sqrt{2(m+1)}}$$

Interestingly enough, the above approximate solution predicts that the oscillator makes only a finite number of waves as $m > 1$ and $t \to \infty$. Figures 8.14 and 8.15 illustrate damped responses of the oscillator with two different degrees of nonlinearity, $m = 3$ and $m = 7$, respectively. As follows from the diagrams, the approximate analytical solution and numerical one are matching relatively well, especially at higher exponent, $m = 7$. In particular, this justifies the idea of using the triangle wave in strongly nonlinear cases, when the oscillator becomes close to the standard vibroimpact model.

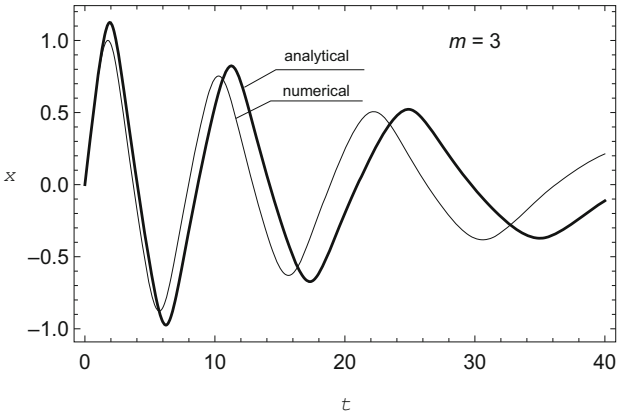

Fig. 8.14 Approximate analytical and numerical solutions of the damped oscillator with cubic power form characteristic; $C = 1.5$, $\mu = 0.05$

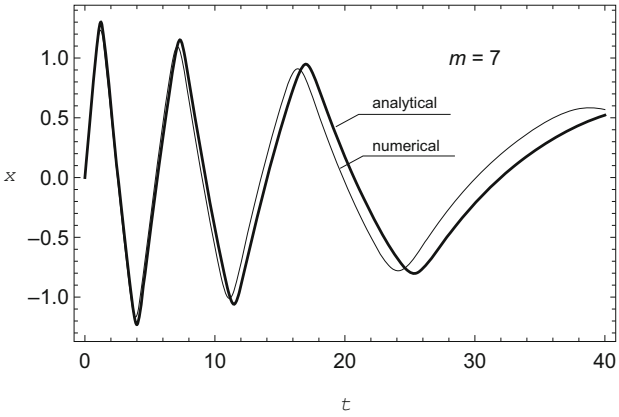

Fig. 8.15 Approximate analytical and numerical solutions of the damped oscillator with the seventh degree power form characteristic; $C = 1.5$, $\mu = 0.05$

8.6.1 Remark on NSTT Combined with Two-Variable Expansion

In general, the iterative process of triangle wave expansions and the averaging procedure can be separated. Moreover, the stage of triangle wave time substitution does not impose any specific method of analyses. Let us apply the method of two-variable expansions directly to the nonlinear boundary value problem (8.115) and (8.116) by means of the asymptotic series

$$\begin{aligned} X &= X_0(\tau, t^0) + \mu X_1(\tau, t^0) + \mu^2 X_2(\tau, t^0) + \cdots \\ Y &= Y_0(\tau, t^0) + \mu Y_1(\tau, t^0) + \mu^2 Y_2(\tau, t^0) + \cdots \end{aligned} \tag{8.124}$$

and

$$\omega = \omega_0(t^0) + \mu\omega_1(t^0) + \mu^2\omega_2(t^0) + \cdots$$
$$H = H_0 + \mu H_1 + \mu^2 H_2 + \ldots \tag{8.125}$$

where $H_i = 2\omega_i\left(1 + \partial/\partial t^0\right) + d\omega_i/dt^0$.

Substituting (8.124) and (8.125) into (8.115) and (8.116), and matching coefficients of like powers of μ, gives, in particular,

$$\omega_0^2 \frac{\partial^2 X_0}{\partial \tau^2} = -R_f^{(0)}(X_0, Y_0), \quad \frac{\partial X_0}{\partial \tau}|_{\tau=\pm 1} = 0$$
$$\omega_0^2 \frac{\partial^2 Y_0}{\partial \tau^2} = -I_f^{(0)}(X_0, Y_0), \quad Y_0|_{\tau=\pm 1} = 0 \tag{8.126}$$

and

$$\omega_0^2 \frac{\partial^2 X_1}{\partial \tau^2} = -R_f^{(1)}(X_0, Y_0, X_1, Y_1) - 2\omega_0\omega_1 \frac{\partial^2 X_0}{\partial \tau^2} - H_0 \frac{\partial Y_0}{\partial \tau}$$
$$\frac{\partial X_1}{\partial \tau}|_{\tau=\pm 1} = 0$$
$$\omega_0^2 \frac{\partial^2 Y_1}{\partial \tau^2} = -I_f^{(1)}(X_0, Y_0, X_1, Y_1) - 2\omega_0\omega_1 \frac{\partial^2 Y_0}{\partial \tau^2} - H_0 \frac{\partial X_0}{\partial \tau} \tag{8.127}$$
$$Y_1|_{\tau=\pm 1} = 0$$

where $R_f^{(0)}$, $R_f^{(1)}$, ... and $I_f^{(0)}$,$I_f^{(1)}$, ... are determined by the expansions

$$R = R_f^{(0)} + \mu R_f^{(1)} + \mu^2 R_f^{(2)} + \ldots$$
$$I = I_f^{(0)} + \mu I_f^{(1)} + \mu^2 I_f^{(2)} + \ldots$$

By taking into account the assumptions on $f(x)$ in Eq. (8.112), one can represent solution of problem (8.126) in the following general form

$$X_0 = X_0(\tau, A, \omega_0), \quad Y_0 \equiv 0 \tag{8.128}$$

where $A = A(t^0)$ is an arbitrary function of the slow time scale, which is coupled with the frequency ω_0 through the boundary condition

$$\frac{\partial X_0(\tau, A, \omega_0)}{\partial \tau}|_{\tau=1} = 0 \tag{8.129}$$

In general, this relationship determines the implicit function $\omega_0 = \omega_0(t^0)$. Now substituting solution (8.128) in (8.127) gives equations

$$\omega_0^2 \frac{\partial^2 X_1}{\partial \tau^2} + f'(X_0) X_1 = -2\omega_0 \omega_1 \frac{\partial^2 X_0}{\partial \tau^2} \tag{8.130}$$

and

$$\omega_0^2 \frac{\partial^2 Y_1}{\partial \tau^2} + f'(X_0) Y_1 = -H_0 \frac{\partial X_0}{\partial \tau} \tag{8.131}$$

Let us consider Eq. (8.131). The best choice would be achieved by setting the right-hand side to zero and therefore making possible the solution $Y_1 \equiv 0$, which is consistent with zero-order solution (8.128) and provides a better smoothness property of the corresponding solution at this stage; see condition (8.119). Note that the right-hand side cannot be always made zero for any τ unless the zero-order solution admits separation of the variables t^0 and τ. However, it is still possible to minimize the right-hand side of Eq. (8.131) by making it orthogonal to solution of the corresponding homogeneous equation, $\partial X_0/\partial \tau$, according to condition

$$\frac{1}{2} \int_{-1}^{1} \frac{\partial X_0}{\partial \tau} H_0 \frac{\partial X_0}{\partial \tau} d\tau \equiv \left\langle \frac{\partial X_0}{\partial \tau} H_0 \frac{\partial X_0}{\partial \tau} \right\rangle = 0 \tag{8.132}$$

Taking into account the expression $H_0 = 2\omega_0 \left(1 + \partial/\partial t^0\right) + d\omega_0/dt^0$ and condition (8.132) gives

$$\omega_0 \left\langle \left(\frac{\partial X_0}{\partial \tau} \right)^2 \right\rangle = C \exp(-2t^0) \tag{8.133}$$

where C is an arbitrary constant.

It can be shown that the condition (8.132) occurs also in a rigorous mathematical way based on the boundary conditions for Y_1. At least, this can be easily verified in the linear case, $f(x) \equiv x$.

8.6.2 *Oscillator with Two Nonsmooth Limits*

Consider the following generalization of Eq. (8.120)

$$\ddot{x} + 2\mu \dot{x} + \operatorname{sgn}(x)|x|^{\alpha} = 0 \tag{8.134}$$

where α is a non-negative real number; see comments to Eq. (8.79).

In this case, zero-order solution (8.128) can be obtained in the form (8.78),

$$x(t) = A(t^0)\mathrm{sgn}(\tau(\varphi)) \times \left[|\tau(\varphi)| - \frac{|\tau(\varphi)|^{\alpha+2}}{\alpha+2} + \frac{\alpha}{2(\alpha+2)}\left(\frac{|\tau(\varphi)|^{2\alpha+3}}{2\alpha+3} - \frac{|\tau(\varphi)|^{\alpha+2}}{\alpha+2}\right)\right] \tag{8.135}$$

$$\dot{\varphi}(t) = \omega_0(t^0), \quad t^0 = \mu t$$

where the functions $A(t^0)$ and $\omega_0(t^0)$ are coupled by relation (8.41) as

$$\omega_0 = \frac{1}{a} = \frac{A^{(\alpha-1)/2}}{\sqrt{\alpha+1}}\left\{1 + \frac{\alpha}{2(\alpha+2)}\left[1 + \frac{(\alpha+1)^2}{(\alpha+2)(2\alpha+3)}\right]\right\}^{-1/2} \tag{8.136}$$

Equations (8.136) and (8.133) admit exact solution

$$A = C\exp\left(-\frac{4\mu t}{3+\alpha}\right), \quad \varphi = \varphi_\infty\left[1 - \exp\left(-2\mu\frac{\alpha-1}{\alpha+3}t\right)\right] \tag{8.137}$$

where C is a new arbitrary constant and

$$\varphi_\infty = \frac{1}{2\mu}\frac{\alpha+3}{\alpha-1}\frac{C^{(\alpha-1)/2}(2+\alpha)\sqrt{2(3+2\alpha)}}{\sqrt{(\alpha+1)\left(7\alpha^3+31\alpha^2+47\alpha+24\right)}} \tag{8.138}$$

It follows from expressions (8.137) and (8.138) that the linear system, $\alpha = 1$, plays the role of a boundary between the two strongly nonlinear areas

$$N_0 = \{\alpha : 0 \le \alpha << 1\} \quad \text{and} \quad N_\infty = \{\alpha : 1 << \alpha < \infty\} \tag{8.139}$$

In other words, we show that the number $\alpha = 1$ separates two qualitatively different regions of the dynamics determined by the influence of different nonsmooth limits of the potential well; see Fig. 8.16 for illustration. In particular, if $\alpha > 1$, then the phase variable φ has the finite limit φ_∞ as $t \to \infty$. In contrast, if $\alpha < 1$, then the phase with its temporal rate is exponentially growing, as the amplitude decays and the system approaches the bottom of the potential well. The physical meaning of this effect is most clear from the limit case $\alpha \to 0$, which is discussed below.

Figures 8.17, 8.18, and 8.19, 8.20 illustrate solution (8.135) through (8.138) for large and small exponents α, respectively. The diagrams suggest quite a good agreement with numerical solution in *both* branches of the exponent (8.139). The numerical solutions shown by dashed lines were obtained by the standard solver *NDSolve* built in *Mathematica*®. Figure 8.17 also shows that some divergence between the curves occurs when the amplitude is decreased to the level about $A = 0.6$. Below this level, the condition of small damping (8.121) is not guaranteed any more. In contrast, the curves are in a better match for smaller amplitudes if $\alpha < 1$; see Fig. 8.19. In this case, the amplitude decay just strengthens condition (8.121).

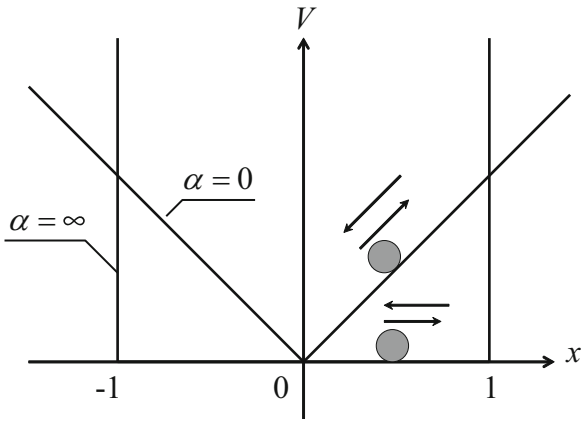

Fig. 8.16 Potential energy representation for the two limit oscillators

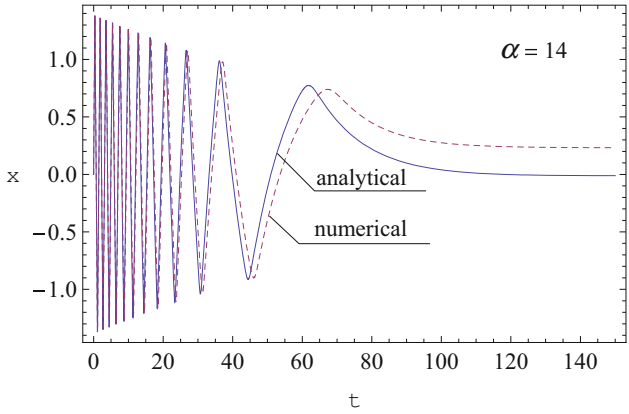

Fig. 8.17 Temporal mode shape of the vibration for $\alpha \in N_\infty$, $C = 1.5$, and $\mu = 0.04$; here and below, the dashed line represents numerical solutions

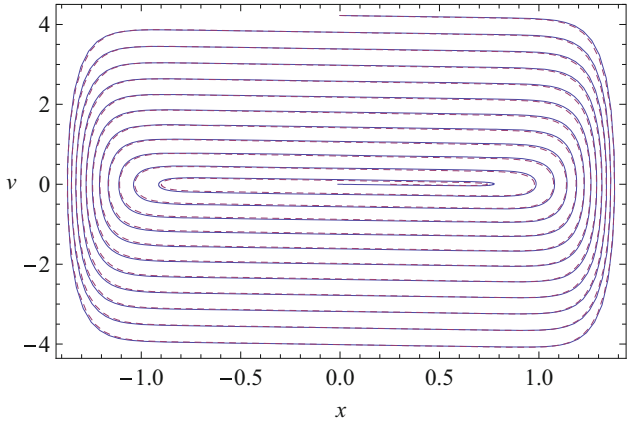

Fig. 8.18 Phase plane diagram for $\alpha \in N_\infty$

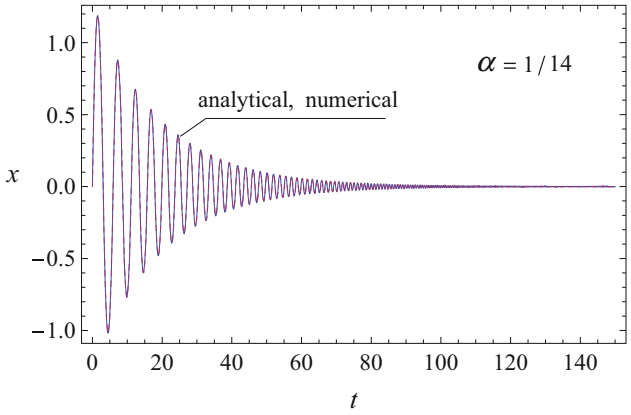

Fig. 8.19 Temporal mode shape of the vibration for $\alpha \in N_0$, $C = 2.5$, and $\mu = 0.04$

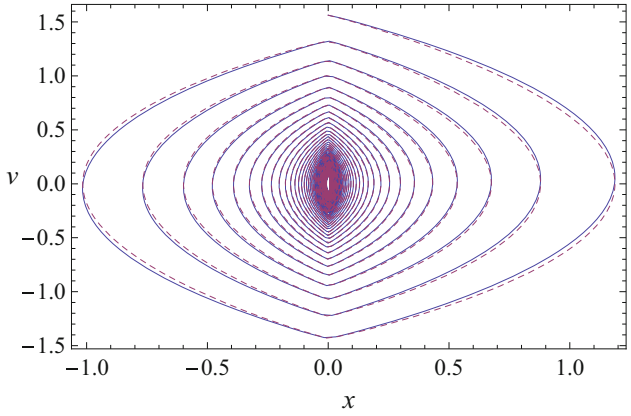

Fig. 8.20 Phase plane diagram for $\alpha \in N_0$

The phase plane diagrams shown in Figs. 8.18 and 8.20 have qualitatively different shapes as dictated by the influence of different nonsmooth limits of the potential well; see Fig. 8.16. Let us show now that solution (8.135) captures both nonsmooth limits $\alpha \to 0$ and $\alpha \to \infty$.

For a physically meaningful transition to the limits, let us express the arbitrary parameter C through the initial velocity $v_0 = \dot{x}|_{t=0}$,

$$C = \left[\frac{v_0^2 \, (\alpha + 1) \left(7\alpha^3 + 31\alpha^2 + 47\alpha + 24\right)}{2(\alpha + 2)^2 (2\alpha + 3)} \right]^{1/(\alpha+1)}$$

and consider the two different cases.

1) As $\alpha \to \infty$, the solution (8.135) through (8.138) gives

$$x = \tau(\varphi) \qquad (8.140)$$
$$\varphi = \frac{v_0}{2\mu}\left[1 - \exp(-2\mu t)\right]$$

Solution (8.140) *exactly* describes the system motion in the square potential well.
2) When $\alpha \to 0$, expressions (8.135) through (8.138) are reduced to

$$x = v_0^2 \exp\left(-\frac{4}{3}\mu t\right)\tau(\varphi)\left(1 - \frac{|\tau(\varphi)|}{2}\right) \qquad (8.141)$$
$$\varphi = \frac{3}{2\mu v_0}\left[\exp\left(\frac{2}{3}\mu t\right) - 1\right]$$

where the identity $\mathrm{sgn}[\tau(\varphi)]|\tau(\varphi)| \equiv \tau(\varphi)$ has been taken into account.

If, in addition $\mu = 0$, then solution (8.141) also *exactly* describes the system dynamics with another nonsmooth limit of the potential energy, $|x|$, as shown in Fig. 8.16. If $\mu \neq 0$, then substituting solution (8.141) into the differential equation of motion gives an error $O(\mu^2)$. In terms of first-order asymptotic solutions, the error of order μ occurs on the time period of order $1/\mu$. Therefore, solution (8.141) exactly captures the carrying shape of the vibration but gives only asymptotic estimate for the exponential decay.

Note that the error of solution (8.135) is due to the error of the iterative procedure for elastic vibrations and the error of asymptotic for energy dissipation. As shown above, the error of successive approximations vanishes as either $\alpha \to \infty$ or $\alpha \to 0$, but the error of asymptotic vanishes only as $\alpha \to \infty$.

Finally, let us discuss the qualitative difference of the dynamics in the parameter intervals N_0 and N_∞. As follows from Eq. (8.137), for $\alpha \in N_0$, the phase of vibration and the corresponding frequency are exponentially increasing in the slow time scale μt . The physical meaning of this phenomenon becomes most clear in the limit case $\alpha = 0$. In this case, according to solution (8.141), the amplitude and frequency are, respectively,

$$A(\mu t) = \frac{v_0^2}{2}\exp\left(-\frac{4}{3}\mu t\right) \quad \text{and} \quad \dot{\varphi} = \frac{1}{v_0}\exp\left(\frac{2}{3}\mu t\right) = \frac{1}{\sqrt{2A(\mu t)}} \qquad (8.142)$$

Expressions (8.142) describe increasingly rapid vibrations—"dither"—near the corner of the potential energy $|x|$ as the amplitude approaches zero. This result is confirmed by the much earlier analysis of the corresponding conservative case [103]. In contrast, when $\alpha \in N_\infty$, the oscillator makes a limited number of cycles such that the phase φ remains bounded for any time t. Again, the most clear interpretation is obtained in the limit case $\alpha \to \infty$, when, as follows from (8.140), the phase variable $\varphi(t)$ represents the total distance passed by the particle by time t, and $\dot{\varphi} = v$ is the absolute value of the velocity. Since the barriers are perfectly elastic, the particle

reflects with no energy loss, and the velocity $v(t)$ remains continuous function of time described by the linear differential equation $\dot{v} + 2\mu v = 0$ or $\ddot{\varphi} + 2\mu\dot{\varphi} = 0$. Under the initial conditions $\varphi(0) = 0$ and $\dot{\varphi}(0) = v_0$, one obtains exactly solution (8.140).

In conclusion, the explicit analytical solution for a class of strongly nonlinear oscillators with viscous damping is introduced. Two different nonsmooth functions involved into the solution are associated with two different nonsmooth limits of the oscillator. As a result, the solution is drastically simplified to give the best match with numerical tests if approaching any of the two limits.

8.7 Bouncing Ball in Viscous Media

In this section, we consider a small ball of mass m falling under the gravity force onto a horizontal plane. In addition to the gravity, the ball is subjected to the linear damping with the coefficient c. Impacts with the plane are inelastic with the restitution coefficient k. The vertical coordinate $z(t)$ therefore is described by the following equations of motion

$$\begin{aligned} m\ddot{z} &= -mg - c\dot{z} \quad (z \neq 0) \\ \dot{z}_+ &= -k\dot{z}_- \quad (z = 0) \end{aligned} \tag{8.143}$$

where $\dot{z}_-$ and $\dot{z}_+$ are velocities right before and immediately after the impact, respectively.

Let h be a natural spatial scale of the system. This can be, for instance, the maximal height that has been reached by the ball during the first cycle. Introducing the coordinate transformation $z = h|x|$ and scaling the time as $t = \sqrt{h/g}\,p$ bring Eq. (8.143) to the form [256]

$$\begin{aligned} &\frac{d^2x}{dp^2} + 2\mu\frac{dx}{dp} + \mathrm{sgn}x = 0 \\ &\left(\frac{dx}{dp}\right)_+ - \left(\frac{dx}{dp}\right)_- = (1-k)\left(\frac{dx}{dp}\right)_- \end{aligned} \tag{8.144}$$

where

$$\mu = \frac{1}{2}\frac{c}{m}\sqrt{\frac{h}{g}}$$

In the particular case $k = 1$, solution (8.141) becomes applicable to Eq. (8.144). Then, returning back to the original notations of Eq. (8.143) gives

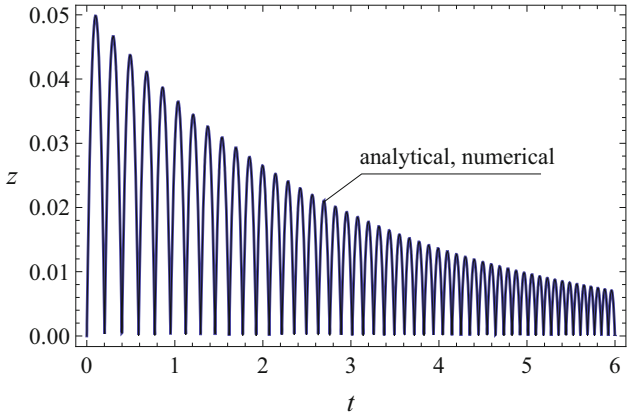

Fig. 8.21 NSTT analytical and direct numerical solutions for the height of bouncing ball under the linear dissipation condition; $m = 1.0$, $c = 0.5$, $z(0) = 0$, and $\dot{z}(0) = 1.0$

$$z(t) = C \exp\left(-\frac{2c}{3m}t\right)\left[|\tau(\varphi)| - \frac{1}{2}\tau^2(\varphi)\right] \tag{8.145}$$

$$\varphi(t) = \sqrt{\frac{g}{C}}\frac{3m}{c}\left[\exp\left(\frac{c}{3m}t\right) - 1\right]$$

where C is a new arbitrary constant.

If $C = \dot{z}_0^2/g$, then solution (8.145) satisfies the specific initial conditions $z(0) = 0$ and $\dot{z}(0) = \dot{z}_0$. One more arbitrary constant can be introduced by shifting the time, $t- > t + t_0$, that would allow to consider non-zero initial height of the ball. The effectiveness of solution (8.145) is illustrated by its comparison to the corresponding numerical solution in Fig. 8.21.

8.8 The Kicked Rotor Model

The so-called kicked rotor model is introduced in physics as a relatively simple essentially nonlinear model for chaotic behavior of systems, where one variable may be either bounded or unbounded in phase space [27, 95, 127]. The kicked rotor is described, in some units, by Hamiltonian

$$H = \frac{1}{2}I^2 + K\cos\theta \sum_{n=-\infty}^{\infty} \delta(t - n) \tag{8.146}$$

where I is the angular momentum, θ is the conjugate angle, and K is the stochasticity parameter that determines qualitative features of the dynamics.

The sequence of impulses in (8.146) can be expressed through the triangle wave $\tau = \tau\,(2t-1)$ in the form

$$\sum_{n=-\infty}^{\infty} \delta\,(t-n) = -\frac{1}{2}\tau\,(2t-1)\,\tau''\,(2t-1) \tag{8.147}$$

where primes denote differentiation with respect to the entire argument of a function, $2t-1$.

Note that the only role of the first multiplier, $\tau\,(2t-1)$, on the right-hand side is to provide pulses with the same sign. Hence (8.146) takes the form

$$H = \frac{1}{2}I^2 - \frac{1}{2}K\tau\,(2t-1)\,\tau''\,(2t-1)\cos\theta \tag{8.148}$$

The corresponding differential equation of motion is

$$\ddot{\theta} = -\frac{1}{2}K\tau\tau''\sin\theta \tag{8.149}$$

A family of solutions of the period $T = 2$ admits NSTT representation by introducing the triangle wave time argument, τ,

$$\theta = \theta(\tau) \tag{8.150}$$

Substituting (8.150) in (8.149) gives

$$\frac{d^2\theta}{d\tau^2} = -\left(\frac{1}{8}K\tau\sin\theta + \frac{d\theta}{d\tau}\right)\tau''$$

Eliminating the singular term τ'' leads to the boundary condition

$$\tau = \pm 1: \qquad \frac{d\theta}{d\tau} = -\frac{1}{8}K\tau\sin\theta \tag{8.151}$$

and the differential equation

$$\frac{d^2\theta}{d\tau^2} = 0 \tag{8.152}$$

The boundary-value problem (8.151) and (8.152) admits solution

$$\theta = A\tau\,(2t-1) + B \tag{8.153}$$

where A and B appear to be coupled by the set of equations

$$A = -\frac{1}{8}K \sin(A \pm B) \tag{8.154}$$

or

$$A = -\frac{1}{8}K \sin A \cos B \tag{8.155}$$

and

$$\cos A \sin B = 0 \tag{8.156}$$

In particular, Eq. (8.155) shows that the number of periodic solutions of the period $T = 2$ is growing as the parameter K increases.

Chapter 9
Strongly Nonlinear Waves

This short chapter deals with modulated waves described by strongly nonlinear Klein-Gordon equation. A mechanical equivalent for this model can be represented by the infinite linear string on elastic foundation. In this case, the carrying wave can be approximated by polynomials or other elementary functions of the triangle wave based on the algorithms of the previous chapter. Then the differential equations for slow varying modulations are derived by using the Whitham assumptions and the specific boundary conditions associated with nonsmooth argument substitutions.

9.1 Wave Processes in One-Dimensional Systems

A one-dimensional wave can be described by the function

$$u = u(\theta, x, t) \tag{9.1}$$

where $\theta = \theta(x, t)$ is a phase variable and x and t are the coordinate and time, respectively.

In the stationary case, the phase variable is usually the only argument of the wave shape function $u = u(\theta)$, where $\theta = \omega t - kx$ with temporal and spatial wave numbers, ω and k, respectively, so that

$$\frac{\partial \theta}{\partial t} = \omega \quad \text{and} \quad \frac{\partial \theta}{\partial x} = -k \tag{9.2}$$

Function (9.1) includes also the variables x and t explicitly in order to describe wave modulation effects. Therefore, we assume that the dependence upon explicit x and t is slow. Such an assumption can be formalized by means of the formal auxiliary parameter ε [151, 245]

V. N. Pilipchuk, *Oscillators and Oscillatory Signals from Smooth to Discontinuous*,
https://doi.org/10.1007/978-3-031-37788-4_9

$$u = u(\theta, x^0, t^0) \tag{9.3}$$

where $x^0 = \varepsilon x,\ t^0 = \varepsilon t$, and relationships (9.2) take now the form

$$\frac{\partial \theta}{\partial t} = \omega(x^0, t^0) \quad \text{and} \quad \frac{\partial \theta}{\partial x} = -k(x^0, t^0) \tag{9.4}$$

Let the wave shape function u be periodic with respect to θ with the period $T = 4$. In this case, the triangle wave phase argument can be introduced as follows $\tau = \tau(\theta)$:

$$u = U(\tau, x^0, t^0) + V(\tau, x^0, t^0)e \tag{9.5}$$

where $e = e(\theta) = \tau'(\theta)$ is the square wave of the phase variable.

9.2 Klein-Gordon Equation

For illustration purposes, we consider the Klein-Gordon equation

$$\frac{\partial^2 u}{\partial t^2} - \frac{\partial^2 u}{\partial x^2} + f(u) = 0 \tag{9.6}$$

where $f(u)$ is an odd function.

Substituting (9.5) in (9.6) and taking into account (9.4) give

$$\begin{aligned} \left(\omega^2 - k^2\right) \frac{\partial^2 U}{\partial \tau^2} &= -R_f(U, V) - \varepsilon H \frac{\partial V}{\partial \tau} - \varepsilon^2 L U \\ \left(\omega^2 - k^2\right) \frac{\partial^2 V}{\partial \tau^2} &= -I_f(U, V) - \varepsilon H \frac{\partial U}{\partial \tau} - \varepsilon^2 L V \end{aligned} \tag{9.7}$$

$$\begin{aligned} \frac{\partial U}{\partial \tau}|_{\tau=\pm 1} &= 0 \\ V|_{\tau=\pm 1} &= 0 \end{aligned} \tag{9.8}$$

where

$$H \equiv 2\left(\omega \frac{\partial}{\partial t^0} + k \frac{\partial}{\partial x^0}\right) + \frac{\partial \omega}{\partial t^0} + \frac{\partial k}{\partial x^0}$$

$$L \equiv \frac{\partial^2}{\partial t^{02}} - \frac{\partial^2}{\partial x^{02}}$$

and

$$R_f = \frac{1}{2}[f(U+V) + f(U-V)]$$
$$I_f = \frac{1}{2}[f(U+V) - f(U-V)]$$

Analogously to the case of strongly nonlinear damped oscillator considered in the previous chapter, we represent solution in the form of series

$$U(\tau, x^0, t^0) = U_0(\tau, x^0, t^0) + \varepsilon U_1(\tau, x^0, t^0) + \dots$$
$$V(\tau, x^0, t^0) = V_0(\tau, x^0, t^0) + \varepsilon V_1(\tau, x^0, t^0) + \dots \tag{9.9}$$

Substituting (9.9) into (9.7) and (9.9), and equating coefficients of like powers of ε, gives in first two steps

$$\left(\omega^2 - k^2\right)\frac{\partial^2 U_0}{\partial \tau^2} = -f(U_0)$$
$$V_0 \equiv 0 \tag{9.10}$$

$$\frac{\partial U_0}{\partial \tau}|_{\tau=1} = 0 \tag{9.11}$$

where $U_0(-\tau) = -U_0(\tau)$ due to oddness of the function $f(U_0)$, and

$$\left(\omega^2 - k^2\right)\frac{\partial^2 U_1}{\partial \tau^2} = -f'(U_0)U_1$$
$$\left(\omega^2 - k^2\right)\frac{\partial^2 V_1}{\partial \tau^2} = -f'(U_0)V_1 - H\frac{\partial U_0}{\partial \tau} \tag{9.12}$$

$$\frac{\partial U_1}{\partial \tau}|_{\tau=\pm 1} = 0$$
$$V_1|_{\tau=\pm 1} = 0 \tag{9.13}$$

The generating solution is obtained from (9.10) in the following general form

$$U_0 = U_0(\tau, A, \omega^2 - k^2) \tag{9.14}$$

where A, ω, and k are functions of the slow variables x^0 and t^0.

The functions $A(x^0, t^0)$, $\omega(x^0, t^0)$, and $k(x^0, t^0)$ are coupled by the boundary condition (9.11)

$$\frac{\partial U_0(\tau, A, \omega^2 - k^2)}{\partial \tau}|_{\tau=1} = 0 \tag{9.15}$$

and by the condition of solvability of the boundary value problem (9.12) for V_1,

$$\int_{-1}^{1} \frac{\partial U_0}{\partial \tau} H \frac{\partial U_0}{\partial \tau} d\tau = 2\left\langle \frac{\partial U_0}{\partial \tau} H \frac{\partial U_0}{\partial \tau} \right\rangle = 0$$

or

$$\frac{\partial}{\partial t^0}\left[\omega\left\langle\left(\frac{\partial U_0}{\partial \tau}\right)^2\right\rangle\right] + \frac{\partial}{\partial x^0}\left[k\left\langle\left(\frac{\partial U_0}{\partial \tau}\right)^2\right\rangle\right] = 0 \tag{9.16}$$

Example 9.2.1 Consider the equation

$$\frac{\partial^2 u}{\partial t^2} - \frac{\partial^2 u}{\partial x^2} + \operatorname{sgn}(u)|u|^\alpha = 0 \tag{9.17}$$

where α is a real positive number. In this case, the generating solution is obtained analogously to the case of oscillator with two nonsmooth limits, considered in Chap. 8, by replacing ω_0^2 with $\omega^2 - k^2$. In particular,

$$\omega^2 - k^2 = \frac{A^{\alpha-1}}{\alpha+1}\left\{1 + \frac{\alpha}{2(\alpha+2)}\left[1 + \frac{(\alpha+1)^2}{(\alpha+2)(2\alpha+3)}\right]\right\}^{-1} \tag{9.18}$$

whereas Eq. (9.16) gives

$$\frac{\partial(\omega A^2)}{\partial t} + \frac{\partial(kA^2)}{\partial x} = 0 \tag{9.19}$$

Equations (9.18) and (9.19) have been written in terms of the original time and coordinate by setting the auxiliary parameter to unity, $\varepsilon = 1$. However, according to the basic assumption, $A = A(t, x)$, $\omega = \omega(t, x)$, and $k = k(t, x)$ still should be treated as slow functions as compared to $\tau(\theta)$.

Chapter 10
Impact Modes and Parameter Variations

In this chapter, new parameter variation and averaging tools are introduced for impact modes. It is also shown that a specific combination of two impact modes gives another impact mode. The number of impact modes depends on the number of constraints and therefore can significantly exceed the number of degrees of freedom. The corresponding manipulations with impact modes become possible due to the availability of closed-form exact solutions obtained by means of the triangular sine temporal substitution for impulsively loaded and vibroimpact systems. In particular, the idea of van der Pol and averaging tool is adapted for the case of impact oscillator. For illustrating purposes, a model of coupled harmonic and impact oscillators is considered. Then, mass-spring systems with multiple impacting particles are considered in order to illustrate impact localization phenomena on high-energy levels.

10.1 An Introductory Example

Vibration modes with impacts have been under study for several years [23, 182, 242, 249]. In practical terms, such studies deal with the dynamics of elastic structures whose amplitudes are limited by stiff constraints. These may be designed intentionally or occur due to a deterioration of joints. As a result, such kinds of dynamics are often accompanied by a rattling noise or dither during operating regimes of vehicles or machine tools. From the theoretical standpoint, the interest to such problems is driven by the question what happens to linear normal modes as the energy of elastic vibrations becomes sufficient for reaching the constraints. Interestingly enough, some of the analytical approaches developed in the area recently found applications in molecular dynamics [68]. However, due to strong nonlinearities of the impact dynamics, most of the results relate to periodic particular solutions according to the idea of nonlinear normal modes [241]. Let us recall that the importance of linear

V. N. Pilipchuk, *Oscillators and Oscillatory Signals from Smooth to Discontinuous*,
https://doi.org/10.1007/978-3-031-37788-4_10

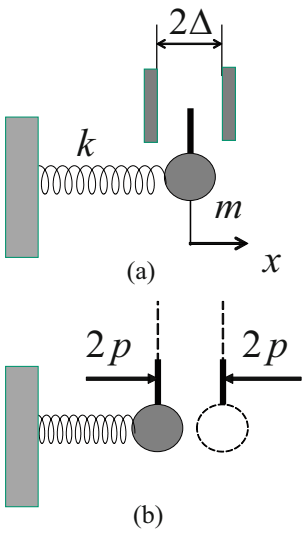

Fig. 10.1 The oscillator with bilateral rigid barriers (on the left) is replaced by the oscillator under the periodic series of external impulses (on the right)

normal modes is emphasized by the linear superposition principle as well as the parameter variation and averaging methods for weakly nonlinear cases.

Let us consider a one-degree-of-freedom free harmonic oscillator between two absolutely rigid barriers. A mechanical model of such an oscillator can be represented as a mass-spring model with two-sided amplitude limiters as shown in Fig. 10.1a.

The interaction with the barriers at $x = \pm\Delta$ is assumed to be perfectly elastic, and the system is represented in the form

$$\ddot{x} + \Omega_0^2 x = 0, \quad |x| \leq \Delta \tag{10.1}$$

Since the normal mode regimes are periodic by their definition, then the reaction of constraints can be treated as a periodic series of external impulses acting on the masses of the system.

Applying this remark to the one-degree-of-freedom system as it is shown in Fig. 10.1b, the related differential equation of motion is written in the *linear* form

$$\begin{aligned} \ddot{x} + \Omega_0^2 x &= 2p \sum_{k=-\infty}^{\infty} \left[\delta\left(\omega t + 1 - 4k + \alpha\right) - \delta\left(\omega t - 1 - 4k + \alpha\right)\right] \\ &= p\tau''\left(\omega t + \alpha\right) \end{aligned} \tag{10.2}$$

where $\delta(\xi)$ is the Dirac function, $\tau(\xi)$ is the triangular sine wave, and $2p$, ω, and α will be interpreted as arbitrary parameters.

For further convenience, the right-hand side of Eq. (10.2) is expressed through second-order generalized derivative of the triangular sine wave with respect to the

entire argument, $\omega t + \alpha$. The parameter ω will be called a frequency parameter, although it differs by the factor $\pi/2$ from the regular trigonometric frequency, $\Omega = (\pi/2)\,\omega$. Further both parameters, ω and Ω, may be used. In contrast to system (10.1), the auxiliary system (10.2) is linear but not completely equivalent to the original one as follows from the analyses below.

Representing unknown steady-state periodic solution in the form

$$x = X(\tau), \quad \tau = \tau(\omega t + \alpha) \tag{10.3}$$

gives the boundary value problem with no singular terms,

$$\omega^2 X''(\tau) + \Omega_0^2 X(\tau) = 0 \tag{10.4}$$
$$X'(\tau)\,|_{\tau=\pm 1} = p\omega^{-2}$$

and the related solution is represented in the triangle wave time form [178]

$$x = \frac{p}{\omega^2}\frac{\sin[\gamma\tau(\omega t + \alpha)]}{\gamma\cos\gamma}, \qquad \gamma = \frac{\Omega_0}{\omega} \tag{10.5}$$

This solution can be verified by direct substitution of expression (10.5) into the equation of motion (10.2).

A connection between solution (10.5) and vibration of the original system with stiff constraints is established by imposing the conditions:

- *The impulses on the right-hand side of Eq. (10.2) act when the mass strikes the limiters*

$$x = \pm\Delta \text{ if } \tau = \pm 1 \Longleftrightarrow \tau'' \neq 0 \tag{10.6}$$

- *The system cannot penetrate through the limiters; therefore,*

$$|x| \leq \Delta \text{ for all } \tau \in [-1, 1] \tag{10.7}$$

Substituting solution (10.5) into condition (10.6) determines the parameter p

$$p = \Delta\omega^2\gamma\cot\gamma \tag{10.8}$$

Substituting now (10.8) in (10.5) gives solution in the final form

$$x(t) = \Delta\frac{\sin[\gamma\tau(\omega t + \alpha)]}{\sin\gamma} \tag{10.9}$$

Obviously, solution (10.9) satisfies condition (10.6) automatically. The related parameter p (10.8) will further be treated as an eigenvalue of the nonlinear (impact)

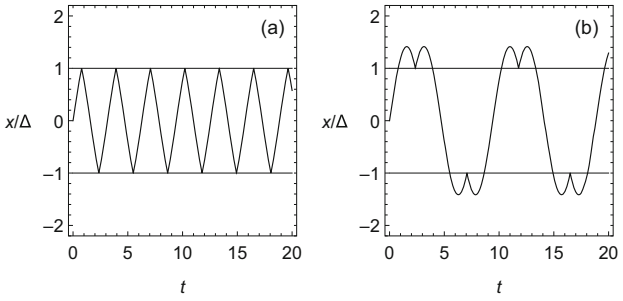

Fig. 10.2 Real (**a**) and "phantom" (**b**) solutions corresponding to the first (smallest) and second roots, respectively, $\gamma_1 = 1.1502$ and $\gamma_2 = -1.1502 + \pi$. The total energy level is $E = 1.2E_*$

problem. Other parameters, ω and α, are determined by the initial conditions. Let us assume that $x(0) = 0$ and thus $\alpha = 0$. As a result, the total energy of the oscillator per unit mass is expressed through the initial velocity as $E = [\dot{x}(0)]^2/2$. Then, taking into account (10.9) and making some analytical manipulations give

$$\gamma = \pm\frac{1}{2}\arccos\left(1 - \frac{\Omega_0^2\Delta^2}{E}\right) + k\pi, \qquad k = 0, 1, \ldots. \tag{10.10}$$

The right-hand side of expression (10.10) is a sequence of real numbers if the total energy is above its critical value, $E \geq E_* = \Omega_0^2\Delta^2/2$, such that the oscillator can reach the constraints. However, not all of the real numbers ω lead to real motions of the original system. Since the auxiliary system (10.2) has no limiters, then condition (10.6) does not guarantee that the oscillator will remain inside the region $|x| \leq \Delta$ during the period of vibration. Therefore, condition (10.7) must be verified as well. Such a verification implemented for solution (10.9) shows that condition (10.7) is satisfied only for the smallest root in set (10.10). Figure 10.2 illustrates the temporal mode shapes corresponding to the first two roots γ. It is seen that the second solution (on the right) violates condition (10.7) while satisfies condition (10.6).

Remark 10.1.1 Note that the above approach can be applied to the case of unilateral limiters. Let us remove, for instance, the left limiter and consider the oscillator (10.1) under the condition $x \leq \Delta$. In this case, the boundary conditions in (10.4) should be modified as

$$X'(\tau)\,|_{\tau=\pm1} = \pm p\omega^{-2} \tag{10.11}$$

Such a periodic change of sign effectively switches the directions of positive δ-functions on the right-hand side of Eq. (10.2). As a result, the solution takes the form

$$x(t) = \Delta \frac{\cos\left[\gamma\tau\left(\omega t + \alpha\right)\right]}{\cos\gamma} \tag{10.12}$$

where the period and the related fundamental frequency are $T = 2/\omega$ and $\Omega = \pi\omega$, respectively.

10.2 Parameter Variation and Averaging

In order to illustrate the idea of parameter variations for solution (10.9), let us include the viscous damping into the model and represent the differential equations of motion between the constraints in the form

$$\begin{aligned} \dot{x} &= v \\ \dot{v} &= -2\zeta\Omega_0 v - \Omega_0^2 x \\ |x| &\le \Delta \end{aligned} \tag{10.13}$$

where ζ is the damping ratio.

In this case, the triangle wave frequency, ω, in solution (10.9) is not constant any more, although the amplitude of the vibration remains constant as long as the oscillator is in the impact regime. The corresponding parameter variation is implemented as a change of the state variables $\{x(t), v(t)\} \to \{\gamma(t), \phi(t)\}$, dictated by solution (10.9)

$$x = \Delta \frac{\sin(\gamma\tau)}{\sin\gamma}, \qquad v = \Omega_0 \Delta \frac{\cos(\gamma\tau)}{\sin\gamma} e \tag{10.14}$$

where $\tau = \tau(\phi)$ and $e = \tau'(\phi)$ depend upon the fast phase $\phi = \phi(t)$ and $\gamma = \gamma(t)$ determines a relatively slow evolution of the temporal mode shape of the vibration.

Substituting (10.14) in (10.13) satisfies the constraint condition automatically and the system of two differential equations for new state variables

$$\begin{aligned} \dot{\gamma} &= 2\zeta\Omega_0 \cos^2\gamma\tau \tan\gamma \\ \dot{\phi} &= \frac{\Omega_0}{\gamma}[1 + \zeta(\sin 2\gamma\tau - 2\tau\cos^2\gamma\tau\tan\gamma)e] \end{aligned} \tag{10.15}$$

Below, the first-order averaging procedure is applied. Notice that the right-hand side of Eq. (10.15) is periodic with respect to the phase ϕ. As proved in Chap. 4, the averaging can be conducted with respect to the variable τ over its interval $-1 \le \tau \le 1$. As a result, one obtains

$$\dot{\gamma} = \zeta \Omega_0 \left(1 + \frac{\sin 2\gamma}{2\gamma}\right) \tan\gamma = 2\zeta\Omega_0 \left(\gamma + \frac{4}{45}\gamma^5\right) + O(\gamma^6)$$
$$\dot{\phi} = \frac{\Omega_0}{\gamma} \tag{10.16}$$

Ignoring the residual terms $O(\gamma^6)$ gives a separable equation with explicit closed-form solution for the frequency ratio

$$\gamma = \exp(2\zeta\Omega_0 t)\left[\frac{45}{4}\frac{r_0}{1 - r_0\exp(8\zeta\Omega_0 t)}\right]^{1/4} \tag{10.17}$$

The corresponding phase ϕ is obtained by using *Mathematica* package in terms of special functions

$$\phi = \Omega_0 \int_0^t \frac{dt}{\gamma} = \frac{1}{2\zeta}\left(\frac{4}{45r_0}\right)^{1/4}$$
$$\times \left\{ {}_2F_1\left[-\frac{1}{4}, -\frac{1}{4}; \frac{3}{4}; r_0\right] - \exp(-2\zeta\Omega_0 t)\right.$$
$$\left. \times [1 - r_0\exp(8\zeta\Omega_0 t)]^{5/4}\, {}_2F_1\left[1, 1; \frac{3}{4}; r_0\exp(8\zeta\Omega_0 t)\right]\right\} \tag{10.18}$$

where ${}_2F_1$ is Hypergeometric function [4] and r_0 is a constant parameter, which is calculated through the initial frequency ratio $\gamma_0 = \Omega_0/\dot{\phi}(0)$ as $r_0 = 4/(4+45\gamma_0^{-4})$.

Keeping the leading-order term only on the right-hand side of the first equation in (10.16) gives solution

$$\gamma = \gamma_0 \exp(2\zeta\Omega_0 t)$$
$$\phi = \frac{1}{2\zeta\gamma_0}[1 - \exp(-2\zeta\Omega_0 t)] \tag{10.19}$$

A simple asymptotic analysis of expressions (10.14) and the remark after expression (10.10) gives the parameter interval, $0 < \gamma < \pi/2$, within which the impact dynamics takes place. The vibration mode shapes close to the triangular wave near the left edge of the interval, but, as the energy dissipates and the parameter γ approaches $\pi/2$, vibrations become close to harmonic. The total energy is expressed through the parameter γ in the form

$$E = \frac{1}{2}\left(\frac{\Omega_0\Delta}{\sin\gamma}\right)^2 \tag{10.20}$$

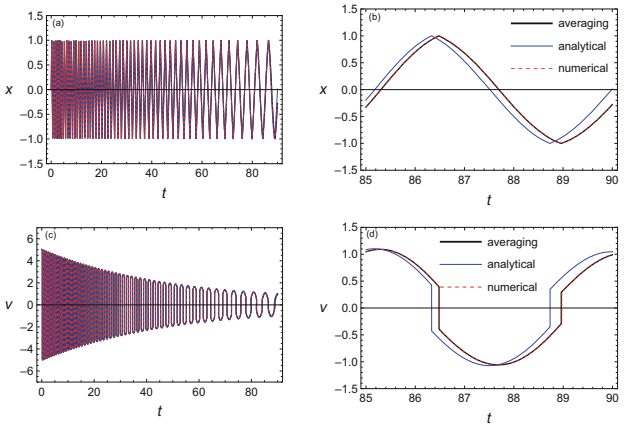

Fig. 10.3 The time history of the impact oscillator according to the numerical solution of "exact equations" (10.15), averaged Eqs. (10.16) without polynomial expansion, and the analytical closed-form solution given by (10.14), (10.17), and (10.18); the parameters are $\gamma_0 = 0.2$, $\zeta = 0.01$, $\omega_0 = 1.0$, and $\Delta = 1.0$

The duration of the impact stage of the dynamics is estimated via solution (10.19) as

$$\gamma(t_{\max}) = \frac{\pi}{2} \Longrightarrow t_{\max} = \frac{1}{2\zeta\Omega_0} \ln \frac{\pi}{2\gamma_0} \tag{10.21}$$

where $\gamma_0 = \gamma(0)$.

As follows from Fig. 10.3, the above averaging procedure leads to practically no error of the time history record within the entire interval of validity of the approach. The analytical solution based on the reduced model gives some deviation from the exact curve at the end of the impact stage of the dynamics. Notice that there is no impact interactions with the constraints for $t > t_{\max}$, where the model becomes harmonic oscillator whose amplitude exponentially decays due to the energy dissipation. At this stage, transformation (10.14) is not valid any more, nor there is any need in transformations. Still the question occurs about such solutions that would be capable of describing both impact and non-impact stages within the same closed-form expressions.

10.3 Two-Degrees-of-Freedom Model

Let us obtain first the impact mode solutions for the model shown in Fig. 10.4 under no damping condition, $c = 0$. For the sake of simplicity, let us also assume that $k_1 = k_2 = k$. On the impact normal mode motions, the system can be effectively replaced by

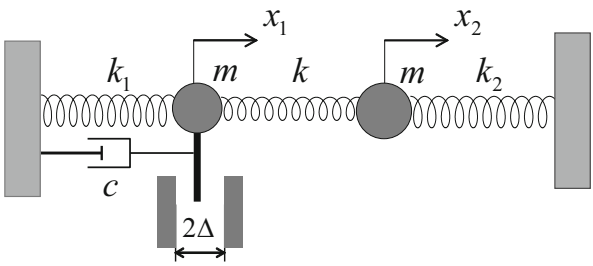

Fig. 10.4 The two-degrees-of-freedom model with viscous damping in the impact subcomponent

$$\begin{aligned} \ddot{x}_1 + \Omega_0^2 (2x_1 - x_2) &= p_1 \tau''(\omega t + \alpha) \\ \ddot{x}_2 + \Omega_0^2 (2x_2 - x_1) &= 0 \end{aligned} \tag{10.22}$$

where $\Omega_0^2 = k/m$ and the parameters ω and p_1 must provide the following condition

$$|x_1| \le \Delta \tag{10.23}$$

The impact mode solution is represented in the form

$$x_n(t) = X_n(\tau); \qquad \tau = \tau(\omega t), \qquad n = 1, 2 \tag{10.24}$$

Substituting (10.24) in (10.22) and eliminating the singular term $e'(\omega t)$ give the linear boundary value problem

$$\begin{aligned} \omega^2 X_1'' + \Omega_0^2 (2X_1 - X_2) &= 0 \\ \omega^2 X_2'' + \Omega_0^2 (2X_2 - X_1) &= 0 \end{aligned} \tag{10.25}$$

$$\begin{aligned} X_1'|_{\tau=\pm 1} &= p_1 \omega^{-2} \\ X_2'|_{\tau=\pm 1} &= 0 \end{aligned} \tag{10.26}$$

The corresponding solution has the form

$$\begin{aligned} X_1 &= \frac{p_1}{2\gamma\omega^2} \left[\frac{\sin(\gamma\tau)}{\cos\gamma} + \frac{\sqrt{3}}{3} \frac{\sin(\sqrt{3}\gamma\tau)}{\cos(\sqrt{3}\Omega_0/\omega)} \right] \\ X_2 &= \frac{p_1}{2\gamma\omega^2} \left[\frac{\sin(\gamma\tau)}{\cos\gamma} - \frac{\sqrt{3}}{3} \frac{\sin(\sqrt{3}\gamma\tau)}{\cos(\sqrt{3}\gamma)} \right] \end{aligned} \tag{10.27}$$

where $\gamma = \Omega_0/\omega$ and the "eigenvalue" p is determined by substituting X_1 into

$$X_1|_{\tau=\pm 1} = \pm\Delta \tag{10.28}$$

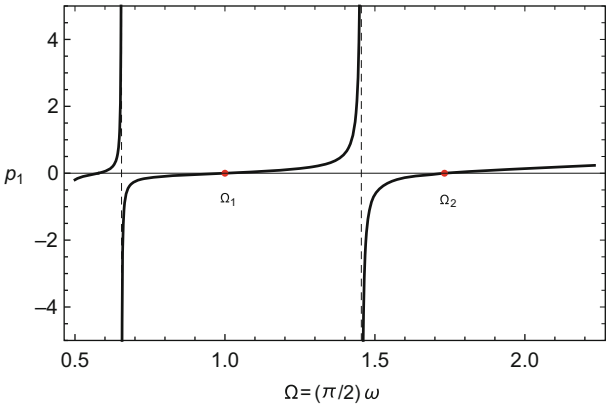

Fig. 10.5 Constraint reaction parameter p_1 versus the fundamental frequency of vibration $\Omega = (\pi/2)\,\omega$ in the case of two mass-spring model with one constrained mass; the model parameters are: $\Omega_0 = 1.0$, $\Delta = 0.2$

This gives

$$p_1 = 2\gamma\omega^2\Delta[\tan\gamma + (\sqrt{3}/3)\tan(\sqrt{3}\gamma)]^{-1} \tag{10.29}$$

In order to insure that solutions (10.27) and (10.29) describe real motions, condition (10.7) must be verified.

As follows from Fig. 10.5, the reaction impulses from amplitude limiters are positive, e.g., reflecting the mass whenever the fundamental frequency of vibrations, $\Omega = (\pi/2)\,\omega$, is on the right of any of the eigenfrequencies of the linear spectrum, $\Omega_1 = \Omega_0$ or $\Omega_2 = \sqrt{3}\Omega_0$. Note that, while on the right, Ω should still be close enough to Ω_1 in order to stay away from the next frequency, Ω_2. The situation is quite different on the right of second frequency Ω_2, corresponding to the antiphase mode. Its right neighborhood extends to the infinity with no "obstacles." It will be shown below that the condition $\Omega \gg \Omega_2$ provides the so-called mode localization. The energy outflow from such a localized mode is prevented by the impossibility of internal resonance with any of the linear modes. Recall that the damping is ignored here. In reality, the high frequency Ω cannot be maintained unless a proper energy inflow into the system is provided.

For numerical validating purposes, Fig. 10.6a, c illustrates the impact mode shapes[1] (10.27) at two different vibration frequencies Ω, such that $\Omega_1 < \Omega \ll \Omega_2$ and $\Omega_2 \ll \Omega$. In different color, the diagrams also show profiles obtained by numerical solution of a model with "soft" amplitude limiters represented by the elastic strongly nonlinear restoring force $p(t) = [x_1(t)/\alpha\Delta]^{2n-1}$, where $n = 9$ and

[1] For a better visualization purpose, here and below, displacements of mass-spring models are shown as vertical.

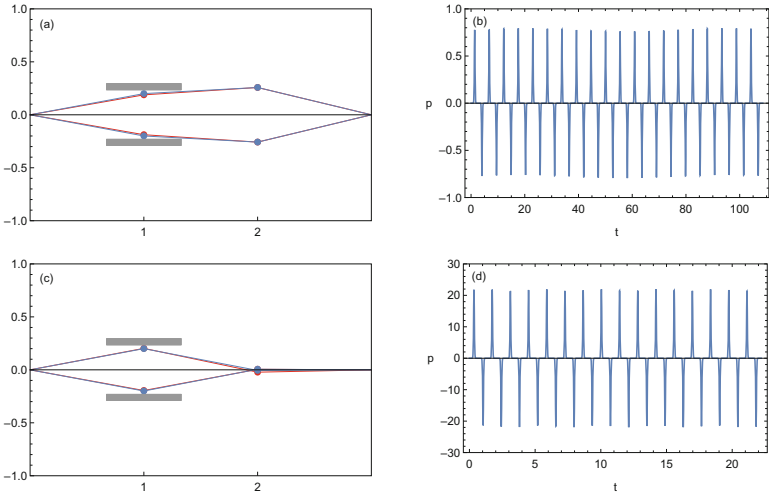

Fig. 10.6 Impact mode profiles (**a**), (**c**) and the restoring pulses (**b**), (**d**) in the right neighborhoods of the linear eigenfrequencies of the two mass-spring model with amplitude limiters imposed on the first mass; the parameters are $\Delta = 0.2$, $\Omega_0 = 1.0$, (a-b): $\omega = (2/\pi)\Omega_1 + 0.1$, and (**c**)–(**d**): $\omega = (2/\pi)\Omega_2 + 2.5$

$\alpha = 0.968$ is a numerical factor compensating the smoothing effect. An optimal number α would be obviously different for different energy levels.

10.4 A Double-Pendulum with Amplitude Limiters

The top mass m_1 of a free double-pendulum, as shown in Fig. 10.7, oscillates between the two absolutely stiff constraints providing small angular amplitudes of the top pendulum

$$\left|\varphi_1\right| \le \Delta_1 \ll 1 \tag{10.30}$$

For comparison reason, we also use a "soft version" of constraints (10.30) represented by the potential energy, which provides a fast-growing restoring force near the boundaries $\varphi_1 = \pm\Delta_1$

$$V(\varphi_1) = \frac{\beta}{2n}\left(\frac{\varphi_1}{\Delta_1}\right)^{2n}, \qquad n \gg 1 \tag{10.31}$$

where α is a positive constant parameter measured in energy units and n is an integer.

Assuming that the both rods of the double pendulum are massless and have the same length l gives the system Lagrangian

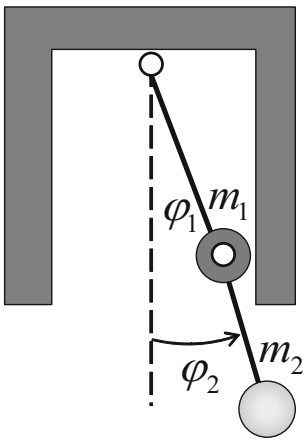

Fig. 10.7 Double pendulum with bilateral constraints

$$L = \frac{1}{2}l^2\left[(m_1+m_2)\dot{\varphi}_1^2 + 2m_2\dot{\varphi}_1\dot{\varphi}_2\cos(\varphi_1-\varphi_2) + m_2\dot{\varphi}_2^2\right]$$
$$-gl\left[m_1(1-\cos\varphi_1) + m_2(2-\cos\varphi_1-\cos\varphi_2)\right] - V(\varphi_1) \quad (10.32)$$

Due to the constraint condition, the angle φ_1 must be small. Assuming that the angle φ_2 is also small, let us approximate Lagrangian (10.32) by its quadratic form while keeping the term $V(\varphi_1)$ unchanged since the maximum ratio φ_1/Δ_1 is of order one. Using $\sqrt{g/l}t$ as a new temporal argument under the original notation t and rescaling the corresponding Euler-Lagrange equations, respectively, give

$$\mu^2\ddot{\varphi}_1 + \ddot{\varphi}_2 + \mu^2\varphi_1 = -\beta_1\left(\frac{\varphi_1}{\Delta_1}\right)^{2n-1}$$
$$\ddot{\varphi}_1 + \ddot{\varphi}_2 + \varphi_2 = 0 \quad (10.33)$$

where $\mu^2 = 1 + m_1/m_2$ and $\beta_1 = \beta/(m_2 g l \Delta_1)$ are unitless parameters and dots indicate differentiation with respect to the new temporal argument.

We seek a family of (impact mode) periodic solutions on which the reaction of constraints represents a periodic sequence of δ-functions. For that reason, we switch from system (10.32) to a linear non-autonomous system by replacing the nonlinear term as

$$-\beta_1\left(\frac{\varphi_1}{\Delta_1}\right)^{2n-1} \to p_1\tau''(\omega t+\alpha) \quad (10.34)$$

The linearized system (10.33) has normal mode vectors and natural frequencies

$$\mathbf{e}_1 = \frac{1}{\sqrt{2\mu\,(\mu+1)}}\begin{pmatrix}1\\ \mu\end{pmatrix}, \quad \Omega_1 = \sqrt{\frac{\mu}{\mu+1}}$$

$$\mathbf{e}_2 = \frac{1}{\sqrt{2\mu\,(\mu-1)}}\begin{pmatrix}1\\-\mu\end{pmatrix}, \quad \Omega_2 = \sqrt{\frac{\mu}{\mu-1}} \tag{10.35}$$

where the modal vectors satisfy the orthogonality condition, $\mathbf{e}_j^T M \mathbf{e}_i = \delta_{ji}$, with respect to the inertia matrix

$$M = \begin{pmatrix}\mu^2 & 1\\ 1 & 1\end{pmatrix}$$

Transition to the principal coordinates $\{q_1, q_2\}$ is given by

$$\begin{pmatrix}\varphi_1\\ \varphi_2\end{pmatrix} = q_1\mathbf{e}_1 + q_2\mathbf{e}_2 \tag{10.36}$$

and

$$\begin{aligned}\ddot{q}_1 + \Omega_1^2 q_1 &= \frac{p_1}{\sqrt{2\mu\,(\mu+1)}}\tau''(\omega t+\alpha)\\ \ddot{q}_2 + \Omega_2^2 q_2 &= \frac{p_1}{\sqrt{2\mu\,(\mu-1)}}\tau''(\omega t+\alpha)\end{aligned} \tag{10.37}$$

Now two-parameter families of periodic solutions for both independent oscillators (10.37) can be obtained as described in Sect. 10.1 by means of the triangle wave temporal substitution, $\tau = \tau(\omega t + \alpha)$. Substituting such solutions in (10.36) and determining the impulse parameter p_1 from the condition $\varphi_1|_{\tau=1} = \Delta_1$ bring the solution to its final form (Fig. 10.8)

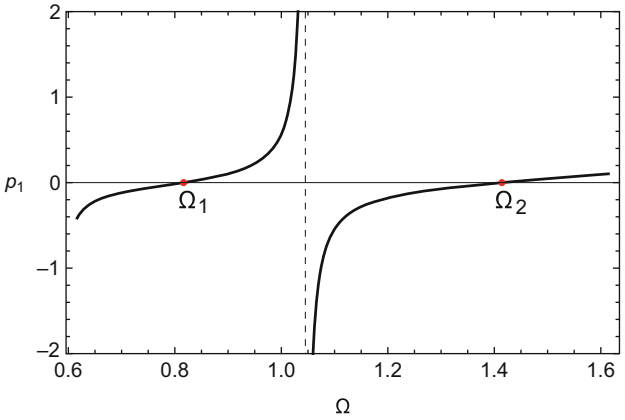

Fig. 10.8 The restoring impulse parameter versus the fundamental frequency of the double-pendulum impact mode vibration, $\Omega = (\pi/2)\,\omega$

$$p_1 = 2\gamma_1 \Delta_1 \mu(\mu+1)\omega^2 \left[\tan\gamma_1 + \left(\gamma_2/\gamma_1\right)\tan\gamma_2\right]^{-1} \tag{10.38}$$
$$= 2\Delta_1 \mu(\mu+1)\Omega_1 \omega \left[\tan\frac{\Omega_1}{\omega} + \frac{\Omega_2}{\Omega_1}\tan\frac{\Omega_2}{\omega}\right]^{-1}$$

and

$$\begin{pmatrix}\varphi_1\\ \varphi_2\end{pmatrix} = \Delta_1 \left[\tan\gamma_1 + \frac{\gamma_2}{\gamma_1}\tan\gamma_2\right]^{-1} \times \tag{10.39}$$

$$\left[\begin{pmatrix}1\\ \mu\end{pmatrix}\frac{\sin\left[\gamma_1\tau\,(\omega t+\alpha)\right]}{\cos\gamma_1} + \frac{\gamma_2}{\gamma_1}\begin{pmatrix}1\\ -\mu\end{pmatrix}\frac{\sin\left[\gamma_2\tau\,(\omega t+\alpha)\right]}{\cos\gamma_2}\right]$$

where $\gamma_{1,2} = \Omega_{1,2}/\omega$ and the relationships $\mu - 1 = \mu\Omega_2^{-2}$ and $\mu + 1 = \mu\Omega_1^{-2}$ have been used in manipulations.

Note that the frequency of first impact mode must be close enough to the first linear frequency Ω_1 to insure that it is still away from the left neighborhood of the next frequency, Ω_2. In the current case, Ω_2 is the highest frequency; therefore its right neighborhood has no upper boundary. As a result, the highest impact mode becomes spatially localized as its frequency parameter grows. The localization admits explicit estimation by the asymptotic expansion

$$\frac{\varphi_2}{\varphi_1}|_{\tau=1} = \mu\left(\tan\gamma_1 - \frac{\gamma_2}{\gamma_1}\tan\gamma_2\right)\left(\tan\gamma_1 + \frac{\gamma_2}{\gamma_1}\tan\gamma_2\right)^{-1}$$
$$= -1 - \frac{1}{3}\omega^{-2} - O\left(\omega^{-4}\right) \tag{10.40}$$

It follows from (10.40) that $(\varphi_2/\varphi_1)\,|_{\tau=1} \to -1$ as $\omega \to \infty$, so that the amplitude of the bottom mass becomes negligibly small, whereas the upper mass has the amplitude determined by the angular limiters. Figures 10.9 and 10.10 illustrate the impact mode profiles above first and second eigenfrequency of the linear spectrum, respectively. The results of numerical integration are obtained for the soft amplitude limiters represented by the high-degree potential energy (10.31) with the parameters $n = 20$ and $\beta = 0.702145$.

10.5 Averaging in the 2DOF System

Let us consider now the model shown in Fig. 10.4. The coefficient of restitution for the impact interactions is assumed to be unity, while a relatively slow energy dissipation is possible due to the viscous damping. Also, the base springs have equal stiffness, and the coupling between the oscillators is weak, such that $k_1 = k_2 =$

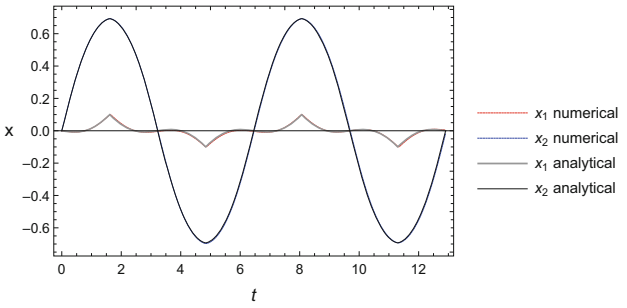

Fig. 10.9 Horizontal displacements of the top (x_1) and bottom (x_2) masses of the double-pendulum near the lower frequency of the linear spectrum, $\omega = (2/\pi)\Omega_1 + 0.1$; the system parameters are $l = 1.0$, $\Delta_1 = 0.1$, and $\mu = 2.0$

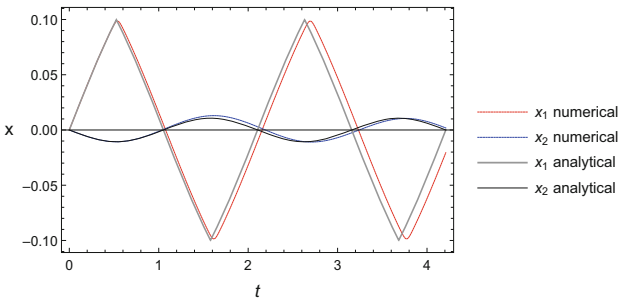

Fig. 10.10 Same as Fig. 10.9 for the frequency $\omega = (2/\pi)\Omega_2 + 1.0$; the trend to impact mode localization is developed

$K >> k$. In order to introduce the corresponding parameter variation technique, let us represent the differential equations of motion in the following general form

$$\begin{aligned}
\dot{x}_1 &= v_1 \\
\dot{v}_1 &= -f_1(x_1, x_2, v_1, v_2) + pe'(\phi) \\
\dot{x}_2 &= v_2 \\
\dot{v}_2 &= -f_2(x_1, x_2, v_1, v_2)
\end{aligned} \tag{10.41}$$

where $pe'(\phi) = p\tau''(\phi)$ and

$$\begin{aligned}
f_1(x_1, x_2, v_1, v_2) &= 2\zeta\Omega_0 v_1 + \Omega_0^2 x_1 + \beta(x_1 - x_2) \\
f_2(x_1, x_2, v_1, v_2) &= \Omega_0^2 x_2 - \beta(x_1 - x_2)
\end{aligned} \tag{10.42}$$

are impact and linear force components per unit mass, $\beta = k/m$ is the parameter of coupling, $\zeta = c/(2\Omega_0 m)$ is the damping ratio, and $\Omega_0 = \sqrt{K/m}$.

The idea of parameter variations is implemented below as a change of the state variables

$$\{x_1(t), v_1(t), x_2(t), v_2(t)\} \to \{\gamma(t), \phi(t), A(t), B(t)\}$$

according to expressions

$$\begin{aligned} x_1 &= \Delta \frac{\sin(\gamma\tau)}{\sin\gamma} \\ v_1 &= \Omega_0 \Delta \frac{\cos(\gamma\tau)}{\sin\gamma} e \\ x_2 &= A \sin\frac{\pi\tau}{2} + B\cos\frac{\pi\tau}{2} e \\ v_2 &= \Omega_0 \left(A\cos\frac{\pi\tau}{2} e - B\sin\frac{\pi\tau}{2} \right) \end{aligned} \tag{10.43}$$

where $\tau = \tau(\phi)$ and $e = e(\phi)$.

It is assumed in (10.43) that the principal frequency of the vibration, $d\phi/dt$, is dictated by the impact subcomponent rather than by a natural frequency of the corresponding linearized system. However, the scaling factor Ω_0 is still used in order to indicate the dominant oscillator of the dynamic process under consideration. Notice that $x_1$and v_1 are transformed analogously to (10.14), whereas the transformation of x_2 are v_2 is based on the standard general solution of the harmonic oscillator represented however in the nonsmooth temporal transformation form.

Substituting (10.43) in (10.41) gives

$$\begin{aligned} \dot\gamma &= \frac{e}{\Omega_0\Delta}\cos\gamma\tau \left(f_1 \sin\gamma - \Omega_0^2 \Delta \sin\gamma\tau \right) \tan\gamma \\ \dot\phi &= \frac{1}{\gamma\Omega_0\Delta}[f_1 \sin\gamma(\sin\gamma\tau - \tau\cos\gamma\tau\tan\gamma) \\ &\quad + \Omega_0^2\Delta\cos\gamma\tau(\cos\gamma\tau + \tau\sin\gamma\tau\tan\gamma)] \\ \dot A &= -\frac{1}{2}\left[\Omega_0(1-\cos\pi\tau) - \pi\dot\phi\right] B \\ &\quad + \left(\frac{1}{2}\Omega_0 A\sin\pi\tau - \frac{1}{\Omega_0} f_2 \cos\frac{\pi\tau}{2} \right) e \\ \dot B &= \frac{1}{2}\left[\Omega_0(1+\cos\pi\tau) - \pi\dot\phi\right] A + \frac{1}{\Omega_0} f_2 \sin\frac{\pi\tau}{2} - e\frac{1}{2}\Omega_0 B\sin\pi\tau \end{aligned} \tag{10.44}$$

where the functions f_1 and f_2 are expressed through the new variables by substitution (10.43) in (10.42) and the impact term $pe'(\phi)$ has been eliminated by setting (compare with (10.8))

$$p = p(t) = \Delta\Omega_0\dot{\phi}(t)\cot\gamma(t) \tag{10.45}$$

Further reduction of system (10.44) includes two major steps, such as averaging with respect to the fast phase ϕ and applying the power series expansion with respect to the parameter γ. Since the periodic functions in Eq. (10.44) are expressed through the triangular sine wave $\tau(\phi)$, then the averaging can be implemented by considering τ as an argument of the averaging as described in Chap. 4. Then, truncating the power series expansions with respect to γ gives

$$\begin{aligned}
\dot{\gamma} &= 2\zeta\Omega_0\gamma - \frac{2\beta}{\pi\Omega_0}\frac{B}{\Delta}\gamma^2 + O(\gamma^3)\\
\dot{\phi} &= \frac{\Omega_0}{\gamma} - \frac{2\beta}{45\Omega_0}\left(1 - 60\frac{12-\pi^2}{\pi^4}\frac{A}{\Delta}\right)\gamma^3 + O(\gamma^4)\\
\dot{A} &= -\left(\Omega_0 + \frac{\beta}{2\Omega_0} - \frac{\pi}{2}\dot{\phi}\right)B\\
\dot{B} &= \left(\Omega_0 + \frac{\beta}{2\Omega_0} - \frac{\pi}{2}\dot{\phi}\right)A - \frac{4\beta\Delta}{3\Omega_0}\frac{12-\pi^2}{\pi^4}\gamma^2 - \frac{4\beta\Delta}{\pi^2\Omega_0} + O(\gamma^3)
\end{aligned} \tag{10.46}$$

Approximate Eqs. (10.46) describe only one-way interaction between the oscillators so that the first two equations can be easily solved analytically; see the above one-degree-of-freedom case. Then, substituting the result into the next two equations gives a linear set of equations with variable coefficients for $A(t)$ and $B(t)$, which can also be considered analytically. Let us skip such kind of analysis but illustrate the final result in Fig. 10.11. The diagrams show the energy versus time of the second oscillator based on numerical solutions for three different sets of equations, such as exact Eqs. (10.44), the equations obtained by averaging (not described here), and the reduced set (10.46). The solutions are in quite a good match most of the time interval; however, the solution of truncated set (10.46) shows some error near the end of the interval. This happens because the parameter γ is slowly approaching its limit magnitude $\pi/2$, at which the first oscillator stops interacting with the constraints and the entire system becomes linear. Remind that Eq. (10.46) was obtained by truncating the polynomial expansions in the neighborhood of $\gamma = 0$; as a result, the accuracy of the equations is low near the point $\gamma = \pi/2$. The precision can be significantly improved by keeping few more terms of the power series with respect to γ.

10.6 Impact Modes in Multiple Degrees of Freedom Systems

Let us consider the N-degrees-of-freedom conservative system described by the coordinate vector $\mathbf{x} = (x_1, \ldots, x_N)^T \in R^N$. The corresponding mass-spring model is shown in Fig. 10.12. It is assumed that displacements of the ath mass are limited

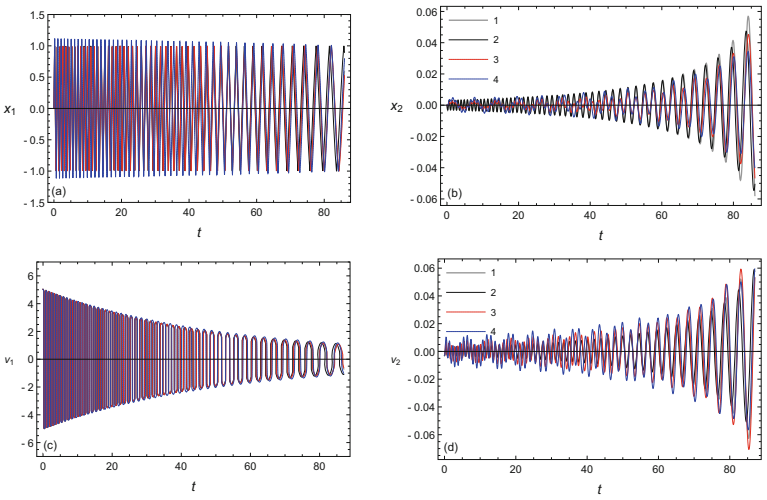

Fig. 10.11 Numerical validation of the transformed and averaged equations: (**a**)–(**b**)—mass1 and (**d**)–(**c**)—mass2. Curves: 1, averaged Eqs. (10.44); 2, the averaged equations followed by polynomial expansions (10.46); 3, Eqs. (10.44) without averaging; and 4, soft-wall approximation. The initial conditions and model parameters are as follows: $\gamma(0) = 0.2$, $\phi(0) = 0.0$, $A(0) = -0.003$, $B(0) = 0$, $\zeta = 0.01$, $\Omega_0 = 1.0$, $\Delta = 1.0$

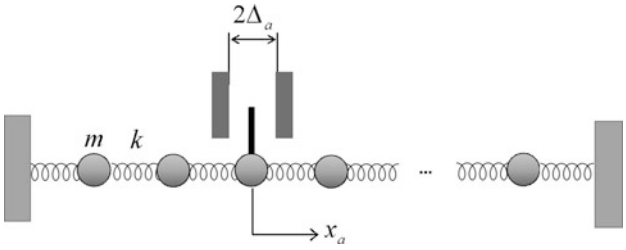

Fig. 10.12 The mass-spring model of a discrete elastic system with displacement limiters

by perfectly stiff elastic constraints, such that $|x_a| \leq \Delta_a$ or, in the matrix form,

$$\left|\mathbf{I}_a^T \mathbf{x}\right| \leq \Delta_a \tag{10.47}$$

where $\mathbf{I}_a = \left(0, \ldots, \underset{a}{1}, \ldots, 0\right)^T$.

Inside the domain (10.47), the differential equations of motion are assumed to be linear

$$M\ddot{\mathbf{x}} + K\mathbf{x} = 0 \tag{10.48}$$

where M and K are constant mass and stiffness $N \times N$ -matrixes, respectively.

The form of matrix equation (10.48) is general enough to describe different models, not necessarily mass-spring chains; see the first example below. In order to obtain impact mode solutions, the systems (10.47) and (10.48) are replaced by the following impulsively forced linear system under no constraints condition

$$M\ddot{\mathbf{x}} + K\mathbf{x} = p\mathbf{I}_a \tau''(\omega t + \alpha) \tag{10.49}$$

where p is a priori unknown "eigenvalue" and ω and α are arbitrary constant parameters.

A family of periodic solutions of the period $T = 4/\omega$ can be found as a linear superposition of solutions (10.5) for each of the N linear modes of system (10.48) with appropriate replacement of the parameters

$$\mathbf{x}(t) = \frac{p}{\omega^2} \sum_{j=1}^{N} \left(\mathbf{e}_j^T \mathbf{I}_a\right) \mathbf{e}_j \frac{\sin[\gamma_j \tau\,(\omega t + \alpha)]}{\gamma_j \cos \gamma_j}; \qquad \gamma_j = \frac{\Omega_j}{\omega} \tag{10.50}$$

where $\mathbf{e}_j$ and Ω_j are the jth normal mode and the natural frequency of linear system (10.48); it is assumed that $\Omega_i < \Omega_j$ when $i < j$, and the linear normal modes are normalized as

$$\mathbf{e}_j^T M \mathbf{e}_i = \delta_{ji} \tag{10.51}$$

where δ_{ji} is the Kronecker symbol.

The impulses act at those time instances when the ath mass interacts with the constraints; in other terms,

$$\mathbf{I}_a^T \mathbf{x} = \pm \Delta_a \text{ when } \tau = \pm 1 \tag{10.52}$$

Substituting (10.50) into (10.52), one obtains the related "eigenvalue"

$$p = \Delta_a \omega^2 \left[\sum_{j=1}^{N} (\mathbf{e}_j^T \mathbf{I}_a)^2 \frac{\tan \gamma_j}{\gamma_j} \right]^{-1} \tag{10.53}$$

where $\mathbf{e}_j^T \mathbf{I}_a$ is the ath component of the jth linear mode vector.

Substituting (10.53) into (10.50) gives a two-parameter family of the periodic solutions for the impact modes. The parameter α is an arbitrary phase shift, whereas the frequency parameter ω is subjected to some restrictions due to condition (10.47). As shown in [182], condition (10.47) is satisfied when the principal frequency of vibration, $\Omega = (\pi/2)\,\omega$, exceeds the highest frequency of the linear spectrum, $\Omega > \Omega_N$. The corresponding impact mode represents an extension of the highest linear normal mode, in which any two neighboring masses vibrate out of phase. Such an impact mode becomes spatially localized as $\Omega \to \infty$. This result was obtained also by qualitative methods in [249]. Condition (10.47) may be satisfied also when the

frequency Ω is located in a small enough right neighborhood of any frequency Ω_j and, in addition, Ω_i/Ω_j is not an odd number for all $i \neq j$. The idea of the proof is to find such cases when $\mathbf{I}_a^T\mathbf{x}$ is a monotonic function of τ on the interval $-1 \leq \tau \leq 1$, and hence condition (10.52) at the boundaries guarantees that inequality (10.47) holds inside the entire interval.

Generally, the impact modes appear to have quite a complicated spectral structure. Therefore, a detailed investigation may be required in order to formulate *necessary and sufficient* conditions of impact mode existence. However, a sufficient condition of *non-existence* can be formulated by using the physical meaning of the parameter p. Namely, if an impact mode exists, then the inequality $p(\omega) > 0$ holds. Indeed, the parameter p (10.53) cannot be negative for any real impact vibrating regime as a reaction of constraint, because it cannot be directed *toward* the barrier. Thus impact modes cannot exist when $p(\omega) < 0$.

Note that investigation of stability properties of the impact modes is rather a separate subject. Later we discuss it based on a mass-spring chain model in a semi-qualitative way.

10.7 Systems with Multiple Impacting Particles

Let us consider the case of two particles, say the ath and bth, under the constraint conditions. These conditions are $|x_a| \leq \Delta_a$ and $|x_b| \leq \Delta_b$ or, in the vector notations,

$$\left|\mathbf{I}_a^T\mathbf{x}\right| \leq \Delta_a \text{ and } \left|\mathbf{I}_b^T\mathbf{x}\right| \leq \Delta_b \tag{10.54}$$

In this case, the impulsive excitation on the right-hand side of the auxiliary equation must act on both ath and bth particles, so that the equation takes the form

$$M\ddot{\mathbf{x}} + K\mathbf{x} = (p_a\mathbf{I}_a + p_b\mathbf{I}_b)\tau''(\omega t + \alpha) \tag{10.55}$$

where p_a and p_b are parameters to be determined.

The related solution includes terms related to p_a and p_b and can be represented in the form

$$\mathbf{x}(t) = \frac{1}{\omega^2}\sum_{j=1}^{N}\left[p_a\left(\mathbf{e}_j^T\mathbf{I}_a\right)\mathbf{e}_j + p_b\left(\mathbf{e}_j^T\mathbf{I}_b\right)\mathbf{e}_j\right]\frac{\sin[\gamma_j\tau(\omega t+\alpha)]}{\gamma_j\cos\gamma_j} \tag{10.56}$$

Following the idea of normal modes, let us assume that the impact mode periodic motion is accompanied by *synchronous* impacts of both particles with the constraints according to conditions

$$\mathbf{I}_a^T\mathbf{x} = \pm\Delta_a \text{ and } \mathbf{I}_b^T\mathbf{x} = \pm\Delta_b \text{ when } \tau = \pm 1 \tag{10.57}$$

Substituting (10.56) in (10.57) gives linear algebraic equations with respect to p_a and p_b in the form

$$\begin{aligned} k_{aa}\, p_a + k_{ab}\, p_b &= \Delta_a \\ k_{ba}\, p_a + k_{bb}\, p_b &= \Delta_b \end{aligned} \tag{10.58}$$

where

$$k_{ab} = \frac{1}{\omega^2} \sum_{j=1}^{N} \left(\mathbf{e}_j^T \mathbf{I}_a\right) \left(\mathbf{e}_j^T \mathbf{I}_b\right) \frac{\tan \gamma_j}{\gamma_j} \tag{10.59}$$

Expressions (10.56) and (10.58) give a formal impact mode solution, which indeed describes an impact mode when the determinant of system (10.58) is non-zero and condition (10.54) holds. Solution (10.56) can be viewed as a strongly nonlinear superposition of the two basic impact modes with a single impacting mass.

10.7.1 Mass-Spring Chain

One Impact Particle

Let us consider a mass-spring chain of N identical particles under the constraint condition

$$m\ddot{x}_n + k\left(-x_{n-1} + 2x_n - x_{n+1}\right) = 0; \qquad n = 1, \ldots, N \tag{10.60}$$

$$x_0 = x_{N+1} = 0; \qquad |x_a| \le \Delta_a; \qquad 1 < a < N \tag{10.61}$$

where k and m are the stiffness of each spring and the mass of each particle, respectively.

The corresponding impulsively loaded linear system is represented as

$$\ddot{x}_n + \Omega_0^2\left(-x_{n-1} + 2x_n - x_{n+1}\right) = p\delta_{an}\tau''(\omega t + \alpha) \tag{10.62}$$

where $\Omega_0 = \sqrt{k/m}$ is a common physical factor for all the eigenfrequencies and the parameter of impulses p is measured per unit mass.

In this case, the corresponding linear modes and their frequencies are described exactly by expressions

$$\mathbf{e}_j = \sqrt{\frac{2}{N+1}} \left(\sin\frac{\pi j}{N+1}, \ldots, \sin\frac{N\pi j}{N+1}\right)^T \tag{10.63}$$

$$\Omega_j = 2\Omega_0 \sin \frac{\pi j}{2(N+1)}$$

where $j = 1, \ldots, N$.

Note that $j = 1+N$ formally gives the relationship[2] $\Omega_{N+1} = 2\Omega_0$, which is used below for convenience of analytical manipulations. The basis vectors of principal coordinates are normalized as $\mathbf{e}_j^T \mathbf{e}_i = \delta_{ji}$ since the inertia matrix of system (10.62) is an identity matrix. The ath component of the jth normal mode vector is therefore

$$\mathbf{e}_j^T \mathbf{I}_a = \sqrt{\frac{2}{N+1}} \sin \frac{a\pi j}{N+1} \tag{10.64}$$

where the matrix column $\mathbf{I}_a = \left(0, \ldots, \underset{a}{1}, \ldots, 0\right)^T$ was used first in (10.47).

Now adaptation of solution (10.50) and (10.53) gives in component-wise form

$$x_n = \frac{2p_a}{(N+1)\omega^2} \sum_{j=1}^{N} \sin \frac{\pi nj}{N+1} \sin \frac{\pi aj}{N+1} \frac{\sin[\gamma_j \tau\,(\omega t + \alpha)]}{\gamma_j \cos \gamma_j} \tag{10.65}$$

$(n = 1, \ldots, N)$

and

$$p_a = \Delta_a \omega^2 \left[\frac{2}{(N+1)} \sum_{j=1}^{N} \sin^2 \frac{\pi aj}{N+1} \frac{\tan \gamma_j}{\gamma_j} \right]^{-1} \tag{10.66}$$

where $\gamma_j = \Omega_j/\omega = (\pi/2)\Omega_j/\Omega$; recall that the period of triangle wave τ of is normalized to four.

For numerical illustrations below, we always set $\Omega_0 = \sqrt{k/m} = 1.0$. As follows from Eq. (10.62), the factor Ω_0 can be removed from the system by rescaling the time argument and the parameter ω. A numerical illustration of the dependence $p_a(\omega)$ and an example of the impact mode amplitude profile are given in Fig. 10.13a and b, respectively (see also Fig. 10.14). Recall that the frequency parameter ω value must provide the condition $p_a(\omega) > 0$ for the assumed restoring impulses of the amplitude limiters.

Internal Resonances

Let us discuss physical specifics in a qualitative way based on a typical temporal mode shape of an uncoupled impact oscillator

[2] Note that this is just a suitable notation since the $(N+1)$th frequency does not physically exist.

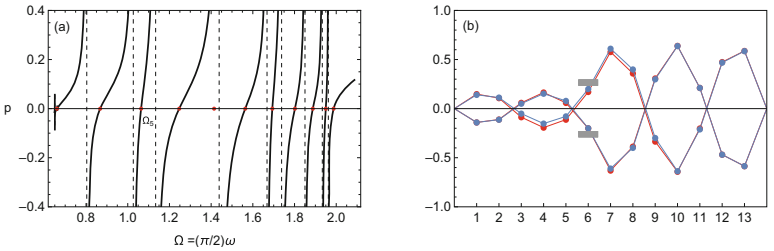

Fig. 10.13 Numerical verification of the existence of impact mode: (**a**) restoring pulses p_6 versus the fundamental frequency of vibration, Ω, for the case of one vibroimpact particle $a = 6$ ($\Delta_6 = 0.2$) of the chain of $n = 13$ particles, where the dots represent natural frequencies of the linear chain, Ω_i ($i = 3, \ldots, 13$); (**b**) the corresponding mode shape profiles for $\omega = (2/\pi)\Omega_5 + 0.02$ obtained from the analytical solution (blue) and numerical solution (red) for the soften restoring pulses represented by the force $\sim 2.18747(x_6/\Delta_6)^{17}$

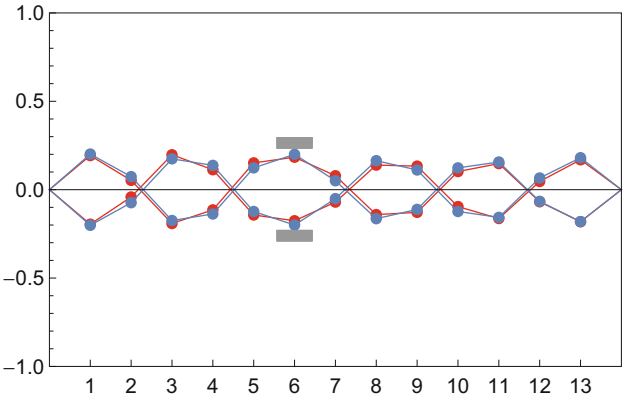

Fig. 10.14 Same as Fig. 10.13b for the case $\omega = (2/\pi)\Omega_6 + 0.02$

$$x(t) = \Delta \frac{\sin[\gamma\tau(\omega t)]}{\sin\gamma}; \qquad 0 < \gamma \le \frac{\pi}{2} \tag{10.67}$$

where γ is the parameter characterizing the energy level as shown in (10.20).

Recall that the upper boundary $\gamma = \pi/2$ corresponds to the grazing regime with the sine wave temporal shape. When $\gamma \to 0$, we have the triangle wave of an infinitely large frequency, since $\omega = O(\gamma^{-1})$ as follows from (10.5): ω and γ in (10.67) are coupled such that $\omega\gamma$ is equal to the fixed natural frequency of the oscillator without the effect of constraints. Obviously the intensive vibroimpact oscillation makes the effect of the linear part of restoring force on the time history of vibration negligible.

Let us consider the Fourier expansion of function (10.67)

$$x(t) = \Delta \sum_{s=1}^{\infty} b_s \sin[(2s-1)\Omega t], \qquad \Omega = \frac{\pi}{2}\omega \tag{10.68}$$

where Ω is the fundamental trigonometric frequency of vibration and

$$b_s = \frac{8(-1)^{s+1}\gamma \cot \gamma}{(2s-1)^2\pi^2 - 4\gamma^2} \tag{10.69}$$

The amplitude b_s is defined for any γ despite of the uncertainty at $\gamma = (2s - 1)\pi/2$, where the corresponding limit must be calculated. For illustrating purposes, let us consider the chain model described by Eq. (10.62) by imposing the temporal mode shape (10.68) on the vibroimpact particle $n = a$ as $x_a(t) = x(t)$. From the physical standpoint, such an assumption ignores the feedback from the rest of the chain to the particle $n = a$. The feedback vanishes in the asymptotic limit of intensive impacts, $\omega \to \infty$, which can be seen explicitly after switching to the phase variable ωt in Eq. (10.62). The kinematic constraint on the displacement $x_a(t)$ effectively splits the chain into two shorter chains with $N_1 = a - 1$ and $N_2 = N - a$ particles. Each of the two chains has one end fixed and another one oscillating according to dependence (10.68). Both chains obey the differential equations of the same form with either $N = N_1$ or $N = N_2$

$$\ddot{x}_n + \Omega_0^2 (-x_{n-1} + 2x_n - x_{n+1}) = \delta_{Nn}\Omega_0^2 \Delta \sum_{s=1}^{\infty} b_s \sin[(2s-1)\Omega t] \tag{10.70}$$

where δ_{Nn} is Kronecker's symbol, $n = 1, \ldots, N$, and $N = N_\alpha$ ($\alpha = 1, 2$).

System (10.70) is solved by taking into account (10.63) and switching to the principal coordinates q as

$$\mathbf{x} = \sum_{j=1}^{N} q_j(t)\mathbf{e}_j \tag{10.71}$$

gives the differential equation for the jth mode

$$\ddot{q}_j + \Omega_j^2 q_j = \Omega_0^2 \left(\mathbf{e}_j^T \mathbf{I}_N\right) \Delta \sum_{s=1}^{\infty} b_s \sin[(2s-1)\Omega t] \tag{10.72}$$

The corresponding steady-state (particular) solution is

$$q_j = \Omega_0^2 (\mathbf{e}_j^T \mathbf{I}_N) \Delta \sum_{s=1}^{\infty} \frac{b_s \sin[(2s-1)\Omega t]}{\Omega_j^2 - (2s-1)^2\Omega^2} \tag{10.73}$$

where

$$\mathbf{e}_j^T \mathbf{I}_N = \sqrt{\frac{2}{N_\alpha + 1}} \sin \frac{N_\alpha \pi j}{N_\alpha + 1}$$

$$\Omega_j = 2\Omega_0 \sin \frac{\pi j}{2(N_\alpha + 1)}; \qquad \alpha = 1, 2 \tag{10.74}$$

Taking into account (10.74) and the numbers $N_1 = a - 1$ and $N_2 = N - a$ gives

$$\Omega = \frac{\pi}{2}\omega = \frac{2\Omega_0}{2s - 1} \sin \frac{\pi j}{2a}; \qquad j = 1, \ldots, N_1 \tag{10.75}$$

$$\Omega = \frac{\pi}{2}\omega = \frac{2\Omega_0}{2s - 1} \sin \frac{\pi j}{2(N - a + 1)}; \qquad j = 1, \ldots, N_2 \tag{10.76}$$

where $1 < a < N$ and $s = 1, 2, \ldots$.

Since resonance frequencies (10.75) and (10.76) are obtained by splitting the chain in two separate pieces by inserting the vibroimpact oscillator in between two subsystems and ignoring possible feedback, then let us clarify how "exact solution" (10.65) does behave under the input frequencies estimated by (10.75) and (10.76). Note that, in contrast to solution (10.73), solution (10.65) does not have singularities at frequencies (10.75) and (10.76). Still Fig. 10.15 depicts sharp increases of the corresponding amplitudes confirmed also by the results of numerical integration under soften constraint conditions. Further, Fig. 10.16 illustrates the trend to impact mode localization as the input frequency ω exceeds the highest resonance frequency by about 6%. The fragment (a) shows a match of mode profiles obtained from different solutions and represented by different colors on the same graph. Recall that solution (10.73) is applied separately to the left and right parts of the chain by using (10.74) with $\alpha = 1$ and $\alpha = 2$, respectively. Also, modal vectors (10.63) must be calculated separately for the numbers of particles N_1 and N_2, respectively. Finally, when switching back to the coordinates $\mathbf{x}$ by means of expansion (10.71), the particles of the right part of the chain, which is after the inserted vibroimpact particle, $n = a$, must be taken in the reverse way: $n =$

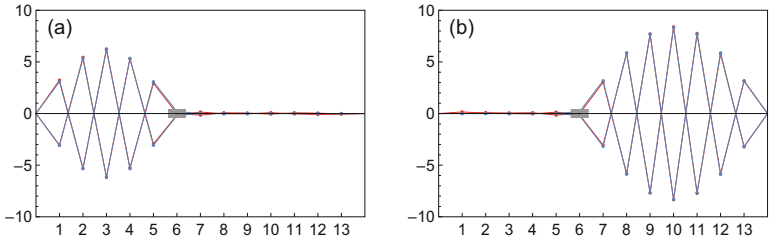

Fig. 10.15 Impact mode profiles associated with resonance frequencies: (**a**) (10.75) for $\omega = 1.22985$ ($j = N_1$) and (**b**) (10.76) for $\omega = 1.24877$ ($j = N_2$); both shapes are obtained for the chain parameters: $n = 13$, $a = 6$, $\Delta_6 = 0.2$, and $\Omega_0 = 1.0$, using analytical solution (10.65) and numerical integration with constraints replaced by the restoring force $1.73828(x_6/\Delta_6)^{17}$

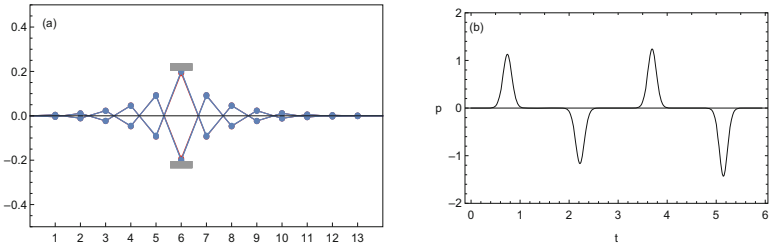

Fig. 10.16 Validation of analytical solutions for the frequency, $\omega = 1.34877$ ($j = N_2$): (**a**) impact mode profiles obtained from solutions (10.65), (10.71)–(10.73), and numerical solution for the chain with soft amplitude limiters described by the restoring force replaced by the restoring force $1.73828(x_6/\Delta_6)^{17}$, and (**b**) initial phase of the restoring pulses from the soft amplitude limiters

$N_2,\ldots,1$. The fragment (b) of Fig. 10.16 illustrates the temporal profile of restoring pulses produced by the soften amplitude limiters. Obviously such pulses are not perfectly localized, and their timing cannot perfectly match the collision times dictated by the auxiliary system (10.62) through the frequency ω. As a result, the smoothed pulses (Fig. 10.16b) may eventually desynchronize and corrupt the spatial mode profile as compared to the analytical predictions. A long-term simulation nonetheless confirms that the localization of amplitude envelope is maintained. This happens because, for the given frequency ω, the spectrum of vibroimpact oscillator has no intersections with the natural spectra of both left and right parts of the chain. As a result, no more or less significant energy exchange between the vibroimpact oscillator and the rest of the chain can occur.

Two Impact Particles

Since the auxiliary system (10.62) is linear, then adding more impulsive terms to its right-hand side will result in a linear combination of solutions similar to (10.65). For instance, if two masses, $n = a$ and $n = b$, are interacting with their amplitude limiters, then solution (10.65) is generalized as

$$x_n = \frac{2}{(N+1)\omega^2} \times \sum_{j=1}^{N} \left(p_a \sin\frac{\pi a j}{N+1} + p_b \sin\frac{\pi b j}{N+1} \right) \sin\frac{\pi n j}{N+1} \frac{\sin[\gamma_j \tau\,(\omega t + \alpha)]}{\gamma_j \cos\gamma_j} \quad (n = 1, \ldots, N) \tag{10.77}$$

Recall that the original system is strongly nonlinear due to its inherent impacts. Therefore any conventional linear modal superposition is impossible. In the present case, it follows from the fact that the parameters of restoring pulses, p_a and p_b, are

not independent but coupled by algebraic system (10.58). This system is fortunately linear and thus admits solution

$$p_a = \frac{\Delta_a k_{bb} - \Delta_b k_{ab}}{k_{aa}k_{bb} - k_{ab}k_{ba}}$$
$$p_b = \frac{\Delta_b k_{aa} - \Delta_a k_{ba}}{k_{aa}k_{bb} - k_{ab}k_{ba}} \tag{10.78}$$

where

$$k_{ab} = \frac{2}{(N+1)\omega^2}\sum_{j=1}^{N} \sin\frac{\pi aj}{N+1}\sin\frac{\pi bj}{N+1}\frac{\tan\gamma_j}{\gamma_j}, \qquad \gamma_j = \Omega_j/\omega \tag{10.79}$$

and $\{\Omega_j\}$ is the (linear) natural spectrum of the chain.

Furthermore, for the impulses to be restoring, both numbers, p_a and p_b, must be positive. This imposes certain conditions on the range of frequencies ω as seen from the illustrating example in Fig. 10.17. For instance, both restoring pulses are positive near frequency Ω_9 which is indicated by the fifth red dot from the left. Then, Fig. 10.18 illustrates the spatial mode shape profile of the corresponding impact vibration given by solution (10.77).

High-Frequency Limits and Impact Localization

Let us show that the impact mode periodic solution (10.65) becomes localized as $\omega \to \infty$ or $\gamma_j \to 0$. First, replacing the trigonometric functions by their asymptotic estimates $\sin(\gamma_j\tau) \sim \gamma_j\tau$, $\cos\gamma_j \sim 1$, and $\tan\gamma_j \sim \gamma_j$ and using the standard trigonometric sums [71] give

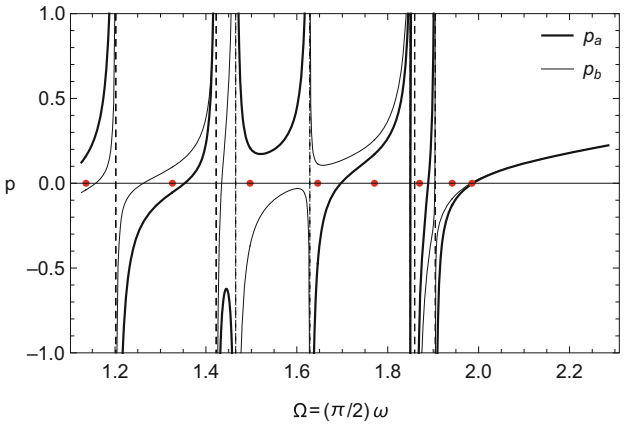

Fig. 10.17 Restoring pulses p_a and p_b versus the fundamental frequency of vibration, Ω, for the case of two vibroimpact particles $a = 5$ and $b = 9$ of the chain of $N = 12$ particles; the dots represent natural frequencies of the linear chain, Ω_i $(i = 5, \ldots, 12)$

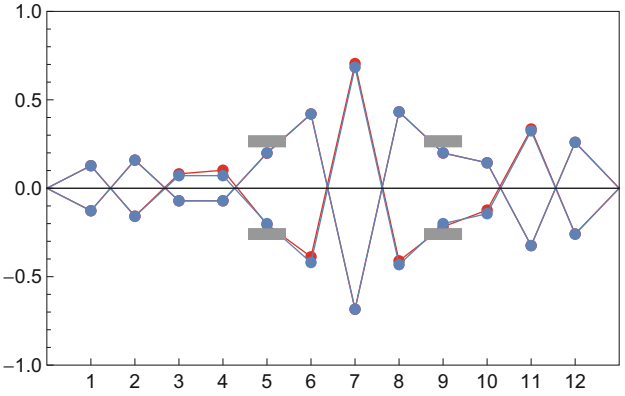

Fig. 10.18 Spatial impact mode shapes for the frequency parameter $\omega = (2/\pi)\Omega_9 + 0.02$ obtained from both analytical (black) and numerical (red) solutions after one cycle of vibration; the numerical integration is using the soften constraints represented by the restoring force $\sim (x_{a,b}/\Delta_{a,b})^{17}$

$$x_n \sim \frac{2p_a}{(N+1)\omega^2} \sum_{j=1}^{N} \sin\frac{\pi nj}{N+1} \sin\frac{\pi aj}{N+1} \tau\,(\omega t + \alpha) \qquad (10.80)$$

$$= \frac{p_a}{\omega^2} \delta_{an} \tau\,(\omega t + \alpha)$$

where δ_{an} is Kronecker's symbol, and

$$p_a \sim \Delta_a \omega^2 \left[\frac{2}{(N+1)} \sum_{j=1}^{N} \sin^2 \frac{\pi aj}{N+1} \right]^{-1} = \Delta_a \omega^2 \qquad (10.81)$$

Substituting then (10.81) in (10.80) gives

$$x_n \sim \Delta_a \delta_{an} \tau\,(\omega t + \alpha) \qquad \text{as} \qquad \omega \to \infty \qquad (10.82)$$

Expression (10.82) shows that the ath particle of the chain vibrates according to the triangle wave temporal mode shape with the infinitely large frequency, whereas all the other particles are at rest. Therefore, the impact mode becomes spatially localized as $\omega \to \infty$.

Let us consider the higher-frequency domain, $(\pi/2)\,\omega >> \Omega_N$, for the above example of mass-spring system with two impact particles, (10.77) through (10.79). In this case, $\tan(\Omega_j/\omega) > 0$ for all $j = 1, \ldots, N$, and therefore, the coefficients k_{ab} (10.79) create the so-called Gram matrix with a non-zero determinant [30], $k_{aa}k_{bb} - k_{ab}k_{ba} \neq 0$. Besides, the asymptotic estimation below confirms this

conclusion. First, the above assumption gives $\gamma_j = \Omega_j/\omega \ll \pi/2$ and the following asymptotic estimate

$$\frac{\sin(\gamma_j \tau)}{\gamma_j \cos\gamma_j} = \tau + \frac{1}{2}\gamma_j^2\left(\tau - \frac{\tau^3}{3}\right) + O\left(\gamma_j^4\right) \tag{10.83}$$

Then substituting (10.83) in (10.77) and using the trigonometric sum [71]

$$\frac{2}{(N+1)}\sum_{j=1}^{N}\sin\frac{\pi n j}{N+1}\sin\frac{\pi a j}{N+1}\gamma_j^2$$

$$= \frac{1}{4}\gamma_{N+1}^2(-\delta_{a,n-1} + 2\delta_{a,n} - \delta_{a,n+1})$$

give

$$x_n = \omega^{-2}\left(p_a\delta_{an} + p_b\delta_{bn}\right)\tau - \frac{1}{8}\omega^{-2}\gamma_{N+1}^2\left(\tau - \frac{\tau^3}{3}\right)\times \tag{10.84}$$

$$\times\left[p_a\left(\delta_{a,n-1} - 2\delta_{an} + \delta_{a,n+1}\right) + p_b\left(\delta_{b,n-1} - 2\delta_{bn} + \delta_{b,n+1}\right)\right] + O\left(\omega^{-6}\right)$$

The parameters of restoring pulses, $\{p_a, p_b\}$, are determined from (10.79), where

$$k_{ab} = \omega^{-2}\delta_{ab} - \frac{1}{12}\omega^{-2}\gamma_{N+1}^2\left(\delta_{a,b-1} - 2\delta_{ab} + \delta_{a,b+1}\right) + O\left(\omega^{-6}\right) \tag{10.85}$$

Since $\omega^{-2}\gamma_{N+1}^2 = O(\omega^{-4})$, we have $k_{ab} = \omega^{-2}\delta_{ab}$ in the leading order approximation. Therefore, $\{p_a, p_b\} = \omega^2\{\Delta_a, \Delta_b\}$as $\omega \to \infty$. In this limit, the vibration energy becomes localized on the two particles vibrating between the barriers with the triangle wave temporal shape

$$x_n \sim \left(\Delta_a\delta_{an} + \Delta_b\delta_{bn}\right)\tau\left(\omega t + \alpha\right) \quad \text{as} \quad \omega \to \infty \tag{10.86}$$

According to (10.86), the particles with numbers $n \neq a$ and $n \neq b$ are at rest. However, they oscillate with amplitudes of different orders of ω^{-2} when the parameter ω takes a large but finite value. Expansion (10.84) also shows that the temporal mode shapes of particles $n = a$ and $n = b$ are nonsmooth and getting closer to the triangle wave as the frequency ω increases. The temporal mode shapes of the nearest particles, $n = a \pm 1$ and $n = b \pm 1$, have amplitudes of order ω^{-2} and appear to be twice continuously differentiable with respect to time, t. In particular, calculating directly first two derivatives and taking into account that $\tau'^2 = 1$ give

$$\frac{d}{dt}\left(\tau-\frac{\tau^3}{3}\right)=\omega\left(1-\tau^2\right)\tau'\in C^1(R)$$

$$\frac{d^2}{dt^2}\left(\tau-\frac{\tau^3}{3}\right)=\omega^2\left[-2\tau\tau'^2+\underline{\left(1-\tau^2\right)\tau''}\right]=-2\omega^2\tau\in C(R)$$

where prime denotes differentiation with respect to the whole argument of the triangle wave, $\tau' \equiv d\tau/d(\omega t+\alpha)$; recall that the underlined terms are zero[3] because $1-\tau^2=0$ on the set of points $\{t:\tau(\omega t+\alpha)=\pm 1\}$, where $\tau''\neq 0$.

The Case of Multiple Impact Particles

A formal extension of relationships (10.56) through (10.59) on the case of multiple vibroimpact particles is quite straightforward. For instance, solution (10.56) is generalized as

$$x_n(t)=\frac{1}{\omega^2}\sum_{j=1}^{N}\sum_{i\in\sigma}p_i(\mathbf{e}_j^T\mathbf{I}_i)(\mathbf{e}_j\mathbf{I}_n)\frac{\sin[\gamma_j\tau(\omega t+\alpha)]}{\gamma_j\cos\gamma_j}=\frac{2}{(N+1)\omega^2}\times$$

$$\times\sum_{j=1}^{N}\sum_{i\in\sigma}p_i\sin\frac{\pi ij}{N+1}\sin\frac{\pi nj}{N+1}\frac{\sin[\gamma_j\tau(\omega t+\alpha)]}{\gamma_j\cos\gamma_j} \qquad (10.87)$$

$$(n=1,\ldots,N)$$

where the inner summation index covers locations of the vibroimpact particles, $\sigma\subset\{1,\ldots,N\}$.

As a result, system (10.58) takes the form

$$\sum_{i\in\sigma}k_{in}p_i=\Delta_n,\qquad n\in\sigma \qquad (10.88)$$

where

$$k_{in}=\frac{1}{\omega^2}\sum_{j=1}^{N}(\mathbf{e}_j^T\mathbf{I}_i)(\mathbf{e}_j^T\mathbf{I}_n)\frac{\tan\gamma_j}{\gamma_j} \qquad (10.89)$$

$$=\frac{2}{(N+1)\omega^2}\sum_{j=1}^{N}\sin\frac{\pi ij}{N+1}\sin\frac{\pi nj}{N+1}\frac{\tan\gamma_j}{\gamma_j}$$

are the elements of $n_\sigma\times n_\sigma$ square matrix, where n_σ is length of the list σ.

[3] It gives a zero contribution into the related integrals of the theory of distributions.

10.8 Modeling the Energy Loss at Perfectly Stiff Barriers

In this section, we follow reference [191], where the methodology of the present chapter was generalized on the case of inelastic interactions with amplitude limiters. The present modeling is based on the assumption that both the moving mass and barriers (walls) are perfectly stiff. An illustrating one degree-of-freedom model is shown in Fig. 10.1. In other words, (elastoplastic) collision deformations are assumed to be negligible as compared to rigid-body displacements, while each collision event happens momentarily. Nevertheless, even under such assumptions, terms *elastic* and *inelastic* (*plastic*) collisions are typically used in the literature in order to characterize reversible and irreversible parts of the kinetic energy, respectively. A one-dimensional collision of a moving mass with stiff obstacles is described in a phenomenological way as a discontinuity of the velocity changing its direction and magnitude as

$$\dot{x}(t_i + 0) = -k\dot{x}(t_i - 0), \qquad 0 \le k \le 1 \tag{10.90}$$

where t_i is the collision time and k is the so-called coefficient of restitution, which is further represented in the form

$$k = 1 - \varepsilon \tag{10.91}$$

According to (10.91), $\varepsilon = 0$ means an elastic collision with no energy loss, whereas $\varepsilon = 1$ is a perfectly plastic limit, when all the kinetic energy momentarily dissipates as the particle strikes an obstacle. In this section, the energy loss due to collisions is assumed to be small so that

$$0 < \varepsilon \ll 1 \tag{10.92}$$

Note that condition (10.90) fixes the time arrow of the dynamics by breaking the time symmetry $t \longrightarrow -t$ similarly to the viscous term $2\zeta\Omega\dot{x}$ of the linear oscillator $\ddot{x} + 2\zeta\Omega\dot{x} + \Omega^2 x = 0$. On first look, such temporal asymmetry creates an obstacle for describing the vibroimpact dynamics in terms of the new time argument τ, which is viewed as an *oscillating time* periodically changing its direction in a reversible way. In other words, when dealing with the time argument τ, it is difficult to specify the *before* and *after* subdomains. Nonetheless, as a first step, let us show that the representation $x = X(\tau) + Y(\tau)e$ with $\tau = \tau(\omega t)$ and $e = e(\omega t)$ can geometrically comply with condition (10.90) assuming that a system, which is described with the coordinate $x(t)$, can maintain its periodicity due to some energy inflows. Using the differentiation rules for a continuous coordinate x gives the velocity $\dot{x} = [Y'(\tau) + X'(\tau)e]\omega$. Let us assume that collisions take place whenever $\tau = \pm 1$, and, for certainty reason, consider a collision time t_i, such that $\tau(\omega t_i) = -1$. When passing through such time point t_i, the function e switches its value from $e = -1$ to $e = +1$ as seen from the diagrams for the basis functions in Fig. 1.8. Therefore, after

cancelling the common factor ω on both sides, condition (10.90) takes the form

$$\tau = -1: \quad Y' + X' = -k\left(Y' - X'\right) \tag{10.93}$$

Now, taking into account that the function e switches its value from $e = +1$ to $e = -1$ when passing through the amplitude points, at which $\tau\ (\omega t_i) = +1$, gives

$$\tau = +1: \quad Y' - X' = -k\left(Y' + X'\right) \tag{10.94}$$

Boundary conditions (10.93) and (10.94) represent an analog of the collision model (10.90) brought by the replacement of temporal argument, $t \longrightarrow \tau$. It is shown in the next section that Eqs. (10.93) and (10.94) adequately describe the vibroimpact dynamics with energy losses caused by collisions with the barriers.

10.8.1 Free Vibrations with Impact Energy Losses

Let us consider the free vibroimpact model as shown in Fig. 10.1a. The differential equation of motion with the constraint condition is represented in the form

$$\ddot{x} + \Omega^2 x = 0, \quad |x| \leq \Delta \tag{10.95}$$

where $\Omega^2 = k/m$, and it is now assumed that the impact energy loss condition (10.90) is taking place whenever $x = \pm\Delta$.

The corresponding effective model (Fig. 10.1b) is described by

$$\ddot{x} + \Omega^2 x = pe'(\varphi) \tag{10.96}$$

In the present case of free vibrations, the frequency $\omega = \dot{\varphi}(t)$ is not fixed by the external load any more. Attributed to the bead's velocity, the quantity ω determines the temporal scale of vibrating process. Generally speaking, in the present relatively simple case, when no external forces are acting, the frequency ω can be assumed to be constant in between any two interactions with the constraints in order to find an exact piecewise solution. This can be done directly with no transition to the oscillating temporal argument τ. However, our goal is to obtain a closed-form solution using the idea of separation of motions. For that reason, the function $\omega(t)$ must be interpreted as a continuously decaying quantity during the entire time range of the process. The decay rate is associated with the energy loss due to collisions with the barriers and assumed to be relatively slow by imposing the condition (10.92). Since the mass velocity is gradually decreasing, the quantity p in Eq. (10.96) characterizing the intensity of interaction with the amplitude limiters, is considered as time dependent too. Based on the above remarks, a frequency modulated solution of Eq. (10.96) can be represented as

$$x = X(\tau) + Y(\tau)e, \tau = \tau(\varphi), e = e(\varphi) \tag{10.97}$$

where $\varphi = \varphi(t)$ is a phase function to be determined.

First time derivative of (10.97) is

$$\dot{x} = [Y'(\tau) + X'(\tau)e + Y(\tau)e'(\varphi)]\omega \tag{10.98}$$

where the notation $\dot{\varphi} = \omega$ is used.

Eliminating the formal singularity of differentiation $e'(\varphi)$ by imposing the boundary condition

$$\tau = \pm 1: \quad Y = 0 \tag{10.99}$$

and then substituting (10.97) and (10.98) in (10.96) gives the relationship

$$(\omega^2 X'' + \Omega^2 X + Y'\dot{\omega}) + (\omega^2 Y'' + \Omega^2 Y + X'\dot{\omega})e + (X'\omega^2 - p)e'(\varphi) = 0$$

leading to the boundary condition

$$\tau = \pm 1: \quad X'\omega^2 = p \tag{10.100}$$

and two equations

$$\begin{aligned} \omega^2 X'' + \Omega^2 X + Y'\dot{\omega} &= 0 \\ \omega^2 Y'' + \Omega^2 Y + X'\dot{\omega} &= 0 \end{aligned} \tag{10.101}$$

Note that the boundary value problem, (10.99), (10.100), and (10.101), for X and Y has two more unknown functions, $\omega(t)$ and $p(t)$. In order to complete the formulation, the energy loss conditions, (10.93) and (10.94), must be added as

$$\tau = \pm 1: \quad Y' \mp X' = -(1-\varepsilon)\left(Y' \pm X'\right), \quad \varepsilon = 1 - k \tag{10.102}$$

The present class of solutions is such that the amplitude limiters are reached when $\tau = \pm 1$; then taking into account (10.99) gives

$$\tau = \pm 1: \quad x = X = \pm\Delta \tag{10.103}$$

Finally, the problem formulation includes two second-order differential equations (10.101) and a set of conditions (10.99), (10.100), (10.102), and (10.103) with no discontinuities. Note that condition (10.100) includes two equations determining just one unknown quantity p. However, it is sufficient to satisfy just one equation in (10.100) and one equation in (10.103) as soon as the X-component of solution is odd with respect to τ.

Further, let us assume that the energy of the oscillator is sufficient for reaching the amplitude limiters during the time interval of interest. The evolution of such a vibrating process is assumed to have the slow temporal scale $\eta = \varepsilon t$. This phase of the process will end up with the so-called grazing state of harmonic oscillations with no energy loss since model (10.95) has no explicit damping terms. During this second phase, the frequency parameter ω becomes constant, whereas the intensity of interactions with the limiters is vanishing, $p = 0$. Since the amplitude remains fixed, let us represent the temporal shape of vibrations in the form of asymptotic expansions without explicitly present slow scale η as

$$\begin{aligned} X(\tau) &= X_0(\tau) + X_1(\tau)\varepsilon + X_2(\tau)\varepsilon^2 + O\left(\varepsilon^3\right) \\ Y(\tau) &= Y_0(\tau) + Y_1(\tau)\varepsilon + Y_2(\tau)\varepsilon^2 + O\left(\varepsilon^3\right) \end{aligned} \tag{10.104}$$

where $\tau = \tau(\varphi)$ and

$$\omega = \dot{\varphi}(t) = \omega_0(\eta) + \omega_1(\eta)\varepsilon + \omega_2(\eta)\varepsilon^2 + O\left(\varepsilon^3\right) \tag{10.105}$$

$$p = p(t) = p_0(\eta) + p_1(\eta)\varepsilon + p_2(\eta)\varepsilon^2 + O\left(\varepsilon^3\right) \tag{10.106}$$

$$\eta = \varepsilon t$$

Expansions (10.104), (10.105), and (10.106) produce the leading order boundary value problem given by equations

$$X_0'' + \lambda^2 X_0 = 0, \quad Y_0'' + \lambda^2 Y_0 = 0 \tag{10.107}$$

under the boundary conditions

$$\tau = \pm 1: \quad X_0 = \pm\Delta, \quad X_0'\omega_0^2 = p_0, \quad Y_0 = 0, \quad Y_0' = 0 \tag{10.108}$$

Solution of this linear boundary value problem can be represented in the form

$$X_0 = \Delta\frac{\sin\lambda\tau}{\sin\lambda}, \quad Y_0 \equiv 0, \quad p_0 = \frac{\Omega^2\Delta}{\lambda\tan\lambda} \tag{10.109}$$

where the time-dependent "frequency ratio" $\lambda = \lambda(\eta)$ is introduced as

$$\lambda = \frac{\Omega}{\omega_0} \tag{10.110}$$

with yet unknown function $\omega_0 = \omega_0(\eta)$.

Recall that the period of triangle wave is normalized to $T = 4$. Therefore, the "real" frequency ratio is $(2/\pi)\lambda$ with the numerical factor $2/\pi$, which is somewhat inconvenient to carry through manipulations. The physical meaning of quantity λ

will be discussed later. Further, once the function $\lambda = \lambda(\eta)$ is determined, the dependence $\omega_0 = \omega_0(\eta)$ becomes known from (10.110). Now taking into account solution (10.109) leads to the differential equations of the first-order approximation in the form

$$X_1'' + \lambda^2 X_1 = 2\omega_1 \lambda^3 \frac{\Delta}{\Omega} \frac{\sin \lambda\tau}{\sin \lambda}$$
$$Y_1'' + \lambda^2 Y_1 = -\lambda \frac{d\lambda}{d\eta} \frac{\Delta}{\Omega} \frac{\cos \lambda\tau}{\sin \lambda} \tag{10.111}$$

under the boundary conditions at $\tau = \pm 1$:

$$Y_1 = 0$$
$$Y_1' = \pm\frac{1}{2} X_0' + \left(\frac{1}{2} - \lambda \frac{\omega_1}{\Omega}\right) Y_0' = \pm\frac{1}{2}\lambda\Delta \cot \lambda \tag{10.112}$$
$$X_1 = 0$$
$$X_1' = \left(\frac{\lambda}{\Omega}\right)^2 - 2\lambda \frac{\omega_1}{\Omega} X_0' = p_1 \left(\frac{\lambda}{\Omega}\right)^2 - 2\omega_1 \lambda^2 \frac{\Delta}{\Omega} \cot \lambda$$

where $\omega_1(\eta)$, $\lambda(\eta)$, and $p_1(\eta)$ are yet unknown functions.

Solution of the boundary value problem (10.111) and (10.112) is

$$X_1 = 0, \quad Y_1 = -\frac{\Delta}{2\Omega} \frac{d\lambda}{d\eta} \left(\frac{\cos \lambda\tau}{\cos \lambda} - \tau \frac{\sin \lambda\tau}{\sin \lambda}\right) \tag{10.113}$$

provided that $\omega_1(\eta) \equiv 0$ and $p_1(\eta) \equiv 0$.

Substituting Y_1 in the second equation of the set (10.112) leads to the following first-order differential equation

$$\frac{d\lambda}{d\eta} = \frac{\Omega}{2}(1 + \cos 2\lambda) \left(1 + \frac{\sin 2\lambda}{2\lambda}\right)^{-1} \tag{10.114}$$

Assuming that $\lambda(\eta)$ is determined from (10.114) and taking into account (10.110) give the fast phase

$$\varphi = \Omega \int_0^t \frac{dt}{\lambda(\varepsilon t)} \tag{10.115}$$

Substituting zero- and first-order solutions, (10.109) and (10.113), in (10.104) and then (10.97) and (10.98) gives solution in the first asymptotic order as

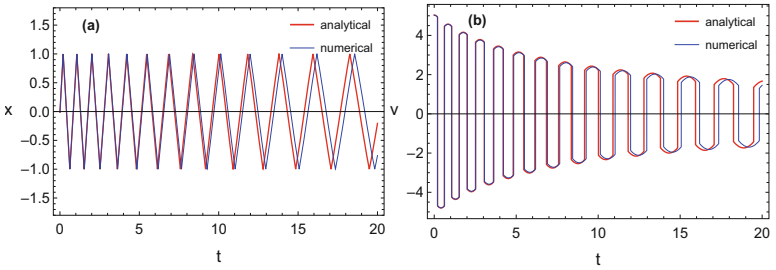

Fig. 10.19 The result of direct numerical integration and analytical approximation in first asymptotic order of ε under parameters: $\Omega = 1.0$, $\Delta = 1.0$, $\varepsilon = 0.05$, and $\omega_0(0) = 5.0$

$$x(t) = \Delta\left[\frac{\sin\lambda\tau}{\sin\lambda} - \frac{\varepsilon}{2\Omega}\frac{d\lambda}{d\eta}\left(\frac{\cos\lambda\tau}{\cos\lambda} - \tau\frac{\sin\lambda\tau}{\sin\lambda}\right)e\right] \tag{10.116}$$

$$v(t) = \Omega\Delta\left\{e\frac{\cos\lambda\tau}{\sin\lambda} + \frac{\varepsilon}{2\Omega}\frac{d\lambda}{d\eta}\left[\tau\frac{\cos\lambda\tau}{\sin\lambda} + \left(\frac{\sin\lambda\tau}{\lambda\sin\lambda} + \frac{\sin\lambda\tau}{\cos\lambda}\right)\right]\right\}$$

where $\tau = \tau(\varphi)$ and $e = e(\varphi)$ are the triangle and square waves, respectively.

Although the differential equation (10.114) is separable, the corresponding quadrature is hardly possible to find within the class of elementary functions. However, it is still well suited for a numerical solution due to the slow temporal scale $\eta = \varepsilon t$.

Solution (10.116) is illustrated in Fig. 10.19 in comparison with the result of direct numerical integration using the *Mathematica*$^{(R)}$ solver:

$$\text{NDSolve}\left[\begin{array}{c}\left\{\begin{array}{l}x''(t) + \Omega^2 x(t) = 0, x(0) = x_0, x'(0) = v_0,\\ \text{WhenEvent}\left[x(t) = \Delta, x'(t) \to -kx'(t)\right],\\ \text{WhenEvent}\left[x(t) = -\Delta, x'(t) \to -kx'(t)\right]\end{array}\right\}, \{x, t\}, \{t, 0, 15\},\\ \text{MaxSteps} \to \infty, \text{PrecisionGoal} \to 20\end{array}\right]$$

The initial conditions were calculated from (10.116) at $t = 0$. The analytical solution appeared to be in sufficient match with the numerical solution. There is some gradually developing phase shift, which is a typical effect of asymptotic approximations of frequencies in nonlinear vibrations. Let us recall that the temporal dependence for phase φ is derived from the boundary conditions, which is an essentially different way as compared to the perturbation methods in nonlinear vibrations of smooth systems [104, 151]. For that reason, note the presence of the so-called secular term with respect to τ in solution (10.116), which is still periodic with respect to the phase φ. As seen in Fig. 10.20, the intensity of strikes against the amplitude limiters, characterized by the quantity p, is diminishing with time, whereas the period of oscillations T_{imp} approaches the natural period of

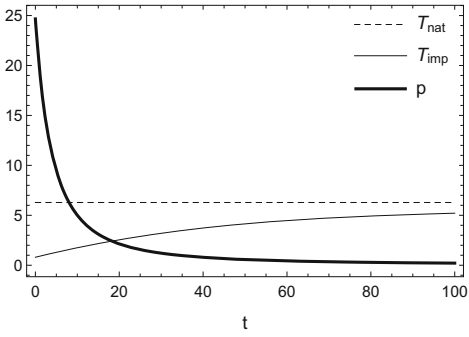

Fig. 10.20 The natural period of oscillator without impacts $T_{nat} = 2\pi/\Omega$, the period of vibroimpact cycle $T_{imp} = 4/\omega$, and the parameter of intensity of strikes against the amplitude limiters, p

unconstrained oscillator, T_{nat}. As already mentioned above, the reason is that no energy loss is assumed in between the limiters, and the system should eventually reach some "grazing" regime with near-zero impact pulses but still the same amplitude [43]. Let us support the above remarks by considering two different asymptotic cases, corresponding to high and low energy limits.

Case 1 Consider the limit $\lambda = \Omega/\omega_0 \to 0$ corresponding to either a very high initial kinetic energy or a very weak spring of the oscillator. In this case, Eq. (10.114) takes the form $d\lambda/d\eta = \Omega/2$ and gives the solution $\lambda = \Omega\eta/2 + \lambda(0)$ leading to

$$\omega_0 = \omega_0(0)\left[1 + \frac{1}{2}\omega_0(0)\eta\right]^{-1}, \quad \eta = \varepsilon t \tag{10.117}$$

and, finally,

$$\varphi = \frac{2}{\varepsilon}\ln\left[1 + \frac{1}{2}\omega_0(0)\varepsilon t\right] \tag{10.118}$$

Then solution (10.116) of the first asymptotic order is reduced to

$$x(t) = \Delta\left[\tau - \frac{1}{4}\varepsilon\left(1 - \tau^2\right)e\right], \quad \tau = \tau(\varphi), \quad e = e(\varphi) \tag{10.119}$$

where the role of "imaginary" term of order ε is to compensate deviations from straight lines between reflections against the barriers. Such deviations are due to the *continuous* representation for the phase $\varphi(t)$.

Solution (10.119) is close to the triangle wave of the gradually increasing period

$$T = \frac{4}{\omega_0(0)}\left[1 + \frac{1}{2}\omega_0(0)\varepsilon t\right] \tag{10.120}$$

Note that, according to relationship (10.117), the frequency should eventually drop to zero. This cannot happen, however, because the frequency has its lower

boundary, which is the natural frequency of harmonic oscillator itself with no interaction with amplitude limiters. For that reason, let us consider the dynamics near its low energy limit.

Case 2 The "grazing" dynamics is reached when the frequency of vibration becomes equal to the natural frequency of the oscillator, $\lambda = \Omega/\omega_0 \to \pi/2$, while the amplitude is still equal to Δ. In this case, solution (10.116) describes the harmonic temporal shape with respect the phase φ:

$$x(t) \to \Delta \sin\left[\frac{\pi}{2}\tau(\varphi)\right] \equiv \Delta \sin\left(\frac{\pi}{2}\varphi\right) \quad \text{as} \quad \lambda \to \pi/2 \tag{10.121}$$

Therefore, in this limit, the term of order ε disappears from solution (10.116) due to Eq. (10.114). Now, introducing the detuning $\rho = \pi/2 - \lambda$ and considering a small neighborhood of $\lambda = \pi/2$ bring Eq. (10.114) to the form

$$\frac{d\rho}{d\eta} = -\Omega\rho^2 + O(\rho^3) \tag{10.122}$$

with general solution $\rho = (\Omega\eta + C)^{-1}$, where C is an arbitrary constant, which is expressed through $\omega_0(0)$ by means of the equation $\lambda = \Omega/\omega_0 = \pi/2 - (\Omega\varepsilon t + C)^{-1}$. Then substituting $\lambda(\varepsilon t)$ in (10.115) and conducting integration give the phase of asymptotic solution (10.121) as

$$\frac{\pi}{2}\varphi = \Omega t + \frac{2}{\varepsilon\pi}\ln\left\{1 + \frac{\pi^2}{4}\varepsilon t\left[\omega_0(0) - \frac{2}{\pi}\Omega\right]\right\} \tag{10.123}$$

Solution (10.123) obviously holds under the condition $\omega_0(0) > (2/\pi)\Omega$, which means that initially the system must be within the impact domain. In this case, the leading term of phase is estimated by $(\pi/2)\varphi \sim \Omega t$ as $t \to \infty$, and therefore $x \sim \Delta \sin \Omega t$.

10.8.2 Bouncing Ball

Let $z = z(t)$ be the vertical upward directed coordinate of a perfectly stiff small bead, which is falling down from its initial position $z(0) = H > 0$ with zero initial velocity (Fig. 10.21). At $z = 0$, the bead reflects against the perfectly stiff floor with the coefficient of restitution $k = 1 - \varepsilon$, where $0 < \varepsilon \ll 1$. Then the bead continues to bounce until all of its energy is lost. The differential equation of motion between reflections and collision conditions is, respectively,

$$\ddot{z} = -g, \quad z \geq 0 \tag{10.124}$$

Fig. 10.21 Bouncing ball

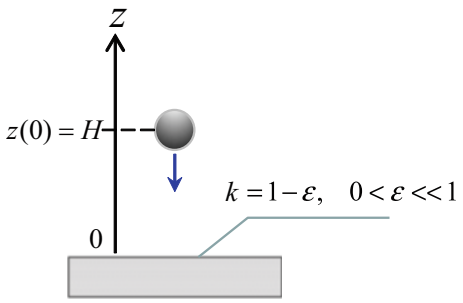

and

$$z = 0: \quad \dot{z}(t_i + 0) = -(1 - \varepsilon)\dot{z}(t_i - 0) \tag{10.125}$$

where g is acceleration due to gravity.

A presence of the linear viscosity in Eq. (10.124) would technically complicate the process of asymptotic integration although with no major effect on the analytical procedure, which is described below.

This problem has an exact piecewise parabolic solution, which is used at the end of this section for comparison reason. We use this exactly solvable problem for illustration of NSTT formalism leading to an asymptotic closed-form solution. Although the present model seems to be easier than (10.95)–(10.90), the asymptotic expansions must be generalized due to both amplitude and frequency modulation effects. The "equivalent" model, in which the reaction of constraint is represented by external pulses, takes the form

$$\ddot{z} = -g - p\,\mathrm{sgn}(\tau)e' \tag{10.126}$$

where $\tau = \tau(\varphi)$, $e' = de(\varphi)/d\varphi$, and the factor $\mathrm{sgn}(\tau)$ is to maintain the upward direction of the impulsive reaction from the stiff ground at $z = 0$.

In order to describe the combined amplitude-frequency modulation, representation (10.97) is generalized by showing the slow temporal scale, $\eta = \varepsilon t$, explicitly as

$$z = X(\tau, \eta) + Y(\tau, \eta)e \tag{10.127}$$

Further manipulations resemble the formalism of two variable expansions with an essential difference though. In particular, the differential equations of evolutionary component emerge from the boundary conditions whose role is in cancellation of δ-functions rather than eliminating resonance terms. Differentiating function (10.127) with respect to time t gives

$$\dot{z} = \frac{\partial Y}{\partial \tau}\omega + \varepsilon\frac{\partial X}{\partial \eta} + \left(\frac{\partial X}{\partial \tau}\omega + \varepsilon\frac{\partial Y}{\partial \eta}\right)e \tag{10.128}$$

$$\tau = \pm 1: \quad Y = 0 \tag{10.129}$$

Now substituting (10.128) in (10.126) and equating separately continuous, stepwise discontinuous, and impulsive groups of terms to zero in a similar to the previous section way give

$$\begin{aligned}
\frac{\partial^2 X}{\partial \tau^2}\omega^2 + \frac{\partial Y}{\partial \tau}\dot{\omega} &= -2\varepsilon\frac{\partial^2 Y}{\partial \tau \partial \eta}\omega - \varepsilon^2\frac{\partial^2 X}{\partial \eta^2} - g \\
\frac{\partial^2 Y}{\partial \tau^2}\omega^2 + \frac{\partial X}{\partial \tau}\dot{\omega} &= -2\varepsilon\frac{\partial^2 X}{\partial \tau \partial \eta}\omega - \varepsilon^2\frac{\partial^2 Y}{\partial \eta^2}
\end{aligned} \tag{10.130}$$

$$\tau = \pm 1: \quad \frac{\partial X}{\partial \tau}\omega^2 = \mp p$$

where $\omega = \dot{\varphi}$, condition (10.129) has been taken into account, and solvability of the third equation for p can be provided by imposing oddness on the derivative $\partial X/\partial \tau$ with respect to the argument τ as

$$\frac{\partial X}{\partial \tau}|_{\tau=1} = -\frac{\partial X}{\partial \tau}|_{\tau=-1} \tag{10.131}$$

It is natural to assume that the ball strikes the ground $z = 0$ whenever $\tau = \pm 1$. Then taking into account condition (10.129) gives

$$\tau = \pm 1: \quad z = X + Ye = X = 0 \tag{10.132}$$

Finally, using velocity (10.128) in (10.125) and following justifications of relationships (10.93) and (10.94) give

$$\begin{aligned}
\tau = \pm 1: \quad & \omega\left(\frac{\partial Y}{\partial \tau} \mp \frac{\partial X}{\partial \tau}\right) + \varepsilon\frac{\partial X}{\partial \eta} \\
&= -(1-\varepsilon)\left[\omega\left(\frac{\partial Y}{\partial \tau} \pm \frac{\partial X}{\partial \tau}\right) + \varepsilon\frac{\partial X}{\partial \eta}\right]
\end{aligned} \tag{10.133}$$

where the term $\partial Y/\partial \eta$ has been excluded due to condition (10.129).

Let us seek solution of the boundary value problem (10.130), (10.129), (10.133), and (10.132) in the form of asymptotic series

$$\begin{aligned}
X(\tau, \eta) &= X_0(\tau, \eta) + X_1(\tau, \eta)\varepsilon + X_2(\tau, \eta)\varepsilon^2 + O\left(\varepsilon^3\right) \\
Y(\tau, \eta) &= Y_0(\tau, \eta) + Y_1(\tau, \eta)\varepsilon + Y_2(\tau, \eta)\varepsilon^2 + O\left(\varepsilon^3\right) \\
\omega &= \dot{\varphi}(t) = \omega_0(\eta) + \omega_1(\eta)\varepsilon + \omega_2(\eta)\varepsilon^2 + O\left(\varepsilon^3\right)
\end{aligned} \tag{10.134}$$

In the leading order approximation, the boundary value problem

$$\frac{\partial^2 X_0}{\partial \tau^2} = -\frac{g}{\omega_0^2}, \quad \frac{\partial^2 Y_0}{\partial \tau^2} = 0 \tag{10.135}$$

$$\tau = \pm 1: \quad X_0 = 0, \quad Y_0 = 0, \quad \frac{\partial Y_0}{\partial \tau} = 0 \tag{10.136}$$

has solution

$$X_0 = \frac{g(1-\tau^2)}{2\omega_0^2}, \quad Y_0 = 0 \tag{10.137}$$

where condition (10.131) was taken into account.

Note that, in zero-order approximation, $\varepsilon = 0$, the physical assumption on energy loss, which is described by the boundary conditions (10.133), produced the equality $\partial Y_0/\partial \tau = 0$ at $\tau = \pm 1$in (10.136), which is satisfied automatically by the trivial solution for Y_0. Since the parameter ε itself characterizes the velocity drop at impact times, then the zero-order approximation $\varepsilon = 0$ cannot depict the effect of energy decay. This is why the dependence $\omega_0(\eta)$ still remains unknown and will be determined at the next step of asymptotic procedure.

Now taking into account (10.137) leads to the first-order boundary value problem

$$\begin{aligned}
\frac{\partial^2 X_1}{\partial \tau^2} &= -\frac{1}{\omega_0^2}\left(\frac{d\omega_0}{d\eta}\frac{\partial Y_0}{\partial \tau} + 2\omega_0 \frac{\partial^2 Y_0}{\partial \tau \partial \eta} + 2\omega_0\omega_1 \frac{\partial^2 X_0}{\partial \tau^2}\right) \\
&\equiv \frac{2g\omega_1}{\omega_0^3} \\
\frac{\partial^2 Y_1}{\partial \tau^2} &= -\frac{1}{\omega_0^2}\left(\frac{d\omega_0}{d\eta}\frac{\partial X_0}{\partial \tau} + 2\omega_0 \frac{\partial^2 X_0}{\partial \tau \partial \eta} + 2\omega_0\omega_1 \frac{\partial^2 Y_0}{\partial \tau^2}\right) \\
&\equiv -\frac{3g\tau}{\omega_0^4}\frac{d\omega_0}{d\eta}
\end{aligned} \tag{10.138}$$

$$\tau = \pm 1: \quad X_1 = 0, \quad Y_1 = 0 \tag{10.139}$$

whose solution is obtained by the direct integration as

$$X_1 = \frac{g\omega_1}{\omega_0^3}(\tau^2 - 1), \quad Y_1 = \frac{g}{2\omega_0^4}\frac{d\omega_0}{d\eta}(\tau - \tau^3) \tag{10.140}$$

Conditions of the velocity drop (10.133) combine now both zero- and first-order terms as

$$\tau = +1: \quad \omega_0 \left(\frac{\partial X_0}{\partial \tau} + \frac{\partial Y_0}{\partial \tau} - 2\frac{\partial Y_1}{\partial \tau} \right) - 2 \left(\frac{\partial X_0}{\partial \eta} + \omega_1 \frac{\partial Y_0}{\partial \tau} \right)$$

$$\equiv -\frac{g}{\omega_0^3} \left(\omega_0^2 - 2\frac{d\omega_0}{d\eta} \right) = 0 \tag{10.141}$$

$$\tau = -1: \quad \omega_0 \left(\frac{\partial X_0}{\partial \tau} - \frac{\partial Y_0}{\partial \tau} + 2\frac{\partial Y_1}{\partial \tau} \right) + 2 \left(\frac{\partial X_0}{\partial \eta} + \omega_1 \frac{\partial Y_0}{\partial \tau} \right)$$

$$\equiv \frac{g}{\omega_0^3} \left(\omega_0^2 - 2\frac{d\omega_0}{d\eta} \right) = 0 \tag{10.142}$$

It is seen that the quantity $\omega_1(\eta)$ disappears from these conditions, and both equalities are satisfied by just one separable differential equation

$$\frac{d\omega_0}{d\eta} = \frac{1}{2}\omega_0^2 \tag{10.143}$$

This gives zero-order approximation for the frequency function as

$$\omega_0 = \omega_0(0) \left[1 - \frac{1}{2}\omega_0(0)\eta \right]^{-1}, \quad \eta = \varepsilon t \tag{10.144}$$

Recall that the first-order term $\omega_1(\eta)$ has disappeared from the condition of velocity drop (10.141)–(10.142) and still remains arbitrary. As follows from (10.140), the term $\omega_1(\eta)$ determines the amplitude of approximation X_1. However, the parabolic shape described by the function $X_1(\tau)$ is already captured by zero-order approximation $X_0(\tau)$. Let us therefore take $X_1 \equiv 0$ by setting $\omega_1(\eta) \equiv 0$ as soon as no more steps of the asymptotic procedure will be conducted in present illustrating example. Note the discrete energy loss is described by function (10.144) in a continuous way by "corrupting" the temporal mode shape of the process $z(t)$ in between impact times. As a result, the Y-component of solution comes into play in order to correct such a side effect. This is clearly seen from solution (10.140) for Y_1, which would be zero if the quantity $\omega_0(\eta)$ was constant.

Now substituting both zero- and first-order approximations in (10.134) gives

$$z = \frac{g}{2\omega_0^2}(1 - \tau^2) \left(1 + \frac{1}{2}\varepsilon\tau e \right); \quad \tau = \tau(\varphi), \quad e = e(\varphi) \tag{10.145}$$

where $\omega_0 = \omega_0(\varepsilon t)$ is given by (10.144) and phase φ is determined by integration from the differential equation $\dot{\varphi}(t) = \omega_0(\varepsilon t)$.

Solution (10.145) links the initial height H to yet arbitrary $\omega_0(0)$ as

$$z(0) = \frac{g}{2[\omega_0(0)]^2} = H \quad \text{or} \quad \omega_0(0) = \sqrt{\frac{g}{2H}} \tag{10.146}$$

Finally, substituting ω_0 from (10.144) in solution (10.145) and taking into account (10.146) give

$$z(t) = H\left(1 - \frac{1}{2}\sqrt{\frac{g}{2H}}\varepsilon t\right)^2 \left(1 - \tau^2\right)\left(1 + \frac{1}{2}\varepsilon\tau e\right) \tag{10.147}$$

where $\tau = \tau(\varphi)$ and $e = e(\varphi)$ and the phase $\varphi = \varphi(t)$ is obtained from (10.144) by integration under the initial condition $\varphi(0) = 0$ in the form

$$\varphi = -\frac{2}{\varepsilon}\ln\left(1 - \frac{1}{2}\sqrt{\frac{g}{2H}}\varepsilon t\right) \tag{10.148}$$

As follows from solution (10.147) and (10.148), the bouncing process ends at

$$t_{\max} = \sqrt{\frac{2H}{g}}\frac{2}{\varepsilon} \tag{10.149}$$

Note that same result (10.149) was obtained in the reference [256] however, by using a different analytical tool based on the space unfolding coordinate transformation with averaging with respect the fast phase. Considering exact piecewise parabolic solution gives the duration of the bouncing process [73], which is in match with (10.149) when $0 < \varepsilon << 1$:

$$t_{\max} = \sqrt{\frac{2H}{g}}\frac{1+k}{1-k} = \sqrt{\frac{2H}{g}}\frac{2+\varepsilon}{\varepsilon} \sim \sqrt{\frac{2H}{g}}\frac{2}{\varepsilon}$$

However, temporal shapes of the above three solutions are somewhat different as it is seen from Fig. 10.22.

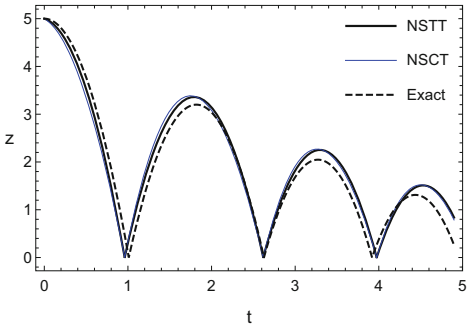

Fig. 10.22 Bouncing ball vertical coordinate versus time obtained by three different methods: nonsmooth temporal transformations (NSTT), nonsmooth coordinate transformation (NSCT), and exact solution

Chapter 11
Singular Trajectories of Forced Vibrations

As shown earlier by Zhuravlev [255], harmonically loaded linear conservative systems possess an alternative physically reasonable basis, which is generally different from that associated with the conventional concept of principal coordinates. Briefly, such a basis determines directions of harmonic loads along which the system response is equivalent to a single oscillator. The corresponding definition (singular directions of forced vibrations) is losing sense in nonlinear case, when the linear tool of eigenvectors becomes inapplicable. However, it will be shown in this chapter that nonlinear formulation is still possible in terms of eigenvector-functions of time given by NSTT boundary value problems. Physical meaning of the corresponding nonlinear definitions for both discrete and continual models is discussed.

11.1 Introductory Remarks

The theory of linear normal modes defines a natural basis in the configuration space of linear conservative systems. The corresponding directions are associated with a set of independent harmonic oscillators. The number of such oscillators is infinite, if the original system is continuous. In the latter case, the modal analysis provides reduction of a continuous system to the related discrete set of harmonic oscillators. As it is known, the normal modes are defined for a class of unforced systems; therefore only initial conditions select those oscillators that will be excited during the dynamical process. Practically, a normal mode regime must be supported by some external loading due to inevitable energy dissipation. However, the theory does not identify directly such external forces. Let $\psi_j(y)$ be, for instance, the jth mode shape of a beam. Generally speaking, the external loading of the same profile, $\psi_j(y)$, will excite not only the jth mode but also some others, unless the mass per unit length of the beam is constant. From the mathematical viewpoint, this is due to

V. N. Pilipchuk, *Oscillators and Oscillatory Signals from Smooth to Discontinuous*,
https://doi.org/10.1007/978-3-031-37788-4_11

the mass density, say $\rho(y)$, participating as a weighting factor in the orthogonality condition

$$\langle \psi_i(y)\rho(y)\psi_j(y)\rangle = 0, \qquad i \neq j \tag{11.1}$$

The question therefore is what kind of external force must be applied to a mechanical system in order to generate a normal mode type of motion when all the system particles coherently vibrate with the same frequency? Following reference [255], let us consider first the linear case assuming that the linear n-degrees-of-freedom forced system oscillates as a single harmonic oscillator in such a manner that the coordinates vector $\mathbf{x}(t)$ and the force vector $\mathbf{p}(t)$ are collinear to the same constant vector $\mathbf{q}$ with a constant length ratio μ as follows

$$\mathbf{x} = \mathbf{q}\sin\Omega t, \quad \mathbf{p} = \mu\mathbf{q}\sin\Omega t \tag{11.2}$$

In the case of forced vibration, the frequency Ω is rather predetermined by the external loading and therefore should not play the role of eigenvalue. It was shown in [255] that the coefficient of proportionality μ can play such a role instead. In a regular case, the coefficient μ has exactly n eigenvalues, whereas the vector $\mathbf{q}$ determines the corresponding "principal directions" according to the definition of reference [255]. Note that the principal directions are always orthogonal regardless the mass matrix of the system. Such an approach therefore determines a new natural basis for external forces from the standpoint of system considered. This, of course, should not be viewed as a substitute for the theory of normal modes; however, some non-autonomous problems can be naturally solved by making use of the above complementary basis. In nonlinear cases, definition (11.2) is inapplicable, and the above notion of principal directions loses its sense. However, it was shown in [175] that the basic idea still can be generalized by considering *trajectories* instead of *directions*. Also a mixed spatiotemporal consideration must be applied since spatial and temporal coordinates are not separable in nonlinear cases and the related vibration and forcing are generally neither harmonic in time nor similar in space. There are some practically important formulations of the problem for the case of nonlinear forced vibration, which could be qualified as inverse or semi-inverse approaches. The related methods select practically reasonable external forces that generate simple enough dynamics. For example, Harvey [77] considered "natural forcing functions" proportional to the nonlinear restoring force of the forced Duffing oscillator. The notion of "exact steady state" was defined by Rosenberg [210] for a strongly nonlinear single degree of freedom system as a vibration with the cosine-wave temporal shape of the period of external force. The corresponding forcing function is determined under some initial conditions. Kinney and Rosenberg [105] considered systems with many degrees of freedom.

11.2 Principal Directions of Linear Forced Systems

Let us illustrate first the basic idea of reference [255] by considering the linear n-degrees-of-freedom forced system

$$M\ddot{\mathbf{x}} + K\mathbf{x} = \mathbf{p}(\Omega t), \quad \mathbf{x}(t) \in R^n \tag{11.3}$$

where M and K are constant mass and stiffness $n \times n$ matrixes, respectively, $\mathbf{p}(\Omega t)$ is a periodic vector force of the period $T = 2\pi$ with respect to Ωt, and the upper dot means differentiation with respect to time, t.

Substituting (11.2) in (11.3) gives the eigenvalue problem with respect to the parameter μ and vector $\mathbf{q}$ in the form

$$-\Omega^2 M\mathbf{q} + K\mathbf{q} = \mu\mathbf{q} \tag{11.4}$$

Let $\mathbf{q} = \mathbf{v}_s$ and $\mu = \mu_s$ be the sth eigenvector and eigenvalue, respectively, $s = 1, \ldots, n$. The eigenvectors $\mathbf{v}_s$ are orthogonal and can be normalized by condition

$$\mathbf{v}_i^T \mathbf{v}_j = \delta_{ij} \tag{11.5}$$

where δ_{ij} is the Kronecker symbol.

Therefore, the set of vectors $\mathbf{v}_s$ determine a natural basis for the case of forced vibrations. Let, for instance, the external force be $\mathbf{p} = \mathbf{Q}\sin\Omega t$, where $\mathbf{Q} \in R^n$ is an arbitrary constant vector. In this case, the corresponding steady-state (particular) solution is written as

$$\mathbf{x} = \sum_s \frac{(\mathbf{v}_s^T \mathbf{Q})}{\mu_s}\mathbf{v}_s \sin\Omega t \tag{11.6}$$

Now, let $\mathbf{e}_s$ and Ω_s be conventional linear normal modes and natural frequencies of the system. (The related eigenvalue problem is obtained from (11.4) by setting $\mu = 0$.) As follows from the linear theory, the normal mode vectors are orthogonal with respect to the mass matrix M so that the normalization condition can be represented in the form

$$\mathbf{e}_i^T M\mathbf{e}_j = \delta_{ij} \tag{11.7}$$

Using the normal mode basis for the above steady state gives

$$\mathbf{x} = \sum_s \frac{(\mathbf{e}_s^T \mathbf{Q})}{\Omega_s^2 - \Omega^2}\mathbf{e}_s \sin\Omega t \tag{11.8}$$

Since the uniqueness theorem holds, expansions (11.6) and (11.8) must represent the same solution, and therefore,

$$\sum_s \frac{\left(\mathbf{v}_s^T \mathbf{Q}\right)}{\mu_s} \mathbf{v}_s = \sum_s \frac{\left(\mathbf{e}_s^T \mathbf{Q}\right)}{\Omega_s^2 - \Omega^2} \mathbf{e}_s \tag{11.9}$$

Let the external force amplitude vector $\mathbf{Q}$ be directed along one of the *principal directions*. Then, expansion (11.6) will include only one term, whereas expansion (11.8) still includes all n terms.

Now, let us consider the case, when the mass matrix is equal to the identity matrix, $M = E$. In this particular case, expression (11.4) takes the standard form of the eigenvalue problem for normal modes with respect to the eigenvalue parameter $\Omega^2 + \mu$

$$-\left(\Omega^2 + \mu\right) E\mathbf{q} + K\mathbf{q} = \mathbf{0} \tag{11.10}$$

As follows from (11.10), the eigenvalues of free and forced vibration are coupled by expression

$$\Omega^2 + \mu_s = \Omega_s^2, \quad s = 1, \ldots, n \tag{11.11}$$

It is seen that each eigenvalue of forced vibration, $\mu_s = \Omega_s^2 - \Omega^2$, is a monotonically decreasing function of the external frequency Ω with only one zero at $\Omega = \Omega_s$.

11.3 Definition for Singular Trajectories of Nonlinear Discrete Systems

Let us consider the nonlinear case

$$M\ddot{\mathbf{x}} + K\mathbf{x} + \varepsilon \mathbf{f}(\mathbf{x}) = \mathbf{p}(\Omega t), \qquad \mathbf{x}(t) \in R^n \tag{11.12}$$

where $\mathbf{f}(\mathbf{x})$ is an analytic nonlinear vector-function such that $\mathbf{f}(-\mathbf{x}) = -\mathbf{f}(\mathbf{x})$, ε is a small positive parameter, and the forcing function and matrixes are defined in Eq. (11.3).

If $\varepsilon \neq 0$, then the concept of *singular directions* of forced vibrations is not applicable anymore; however it is still possible to consider *principal trajectories* instead based on the following:

Definition 11.3.1 Trajectories of periodic motions of the period $T = 2\pi/\Omega$ on which mechanical system (11.12) behaves as a Newtonian particle in R^n, namely, the external force and acceleration vectors are coupled by the Newton second law,

$$m\ddot{\mathbf{x}}(t) = \mathbf{p}(\Omega t) \tag{11.13}$$

will be called *singular trajectories* of forced vibrations.

In Eq. (11.13), m is a priori unknown effective mass parameter. The effective mass m and the force $\mathbf{p}(\Omega t)$ must be chosen in order to make Eqs. (11.12) and (11.13) compatible.

Note that, in the linear case, the above definition still gives principal *directions* of forced vibrations (11.2) after representing the mass parameter as follows

$$m = -\frac{\mu}{\Omega^2} \tag{11.14}$$

Indeed, substituting expression $\mathbf{x}(t) = \mathbf{q} \sin \Omega t$ in Eq. (11.13) and taking into account expression (11.14) give definition (11.2) in the form $\mathbf{p} = \mu \mathbf{x}$. In contrast to linear case (11.2), definition (11.13) admits non-harmonic temporal shapes.

The current definition itself does not imply that the system is weakly nonlinear. However, if the parameter ε is small, then explicit solutions can be obtained in terms of conventional asymptotic expansions as described in the next section.

As mentioned, the concept of principal trajectories seems to relate to the idea of "natural forcing functions" introduced in [77] for the Duffing oscillator. Let us consider now a multidimensional case from that point of view.

Applying definition (11.13) to the general nonlinear system

$$M\ddot{\mathbf{x}} + \mathbf{F}(\mathbf{x}) = \mathbf{p}(\Omega t) \tag{11.15}$$

and eliminating the acceleration give the external forcing vector-function as a linear transformation of the restoring force in the form

$$\mathbf{p}(\Omega t) = \left(E - \frac{1}{m} M\right)^{-1} \mathbf{F}(\mathbf{x}) \tag{11.16}$$

where the matrix of the transformation includes the identity matrix E and the effective mass parameter m.

Relationship (11.16) can be viewed as a vector version of the concept of natural forcing functions.

On the other hand, using the definition for principal trajectories and excluding the external forcing vector $\mathbf{p}(\Omega t)$ from the equation of motion give an auxiliary free system described by the differential equation of motion

$$(M - mE)\ddot{\mathbf{x}} + \mathbf{F}(\mathbf{x}) = \mathbf{0}$$

The idea of transforming the forced problem to a free vibration problem by imposing the form of excitation was used also in [40] with illustrations on two-degree-of-freedom systems based on an essentially different methodology though.

11.4 Asymptotic Expansions for Principal Trajectories

In order to make Eqs. (11.12) and (11.13) compatible, let us eliminate the forcing vector-function $\mathbf{p}(\Omega t)$ and thus consider equation

$$M\ddot{\mathbf{x}} + K\mathbf{x} + \varepsilon \mathbf{f}(\mathbf{x}) = m\ddot{\mathbf{x}}(t) \tag{11.17}$$

A family of periodic solutions that give principal directions of linearized system as $\varepsilon \to 0$ will be considered. Let us represent such solutions (principal trajectories) in the following parametric form

$$\mathbf{x} = \mathbf{X}(\tau) \tag{11.18}$$

where $\tau = \tau(\omega t)$ is the triangular sine wave of the period of external loading, $T = 2\pi/\Omega = 4/\omega$.

Substituting (11.18) into (11.17) gives

$$L\mathbf{X} + \varepsilon f(\mathbf{X}) = \omega^2 m\mathbf{X}'' \tag{11.19}$$

$$L \equiv \omega^2 M \frac{d^2}{d\tau^2} + K$$

under the boundary condition

$$\mathbf{X}'(\tau)\,|_{\tau=\pm 1} = 0 \tag{11.20}$$

As mentioned above, the temporal and spatial variables generally are not separable any more in nonlinear cases; therefore it is impossible to obtain an exact nonlinear version of the eigenvector problem (11.4). As a result, both temporal and spatial mode shapes must be corrected on each step of the related asymptotic process as described below.

Remind that the differential operator L in Eq. (11.19) includes the frequency parameter Ω fixed, whereas the mass m is an eigenvalue to be determined.

Let m_a and $\mathbf{e}_a(\tau)$ be the eigenvalue and eigenvector of the linearized problem, $\varepsilon = 0$, respectively,

$$\begin{aligned} L\mathbf{e}_a &= m_a^2 \omega^2 \mathbf{e}_a'' \\ \mathbf{e}_a' \;|\; _{\tau=\pm 1} &= 0 \end{aligned} \tag{11.21}$$

where the index $a = \{s, j\}$ consists of spatial and temporal mode shape numbers, $s = 1, \ldots, n$ and $j = 1, \ldots$, respectively.

The scalar product of any two vector-functions $\mathbf{x} = \mathbf{x}(\tau)$ and $\mathbf{y} = \mathbf{y}(\tau)$ will be defined as follows

$$\langle \mathbf{x}, \mathbf{y} \rangle = \frac{1}{2} \int_{-1}^{1} \mathbf{x}^T \mathbf{y} d\tau$$

Let us represent solution of the weakly nonlinear eigenvalue problem (11.19) and (11.20) in the following form of asymptotic expansions

$$\mathbf{X}(\tau) = A\mathbf{e}_a(\tau) + \varepsilon \mathbf{X}^{(1)}(\tau) + O\left(\varepsilon^2\right) \tag{11.22}$$

$$m = m_a + \varepsilon \eta_1 + O\left(\varepsilon^2\right)$$

Then substituting (11.22) in (11.19) and (11.20), and matching the coefficients of the first order of ε, gives equation

$$L\mathbf{X}^{(1)} - \omega^2 m_a \mathbf{X}^{(1)\prime\prime} = -f\left(A\mathbf{e}_a\right) + \omega^2 \eta_1 A\mathbf{e}_a'' \tag{11.23}$$

and boundary condition

$$\mathbf{X}^{(1)\prime}\,|_{\tau=\pm 1} = 0 \tag{11.24}$$

Following the idea of perturbations for eigenvalue problems [44], let us represent solution of Eq. (11.23)

$$\mathbf{X}^{(1)} = \sum_{b \neq a} a_b^{(1)} \mathbf{e}_b(\tau) \tag{11.25}$$

where $b = \{r, i\}$ is a double index, $a_b^{(1)}$ is yet unknown constant coefficient, and boundary condition (11.24) is automatically satisfied.

Let us assume the following normalization condition for the eigenvector-functions

$$\left\langle \mathbf{e}_a'(\tau), \mathbf{e}_b'(\tau) \right\rangle = \begin{cases} 0, & b \neq a \\ 1, & b = a \end{cases} \tag{11.26}$$

Substituting (11.25) in (11.23) and taking into account (11.26) determine the coefficients $a_b^{(1)}$ and η_1. As a result, expansions (11.22) give first-order asymptotic solution

$$\mathbf{X} = A\mathbf{e}_a + \frac{\varepsilon}{\omega^2} \sum_{b \neq a} \frac{\langle \mathbf{e}_b, f\left(A\mathbf{e}_a\right) \rangle \mathbf{e}_b}{m_b - m_a} + O\left(\varepsilon^2\right) \tag{11.27}$$

$$m = m_a - \frac{\varepsilon}{\omega^2} \frac{\langle \mathbf{e}_a, f\left(A\mathbf{e}_a\right) \rangle}{A} + O\left(\varepsilon^2\right)$$

As follows from the form of solution (11.27), all the coefficients are uniquely determined under the condition that $m_a \neq m_b$ for $a \neq b$. The possibility of degeneration, namely, $m_a = m_b$ for $a \neq b$, depends on the inner properties of the system and the frequency parameter ω. The related examples were considered earlier [175, 181].

11.5 Extension on Continuous Systems

Let us consider a one-dimensional elastic system whose vibration is described by some function $u = u(t, y)$. For certainty reason, let us consider a nonlinear string of the length l under external distributed loading described by the partial differential equation and boundary conditions

$$Lu+\varepsilon f[u] = p(\Omega t, y), \qquad 0 < y < l \tag{11.28}$$

$$u(t, 0) = u(t, l) = 0 \tag{11.29}$$

$$L \equiv \rho(y)\frac{\partial^2}{\partial t^2} - T\frac{\partial^2}{\partial y^2} \tag{11.30}$$

where L is the differential self-adjoint operator of linear string, $\rho(y)$ is a mass per unit length parameter, T is a constant tensile force, $f[u]$ is a nonlinear operator acting in the corresponding function space of configurations, ε is a small parameter, and $p(\Omega t, y)$ is the external forcing function, which is assumed to be 2π-periodic with respect to Ωt.

Now keeping in mind expressions (11.28) through (11.30), let us introduce

Definition 11.5.1 Periodic forced vibrations of a continuous system, in which the system motion is equivalent to a particle in the function space of configurations described by the second Newton law,

$$\sigma\frac{\partial^2 u(t, y)}{\partial t^2} = p(\Omega t, y) \tag{11.31}$$

will be called a *principal mode of forced vibration.*

In one-dimensional cases, σ is a priori unknown effective mass per unit length. Substituting (11.31) in (11.28) gives the following partial differential equation for principal modes of forced vibrations

$$Lu+\varepsilon f[u] = \sigma\frac{\partial^2 u}{\partial t^2} \tag{11.32}$$

Introducing the triangular wave time substitution as $\tau = \tau(\omega t)$ and $u(t, y) = U(\tau, y)$ gives

$$LU + \varepsilon f(U) = \omega^2 \sigma \frac{\partial^2 U}{\partial \tau^2} \tag{11.33}$$

$$L \equiv \omega^2 \rho(y) \frac{\partial^2}{\partial \tau^2} - T \frac{\partial^2}{\partial y^2}$$

The boundary conditions are formulated for both temporal and spatial variables as

$$U(\tau, 0) = U(\tau, l) = 0 \tag{11.34}$$

and

$$\frac{\partial U(\tau, l)}{\partial \tau} \mid_{\tau=\pm 1} = 0 \tag{11.35}$$

respectively.

In this case, the scalar product of two functions $U = U(\tau, y)$ and $V = V(\tau, y)$ from the configuration space can be defined as

$$\langle U, V \rangle = \frac{1}{2l} \int_{-1}^{1} \int_{0}^{l} UV d\tau dy \tag{11.36}$$

Further, a weakly nonlinear asymptotic procedure can be developed analogously to the above discrete case.

Chapter 12
NSTT and Shooting Method for Periodic Motions

In this chapter, two-dimensional shooting diagrams are introduced for visualization of manifolds of periodic solutions and their bifurcations. A general class of nonlinear oscillators under smooth, nonsmooth, and impulsive loadings is considered. The corresponding boundary value problems are formulated by introducing the triangular wave temporal argument. Duffing oscillator with no linear stiffness (Ueda circuit) is considered for illustration. It is shown that the temporal mode shape of the loading is responsible for qualitative features of the dynamics, such as transitions from regular and random motions. The important role of unstable periodic orbits is discussed.

12.1 Introductory Remarks

Periodic solutions and their bifurcation diagrams often reveal important qualitative features of the dynamics even though the system motion is not expected to be periodic. In particular, the number of periodic orbits and their distribution and properties reveal the structure of chaotic orbits; see, for instance, works [19, 72, 160] and references therein. Direct numerical tools for detection and construction of periodic orbits based on the mapping approach can be found in the book [162] and paper [74]. Different formulations in terms of boundary value problems for ordinary differential equations are described in [17]. Theoretical and applied results regarding periodic motions, bifurcations, and chaos are reported in [21] and [247].

In this chapter, a special two-dimensional visualization of the shooting method is introduced in order to incorporate the general two-component NSTT as a preliminary analytical stage [185]. Note that the same approach using the one-component NSTT was suggested earlier in [201] and implemented in *Mathematica*® interface [25]. In particular, subharmonic orbits of the forced pendulum and bifurcation diagrams were obtained by examining the shooting curves and their

V. N. Pilipchuk, *Oscillators and Oscillatory Signals from Smooth to Discontinuous*,
https://doi.org/10.1007/978-3-031-37788-4_12

zeros. Subharmonic orbits of a strongly nonlinear oscillator forced by closely spaced harmonics were investigated in [217]. The NSTT followed by shooting method was applied to study the resonance capture dynamics.

Let us consider a multi-dimensional oscillator described be the differential equation

$$F(\ddot{x}, \dot{x}, x, t) = 0 \tag{12.1}$$

where $x\,(t) \in R^n$ and the vector-function $F \in R^n$ is periodic with respect to time t with the period $T = 4a$.

In this work, different kinds of temporal discontinuity in the differential equations of motion will be considered. In order to satisfy the related mathematical requirements, the left-hand side of Eq. (12.1) must be interpreted in term distributions [225]

$$\int_{-\infty}^{\infty} F(\ddot{x}, \dot{x}, x, t)\varphi\,(t)\,dt = 0 \tag{12.2}$$

where $\varphi\,(t)$ is any sufficiently smooth testing function.

However, at this point, let us assume that the function $F(\ddot{x}, \dot{x}, x, t)$ is regular with no singular terms involved.

Let us consider periodic solutions of the period T by means of the coordinate complexification (NSTT)

$$x \to \{X, Y\}: \qquad x = X\,(\tau) + Y\,(\tau)\,\tau' \tag{12.3}$$

where $\tau = \tau\,(t/a)$ the triangular sine wave of the period $T = 4a$ and $\tau' = d\tau\,(t/a)\,/d\,(t/a)$ is its first generalized derivative, which is a stepwise discontinuous function at the time instances

$$\Lambda = \{t : \tau\,(t/a) = \pm 1\} \tag{12.4}$$

As discussed in this book, the above discontinuities can be suppressed by the condition $Y\,(\pm 1) = 0$, which is the necessary condition of continuity of the original coordinates $x(t)$. Then, assuming for a while no infinite discontinuities in F, substituting (12.3) in (12.1), using the algebraic properties of representation (12.3) as well as other NSTT rules, gives the boundary value problem

$$F\left(\frac{X'' + Y''}{a^2}, \frac{X' + Y'}{a}, \frac{X + Y}{a}, a\tau\right) = 0 \tag{12.5}$$

$$F\left(\frac{X'' - Y''}{a^2}, -\frac{X' - Y'}{a}, \frac{X - Y}{a}, 2a - a\tau\right) = 0 \tag{12.6}$$

$$Y|_{\tau=\pm1} = 0, \qquad X'|_{\tau=\pm1} = 0 \tag{12.7}$$

where the prime used with X and Y means differentiation with respect to τ.

Both Eqs. (12.5) and (12.6) are easily derived by the corresponding algebraic manipulations, whereas boundary conditions (12.7) represent the result of elimination of the singular term $\tau''(t/a)$ when substituting (12.3) in (12.1). In some cases, such a singular term can be employed though in order to eliminate singularities from original equations; see below.

Despite of a relatively complicated form of Eqs. (12.5) and (12.6), the new formulation brings some advantages due to the fact that the new temporal variable τ is bounded and automatically accounts for periodicity of solutions regardless their temporal shapes. This property appears to be important in those cases when the solutions do not represent a final stage of investigation but must be used for further analyses. The dimension increase is often compensated by an effective decrease of the temporal interval of the problem, since the range $-1 \leqslant \tau \leqslant 1$ is covered by the original time domain $-a \leqslant t \leqslant a$, which is twice shorter than the whole period $T = 4a$. Moreover, there are many cases when the number of equations can be reduced to that of the original system due to the symmetry of equations. If, for instance, the vector-function $F(\ddot{x}, \dot{x}, x, t)$ is even with respect to the velocity $\dot{x}$ or includes no velocity at all, and the explicit dependence on time t produces zero "imaginary component," then boundary value problem (12.5) through (12.7) admits a family of solutions on which

$$Y \equiv 0, \qquad F\left(\frac{X''}{a^2}, \frac{X'}{a}, \frac{X}{a}, a\tau\right) = 0 \tag{12.8}$$

$$X'|_{\tau=\pm1} = 0 \tag{12.9}$$

The particular case (12.8) and (12.9) was investigated numerically by the shooting method in [201] and [224] based on a single- and multiple-degrees-of freedom systems, respectively. It should be noted that no special requirements are imposed on numerical methods or packages for solving the above boundary-value problems. However, the shooting algorithm in the *Mathematica*® interface provides a physically meaningful way of visualization of periodic solutions due to the specific combination analytical and numerical commands.

12.2 Problem Formulation

Let assume now that the system loading may include a periodic series of Dirac δ-functions acting at times Λ(12.4). As is known [63], Dirac δ-functions can participate in nonlinear differential equations only as summands because nonlinear manipulations with δ-functions are physically meaningless, except special concepts

[138]. Therefore, the original equation (12.1) must be concretized as

$$\ddot{x} + f(x, \dot{x}, t) = q(t) \tag{12.10}$$

where

$$q(t) = Q(\tau(t/a)) + P(\tau(t/a))\,\tau'(t/a) + p(\tau(t/a))\,\tau''(t/a) \tag{12.11}$$

and

$$\begin{aligned} \tau''(t/a) &= d^2\tau(t/a)/d(t/a)^2 \\ &= 2\sum_{k=-\infty}^{\infty}\left[\delta\left(\frac{t}{a}+1-4k\right) - \delta\left(\frac{t}{a}-1-4k\right)\right] \end{aligned} \tag{12.12}$$

In Eq. (12.10), the function $f(x, \dot{x}, t)$ may still include parametric terms of the period $T = 4a$ with possible stepwise discontinuities on Λ. The acceleration $\ddot{x}$ also participates as a summand, since it must have the same kind of singularities as the external forcing function, $q(t)$. According to the distribution theory [208], $p(\tau(t/a))$ must be at least continuous on Λ; otherwise the "product" $p(\tau)\,\tau''$ cannot be treated as a distribution. Note that behavior of the function $p(\tau(t/a))$ between the times Λ is arbitrary, since only values $p(-1)$ and $p(1)$ contribute into the expression

$$\begin{aligned} &p(\tau(t/a))\,\tau''(t/a) \\ &= 2\sum_{k=-\infty}^{\infty}\left[p(-1)\,\delta\left(\frac{t}{a}+1-4k\right) - p(1)\,\delta\left(\frac{t}{a}-1-4k\right)\right] \end{aligned} \tag{12.13}$$

The numbers $p(-1)$ and $p(1)$ control the "amplitudes" and directions of the δ-functions. For example, all the pulses can be positively co-directed by setting $p(\tau) = -\operatorname{sign}\tau$.

Remark 12.2.1 Expressions (12.3) and (12.11) represent particular cases of the truncated series

$$q(t) = \sum_{k=0}^{N} P_k(\tau(t/a))\,d^k\tau(t/a)/d(t/a)^k \tag{12.14}$$

where $P_k(\tau(t/a))$ must be at least $k-2$ times continuously differentiable in the neighborhood of points $t = \pm a$. Although physical interpretation of the higher-order terms in (12.14) is not straightforward, such terms still can occur after reducing the number of equations from the entire system. In cases (12.10) and (12.11), one has $N = 2$, and therefore the velocity vector $\dot{x}$ must be stepwise discontinuous. Further, if $N = 3$, then the velocity $\dot{x}$ includes singular terms, and the

function $f(x, \dot{x}, t)$ in Eq. (12.10) must be linear with respect to $\dot{x}$. If $N = 4$, then the function $f(x, \dot{x}, t)$ must be linear also with respect to the position vector x provided that any parametric terms are sufficiently smooth functions of time. Therefore, only linear systems can be considered if $N \geq 4$.

Since the basis elements $\{1, \tau', \tau''\}$ represent functions of different classes of smoothness, then substituting (12.3) and (12.11) in (12.10) gives separately

$$a^{-2}X'' + R_f\left(X, Y, X', Y', \tau\right) = Q(\tau) \tag{12.15}$$

$$a^{-2}Y'' + I_f\left(X, Y, X', Y', \tau\right) = P(\tau) \tag{12.16}$$

and

$$a^{-2}X' \,|_{\tau=\pm 1} = p(\pm 1) \tag{12.17}$$

where

$$\left\{\begin{matrix} R_f \\ I_f \end{matrix}\right\} = \frac{1}{2}\left[f\left(X + Y, \ \frac{X' + Y'}{a}, a\tau\right) \pm f\left(X - Y, \ -\frac{X' - Y'}{a}, 2a - a\tau\right)\right] \tag{12.18}$$

Note that the singular term $a^{-1}Y\tau''$ is eliminated from the velocity vector $\dot{x}(t)$ by imposing another boundary condition

$$Y \,|_{\tau=\pm 1} = 0 \tag{12.19}$$

The boundary value problem (12.15) through (12.19) includes no singular or discontinuous functions; therefore standard numerical codes and packages can be applied with no specific constraints on their choice.

In general, Eqs. (12.15) and (12.16) are coupled. Although the equations can be decoupled by introducing the new unknown functions, $X(\tau) + Y(\tau)$ and $X(\tau) - Y(\tau)$, the boundary conditions will become coupled. There are two special cases, however, when the entire problem can be reduced. If, for instance, $f(x, \dot{x}, t) = f(x, -\dot{x}, 2a - t)$ and $P(\tau) \equiv 0$, then the problem admits a family of solutions such that

$$Y \equiv 0, \quad a^{-2}X'' + f\left(X, \ X'/a, a\tau\right) = Q(\tau) \tag{12.20}$$

under the boundary condition (12.17).

In case $f(x, \dot{x}, t) = -f(-x, \dot{x}, 2a - t)$, $Q(\tau) \equiv 0$ and $p(\tau) \equiv 0$, then one can consider another family of solutions on which

$$X \equiv 0, \quad a^{-2}Y'' + f\left(Y, \ Y'/a, a\tau\right) = P(\tau) \tag{12.21}$$

under the boundary condition (12.19).

This chapter nevertheless focuses on the general two-component problem (12.15) through (12.19).

12.3 Sample Problems and Discussion

12.3.1 Smooth Loading

The Duffing-Ueda oscillator [236] under the periodic loading of different temporal shapes will be considered below.

Let us start with the standard case of sine wave voltage

$$\ddot{x} + \zeta \dot{x} + x^3 = B \sin \Omega t \tag{12.22}$$

where ζ, B, and Ω are constant parameters.

In this case, the differential equations (12.15) and (12.16) take the form

$$a^{-2} X'' + \zeta a^{-1} Y' + X^3 + 3XY^2 = B \sin \frac{\pi \tau}{2} \tag{12.23}$$

$$a^{-2} Y'' + \zeta a^{-1} X' + Y^3 + 3X^2 Y = 0 \tag{12.24}$$

where $a = \pi/(2\Omega)$ is a quarter of the loading period, and the boundary conditions are

$$Y\,|_{\tau=\pm 1} = 0, \quad X'\,|_{\tau=\pm 1} = 0 \tag{12.25}$$

The shooting method can be applied now as follows. First, the differential equations (12.23) and (12.24) are solved under the *initial conditions*

$$X(-1) = g, \quad X'(-1) = 0 \tag{12.26}$$

$$Y(-1) = 0, \quad Y'(-1) = h \tag{12.27}$$

where g and h are numbers to be determined in order to satisfy boundary conditions (12.25).

Let us represent solution of the initial value problem (12.23), (12.24), (12.26), and (12.27) in the following general form

$$X = X(\tau; g, h), \quad Y = Y(\tau; g, h) \tag{12.28}$$

By the idea of shooting method, the initial value problem (12.23), (12.24), (12.26), and (12.27) must be iteratively solved multiple times at different g and h until sufficient precision has been reached for boundary conditions (12.25) at right end $\tau = 1$,

$$\frac{\partial X(\tau; g, h)}{\partial \tau}|_{\tau=1} \equiv G(g, h) = 0 \qquad (12.29)$$
$$Y(\tau; g, h)|_{\tau=1} \equiv H(g, h) = 0$$

When dealing with the particular cases (12.20) or (12.21), such a procedure is not difficult since one has only one equation with a single unknown, $G(g) = 0$ or $H(h) = 0$. Multidimensional cases, such as (12.29), appear to be more difficult and time-consuming. From this point of view, the important feature of *Mathematica* is that it is possible to program the functions $G(g, h)$ and $H(g, h)$ explicitly in such a way that the arguments g and h are included into the numerical solver of differential equations. This can be done as follows.[1] First, the numerical solution is defined as a function of the arguments g and h according to the command

sol[g_, h_]:=NDSolve[{eqX, eqY,

X[-1]==g, X′[-1] == 0, Y[-1] == 0, Y′[-1] == h}, {X,Y}, {τ,-1,1}];

where eqX and eqY are Eqs. (12.23) and (12.24), respectively.

Then, the functions $G(g, h)$ and $H(g, h)$ are defined as follows

G[g_, h_]:=X′[1]/.sol[g, h][[1]];

H[g_, h_]:=Y[1]/.sol[g, h][[1]];

As a result, the functions $G(g, h)$ and $H(g, h)$ can be considered as usual functions of two arguments. In particular, intersections of two manifolds (12.29) can be located and determined by using the commands *ContourPlot* and *FindRoot,* respectively. Each of the determined roots of Eq. (12.29) represents a periodic solution of the original equation. If the loading amplitude B is a control parameter, then the evolution of diagrams $G(g, h; B) = 0$ and $H(g, h; B) = 0$ represents the corresponding structural changes in the set of periodic solutions.

Figure 12.1 gives an example of such a diagram. The parameters were chosen in order to provide conditions for the "randomly transitional" process in terms of work [236]. The diagram clearly shows five intersections between the two different families of curves. The corresponding solutions of the input period $T = 4a = 2\pi$ are shown in Figs. 12.2 and 12.3.

Direct numerical solutions of the corresponding estimates for Floquet multipliers show that first four periodic solutions, (a) through (d), are unstable and only one solution (e) is stable. Solution (e) was detected by direct analog and digital computer simulations reported in [236], whereas solutions (a) through (d) were unlisted. Instead, a "non-reproducible trajectory" as a realization of the "randomly transitional" process was represented in the xv-plane. Such a trajectory can be

[1] See Appendix 4 for the related algorithms.

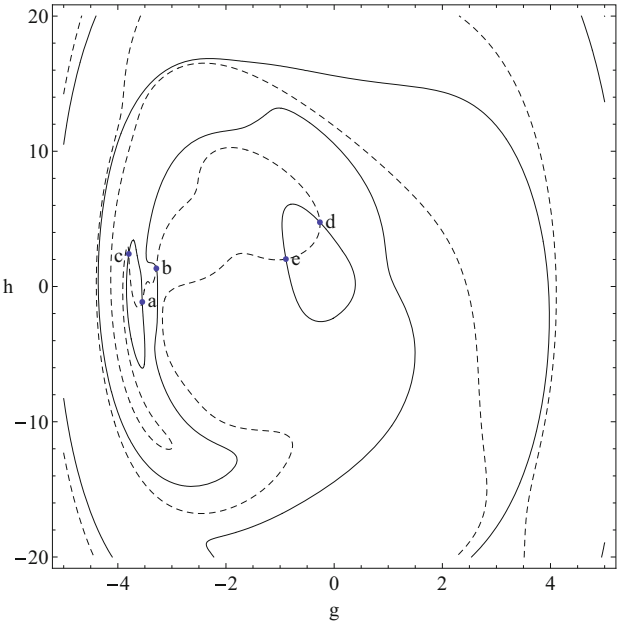

Fig. 12.1 The curves $G(g, h) = 0$ (continuous) and $H(g, h) = 0$ (dashed) and their intersections for the Ueda oscillator under the sine wave input and the following parameters: $\zeta = 0.1$, $B = 12$, and $\omega = 1$ (0.1592 Hz)

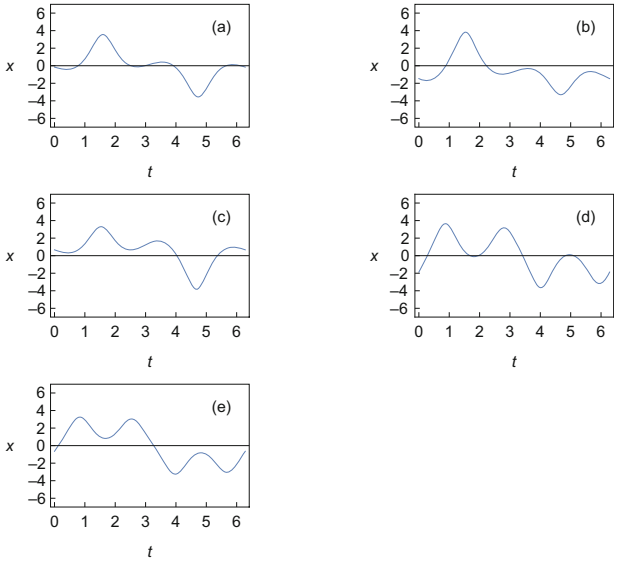

Fig. 12.2 The temporal mode shapes of periodic solutions

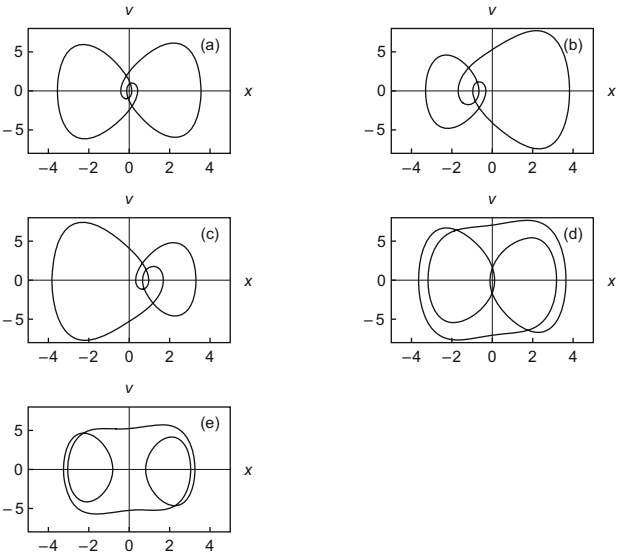

Fig. 12.3 The projections of periodic trajectories on xv-planes

treated as a chaotic drift around the first three unstable motions (a), (b), and (c). However, high-order periodic solutions may also affect the dynamics of chaotic drift [19].

Figure 12.3 shows what actually happens when trying to numerically reproduce an unstable periodic orbit, say (a). Neither the shooting algorithm nor computer codes allow to perfectly introduce the initial conditions; therefore it is unlikely that the oscillator will remain on the unstable orbit. After few cycles, the system leaves the orbit (a) for the "randomly transitional" drift around the all three unstable orbits (a), (b), and (c) with "no certain choice" between them. The long-term time history and the corresponding spectrogram of this motion, represented in Fig. 12.4, confirm its random character during quite a long period of time.

Although preliminary qualitative information about stability or instability of periodic solutions can be obtained by direct numerical tests, one can quantify stability properties based on the well-known Floquet theory in terms of the characteristic multipliers [76, 145]. In order to remind the principals, let us consider periodic solution $x(t)$ of the Eq. (12.10),where $f(x, \dot{x}, t) = f(x, \dot{x}, t + T)$, $q(t) = q(t + T)$, and the period is $T = 4a$.

A variation of the solution $x(t)$, say $u(t)$, is described by the linear differential equation with periodic coefficients

$$\ddot{u} + q_1(t)\dot{u} + q_2(t)u = 0$$

where $q_1(t) = \partial f(x, \dot{x}, t)/\partial \dot{x}$ is assumed to be independent on $\dot{x}$ and $q_2(t) = \partial f(x, \dot{x}, t)/\partial x$.

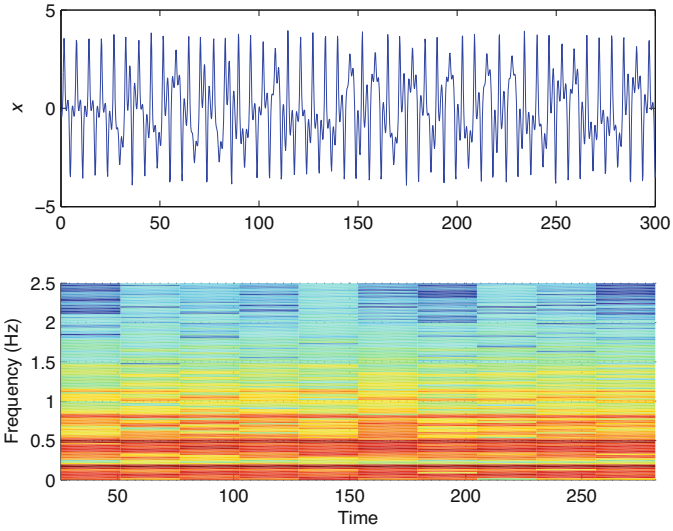

Fig. 12.4 The time history record and its spectrogram (in Hz) for Ueda oscillator after the direct numerical integration. The parameters are $\zeta = 0.1$, $\omega = 1.0$, and $B = 12.0$

Then substitution

$$u = y(t) \exp\left(-\frac{1}{2}\int_0^t q_1(z)dz\right)$$

gives

$$\ddot{y} + p(t)y = 0 \tag{12.30}$$

where

$$p(t) = q_2(t) - \frac{1}{4}[q_1(t)]^2 - \frac{1}{2}\dot{q}_1(t)$$

As known from the Floquet theory, stability of solution is determined by the Floquet multipliers

$$\mu_{1,2} = A \pm \sqrt{A^2 - 1} \tag{12.31}$$

where $A = [y_1(T) + \dot{y}_2(T)]/2$ and $y_1(t)$ and $y_2(t)$ are two fundamental solutions of Eq. (12.30) given by the initial conditions

$$y_1(0) = 1, \quad \dot{y}_1(0) = 0$$

$$y_2(0) = 0, \quad \dot{y}_2(0) = 1$$

Based on the number A, the solution $x(t)$ is unstable if $A^2 > 1$, and it is stable if $A^2 < 1$. In case $A^2 = 1$, there exists a periodic solution of Eq. (12.30).

Now, let $x(t)$ be a periodic solution of Eq. (12.22). The corresponding variational equation is

$$\ddot{u} + \zeta \dot{u} + 3x^2 u = 0 \tag{12.32}$$

where $u = u(t)$ is a small variation of the solution $x = x(t)$.

After the standard substitution $u(t) = y(t)\exp(-\zeta t/2)$ Eq. (12.32) takes the form

$$\ddot{y} + \left(3x^2 - \frac{\zeta^2}{4}\right) y = 0$$

Taking into account the form of solution (12.3) gives the variational equation with periodic coefficient

$$\ddot{y} + [U(\tau(t/a)) + V(\tau(t/a))\tau'(t/a)]y = 0 \tag{12.33}$$

where $U(\tau) = 3X^2(\tau) + 3Y^2(\tau) - \zeta^2/4$ and $V(\tau) = 6X(\tau)Y(\tau)$.

Note that the periodic coefficient in Eq. (12.33) is continuous with respect to time t since $V(\pm 1) = 0$ due to the boundary conditions (12.25). By using the numerical solutions of Eq. (12.33), one obtains the number A for every solution

$$A_a = 10.5155,\ A_b = -2.63747,\ A_c = -2.63749$$

$$A_d = 1.70201, \text{ and } A_e = 0.143507 \tag{12.34}$$

where the index corresponds to the type of periodic solution of the original equation; see Figs. 12.1, 12.2, and 12.3. These numbers confirm that only solution (e) is stable.

12.3.2 Stepwise Discontinuous Input

Let us consider now the case of discontinuous periodic input of the square wave temporal shape

$$\ddot{x} + \zeta \dot{x} + x^3 = B\frac{d\tau\,(t/a)}{d\,(t/a)} \tag{12.35}$$

where a is a quarter of the input period.

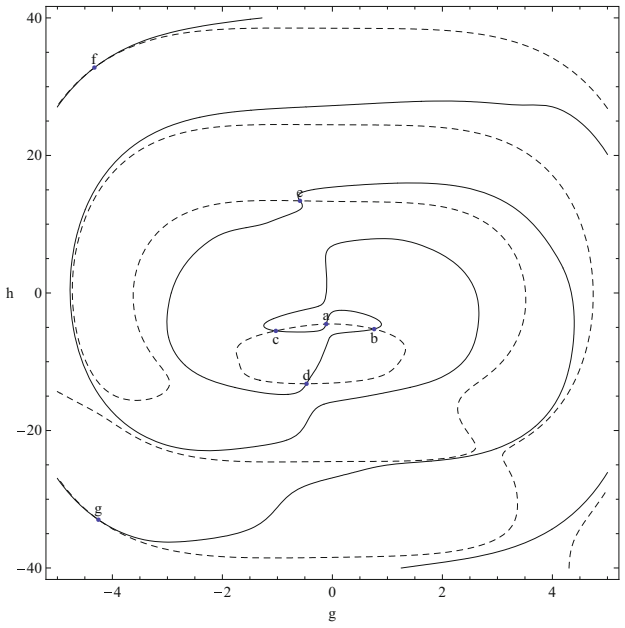

Fig. 12.5 The curves $G(g, h) = 0$ (continuous) and $H(g, h) = 0$ (dashed) for the Ueda oscillator under the stepwise input and the following parameters: $\zeta = 0.05$, $B = 7.4$, and $\omega = 1$

In this case, the right-hand side of Eqs. (12.23) and (12.24) are modified so that the equations take the form

$$a^{-2}X'' + \zeta a^{-1}Y' + X^3 + 3XY^2 = 0 \tag{12.36}$$

$$a^{-2}Y'' + \zeta a^{-1}X' + Y^3 + 3X^2Y = B \tag{12.37}$$

under the homogeneous boundary conditions (12.25).

Figure 12.5 shows the shooting diagram under the fixed parameters $\Omega = \pi/(2a) = 1$ (0.1592 Hz), $B = 7.4$, and $\zeta = 0.05$. In this case, there are seven intersections between the two families of curves and therefore seven periodic solutions of the period $T = 4a$ as shown in Figs. 12.6 and 12.7.

Note that, under the same parameters, the system response on the square wave input shows new features compared to those under the sine wave input [185]. For example, after few cycles along the orbit (a), the system starts its drift around the first three solutions, (a), (b), and (c). At this stage, the dynamics resembles that under the sine wave input. Further, however, after several random "jumps" between the orbits (a), (b), and (c), the system becomes eventually attracted by the stable orbit (e). The direct numerical solution, represented in Fig. 12.8, clearly shows all three stages of the time and spectral histories of the dynamics.

To clarify stability properties, Floquet theory can be applied analogously to the case of the sine wave input.

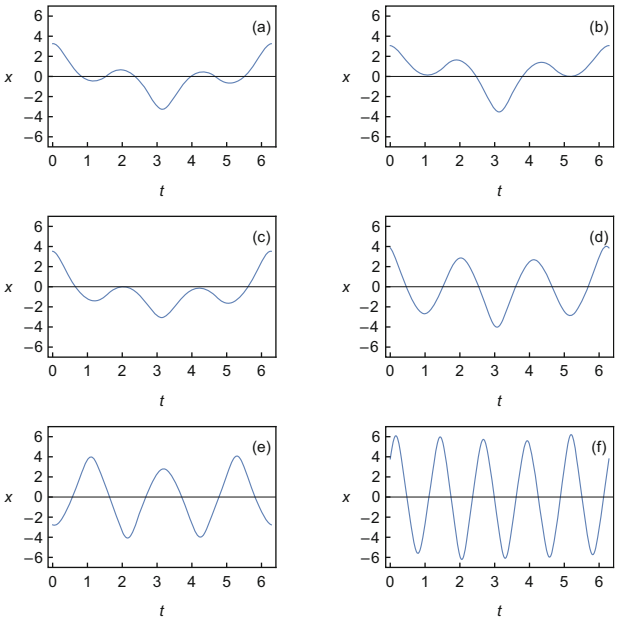

Fig. 12.6 The temporal mode shapes of periodic solutions of Ueda circuit under the stepwise input

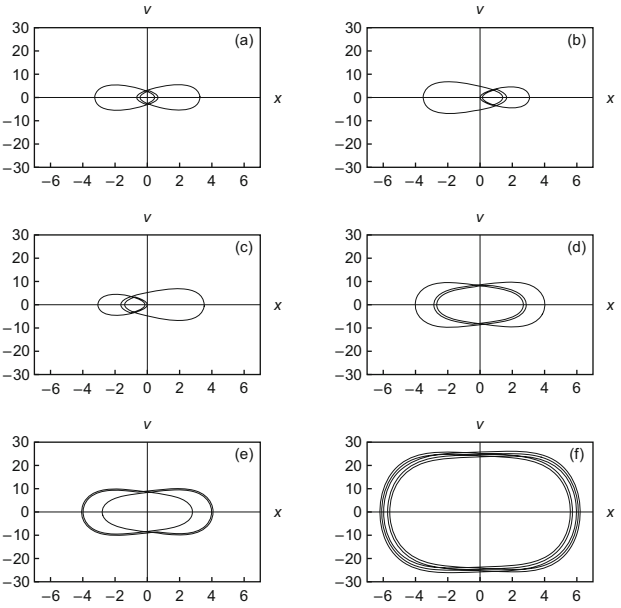

Fig. 12.7 The projections of periodic trajectories on $x\,v$-planes

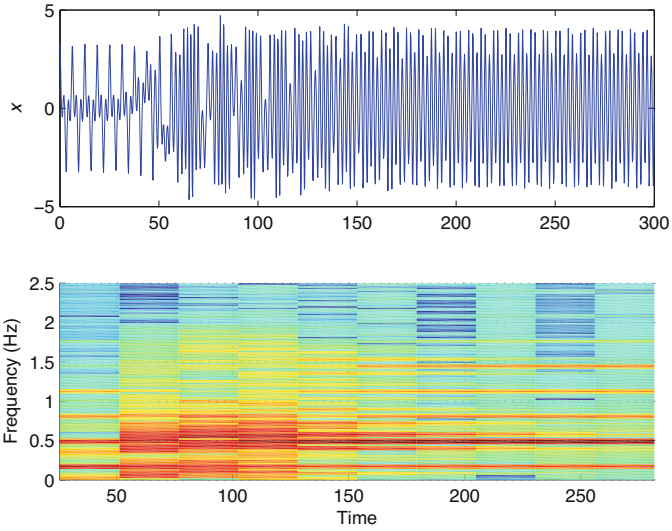

Fig. 12.8 The time history record and its spectrogram (in Hz) for evolution of the solution (a) under the stepwise voltage of the amplitude $B = 7.4$

12.3.3 Impulsive Loading

Let us consider the same oscillator loaded by the periodic series of pulses

$$\ddot{x} + \zeta\dot{x} + x^3 = p\tau'' \qquad (12.38)$$
$$= 2p\sum_{k=-\infty}^{\infty}\left[\delta\left(\frac{t}{a} + 1 - 4k\right) - \delta\left(\frac{t}{a} - 1 - 4k\right)\right]$$

where $p = p(\pm 1) = B = const.$

In this case, both Eqs. (12.36) and (12.37) should have zero right-hand side; however, the non-homogeneous version of the boundary condition (12.17) must be imposed in order to eliminate the pulses. The second expression in (12.26) and the first one in (12.29) must be modified as $X'(-1) = a^2 B = [\pi/(2\Omega)]^2 B$ and $G(g,h) = a^2 B = [\pi/(2\Omega)]^2 B$, respectively. Therefore, the singular terms are eliminated from the system due to the triangle wave time, and the shooting procedure can be applied in the same fashion as that under the smooth input. The shooting diagram and the corresponding periodic solutions are shown in Figs. 12.9, 12.10, and 12.11, respectively.

The projections of the phase trajectories show discontinuities of the velocity on the xv-plane caused by the external pulses. The last four projections, (h) through (k), can be qualified as "quasi free" vibrations sustained by the pulses. In the shooting

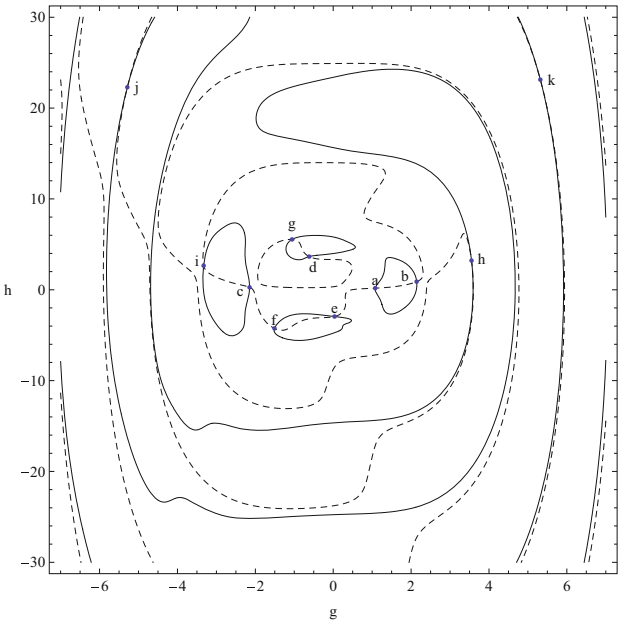

Fig. 12.9 The curves $G(g, h) = 0$ (continuous) and $H(g, h) = 0$ (dashed) for Ueda circuit under the impulsive input and parameters: $\zeta = 0.05$, $B = 1.4$, and $\Omega = 1$

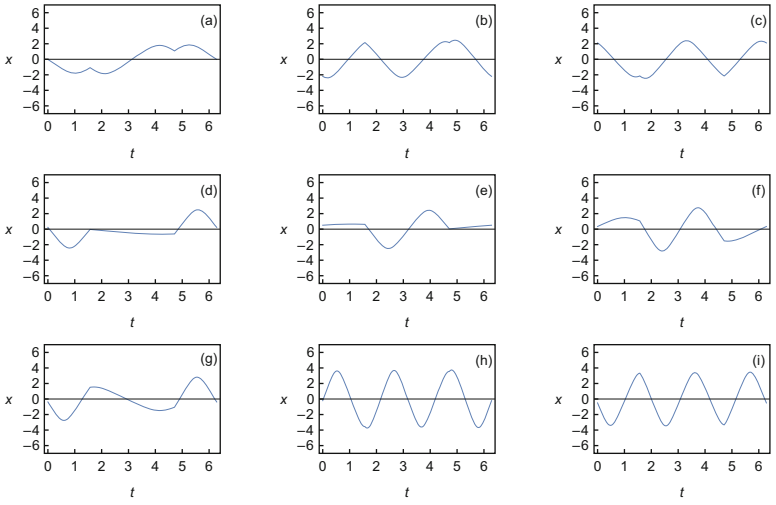

Fig. 12.10 The temporal mode shapes of periodic solutions of Ueda circuit under the impulsive input

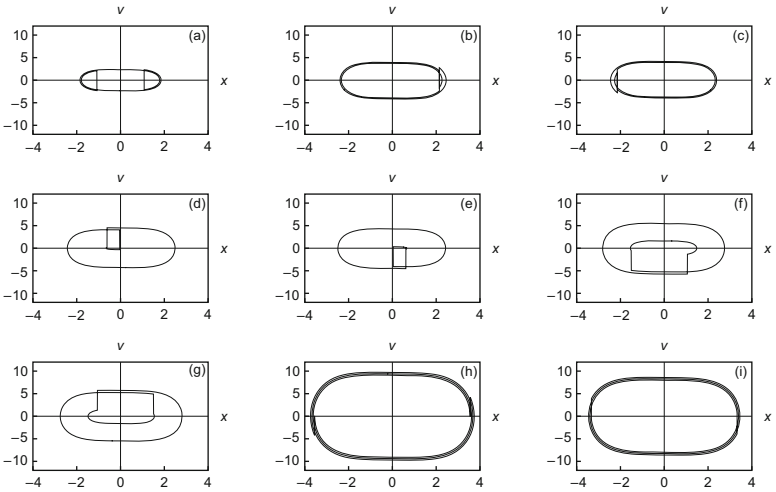

Fig. 12.11 The projections of periodic trajectories on xv-planes

diagram represented in Fig. 12.9, the related intersections are difficult to determine due to a very small angle between the intersecting curves.

12.4 Other Applications

12.4.1 Periodic Solutions of the Period—n

The above sections deal with periodic solutions with the input period $T = 4a$. In order to capture "subharmonic" solutions of the period nT, the components of representation (12.3) must be taken in the form

$$\begin{aligned} X(\tau) &= \frac{1}{2}\left[x(na\tau) + x(2na - na\tau)\right] \\ Y(\tau) &= \frac{1}{2}\left[x(na\tau) - x(2na - na\tau)\right] \end{aligned} \tag{12.39}$$

where $\tau = \tau(t/(na))$.

For instance, applying (12.39) to the sine wave $\sin \Omega t$ gives

$$\begin{aligned} \sin \Omega t = &\frac{1}{2}\left[\sin\frac{n\pi\tau}{2} + \sin\left(n\pi - \frac{n\pi\tau}{2}\right)\right] \\ &+\frac{1}{2}\left[\sin\frac{n\pi\tau}{2} - \sin\left(n\pi - \frac{n\pi\tau}{2}\right)\right]\tau' \end{aligned} \tag{12.40}$$

$$= \frac{1}{2}\sin\frac{n\pi\tau}{2}\left\{\left[1+(-1)^{n+1}\right]+\left[1-(-1)^{n+1}\right]\tau'\right\}$$

where $\tau' = d\tau(t/(na))/d(t/(na))$ and $a = \pi/(2\Omega)$.

According to representation (12.40), Eqs. (12.23) and (12.24) must be modified as follows

$$\begin{aligned}
&(na)^{-2}X'' + \zeta(na)^{-1}Y' + X^3 + 3XY^2 \\
&= \frac{B}{2}\left[1+(-1)^{n+1}\right]\sin\frac{n\pi\tau}{2} \\
&(na)^{-2}Y'' + \zeta(na)^{-1}X' + Y^3 + 3X^2Y \\
&= \frac{B}{2}\left[1-(-1)^{n+1}\right]\sin\frac{n\pi\tau}{2}
\end{aligned} \tag{12.41}$$

The right-hand side of these equations shows that direct replacement $a \to na$ in (12.23) and (12.24) would not work.

If $n = 1$, then Eqs. (12.41) takes the form (12.23) and (12.24), but if $n > 1$, Eqs. (12.41) can give new solutions in addition to those described by Eqs. (12.23) and (12.24). The corresponding calculations however become time-consuming and give complicated diagrams as the number n increases.

12.4.2 Two-Degrees-of-Freedom Systems

Using the above two-dimensional geometrization of shooting diagrams enables one of considering special cases of two-degrees-of-freedom systems based on Eqs. (12.20) or (12.21). For example, Eq. (12.20) can be treated as an equation with respect to the two-component vector-function $X = \{X_1(\tau), X_2(\tau)\}$. Such an interpretation leads to two scalar equations

$$\begin{aligned}
a^{-2}X_1'' + f_1(X_1, X_2, X_1'/a, X_2'/a, a\tau) &= Q_1(\tau) \\
a^{-2}X_2'' + f_2(X_1, X_2, X_1'/a, X_2'/a, a\tau) &= Q_2(\tau)
\end{aligned} \tag{12.42}$$

In this case, the shooting procedure should be based on the initial conditions at $\tau = -1$,

$$\begin{aligned}
X_1(-1) &= g, \quad X_1'(-1) = 0 \\
X_2(-1) &= h, \quad X_2'(-1) = 0
\end{aligned} \tag{12.43}$$

where the numbers g and h are determined to satisfy the boundary conditions on the right end of the interval $-1 \le \tau \le 1$,

$$\frac{\partial X_1(\tau; g, h)}{\partial \tau}|_{\tau=1} \equiv G(g, h) = 0$$
$$\frac{\partial X_2(\tau; g, h)}{\partial \tau}|_{\tau=1} \equiv H(g, h) = 0 \tag{12.44}$$

In this case, every solution g and h of system (12.44) gives the initial position on the configuration plane X_1X_2 at which the system starts with zero velocity its periodic motion of the period $T = 4a$.

12.4.3 Autonomous Case

The nonlinear normal modes represent an important class of periodic motions. The related references and description of analytical methods can be found in [136] and [241]. Analogously to the linear theory, the basic nonlinear normal mode solutions are given by the class of autonomous conservative systems. In this case, Eq. (12.42) takes the form

$$a^{-2}X_1'' + f_1(X_1, X_2) = 0$$
$$a^{-2}X_2'' + f_2(X_1, X_2) = 0 \tag{12.45}$$

The form of Eqs. (12.45) is easier than (12.42), but the parameter a becomes unknown. It is possible to avoid determining the parameter a by considering it as a control parameter for tracking the evolution of shooting diagrams. Alternatively, the parameter a can be considered as a shooting parameter by imposing one constraint on the parameters g or h. Let us consider, for instance, the system trajectories in the configuration plane X_1X_2. Introducing the amplitude $A = \sqrt{g^2 + h^2}$ in (12.43) gives

$$X_1(-1) = A\cos\varphi$$
$$X_2(-1) = A\sin\varphi$$

where the angle φ ($0 \leq \varphi < 2\pi$) together with the parameter a can play the role of a new unknowns to be determined by shooting whereas the amplitude A is considered as a control parameter.

Chapter 13
Essentially Non-periodic Processes

This chapter describes a possible physical basis for NSTT in case of essentially non-periodic processes. The physical time is structured to match the one-dimensional dynamics of rigid-body chain of identical particles. Namely, the continuous "global" time is associated with the propagation of linear momentum, whereas a sequence of nonsmooth "local" times describe behaviors of individual physical particles. Such an idea helps to incorporate temporal symmetries of the dynamics into differential equations of motion in many other cases of regular or irregular sequences of internal impacts or external pulses. Since the local times are bounded, a much wider set of analytical tools becomes possible, whereas matching conditions are generated automatically by the corresponding time substitution.

13.1 Nonsmooth Time Decomposition and Pulse Propagation in a Chain of Particles

The periodic version of NSTT employs basis functions generated by the most simple impact oscillator. This is based on the fact that the triangle and square waves capture general temporal symmetries of periodic processes regardless specifics of individual vibrating systems. Below, a non-periodic pair of nonsmooth functions is considered, such as the ramp function,

$$s\left(t;d\right)=\frac{1}{2}\left(d+\left|t\right|-\left|t-d\right|\right) \tag{13.1}$$

and its first-order generalized derivative, $\dot{s}\left(t;d\right)$, with respect to the temporal argument, t; see Figs. 13.1 and 13.2, respectively.

Such kind of functions play an important role in signal analyses [98].

V. N. Pilipchuk, *Oscillators and Oscillatory Signals from Smooth to Discontinuous*,
https://doi.org/10.1007/978-3-031-37788-4_13

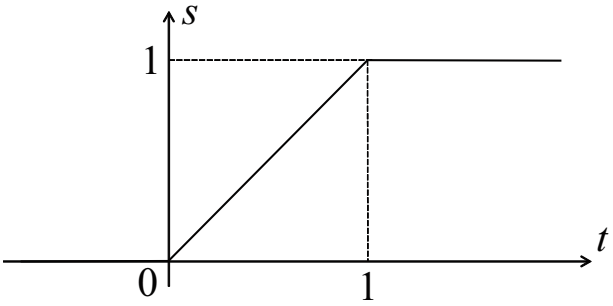

Fig. 13.1 The unit slope ramp function at $d = 1.0$

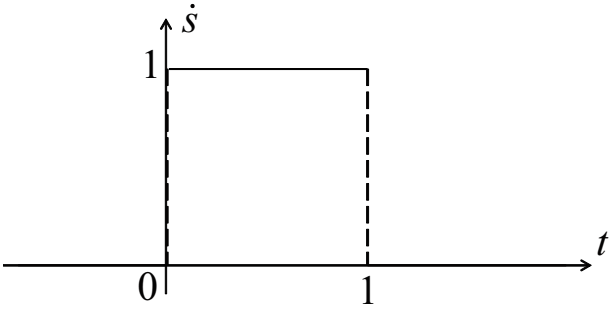

Fig. 13.2 First derivative of the ramp function

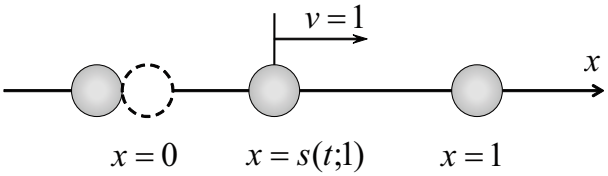

Fig. 13.3 Physical meaning of the ramp function: $s(t; 1)$ describes position of the bead struck by another bead from the left and moving until it strikes the next bead of the same mass

Possible physical interpretation of these functions is represented in Fig. 13.3. Namely, the function $s\,(t, d)$ can be treated as a coordinate of a particle, say a very small perfectly stiff bead, initially located at the origin $x = 0$. At the time instance $t = 0$, this bead is struck by the identical bead with the velocity $v = 1$. After the linear momentum exchange, the reference bead starts moving until it stopped by the third bead $x = d$; in our case $d = 1$.

Now, let us consider an infinite chain of the identical perfectly stiff beads located regularly on a straight line at the points x_i $(i = 0, 1, ...)$. No energy loss is assumed so that any currently moving bead has the same velocity. As a result, the linear

momentum is translated with the constant speed $v = 1$, whereas the beads are interacting at the time instances $t_i = x_i$. Making the temporal shift $t \to t - t_i$ in function (13.1) gives

$$s_i(t) = s(t - t_i, d_i) = \frac{1}{2}(d_i + |t - t_i| - |t - t_{i+1}|) \tag{13.2}$$

where $d_i = t_{i+1} - t_i$.

Due to the unit velocity, function (13.2) can play the role of "local" time for the bead moving within the interval $x_i < x < x_{i+1}$ during the "global" time interval $t_i < t < t_{i+1}$. The term "local" means that the temporal variable s_i starts at zero when the "global" time, t, has reached the point $t = t_i$.

In other words, *the global temporal variable is associated with the linear momentum, whereas all the local temporal variables are attached to the physical bodies.*

For any sequence of time instances, $\Lambda = \{t_0, t_1, ...\}$, the global time, $t \in (t_0, \infty)$, can be expressed through the sequence of local times, $\{s_i\}$, as

$$t = \sum_{i=0}^{\infty} (t_i + s_i)\,\dot{s}_i \tag{13.3}$$

where the derivatives $\dot{s}_i$ satisfy the relationship

$$\dot{s}_i \dot{s}_j = \dot{s}_i \delta_{ij} \tag{13.4}$$

Practically, equality (13.3) is always a finite sum because temporal intervals of physical processes always have finite upper bounds. This equality can be verified analytically within an arbitrary interval, $t_i < t < t_{i+1}$, by means of definitions (13.1) and (13.2), although its geometrical meaning is quite clear from the graphs of participating functions. Formally differentiating both sides of equality (13.3) with respect to t and taking into account (13.4) give

$$1 = \sum_{i=0}^{\infty} \dot{s}_i + t_0 \delta(t - t_0) \tag{13.5}$$

Hence,

$$\sum_{i=0}^{\infty} \dot{s}_i = 1 \qquad (t > t_0) \tag{13.6}$$

Equality (13.6) holds based on the definition for $\dot{s}_i$ as illustrated in Fig. 13.2. Note that the right-hand side of expansion (13.3) can be viewed as an element of algebra with the orthogonal basis $\{s_i\}$ and multiplication rule (13.4). This significantly eases different manipulations with the temporal variable (13.3), for instance,

$$t^n = \sum_{i=0}^{\infty} (t_i + s_i)^n \dot{s}_i, \quad n = 1, 2, ... \tag{13.7}$$

or, generally,

$$x(t) = \sum_{i=0}^{\infty} x(t_i + s_i)\dot{s}_i \equiv \sum_{i=0}^{\infty} X_i(s_i)\dot{s}_i \tag{13.8}$$

Since the right-hand sides of (13.7) and (13.8) have the same structure as the argument t itself, then the following functional linearity holds for a general function g

$$g\left(\sum_{i=0}^{\infty} X_i \dot{s}_i\right) = \sum_{i=0}^{\infty} g(X_i)\dot{s}_i \tag{13.9}$$

Now, differentiating (13.8) with respect to time t, and taking into account that $s_i(t_i) = 0$ and $s_{i-1}(t_i) = d_{i-1}$, gives

$$\begin{aligned}\dot{x}(t) &= \sum_{i=0}^{\infty} X_i'(s_i)\dot{s}_i + \sum_{i=0}^{\infty} X_i(s_i)[\delta(t - t_i) - \delta(t - t_{i+1})] \\ &= \sum_{i=0}^{\infty} X_i'(s_i)\dot{s}_i + \sum_{i=0}^{\infty} [X_i(0) - X_{i-1}(d_{i-1})]\delta(t - t_i)\end{aligned} \tag{13.10}$$

where $X_{-1}(d_{-1}) = 0$.

Therefore, all the δ—functions are eliminated from (13.10) under condition, which can be qualified as a necessary condition of continuity for $x(t)$

$$X_i(0) - X_{i-1}(d_{i-1}) = 0 \tag{13.11}$$

Under condition (13.11), the derivative $\dot{x}(t)$ has the same algebraic structure as the function $x(t)$ itself. As a result, transformation (13.3) can be applied to a general class of dynamical systems. Moreover, in the case of impulsively loaded systems, the sequences of δ-functions in (13.10) can be utilized for eliminating the corresponding singularities from dynamical systems.

13.2 Impulsively Loaded Dynamical Systems

Let us consider a dynamical system subjected to an arbitrary sequence of impulses, applied to the system at time instances $\Lambda = \{t_0, t_1, \ldots\}$,

$$\dot{\mathbf{x}} = \mathbf{f}(\mathbf{x}, t) + \sum_{i=0}^{\infty} \mathbf{p}_i \delta(t - t_i), \qquad \mathbf{x}(t) \in R^n \tag{13.12}$$

$$\mathbf{x} \equiv 0, \qquad t < t_0 \tag{13.13}$$

where $\mathbf{f}(\mathbf{x}, t)$ is a sufficiently smooth vector-function and $\mathbf{p}_i$ is vector characterizing magnitudes and directions of the impulses.

In particular case, when $t_0 = 0$, and $\mathbf{p}_i = \mathbf{0}$ $(i = 1, \ldots)$, systems (13.12) and (13.13) become equivalent to the following initial value problem

$$\dot{\mathbf{x}} = \mathbf{f}(\mathbf{x}, t), \qquad \mathbf{x}(0) = \mathbf{p}_0 \tag{13.14}$$

Below, solution of the initial value problem (13.12) and (13.13) is introduced in the specific form based on the operator Lie associated with dynamical system (13.14)

$$\begin{aligned} A &= \mathbf{f}(\mathbf{x}, t) \frac{\partial}{\partial \mathbf{x}} + \frac{\partial}{\partial t} \\ &= f_1(\mathbf{x}, t) \frac{\partial}{\partial x_1} + \ldots. + f_n(\mathbf{x}, t) \frac{\partial}{\partial x_n} + \frac{\partial}{\partial t} \end{aligned} \tag{13.15}$$

It is known, for instance, that the exponent of operator (13.15) produces temporal shifts as follows

$$\begin{aligned} e^{zA}\mathbf{f}(\mathbf{x}(t), t) &= \mathbf{f}(\mathbf{x}(t + z), t + z) \\ &= \mathbf{f}(\mathbf{x}, t) + \left[\mathbf{f}(\mathbf{x}, t) \frac{\partial \mathbf{f}(\mathbf{x}, t)}{\partial \mathbf{x}} + \frac{\partial (\mathbf{x}, t)}{\partial t}\right] z + O(z^2) \end{aligned} \tag{13.16}$$

Proposition 13.2.1 *Solution of the initial value problem (13.12) and (13.13) can be represented in the form*

$$\mathbf{x}(t) = \sum_{i=0}^{\infty} [\mathbf{a}_{i-1} + \mathbf{p}_i + \mathbf{F}(\mathbf{a}_{i-1} + \mathbf{p}_i, t_i, s_i(t))] \dot{s}_i(t) \tag{13.17}$$

where $\mathbf{a}_i = \mathbf{x}(t_{i+1})$ *is the sequence of constant vectors determined by the mapping*

$$\begin{aligned} \mathbf{a}_{-1} &= 0 \\ \mathbf{a}_i &= \mathbf{a}_{i-1} + \mathbf{p}_i + \mathbf{F}(\mathbf{a}_{i-1} + \mathbf{p}_i, t_i, d_i); \qquad i = 1, 2, \ldots \end{aligned} \tag{13.18}$$

and the function F *is defined by*

$$\mathbf{F}(\mathbf{x}, t, z) = \int_0^z e^{zA}\mathbf{f}(\mathbf{x}, t)\, dz \tag{13.19}$$

where A *is the operator Lie (13.15).*

Proof Substituting vector analogs of expressions (13.8), and (13.10) into the differential equation of motion (13.12) and taking into account (13.9) give

$$\sum_{i=0}^{\infty}\{[\mathbf{X}_i'(s_i)-\mathbf{f}(\mathbf{X}_i(s_i),t_i+s_i)]\dot{s}_i+$$

$$[\mathbf{X}_i(0)-\mathbf{X}_{i-1}(d_{i-1})-\mathbf{p}_i]\delta(t-t_i)\}=0 \tag{13.20}$$

The left-hand side of expression (13.20) includes both regular and singular terms. Moreover, the basis elements $\dot{s}_i$ are linearly independent, and all the δ-functions are acting at different time instances. Therefore, Eq. (13.20) gives

$$\mathbf{X}_i'(s_i)=\mathbf{f}(\mathbf{X}_i(s_i),t_i+s_i) \tag{13.21}$$

$$\mathbf{X}_i(0)=\mathbf{X}_{i-1}(d_{i-1})+\mathbf{p}_i=\mathbf{a}_{i-1}+\mathbf{p}_i \tag{13.22}$$

where $\mathbf{a}_{-1}=0$ and $\mathbf{a}_i=\mathbf{X}_i(d_i)$ $(i=0,1,2,...)$. Equation (13.21) can be represented in the integral form

$$\mathbf{X}_i(s_i)=\mathbf{X}_i(0)+\int_0^{s_i}\mathbf{f}(\mathbf{X}_i(z),t_i+z)\,dz \tag{13.23}$$

Since the variable of integration is limited by the interval $0\le z\le s_i$, the integrand in (13.23) can be approximated by the easy to integrate Maclaurin's series with respect to z. Moreover, such a series can be represented in the convenient form of Lie series based on the fact that $\mathbf{X}_i(z)$ are coordinates of the dynamical system with the operator Lie (13.15). As a result, all the coefficients of power series are expressed through the "initial conditions" at $z=0$ $(t=t_i)$ by enforcing the form of the dynamical system. As a result, no high-order derivatives of the coordinates are included anymore into the coefficients of the series. Taking into account the notation $\mathbf{X}_i(s_i)=\mathbf{x}(t_i+s_i)$, and expressions (13.16) and (13.19), brings (13.23) to the form

$$\begin{aligned}\mathbf{X}_i(s_i)&=\mathbf{X}_i(0)+\int_0^{s_i}e^{zA}\mathbf{f}(\mathbf{x}(t_i),t_i)\,dz\\&=\mathbf{X}_i(0)+\mathbf{F}(\mathbf{x}(t_i),t_i,s_i)\\&=\mathbf{X}_i(0)+\mathbf{F}(\mathbf{X}_i(0),t_i,s_i)\end{aligned} \tag{13.24}$$

Substituting now $\mathbf{X}_i(0)$ from (13.22) in (13.24) gives

$$\mathbf{X}_i(s_i)=\mathbf{a}_{i-1}+\mathbf{p}_i+\mathbf{F}(\mathbf{a}_{i-1}+\mathbf{p}_i,t_i,s_i) \tag{13.25}$$

Finally, substituting (13.25) in expansion (13.8) gives (13.17). Then, substituting $s_i = d_i$ in (13.25) gives (13.18) and thus completes the proof.

Solutions (13.17) and (13.18) should be viewed as a semi-analytic solution, since some numerical tool is required for calculating the discrete mapping (13.18). The central role here belongs to the function $s(t; d)$ (13.1), which is automatically matching all the neighboring pieces of the solution. Note that the distances d_i between times Λ are not necessary small; however, the precision of the solution can be improved by increasing the number of terms of the Lie series $e^{zA}\mathbf{f}(\mathbf{x}, t)$ with respect to z, rather than reducing the distances d_i.

13.2.1 Harmonic Oscillator Under Sequential Impulses

In order to estimate precision of the above procedure, let us consider the particular case in which function (13.19) can be calculated exactly in the closed form due to the presence of exact analytical solution in between the pulses Λ. The differential equation of motion on the entire time range is

$$\ddot{x} + 2\zeta\Omega\dot{x} + \Omega^2 x = \sum_{i=0}^{\infty} p_i \delta(t - t_i) \tag{13.26}$$

In this case, the function $\mathbf{f}(\mathbf{x}, t)$ in Eq. (13.12) becomes

$$\mathbf{f}(\mathbf{x}) = \begin{pmatrix} x_2 \\ -2\zeta\Omega x_2 - \Omega^2 x_1 \end{pmatrix} \tag{13.27}$$

Using the identity $e^{zA}\mathbf{f}(\mathbf{x}(t), t) = \mathbf{f}(\mathbf{x}(t+z), t+z)$ and the exact analytical solution of the corresponding free oscillator gives both components of the vector-function (13.19) in the form

$$\begin{aligned} F_1(\mathbf{x}; z) &= \left[e^{-z\zeta\Omega} \cos\left(z\sqrt{1-\zeta^2}\,\Omega\right) + \frac{\zeta e^{-z\zeta\Omega}}{\sqrt{1-\zeta^2}} \sin\left(z\sqrt{1-\zeta^2}\,\Omega\right) - 1 \right] x_1 \\ &\quad + \frac{e^{-z\zeta\Omega}}{\Omega\sqrt{1-\zeta^2}} \sin\left(z\sqrt{1-\zeta^2}\,\Omega\right) x_2 \\ F_2(\mathbf{x}; z) &= -\frac{\Omega e^{-z\zeta\Omega}}{\sqrt{1-\zeta^2}} \sin\left(z\sqrt{1-\zeta^2}\,\Omega\right) x_1 \\ &\quad + \left[e^{-z\zeta\Omega} \cos\left(z\sqrt{1-\zeta^2}\,\Omega\right) - \frac{\zeta e^{-z\zeta\Omega}}{\sqrt{1-\zeta^2}} \sin\left(z\sqrt{1-\zeta^2}\,\Omega\right) - 1 \right] x_2 \end{aligned} \tag{13.28}$$

In this particular case, properties of mapping (13.18) depend on the following determinant

$$J = \begin{vmatrix} 1 + \partial F_1/\partial x_1 & \partial F_1/\partial x_2 \\ \partial F_2/\partial x_1 & 1 + \partial F_2/\partial x_2 \end{vmatrix} = e^{-2d_i \zeta \Omega} \tag{13.29}$$

Let us introduce the relative error

$$\delta = \left| J - J_{appr} \right| / J \tag{13.30}$$

where J_{appr} is an approximate determinant based on the Lie series expansion (13.16).

Figures 13.4 and 13.5 show diagrams for the relative error δ versus the distance d between any two neighboring impulse times when the highest-order terms kept in Lie series (13.16) are $O(z^2)$ and $O(z^3)$, respectively.

As follows from the diagrams, precision of the discrete mapping essentially depends on both the distance between pulse times and the number of terms kept in the Lie series. As a result, the error due to a large distance can be reduced by increasing the number of terms in the Lie series.

13.2.2 Random Suppression of Chaos

A specific case of the Duffing oscillator with no linear stiffness under sine modulated random impulses was considered in [183]. The corresponding differential equation of motion is represented in the form

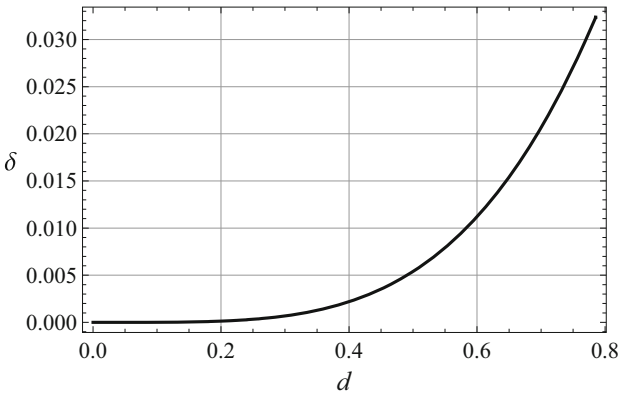

Fig. 13.4 Relative error of the determinant based on the truncated Lie series including terms of order $O(z^2)$

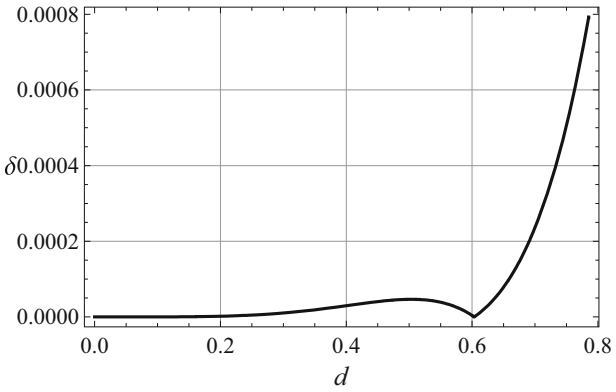

Fig. 13.5 Relative error of the determinant based on the truncated Lie series including terms of order $O(z^3)$

$$\ddot{x} + \zeta \dot{x} + x^3 = B \sin t \sum_{i=0}^{\infty} \delta (t - t_i) \tag{13.31}$$

where ζ is a constant linear damping coefficient and B is the amplitude of modulation.

Distances between any two sequential impulse times are given by

$$d_i = t_{i+1} - t_i = \frac{\pi}{12} \left(1 + \beta \eta_i\right)$$

where η_i is random real number homogeneously distributed on the interval $[-1, 1]$ and β is a small positive number, $0 < \beta \ll 1$.

Introducing the state vector $\mathbf{x} = (x, \dot{x})^T \equiv (x_1, x_2)^T$ brings system (13.31) to the standard form (13.12), where

$$\mathbf{f}(\mathbf{x}) = \begin{pmatrix} x_2 \\ -\zeta x_2 - x_1^3 \end{pmatrix}, \quad \mathbf{p}_i = \begin{pmatrix} 0 \\ B \sin t_i \end{pmatrix}$$

Note that oscillator (13.31) represents of course a modified version of the well-known oscillator, $\ddot{x} + \zeta \dot{x} + x^3 = B \sin t$, considered first by Ueda [236] as a model of nonlinear inductor in electrical circuits—the Ueda circuit. In particular, the result of work [236], as well as many further investigations of similar models, reveals the existence of stochastic attractors often illustrated by the Poincaré diagrams [147]. Similar diagrams obtained under non-regular snapshots can be qualified as "stroboscopic" diagrams. The results of the computer simulations described in [183] show that some irregularity of the pulse times can be used for the purposes of a more clear observation of the system orbits in the stroboscopic diagrams. When

repeatedly executing the numerical code, under the same input conditions, such a small disorder in the input results some times in a less noisy and more organized stroboscopic diagrams. However, such phenomenon itself was found to be a random event whose "appearance" depends on the level of pulse randomization as well as the number of iterations.

Chapter 14
Spatially Oscillating Structures

This chapter illustrates applications of nonsmooth argument substitutions to modeling spatially oscillating structures such as one-dimensional elastic rods with periodic discrete inclusions and two- or three-dimensional acoustic media with periodic nonsmooth boundary sources of waves. Whenever the corresponding global spatial domains are infinite or cyclical, the related analytical manipulations are similar to those conducted with dynamical systems. The idea of structural homogenization is implemented through the two-variable expansions, where the fast scale is represented by the triangular periodic wave. As a result, closed-form analytical solutions are derived despite of the presence of discrete inclusions or external discontinuous loads. Static and dynamic problems of elasticity dealing with nonsmooth periodic structures are often considered in the literature due to their practical importance; see reviews in [10, 11, 100] for introduction and references. Such problems can also be considered by means of the nonsmooth argument transformations. In this case though, the transformation must be applied to the spatial independent variable related to coordinate along which the structure under consideration is periodic. Such an approach was introduced in [174] for a string on discrete elastic foundation, although the complete description of the tool was given later for the corresponding nonlinear case [199, 200, 213].

14.1 Spatial Triangle Wave Argument

14.1.1 Infinite String on a Discrete Elastic Foundation

For illustrating purpose, let us consider the dynamics of an infinite string on a discrete nonlinearly elastic foundation described by equation

V. N. Pilipchuk, *Oscillators and Oscillatory Signals from Smooth to Discontinuous*,
https://doi.org/10.1007/978-3-031-37788-4_14

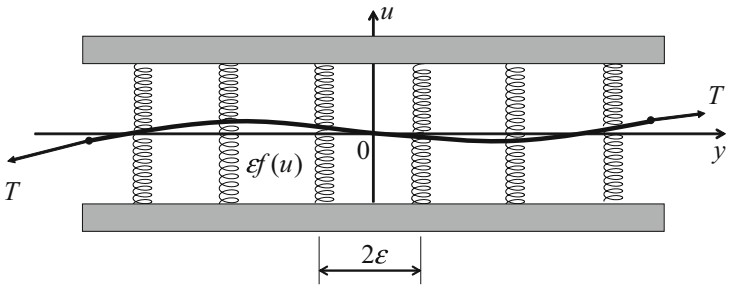

Fig. 14.1 Linear string on the discrete regular set of nonlinearly elastic springs

$$\rho\frac{\partial^2 u}{\partial t^2} - T\frac{\partial^2 u}{\partial y^2} + 2f(u)\sum_{k=-\infty}^{\infty}\delta\left(\frac{y}{\varepsilon} - 1 - 2k\right) = q\left(\frac{y}{\varepsilon}, y, t\right) \tag{14.1}$$

$$(-\infty < y < \infty)$$

where ρ is the mass density per unit length; T is a constant tension; $q(y/\varepsilon, y, t)$ is the body force or external loading, which is assumed to be periodic in the "fast spatial scale" y/ε $(0 < \varepsilon \ll 1)$ with the period normalized to four; and a similar assumption is made with respect to the transverse displacement of the string $u = u(y/\varepsilon, y, t)$; see Fig. 14.1 for illustration.

Note that Eq. (14.1) does not allow for a point-wise interpretation due to the presence of Dirac δ-function. Both sides of the equation therefore must be interpreted as distributions producing the same output if applied to the same testing function. Correctness of such type of modeling was intensively discussed in the literature; see, for instance, [65]. Omitting details, the series of δ-functions in Eq. (14.1) has a certain meaning if the function $f(u(y/\varepsilon, y, t))$ is at least continuous in the neighborhoods of points $y = \varepsilon(1 + 2k)$ with respect to the spatial argument, y, for every k. Note that such a continuity condition is guaranteed by the form of Eq. (14.1). If, for instance, the displacement u was stepwise discontinuous at $y = \varepsilon(1 + 2k)$, then the derivative $\partial^2 u/\partial y^2$ would produce uncompensated first derivatives of the δ-function. Therefore, the displacement u is at least continuous function of the coordinate y in a match with the physical meaning of the model. Moreover, it will be shown below that introducing the space folding spatial argument, $\tau = \tau(y/\varepsilon)$, eliminates the singularities from Eq. (14.1) and hence takes the problem in the frameworks of classical theory of differential equations. First, the set of localized restoring forces of the elastic foundation are expressed through second derivative of the triangular wave as

$$2f(u)\sum_{k=-\infty}^{\infty}\delta\left(\frac{y}{\varepsilon} - 1 - 2k\right) = -f(u)\mathrm{sgn}(\tau)\tau''\left(\frac{y}{\varepsilon}\right) \tag{14.2}$$

where the derivative τ'' is taken with respect to the entire argument y/ε and $\text{sgn}(\tau)$ is introduced to make all the δ-functions positive, since the foundation reaction forces must be restoring.

Now both the displacement u and the external loading function q are represented as elements of the hyperbolic algebra

$$\begin{aligned} u &= U(\tau, y, t) + V(\tau, y, t)e \\ q &= Q(\tau, y, t) + P(\tau, y, t)e \\ e &= e\,(y/\varepsilon) \equiv d\tau(y/\varepsilon)/d(y/\varepsilon) \end{aligned} \tag{14.3}$$

where the components Q and P are known, whereas X and Y are new unknown functions.

Finally, substituting (14.2) and (14.3) in Eq. (14.1) and using the differential and algebraic rules of nonsmooth argument substitutions (Chap. 4) give the differential equations and boundary conditions as, respectively,

$$\frac{\partial^2 U}{\partial \tau^2} = -2\varepsilon \frac{\partial^2 V}{\partial y \partial \tau} + \varepsilon^2 \left(\frac{\rho}{T} \frac{\partial^2 U}{\partial t^2} - \frac{\partial^2 U}{\partial y^2} - \frac{Q}{T} \right) \tag{14.4}$$

$$\frac{\partial^2 V}{\partial \tau^2} = -2\varepsilon \frac{\partial^2 U}{\partial y \partial \tau} + \varepsilon^2 \left(\frac{\rho}{T} \frac{\partial^2 V}{\partial t^2} - \frac{\partial^2 V}{\partial y^2} - \frac{P}{T} \right) \tag{14.5}$$

and

$$\tau = \pm 1 : V = 0 \tag{14.6}$$

$$\tau = \pm 1 : \frac{\partial U}{\partial \tau} = \mp \frac{\varepsilon^2}{T} f(U) \tag{14.7}$$

where the form of boundary condition (14.7) was eased by enforcing condition (14.6).

In contrast to Eq. (14.1), the above boundary value problem, (14.4) through (14.7), is free of the δ-function singularities. Therefore, conventional methods of asymptotic integration, such as two-variable expansions, can be applied after a proper modification to account for the problem specifics. Regardless of the types of algorithms, solutions are represented in the form of asymptotic series

$$\begin{aligned} U(\tau, y, t) &= \sum_{k=0}^{\infty} \varepsilon^k U_k(\tau, y, t) \\ V(\tau, y, t) &= \sum_{k=0}^{\infty} \varepsilon^k V_k(\tau, y, t) \end{aligned} \tag{14.8}$$

As just noticed, problem formulations based on Eqs. (14.4) through (14.7) possess certain advantages as compared to Eq. (14.1). For instance, the influence of infinite discontinuities in Eq. (14.1) is captured by the form of substitution (14.3). Also, the structural discreteness of the nonlinear elastic foundation (14.2) is associated with the new spatial variable τ restricted in the range $-1 \le \tau \le 1$. As a result, polynomial expansions with respect to the coordinate τ will not be affecting the regularity of asymptotic expansions (14.8) in terms of the original fast scale y/ε. In other words, the structural periodicity will be maintained in a wide range of asymptotic algorithms due to the inherent periodicity of the coordinate $\tau = \tau(y/\varepsilon)$.

Note that partial differential Eqs. (14.4) and (14.5) are coupled, whereas boundary conditions (14.6) and (14.7) are decoupled with respect to the unknowns U and V. It is usually more convenient to decouple equations by introducing new unknown functions, say $X = U + V$ and $Y = U - V$. Then Eqs. (14.4) and (14.5) take the form

$$\frac{\partial^2 X}{\partial \tau^2} = -2\varepsilon \frac{\partial^2 X}{\partial y \partial \tau} + \varepsilon^2 \left(\frac{\rho}{T} \frac{\partial^2 X}{\partial t^2} - \frac{\partial^2 X}{\partial y^2} - \frac{Q+P}{T} \right) = 0 \tag{14.9}$$

$$\frac{\partial^2 Y}{\partial \tau^2} = 2\varepsilon \frac{\partial^2 Y}{\partial y \partial \tau} + \varepsilon^2 \left(\frac{\rho}{T} \frac{\partial^2 Y}{\partial t^2} - \frac{\partial^2 Y}{\partial y^2} - \frac{Q-P}{T} \right) = 0 \tag{14.10}$$

This is obviously transition to the idempotent basis, $\{1, e\} \longrightarrow \{e_+, e_-\}$, as described in Sect. 4.2.1

$$\begin{aligned} u &= U + Ve = U(e_+ + e_-) + V(e_+ - e_-) \\ &= (U+V)e_+ + (U-V)e_- = Xe_+ + Ye_- \end{aligned}$$

Equations (14.9) and (14.10) have the same structure, except for signs of two terms. Therefore, it is sufficient to solve just one of the equations. Then, solution of another equation can be written by analogy.

14.1.2 Doubling the Array of Springs

The mechanical model, which is shown in Fig. 14.2, was considered in [198] based on the generalized (asymmetric) version of the triangle wave in different notations. In contrast to the model shown in Fig. 14.1, the support sprigs are linearly elastic and shifted in a dipole-wise manner, such that the differential equation of motion with respect to the string deflection $u = u(t, y)$ has the form

$$\rho \frac{\partial^2 u}{\partial t^2} - T \frac{\partial^2 u}{\partial y^2} - \frac{k}{\varepsilon}(1-\gamma^2) u \, \mathrm{sgn}[\tau(\xi, \gamma)] \frac{\partial^2 \tau(\xi, \gamma)}{\partial \xi^2} = 0 \tag{14.11}$$

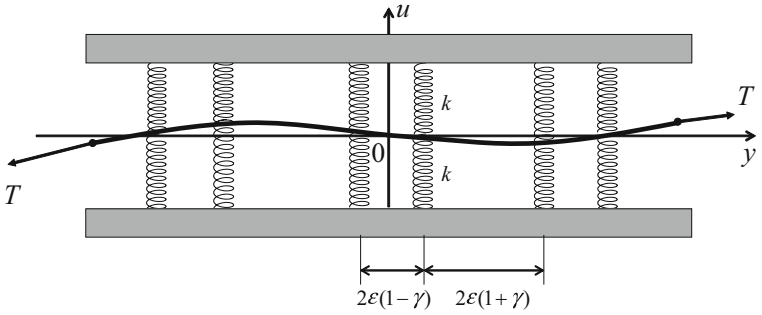

Fig. 14.2 Linear string on the discrete periodic set of linearly elastic dipole-wise shifted springs of the stiffness k

$$\left(-\infty < y < \infty, \qquad \xi = \frac{y}{\varepsilon}\right)$$

where the triangular wave with different positive and negative slopes is given by (Fig. 14.7)

$$\tau = \quad \tau(\xi, \gamma) = \begin{cases} \xi/(1-\gamma) & \text{for } -1+\gamma \le \xi \le 1-\gamma \\ (-\xi+2)/(1+\gamma) & \text{for } 1-\gamma \le \xi \le 3+\gamma \end{cases} \tag{14.12}$$

$$\forall \xi : \qquad \tau(\xi+4, \gamma) = \tau(4, \gamma), \qquad -1 < \gamma < 1$$

Schwartz derivatives of function (14.12), $e = \partial\tau(\xi, \gamma)/\partial\xi$, satisfy the following relationships

$$e^2 = \alpha + \beta e \tag{14.13}$$

$$e\frac{\partial e}{\partial \xi} = \frac{1}{2}\beta\frac{\partial e}{\partial \xi} \tag{14.14}$$

$$\frac{\partial e}{\partial \xi} = 2\alpha \sum_{k=-\infty}^{\infty} [\delta(\xi + 1 - \gamma - 4k) - \delta(\xi - 1 + \gamma - 4k)] \tag{14.15}$$

where $\alpha = 1/\left(1-\gamma^2\right)$ and $\beta = 2\gamma\alpha$.

Let us represent the string deflection in the form

$$u = U(\tau, y, t) + V(\tau, y, t)e \tag{14.16}$$

where $\tau = \tau(\xi, \gamma)$ and $e = \partial\tau(\xi, \gamma)/\partial\xi$.

The components of representation (14.16), U and V, depend on the coordinate y both explicitly and through the triangular wave function τ in such a way that the

complete partial derivative $\partial u/\partial y$, including the dependence $\xi = y/\varepsilon$, is equivalent to applying the differential matrix operator

$$D = \varepsilon^{-1} \begin{bmatrix} \varepsilon\partial/\partial y & \alpha\partial/\partial\tau \\ \partial/\partial\tau & \beta\partial/\partial\tau + \varepsilon\partial/\partial y \end{bmatrix} \tag{14.17}$$

to the vector column of the components U and V

$$\frac{\partial u}{\partial y} \Longleftrightarrow D \begin{bmatrix} U \\ V \end{bmatrix} \tag{14.18}$$

under the condition

$$\tau = \pm 1 : V = 0 \tag{14.19}$$

The regular part of the second derivative can be calculated by means of the relationship

$$\frac{\partial^2 u}{\partial y^2} \Longleftrightarrow D^2 \begin{bmatrix} U \\ V \end{bmatrix} \tag{14.20}$$

However, second derivative of the triangular wave function must be preserved in order to eliminate the same kind of singularity from Eq. (14.11). So, substituting (14.16) in (14.11) and collecting separately terms related to different elements of the basis $\{1, e\}$ give

$$\rho \frac{\partial^2 U}{\partial t^2} - T \times \left[\left(\frac{\alpha}{\varepsilon^2} \frac{\partial^2}{\partial \tau^2} + \frac{\partial^2}{\partial y^2} \right) U + \left(\frac{\alpha\beta}{\varepsilon^2} \frac{\partial^2}{\partial \tau^2} + \frac{2\alpha}{\varepsilon} \frac{\partial^2}{\partial \tau \partial y} \right) V \right] = 0 \tag{14.21}$$

$$\rho \frac{\partial^2 V}{\partial t^2} - T \times \left[\left(\frac{\beta}{\varepsilon^2} \frac{\partial^2}{\partial \tau^2} + \frac{2}{\varepsilon} \frac{\partial^2}{\partial \tau \partial y} \right) U + \left(\frac{\alpha + \beta^2}{\varepsilon^2} \frac{\partial^2}{\partial \tau^2} + \frac{2\beta}{\varepsilon} \frac{\partial^2}{\partial \tau \partial y} + \frac{\partial^2}{\partial y^2} \right) V \right] = 0 \tag{14.22}$$

under the additional to (14.19) condition

$$\tau = \pm 1 : -\frac{T}{\varepsilon^2} \left(\frac{\partial U}{\partial \tau} + \beta \frac{\partial V}{\partial \tau} \right) = \pm \frac{k}{\varepsilon} (1 - \gamma^2) U \tag{14.23}$$

Note that some terms have been eliminated from condition (14.23) by taking into account condition (14.19).

Further analysis of the boundary value problems (14.19) and (14.21) through (14.23) can be implemented by using the asymptotic approach [199] considering ε as a small parameter.

Similar version of the transformation was employed for statics of layered composites in [227].

14.1.3 Elastic Ring Under Periodic Array of Compressive Loads

The buckling of a circular ring loaded by a discrete regular set of concentrated compressive forces was considered in [239]; see Fig. 14.3. Taking into account identity (14.2), the differential equation of equilibrium of such ring can be represented in the form

$$\frac{dy}{dt} = f(y) - \lambda \sum_{k=-\infty}^{\infty} \delta\left(2\frac{t}{\varepsilon} - 1 - 2k\right) \equiv f(y) + \frac{1}{2}\lambda \mathrm{sgn}(\tau)\tau'' \tag{14.24}$$

where $t = s/R$ $(0 \le t \le 2\pi)$ is the arc length of the undeformed ring axis per radius; $y = y(t)$ is a six-component vector-function characterizing elastic states of the ring; $f(y)$ is a vector-function of the elastic states describing both geometrical and physical properties of the ring; $\tau = \tau(2t/\varepsilon)$ is the triangular sine wave of the period $T = 2\varepsilon$ and prime means its Schwartz derivative; ε is a small parameter, as compared to unity, characterizing the distance between loads (Fig. 14.3); λ is

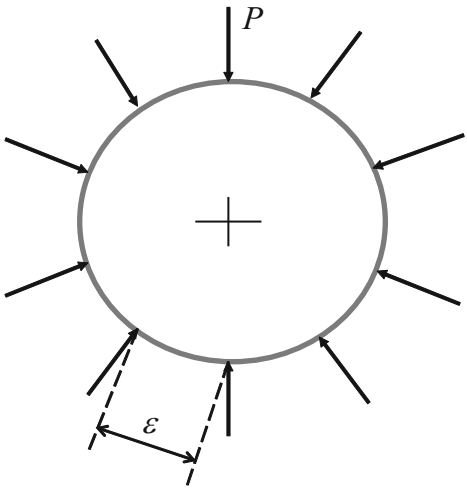

Fig. 14.3 The circular ring, whose radius is scaled to unity, under the discrete regular set of compressive radial forces, where $\varepsilon = 2\pi/N \ll 1$ and N is the number of forces

a dimensionless parameter which is proportional to the load P; and conditions of periodicity are imposed on the vector-function: $y(t + 2\pi) = y(t)$. This periodicity is associated with the formally infinite limits of summation in Eq. (14.24). Shifting the arclength t by 2π is equivalent to shifting the summation index as $k \longrightarrow k + N$. Obviously, the wave length of buckling is not necessarily equal to the spatial period of loading.

Further, the unknown vector-function is represented as an element of the hyperbolic algebra

$$y = X(t, \tau) + Y(t, \tau)e, \qquad e = e(2t/\varepsilon) \tag{14.25}$$

Substituting (14.25) in Eq. (14.24) gives

$$\frac{2}{\varepsilon}\frac{\partial Y}{\partial \tau} + \frac{\partial X}{\partial t} - R(X, Y) + \left[\frac{2}{\varepsilon}\frac{\partial X}{\partial \tau} + \frac{\partial Y}{\partial t} - I(X, Y)\right]e + \left[\frac{2}{\varepsilon}Y - \frac{1}{2}\lambda \mathrm{sgn}(\tau)\right]e' = 0 \tag{14.26}$$

or

$$\frac{\partial Y}{\partial \tau} = \frac{1}{2}\varepsilon\left[R(X, Y) - \frac{\partial X}{\partial t}\right]$$
$$\frac{\partial X}{\partial \tau} = \frac{1}{2}\varepsilon\left[I(X, Y) - \frac{\partial Y}{\partial t}\right] \tag{14.27}$$

and

$$\tau = \pm 1 : Y = \pm\frac{1}{4}\varepsilon\lambda \tag{14.28}$$

where

$$R(X, Y) = \frac{1}{2}[f(X + Y) + f(X - Y)]$$
$$I(X, Y) = \frac{1}{2}[f(X + Y) - f(X - Y)]$$

Recall that the role of boundary conditions (14.28) is to eliminate the δ-function singularities, $e' = \tau''$, from Eq. (14.26). The resultant boundary value problem, (14.27)–(14.28), was analyzed by means of regular asymptotic expansions in [239]. Based on the asymptotic solutions, the load discreteness effects on the critical load and postbuckling states of the ring were estimated.

14.2 Homogenization of One-Dimensional Periodic Structures

Let us consider a one-dimensional 4ε-periodic structure whose static elastic states are described by the vector-function $z = z(y) \in R^n$ that depends upon the longitudinal coordinate y attached to the undeformed structure. The number of vector components n can always be increased in such a way that the differential equation of equilibrium takes the form of first-order differential equation, for instance, as follows

$$\frac{dz}{dy} = f(z, y, \xi) + p(y)e'(\xi), \; e(\xi) = \tau'(\xi) \tag{14.29}$$

Here the spatial scale $\xi = y/\varepsilon$ associates with the structural periodicity, the vector-function $f(z, y, \xi) \in R^n$ is continuous with respect to z and y, but it is allowed to be stepwise discontinuous with respect to ξ at the points $\{\xi : \tau(\xi) = \pm 1\}$, and $p(y) \in R^n$ is a continuous vector-function describing the amplitude modulation of the localized loading.

Example 14.2.1 In terms of the matrixes,

$$z = \begin{bmatrix} u(y) \\ v(y) \end{bmatrix}, \; p(y) = \begin{bmatrix} 0 \\ q(y)/(2\varepsilon) \end{bmatrix} \tag{14.30}$$

$$f = \begin{bmatrix} v(y)/\{EF[1 + \alpha e(\xi)]\} \\ 0 \end{bmatrix}$$

Equation (14.29) describes an elastic rod whose cross-sectional area is a piecewise constant periodic function of the longitudinal coordinate as it is shown in Fig. 14.4. Substituting (14.30) in (14.29) and eliminating then $v(y)$ give the second-order differential equation of equilibrium of the rod

$$\frac{d}{dy}\left[EF\,[1 + \alpha e(\xi)]\,\frac{du}{dy}\right] = \frac{1}{2\varepsilon}q(y)e'(\xi) \tag{14.31}$$

Now let us consider the vector-form equation in its general form (14.29). Nonsmooth two-variable expansions will be used by considering the triangular wave

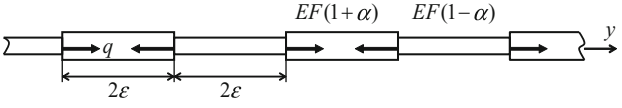

Fig. 14.4 An elastic rod with a periodic nonsmoothly varying cross-sectional area and concentrated loading

oscillating coordinate $\tau = \tau(\xi)$ and the original coordinate $\eta \equiv y$ as fast and slow spatial scales, respectively, provided that the following assumption holds

$$\varepsilon << 1 \tag{14.32}$$

Let us represent solutions of Eq. (14.29) in the form

$$z = X(\tau, \eta) + Y(\tau, \eta)e \tag{14.33}$$

Substituting (14.33) in Eq. (14.29) gives

$$\frac{\partial Y}{\partial \tau} + \varepsilon \left(\frac{\partial X}{\partial \eta} - R_f \right) + \left[\frac{\partial X}{\partial \tau} + \varepsilon \left(\frac{\partial Y}{\partial \eta} - I_f \right) \right] e + [Y - \varepsilon p(\eta)]e' = 0 \tag{14.34}$$

where

$$\left.\begin{array}{l} R_f\,(X, Y, \tau, \eta) \\ I_f\,(X, Y, \tau, \eta) \end{array}\right\} = \frac{1}{2}[f(X + Y, \tau, \eta) \pm f(X - Y, 2 - \tau, \eta)] \tag{14.35}$$

Expression (14.34) is equivalent to the following boundary value problem with no discontinuities

$$\begin{aligned} \frac{\partial X}{\partial \tau} + \varepsilon \left(\frac{\partial Y}{\partial \eta} - I_f \right) &= 0 \\ \frac{\partial Y}{\partial \tau} + \varepsilon \left(\frac{\partial X}{\partial \eta} - R_f \right) &= 0 \end{aligned} \tag{14.36}$$

$$\tau = \pm 1 : Y = \varepsilon p(\eta) \tag{14.37}$$

Let us represent solutions of the boundary value problem, (14.36) and (14.37), in the form of asymptotic series with respect to ε

$$\begin{aligned} X &= \sum_{i=0}^{\infty} \varepsilon^i X^i(\tau, \eta) \\ Y &= \sum_{i=0}^{\infty} \varepsilon^i Y^i(\tau, \eta) \end{aligned} \tag{14.38}$$

where the functions X^i and Y^i are to be sequentially determined.

Substituting (14.38) in (14.35) generates power series expansions

$$R_f = R_f^0 + \varepsilon R_f^1 + \varepsilon^2 R_f^2 + \ldots \tag{14.39}$$

$$I_f = I_f^0 + \varepsilon I_f^1 + \varepsilon^2 I_f^2 + \ldots$$

where the following notations are used

$$R_f^i = \frac{1}{i!}\frac{\partial^i R_f}{\partial \varepsilon^i}|_{\varepsilon=0}, \qquad I_f^i = \frac{1}{i!}\frac{\partial^i I_f}{\partial \varepsilon^i}|_{\varepsilon=0}$$

Substituting (14.38) in (14.36) and (14.37), then matching the coefficients of the same powers of ε, gives the corresponding sequence of equations and boundary conditions. In particular, zero-order problem takes the form

$$\frac{\partial X^0}{\partial \tau} = 0, \quad \frac{\partial Y^0}{\partial \tau} = 0 \tag{14.40}$$

and

$$\tau = \pm 1 : Y^0 = 0 \tag{14.41}$$

As follows from (14.40), the generating solution is independent on the fast oscillating scale τ. Therefore, taking into account (14.41) gives solution

$$X^0 = A^0(\eta), \qquad Y^0 \equiv 0 \tag{14.42}$$

where A^0 is an arbitrary vector-function of the slow coordinate that will be determined on the next step of the asymptotic procedure.

So, collecting the terms of order ε gives the differential equations and boundary conditions in the form, respectively,

$$\frac{\partial X^1}{\partial \tau} = I_f^0 - \frac{\partial Y^0}{\partial \eta} = I_f(A^0, 0, \tau, \eta) \tag{14.43}$$

$$\frac{\partial Y^1}{\partial \tau} = R_f^0 - \frac{\partial X^0}{\partial \eta} = R_f(A^0, 0, \tau, \eta) - \frac{dA^0}{d\eta} \tag{14.44}$$

and

$$\tau = \pm 1 : Y^1 = p(\eta) \tag{14.45}$$

Integrating Eqs. (14.43) and (14.44) gives first-order terms of the asymptotic solution

$$X^1 = \int_0^\tau I_f^0 d\tau + A^1(\eta) \tag{14.46}$$

$$Y^1 = \int_{-1}^{\tau} R_f^0 d\tau - \frac{dA^0}{d\eta}(\tau + 1) + p(\eta)$$

where A^1 is a new arbitrary vector-function of the slow spatial scale η and the limits of integration for Y^1 are chosen in such a manner that boundary condition (14.45) is satisfied automatically at the point $\tau = -1$, whereas another point, $\tau = 1$, gives equation

$$\frac{dA^0}{d\eta} = \frac{1}{2}\int_{-1}^{1} R_f^0 d\tau \equiv \left\langle R_f^0 \right\rangle \tag{14.47}$$

Note that the "slow scale" Eq. (14.47) was obtained by satisfying the boundary condition in contrast to the conventional scheme of two-variable expansions in which such kind of equations are obtained by eliminating the so-called resonance terms.

Enforcing now Eq. (14.47) brings the component Y^1 to the final form

$$Y^1 = \int_{-1}^{\tau} \left(R_f^0 - \left\langle R_f^0 \right\rangle \right) d\tau + p(y^0) \tag{14.48}$$

At this stage, expressions (14.46) through (14.48) determine the first-order terms of the asymptotic solution; however, the slow scale vector-function $A^1(\eta)$ still remains unknown. The corresponding ordinary differential equation is obtained on the next stage from the boundary condition for Y^2 and can be represented in the form

$$\frac{dA^1}{d\eta} = \left\langle \frac{\partial R_f^0}{\partial A^0} \right\rangle A^1 + F^1(A^0, \eta) \tag{14.49}$$

where $\partial R_f^0 / \partial A^0$ is the Jacobian matrix and the vector-function F^1 is known.

Note that Eq. (14.49) is linear. Moreover, on the next steps, equations for the vector-functions A^2, A^3,... will be of the same linear structure, including the same Jacobian matrix.

14.3 Second-Order Equations

Let us consider now the second-order differential equation with respect to the vector-function $z(y) \in R^n$, however, in the linear form

$$\frac{d^2z}{dy^2} + [q(\xi, y) + p(y)e'(\xi)]z = g(\xi, y) + r(y)e'(\xi) \tag{14.50}$$

$$\tau = \tau(\xi), \qquad e = \tau'(\xi), \qquad \xi = y/\varepsilon$$

where q and p are $n \times n$-matrixes, g and r are n-dimensional vector-functions, and ξ is the fast spatial scale.

Based on the assumptions of the previous section, the functions q and g and solutions of Eq. (14.50) can be represented in the form, respectively,

$$\begin{aligned} q(\xi, y) &= Q(\tau, \eta) + P(\tau, \eta)e \\ g(\xi, y) &= G(\tau, \eta) + F(\tau, \eta)e \\ \eta &\equiv y \end{aligned} \tag{14.51}$$

and

$$z(y) = X(\tau, \eta) + Y(\tau, \eta)e \tag{14.52}$$

where η and τ represent the slow and fast spatial scales, respectively.

Substituting (14.51) and (14.52) in Eq. (14.50) and conducting differential and algebraic manipulations of NSTT lead to the boundary value problem

$$\frac{\partial^2 X}{\partial \tau^2} = -2\varepsilon \frac{\partial^2 Y}{\partial \tau \partial \eta} - \varepsilon^2 \left(\frac{\partial^2 X}{\partial \eta^2} + QX + PY - G \right) \tag{14.53}$$

$$\frac{\partial^2 Y}{\partial \tau^2} = -2\varepsilon \frac{\partial^2 X}{\partial \tau \partial \eta} - \varepsilon^2 \left(\frac{\partial^2 Y}{\partial \eta^2} + PX + QY - F \right) \tag{14.54}$$

and

$$\tau = \pm 1 : \frac{\partial X}{\partial \tau} = \varepsilon^2 [r(y) - p(y)X], \qquad Y = 0 \tag{14.55}$$

Further, representing the solution of the boundary value problem (14.53), (14.54), and (14.55) in the form of asymptotic series (14.38) gives a sequence of boundary value problems, in which first two steps appear to have quite trivial solutions, such as

$$X^0 = B^0(\eta), \quad Y^0 \equiv 0$$

and

$$X^1 \equiv 0, \quad Y^1 \equiv 0$$

where B^0 is an arbitrary function of the slow argument η.

As a result, first two non-trivial steps of the averaging procedure give

$$z = B^0(\eta) + \varepsilon^2[X^2(\tau, \eta) + Y^2(\tau, \eta)e] + O(\varepsilon^3) \tag{14.56}$$

where, in second order of ε, the solution components are

$$X^2 = \int_{-1}^{\tau} (\tau - s)[G(s, \eta) - \langle G(\tau, \eta)\rangle \tag{14.57}$$

$$-(Q(s, \eta) - \langle Q(\tau, \eta)\rangle)B^0]ds + (r - pB^0)\tau + B^2(\eta)$$

$$Y^2 = \int_{-1}^{\tau} [(\tau - s)(F(s, \eta) - P(s, \eta)B^0) \tag{14.58}$$

$$-\langle(1 - \tau)(F(\tau, \eta) - P(\tau, \eta)B^0)\rangle]ds$$

Here, notation $< \bullet >$ means averaging with respect to τ as defined in (14.47); the vector-function $B^0 = B^0(\eta)$ satisfies equation

$$\frac{d^2B^0}{d\eta^2} + \langle Q(\tau, \eta)\rangle B^0 = \langle G(\tau, \eta)\rangle \tag{14.59}$$

The new arbitrary function of the slow coordinate, $B^2(\eta)$, has to be defined on the next step of the procedure.

Note that the δ-function impulses generated by the derivative $e'(\xi)$ are switching their directions twice per one period of the triangular wave. In many practical cases though, the direction of impulses may remain constant. The corresponding reformulation of the problem can be implemented by introducing the factor -sgn(τ) into the differential equation as follows

$$\frac{d^2z}{dy^2} + [q(\xi, y) - p(y)\mathrm{sgn}(\tau)e'(\xi)]z = g(\xi, y) + r(y)\mathrm{sgn}(\tau)e'(\xi) \tag{14.60}$$

Now, in Eq. (14.60), the term $\mathrm{sgn}(\tau)e'(\xi)$ generates δ-functions of the same direction, whereas the boundary condition (14.55) for the X-component takes the form

$$\tau = \pm 1 : \frac{\partial X}{\partial \tau} = \mp\varepsilon^2[r(y) - p(y)X] \tag{14.61}$$

The form of expressions (14.57) and (14.59) is modified as, respectively,

$$X^2 = \int_{-1}^{\tau} (\tau - s)[G(s,\eta) - \langle G(\tau,\eta)\rangle \tag{14.62}$$

$$-(Q(s,\eta) - \langle Q(\tau,\eta)\rangle)B^0]ds - \frac{\tau^2}{2}(r - pB^0) + B^2(\eta)$$

and,

$$\frac{d^2B^0}{d\eta^2} + (\langle Q(\tau,\eta)\rangle + p)B^0 = \langle G(\tau,\eta)\rangle + r \tag{14.63}$$

where $\eta \equiv y$ and the component Y^2 is still described by (14.58).

Example 14.3.1 Let us consider an infinite beam resting on a discrete foundation represented by the periodic set of linearly elastic springs of stiffness c. The corresponding differential equation of equilibrium is

$$EI\frac{d^4w}{dx^4} + \frac{c}{a}w\sum_{k=-\infty}^{\infty}\delta\left(\frac{x}{a} - 1 - 2k\right) = f\left(\frac{x}{L}\right) \tag{14.64}$$

$$(-\infty < x < \infty)$$

Let us introduce the following dimensionless values

$$y = \frac{x}{L},\ \xi = \frac{y}{\varepsilon},\quad W = \frac{w}{a},\ \gamma = \frac{cL^4}{aEI}$$

where $\varepsilon = a/L << 1$. As a result the above Eq. (14.64) for the beam's center line takes the form

$$\frac{d^4W}{dy^4} - \frac{1}{2}\gamma\,\mathrm{sgn}[\tau(\xi)]e'(\xi)\,W = \frac{\gamma}{c}f(y) \tag{14.65}$$

This equation becomes equivalent to (14.60), after the following substitutions

$$z = \begin{bmatrix} W \\ W'' \end{bmatrix},\quad q = \begin{bmatrix} 0 & -1 \\ 0 & 0 \end{bmatrix},\ p = \frac{\gamma}{2}\begin{bmatrix} 0 & 0 \\ 1 & 0 \end{bmatrix},\ g = \frac{\gamma}{c}f(y)\begin{bmatrix} 0 \\ 1 \end{bmatrix}$$

and $r \equiv 0$. Note that q and g do not have "imaginary parts" in hyperbolic elements (14.51); therefore $G \equiv g$, $Q \equiv q$, $P \equiv 0$, and $F \equiv 0$. Inserting these values in (14.62) and (14.58), one finally obtains

$$z = B^0(y) + \frac{1}{2}\varepsilon^2\tau^2(\xi)\, pB^0(y) + O\left(\varepsilon^3\right)$$

or

$$\begin{bmatrix} W \\ W'' \end{bmatrix} = \left\{ \begin{bmatrix} 1 & 0 \\ 0 & 1 \end{bmatrix} + \frac{1}{4}\gamma\varepsilon^2\tau^2\left(\frac{y}{\varepsilon}\right) \begin{bmatrix} 0 & 0 \\ 1 & 0 \end{bmatrix} \right\} \begin{bmatrix} B_1^0 \\ B_2^0 \end{bmatrix} + O\left(\varepsilon^3\right) \tag{14.66}$$

where the term $\varepsilon^2 B^2(y)$ is ignored compared to the leading-order term $B^0(y)$; however, the terms of order ε^2 describing the discreteness effects are maintained. The matrix-column $B^0 = [B_1^0,\ B_2^0]^T$ is determined from Eq. (14.63). In a component-wise form, this equation reads

$$\frac{d^2}{dy^2}\begin{bmatrix} B_1^0 \\ B_2^0 \end{bmatrix} + \frac{1}{2}\begin{bmatrix} 0 & -2 \\ \gamma & 0 \end{bmatrix}\begin{bmatrix} B_1^0 \\ B_2^0 \end{bmatrix} = \frac{\gamma}{c}\begin{bmatrix} 0 \\ f(y) \end{bmatrix} \tag{14.67}$$

This system is equivalent to

$$\frac{d^4 B_1^0}{dy^4} + \frac{\gamma}{2} B_1^0 = \frac{\gamma}{c} f(y) \tag{14.68}$$

and $B_2^0 = d^2 B_1^0/dy^2$. Note that Eq. (14.68) is the result of a homogenization of Eq. (14.65) with respect to the fast spatial scale ξ. In other words, Eq. (14.68) describes an elastic beam resting on the effectively continuous elastic foundation. In order to illustrate the asymptotic solution, let us consider the case of sine-wave loading, $f(x/L) \equiv q_0 \sin(\pi x/L)$, where q_0 =const. Taking into account only the leading order "slow" and "fast" components gives the bending moment in terms of the original variables

$$M(x) = EI\frac{d^2 w}{dx^2} = -M_0\left[1 - \gamma\left(\frac{a}{2\pi L}\right)^2 \tau^2\left(\frac{x}{a}\right)\right] \sin\frac{\pi x}{L} \tag{14.69}$$

where $M_0 = 2q_0\pi^2 L^2/(2\pi^4 + \gamma)$. The bending moment diagram is given in Fig. 14.5.

Finally, note that the homogenization procedure described in [31] gives the resultant equation in a slow spatial scale and a so-called cell problem in the fast scale. In the above approach, the analog of cell problem associates with the fast oscillating spatial scale given by the triangle wave function $\tau(y/\varepsilon)$. As a result, solution for the cell problem automatically unfolds on the entire structure so that the fast and slow components of elastic states are eventually expressed though the same coordinate in a closed form. Every cell of the infinite array of cells is associated with same standard interval $-1 < \tau < 1$. Further clarifications are given in the next section.

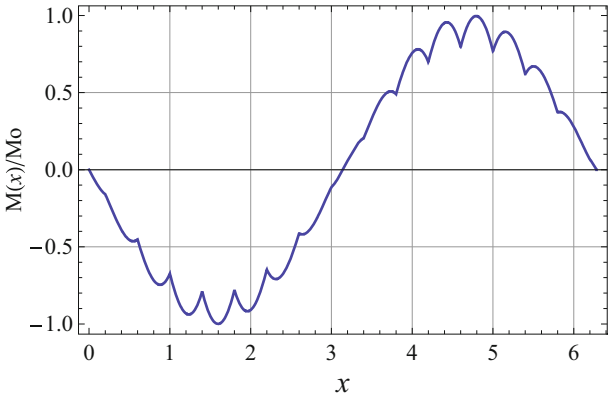

Fig. 14.5 Bending moment of the beam on the discrete elastic foundation; numerical values of the parameters are as follows: $L = \pi$, $a = 0.2$, and $\gamma = 1948.0$

14.4 Wave Propagation in 1D Periodic Layered Composites

Propagation of waves in periodic media has been of significant interest in various branches of optics, acoustics, and elastodynamics for several decades due to a widening area of practical applications for composite materials and extensive usage of periodic structures in civil engineering [12, 13, 31, 47, 118, 154, 159, 215, 216]. Periodicity in material properties can serve for passive control of wave propagation in different micro- and macro-systems. Basic physical formulations and analytical methodologies are systemized and documented, for instance, in [35, 36, 56]. Although linear problems may possess exact solutions, different approximate methods are quite popular by two major reasons. First, typical exact solutions are usually represented as a combination of local solutions describing separate layers (cells), while global characterization of propagating waves is of main interest. Second, the exact approaches are usually difficult to extend on even weakly nonlinear materials. Note that the wave dynamics of layered structures possess typical properties of waves in continuous materials and those in discrete lattices, as confirmed by the presence of so-called pass bands and stop bands in dispersion curves. Despite of the extra complexity, such specifics widen the set of analytical, numerical, and experimental tools. This section is based on reference [194].

14.4.1 Governing Equations and Zero-Order Homogenization

Let us consider longitudinal waves propagating along the infinitely periodic composite rod consisting of alternating layers of two elastic materials as shown at the top of Fig. 14.6. The governing one-dimensional wave equation is

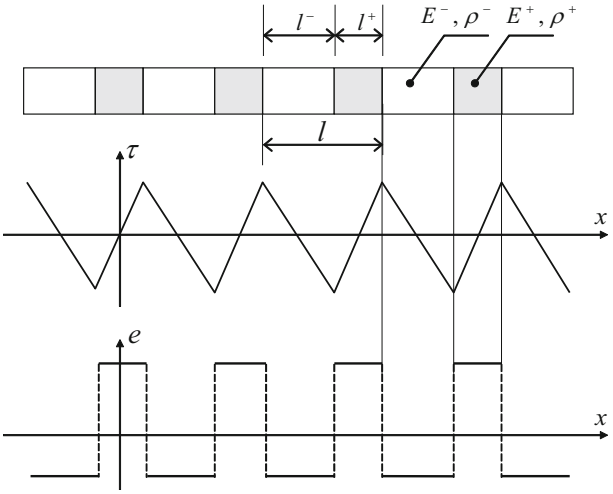

Fig. 14.6 1D periodic composite media with the corresponding basis functions, τ and e; see also Fig. 4.1 of Sect. 4.1.8 for details

$$\rho^{\pm}\frac{\partial^2 u^{\pm}(t,x)}{\partial t^2} - E^{\pm}\frac{\partial^2 u^{\pm}(t,x)}{\partial x^2} = 0 \tag{14.70}$$

where $E^{\pm}$ are Young's moduli; $\rho^{\pm}$ are mass densities; and $u^{\pm}(t,x)$ are displacements; the superscript "+" or "−" indicates different types of layers. Since both types of layers are assumed to be linearly elastic, the longitudinal stress is given by Hooke's law

$$\sigma^{\pm}(t,x) = E^{\pm}\frac{\partial u^{\pm}(t,x)}{\partial x} \tag{14.71}$$

In the case of the perfect bonding between the layers, Eq. (14.70) must be considered under the following continuity conditions at the layer interfaces $x = x_n$

$$u^-(t,x_n) = u^+(t,x_n) \tag{14.72}$$

$$\sigma^-(t,x_n) = \sigma^+(t,x_n) \tag{14.73}$$

$$(n = 0, \pm 1, \pm 2, ...)$$

Due to linearity of the boundary value problem, (14.70) through (14.73), the Floquet-Bloch approach [36] gives the exact dispersion relation [13]. However, when elastic waves are considerably longer than typical cells of the material, the idea of homogenization can be used for easing estimations of global elastodynamic properties of composite structures. In such case, a natural small parameter character-

izing the rate of heterogeneity and the corresponding scales for spatial coordinates can be introduced as

$$\varepsilon = \frac{l}{L} << 1, \qquad \eta = x, \qquad \xi = \frac{x}{\varepsilon} \tag{14.74}$$

where ε is a unitless heterogeneity parameter, l is a cell (layer) thickness, L is the wave length, η is identical to the original coordinate x associated with the spatial scale of the propagating wave, and ξ is another coordinate, associated with the spatial scale of heterogeneity.

Asymptotic homogenization procedures are usually designed in such way that ξ is a *local* coordinate attached to a typical cell of the material, and the corresponding "cell problem" is assumed to depend slowly upon the *global* coordinate η. As a result, the effect of structural periodicity becomes somewhat shadowed in the solution despite the fact that considering a single *arbitrary* cell is justified by periodicity.

Note that a *quasi static* homogenization, corresponding to the limit $\varepsilon \longrightarrow 0$, can be conducted by calculating the effective Young's modulus and mass density of a single elementary cell composed of two different layers. For instance, neglecting the inertia term in Eq. (14.70) gives general solution in the form $u^{\pm} = A^{\pm}x + B^{\pm}$, where $A^{\pm}$ and $B^{\pm}$ are arbitrary constants and $x = 0$ corresponds to the boundary between two different layers. Two of the four constants are eliminated from this solution due to the continuity of displacement and stress at the boundary $x = 0$. Then, calculating the effective strain of the entire cell of two layers, $\epsilon = \left(u^{+}|_{x=l^{+}} - u^{-}|_{x=l^{-}}\right)/l$, gives the effective Young's modulus

$$E_0 = \frac{\sigma^{+}}{\epsilon} = \frac{\sigma^{-}}{\epsilon} = \frac{E^{-}E^{+}}{E^{-}(1-s) + E^{+}s} \tag{14.75}$$

where the parameter $s = l^{-}/l$ describes the "inner geometry" of cells, $l = l^{+} + l^{-}$.

The effective mass density of the cell is given by

$$\rho_0 = \frac{\rho^{+}l^{+} + \rho^{-}l^{-}}{l} = \rho^{-}s + \rho^{+}(1-s) \tag{14.76}$$

Due to the structural periodicity of the composite rod, all the cells must have the same effective Young's modus and mass density. This actually means that the rod is homogenized, and therefore its partial differential equation takes the form

$$\rho_0 \frac{\partial^2 u_0(t,x)}{\partial t^2} - E_0 \frac{\partial^2 u_0(t,x)}{\partial x^2} = 0 \tag{14.77}$$

However, this equation is justified only for very long waves, since it ignores the dispersion of waves caused by their scattering at the boundaries between different layers. Also the heterogeneity effect on wave shapes cannot be captured by the function $u_0(t,x)$.

14.4.2 Structure Attached Triangle Wave Coordinate

Following publication [194], we introduce the periodic nonsmooth coordinate

$$(-\infty, \infty) \ni \xi \longrightarrow \tau \in [-1, 1]: \qquad \tau = \tau\left(\frac{4\xi}{L}, \gamma\right) \tag{14.78}$$

where τ is a triangle wave whose geometry is linked to the structural periodicity of composite as shown in Fig. 14.6.

The period of function (14.78) with respect to the original coordinate x is equal to the length of one cell, l, because $4\xi/L = 4x/l$. Such a space folding coordinate transformation incorporates micro-structural specifics of the material into the differential equations of elastodynamics on the preliminary phase of analysis. The shape of function (14.78) is controlled by the parameter

$$\gamma = -1 + 2s, \quad s = \frac{l^-}{l} \tag{14.79}$$

where the ratio s is defined in (14.76) in such a way that, when the thickness of different layers is the same, $l^- = l^+$, then $\gamma = 0$, and hence function (14.78) describes the triangle wave.

Recall that function (14.78) is non-differentiable at points $\{\xi : \tau = \pm 1\}$ and non-invertible on the entire period. Therefore, using τ as a new independent variable requires a specific complexification of the unknown displacement function u as

$$u(t, x) = U^+(t, \eta, \tau)e_+ + U^-(t, \eta, \tau)e_- \tag{14.80}$$

where the algebraic basis is

$$e_\pm = \frac{1}{2}[1 \mp \gamma \pm (1 - \gamma^2)e] \tag{14.81}$$

and e is a generalized derivative of the triangle wave function (14.78)

$$e = e\left(\frac{4\xi}{L}, \gamma\right) = \partial\tau\left(\frac{4\xi}{L}, \gamma\right)/\partial\left(\frac{4\xi}{L}\right) \tag{14.82}$$

In Eq. (14.81), the parameter of asymmetry γ normalizes the range of change for the basis elements to the standard intervals, $0 \le e_+ \le 1$ and $0 \le e_- \le 1$, as illustrated in Fig. 14.7.

Differentiating (14.80) with respect to the original coordinate x gives yet again the element of the same algebraic structure

$$\frac{\partial u}{\partial x} = D_+U^+e_+ + D_-U^-e_- \tag{14.83}$$

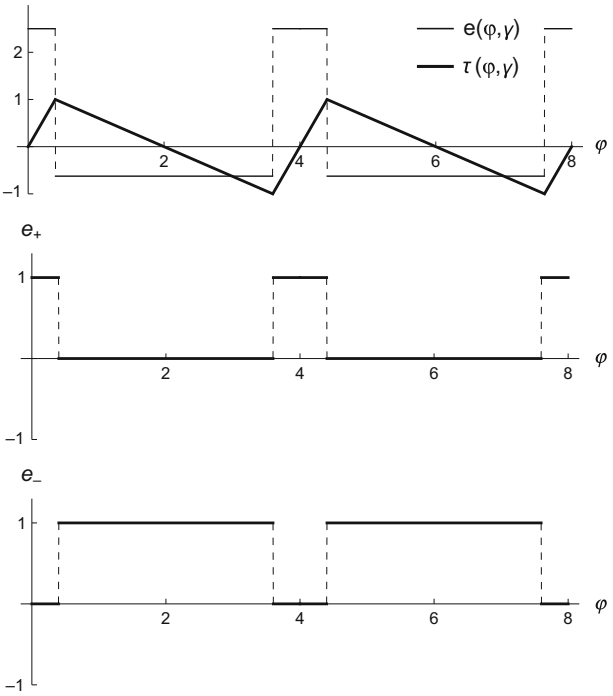

Fig. 14.7 Example of idempotent basis generated by the function $\tau(\varphi, \gamma)$ for $\gamma = 0.6$

where $D^{\pm}$ are linear differential operators,

$$D_{\pm} \equiv \frac{\partial}{\partial \eta} \pm \frac{4}{\varepsilon L(1 \mp \gamma)} \frac{\partial}{\partial \tau}$$

and the following displacement continuity condition is imposed

$$(U^{+} - U^{-})|_{\tau=\pm 1} = 0 \tag{14.84}$$

Condition (14.84) eliminates the δ-function singularities caused by differentiation of the stepwise discontinuous functions $e_{\pm}$ in (14.80). In terms of the original variables, such elimination of singularity is obviously equivalent to the displacement continuity condition.

In compliance with (14.80), the mass density ρ and Young's modulus E are represented in the same algebraic form

$$\begin{aligned} \rho &= \rho^{+} e_{+} + \rho^{-} e_{-} \\ E &= E^{+} e_{+} + E^{-} e_{-} \end{aligned} \tag{14.85}$$

Taking into account (14.83) and (14.85) gives the following expression for stress

$$\sigma = E\frac{\partial u}{\partial x} = E^+ D_+ U^+ e_+ + E^- D_- U^- e_- \equiv \sigma^+ e_+ + \sigma^- e_- \tag{14.86}$$

where orthogonality of the basis elements, $e_+ e_- = 0$, was used; see Fig. 14.7.

Analogously, combining (14.80) and (14.85) brings the inertia force to the form

$$\rho\frac{\partial^2 u}{\partial t^2} = \rho^+\frac{\partial^2 U^+}{\partial t^2}e_+ + \rho^-\frac{\partial^2 U^-}{\partial t^2}e_- \tag{14.87}$$

Expressions (14.86) and (14.87) enable one of describing the composite rod by a "single" partial differential equation in the standard form

$$\rho\frac{\partial^2 u}{\partial t^2} - \frac{\partial \sigma}{\partial x} = 0 \tag{14.88}$$

Now applying the differentiation rule (14.83)–(14.84) to the stress σ gives

$$\left(\rho^+\frac{\partial^2 U^+}{\partial t^2} - E^+ D_+^2 U^+\right)e_+ + \left(\rho^-\frac{\partial^2 U^-}{\partial t^2} - E^- D_-^2 U^-\right)e_- = 0$$

or

$$\rho^\pm\frac{\partial^2 U^\pm}{\partial t^2} - E^\pm D_\pm^2 U^\pm = 0 \tag{14.89}$$

under condition

$$(\sigma^+ - \sigma^-)|_{\tau=\pm 1} = (E^+ D_+ U^+ - E^- D_- U^-)|_{\tau=\pm 1} = 0 \tag{14.90}$$

The boundary condition (14.90) occurs in a similar way to (14.84) as a result of elimination of singularity caused by differentiation of the stress function (14.86). From the physical standpoint, this is equivalent to the continuity of stress at bonding interfaces. Note that, during the procedure of asymptotic integration described below, it is convenient to deal with the continuity conditions in the form

$$(U^+ - U^-)|_{\tau=1} \pm (U^+ - U^-)|_{\tau=-1} = 0 \tag{14.91}$$

and

$$(E^+ D_+ U^+ - E^- D_- U^-)|_{\tau=1} \pm (E^+ D_+ U^+ - E^- D_- U^-)|_{\tau=-1} = 0 \tag{14.92}$$

Equation (14.89) under the boundary conditions (14.91) and (14.92) represents the final result of transition to the structure-based coordinate τ. As compared to the boundary value problem (14.70) through (14.73), the resultant problem still

has the same dimension. However, representation (14.80) eventually provides a closed-form description combining both global and local specifics of wave shapes. In addition, the boundary conditions of continuity for the displacement and stress occur automatically as a result of elimination singularities of their derivatives.

Remark Note that, due to the "functional linearity" property, the above formulation remains valid for nonlinear cases as well. For instance, let the stress-strain relationship for every "positive" layer be described by

$$\sigma^+(t,x) = F\left(\epsilon^+, \frac{\partial \epsilon^+}{\partial t}\right) \tag{14.93}$$

where $\epsilon^+ = \partial u^+/\partial x$ and F is a nonlinear function.

Assuming that every "negative" layer is linearly elastic and conducting the derivations gives the boundary value problem

$$\rho^+ \frac{\partial^2 U^+}{\partial t^2} - D_+\left[F\left(D_+U^+, D_+\frac{\partial U^+}{\partial t}\right)\right] = 0$$
$$\rho^- \frac{\partial^2 U^-}{\partial t^2} - E^- D_-^2 U^- = 0 \tag{14.94}$$

and

$$\left[F\left(D_+U^+, D_+\frac{\partial U^+}{\partial t}\right) - E^- D_- U^-\right]|_{\tau=\pm 1} = 0 \tag{14.95}$$
$$(U^+ - U^-)|_{\tau=\pm 1} = 0$$

Note that nonlinearities may lead to inevitable technical complications unrelated to the key elements of the suggested formulation.

14.4.3 Algorithm of Asymptotic Integration

Let us seek solution of the boundary value problem (14.89), (14.91), and (14.92) in the form of asymptotic expansions

$$U^\pm = u_0(t,\eta) + \sum_{i=1}^{4} \varepsilon^i U_i^\pm(t,\eta,\tau) + O(\varepsilon^5) \tag{14.96}$$

where ε is the heterogeneity parameter defined in (14.74).

Note that the adopted asymptotic order provides sufficient details of the corresponding homogenized equation, whose asymptotics appear to be delayed by two steps of iterations. The time variable preserves its original scale, and zero-order

(generating) term $u_0(t,\eta)$ is assumed to be the same for both components $U^{\pm}$ and hence independent on the coordinate τ. When substituted in (14.80), this term gives

$$u(t,x) = u_0(t,\eta)(e_+ + e_-) + O(\varepsilon) = u_0(t,\eta) + O(\varepsilon) \tag{14.97}$$

due to the property $e_+ + e_- = 1$, as explained by Fig. 14.7.

Further, substituting (14.96) in Eq. (14.89) and the boundary conditions, (14.91) and (14.92) and then matching terms of the same order of ε give a sequence of linear boundary value problems. At every step of iterations, the mathematical structure of differential equations remains the same and takes the form

$$\frac{\partial^2 U_i^{\pm}(t,\eta,\tau)}{\partial \tau^2} = f_i^{\pm}(t,\eta,\tau) \tag{14.98}$$

where the dependence $f_i^{\pm}(t,\eta,\tau)$ on τ is polynomial, which is known as soon as all the previous iterations have been processed, and the dependencies on t and η are combined of different derivatives of $u_0(t,\eta)$.

General solution of Eq. (14.98) can be represented in the integral form

$$U_i^{\pm}(t,\eta,\tau) = \int_0^{\tau} f_i^{\pm}(t,\eta,s)(\tau - s)ds + A_i^{\pm}(t,\eta)\tau + B_i^{\pm}(t,\eta) \tag{14.99}$$

where $A_i^{\pm}(t,\eta)$ and $B_i^{\pm}(t,\eta)$ are four arbitrary functions of the slow arguments.

On the i-iteration, the boundary conditions are not uniquely solvable for all the four unknowns, $A_i^{\pm}(t,\eta)$ and $B_i^{\pm}(t,\eta)$. Three of the four boundary conditions determine $A_i^{\pm}(t,\eta)$ with the following coupling

$$B_i^{+}(t,\eta) = B_i^{-}(t,\eta) \tag{14.100}$$

while the fourth boundary condition can be represented in the form

$$(E^{+}D_{+}U^{+} - E^{-}D_{-}U^{-})|_{\tau=-1}^{\tau=1} = 0 \tag{14.101}$$

where the typical symbol of double substitution is used.

Due to the property, $e_+ + e_- = 1$, the terms $B_i^{\pm}(t,\eta)$ in (14.99) contribute some correction into still arbitrary generating term $u_0(t,\eta)$ (14.96) and thus can be ignored. Boundary condition (14.101) plays a specific role. It is intentionally kept unsatisfied as long as the generating term $u_0(t,\eta)$ is maintained arbitrary. Once a sufficient number of iterations have been processed, the corresponding truncated series is substituted in (14.101) that leads to the homogenized equation for $u_0(t,\eta)$. Note that no operators of averaging are imposed on the original differential equation (14.88). Instead, the homogenized model is generated by the boundary condition

(14.101), which is one of the two continuity conditions for the stress function (14.90).

14.4.4 Homogenized Equation and Solution

Conducting the first four steps of the asymptotic procedure, as described in the previous section, gives the asymptotic solution in the form

$$u(t,x) = u_0(t,x) + \varepsilon u_1(t,x)\tau + \varepsilon^2\left[u_2^+(t,x)e_+ + u_2^-(t,x)e_-\right]\frac{\tau^2-1}{2} + \varepsilon^3\left[\left(u_3^+(t,x)e_+ + u_3^-(t,x)e_-\right)\frac{\tau^3}{6} + \left(A_3^+(t,x)e_+ + A_3^-(t,x)e_-\right)\tau\right] + O(\varepsilon^4) \tag{14.102}$$

where $\eta \equiv x$ $(-\infty < x < \infty)$, $\tau = \tau(4x/l, \gamma)$, and $e_\pm = e_\pm(4x/l, \gamma)$, and different functions of the arguments t and x are sequentially expressed through derivatives of the generating solution $u_0(t,x)$ as

$$u_1 = \frac{L}{4}\frac{\left(1-\gamma^2\right)\left(E^- - E^+\right)}{(1-\gamma)E^- + (1+\gamma)E^+}\frac{\partial u_0}{\partial x}$$

$$u_2^\pm = \mp\frac{L(1\mp\gamma)}{16E^\pm}\left[8E^\pm\frac{\partial u_1}{\partial x} \mp L(1\mp\gamma)\left(\rho^\pm\frac{\partial^2 u_0}{\partial t^2} - E^\pm\frac{\partial^2 u_0}{\partial x^2}\right)\right]$$

$$u_3^\pm = \mp\frac{L(1\mp\gamma)}{16E^\pm}\left[8E^\pm\frac{\partial u_2^\pm}{\partial x} \mp L(1\mp\gamma)\left(\rho^\pm\frac{\partial^2 u_1}{\partial t^2} - E^\pm\frac{\partial^2 u_1}{\partial x^2}\right)\right]$$

$$A_3^\pm = -\frac{3(1\pm\gamma)E^\pm u_3^\pm + (1\mp\gamma)E^-\left(u_3^\pm + 2u_3^\mp\right)}{6\left[(1-\gamma)E^- + (1+\gamma)E^+\right]}$$

The asymptotic order of solution (14.102) is high enough for practical estimations of the heterogeneity effects on wave shapes. One more iteration has to be processed though in order to see such effects in terms of the homogenized equation, which is obtained by substituting the components $U^\pm$ (14.99) into the boundary condition (14.101)

$$\rho_0\frac{\partial^2 u_0(t,x)}{\partial t^2} = E_0\frac{\partial^2 u_0(t,x)}{\partial x^2} + (\varepsilon L)^2 E_2\frac{\partial^4 u_0(t,x)}{\partial x^4} + O(\varepsilon^4) \tag{14.103}$$

The effective parameters are determined by collecting terms with different derivatives and summarized as

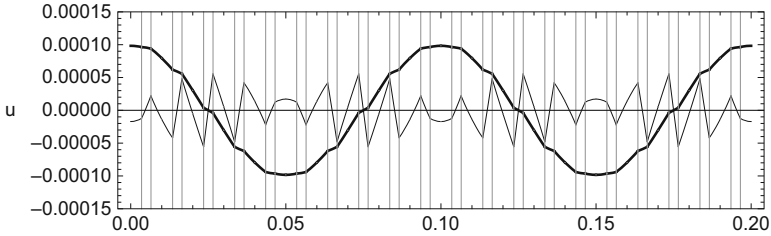

Fig. 14.8 Spatial shape of the propagating wave through the composite rod obtained from third-order asymptotic solution (14.102) (thick line) and correction to the homogenized solution with the amplitude zoomed by factor ε^{-1} (thin line); $E^+ = 7\cdot 10^{10}$ N/m^2, $E^- = 21\cdot 10^{10}$N/m^2, $\rho^- = 7800$ kg/m^3, $\rho^+ = 2700$ kg/m^3, $l = 0.01$ m, $L = 0.1$ m, ($\varepsilon = 0.1$), $\gamma = -0.4$

$$\rho_0 = \frac{1}{2}\left[(1+\gamma)\rho^- + (1-\gamma)\rho^+\right]$$
$$E_0 = \frac{2E^-E^+}{(1-\gamma)E^- + (1+\gamma)E^+} \tag{14.104}$$
$$E_2 = \frac{1}{6}\frac{\left(1-\gamma^2\right)^2 E^-E^+\left(E^-\rho^- - E^+\rho^+\right)^2}{\left[(1-\gamma)E^- + (1+\gamma)E^+\right]^3\left[(1+\gamma)\rho^- + (1-\gamma)\rho^+\right]^2}$$

Note that substituting (14.79) in E_0 and ρ_0 gives (14.75) and (14.76), respectively. Therefore, Eq. (14.103) is reduced to Eq. (14.77) as $\varepsilon \longrightarrow 0$. Otherwise, the term of order ε^2 describes the effect of wave dispersion due to the structural heterogeneity of the rod. After substitution (14.79), the effective parameters (14.104) coincide those obtained in [64] and [12] by different methods. However, the main target of this section is "closed-form" solution (14.102) describing both local and global wave shapes within the same expression. As a result, it is possible to visualize cell to cell transitions over the long wave length as shown in Fig. 14.8. Some features, such as beating effects in the nonsmooth component of solution, would be difficult to observe by other means. Besides, Fig. 14.8 validates the asymptotic property of expansion (14.102) since the maxima of correction terms, $u - u_0$, even with magnifying factor $\varepsilon^{-1} = 10$ are about 50% below the wave amplitude.

14.5 Acoustic Waves from Nonsmooth Periodic Boundary Sources

This section deals with two-dimensional acoustic waves propagating from a discontinuous periodic source located at the boundary of half-infinite space. It is shown that introducing the triangular wave function as a specific spatial coordinate

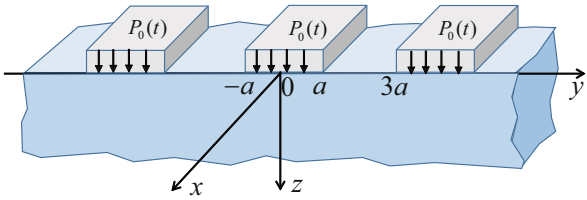

Fig. 14.9 A half-infinite acoustic media excited by the stepwise discontinuous periodic pressure source at the upper boundary

naturally eliminates discontinuities from the boundary condition associated with the active boundary.

For illustrating purposes, let us consider the case of two-dimensional stationary waves propagating in the half-infinite media from a piecewise-linear periodic boundary source as shown in Fig. 14.9.

Let us describe acoustic waves by the linear wave equation in the standard form

$$\frac{1}{c_f^2}\frac{\partial^2 P}{\partial t^2} = \frac{\partial^2 P}{\partial x^2} + \frac{\partial^2 P}{\partial y^2} + \frac{\partial^2 P}{\partial z^2} \tag{14.105}$$

where P is a pressure deviation from the static equilibrium pressure; x, y, z, and t are spatial coordinates and time, respectively; and c_f is the speed of sound in the media.

Further, the plane problem is considered when $P = P(t, y, z)$, and therefore, $\partial^2 P/\partial x^2 = 0$. Such an assumption can be justified by sufficiently long piezoelectric rods whose characteristics are constant along the x-coordinate. Suppose that the pressure generated by the rods near the boundary is $P_0 = A \sin \Omega t$, where A and Ω are constant amplitude and frequency, respectively.

Let the boundary condition at $z = 0$ to have the form

$$P(t, y, 0) = \begin{cases} P_0(t) & \text{for } (4n-1)\,a \le y \le (4n+1)\,a \\ 0 & \text{for } (4n+1)\,a \le y \le (4n+3)\,a \end{cases} \tag{14.106}$$

$$n = 0, \pm 1, \pm 2, \ldots$$

Note that, based on what is actually known near the fluid-source interface, the boundary condition can also be formulated for pressure derivatives. From the mathematical standpoint, this do not affect much the solution procedure though.

Let us seek the steady-state solution, which is periodic with respect to t and y and remains bounded as $z \to \infty$.

Since the boundary condition is periodic along y-coordinate with period $T = 4a$, then, according to the idea of nonsmooth argument transformation, the triangular wave periodic coordinate is introduced as $y \to \tau(y/a)$. As a result, the boundary condition (14.106) and yet unknown solution are represented as, respectively,

$$P(t, y, z)|_{z=0} = \frac{1}{2}P_0(t) + \frac{1}{2}P_0(t)\,\tau'\left(\frac{y}{a}\right) \tag{14.107}$$

and

$$P(t, y, z) = P_1(t, \tau(y/a), z) + P_2(t, \tau(y/a), z)\tau'(y/a) \tag{14.108}$$

where the components P_1 and P_2 are considered as new unknown functions.

Taking into account the expression $[\tau'(y/a)]^2 = 1$ gives first generalized derivative of the original unknown function in the form

$$\frac{\partial P}{\partial y} = \frac{1}{a}\frac{\partial P_2}{\partial \tau} + \frac{1}{a}\frac{\partial P_1}{\partial \tau}\tau'\left(\frac{y}{a}\right) + \frac{1}{a}P_2\tau''\left(\frac{y}{a}\right) \tag{14.109}$$

Since the function $P(t, y, z)$ has to be continuous with respect to y in the unbounded open region $z > 0$, then the periodic singular term τ'' in (14.109) must be eliminated by imposing condition

$$P_2|_{\tau=\pm 1} = 0 \tag{14.110}$$

Analogously, second derivative takes the form

$$\frac{\partial^2 P}{\partial y^2} = \frac{1}{a^2}\frac{\partial^2 P_1}{\partial \tau^2} + \frac{1}{a^2}\frac{\partial^2 P_2}{\partial \tau^2}\tau'\left(\frac{y}{a}\right) \tag{14.111}$$

under the condition

$$\frac{\partial P_1}{\partial \tau}|_{\tau=\pm 1} = 0 \tag{14.112}$$

Note that both derivatives, (14.109) and (14.111), as well as the original function (14.108) appear to have the same algebraic structure of hyperbolic numbers. Obviously, differentiation with respect to t and z preserves such a structure as well. As a result, substituting the second derivatives into differential equation (14.105) and collecting separately terms related to each of the basis elements $\{1, \tau'\}$ give two partial differential equations for the components of representation (14.108)

$$\frac{1}{c_f^2}\frac{\partial^2 P_i}{\partial t^2} = \frac{1}{a^2}\frac{\partial^2 P_i}{\partial \tau^2} + \frac{\partial^2 P_i}{\partial z^2} \tag{14.113}$$

$$(i = 1, 2)$$

Substituting then (14.108) in (14.107) gives the corresponding set of boundary conditions

$$P_i(t, \tau, z)|_{z=0} = \frac{1}{2}P_0(t) = \frac{1}{2}A\sin\Omega t \tag{14.114}$$

Now Eqs. (14.113) and boundary conditions (14.110), (14.112), and (14.114) constitute two independent boundary value problems for the components P_1 and P_2. *However, the result achieved is that no discontinuous functions are present anymore in the boundary conditions*.

Solving the above boundary value problems by the standard method of separation of variables gives finally

$$P(t, y, z) = \frac{1}{2} A \sin \Omega \left(t - \frac{z}{c_f} \right)$$
$$+A \left\{ \sum_{k=1}^{m} \frac{(-1)^{k-1}}{(k - 1/2)\,\pi} \sin \Omega\,(t - K_k z) \cos \left[\left(k - \frac{1}{2} \right) \pi \tau \left(\frac{y}{a} \right) \right] \right. \tag{14.115}$$
$$\left. + \sum_{k=m+1}^{\infty} \frac{(-1)^{k-1}}{(k - 1/2)\,\pi} \sin \Omega t \exp\left(-\chi_k z\right) \cos \left[\left(k - \frac{1}{2} \right) \pi \tau \left(\frac{y}{a} \right) \right] \right\} \tau' \left(\frac{y}{a} \right)$$

where

$$K_k = \sqrt{\left(\frac{\Omega}{c_f} \right)^2 - \left(k - \frac{1}{2} \right)^2 \left(\frac{\pi}{a} \right)^2}, \qquad k = 1, ..., m$$
$$\chi_k = \sqrt{\left(k - \frac{1}{2} \right)^2 \left(\frac{\pi}{a} \right)^2 - \left(\frac{\Omega}{c_f} \right)^2}, \qquad k = m + 1, ...$$

and m is the maximum number at which the expression under the first square root is still positive.

A three-dimensional illustration of solution (14.115) is given by Figs. 14.10 and 14.11 for two different magnitudes of the frequency Ω. Besides, it is seen that shorter waves are carrying the information about the discreteness of the wave source for a longer distance from the source.

Note that solution (14.115) could be obtained in terms of the standard trigonometric expansions by applying the method of separation of variables directly to the original problem, (14.105) and (14.106). However, the derivation of solution (14.115) implies no integration of discontinuous functions, since all the discontinuities have been captured in advance by transformation (14.108).

It is also worth to note that the terms of series (14.115) are calculated on the standard interval, $-1 \le \tau \le 1$, which is covered by one half of the total period, whereas the standard Fourier expansions must be built over the entire period. This is due to the fact that representation (14.108) automatically unfolds the half-period domain on the infinite spatial interval.

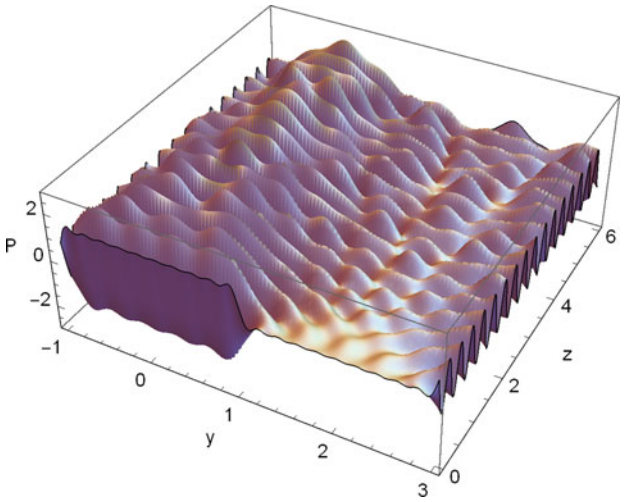

Fig. 14.10 Acoustic wave surface for the set of parameters : $c_f = 10.0$, $a = 1$, $\Omega = 172$, $t = 3$, and $A = 2$

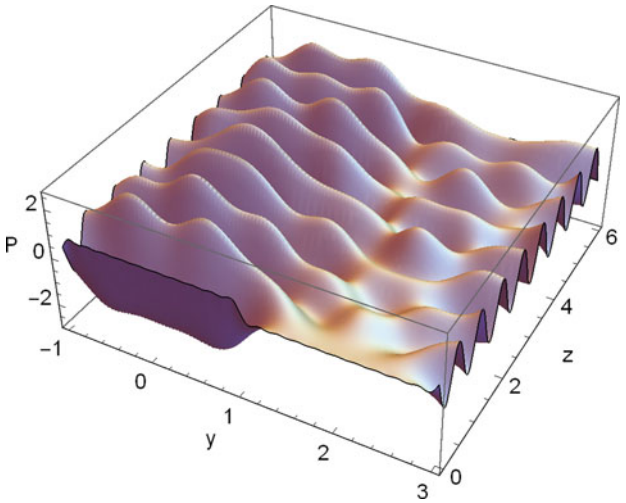

Fig. 14.11 Acoustic wave surface for the set of parameters: $c_f = 10.0$, $a = 1$, $\Omega = 86$, $t = 3$, and $A = 2$

14.6 Spatiotemporal Periodicity

As a possible generalization of the approach, let us consider, for instance, the boundary condition in the form

$$P(t, y, z)|_{z=0} = f(t, y) \tag{14.116}$$

where the function f is periodic with temporal period $T_t = 2\pi/\Omega$ and spatial period $T_y = 4a$.

Introducing the triangular wave spatial argument, $\tau_y = \tau(y/a)$, gives

$$f(t, y) = F_1(t, \tau(y/a)) + F_2(t, \tau(y/a))\tau'(y/a) \tag{14.117}$$

where

$$\begin{aligned} F_1(t, \tau_y) &= \frac{1}{2}[f(t, a\tau_y) + f(t, 2a - a\tau_y)] \\ F_2(t, \tau_y) &= \frac{1}{2}[f(t, a\tau_y) - f(t, 2a - a\tau_y)] \end{aligned} \tag{14.118}$$

In a similar way, introducing the triangular wave temporal argument, $\tau_t = \tau(2\Omega t/\pi)$, into both of the components, F_1 and F_2, gives eventually expression of the form

$$f(t, y) = f_0(\tau_t, \tau_y)e_0 + f_1(\tau_t, \tau_y)e_1 + f_2(\tau_t, \tau_y)e_2 + f_3(\tau_t, \tau_y)e_3 \tag{14.119}$$

where components $f_i(\tau_t, \tau_y)$ are uniquely determined by rule (14.118) applied to each of the two arguments, and the following basis is introduced

$$\begin{aligned} e_0 &= 1 \\ e_1 &= \tau'(2\Omega t/\pi) \\ e_2 &= \tau'(y/a) \\ e_3 &= e_1 e_2 \end{aligned} \tag{14.120}$$

Basis (14.120) obeys the table of products

$$\begin{array}{cccccc} \times & e_0 & e_1 & e_2 & e_3 \\ e_0 & 1 & e_1 & e_2 & e_3 \\ e_1 & e_1 & 1 & e_3 & e_2 \\ e_2 & e_2 & e_3 & 1 & e_1 \\ e_3 & e_3 & e_2 & e_1 & 1 \end{array} \tag{14.121}$$

Now, the acoustic pressure is represented in the similar to (14.119) form

$$P(t, y, z) = P_0(\tau_t, \tau_y, z)e_0 + P_1(\tau_t, \tau_y, z)e_1 + P_2(\tau_t, \tau_y, z)e_2 + P_3(\tau_t, \tau_y, z)e_3 \tag{14.122}$$

Regarding the problem described in the previous section, the components of representation (14.122) can be obtained as an exercise by introducing the argument τ_t directly into solution (14.115). However, formulations based on representation (14.122) become technically reasonable whenever the boundary pressure is adequately described by the functions τ_t and τ_y or their different combinations, for instance, polynomials. In such cases, polynomial approximations with respect to the bounded arguments may appear to be more effective as compared to Fourier expansions. Let us, for instance, $P_0(t)$ describes the periodic sequence of rectangular spikes of the amplitude A,

$$P_0(t) = \frac{1}{2}A\left[1 + \tau'\left(\frac{2\Omega}{\pi}t\right)\right] \equiv \frac{1}{2}A(1 + e_1) \tag{14.123}$$

Then, boundary condition (14.107) takes the form

$$P(t, y, z)|_{z=0} = \frac{1}{4}A(1 + e_1)(1 + e_2) \equiv \frac{1}{4}A(e_0 + e_1 + e_2 + e_3) \tag{14.124}$$

where the basis elements $\{e_0, e_1, e_2, e_3\}$ are given by (14.120) and the table of products (14.121) is taken into account.

Now, substituting representation (14.122) in (14.124) gives the boundary conditions for its components at $z = 0$ as follows

$$P_i(\tau_t, \tau_y, 0) = \frac{1}{4}A; \quad i = 0,...,3$$

Finally, the three-dimensional case can be considered by adding periodicity of the source along the x-direction at the boundary $z = 0$ and introducing the corresponding triangular wave argument, say τ_x. The corresponding rules for algebraic manipulations would be analogous to those generated by the arguments τ_t and τ_y. However, necessary details are illustrated below on another model.

14.7 Membrane on a Two-Dimensional Periodic Foundation

Consider an infinite membrane resting on a linearly elastic foundation of the stiffness $K(x, y)$ under the transverse load $q(x, y)$. Assuming that both the stiffness

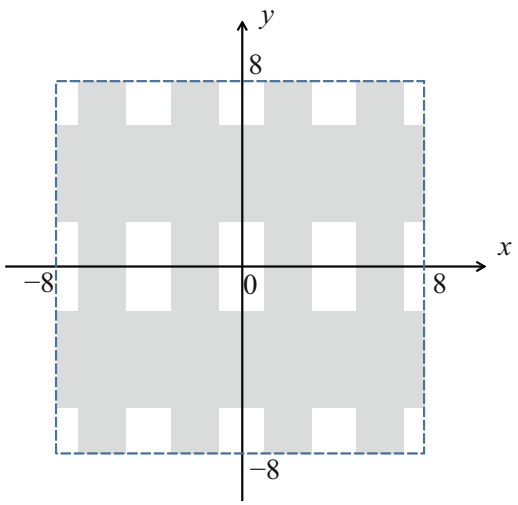

Fig. 14.12 Fragment of the map of periodic elastic foundation; $a = 1.0$ and $b = 2.0$

K and load q are measured per unit membrane tension T, the partial differential equation of equilibrium is represented in the form

$$\Delta u - K(x, y)u = q(x, y) \tag{14.125}$$

$$\Delta = \frac{\partial^2}{\partial x^2} + \frac{\partial^2}{\partial y^2}$$

where $u = u(x, y)$ is the membrane transverse deflection.

The foundation is assumed to be stepwise discontinuous and periodic along each of the coordinates as described by the function

$$K(x, y) = \frac{k}{4}\left[1 + \tau'\left(\frac{x}{a}\right)\right]\left[1 + \tau'\left(\frac{y}{b}\right)\right] \tag{14.126}$$

With reference to Fig. 14.12, function (14.126) is defined on the infinite plane, such that

$$K(x, y) = \begin{cases} 0 & (x, y) \in \text{any "dark field"} \\ k & (x, y) \in \text{any "light field"} \end{cases} \tag{14.127}$$

In the same way, Fig. 14.13 provides maps for the elements of basis

$$\begin{aligned} e_0 &= 1 \\ e_1 &= \tau'(x/a) \\ e_2 &= \tau'(y/b) \end{aligned} \tag{14.128}$$

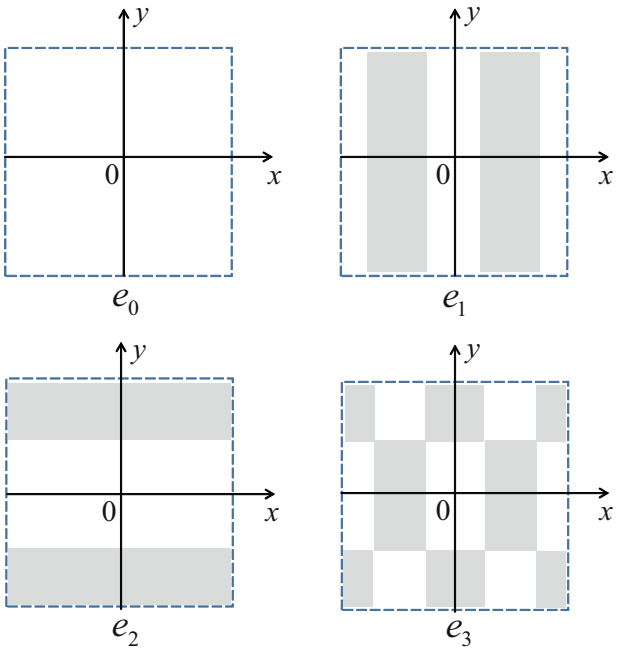

Fig. 14.13 The standard basis map: each of the elements is equal to unity within light domains and zero within dark domains; square areas $[-4 < x < 4, -4 < y < 4]$ are shown under the parameters $a = 1$ and $b = 2$

$$e_3 = e_1 e_2$$

The above table of products (14.121) is still valid for basis (14.128). As a result, function (14.126) takes eventually the form

$$K(x, y) = \frac{k}{4}(e_0 + e_1 + e_2 + e_3) \tag{14.129}$$

Now let us represent the membrane deflection in the form

$$\begin{aligned} u(x, y) = {} & X(\tau_x, \tau_y, x, y)e_0 + Y(\tau_x, \tau_y, x, y)e_1 \\ & + Z(\tau_x, \tau_y, x, y)e_2 + W(\tau_x, \tau_y, x, y)e_3 \end{aligned} \tag{14.130}$$

where $\tau_x = \tau(x/a)$ and $\tau_y = \tau(y/b)$ are triangular waves whose lengths are determined by the periods of foundation along $x-$ and $y-$ direction, respectively; scales of the explicitly present variables, x and y, are associated with the scales of loading $q(x, y)$, which is assumed to be slow as compared to the spatial rate of foundation.

Note that both linear and nonlinear algebraic manipulations with combinations of type (14.130) are dictated by the table of products (14.121). For example, taking into account (14.129) and (14.130) gives

$$Ku = \frac{k}{4}(X + Y + Z + W)(e_0 + e_1 + e_2 + e_3) \tag{14.131}$$

High-order derivatives of (14.130) are simplified by using the table of products (14.121) and introducing specific differential operators as follows.

First, using the chain rule gives

$$\frac{d\tau_x}{dx} = \frac{1}{a}\tau'(x/a) = \frac{1}{a}e_1 \tag{14.132}$$

$$\frac{d\tau_y}{dy} = \frac{1}{b}\tau'(y/a) = \frac{1}{b}e_2 \tag{14.133}$$

Then, taking into account (14.121), (14.128), (14.132), and (14.133) gives first derivatives of (14.130) in the form

$$\begin{aligned}\frac{\partial u}{\partial x} = &\left(\frac{1}{a}\frac{\partial Y}{\partial \tau_x} + \frac{\partial X}{\partial x}\right)e_0 + \left(\frac{1}{a}\frac{\partial X}{\partial \tau_x} + \frac{\partial Y}{\partial x}\right)e_1 \\ &+ \left(\frac{1}{a}\frac{\partial W}{\partial \tau_x} + \frac{\partial Z}{\partial x}\right)e_2 + \left(\frac{1}{a}\frac{\partial Z}{\partial \tau_x} + \frac{\partial W}{\partial x}\right)e_3 \\ &+ \frac{1}{a}(Y + We_2)\frac{de_1(x/a)}{d(x/a)}\end{aligned} \tag{14.134}$$

$$\begin{aligned}\frac{\partial u}{\partial y} = &\left(\frac{1}{b}\frac{\partial Z}{\partial \tau_y} + \frac{\partial X}{\partial y}\right)e_0 + \left(\frac{1}{b}\frac{\partial W}{\partial \tau_y} + \frac{\partial Y}{\partial y}\right)e_1 \\ &+ \left(\frac{1}{b}\frac{\partial X}{\partial \tau_y} + \frac{\partial Z}{\partial y}\right)e_2 + \left(\frac{1}{b}\frac{\partial Y}{\partial \tau_y} + \frac{\partial W}{\partial y}\right)e_3 \\ &+ \frac{1}{b}(Z + We_1)\frac{de_2(y/b)}{d(y/b)}\end{aligned} \tag{14.135}$$

Last addends in (14.134) and (14.135) include derivatives of the stepwise discontinuous functions $e_1(x/a)$ and $e_2(y/b)$. Such derivatives are expressed through Dirac δ-functions and therefore must be excluded from the expressions (14.134) and (14.135) due to continuity of the original function $u(x, y)$. The δ-functions are eliminated under the boundary conditions

$$\begin{aligned}Y|_{\tau_x=\pm 1} &= 0 \\ W|_{\tau_x=\pm 1} &= 0\end{aligned} \tag{14.136}$$

and

$$Z|_{\tau_y=\pm 1} = 0$$
$$W|_{\tau_y=\pm 1} = 0 \tag{14.137}$$

The rest of terms in (14.134) and (14.135) represent linear combinations of the basis $\{e_0, e_1, e_2, e_3\}$. In order to formalize the differentiation procedure, let us associate expansion (14.130) with the vector-column

$$\mathbf{u} = \begin{bmatrix} X \\ Y \\ Z \\ W \end{bmatrix} \tag{14.138}$$

In a similar way, let us introduce the vector-columns $\mathbf{u}_x$ and $\mathbf{u}_y$ associated with derivatives (14.134) and (14.135) under conditions (14.136) and (14.137), respectively,[1]

$$\mathbf{u}'_x = \mathbf{D}_x \mathbf{u}$$
$$\mathbf{u}'_y = \mathbf{D}_y \mathbf{u} \tag{14.139}$$

where

$$\mathbf{D}_x = \begin{bmatrix} \partial/\partial x & a^{-1}\partial/\partial\tau_x & 0 & 0 \\ a^{-1}\partial/\partial\tau_x & \partial/\partial x & 0 & 0 \\ 0 & 0 & \partial/\partial x & a^{-1}\partial/\partial\tau_x \\ 0 & 0 & a^{-1}\partial/\partial\tau_x & \partial/\partial x \end{bmatrix} \tag{14.140}$$

and

$$\mathbf{D}_y = \begin{bmatrix} \partial/\partial y & 0 & b^{-1}\partial/\partial\tau_y & 0 \\ 0 & \partial/\partial y & 0 & b^{-1}\partial/\partial\tau_y \\ b^{-1}\partial/\partial\tau_y & 0 & \partial/\partial y & 0 \\ 0 & b^{-1}\partial/\partial\tau_y & 0 & \partial/\partial y \end{bmatrix} \tag{14.141}$$

These differential matrix operators automatically generate high-order derivatives of combination (14.130) provided that necessary smoothness (boundary) conditions hold. For instance, the components of expansion for Δu are given by the elements of vector-column $(\mathbf{D}_x^2 + \mathbf{D}_y^2)\mathbf{u}$ under conditions

[1] Note that $\mathbf{u}'_x$ is not $\partial\mathbf{u}/\partial x$.

$$\left(\frac{1}{a}\frac{\partial X}{\partial \tau_x}+\frac{\partial Y}{\partial x}\right)|_{\tau_x=\pm 1}=0$$
$$\left(\frac{1}{a}\frac{\partial Z}{\partial \tau_x}+\frac{\partial W}{\partial x}\right)|_{\tau_x=\pm 1}=0 \tag{14.142}$$

$$\left(\frac{1}{b}\frac{\partial X}{\partial \tau_y}+\frac{\partial Z}{\partial y}\right)|_{\tau_y=\pm 1}=0$$
$$\left(\frac{1}{b}\frac{\partial Y}{\partial \tau_y}+\frac{\partial W}{\partial y}\right)|_{\tau_y=\pm 1}=0 \tag{14.143}$$

Consider now the particular case $a=b=\varepsilon \ll 1$. Following the differentiation and algebraic manipulation rules as introduced above, and substituting (14.130) in (14.125), gives

$$\begin{aligned}
&\Delta_\tau X+2\varepsilon\left(\frac{\partial^2 Y}{\partial \tau_x \partial x}+\frac{\partial^2 Z}{\partial \tau_y \partial y}\right)+\varepsilon^2(\Delta X-F)=\varepsilon^2 q(x,y)\\
&\Delta_\tau Y+2\varepsilon\left(\frac{\partial^2 X}{\partial \tau_x \partial x}+\frac{\partial^2 W}{\partial \tau_y \partial y}\right)+\varepsilon^2(\Delta Y-F)=0\\
&\Delta_\tau Z+2\varepsilon\left(\frac{\partial^2 W}{\partial \tau_x \partial x}+\frac{\partial^2 X}{\partial \tau_y \partial y}\right)+\varepsilon^2(\Delta Z-F)=0\\
&\Delta_\tau W+2\varepsilon\left(\frac{\partial^2 Z}{\partial \tau_x \partial x}+\frac{\partial^2 Y}{\partial \tau_y \partial y}\right)+\varepsilon^2(\Delta W-F)=0
\end{aligned} \tag{14.144}$$

where $\Delta_\tau=\partial^2/\partial\tau_x^2+\partial^2/\partial\tau_y^2$, $\Delta=\partial^2/\partial x^2+\partial^2/\partial y^2$, and symbol F denotes the following group of terms related to the elastic foundation

$$F\equiv\frac{1}{4}k(X+Y+Z+W) \tag{14.145}$$

Boundary conditions (14.142) and (14.143) can be simplified due to (14.136) and (14.137). As a result, the complete set of boundary conditions takes the form

$$\begin{aligned}
\frac{\partial X}{\partial \tau_x}|_{\tau_x=\pm 1}&=0, \quad \frac{\partial X}{\partial \tau_y}|_{\tau_y=\pm 1}=0\\
Y|_{\tau_x=\pm 1}&=0, \quad \frac{\partial Y}{\partial \tau_y}|_{\tau_y=\pm 1}=0\\
\frac{\partial Z}{\partial \tau_x}|_{\tau_x=\pm 1}&=0, \quad Z|_{\tau_y=\pm 1}=0\\
W|_{\tau_x=\pm 1}&=0, \quad W|_{\tau_y=\pm 1}=0
\end{aligned} \tag{14.146}$$

Note that Eq. (14.144) has constant coefficients, whereas the stepwise discontinuities of foundation have been absorbed by the triangular wave arguments τ_x and τ_y. The corresponding boundary conditions (14.146) generate a so-called "cell problem" [100] within the rectangular domain $\{-1 \le \tau_x \le 1, -1 \le \tau_y \le 1\}$. Therefore, the arguments τ_x and τ_y locally describe the fast varying component of membrane shape. In contrast, the explicitly present coordinates x and y describe the slow component in the infinite plane $\{-\infty < x < \infty, -\infty < y < \infty\}$. Finally, the increase in number of Eqs. (14.144) of-course complicates solution procedures from the technical standpoint. However, the obvious symmetry of equations helps to ease the corresponding derivations. For instance, Eqs. (14.144) can be decoupled by introducing new unknown functions $U_i = U_i(\tau_x, \tau_y, x, y)$ $(i = 1, .., 4)$ as follows

$$\begin{aligned} U_1 &= X + Y + Z + W \\ U_2 &= X + Y - Z - W \\ U_3 &= X - Y + Z - W \\ U4 &= X - Y - Z + W \end{aligned} \tag{14.147}$$

Linear transformation (14.147) however makes boundary conditions (14.146) coupled. New boundary conditions are given by the inverse substitution in (14.146)

$$\begin{aligned} X &= \frac{1}{4}(U_1 + U_2 + U_3 + U_4) \\ Y &= \frac{1}{4}(U_1 + U_2 - U_3 - U_4) \\ Z &= \frac{1}{4}(U_1 - U_2 + U_3 - U_4) \\ W &= \frac{1}{4}(U_1 - U_2 - U_3 + U_4) \end{aligned} \tag{14.148}$$

Note that transformation (14.147) can be effectively incorporated at the very beginning of transformations by using the idempotent basis as described in the next section.

14.8 The Idempotent Basis for Two-Dimensional Structures

The two-dimensional idempotent basis is introduced as follows

$$i_1 = e_1^+ e_2^+ = \frac{1}{4}(e_0 + e_1)(e_0 + e_2) = \frac{1}{4}(e_0 + e_1 + e_2 + e_3)$$

$$
\begin{aligned}
i_2 &= e_1^+ e_2^- = \frac{1}{4}(e_0 + e_1)(e_0 - e_2) = \frac{1}{4}(e_0 + e_1 - e_2 - e_3) \\
i_3 &= e_1^- e_2^+ = \frac{1}{4}(e_0 - e_1)(e_0 + e_2) = \frac{1}{4}(e_0 - e_1 + e_2 - e_3) \\
i_4 &= e_1^- e_2^- = \frac{1}{4}(e_0 - e_1)(e_0 - e_2) = \frac{1}{4}(e_0 - e_1 - e_2 + e_3)
\end{aligned} \tag{14.149}
$$

where the standard basis e_i is defined by (14.128) and the table of products (14.121), and the following notations for one-dimensional idempotent basis are used

$$
\begin{aligned}
e_k^{\pm} &= \frac{1}{2}(e_0 \pm e_k) \\
e_k^+ e_k^- &= 0; \quad (k = 1, 2)
\end{aligned} \tag{14.150}
$$

The main reason for using basis (14.149) is that its table of products has the normalized diagonal form

$$
i_k i_n = \delta_{kn} \tag{14.151}
$$

where δ_{kn} is the Kronecker symbol.

The geometrical meaning of property (14.151) follows from the maps in Fig. 14.14.

In this basis, representation (14.130) takes the form

$$
u(x, y) = \sum_{k=1}^{4} U_k(\tau_x, \tau_y, x, y) i_k \tag{14.152}
$$

As a result,

$$
f\left(\sum_{k=1}^{4} U_k i_k\right) = \sum_{k=1}^{4} f(U_k) i_k \tag{14.153}
$$

where f is practically any function, linear or nonlinear.

First-order partial derivatives of representation (14.153) are obtained as follows

$$
\begin{aligned}
&\frac{\partial u(x, y)}{\partial x} \\
&= \sum_{k=1}^{4} \left[\frac{1}{a} \frac{\partial U_k(\tau_x, \tau_y, x, y)}{\partial \tau_x} e_1 i_k + \frac{\partial U_k(\tau_x, \tau_y, x, y)}{\partial x} i_k + U_k(\tau_x, \tau_y, x, y) \frac{\partial i_k}{\partial x} \right]
\end{aligned} \tag{14.154}
$$

Further, taking into account (14.149) and (14.150), gives

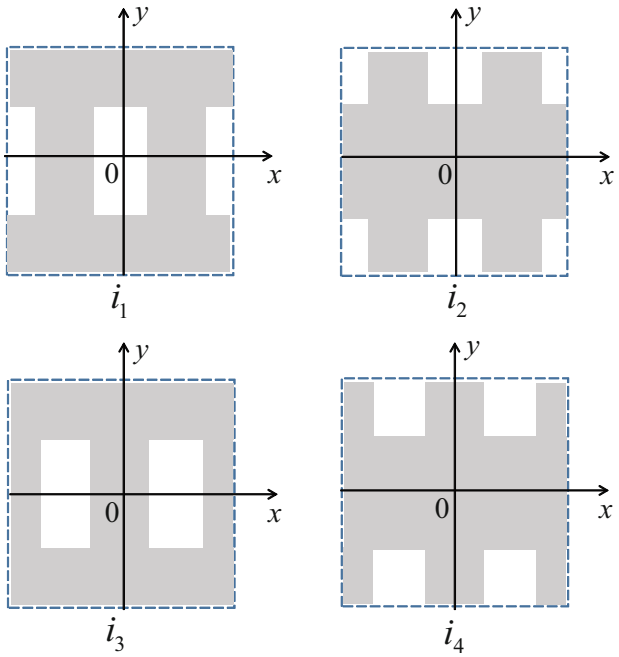

Fig. 14.14 The map of idempotent basis: each of the elements is equal to unity within light domains and zero within dark domains; square areas $[-4 < x < 4, -4 < y < 4]$ are shown under the parameters $a = 1$ and $b = 2$

$$
\begin{aligned}
e_1 i_1 &= (e_1^+ - e_1^-) e_1^+ e_2^+ = i_1 \\
e_1 i_2 &= (e_1^+ - e_1^-) e_1^+ e_2^- = i_2 \\
e_1 i_3 &= (e_1^+ - e_1^-) e_1^- e_2^+ = -i_3 \\
e_1 i_4 &= (e_1^+ - e_1^-) e_1^- e_2^- = -i_4
\end{aligned}
$$

and

$$
\begin{aligned}
\frac{\partial i_1}{\partial x} &= \frac{\partial e_1^+}{\partial x} e_2^+ = \frac{1}{2} \frac{\partial e_1}{\partial x} e_2^+ \\
\frac{\partial i_2}{\partial x} &= \frac{\partial e_1^+}{\partial x} e_2^- = \frac{1}{2} \frac{\partial e_1}{\partial x} e_2^- \\
\frac{\partial i_3}{\partial x} &= \frac{\partial e_1^-}{\partial x} e_2^+ = -\frac{1}{2} \frac{\partial e_1}{\partial x} e_2^+ \\
\frac{\partial i_4}{\partial x} &= \frac{\partial e_1^-}{\partial x} e_2^- = -\frac{1}{2} \frac{\partial e_1}{\partial x} e_2^-
\end{aligned}
$$

As a result, derivative (14.154) takes the form

$$\begin{aligned}\frac{\partial u}{\partial x} &= \left(\frac{1}{a}\frac{\partial U_1}{\partial \tau_x} + \frac{\partial U_1}{\partial x}\right) i_1 + \left(\frac{1}{a}\frac{\partial U_2}{\partial \tau_x} + \frac{\partial U_2}{\partial x}\right) i_2 \\ &+ \left(-\frac{1}{a}\frac{\partial U_3}{\partial \tau_x} + \frac{\partial U_3}{\partial x}\right) i_3 + \left(-\frac{1}{a}\frac{\partial U_4}{\partial \tau_x} + \frac{\partial U_4}{\partial x}\right) i_4 \\ &+ \frac{1}{2}(U_1 - U_3)\frac{\partial e_1}{\partial x} e_2^+ + \frac{1}{2}(U_2 - U_4)\frac{\partial e_1}{\partial x} e_2^-\end{aligned} \tag{14.155}$$

Analogously, one obtains

$$\begin{aligned}\frac{\partial u}{\partial y} &= \left(\frac{1}{b}\frac{\partial U_1}{\partial \tau_y} + \frac{\partial U_1}{\partial y}\right) i_1 + \left(-\frac{1}{b}\frac{\partial U_2}{\partial \tau_y} + \frac{\partial U_2}{\partial y}\right) i_2 \\ &+ \left(\frac{1}{b}\frac{\partial U_3}{\partial \tau_y} + \frac{\partial U_3}{\partial y}\right) i_3 + \left(-\frac{1}{b}\frac{\partial U_4}{\partial \tau_y} + \frac{\partial U_4}{\partial y}\right) i_4 \\ &+ \frac{1}{2}(U_1 - U_2)\frac{\partial e_2}{\partial y} e_1^+ + \frac{1}{2}(U_3 - U_4)\frac{\partial e_2}{\partial y} e_1^-\end{aligned} \tag{14.156}$$

Let us introduce vector, associated with expansion (14.152), and the corresponding differential matrix operators as, respectively,

$$\mathbf{u} = \begin{bmatrix} U_1 \\ U_2 \\ U_3 \\ U_4 \end{bmatrix} \tag{14.157}$$

and

$$\mathbf{D}_x = \begin{bmatrix} \frac{1}{a}\frac{\partial}{\partial \tau_x} + \frac{\partial}{\partial x} & 0 & 0 & 0 \\ 0 & \frac{1}{a}\frac{\partial}{\partial \tau_x} + \frac{\partial}{\partial x} & 0 & 0 \\ 0 & 0 & -\frac{1}{a}\frac{\partial}{\partial \tau_x} + \frac{\partial}{\partial x} & 0 \\ 0 & 0 & 0 & -\frac{1}{a}\frac{\partial}{\partial \tau_x} + \frac{\partial}{\partial x} \end{bmatrix} \tag{14.158}$$

$$\mathbf{D}_y = \begin{bmatrix} \frac{1}{b}\frac{\partial}{\partial \tau_y} + \frac{\partial}{\partial y} & 0 & 0 & 0 \\ 0 & -\frac{1}{b}\frac{\partial}{\partial \tau_y} + \frac{\partial}{\partial y} & 0 & 0 \\ 0 & 0 & \frac{1}{b}\frac{\partial}{\partial \tau_y} + \frac{\partial}{\partial y} & 0 \\ 0 & 0 & 0 & -\frac{1}{b}\frac{\partial}{\partial \tau_y} + \frac{\partial}{\partial y} \end{bmatrix} \tag{14.159}$$

Substituting (14.152) into the original Eq. (14.125), using the differentiation rules for idempotent basis, and assuming that $a = b = \varepsilon$, gives

$$\begin{aligned}
&\Delta_\tau U_1 + 2\varepsilon\left(\frac{\partial^2 U_1}{\partial\tau_x\partial x} + \frac{\partial^2 U_1}{\partial\tau_y\partial y}\right) + \varepsilon^2\Delta U_1 = \varepsilon^2[q(x,y) + kU_1]\\
&\Delta_\tau U_2 + 2\varepsilon\left(\frac{\partial^2 U_2}{\partial\tau_x\partial x} - \frac{\partial^2 U_2}{\partial\tau_y\partial y}\right) + \varepsilon^2\Delta U_2 = \varepsilon^2 q(x,y)\\
&\Delta_\tau U_3 - 2\varepsilon\left(\frac{\partial^2 U_3}{\partial\tau_x\partial x} - \frac{\partial^2 U_3}{\partial\tau_y\partial y}\right) + \varepsilon^2\Delta U_3 = \varepsilon^2 q(x,y)\\
&\Delta_\tau U_4 - 2\varepsilon\left(\frac{\partial^2 U_4}{\partial\tau_x\partial x} + \frac{\partial^2 U_4}{\partial\tau_y\partial y}\right) + \varepsilon^2\Delta U_4 = \varepsilon^2 q(x,y)
\end{aligned} \tag{14.160}$$

where the notations Δ_τ and Δ have the same meaning as those in Eqs. (14.144).

Equations (14.160) are decoupled, at cost of coupling the boundary conditions though

$$\begin{aligned}
&\frac{\partial(U_1 - U_3)}{\partial\tau_x}|_{\tau_x=\pm1} = 0, \quad \frac{\partial(U_1 - U_2)}{\partial\tau_y}|_{\tau_y=\pm1} = 0\\
&(U_1 - U_3)|_{\tau_x=\pm1} = 0, \quad (U_1 - U_2)|_{\tau_y=\pm1} = 0\\
&\frac{\partial(U_2 - U_4)}{\partial\tau_x}|_{\tau_x=\pm1} = 0, \quad \frac{\partial(U_3 - U_4)}{\partial\tau_y}|_{\tau_y=\pm1} = 0\\
&(U_2 - U_4)|_{\tau_x=\pm1} = 0, \quad (U_3 - U_4)|_{\tau_y=\pm1} = 0
\end{aligned} \tag{14.161}$$

Note that both boundary value problems (14.144) through (14.146) and (14.160) through (14.161) implement the transition from two to four spatial arguments: $\{x, y\} \to \{\tau_x, \tau_y, x, y\}$. The arguments τ_x and τ_y naturally relate to cell problems and incorporate the corresponding elastic components within the class of closed-form solutions.

Finally, let us introduce two-dimensional idempotent basis generated by the triangular asymmetric wave; see Fig. 14.15. First, following definitions of Chap. 4, let us introduce one-dimensional idempotents associated with x and y coordinates

$$\begin{aligned}
e_i^+ &= \frac{1}{2}\left[1 - \gamma_i + \left(1 - \gamma_i^2\right)e_i\right]\\
e_i^- &= \frac{1}{2}\left[1 + \gamma_i - \left(1 - \gamma_i^2\right)e_i\right]\\
(i &= 1, 2)
\end{aligned} \tag{14.162}$$

where $e_1 = \partial\tau(x/a, \gamma_1)/\partial(x/a)$ and $e_2 = \partial\tau(y/b, \gamma_2)/\partial(y/b)$.

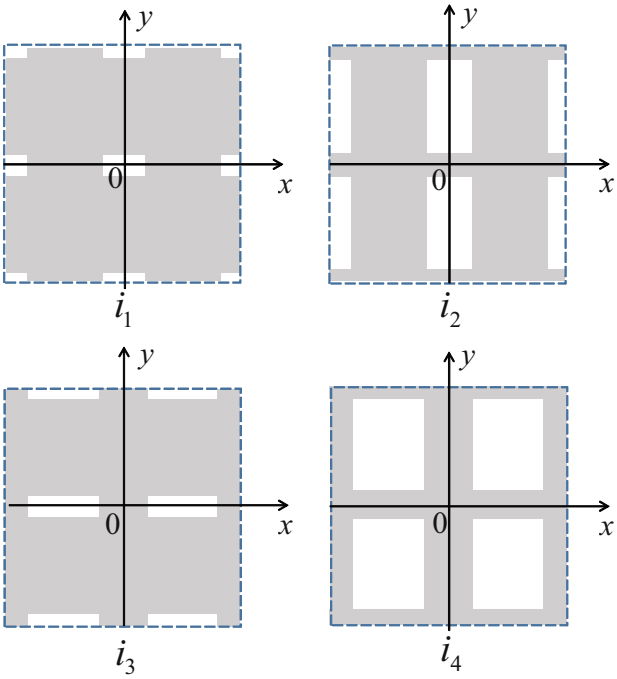

Fig. 14.15 The map of idempotent basis generated by the asymmetric triangular waves with parameters: $a = b = 1.0$, $\gamma_1 = 0.2$, and $\gamma_2 = 0.6$; each of the elements is equal to unity within light domains and zero within dark domains; square areas $[-4 < x < 4, -4 < y < 4]$ are shown

Now the two-dimensional idempotent basis is given by $i_1 = e_1^+ e_2^+$, $i_2 = e_1^+ e_2^-$, $i_3 = e_1^- e_2^+$, and $i_4 = e_1^- e_2^-$, although further expansions shown in (14.149) are not valid any more.

Appendix 1

APPENDIX 1: Mathematica$^{(R)}$ **notebook for sawtooth power-series solutions for the oscillator** $\partial_{t,t}X + X^m = 0$.

This module builds triangle wave power series solutions.

The module admits modification for polynomial restoring force characteristics.

In[4]:=
```
(* n – the number of iterations *)
(* m – the exponent *)
STSR[n_, m_] := Module[{f, h, RHS, ϵ, suc, x, X, H},
  f[x_] := x^m;
  h = Sum[ϵ^i H_i, {i, 0, n}];
  RHS = -ϵ h f[Sum[ϵ^i X_i[ξ], {i, 0, n}]];
  suc = Cancel[Coefficient[Normal[Series[RHS, {ϵ, 0, n}]], Table[ϵ^i, {i, 1, n}]]];
  X_0[ξ_] := A ξ;
  Do[X_k[τ_] =
    Integrate[suc[[k]] (-ξ + τ), {ξ, 0, τ}, Assumptions → τ > 0 && Re[m] > -1], {k, 1, n}];
  H_0 = H_0 /. Solve[∂_τ (X_0[τ] + X_1[τ]) == 0 /. τ → 1, H_0][[1]];
  Do[H_k = H_k /. Solve[∂_τ X_(k+1)[τ] == 0 /. τ → 1, H_k][[1]], {k, 1, n - 1}];
  {Table[X_k[τ], {k, 0, n}], Table[H_k, {k, 0, n - 1}]}]
```

Successive approximations:

In[2]:=
```
n = 3;
AnalyticalSolution = STSR[n, α];
Do[X_(i-1) = AnalyticalSolution[[1]][[i]], {i, 1, n + 1}];
Do[H_(i-1) = AnalyticalSolution[[2]][[i]], {i, 1, n}];
Do[Print["X", i, "=", X_i // Simplify], {i, 0, n}]
Do[Print["H", i, "=", H_i // Simplify], {i, 0, n - 1}]
```


V. N. Pilipchuk, *Oscillators and Oscillatory Signals from Smooth to Discontinuous*,
https://doi.org/10.1007/978-3-031-37788-4

$$X0 = A\,\tau$$

$$X1 = -\frac{A\,\tau^{2+\alpha}}{2+\alpha}$$

$$X2 = -\frac{A^{1-\alpha}\,\alpha\,\tau^{2+\alpha}\,\left(A^{\alpha}\,(3+2\,\alpha) - (2+\alpha)\,\tau\,(A\,\tau)^{\alpha}\right)}{2\,(2+\alpha)^{2}\,(3+2\,\alpha)}$$

$$X3 = -\frac{A^{1-2\,\alpha}\,\alpha\,\tau^{2+\alpha}\,\left(A^{2\,\alpha}\,(1+\alpha)^{2}\,(4+3\,\alpha) - A^{\alpha}\,\alpha\,\left(8+10\,\alpha+3\,\alpha^{2}\right)\,\tau\,(A\,\tau)^{\alpha} + \left(-2+\alpha+3\,\alpha^{2}+\alpha^{3}\right)\,\tau^{2}\,(A\,\tau)^{2\,\alpha}\right)}{2\,(2+\alpha)^{3}\,(3+2\,\alpha)\,(4+3\,\alpha)}$$

$$H0 = A^{1-\alpha}\,(1+\alpha)$$

$$H1 = \frac{A^{1-\alpha}\,\alpha\,(1+\alpha)}{2\,(2+\alpha)}$$

$$H2 = \frac{A^{1-\alpha}\,\alpha\,(1+\alpha)^{3}}{2\,(2+\alpha)^{2}\,(3+2\,\alpha)}$$

Successive approximation truncated series:

In[8]:=
```
x[n_] := Sum[X_i, {i, 0, n}] /. τ → τ[ξ];
v[n_] := 1/Sqrt[h[n]] ∂_τ (Sum[X_i, {i, 0, n}]) e[ξ] /. τ → τ[ξ];
h[n_] := Sum[H_i, {i, 0, n-1}]
T[n_] := 4 Sqrt[h[n]]
```

Graphs

In[12]:=
```
τ[ξ_] := 2/π ArcSin[Sin[π/2 ξ]];
e[ξ_] := Sign[Cos[π/2 ξ]];
α = 5;  (* exponent *)
A = 1.0;(* 'amplitude' parameter *)
```

In[16]:=
```
plotx = Plot[{x[1], x[2], x[3]}, {ξ, 0, 4},
   PlotStyle → {{Thickness[.001], Blue}, {Thickness[.002], Red}, {Thickness[.006], Gray}},
   Frame → True, FrameLabel → {"t", "x"},
   FrameTicks → {{Automatic, None}, {Automatic, None}}, RotateLabel → False,
   PlotRange → All, LabelStyle → {GrayLevel[0], FontSize → 12},
   PlotLegends → Placed[{"n = 1", "n = 2", "n = 3"}, {Right, Top}],
   ImageSize → 320, AspectRatio → 1 / 2];
plotv = Plot[{v[1], v[2], v[3]}, {ξ, 0, 4},
   PlotStyle → {{Thickness[.001], Blue}, {Thickness[.002], Red}, {Thickness[.006], Gray}},
   Frame → True, FrameLabel → {"t", "v"},
   FrameTicks → {{Automatic, None}, {Automatic, None}}, RotateLabel → False,
   PlotRange → All, LabelStyle → {GrayLevel[0], FontSize → 12},
   PlotLegends → Placed[{"n = 1", "n = 2", "n = 3"}, {Center, Top}],
   ImageSize → 320, AspectRatio → 1 / 2];
GraphicsGrid[{{plotx, plotv}}, ImageSize → 620]
```

Out[18]=

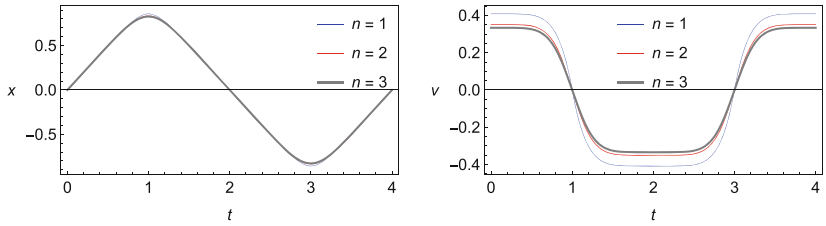

In[19]:=
```
Quit
```

Pade' approximant for the period:

In[1]:=
```
hpade[n_, m1_, m2_] := PadeApproximant[Sum[ϵ^i H_i, {i, 0, n}], {ϵ, 0, {m1, m2}}] /. ϵ → 1

Tpade[n_] := 4 Sqrt[hpade[n, 0, n]]
Tpade[3] (* Example *)
```

Out[3]=

$$4\sqrt{\frac{H_0}{1-\frac{H_1}{H_0}+\frac{H_1^2-H_0 H_2}{H_0^2}+\frac{-H_1^3+2 H_0 H_1 H_2-H_0^2 H_3}{H_0^3}}}$$

```
(* Load the module STSR again now *)
```

In[5]:=
```
α = 5;   (* exponent *)
A = 1.0;(* 'amplitude' parameter *)
n = 10;
AnalyticalSolution = STSR[n, α];
Do[H_(i-1) = AnalyticalSolution[[2]][[i]], {i, 1, n}];

h[n_] := Sum[H_i, {i, 0, n-1}]

T[n_] := 4 Sqrt[h[n]]
```

In[12]:=
```
Tplot = ListPlot[Table[T[i], {i, 1, n}], PlotRange → {6, 14},
   AxesLabel → {"n", "T"}, LabelStyle → {GrayLevel[0], FontSize → 12}];
TPadeplot = ListPlot[Table[Tpade[i], {i, 1, n}], PlotRange → {6, 14},
   AxesLabel → {"n", "T"}, LabelStyle → {GrayLevel[0], FontSize → 12}, PlotStyle → Red];
Show[Tplot, TPadeplot] (* Red - Pade *)
```

Out[14]=

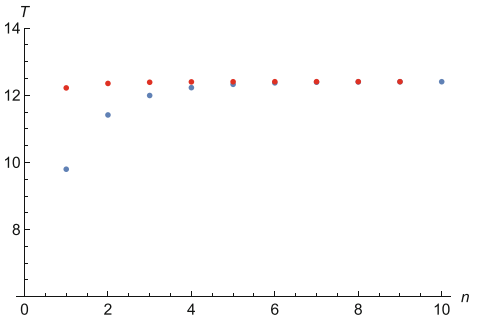

Appendix 2

APPENDIX2: Mathematica$^{(R)}$ **notebook for triangle wave power-series expansion of periodic functions.**

In[1]:=
```
(* f = f[t] - periodic function of the period T *)
```

In[2]:=
```
TauTransform[f_, T_] := Module[{a, s1, s2, RE, IM},
   a = T / 4;
   s1 = {t → a τ};
   s2 = {t → 2 a - a τ};
   RE = 1/2 ((f /. s1) + (f /. s2)) // Simplify; (* X-component *)
   IM = 1/2 ((f /. s1) - (f /. s2)) // Simplify; (* Y-component  *)
   RE + IM e // FullSimplify];
(* m          - "length" of the series; *)
(* smoothness - True or False;          *)
TauSeries[f_, T_, m_, smoothness_] :=
  Module[{a, s1, s2, NLX, NLY, RE, IM, der, TauSpectrum},
   a = T / 4;
   s1 = {t → a τ}; s2 = {t → 2 a - a τ};
   RE = 1/2 ((f /. s1) + (f /. s2)); IM = 1/2 ((f /. s1) - (f /. s2));
   der[F_] := Apply[D, {F, τ }];
   NLX = NestList[der, RE, 2 m + 1] /. {τ → 0};
   NLY = NestList[der, IM, 2 m + 1] /. {τ → 0};
   Do[{KX[2 i - 1] = Sum[NLX[[2 k]]/Factorial[2 k - 2], {k, 1, i}], KX[2 i] = Sum[NLX[[2 k + 1]]/Factorial[2 k - 1], {k, 1, i}],
     KY[2 i - 1] = Sum[NLY[[2 k]]/Factorial[2 k - 1], {k, 0, i}], KY[2 i] = Sum[NLY[[2 k + 1]]/Factorial[2 k], {k, 0, i}]}, {i, -1, m}];
```


V. N. Pilipchuk, *Oscillators and Oscillatory Signals from Smooth to Discontinuous*,
https://doi.org/10.1007/978-3-031-37788-4

```
    If[smoothness, {X → (RE /. {τ → 0}) + Sum[KX[i] (τ^i/i - τ^(i+2)/(i+2)), {i, 1, 2 m}],
      Y → Sum[KY[i] (τ^i - τ^(i+2)), {i, 0, 2 m}]}, {X → Sum[NLX[[k]] τ^(k-1)/Factorial[k-1], {k, 1, 2 m}],
      Y → Sum[NLY[[k]] τ^(k-1)/Factorial[k-1], {k, 1, 2 m}]}];
(* ===== Smoothing, Version2) ================= *)
(* mx - length of the series for X-component    *)
(* kx - smoothing parameter  for X-component    *)
(* my - length of the series for Y-component    *)
(* ky - smoothing parameter  for Y-component    *)
TauSeries2[f_, T_, mx_, kx_, my_, ky_] := Module[{a, s1, s2, RE, IM, A, B,
   eqX, coeffEqX, succCoeffsX, slX, eqY, coeffEqY, succCoeffsY, slY, X, Y},
  a = T / 4;
  s1 = {t → a τ};
  s2 = {t → 2 a - a τ};
  RE = 1/2 ((f /. s1) + (f /. s2)); (* X-component *)
  IM = 1/2 ((f /. s1) - (f /. s2)); (* Y-component  *)
  eqX = Series[RE - Sum[A_i (τ - τ^(2 kx+1)/(2 kx+1))^i, {i, 0, mx}], {τ, 0, mx}] == 0;
  (* X-component truncated series *)
  coeffEqX = LogicalExpand[eqX];
  succCoeffsX = Table[A_i, {i, 0, mx}];
  slX = Solve[coeffEqX, succCoeffsX];
  eqY = Series[IM - (1 - τ^(2 ky)) Sum[B_i τ^i, {i, 0, my}], {τ, 0, my}] == 0;
  (* Y-component truncated series *)
  coeffEqY = LogicalExpand[eqY];
  succCoeffsY = Table[B_i, {i, 0, my}];
  slY = Solve[coeffEqY, succCoeffsY];
  (X + Y e) /. {X → Sum[A_i (τ - τ^(2 kx+1)/(2 kx+1))^i, {i, 0, mx}] /. slX[[1]],
    Y → (1 - τ^(2 ky)) Sum[B_i τ^i /. slY[[1]], {i, 0, my}]}];
```

In[5]:=
```
(* ============= EXAMPLE 1 ============ *)
Clear[α, τ, e]
f[t_] := Sin[π t/2]^3; T = 4;
TauTransform[f[t], T]
```

Out[6]=
$$\sin\left[\frac{\pi\,\tau}{2}\right]^3$$

In[7]:=
```
(* == Expansions without smoothing procedure == *)
fnosmooth[t_, m_] :=
 ((X + Y e) /. TauSeries[f[t], T, m, False]) /. {τ → τ[4 t / T], e → e[4 t / T]}
fnosmooth[t, 5]
```

Out[8]=
$$\frac{1}{8}\pi^3\tau[t]^3-\frac{1}{64}\pi^5\tau[t]^5+\frac{13\pi^7\tau[t]^7}{15\,360}-\frac{41\pi^9\tau[t]^9}{1\,548\,288}$$

In[9]:=
```
(* === Expansions with smoothing procedure === *)
fsmooth[t_, m_] :=
 ((X + Y e) /. TauSeries[f[t], T, m, True]) /. {τ → τ[4 t / T], e → e[4 t / T]}
fsmooth[t, 3]
```

Out[10]=
$$\frac{3}{8}\pi^3\left(\frac{\tau[t]^3}{3}-\frac{\tau[t]^5}{5}\right)+\left(\frac{3\pi^3}{8}-\frac{5\pi^5}{64}\right)\left(\frac{\tau[t]^5}{5}-\frac{\tau[t]^7}{7}\right)$$

In[11]:=
```
(* ====== Defining the basis functions  ====== *)
τ[ξ_] := 2/π ArcSin[Sin[π/2 ξ]];
e[ξ_] := Sign[Cos[π/2 ξ]];
```

In[13]:=
```
(* ========= Convergence with no smoothing  ======= *)
nosmooth =
 Plot[Evaluate[{f[t], fnosmooth[t, 2], fnosmooth[t, 3], fnosmooth[t, 4], fnosmooth[t, 5]},
   {t, 0, 2 T}], PlotStyle → {{Thickness[.005]}, {Thickness[.002], Dashing[{0.01, 0.01}]},
    {Thickness[.002]}, {Thickness[.002]}, {Thickness[.003]}},
  AxesLabel → {"t", "x"}, PlotRange → All, PlotLegends →
   Placed[{"f(t)", "m = 2", "m = 3", "m = 4", "m = 5"}, Right], ImageSize → 320,
  LabelStyle → {GrayLevel[0], FontSize → 12}, PlotLabel → "No smoothing"]
```

Out[13]=

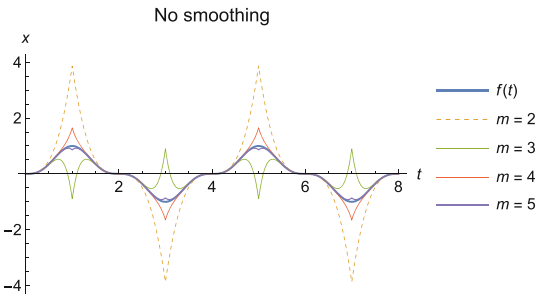

In[14]:=
```
(* ========== Convergence with smoothing  ======== *)
smooth = Plot[Evaluate[{f[t], fsmooth[t, 2], fsmooth[t, 3], fsmooth[t, 4]}, {t, 0, 2 T}],
  PlotStyle → {{Thickness[.005]}, {Thickness[.002], Dashing[{0.01, 0.01}]},
    {Thickness[.002]}, {Thickness[.003]}}, AxesLabel → {"t", "x"}, PlotRange → All,
  PlotLegends → Placed[{"f(t)", "m = 2", "m = 3", "m = 4"}, Right], ImageSize → 320,
  LabelStyle → {GrayLevel[0], FontSize → 12}, PlotLabel → "Smoothing procedure"]
  (* Grid[{{nosmooth,smooth}}] *)
```

Out[14]=

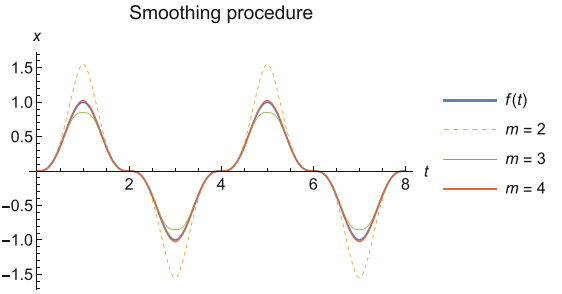

In[15]:=
```
(* ============== EXAMPLE 2 ============ *)
```

In[16]:=
```
Clear[α, τ, e]
f[t_] := 2/(α π) ArcSin[α Sin[π/2 t]] ; T = 4; TauTransform[f[t], T]
```

Out[17]=

$$\frac{2\,\text{ArcSin}\left[\alpha\,\text{Sin}\left[\frac{\pi\,\tau}{2}\right]\right]}{\pi\,\alpha}$$

In[18]:=
```
mx = 5;
kx = 2;
my = 1;
ky = 1;
fser = TauSeries2[f[t], T, mx, kx, my, ky]
```

Out[22]=

$$\tau - \frac{\tau^5}{5} + \frac{1}{24}\left(-\pi^2 + \pi^2\,\alpha^2\right)\left(\tau - \frac{\tau^5}{5}\right)^3 + \frac{\left(384 + \pi^4 - 10\,\pi^4\,\alpha^2 + 9\,\pi^4\,\alpha^4\right)\left(\tau - \frac{\tau^5}{5}\right)^5}{1920}$$

In[23]:=
```
fser = fser /. {τ → τ[4 t / T], e → e[4 t / T]};
τ[ξ_] := 2/π ArcSin[Sin[π/2 ξ]];
e[ξ_] := Sign[Cos[π/2 ξ]];
```

In[26]:=
```
plot1[α1_, α2_] := Plot[{f[t] /. α → α1, fser /. α → α1, f[t] /. α → α2, fser /. α → α2},
   {t, 0, 6 T / 3}, PlotStyle → {{Thickness[.004], Black}, {Thickness[.002], Red, Dashed},
     {Thickness[.006], Gray}, {Thickness[.003], Red, Dashed}}, Frame → True,
   FrameLabel → {"t", "f"}, FrameTicks → {{Automatic, None}, {Automatic, None}},
   RotateLabel → False, PlotRange → All, LabelStyle → {GrayLevel[0], FontSize → 12},
   PlotLegends → Placed[{"α = 0.25", None, "α = 0.98", None}, {Right, Top}],
   ImageSize → 380, AspectRatio → 1 / 2];
plot1[0.25, 0.99]
```

Out[27]=

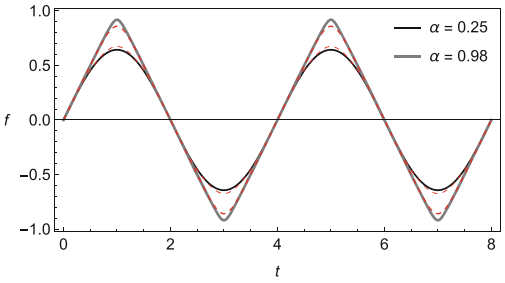

In[28]:=
```
(* ============== EXAMPLE 3 ============ *)
Clear[α, τ, e]
f[t_] := Cos[πt/2] / Sqrt[1 - α^2 Sin[πt/2]^2]; T = 4;
TauTransform[f[t], 4]
```

Out[29]=

$$\frac{\sqrt{2}\ \mathrm{e}\,\mathrm{Cos}\left[\frac{\pi\tau}{2}\right]}{\sqrt{2-\alpha^2+\alpha^2\,\mathrm{Cos}\left[\pi\tau\right]}}$$

In[30]:=
```
mx = 1;
kx = 1;
my = 4;
ky = 2;
fser = TauSeries2[f[t], T, mx, kx, my, ky]
```

Out[34]=

$$\mathrm{e}\left(1-\tau^4\right)\left(1+\frac{1}{8}\left(-\pi^2+\pi^2\alpha^2\right)\tau^2+\frac{1}{384}\left(384+\pi^4-10\,\pi^4\alpha^2+9\,\pi^4\alpha^4\right)\tau^4\right)$$

In[35]:=
```
fser = fser /. {τ → τ[4 t / T], e → e[4 t / T]};
τ[ξ_] := 2/π ArcSin[Sin[π/2 ξ]];
e[ξ_] := Sign[Cos[π/2 ξ]];
```

In[38]:=
```
plot1[α1_, α2_] := Plot[{f[t] /. α → α1, fser /. α → α1, f[t] /. α → α2, fser /. α → α2},
  {t, 0, 5.25 T / 3}, PlotStyle → {{Thickness[.004], Black}, {Thickness[.002], Red, Dashed},
    {Thickness[.006], Gray}, {Thickness[.003], Red, Dashed}}, Frame → True,
  FrameLabel → {"t", "f"}, FrameTicks → {{Automatic, None}, {Automatic, None}},
  RotateLabel → False, PlotRange → All, LabelStyle → {GrayLevel[0], FontSize → 12},
  PlotLegends → Placed[{"α = 0.25", None, "α = 0.98", None}, {Right, Top}],
  ImageSize → 380, AspectRatio → 1 / 2]
plot1[0.25, 0.98]
```

Out[39]=

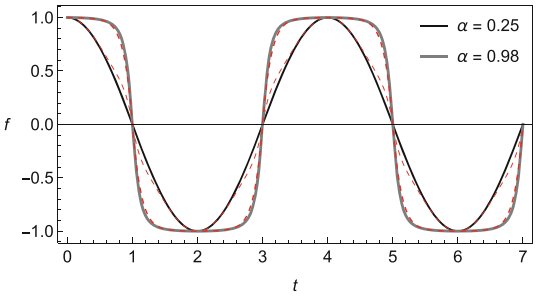

In[40]:=
```
(* ========= EXAMPLE 4: X- and Y-components ========== *)
Clear[α, τ, e]
f[t_] := Log[2 + Cos[t]]
T = 2 π;
Collect[TauTransform[f[t], T], e]
```

Out[43]=

$$\frac{1}{2}\, e\left(-\text{Log}\left[2-\text{Cos}\left[\frac{\pi\,\tau}{2}\right]\right]+\text{Log}\left[2+\text{Cos}\left[\frac{\pi\,\tau}{2}\right]\right]\right)+\frac{1}{2}\left(\text{Log}\left[2-\text{Cos}\left[\frac{\pi\,\tau}{2}\right]\right]+\text{Log}\left[2+\text{Cos}\left[\frac{\pi\,\tau}{2}\right]\right]\right)$$

In[44]:=
```
1/2 Log[4 - Cos[π τ/2]^2] + 1/2 Log[(2 + Cos[π τ/2])/(2 - Cos[π τ/2])] e
```

Out[44]=

$$\frac{1}{2}\, e\,\text{Log}\left[\frac{2+\text{Cos}\left[\frac{\pi\,\tau}{2}\right]}{2-\text{Cos}\left[\frac{\pi\,\tau}{2}\right]}\right]+\frac{1}{2}\,\text{Log}\left[4-\text{Cos}\left[\frac{\pi\,\tau}{2}\right]^2\right]$$

In[45]:=
```
(* == Expansions with no smoothing procedure == *)
fnosmooth[t_, m_] :=
 ((X + Y e) /. TauSeries[f[t], T, m, False]) /. {τ → τ[4 t / T], e → e[4 t / T]}
fnosmooth[t, 1]
fnosmooth[t, 2]
```

Out[46]=

$$\frac{\text{Log}[3]}{2}+\frac{1}{2}\, e\left[\frac{2\,t}{\pi}\right]\text{Log}[3]$$

Out[47]=

$$\frac{\text{Log}[3]}{2}+\frac{1}{24}\,\pi^2\,\tau\left[\frac{2\,t}{\pi}\right]^2+e\left[\frac{2\,t}{\pi}\right]\left(\frac{\text{Log}[3]}{2}-\frac{1}{12}\,\pi^2\,\tau\left[\frac{2\,t}{\pi}\right]^2\right)$$

In[48]:=
```
fsmooth[t_, m_] := ((X + Y e) /. TauSeries[f[t], T, m, True]) /. {τ → τ[4 t / T], e → e[4 t / T]}
fsmooth[t, 1]
```

Out[49]=

$$\frac{\text{Log}[3]}{2}+\frac{1}{12}\pi^2\left(\frac{1}{2}\tau\left[\frac{2t}{\pi}\right]^2-\frac{1}{4}\tau\left[\frac{2t}{\pi}\right]^4\right)+e\left[\frac{2t}{\pi}\right]\left(\frac{1}{2}\text{Log}[3]\left(1-\tau\left[\frac{2t}{\pi}\right]^2\right)+\left(-\frac{\pi^2}{12}+\frac{\text{Log}[3]}{2}\right)\left(\tau\left[\frac{2t}{\pi}\right]^2-\tau\left[\frac{2t}{\pi}\right]^4\right)\right)$$

In[50]:=
```
(* ====== GRAPHS  ====== *)
τ[ξ_] := 2/π ArcSin[Sin[π/2 ξ]];
e[ξ_] := Sign[Cos[π/2 ξ]];
```

In[52]:=
```
nosmooth = Plot[Evaluate[
   {f[t], fnosmooth[t, 2], fnosmooth[t, 3], fnosmooth[t, 4], fnosmooth[t, 5]}, {t, 0, 2 T}],
  PlotStyle → {{Thickness[.005], Blue}, {Thickness[.002], Dashing[{0.01, 0.01}]},
    {Thickness[.002]}, {Thickness[.002]}, {Thickness[.003]}},
  AxesLabel → {"t", "f"}, PlotRange → All, PlotLegends →
   Placed[{"f(t)", "m = 2", "m = 3", "m = 4", "m = 5"}, Right], ImageSize → 320,
  LabelStyle → {GrayLevel[0], FontSize → 12}, PlotLabel → "No smoothing"]
smooth = Plot[Evaluate[{f[t], fsmooth[t, 2], fsmooth[t, 3], fsmooth[t, 4]}, {t, 0, T}],
  PlotStyle → {{Thickness[.005], Black}, {Thickness[.004], Dashing[{0.01, 0.01}], Red},
    {Thickness[.003], Blue}, {Thickness[.002]}}, AxesLabel → {"t", "f"}, PlotRange → All,
  PlotLegends → Placed[{"f(t)", "m = 2", "m = 3", "m = 4"}, {Center, Top}],
  ImageSize → 320, LabelStyle → {GrayLevel[0], FontSize → 12},
  AspectRatio → 0.5, PlotLabel → "Smoothing procedure"]
```

Out[52]=

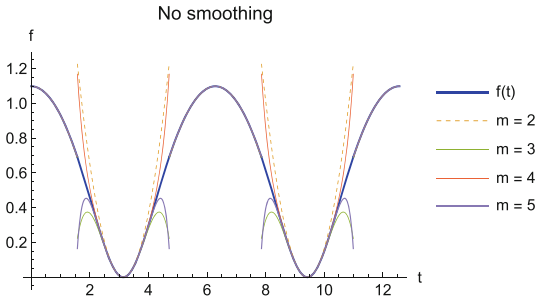

Out[53]=

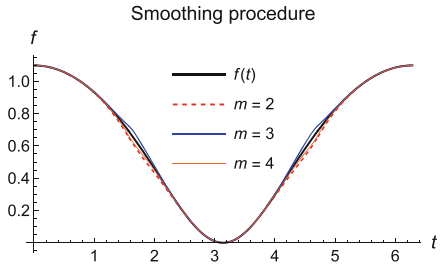

In[54]:=
```
(* ======= Coefficients of smoothed series for X ===== *)
```

In[55]:=
```
Clear[τ, e]
```

In[56]:=
```
mx = 10;
kx = 2;
my = 4;
ky = 2;
eqX = Series[X[τ] - Sum[A_i (τ - τ^(2 kx+1)/(2 kx + 1))^i, {i, 0, mx}], {τ, 0, mx}] == 0;
(* X-component truncated series *)
coeffEqX = LogicalExpand[eqX];
succCoeffsX = Table[A_i, {i, 0, mx}];
slX = Solve[coeffEqX, succCoeffsX];
slX
eqY = Series[Y[τ] - (1 - τ^(2 ky)) Sum[B_i τ^i, {i, 0, my}], {τ, 0, my}] == 0; (* Y-component truncated series *)
coeffEqY = LogicalExpand[eqY];
succCoeffsY = Table[B_i, {i, 0, my}];
slY = Solve[coeffEqY, succCoeffsY];
slY
```

Out[64]=

$$\left\{\left\{A_0 \to X[0],\ A_1 \to X'[0],\ A_2 \to \frac{X''[0]}{2},\ A_3 \to \frac{1}{6} X^{(3)}[0],\right.\right.$$
$$A_4 \to \frac{1}{24} X^{(4)}[0],\ A_5 \to \frac{1}{120}\left(24 X'[0] + X^{(5)}[0]\right),\ A_6 \to \frac{1}{720}\left(144 X''[0] + X^{(6)}[0]\right),$$
$$A_7 \to \frac{504 X^{(3)}[0] + X^{(7)}[0]}{5040},\ A_8 \to \frac{1344 X^{(4)}[0] + X^{(8)}[0]}{40\,320},$$
$$\left.\left.A_9 \to \frac{72\,576 X'[0] + 3024 X^{(5)}[0] + X^{(9)}[0]}{362\,880},\ A_{10} \to \frac{798\,336 X''[0] + 6048 X^{(6)}[0] + X^{(10)}[0]}{3\,628\,800}\right\}\right\}$$

Out[69]=

$$\left\{\left\{B_0 \to Y[0],\ B_1 \to Y'[0],\ B_2 \to \frac{Y''[0]}{2},\ B_3 \to \frac{1}{6} Y^{(3)}[0],\ B_4 \to \frac{1}{24}\left(24 Y[0] + Y^{(4)}[0]\right)\right\}\right\}$$

Appendix 3

APPENDIX 3: Mathematica$^{(R)}$ **NSTT of the *T*-periodic differential equation of the form** $\partial_{t,t}x + f(x, \partial_t x, t) = 0$.

In[1]:=
```
(* See examples below for the meaning of inputs *)

TauTransform[equation_, function_, argument_, period_, basis_] :=
 Module[{sub, eqn, RE, IM},
  sub = {function -> X[τ] + Y[τ] e,
    ∂argument function -> (Y'[τ] + X'[τ] e) / a,
    ∂argument,argument function -> (X''[τ] + Y''[τ] e) / a^2};
  Q = Part[equation, 1] /. sub;
  eqn = ((1/2) ((Q /. t -> a τ) + (Q /. t -> 2 a - a τ))
      + (1/2) ((Q /. t -> a τ) - (Q /. t -> 2 a - a τ)) e) /. a -> period / 4;
  EQNX = Simplify[(1/2) ((eqn /. e -> 1) + (eqn /. e -> -1))];
  EQNY = Simplify[(1/2) ((eqn /. e -> 1) - (eqn /. e -> -1))];
  subid = {X[τ] -> (1/2) (X+[τ] + X-[τ]), Y[τ] -> (1/2) (X+[τ] - X-[τ]),
    X'[τ] -> (1/2) (∂τ X+[τ] + ∂τ X-[τ]), Y'[τ] -> (1/2) (∂τ X+[τ] - ∂τ X-[τ]),
    X''[τ] -> (1/2) ∂τ,τ (X+[τ] + X-[τ]), Y''[τ] -> (1/2) ∂τ,τ (X+[τ] - X-[τ])};
  IDP = Simplify[(EQNX + EQNY) /. subid];
  IDM = Simplify[(EQNX - EQNY) /. subid];
  If[basis == 1, {{EQNX == 0, EQNY == 0}, {Y[1] == 0, Y[-1] == 0, X'[1] == 0, X'[-1] == 0}},
   {{IDP == 0, IDM == 0},
    {X+[1] - X-[1] == 0, X+[-1] - X-[-1] == 0, X+'[1] + X-'[1] == 0, X+'[-1] + X-'[-1] == 0}}]]
```

EXAMPLES

In[2]:=
```
(* If basis = 1, then the output is created in the standard basis {1,e},
otherwise the output is in the idempotent basis {e+,e-}={(1+e)/2,(1-e)/2} *)
```


V. N. Pilipchuk, *Oscillators and Oscillatory Signals from Smooth to Discontinuous*,
https://doi.org/10.1007/978-3-031-37788-4

In[3]:=
```
TauTransform[x''[t] + x[t]^3 == 0, x[t], t, 4 a, 1]
```

Out[3]=
$$\left\{\left\{X[\tau]^3+3\,X[\tau]\,Y[\tau]^2+\frac{X''[\tau]}{a^2}==0,\ 3\,X[\tau]^2\,Y[\tau]+Y[\tau]^3+\frac{Y''[\tau]}{a^2}==0\right\},\right.$$
$$\left.\{Y[1]==0,\ Y[-1]==0,\ X'[1]==0,\ X'[-1]==0\}\right\}$$

In[4]:=
```
TauTransform[x''[t] + x[t]^3 == 0, x[t], t, 4 a, 0]
```

Out[4]=
$$\left\{\left\{X_+[\tau]^3+\frac{X_+''[\tau]}{a^2}==0,\ X_-[\tau]^3+\frac{X_-''[\tau]}{a^2}==0\right\},\right.$$
$$\left.\{-X_-[1]+X_+[1]==0,\ -X_-[-1]+X_+[-1]==0,\ X_-'[1]+X_+'[1]==0,\ X_-'[-1]+X_+'[-1]==0\}\right\}$$

In[5]:=
```
TauTransform[x''[t] + x[t]^3 - P Sin[t] == 0, x[t], t, 2 π, 0]
```

Out[5]=
$$\left\{\left\{-P\,\text{Sin}\left[\frac{\pi\tau}{2}\right]+X_+[\tau]^3+\frac{4\,X_+''[\tau]}{\pi^2}==0,\ -P\,\text{Sin}\left[\frac{\pi\tau}{2}\right]+X_-[\tau]^3+\frac{4\,X_-''[\tau]}{\pi^2}==0\right\},\right.$$
$$\left.\{-X_-[1]+X_+[1]==0,\ -X_-[-1]+X_+[-1]==0,\ X_-'[1]+X_+'[1]==0,\ X_-'[-1]+X_+'[-1]==0\}\right\}$$

In[6]:=
```
TauTransform[x''[t] + x[t]^3 - P Sin[t] == 0, x[t], t, 2 π, 1]
```

Out[6]=
$$\left\{\left\{-P\,\text{Sin}\left[\frac{\pi\tau}{2}\right]+X[\tau]^3+3\,X[\tau]\,Y[\tau]^2+\frac{4\,X''[\tau]}{\pi^2}==0,\ 3\,X[\tau]^2\,Y[\tau]+Y[\tau]^3+\frac{4\,Y''[\tau]}{\pi^2}==0\right\},\right.$$
$$\left.\{Y[1]==0,\ Y[-1]==0,\ X'[1]==0,\ X'[-1]==0\}\right\}$$

In[7]:=
```
(* If present, the function e=e(4t/T) must be shown with no argument;
derivatives de/dt are not allowed by this code,
but necessary generalizations are easy to implement *)
```

In[8]:=
```
TauTransform[x''[t] + (1 + α e) x[t] + β x[t]^3 == 0, x[t], t, 4 a, 1]
```

Out[8]=
$$\left\{\left\{X[\tau]+\beta\,X[\tau]^3+\alpha\,Y[\tau]+3\,\beta\,X[\tau]\,Y[\tau]^2+\frac{X''[\tau]}{a^2}==0,\right.\right.$$
$$\left.\alpha\,X[\tau]+Y[\tau]+3\,\beta\,X[\tau]^2\,Y[\tau]+\beta\,Y[\tau]^3+\frac{Y''[\tau]}{a^2}==0\right\},$$
$$\left.\{Y[1]==0,\ Y[-1]==0,\ X'[1]==0,\ X'[-1]==0\}\right\}$$

In[9]:=
```
TauTransform[x''[t] + (1 + α e) x[t] + β x[t]^3 == 0, x[t], t, 4 a, 0]
```

Out[9]=
$$\left\{\left\{(1+\alpha)\,X_+[\tau]+\beta\,X_+[\tau]^3+\frac{X_+''[\tau]}{a^2}==0,\ -(-1+\alpha)\,X_-[\tau]+\beta\,X_-[\tau]^3+\frac{X_-''[\tau]}{a^2}==0\right\},\right.$$
$$\left.\{-X_-[1]+X_+[1]==0,\ -X_-[-1]+X_+[-1]==0,\ X_-'[1]+X_+'[1]==0,\ X_-'[-1]+X_+'[-1]==0\}\right\}$$

PROJECT: Using the idempotent basis, find T-periodic solution of the linear oscillator under external and parametric rectangular wave periodic excitation of the period T=4,

$$\partial_{t,t}x+\left(1+\tfrac{1}{2}e(t)\right)\omega^2 x=\text{pe}(t).$$

In[10]:=
```
(* Formulates boundary value problem in the idempotent basis: *)

T = 4;
bvp = TauTransform[x''[t] + ω^2 (1 + 1/2 e) x[t] - p e == 0, x[t], t, T, 0]
```

Out[11]=
$$\left\{\left\{-p+\frac{3}{2}\omega^2\,X_+[\tau]+X_+''[\tau]==0,\ p+\frac{1}{2}\omega^2\,X_-[\tau]+X_-''[\tau]==0\right\},\right.$$
$$\left.\{-X_-[1]+X_+[1]==0,\ -X_-[-1]+X_+[-1]==0,\ X_-'[1]+X_+'[1]==0,\ X_-'[-1]+X_+'[-1]==0\}\right\}$$

In[12]:=
```
(* Solves the boundary value problem analytically: *)

sol = DSolve[bvp, {X+[τ], X-[τ]}, τ] // Simplify
```

Out[12]=
$$\left\{\left\{X_+[\tau] \to \left(4\,p\left(\sqrt{3}\,\text{Cos}\left[\frac{\omega}{\sqrt{2}}\right]^2\text{Sin}\left[\sqrt{\frac{3}{2}}\,\omega\right]^2+\sqrt{3}\,\text{Cos}\left[\sqrt{\frac{3}{2}}\,\omega\right]^2\text{Sin}\left[\frac{\omega}{\sqrt{2}}\right]^2-4\sqrt{3}\,\text{Cos}\left[\sqrt{\frac{3}{2}}\,\omega\right]\text{Cos}\left[\sqrt{\frac{3}{2}}\,\tau\,\omega\right]\text{Sin}\left[\frac{\omega}{\sqrt{2}}\right]^2+\text{Sin}\left[\sqrt{2}\,\omega\right]\left(-2\,\text{Cos}\left[\sqrt{\frac{3}{2}}\,\tau\,\omega\right]\text{Sin}\left[\sqrt{\frac{3}{2}}\,\omega\right]+\text{Sin}\left[\sqrt{6}\,\omega\right]\right)\right)\right)\Big/\left(3\,\omega^2\left(\sqrt{3}-\sqrt{3}\,\text{Cos}\left[\sqrt{2}\,\omega\right]\text{Cos}\left[\sqrt{6}\,\omega\right]+2\,\text{Sin}\left[\sqrt{2}\,\omega\right]\text{Sin}\left[\sqrt{6}\,\omega\right]\right)\right),\right.$$
$$\left.X_-[\tau] \to \left(2\,p\left(\sqrt{3}\left(-3+4\,\text{Cos}\left[\frac{\tau\,\omega}{\sqrt{2}}\right]\text{Sec}\left[\frac{\omega}{\sqrt{2}}\right]\right)\text{Sin}\left[\sqrt{\frac{3}{2}}\,\omega\right]^2-3\,\text{Tan}\left[\frac{\omega}{\sqrt{2}}\right]\left(\left(2-2\,\text{Cos}\left[\frac{\tau\,\omega}{\sqrt{2}}\right]\text{Sec}\left[\frac{\omega}{\sqrt{2}}\right]\right)\text{Sin}\left[\sqrt{6}\,\omega\right]+\sqrt{3}\,\text{Cos}\left[\sqrt{\frac{3}{2}}\,\omega\right]^2\text{Tan}\left[\frac{\omega}{\sqrt{2}}\right]\right)\right)\right)\Big/\left(3\,\omega^2\left(\sqrt{3}\,\text{Sin}\left[\sqrt{\frac{3}{2}}\,\omega\right]^2+\text{Tan}\left[\frac{\omega}{\sqrt{2}}\right]\left(2\,\text{Sin}\left[\sqrt{6}\,\omega\right]+\sqrt{3}\,\text{Cos}\left[\sqrt{\frac{3}{2}}\,\omega\right]^2\text{Tan}\left[\frac{\omega}{\sqrt{2}}\right]\right)\right)\right)\right\}\right\}$$

In[13]:=
```
(* Extracting two components of the solution: *)

X+[τ] = X+[τ] /. sol[[1]];
X-[τ] = X-[τ] /. sol[[1]];
```

In[15]:=
```
(* Back to the original x-t variables: *)
x = X+[τ] 1/2 (1 + e) + X-[τ] 1/2 (1 - e) /. {τ → τ[t], e → e[t]};
v = 1/(T/4) (∂τ X+[τ] 1/2 (1 + e) - ∂τ X-[τ] 1/2 (1 - e)) /. {τ → τ[t], e → e[t]};
```

In[17]:=
```
(* Basis functions: *)
τ[t_] := 2/π ArcSin[Sin[π/2 t]];
e[t_] := Sign[Cos[π/2 t]];
```

In[19]:=
```
(* Parameters and graphic output: *)
ω = 20.0;
p = 1.0;
plot1 = Plot[Evaluate[x, {t, 0, 8}], PlotRange → All,
   FrameLabel → {"t", "x"}, PlotStyle → {{Thickness[.005], Blue}},
   Exclusions -> None, Frame -> True, RotateLabel -> False];
```

In[22]:=
```
(* Validating the code by durect numerical solution: *)
x0 = x /. t → 0;
v0 = v /. t → 0;
dirsol = NDSolve[{y''[t] + ω^2 (1 + 1/2 e[t]) y[t] - p e[t] == 0, y[0] == x0, y'[0] == v0},
   y, {t, 0, 50}, MaxSteps → Infinity];
y = y /. dirsol[[1]];
```

In[26]:=
```
plot2 = Plot[Evaluate[y[t], {t, 0, 8}], PlotRange → All,
   FrameLabel → {"t", "x"}, PlotStyle → {{Thickness[.005], Red, Dashed}},
   Exclusions -> None, Frame -> True, RotateLabel -> False];
```

In[27]:=
```
Show[plot1, plot2]
```

Out[27]=

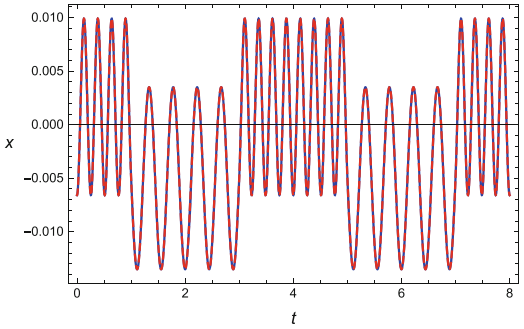

Appendix 4

APPENDIX 4: Mathematica$^{(R)}$ **NSTT & Shooting method for periodic solutions of the oscillator** $\frac{d^2x}{dt^2} + \zeta\frac{dx}{dt} + \epsilon x^3 = B\,e\left[\frac{t}{a}\right]$.

```
p[x_, v_, t_] := ζ v + ϵ x^3;
a = π/(2 ω);

(* Substitution x[t] =
 X[τ[t/a]]+Y[τ[t/a]]*e[t/a] applied to the equation of motion: *)
eqX = (1/a^2 ∂τ,τX[τ] + 1/2 (p[X[τ] + Y[τ], 1/a (∂τ X[τ] + ∂τ Y[τ]), a τ]
        + p[X[τ] - Y[τ], 1/a (-∂τ X[τ] + ∂τ Y[τ]), 2 a - a τ])) == 0 // Simplify;
eqY = (1/a^2 ∂τ,τY[τ] + 1/2 (p[X[τ] + Y[τ], 1/a (∂τ X[τ] + ∂τ Y[τ]), a τ]
        - p[X[τ] - Y[τ], 1/a (-∂τ X[τ] + ∂τ Y[τ]), 2 a - a τ])) == B // Simplify;

(* Parameters: *)
ω = 1.0; ζ = 0.05; ϵ = 1.0; B = 7.4;

Clear[g, h]; dg = 3; dh = 15;
sol[g_, h_] := NDSolve[{eqX, eqY, X[-1] == g, X'[-1] == 0, Y[-1] == 0, Y'[-1] == h},
   {X, Y}, {τ, -1, 1}, MaxSteps → Infinity];
Xn[g_, h_] := X'[1] /. sol[g, h][[1]];
Yn[g_, h_] := Y[1] /. sol[g, h][[1]];

plx = ContourPlot[Xn[g, h], {g, -dg, dg}, {h, -dh, dh}, Contours → {0},
  ContourShading → False, FrameLabel → {"g", "h"}, PlotPoints → 100,
  RotateLabel → False, DisplayFunction → Identity, ContourStyle → {Thickness[0.005]}];
ply = ContourPlot[Yn[g, h], {g, -dg, dg}, {h, -dh, dh}, Contours → {0},
  ContourShading → False, FrameLabel → {"g", "h"}, PlotPoints → 100, RotateLabel → False,
  ContourStyle → {Dashing[{0.01, 0.01}], Blue}, DisplayFunction → Identity];
pxy = Show[plx, ply, DisplayFunction → $DisplayFunction];
```


V. N. Pilipchuk, *Oscillators and Oscillatory Signals from Smooth to Discontinuous*,
https://doi.org/10.1007/978-3-031-37788-4

```
(* Magnified portion of the diagram:  *)
Show[pxy, PlotRange → {{-dg, dg}, {-dh, dh}}]
```

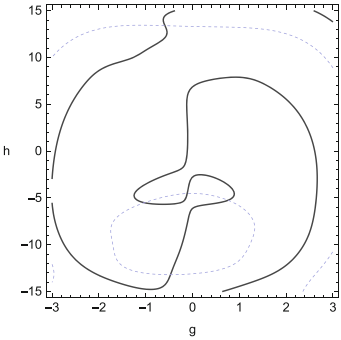


```
(* Find one of the roots: *)

{g, h} = {g, h} /. FindRoot[{Evaluate[Xn[g, h]] == 0, Evaluate[Yn[g, h]] == 0},
    {g, -0.3, 0}, {h, -5, -4}, Evaluated → False]
```

{−0.113352, −4.51958}

```
(* Check precision: *)

sln = NDSolve[{eqX, eqY, X[-1] == g, X'[-1] == 0, Y[-1] == 0, Y'[-1] == h}, {X, Y}, {τ, -1, 1}];
{Y[1], X'[1]} /. sln[[1]]
```

$\{-1.23107 \times 10^{-13}, -4.37359 \times 10^{-14}\}$

```
(* Introduce triangle and rectangle wave functions: *)
τ[t_] := 2/π ArcSin[Sin[π/2 t]];
e[t_] := Sign[Cos[π/2 t]];


(* Comparison to the direct numerical solution of the related Cauchy problem *)

x[t_] := (X[τ[t/a]] + Y[τ[t/a]] * e[t/a]) /. sln[[1]];
v[t_] := 1/a (Y'[τ[t/a]] + X'[τ[t/a]] * e[t/a]) /. sln[[1]];
xxtt = Plot[Evaluate[x[t], {t, 0, 4 a}], PlotRange → All, AxesLabel → {"t", "x"},
  PlotStyle → {{Thickness[.009]}}, DisplayFunction → Identity, RotateLabel -> False];
xxvv = ParametricPlot[Evaluate[{x[t], v[t]}, {t, 0, 4 a}], PlotRange → All,
  AxesLabel → {"x", "v"}, Frame → True, PlotStyle → {{Thickness[.009]}},
  DisplayFunction → Identity, AspectRatio -> 0.57];

Clear[y];
Tmax = 4 a;
dirsol = NDSolve[{∂t,t y[t] + ξ ∂t y[t] + ϵ y[t]^3 == B e[t/a], y[0] == x[0], y'[0] == v[0]},
  y, {t, 0, Tmax}, MaxSteps → Infinity];
y = y /. dirsol[[1]];
yyvv = ParametricPlot[Evaluate[{y[t], y'[t]}, {t, 0, Tmax}],
  PlotRange → All, AxesLabel → {"x", "v"}, PlotStyle → {{Thickness[.001]}},
  PlotPoints → 500, Frame → True, DisplayFunction → Identity, AspectRatio -> 1/2];
Grid[{{xxtt, Show[xxvv, yyvv]}}]
```

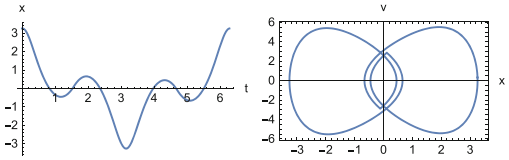

References

1. H.N. Abramson. *The dynamic behavior of liquids in moving contains*. NASA SP-106, 1966.
2. V. Acary and B. Brogliato. *Numerical methods for nonsmooth dynamical systems: Applications in Mechanics and Electronics*. Springer, Berlin, Heidelberg, 2008.
3. U. Andreaus, P. Casini, and F. Vestroni. Non-linear dynamics of a cracked cantilever beam under harmonic excitation. *International Journal of Non-Linear Mechanics*, 42(3):566–575, 2007.
4. G.E. Andrews, R. Askey, and R. Roy. *Special Functions*. Encyclopedia of Mathematics and its Applications. Cambridge University Press, 1999.
5. I.V. Andrianov. Asymptotics of nonlinear dynamical systems with a high degree of nonlinearity. *Doklady Mathematics*, 66(2):270–273, 2002.
6. I.V. Andrianov. The pursuit of simplicity: The scientific heritage of professor Leonid I. Manevitch. *International Journal of Non-Linear Mechanics*, page 103998, 2022.
7. I.V. Andrianov. Why would a biologist need a logarithm? *For the Learning of Mathematics. Communications*, 42(1):11–12, 2022.
8. I.V. Andrianov and J. Awrejcewicz. Methods of small and large δ in the nonlinear dynamics—a comparative analysis. *Nonlinear Dynam.*, 23(1):57–66, 2000.
9. I.V. Andrianov, J. Awrejcewicz, and R.G. Barantsev. Asymptotic approaches in mechanics: New parameters and procedures. *Applied Mechanics Reviews*, 56(1):87–110, 2003.
10. I.V. Andrianov, J. Awrejcewicz, and V.V. Danishevskyy. *Linear and Nonlinear Waves in Microstructured Solids: Homogenization and Asymptotic Approaches*. CRC Press, Boca Raton, 2021.
11. I.V. Andrianov, J. Awrejcewicz, and G.A. Starushenko. *Approximate Models of Mechanics of Composites: An Asymptotic Approach*. CRC Press, Boca Raton, 2024.
12. I.V. Andrianov, V.I. Bolshakov, V.V. Danishevs'kyy, and D. Weichert. Higher order asymptotic homogenization and wave propagation in periodic composite materials. *Proceedings of the Royal Society A: Mathematical, Physical and Engineering Sciences*, 464(2093):1181–1201, 2008.
13. I.V. Andrianov, V.V. Danishevs'kyy, H. Topol, and D. Weichert. Homogenization of a 1d nonlinear dynamical problem for periodic composites. *ZAMM - Journal of Applied Mathematics and Mechanics / Zeitschrift für Angewandte Mathematik und Mechanik*, 91(6):523–534, 2011.
14. I.V. Andrianov and L.I. Manevitch. *Asymptotology: Ideas, Methods, and Applications*. Kluwer Academic Publishers, Dordrecht, Boston, London, 2002.
15. F. Antonuccio. Hyperbolic numbers and the Dirac spinor. http://arxiv.org/abs/hep-th/9812036v1, 1998.

V. N. Pilipchuk, *Oscillators and Oscillatory Signals from Smooth to Discontinuous*,
https://doi.org/10.1007/978-3-031-37788-4

16. V.I. Arnol'd. *Mathematical Methods of Classical Mechanics*. Springer-Verlag, New York, 1978.
17. U.M. Ascher, R.M.M. Mattheij, and R.D. Russell. *Numerical Solution of Boundary Value Problems for Ordinary Differential Equations*, volume 13 of *Classics in Applied Mathematics*. Society for Industrial and Applied Mathematics (SIAM), Philadelphia, PA, 1995. Corrected reprint of the 1988 original.
18. C.P. Atkinson. On the superposition method for determining frequencies of nonlinear systems. *ASME Proceedings of the 4-th National Congress of Applied Mechanics*, pages 57–62, 1962.
19. D. Auerbach, P. Cvitanovic, J.-P. Eckmann, G. Gunaratne, and I. Procaccia. Exploring chaotic motion through periodic orbits. *Phys. Rev. Lett.*, 58(23):2387–2389, 1987.
20. J. Awrejcewicz, I.V. Andrianov, and L.I. Manevitch. *Asymptotic Approaches in Nonlinear Dynamics. New Trends and Applications*. Springer Series in Synergetics. Springer-Verlag, Berlin, 1998.
21. J. Awrejcewicz, A. K. Bajaj, and C.-H. Lamarque, editors. *Nonlinearity, Bifurcation and Chaos: the Doors to the Future. Part II*. World Scientific Publishing Co., Singapore, 1999.
22. J. Awrejcewicz and C.-H. Lamarque. *Bifurcation and Chaos in Nonsmooth Mechanical Systems*. World Scientific, Singapore, 2003.
23. M.A.F. Aziz, A.F. Vakakis, and L.I. Manevitch. Exact solutions of the problem of vibroimpact oscillations of a discrete system with two degrees of freedom. *Journal of Applied Mathematics and Mechanics*, 63(4):527–530, 1999.
24. V.I. Babitsky. *Theory of Vibroimpact Systems and Applications*. Springer-Verlag, Berlin, 1998.
25. T. B. Bahler. *Mathematica for Scientists and Engineers*. Addison-Wesley, New York, 1995.
26. G. A. Baker Jr. and P. Graves-Morris. *Padé Approximants, vol. 59 of Encyclopedia of Mathematics and Its Applications, 2nd edition*. Cambridge University Press, Cambridge, UK, 1987.
27. R. Balescu. *Statistical Dynamics, Matter out of Equilibrium*. Imperial College Press, Singapore, 1997.
28. H. Bateman and A. Erdelyi. *Higher Transcendental Functions*. McGraw-Hill, New York, 1955.
29. J. G. F. Belinfante and B. Kolman. *A survey of Lie groups and Lie algebras with applications and computational methods*. Society for Industrial and Applied Mathematics (SIAM), Philadelphia, PA, 1989. Reprint of the 1972 original.
30. R. Bellman. *Introduction to Matrix Analysis*. McGraw-Hill Company, New York, 1960.
31. A. Bensoussan, J.-L. Lions, and G. Papanicolaou. *Asymptotic Analysis for Periodic Structures*. North-Holland Publishing Co., Amsterdam, 1978.
32. B. Blazejczyk-Okolewska, K. Czolczynski, T. Kapitaniak, and J. Wojewoda. *Chaotic Mechanics in Systems with Impacts and Friction*. World Scientific, 1999.
33. S. Boettcher and C.M. Bender. Nonperturbative square-well approximation to a quantum theory. *Journal of Mathematical Physics*, 31(11):2579–2585, 1990.
34. N. Bogoliubov and Y. Mitropollsky. *Asymptotic Methods in the Theory of Nonlinear Oscillations*. Gordon and Breach, New York, 1961.
35. L. Brekhovskikh. *Waves in Layered Media 2e*. Elsevier, 2012.
36. L. Brillouin. *Wave Propagation in Periodic Structures: Electric Filters and Crystal Lattices*. Dover, 2003.
37. B. Brogliato. *Nonsmooth Mechanics: Models, Dynamics and Control*. Springer-Verlag, London, Berlin, Heidelberg, 1999.
38. B. Brogliato. *Impacts in Mechanical Systems: Analysis and Modelling*. Springer-Verlag, Berlin, 2000.
39. L.A. Bunimovich. Decay of correlations in dynamical systems with chaotic behavior. *Sov. Phys. JETP*, 62:842–852, 1985.
40. T.K. Caughey and A.F. Vakakis. A method for examining steady state solutions of forced discrete systems with strong non-linearities. *International Journal of Non-Linear Mechanics*, 26(1):89–103, 1966.

41. M. Chati, R. Rand, and S. Mukherjee. Modal analysis of a cracked beam. *Journal of Sound and Vibration*, 207:249–270, 1997.
42. S. Chen and S.W. Shaw. Normal modes for piecewise linear vibratory systems. *Nonlinear Dynamics*, 10:135–163, 1996.
43. W. Chin, E. Ott, H.E. Nusse, and C. Grebogi. Grazing bifurcations in impact oscillators. *Phys. Rev. E*, 50:4427–4444, 1994.
44. L. Collatz. *Eigenwertaufgaben mit technischen Anwendungen*. Geest & Portig, Lepizig, 1963.
45. K. Cooper and R. E. Mickens. Generalized harmonic balance/numerical method for determining analytical approximations to the periodic solutions of the $x^{4/3}$ potential. *Journal of Sound and Vibration*, 250:951–954, 2002.
46. V. T. Coppola and R. H. Rand. Computer algebra implementation of Lie transforms for hamiltonian systems: Application to the nonlinear stability of l4. *ZAMM*, 69(9):275–284, 1989.
47. R.V. Craster, J. Kaplunov, and A.V. Pichugin. High-frequency homogenization for periodic media. *Proceedings of the Royal Society A: Mathematical, Physical and Engineering Science*, 466(2120):2341–2362, 2010.
48. L. Cveticanin. Oscillator with strong quadratic damping force. *Publications de L'institut Mathematique (Nouvelle serie)*, 85(99):119–130, 2009.
49. H. Dankowicz and M. R. Paul. Discontinuity-induced bifurcations in systems with hysteretic force interactions. *Journal of Computational and Nonlinear Dynamics*, 4(Article 041009):1–6, 2009.
50. A. Deprit. Canonical transformations depending on a parameter. *Celestial mechanics*, 1(1):12–30, 1969.
51. P.A. Deymier. *Acoustic Metamaterials and Phononic Crystals*. Springer, Berlin-Heidelberg, 2013.
52. M.F. Dimentberg. *Statistical Dynamics of Nonlinear and Time-Varying Systems*. John Wiley & Sons, New York, 1988.
53. M.F. Dimentberg and A.S. Bratus. Bounded parametric control of random vibrations. *Proc. R. Soc. Lond. Ser. A Math. Phys. Eng. Sci.*, 456(2002):2351–2363, 2000.
54. M.F. Dimentberg, D.V. Iourtchenko, and A.S. Bratus'. Transition from planar to whirling oscillations in a certain nonlinear system. *Nonlinear Dynamics*, 23:165–174, 2000.
55. H. Ding and L.Q. Chen. Designs, analysis, and applications of nonlinear energy sinks. *Nonlinear Dynamics*, 100:3061–3107, 2020.
56. W.M. Ewing, W.S. Jardetzky, and F. Press. *Elastic Waves in Layered Media*. Lamont Geological Observatory contribution. McGraw-Hill, 1957.
57. O. M. Faltinsen, O. F. Rognebakke, and A. N. Timokha. Transient and steady-state amplitudes of resonant three-dimensional sloshing in a square base tank with a finite fluid depth. *Physics of Fluids*, 18(1):012103, 2006.
58. M. Feckan and M. Pospisil. On equations with generalized periodic right-hand side. *Ukrainian Mathematical Journal*, 70(2):255–279, 2018.
59. B. Feeny and F.C. Moon. Chaos in a forced dry-friction oscillator: Experiments and numerical modelling. *Journal of Sound and Vibration*, 170(3):303–323, 1994.
60. B.A. Feeny, A. Guran, N. Hinrichs, and K. Popp. A historical review on dry friction and stick-slip phenomena. *ASME Applied Mechanics Reviews*, 51:321–341, 1998.
61. L. Ferrari and C.D.E. Boschi. Nonautonomous and nonlinear effects in generalized classical oscillators: A boundedness theorem. *Physical Review E*, 62(3):R3039–R3042, 2000.
62. A. Fidlin. *Nonlinear Oscillations in Mechanical Engineering*. Springer, Berlin, Heidelberg, 2005.
63. A.F. Filippov. *Differential Equations with Discontinuous Righthand Sides*. Kluwer Academic Publishers Group, Dordrecht, 1988. Translated from the Russian.
64. J. Fish and W. Chen. Space-time multiscale model for wave propagation in heterogeneous media. *Computer Methods in Applied Mechanics and Engineering*, 193(45):4837–4856, 2004.

65. S. Fucik and A. Kufner. *Nonlinear differential equations*. Elsevier, Amsterdam, Oxford, New York, 1980. Studies in Applied Mechanics 2, Elsevier Scientific Publishing Company.
66. O. Gendelman, L.I. Manevitch, A.F. Vakakis, and R. M'Closkey. Energy pumping in nonlinear mechanical oscillators. I. Dynamics of the underlying Hamiltonian systems. *Trans. ASME J. Appl. Mech.*, 68(1):34–41, 2001.
67. O.V. Gendelman. Modeling of inelastic impacts with the help of smooth functions. *Chaos, Solitons and Fractals*, 28:522–526, 2006.
68. O.V. Gendelman and L.I. Manevitch. Discrete breathers in vibroimpact chains: Analytic solutions. *Physical Review E*, 78(026609), 2008.
69. G.E.O. Giacaglia. *Perturbation Methods in Non-Linear Systems*. Springer-Verlag, New York, 1972. Applied Mathematical Sciences, Vol. 8.
70. W. Goldsmith. *Impact: The Theory and Physical Behaviour of Colliding*. Courier Dover Publications, North Chelmsford, 2001.
71. I. S. Gradshteyn and I. M. Ryzhik. *Table of Integrals, Series, and Products (Fifth Edition)*. Academic Press, Boston, 1994.
72. C. Grebogi, E. Ott, and J.A. Yorke. Unstable periodic orbits and the dimensions of multifractal chaotic attractors controlling chaos. *Physical Review A*, 37(5):1711–1724, 1988.
73. D.T. Greenwood. *Principles of Dynamics*. Prentice Hall, 1988.
74. J. Guckenheimer and B. Meloon. Computing periodic orbits and their bifurcations with automatic differentiation. *SIAM J. Sci. Comput.*, 22(3):951–985, 2000.
75. A. Guran, F. Pfeiffer, and K. Popp. *Dynamics with Friction: Modeling, Analysis and Experiments*. World Scientific, 2001.
76. W. Hahn. *Stability of Motion*. Springer Series in Nonlinear Dynamics. Springer-Verlag, New York, 1967.
77. T.J. Harvey. Natural forcing functions in nonlinear systems. *ASME Journal of Applied Mechanics*, 25:352–356, 1958.
78. E. Hascoët, H.J. Herrmann, and V. Loreto. Shock propagation in a granular chain. *Phys. Rev. E*, 59(3):3202–3206, 1999.
79. D. D. Holm and P. Lynch. Stepwise precession of the resonant swinging spring. *SIAM J. Applied Dynamical Systems*, 1(1):44–64, 2002.
80. J. Hong, J.-Y. Ji, and H. Kim. Power laws in nonlinear granular chain under gravity. *Phys. Rev. Lett.*, 82(15):3058–3061, 1999.
81. G. Hori. Theory of general perturbations with unspecified canonical variables. *Publ. Astron. Soc. Japan*, 18(4):287–296, 1966.
82. G.-I. Hori. Mutual perturbations of $1:1$ commensurable small bodies with the use of the canonical relative coordinates. I. In *Resonances in the motion of planets, satellites and asteroids*, pages 53–66. Univ. São Paulo, São Paulo, 1985.
83. H. Hu and Z.-G. Xiong. Oscillations in an $x^{(2m+2)/(2n+1)}$ potential. *Journal of Sound and Vibration*, 259:977–980, 2003.
84. K. H. Hunt and F. R. E. Crossley. Coefficient of restitution interpreted as damping in vibroimpact. *ASME Journal of Applied Mechanics*, 97:440–445, 1975.
85. M.I. Hussein, M.J. Leamy, and M. Ruzzene. Dynamics of phononic materials and structures: Historical origins, recent progress, and future outlook. *Applied Mechanics Review*, 66:040802, 2014.
86. C. M. Hutchins. A history of violin research. *J. Acoust. Soc. Am.*, 73(5):1421–1440, 1983.
87. R.A. Ibrahim. *Liquid Sloshing Dynamics*. Cambridge University Press, New York, 2005.
88. R.A. Ibrahim. *Vibro-Impact Dynamics: Modeling, Mapping and Applications, LNACM 43*. Springer-Verlag, Berlin, Heidelberg, 2009.
89. R.A. Ibrahim, V. I. Babitsky, and M. Okuma, editors. *Vibro-Impact Dynamics of Ocean Systems and Related Problems*. Springer-Verlag, Berlin Heidelberg, 2009.
90. R.A. Ibrahim, V.N. Pilipchuk, and T. Ikeda. Recent advances in liquid sloshing dynamics. *Applied Mechanics Reviews*, 54(2):133–199, 2001.
91. T. Ikeda. Nonlinear parametric vibrations of an elastic structure with a rectangular liquid tank. *Nonlinear Dynamics*, 33:43–70, 2003.

92. T. Ikeda, Y. Harata, and R. Ibrahim. Nonlinear liquid sloshing in square tanks subjected to horizontal random excitation. *Nonlinear Dynamics*, pages 1–15, 2013.
93. T. Ikeda, R. A. Ibrahim, Y. Harata, and T. Kuriyama. Nonlinear liquid sloshing in a square tank subjected to obliquely horizontal excitation. *Journal of Fluid Mechanics*, 700:304–328, 2012.
94. E. L. Ince. *Ordinary Differential Equations*. Dover, New York, 1956.
95. A. Iomin, S. Fishman, and G.M. Zaslavsky. Quantum localization for a kicked rotor with accelerator mode islands. *Physical Review E*, 65(036215), 2002.
96. A. P. Ivanov. *Dynamics of Systems with Mechanical Collisions*. International Program of Education, Moscow, 1997. in Russian.
97. A.P. Ivanov. Impact oscillations: linear theory of stability and bifurcations. *Journal of Sound and Vibration*, 178(3):361–378, 1994.
98. L.B. Jackson. *Signals, Systems, and Transforms*. Addison-Wesley Publishing Company, New York, 1991.
99. D. Jiang, C. Pierre, and S.W. Shaw. Large-amplitude non-linear normal modes of piecewise linear systems. *Journal of Sound and Vibration*, 272:869–891, 2004.
100. A. L. Kalamkarov, I. V. Andrianov, and V. V. Danishevskyy. Asymptotic homogenization of composite materials and structures. *Applied Mechanics Reviews*, 62(030802):1–20, 2009.
101. G. V. Kamenkov. *Izbrannye trudy v dvukh tomakh. Tom. I*. Nauka, Moscow, 1971. Ustoichivost dvizheniya. Kolebaniya. Aerodinamika. [Stability of motion. Oscillations. Aerodynamics], With a biography of G. V. Kamenkov, a survey article on his works by V. G. Veretennikov, A. S. Galiullin, S. A. Gorbatenko and A. L. Kunicyn, and a bibliography, Edited by N. N. Krasovskiĭ.
102. I.L. Kantor, A.S. Solodovnikov, and A. Shenitzer. *Hypercomplex Numbers: an Elementary Introduction to Algebras*. Springer, 1989.
103. H. Kauderer. *Nichtlineare Mechanik*. Springer-Verlag, Berlin, 1958.
104. J. Kevorkian and J. D. Cole. *Multiple scale and singular perturbation methods*. Springer-Verlag, New York, 1996.
105. W.M. Kinney and R.M. Rosenberg. On steady state harmonic vibrations of non-linear systems with many degrees of freedom. *ASME Journal of Applied Mechanics*, 33:406–412, 1966.
106. V.V. Kisil. Induced representations and hypercomplex numbers. *Advances in Applied Clifford Algebras*, 23(2):417–440, 2013.
107. V. Kislovsky, M. Kovaleva, K.R. Jayaprakash, and Y. Starosvetsky. Consecutive transitions from localized to delocalized transport states in the anharmonic chain of three coupled oscillators. *Chaos*, 26:073102, 2016.
108. V. Kislovsky, M. Kovaleva, and Yu. Starosvetsky. Regimes of local energy pulsations in non-linear klein-gordon trimer: Higher dimensional analogs of limiting phase trajectories, 2016.
109. D.M. Klimov and V.Ph. Zhuravlev. *Group-Theoretic Methods in Mechanics and Applied Mathematics*. CRC Press, 2004.
110. A.E. Kobrinskii. *Dynamics of Mechanisms with Elastic Connections and Impact Systems*. Iliffe Books, London, 1969.
111. C. Koch. *Biophysics of Computation. Information Processing in Single Neurons*. Oxford University Press, Oxford, 1999.
112. A.M. Kosevich and A.S. Kovalev. *Introduction to Nonlinear Physical Mechanics (in Russian)*. Naukova Dumka, Kiev, 1989.
113. I. Kovacic. On the use of Jacobi elliptic functions for modelling the response of antisymmetric oscillators with a constant restoring force. *Communications in Nonlinear Science and Numerical Simulation*, 93:105504, 2021.
114. M. Kovaleva, V. Pilipchuk, and L. Manevitch. Nonconventional synchronization and energy localization in weakly coupled autogenerators. *Phys. Rev. E*, 94:032223, 2016.
115. M.A. Kovaleva, L.I. Manevitch, and V.N. Pilipchuk. *Non-linear beatings as non-stationary synchronization of weakly coupled autogenerators*, pages 53–83. In Problems of Nonlinear Mechanics and Physics of Materials. Springer, 2019.

116. P. Kowalczyk, M. Bernardo, A. R. Champneys, S. J. Hogan, M. Homer, P. T. Piiroinen, Yu. A. Kuznetsov, and A. Nordmark. Two-parameter discontinuity-induced bifurcations of limit cycles: Classification and open problems. *International Journal of Bifurcation and Chaos*, 16(3):601–629, 2006.
117. N. Kryloff and N. Bogoliuboff. *Introduction to Non-Linear Mechanics*. Princeton University Press, Princeton, N. J., 1943.
118. M. S. Kushwaha, P. Halevi, G. Martinez, L. Dobrzynski, and B. Djafari-Rouhani. Theory of acoustic band structure of periodic elastic composites. *Phys. Rev. B*, 49:2313–2322, Jan 1994.
119. N.J. Kutz. Mode-locked soliton lasers. *SIAM Review*, 48(4):629–678, 2006.
120. L. D. Landau and E. M. Lifschitz. *Mechanics: Course of the Theoretical Physics, Volume 1. 3rd ed.* Elsevier, Amsterdam, 1976.
121. M.A. Lavrent'ev and B. V. Shabat. *Problemy Gidrodinamiki i ikh Matematicheskie Modeli*. Nauka, Moscow (in Russian), 1977.
122. Y. S. Lee, F. Nucera, A. F. Vakakis, D.M. McFarland, and L. A. Bergman. Periodic orbits, damped transitions and targeted energy transfers in oscillators with vibro-impact attachments. *Physica D*, 238(18):1868–1896, 2009.
123. Y.S. Lee, G. Kerschen, A.F. Vakakis, P. Panagopoulos, L. Bergman, and D.M. McFarland. Complicated dynamics of a linear oscillator with a light, essentially nonlinear attachment. *Physica D*, 204:41–69, 2005.
124. R. I. Leine, Henk Nijmeijer, and Hendrik Nijmeijer. *Dynamics and Bifurcations of Non-Smooth Mechanical Systems*. Springer, 2006.
125. F. L. Lewis, D. M. Dawson, and C. T. Abdallah. *Robot Manipulator Control: Theory and Practice*. CRC Press, 2004.
126. A.M. Liapunov. An investigation of one of the singular cases of the theory of stability of motion, II. *Mathematicheskiy Sbornik*, 17(2):253–333, 1893. [English translation in: A. M. Liapunov. Stability of Motion. Academic Press, 1966, pages 128–184].
127. A. J. Lichtenberg and M. A. Lieberman. *Regular and Stochastic Motion*. Springer, New York, 1983.
128. O. Makarenkov and J.S.W. Lamb. Dynamics and bifurcations of nonsmooth systems: A survey. *Physica D: Nonlinear Phenomena*, 241(22):1826–1844, 2012.
129. I. G. Malkin. *Some problems of the theory of nonlinear oscillations*. U. S. Atomic Energy Commision, Technical Information Service, 1959.
130. M. Manciu, S. Sen, and A.J. Hurd. Impulse propagation in dissipative and disordered chains with power-low repulsive potentials. *Physica D*, 157:226–240, 2001.
131. A.I. Manevich and L.I. Manevitch. *The Mechanics of Nonlinear Systems With Internal Resonances*. Imperial College Press, London, 2005.
132. L. I. Manevitch and A.I. Musienko. Limiting phase trajectory and beating phenomena in systems of coupled nonlinear oscillators. *2nd International Conference on Nonlinear Normal Modes and Localization in Vibrating Systems, Samos, Greece, June 19–23*, pages 25–26, 2006.
133. L.I. Manevitch. New approach to beating phenomenon in coupled nonlinear oscillatory chains. *Archive Appl Mech*, 77(5):301–12, 2007.
134. L.I. Manevitch and O.V. Gendelman. Oscillatory models of vibro-impact type for essentially non-linear systems. *Proceedings of the Institution of Mechanical Engineers, Part C: Journal of Mechanical Engineering Science*, 222(10):2007–2043, 2008.
135. L.I. Manevitch, M.A. Kovaleva, and V.N. Pilipchuk. Non-conventional synchronization of weakly coupled active oscillators. *Europhysics Letters*, 101(5):50002, 2013.
136. L.I. Manevitch, Yu.V. Mikhlin, and V.N. Pilipchuk. *Metod Normalnykh Kolebanii dlya Sushchestvenno Nelineinykh Sistem*. Nauka, Moscow (in Russian), 1989.
137. J. E. Marsden. *Basic Complex Analysis*. Freeman, San Francisco, 1973.
138. V. P. Maslov and G. A. Omel'janov. Asymptotic soliton-like solutions of equations with small dispersion. *Russian Math. Surveys*, 36(3):73–149, 1981.
139. K.H. Matlack, M. Serra-Garcia, A. Palermo, S.D. Huber, and C. Daraio. Designing perturbative metamaterials from discrete models. *Nature Materials*, 17:323–328, 2018.

140. Michael McCloskey. Intuitive physics. *Scientific american*, 248(4):122–131, 1983.
141. R. E. Mickens. Oscillations in an $x^{4/3}$ potential. *J. Sound Vibration*, 246:375–378, 2001.
142. Yu. V. Mikhlin and S. N. Reshetnikova. Dynamical interaction of an elastic system and a vibro-impact absorber. *Mathematical Problems in Engineering*, 2006(Article ID 37980):15 pages, 2006.
143. Yu. V. Mikhlin and A. M. Volok. Solitary transversal waves and vibro-impact motions in infinite chains and rods. *International Journal of Solids and Structures*, 37:3403–3420, 2000.
144. Yu. V. Mikhlin and A. L. Zhupiev. An application of the Ince algebraization to the stability of the non-linear normal vibration modes. *Internat. J. Non-Linear Mech.*, 32(2):393–409, 1997.
145. N. Minorsky. *Introduction to Non-Linear Mechanics*. J.W. Edwards, Ann Arbor, 1947.
146. Yu.A. Mitropol'sky and P.M. Senik. Construction of asymptotic solution of an autonomouse system with strong nonlinearity. *Doklady AN Ukr.SSR (Ukrainian Academy of Sciences Reports)*, 6:839–844, 1961. (in Russian).
147. F.C. Moon. *Chaotic Vibrations*. John Willey & Sons, New York, 1987.
148. J. Moser. Recent developments in the theory of Hamiltonian systems. *SIAM Rev.*, 28(4):459–485, 1986.
149. J.K. Moser. Lectures on Hamiltonian systems. In *Mem. Amer. Math. Soc. No. 81*, pages 1–60. Amer. Math. Soc., Providence, R.I., 1968.
150. R.F. Nagaev and V.N. Pilipchuk. Nonlinear dynamics of a conservative system that degenerates to a system with a singular set. *Journal of Applied Mathematics and Mechanics*, 53(2):145–149, 1989.
151. A.H. Nayfeh. *Perturbation Methods*. John Wiley & Sons, New York-London-Sydney, 1973.
152. A.H. Nayfeh. Perturbation methods in nonlinear dynamics. In *Nonlinear Dynamics Aspects of Particle Accelerators (Santa Margherita di Pula, 1985)*, pages 238–314. Springer, Berlin, 1986.
153. A.H. Nayfeh. *Method of Normal Forms*. John Wiley & Sons Inc., New York, 1993.
154. A.H. Nayfeh. *Wave Propagation in Layered Anisotropic Media: with Application to Composites*. North-Holland Series in Applied Mathematics and Mechanics. Elsevier Science, 1995.
155. A.H. Nayfeh. *Nonlinear Interactions: Analytical Computational, and Experimental Methods*. John Wiley & Sons Inc., New York, 2000.
156. A.H. Nayfeh and B. Balachandran. *Applied Nonlinear Dynamics Analytical, Computational, and Experimental Methods*. John Wiley & Sons Inc., New York, 1995.
157. V.F. Nesterenko. *Dynamics of Heterogeneous Materials*. Springer-Verlag, New York, 2001.
158. S.V. Nesterov. Examples of nonlinear Klein-Gordon equations, solvable in terms of elementary functions. *Proceedings of Moscow Institute of Power Engineering*, 357:68–70, 1978. (in Russian).
159. A. Norris. Waves in periodically layered media: A comparison of two theories. *SIAM Journal on Applied Mathematics*, 53(5):1195–1209, 1993.
160. E. Ott, C. Grebogi, and J.A. Yorke. Controlling chaos. *Phys. Rev. Lett.*, 64(11):1196–1199, 1990.
161. A.M. Ozorio de Almeida. *Hamiltonian Systems: Chaos and Quantization*. Cambridge University Press, Cambridge, 1988.
162. T.S. Parker and L.O. Chua. *Practical Numerical Algorithms for Chaotic Systems*. Springer-Verlag, New York, 1989.
163. F.D. Peat. *Synchronicity: the Bridge Between Matter and Mind*. Bantam Books, New York, 1988.
164. I.C. Percival and D. Richards. *Introduction to Dynamics*. Cambridge University Press, 1982.
165. F. Peterka. *Introduction to Oscillations of Mechanical Systems with Internal Impacts (in Czech)*. Academia, Prague, 1981.
166. F. Pfeiffer. *Mechanical System Dynamics*. Springer, Berlin, Heidelberg, 2008.
167. F. Pfeiffer and C. Glocker. *Multibody Dynamics with Unilateral Contacts*. Wiley, New York, 1996.
168. F. Pfeiffer and A. Kunert. Rattling models from deterministic to stochastic processes. *Nonlinear Dynamics*, 1(1):63–74, 1990.

169. V. Pilipchuk. Stochastic energy absorbers based on analogies with soft-wall billiards. *Nonlinear Dynamics*, 98(4):2671–2685, 2019.
170. V. Pilipchuk. Analytical criterion of a multimodal snap-through flutter of thin-walled panels with initial imperfections. *Nonlinear Dynamics*, 102(3):1181–1195, 2020.
171. V. Pilipchuk. Design of energy absorbing metamaterials using stochastic soft-wall billiards. *Symmetry*, 13:1798, 2021.
172. V.N. Pilipchuk. The calculation of strongly nonlinear systems close to vibroimpact systems. *Journal of Applied Mathematics and Mechanics*, 49(5):572–578, 1985.
173. V.N. Pilipchuk. Transformation of the vibratory systems by means of a pair of nonsmooth periodic functions. *Dopovidi Akademii Nauk Ukrainskoi RSR. Seriya A - Fiziko-Matematichni Ta Technichni Nauki*, 4:36–38, 1988. (in Ukrainian).
174. V.N. Pilipchuk. On the computation of periodic processes in mechanical systems with the impulsive excitation. In *XXXI Sympozjon "Modelowanie w Mechanice", Zeszyty Naukowe Politechniki Slaskiej, Z.107, Gliwice (Poland)*. Politechnica Slaska, 1992.
175. V.N. Pilipchuk. On special trajectories in configuration space of non - linear vibrating systems. *Mekhanika Tverdogo Tela (Mechanics of Solids)*, 3:36–47, 1995.
176. V.N. Pilipchuk. Analytical study of vibrating systems with strong non-linearities by employing saw-tooth time transformations. *Journal of Sound and Vibration*, 192(1):43–64, 1996.
177. V.N. Pilipchuk. Calculation of mechanical systems with pulsed excitation. *Journal of Applied Mathematics and Mechanics*, 60(2):217–226, 1996.
178. V.N. Pilipchuk. Application of special nonsmooth temporal transformations to linear and nonlinear systems under discontinuous and impulsive excitation. *Nonlinear Dynam.*, 18(3):203–234, 1999.
179. V.N. Pilipchuk. Auto-localized modes in array of nonlinear coupled oscillators. *In: Problemy nelineinoi mekhaniki i fiziki materialov, Dnepropetrovsk, Editor A.I. Manevich (ISBN: 966-7476-10-3)*, pages 229–235, 1999.
180. V.N. Pilipchuk. Non-smooth spatio-temporal transformation for impulsively forced oscillators with rigid barriers. *J. Sound Vibration*, 237(5):915–919, 2000.
181. V.N. Pilipchuk. Principal trajectories of the forced vibration for discrete and continuous systems. *Meccanica*, 35(6):497–517, 2000.
182. V.N. Pilipchuk. Impact modes in discrete vibrating systems with bilateral barriers. *International Journal of Nonlinear Mechanics*, 36(6):999–1012, 2001.
183. V.N. Pilipchuk. Non-smooth time decomposition for nonlinear models driven by random pulses. *Chaos, Solitons and Fractals*, 14(1):129–143, 2002.
184. V.N. Pilipchuk. Some remarks on nonsmooth transformations of space and time for oscillatory systems with rigid barriers. *Journal of Applied Mathematics and Mechanics*, 66(1):31–37, 2002.
185. V.N. Pilipchuk. Temporal transformations and visualization diagrams for nonsmooth periodic motions. *International Journal of Bifurcation and Chaos*, 15(6):1879–1899, 2005.
186. V.N. Pilipchuk. A periodic version of Lie series for normal mode dynamics. *Nonlinear Dynamics and System Theory*, 6(2):187–190, 2006.
187. V.N. Pilipchuk. Transient mode localization in coupled strongly nonlinear exactly solvable oscillators. *Nonlinear Dynamics*, 51(1-2):245–258, 2008.
188. V.N. Pilipchuk. Transitions from strongly to weakly-nonlinear dynamics in a class of exactly solvable oscillators and nonlinear beat phenomena. *Nonlinear Dynamics*, 52(4):263–276, 2008.
189. V.N. Pilipchuk. Transition from normal to local modes in an elastic beam supported by nonlinear springs. *Journal of Sound and Vibration*, 322:554–563, 2009.
190. V.N. Pilipchuk. Nonlinear interactions and energy exchange between liquid sloshing modes. *Physica D: Nonlinear Phenomena*, 263(0):21–40, 2013.
191. V.N. Pilipchuk. Closed-form solutions for oscillators with inelastic impacts. *Journal of Sound and Vibration*, 359:154–167, 2015.

192. V.N. Pilipchuk. Effective hamiltonians for resonance interaction dynamics and interdisciplinary analogies. *Procedia IUTAM*, 19:27–34, 2016. IUTAM Symposium Analytical Methods in Nonlinear Dynamics.
193. V.N. Pilipchuk. Friction induced pattern formations and modal transitions in a mass-spring chain model of sliding interface. *Mechanical Systems and Signal Processing*, 147:107119, 2021.
194. V.N. Pilipchuk, I.V. Andrianov, and B. Markert. Analysis of micro-structural effects on phononic waves in layered elastic media with periodic nonsmooth coordinates. *Wave Motion*, 63:149–169, 2016.
195. V.N. Pilipchuk and R.A. Ibrahim. The dynamics of a non-linear system simulating liquid sloshing impact in moving structures. *Journal of Sound and Vibration*, 205(5):593–615, 1997.
196. V.N. Pilipchuk and R.A. Ibrahim. Dynamics of a two-pendulum model with impact interaction and an elastic support. *Nonlinear Dynam.*, 21(3):221–247, 2000.
197. V.N. Pilipchuk and G.A. Starushenko. On the representation of periodic solutions of differential equations by means of an oblique-angled saw-tooth transformation of the argument. *Dopov. Nats. Akad. Nauk Ukr. Mat. Prirodozn. Tekh. Nauki*, 11:25–28, 1997. (in Russian).
198. V.N. Pilipchuk and G.A. Starushenko. A version of non-smooth transformations for one-dimensional elastic systems with a periodic structure. *Journal of Applied Mathematics and Mechanics*, 61(2):265–274, 1997.
199. V.N. Pilipchuk and A.F. Vakakis. Nonlinear normal modes and wave transmission in a class of periodic continuous systems. In *Dynamics and Control of Distributed Systems*, pages 95–120. Cambridge Univ. Press, Cambridge, 1998.
200. V.N. Pilipchuk and A.F. Vakakis. Study of the oscillations of a nonlinearly supported string using nonsmooth transformations. *Journal of Vibration and Acoustics*, 120(2):434–440, 1998.
201. V.N. Pilipchuk, A.F. Vakakis, and M.A.F. Azeez. Study of a class of subharmonic motions using a nonsmooth temporal transformations (NSTT). *Physica D*, 100:145–164, 1997.
202. H. Poincaré. *Science and Hypothesis*. Dover books on science. Dover Publications, 1952.
203. H. Poincaré. *Les méthodes nouvelles de la mécanique céleste. Tome I*. Librairie Scientifique et Technique Albert Blanchard, Paris, 1987. Solutions périodiques. Non-existence des intégrales uniformes. Solutions asymptotiques. [Periodic solutions. Nonexistence of uniform integrals. Asymptotic solutions], Reprint of the 1892 original, With a foreword by J. Kovalevsky, Bibliothèque Scientifique Albert Blanchard. [Albert Blanchard Scientific Library].
204. H. Poincaré. *Science and method*. Thoemmes Press, Bristol, 1996. Translated by Francis Maitland, With a preface by Bertrand Russell, Reprint of the 1914 edition.
205. K. Popp. Non-smooth mechanical systems. *Journal of Applied Mathematics and Mechanics*, 64(5):765–772, 2000.
206. M.I. Qaisi. Non-linear normal modes of a lumped parameter system. *Journal of Sound and Vibration*, 205:205–211, 1997.
207. J. I. Ramos. Piecewise-linearized methods for oscillators with fractional-power nonlinearities. *Journal of Sound and Vibration*, 300:502–521, 2007.
208. R.D. Richtmyer. *Principles of Advanced Mathematical Physics. Vol. II*. Springer-Verlag, New York, 1981. Texts and Monographs in Physics.
209. R.M. Rosenberg. The $Ateb(h)$-functions and their properties. *Quart. Appl. Math.*, 21:37–47, 1963.
210. R.M. Rosenberg. Steady-state forced vibrations. *Internat. J. Non-Linear Mech.*, 1:95–108, 1966.
211. P.F. Rowat and A.I. Selverston. Oscillatory mechanisms in pairs of neurons connected with fast inhibitory synapses. *Journal of Computational Neuroscience*, 4:103–127, 1997.
212. G. Salenger, A.F. Vakakis, O. Gendelman, L. Manevitch, and I. Andrianov. Transitions from strongly to weakly nonlinear motions of damped nonlinear oscillators. *Nonlinear Dynam.*, 20(2):99–114, 1999.
213. G. D. Salenger and A. F. Vakakis. Discreteness effects in the forced dynamics of a string on a periodic array of non-linear supports. *International Journal of Non-Linear Mechanics*, 33(4):659–673, 1998.

214. A.M. Samoĭlenko, A.A. Boĭchuk, and V.F. Zhuravlev. Weakly nonlinear boundary value problems for operator equations with impulse action. *Ukraïn. Mat. Zh.*, 49(2):272–288, 1997.
215. E. Sanchez-Palencia. *Non-Homogeneous Media and Vibration Theory*. Springer, 2014.
216. F. Santosa and W.W. Symes. A dispersive effective medium for wave propagation in periodic composites. *SIAM Journal on Applied Mathematics*, 51(4):984–1005, 1991.
217. T.P. Sapsis and A.F. Vakakis. Subharmonic orbits of a strongly nonlinear oscillator forced by closely spaced harmonics. *Journal of Computational and Nonlinear Dynamics*, 6:011014, 2011.
218. P. Scherz. *Practical Electronics for Inventors*. McGraw-Hill, 2006.
219. O.H. Schmitt. A thermionic trigger. *Journal of Scientific Instruments*, 15(1):24, 1938.
220. G. Sheng, R. Dukkipati, and J. Pang. Nonlinear dynamics of sub-10 nm flying height air bearing slider in modern hard disk recording system. *Mechanism and Machine Theory*, 41:1230–1242, 2006.
221. Y.G. Sinai. Dynamical systems with elastic reflections: ergodic properties of dispersing billiards. *Russian Math. Surveys*, 25:137–189, 1970.
222. V.V. Smirnov, D.S. Shepelev, and L.I. Manevitch. Energy exchange and transition to localization in the asymmetric Fermi-Pasta-Ulam oscillatory chain. *European Physical Journal B*, 86(10):1–9, 1993.
223. G. Sobczyk. The hyperbolic number plane. *The College Mathematics Journal*, 26(4):268–280, 1995.
224. D. S. Sophianopoulos, A. N. Kounadis, and A. F. Vakakis. Complex dynamics of perfect discrete systems under partial follower forces. *Internat. J. Non-Linear Mech.*, 37(6):1121–1138, 2002.
225. I. Stakgold. *Green's Functions and Boundary Value Problems*. Wiley-Interscience, New York, 1979.
226. Yu. Starosvetsky, K.R. Jayaprakash, and A.F. Vakakis. Scattering of solitary waves and excitation of transient breathers in granular media by light intruders and no precompression. *Journal of Applied Mechanics*, 79(1), 11 2011. 011001.
227. G. Starushenko, N. Krulik, and S. Tokarzewski. Employment of non-symmetrical saw-tooth argument transformation method in the elasticity theory for layered composites. *International Journal of Heat and Mass Transfer*, 45:3055–3060, 2002.
228. W.J. Stronge. *Impact Mechanics*. Cambridge University Press, 2000.
229. H. Tao and J. Gibert. Periodic orbits of a conservative 2-DOF vibro-impact system by piecewise continuation: bifurcations and fractals. *Nonlinear Dynamics*, 95:2963–2993, 2019.
230. J. J. Thomsen and A. Fidlin. Near-elastic vibro-impact analysis by discontinuous transformations and averaging. *Journal of Sound and Vibration*, 311:386–407, 2008.
231. J.J. Thomsen. *Vibrations and Stability, 3rd Edition*. Springer Nature Switzerland AG, 2021.
232. S. P. Timoshenko, D.H. Young, and W.Jr. Weaver. *Vibration Problems in Engineering. 4th. ed.* John Wiley, New York, 1974.
233. J. R. Tippetts. Analysis of idealised oscillatory pipe flow. *2nd International Symposium on Fluid - Control, Measurement, Mechanics - and Flow Visualisation, 5-9 September 1988, Sheffield, England*, 1988.
234. M. Toda. Nonlinear lattice and soliton theory. *IEEE Transactions on Circuits and Systems*, 30(8):542–554, 1983.
235. J.D. Turner. On the simulation of discontinuous functions. *Journal of Applied Mechanics*, 68:751–757, 2001.
236. Y. Ueda. Randomly transitional phenomena in the system governed by Duffing's equation. *J. Statist. Phys.*, 20(2):181–196, 1979.
237. S. Ulrych. Relativistic quantum physics with hyperbolic numbers. *Physics Letters B*, 625:313, 2005.
238. I. M. Uzunov, R. Muschall, M. Golles, Yu. S. Kivshar, B. A. Malomed, and F. Lederer. Pulse switching in nonlinear fiber directional couplers. *Phys. Rev. E*, 51:2527–2537, 1995.
239. A. F. Vakakis and T. M. Atanackovic. Buckling of an elastic ring forced by a periodic attay of compressive loads. *ASME Journal of Applied Mechanics*, 66:361–367, 1999.

240. A.F. Vakakis, O.V. Gendelman, L.A. Bergman, D.M. McFarland, G. Kerschen, and Y.S. Lee. *Nonlinear Targeted Energy Transfer in Mechanical and Structural Systems*. Springer-Verlag, Berlin, Heidelberg, 2009.
241. A.F. Vakakis, L.I. Manevitch, Yu.V. Mikhlin, V.N. Pilipchuk, and A.A. Zevin. *Normal Modes and Localization in Nonlinear Systems*. John Wiley & Sons Inc., New York, 1996. A Wiley-Interscience Publication.
242. E.G. Vedenova, L.I. Manevich, and V.N. Pilipchuk. Normal oscillations of a string with concentrated masses on nonlinearly elastic supports. *Journal of Applied Mathematics and Mechanics*, 49(2):153–159, 1985.
243. F. Vestroni, A. Luongo, and A. Paolone. A perturbation method for evaluating nonlinear normal modes of a piecewise linear two-degrees-of-freedom system. *Nonlinear Dynamics*, 54(4):379–393, 2008.
244. S. B. Waluya and W. T. van Horssen. On the periodic solutions of a generalized non-linear Van der Pol oscillator. *Journal of Sound and Vibration*, 268:209–215, 2003.
245. G.B. Whitham. *Linear and Nonlinear Waves*. John Wiley & Sons Inc., New York, 1999. Reprint of the 1974 original.
246. E.T. Whittaker and G.N. Watson. *A Course of Modern Analysis. 4th Edition*. Cambridge University Press, Cambridge (UK), 1986.
247. M. Wiercigroch and B. de Kraker, editors. *Applied Nonlinear Dynamics ans Chaos of Mechanical Systems with Discontinuities*. World Scientific, Singapore, 2000.
248. I.M. Yaglom. *Complex Numbers in Geometry*. Academic Press, 2014.
249. A. A. Zevin. Localization of periodic oscillations in vibroimpact systems. In *XXXV Symposium "Modeling in Mechanics", Gliwice (Poland), 261-266*. Politechnica Slaska, 1996.
250. A.L. Zhupiev and Yu.V. Mikhlin. Stability and branching of normal oscillations forms of nonlinear systems. *Journal of Applied Mathematics and Mechanics*, 45:328–331, 1981.
251. V.F. Zhuravlev. A method for analyzing vibration-impact systems by means of special functions. *Mechanics of Solids*, 11(2):23–27, 1976.
252. V.F. Zhuravlev. Equations of motion of mechanical systems with ideal one-sided links. *Journal of Applied Mathematics and Mechanics*, 42(5):839–847, 1978.
253. V.F. Zhuravlev. The method of Lie series in the motion-separation problem in nonlinear mechanics. *Journal of Applied Mathematics and Mechanics*, 47(4):461–466, 1983.
254. V.F. Zhuravlev. The application of monomial Lie groups to the problem of asymptotically integrating equations of mechanics. *Journal of Applied Mathematics and Mechanics*, 50(3):260–265, 1986.
255. V.F. Zhuravlev. Singular directions in the configuration space of linear vibrating systems. *Journal of Applied Mathematics and Mechanics*, 56(1):13–19, 1992.
256. V.F. Zhuravlev and D.M. Klimov. *Prikladnye Metody v Teorii Kolebanii*. Nauka, Moscow, 1988. Edited and with a foreword by A. Yu. Ishlinskiĭ.
257. Z.T. Zhusubaliyev and Mosekilde E. *Bifurcations and Chaos in Piecewise-Smooth Dynamical Systems*. World Scientific, 2003.

Index

V. N. Pilipchuk, *Oscillators and Oscillatory Signals from Smooth to Discontinuous*,
https://doi.org/10.1007/978-3-031-37788-4